GEORGIA INSTITUTE OF TECHNOLOGY
OFFICE OF RESEARCH ADMINISTRATION

RESEARCH PROJECT INITIATION

Date: July 11, 1974

Project Title: Window and Curtain Wall Performance in High-rise Buildings

Project No: E-16-650/E-20-654

Principal Investigators: Dr. C. S. Martin (CE)
Dr. J. I. Craig (AE)

Sponsor: National Science Foundation

Agreement Period: From 5/15/74 Until 10/31/75* (Grant Expiration)

Type Agreement: Grant No. GK-43455X

Amount:	C.E.		A.E.		Totals
	$30,421	(E-20-654)	$38,379	(E-16-650)	$68,800 NSF Funds
	+3,483	(E-20-328)	4,243	(E-16-343)	7,726 GIT Contri.
	$33,904		$42,622		$76,526 Total

Reports Required:
Annual Letter (if expected renewal is granted)
Final Report

Sponsor Contact Person (s):

Technical Matters

Dr. M. P. Gaus, Head
Engineering Mechanics Section
National Science Foundation
Washington, D. C. 20550

Administrative Matters

(Thru ORA)
Mr. F. G. Naughten
Grants Manager, Area 4
National Science Foundation
Washington, D. C. 20550
Phone: (202) 632-5965

*Proposed project period (12 mos.) ends 5/14/75; all committments to be met by grant expiration date unless formal extension is obtained in advance.

Assigned to: Civil Engineering/Aerospace Engineering

COPIES TO:

- Principal Investigator (2)
- School Director (2)
- Dean of the College
- Director, Research Administration
- Director, Financial Affairs (2) (4)
- Security-Reports-Property Office
- Patent Coordinator
- Library
- Rich Electronic Computer Center
- Photographic Laboratory
- Project File
- Other

RECEIVED AUG 1974 Research Security Office

RA—3 (6—71)

GEORGIA INSTITUTE OF TECHNOLOGY
OFFICE OF CONTRACT ADMINISTRATION

SPONSORED PROJECT TERMINATION

Posted

Date: 5/17/78

Project Title: "Window and Curtainwall Performance in Highrise Buildings"

Project No: E-16-650/E-20-654

Project Director: Dr. J. I. Craig/Dr. C. S. Martin

Sponsor: National Science Foundation

Effective Termination Date: 4/30/77

Clearance of Accounting Charges: 4/30/77

Grant/Contract Closeout Actions Remaining: NONE

_ Final Invoice and Closing Documents
_ Final Fiscal Report
_ Final Report of Inventions
_ Govt. Property Inventory & Related Certificate
_ Classified Material Certificate
_ Other _____

Assigned to: Aerospace Engineering/Civil Engineering (School/Laboratory)

COPIES TO:

Project Director
Division Chief (EES)
School/Laboratory Director
Dean/Director–EES
Accounting Office
Procurement Office
Security Coordinator (OCA) ✓
Reports Coordinator (OCA)
Library, Technical Reports Section
Office of Computing Services
Director, Physical Plant
EES Information Office
Project File (OCA)
Project Code (GTRI)
Other _____

CA–4 (3/76)

LETTER PROGRESS REPORT
NSF Grant GK - 43455x

March 1975

Work on the subject grant to study the performance of windows and curtain walls in highrise buildings was initiated at the beginning of the summer academic quarter, 1974. The initial effort during the first year has been reduced somewhat from the level proposed. This was directly the result of, (a) unexpectedly increased teaching loads, and (b) delays in the completion of the particular highrise building to be studied. Work has proceeded along three lines and the progress to date in each area is summarized in the following sections.

Pressure Simulation Facility: The design of the full-scale wind pressure simulator has been completed. Detail and assembly drawings have been prepared, and final construction work is underway. Preliminary testing of the system is scheduled for the first week in May. The present facility has been extensively redesigned from that proposed in order to extend the performance. The basic design is of a positive displacement type where pressure loads are produced by controlled displacements of several large pistons forming part of the rear wall of a large test chamber (see attachment). The fixture will accept window test assemblies as large as 8 ft. by 15 ft. and is designed to produce pressure fluctuations of up to 50 psf, peak-to-peak, about mean pressures of up to 75 psf at cyclic rates as high as 20 Hz. The driving force is provided by small servo-controlled, 3000 psi hydraulic actuators connected to six large hinged pistons (doors) which cover the rear of the test fixture. The performance at extreme pressure and frequency is obtained by actually producing and controlling a resonance behavior of the pistons and test chamber. The apparatus will operate in a closed-loop fashion using a modified cascade control system and will accept both random and sinusoidal forcing functions.

The system will be initially operated with only two of the six actuators; however, provision has been made and hydraulic capacity provided to handle the remaining four actuators. Four 55 in. by 99 in. by ¼ in. doubly glazed lights along with appropriate sections from the curtain wall used in the building have been acquired and are ready to be installed in the test fixture. The design and preliminary results for this facility will be presented in a Research Summary Report at the 2nd U.S. National Conference on Wind Engineering Research, Ft. Collins, June 1975.

Field Measurement Program: The field measurement study in the 30 story "Tower Place" building has been held up due to delays in the building construction program. It is anticipated that the curtain wall installation will be completed by the end of April so that instrumentation can be moved into the building during late spring. Work to date has centered in the laboratory on the design and construction of the response measurement instruments, particularily on the development of a remote sensing instrument to simultaneously from one side measure the movement of both lights in a doubly-glazed window. This latter instrument has been constructed and is presently being calibrated in the laborato prior to its field use. The basic design uses a narrow collimated light beam from a small He-Ne laser reflected off of the inner and outer lights. Two solid state, linear position-sensitive photo-detectors are used to differentially analyze the movement of the reflected beam, and a simple analog computational circuit is used to derive the normal and angular displacement components. Detail of the design and operation of this instrument will be presented shortly in a paper by the graduate research assistant participating the study.

In a separate program funded by the building owners, a wind tunnel study of the building wind pressure loading was run in the Aerospace Engineering 9 ft. tunnel. All data from these tests have been recorded in computer-compatible

form and will be used for comparison with the full scale response measurements.

Analytical Studies: Analytical studies are being directed at modelling the dynamic response of both single and double-glazed lights. In the first case, the effort is being directed towards properly representing the damping and non-linearily elastic behavior in the boundaries (gaskets) by means of a hybrid finit element appraoch. In the second case, the boundary-coupled response of the two lights in a double-glazed assembly is being modelled and the effect of venting of the gas entrapped between the two plates is being studied.

Dr. L. Z. Emkin has been unable to participate as an associate on the program. His responsibilities, particularily in the analytical modelling, have been assumed as of January 1975 by Dr. Barry Goodno, recently appointed as Assistant Professor of Civil Engineering. A copy of his biosketch is attached.

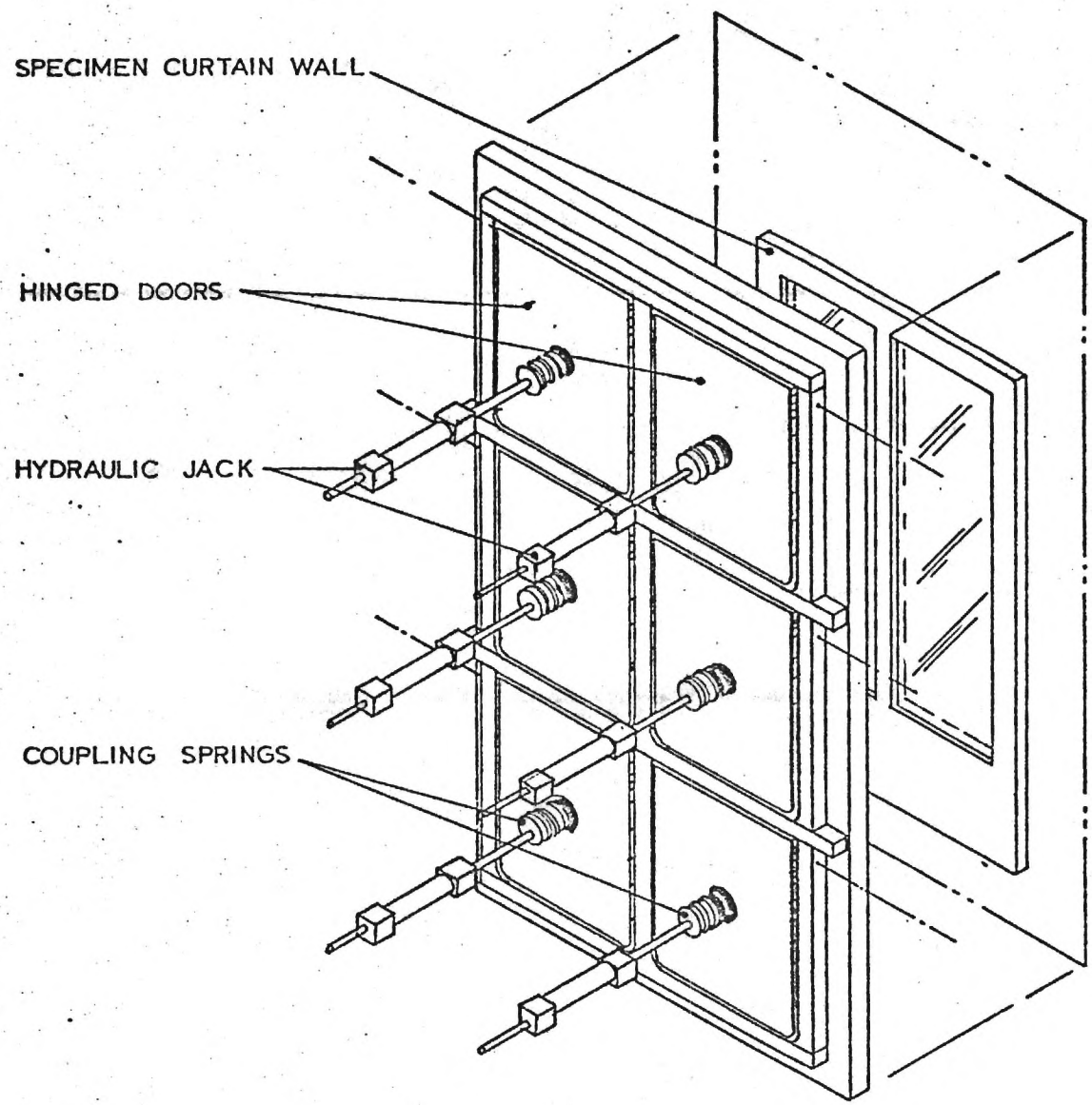

CURTAIN WALL TEST FACILITY

BIOGRAPHICAL SKETCH

Barry John Goodno

Present Position and Address:

Assistant Professor
School of Civil Engineering
Georgia Institute of Technology
Atlanta, Georgia 30332

Date and Place of Birth: July 19, 1947, Madison, Wisconsin

Education:

Bachelor of Science, Civil Engineering, January, 1970
University of Wisconsin, Madison, Wisconsin
Master of Science, Structural Engineering, June, 1971
Stanford University, Stanford, California
Doctor of Philosophy, Civil Engineering, January, 1975
Stanford University, Stanford, California

Professional Society Membership:

American Society of Civil Engineers, (ASCE), Associate Member
Earthquake Engineering Research Institute, (EERI), Member
Seismological Society of America, (SSA), Member
The Society of the Sigma Xi, Member
Engineer-in-Training, (EIT), State of Wisconsin, (June, 1969)

Honor Societies:

Phi Eta Sigma, Chi Epsilon, Tau Beta Pi, Phi Kappa Phi

Employment History:

Assistant Professor, School of Civil Engineering
Georgia Institute of Technology
Atlanta, Georgia
September 1974 to Present

Senior Structural Research Engineer
John A. Blume and Associates, Engineers
San Francisco, California
April to July, 1973

National Science Foundation Teaching
Fellow, Stanford University
Spring Quarter 1972 and Winter Quarter 1973

Structural Engineer
Arnold and O'Sheridan, Inc.
Structural Engineering Consultants
Madison, Wisconsin
Summer 1969, 1970

Student Engineer Trainee
Wisconsin Division of Highways
Madison, Wisconsin
Summer 1966, 1967, 1968

Publications:

Goodno, B. J., and Kost, E. G., Structural Design for Ground Motions: Reduction of Input Energy and Structural Response - Literature Survey, John A. Blume and Associates, Engineers, San Francisco, California, September 1973.

Goodno, B. J., Dynamic Analysis of Suspended-Floor Highrise Buildings Using Super-Elements, thesis presented to the Department of Civil Engineering, Stanford University, Stanford, California, in September, 1974 in partial fulfillment of the requirements for the degree of Doctor of Philosophy.

Current Fields of Interest:

Damping in Highrise Building Structures

Finite - Element Analysis of Shear Walls and Shear Cores in Highrise Buildings

Dynamic Analysis of Floor Systems to Reduce Human Discomfort in Building Structures

Performance of Windows and Cladding in Highrise Building Structures

E76-650

Window and Curtainwall Performance in Highrise Buildings

Final Technical Report
Submitted to the
National Science Foundation
by
Georgia Institute of Technology
School of Aerospace Engineering
School of Civil Engineering

C. S. Martin, Co-principal Investigator
J. I. Craig, Co-principal Investigator
B. J. Goodno, Associate Investigator
R. B. Deo, Post Doctoral Fellow

Grant ENG 73-04216
Starting Date: May 1974
Completion Date: March 1978

Scientific Description of Research and Results

A detailed and comprehensive description of the research and the results obtained from this work are provided in the attached copy of the Final Report. This report covers the field study conducted at a highrise building in Atlanta, the analytical modelling of typical sheer glass cladding (including a full listing of all computer code developed), and the design, construction and use of a full scale laboratory window pressure test facility. The following paragraph provides a brief abstract of the work.

The present study is directed at more precisely characterizing the nature of the local cladding pressure loads in highrise buildings and more accurately modelling the structural response of the cladding to these loads. A combination of full scale field measurements of loads and response, detailed discrete element analytical modelling of the cladding itself, and controlled laboratory simulation and testing have been carried out. A comprehensive measurement methodology is developed and used in the field study to characterize the temporal and spectral features of the differential pressure loading and to assess the causality of these loads for the measured dynamic response of the cladding - in particular large insulating glass windows. The analytical work is centered around the development of a large and detailed discrete element model for the cladding, including its connection to the underlying structure. When the model parameters are adjusted or "calibrated" to laboratory measured values, it is shown that the predicted cladding performance agrees well with field and lab response measurements. Out-of-phase double panel glass plate modes are predicted and are measured. Finally, the design and use of a full-scale laboratory facility for simulating both the static and dynamic features of the cladding pressure loads are described. This facility is used for a detailed modal test of a large double panel window under typical mounting conditions and the results are compared to the present analytical predictions.

List of Publications

1. Deo, R. "An Experimental Investigation of the Performance of Insulating Windows-Wind Loads and Dynamic Response," Ph.D. dissertation, Georgia Tech, June 1977.

2. Wey, J.D., "Properties and Behavior of Window-Frame Assemblies," M.S. thesis, Georgia Tech, September 1976.

3. Craig, J. I., and Palfery, J. G., "Full-Scale Wind Pressure Simulation for Windows and Curtain Wall Structures," ASCE-EMD Specialty Conference on Dynamic Response of Structures: Instrumentation, Testing Methods and System Identification, UCLA, Los Angeles, March 1976.

4. Craig, J. I., Palfery, J.G. and Martin, C. S. "Wind Pressure Simulation and Response Measurement for Windows," proceedings of Second U.S. National Conference on Wind Engineering Research, Colorado State University, Ft. Collins, Colorado, June 1975.

5. Deo, R. and Craig, J. I. "An Optical Technique for the Measurement of Time Dependent Displacements," Advances in Test Measurement, Vol. 15, Instrument Society of America, 1978, pp. 339342.

6. Deo, R. B. and Craig, J. I., "Wind Load Causality for Dynamic Response of Windows," proceedings of the 3rd U.S. National Conference on Wind Engineering Research, University of Florida, Feb. 1978, III - 12-1.

7. Deo, R. B. and Craig, J. I., "Full Scale Measurement of Cladding Pressure," proceedings of the 3rd U.S. National Conference on Wind Engineering Research, University of Florida, Feb. 1978, III -11-1.

8. Goodno, B. J., "Response of Glass Cladding in Highrise Buildings," proceedings of the 3rd U.S. National Conference on Wind Engineering Research, University of Florida, Feb. 1978, p. III-10-1.

9. Goodno, B. J., "Structural Performance of Insulating Windows," submitted for publication in the Journal of the Structural Division, ASCE.

10. Goodno, B. J., "Dynamic Response of Glass Curtain Wall Elements," submitted for publication in the Journal of the Structural Division, ASCE.

11. Craig, J. I., Goodno, B. J. and Deo, R. B., "Window and Curtain Wall Performance in Highrise Buildings," Final Report, NSF Grant ENG 73-04216, Georgia Institute of Technology, GITAER 78-100, SCEGIT 78-170, March 1978.

Theses

One Masters and a Doctoral thesis were completed in support of and with funds provided by the grant. The titles are as follows:

Deo, R. B., "An Experimental Investigation of the Performance of Insulating Windows - - Wind Loads and Dynamic Response," Ph.D. Dissertation, Georgia Institute of Technology, School of Aerospace Engineering, June 1977.

Wey, J. D., "Properties and Behavior of Window - Frame Assemblies," M.S. Thesis, Georgia Institute of Technology, School of Civil Engineering, Sept. 1976.

Inventions

A laser displacement meter, described in Reference #5, was developed to measure the movement of the outer pane of a doubly glazed window from a reference position inside the building. This instrument was not judged to be patentable but the present design is being studied and is now under consideration by others for use in various experimental studies.

Scientific Collaborators at Georgia Institute of Technology

J. I. Craig, Associate Professor, Co-principal Investigator
B. J. Goodno, Assistant Professor, Associate Investigator
C. S. Martin, Professor, Co-principal Investigator
R. B. Deo, Post Doctoral Fellow
J. D. Wey, Graduate Research Assistant
J. G. Palfery, Research Engineer

Comments

The reported work has resulted in the development of a laboratory facility for evaluating the performance of full scale window assemblies under both static and dynamic loads. The work has also promoted the development of a first-class experimental research capability in this area of structural dynamics at Georgia

Tech. Finally, these efforts have led, in part, to the preparation of a new 3 year research proposal to NSF/PFRA which has now been funded. The new grant, ENV 77-04269 is titled, "Influence of Nonstructural Cladding on Dynamic Properties and Response of Highrise Buildings," with co-principal investigators, B. J. Goodno, J. I. Craig, K. M. Will.

Signatures

C. S. Martin	J. I. Craig	B. J. Goodno
Co-principal Investigator	Co-principal Investigator	Associate Investigator

Date: 5/17/78

NATIONAL SCIENCE FOUNDATION
Washington, D.C. 20550

SUMMARY OF COMPLETED PROJECT

Form Approved
OMB No. 99R0013

Please read instructions on reverse carefully before completing this form.

1. INSTITUTION AND ADDRESS	2. NSF PROGRAM	3. PRINCIPAL INVESTIGATOR(S)
Georgia Institute of Technology Atlanta, Georgia	Water Resources, Urban & Environmental Engr.	Dr. J. I. Craig Dr. C. S. Martin

4. AWARD NUMBER	5. DURATION (MOS)	6. AWARD PERIOD	7. AWARDEE ACCOUNT NUMBER
ENG73-04216 A01	36	from 5/15/74 to 4/30/77	E-16-650/E-20-654

8. PROJECT TITLE

"Window and Curtain Wall Performance in Highrise Buildings."

9. SUMMARY (ATTACH LIST OF PUBLICATIONS TO FORM)

The present study is directed at more precisely characterizing the nature of the local cladding pressure loads in highrise buildings and more accurately modelling the structural response of the cladding to these loads. A combination of full scale field measurements of loads and response, detailed discrete element analytical modelling of the cladding itself, and controlled laboratory simulation and testing have been carried out. A comprehensive measurement methodology is developed and used in the field study to characterize the temporal and spectral features of the differential pressure loading and to assess the causality of these loads for the measured dynamic response of the cladding - in particular large insulating glass windows. The analytical work is centered around the development of a large and detailed discrete element model for the cladding, including its connection to the underlying structure. When the model parameters are adjusted or "calibrated" to laboratory measured values, it is shown that the predicted cladding performance agrees well with field and lab response measurements. Out-of-phase double panel glass plate modes are predicted and are measured. Finally, the design and use of a full-scale laboratory facility for simulating both the static and dynamic features of the cladding pressure loads are described. This facility is used for a detailed modal test of a large double panel window under typical mounting conditions and the results are compared to the present analytical predictions.

9. SIGNATURE OF PRINCIPAL INVESTIGATOR/ PROJECT DIRECTOR	TYPED OR PRINTED NAME	DATE
	Dr. J. I. Craig	5/17/78

NSF Form 98A (10-77) SUPERSEDES ALL PREVIOUS EDITIONS

FINAL REPORT

WINDOW AND CURTAIN WALL PERFORMANCE IN HIGH-RISE BUILDINGS

By

J. I. Craig
B. J. Goodno
R. B. Deo

Prepared for

NATIONAL SCIENCE FOUNDATION
DIVISION OF ENGINEERING

GRANT ENG–73–04216

March 1978

GEORGIA INSTITUTE OF TECHNOLOGY
SCHOOL OF AEROSPACE ENGINEERING
SCHOOL OF CIVIL ENGINEERING
ATLANTA, GEORGIA 30332

GITAER-78-100
SCEGIT-78-170

WINDOW AND CURTAIN WALL PERFORMANCE IN HIGH-RISE BUILDINGS

J. I. Craig
B. J. Goodno
R. B. Deo

FINAL REPORT

Grant ENG-73-04216

Prepared for the

National Science Foundation
Division of Engineering

by

GEORGIA INSTITUTE OF TECHNOLOGY
School of Aerospace Engineering
School of Civil Engineering

March 1978

ABSTRACT

The present study is directed at more precisely characterizing the nature of the local cladding pressure loads in highrise buildings and more accurately modelling the structural response of the cladding to these loads. A combination of full scale field measurements of loads and response, detailed discrete element analytical modelling of the cladding itself, and controlled laboratory simulation and testing have been carried out. A comprehensive measurement methodology is developed and used in the field study to characterize the temporal and spectral features of the differential pressure loading and to assess the causality of these loads for the measured dynamic response of the cladding-in particular large insulating windows. The analytical work is centered around the development of a large and detailed discrete element model for the cladding, including its connection to the underlying structure. When the model parameters are adjusted or "calibrated" to laboratory measured values, it is shown that the predicted cladding performance agrees well with field and lab measurements. Out-of-phase double panel glass plate modes are predicted and are measured. Finally, the report describes the design and use of a full scale laboratory facility for simulating both the static and dynamic features of the cladding pressure loads. This facility is used for a detailed modal test of a large double panel window under typical mounting conditions and the results are compared to the present analytical predictions.

TABLE OF CONTENTS

1.0	Introduction	1
	1.1 Background	1
	1.2 Design Considerations	3
	1.3 Statement of Work	8
2.0	Field Study	13
	2.1 Background	13
	2.2 Design Considerations	21
	2.3 Site Specification	26
	(a) Test Site Description	26
	(b) Wind Tunnel Study	29
	2.4 Evaluation Methodology	31
	(a) System Description	32
	(b) Application to Wind Loads and Window Response	44
	(c) Data Processing	53
	(d) Experimental Techniques	64
	2.5 Experimental Results	78
	(a) Parametric Analysis of Wind Loads	79
	(b) Window Response Causality	105
	(c) Window Dynamic Properties	117
3.0	Analytical Investigations	136
	(a) Need for Discrete Element Model	136
	(b) Objectives	137
	3.1 Analytical Model	138
	(a) Description of Discrete Element Model	138
	(b) Structural Assemblage and Condensation	147
	(c) Static Analysis Procedures	155
	(d) Dynamic Analysis Procedures	158
	3.2 Computer Program	165
	(a) Description	165
	(b) Macro-Flow Chart	166
	(c) Notation and Input Guide	169

3.3 Discussion of Results 169
(a) Sample Analyses 175
(b) Nondimensional Ratios 191
(c) Static Analysis Results 194
(d) Dynamic Analysis Results 199
(e) Panel Racking Studies 213
3.4 Double Panel Models 226
(a) Continuum Model 226
(b) Discrete Element Model 233
3.5 Overall Structure Cladding Model 236
3.6 Summary 238
4.0 Laboratory Facility 239
4.1 Background 239
4.2 Design of the Facility 242
4.3 Performance Evaluation 247
4.4 Static Testing 256
(a) Boundary Properties 257
(b) Static Test Results 271
4.5 Dynamic Testing 285
(a) Measurement and Analysis Methodology 285
(b) Dynamic Response Results 290
5.0 Conclusions 299
6.0 References 302

APPENDIX 309

1.0 INTRODUCTION

1.1 Background

The past decade has witnessed considerable activity and progress in the analysis of and design for wind loads on tall buildings. Two important considerations, the effect of terrain roughness and the dynamic aspects of the wind loading itself, are now better understood because of a substantial research effort. Much has been accomplished in expanding our understanding of wind loads on the total structure, however our knowledge, relatively speaking, of the loading and response of windows, curtain walls and architectural details of the building cladding is yet in quite an infant state. To illustrate this it should be noted that design wind loads are usually given for the overall structure but not specifically for the glass panes which are incorporated in the cladding. The fact that such geometric features as corners have been shown to produce substantial changes in local flow conditions dictates that the design wind load for windows and cladding be different than that for the structure as a whole. Furthermore, from a dynamic standpoint the gust loading for a window would not be expected to be the same as that for the sturcture. In a first step, the American National Standards Institute code ANSI A58.1-1972 has recognized the problem and provided for increased design wind pressures in the vicinity of corners or setbacks.

At the same time, increased activity in building design, especially with regard to tall buildings of unusual design, is rapidly extending the engineering state-of-the-art. Unfortunately, engineering knowledge and design methodology in several areas appear to have been surpassed by

architectural innovation. This problem has been particularly evident in the design of building cladding systems which in recent years have become increasingly varied. Cladding in general is considered non-structural, but yet must form a first line of defense for the structure against environmental forces arising from a variety of sources: pressure loads due to wind or sonic boom, impact due to debris, solar thermal loads, seismic loading, and interactive structural loading due to building frame distortions. The complexity and interaction of these factors is shown schematically in Fig. 1.1-1 where a distinction has been made as to source and manner (static, dynamic) of loadings.

In traditional engineering design greater analytical attention has been given to major building components (foundation, frame) than to architectural details such as the cladding or window systems. The principal reason is, of course, that the failure of a major component would be catastrophic. However, the increasingly frequent failure of windows and cladding to perform as intended coupled with the fact that the cladding can now account for 10 - 20% of the initial building cost, has noticeably increased the economic risk of advanced design concepts. A detailed discussion of recent failures would be overly lengthy, but the instances documented by Refs. 1 - 10 clearly underline the fact that a reliable design methodology is lacking. The pattern of failures strongly suggests that wind forces constitute the major consideration for the design of cladding systems. The problem is compounded, however, by the fact that failures have been variously attributed to a number of factors including thermal stressing, inplane loading due to rocking and glazing interference, improper use of cleaning fluid, projectiles,

as well as dynamic effects such as glazing pull-out or interaction between two panes in a double-glazed window.

Clearly, many of the failures of windows and cladding assemblies, reported or not, can be generally attributed to improper design. The solution to these problems is not always so direct, however. While all important factors may not have been considered, it is also possible that some factors were previously unknown. The situation can only be made more acute by the healthy diversification of design and construction present in modern highrise buildings. The use of new materials and advanced construction techniques makes it imperative not only that all significant loads are defined but also that the various response patterns are properly identified and understood.

1.2 Design Considerations

Wind forces are recognized to constitute a major loading in the structural design of tall buildings and there is currently much interest and activity in refining knowledge of these loads. While treatment of the effect of wind loading on the overall structural performance has received wide attention, the localized effects of wind pressure, especially strongly fluctuating pressure, on build cladding has until recently received much less consideration.

In developing rational design procedures for cladding components and systems, much of the work to date has centered on the specification of static wind pressure loads. These figures are often augmented by factors reflecting the expected magnitudes of wind gusts. In some instances account is also taken of the pressure distribution caused by

wind flow around corners and other gross shape features of the structure (11).

Results from extensive testing programs by the two major glass manufacturers in the U. S. form the basis of most design procedures and codes. This data has been obtained exclusively from static testing although charts are available for various equivalent static loads (12). Extensive discussion of these procedures and codes, as well as consideration of wind load prediction and glass strength, formed a major portion of the national conference on building research in 1967 (13 - 15). Wind effects and wind loads on buildings and other structures have been the subject of much more work and several national and international conferences during the past decade have been largely devoted to this topic (16 - 21). While a majority of the reported work has dealt with overall or integrated wind loading, an increasing concern for the nature of localized loading is evident. A comprehensive treatment of these combined factors in current building design is beginning to emerge, and innovations such as buildings designed to minimize, not just withstand, wind loads (22), or specification of windows of a variable size with height for a tall building (23) have been reported.

A rational methodology for designing building cladding and windows in particular has lagged considerably behind, and only recently have attempts been made to characterize the nature of localized loadings (24 - 26). There have been only scattered attempts to ascertain the resultant localized structural response to these forces (27), although at least one experimental facility has been built to simulate the anticipated conditions (28). As far as response characteristics or

failure modes are concerned there is much conjecture but little hard evidence is available. It is observed that pressure loads may in certain circumstances cause window panes to actually be ejected from their glazing but it is often assumed that the force responsible for this is a quasi-static pressure load due largely to wind suction effects. The situation is often augmented by weakness in the mullion or glazing design or by improper installation of the light itself. Instances in which the light does not appear to fracture before leaving the glazing are often recorded and consequently it can be reasonably assumed that glass fracture by itself is not a major consideration in this connection. There has been, however, no real attention directed toward possible dynamic mechanisms which might play a role in this ejection type failure of lights. In fact, the only available reference to dynamic effects in commercial curtain wall designs that we have noted regards the possible psychological effects on building occupants of low frequency (3 - 7 Hz) panel vibrations (29, 30). As human response and discomfort is receiving more and more attention (31), psychological reaction to excessive glass movement must be considered. Regarding the range of natural frequencies of large windows, Pretlove and Bowles (32) have, from a large sampling of window response in Britain, found that a typical large window (88.3 in by 125.8 in) will have a natural frequency of 6 Hz. Although the deflection itself may not be structurally critical, excessive deflections can be of concern to occupants.

An interesting failure mode involving excessive deflection coupled with dynamic response has been suggested in windows that are doubly

glazed. The proposed failure mode, particularly for those windows incorrectly or incompletely installed involves a sharp transient vibration of the panes in which each moves out of phase with the other. If sufficient amplitude is developed, the panes might actually contact with the result that either or both may fail. While the ultimate failure is due to breakage, the initiation might be the result of dynamic response of the window.

In examining the overall design of curtain walls it appears reasonable to inquire as to the possible effects of the vibration behavior of lights as well as other component panels on the structural performance of the assembly. The current procedures for design of building windows principally involves the consideration of the maximum gust loading modified by local shape effects, the resistance of the glazing to rain penetration (and, possible freezing), and the thermal expansion or contraction behavior. The aggregate effect is then considered as a static design load and the glass pane is sized in thickness accordingly. The strength estimations for the panes are based on the statistical results of static tests to failure of numerous laboratory samples (33, 34). There is, of course, an inconsistency in this approach because glass, as it is well known, exhibits a pronounced static fatigue and consequently static failure stresses are often several times lower than those for dynamic loading. Wind loads by their nature represent a dynamic load component and therefore static strength figures may be unduly conservative. This effect is considered to some extent in the specification of a safety factor of 2.5 for this utilization. In contrast, factors of from 5 to 8 are common for static loading that prevails in aquariums or shelving.

The dynamic processes should be present to some degree in curtain wall windows of all sizes but the effects may become more pronounced in larger windows (greater than 20 sq ft). In these cases the natural frequencies are lower and the vibrations are often of higher amplitude. Since pressure loading increases as the square of the dimensions, the restraint forces per unit length along the boundaries are increased in direct proportion to the edge dimensions. This requires correspondingly heavier glazing and magnifies dynamic effects here. Tempered glass because of its strength advantage over annealed plate glass is sometimes used in large windows to conserve weight and hence cost. Unfortunately, the elastic properties (modulus) are largely unaffected by tempering and hence thinner lights possible with this material have lower natural frequencies which aggrevate the boundary restraint problem noted above and which also may produce adverse psychological effects.

Finally, while the previous design considerations have implicitly assumed that the cladding system is essentially nonstructural, it is becoming evident from the results of more refined structural analyses and experimental data that architectural details such as partitions, light walls, etc., may provide measureable structural stiffening and damping action (35 - 39). Building cladding in many instances may also provide similar benefits although it is seldom if ever accounted for. Usually the problem is just the opposite: how to minimize the interactive structural effects and transmit only the direct wind pressure or seismic loads to the structure. On the other hand, cladding is generally composed of thin plate-like elements which may have considerable in-plane load carrying ability and shear strength

that might with proper design be utilized to control structural stiffness or energy dissipation. Because of the lack of adequate knowledge as to precisely how loads are transmitted into and through the cladding, it is not currently feasible to directly utilize this component as more than an environmental barrier.

The formulation of a rational design procedure for modern window and curtain wall construction as can be seen from the brief discussion above involves consideration of a large number of factors. There are numerous sources of dynamic loading on a window and the realtive magnitudes of the factors among themselves as well as compared to static loads have not been established. At the same time, the dynamic response of windows and claddings is not well understood. Clearly, there is currently the need for a fuller understanding and more complete knowledge of these topics. This is especially appropriate because of the more diverse design and sophisticated analysis of tall buildings, involving, for example, detailed computer structural analysis and model wind tunnel testing.

1.3 Statement of Work

The present report describes the results of a two-year program of research aimed at providing some of the answers to the questions raised concerning the localized character of wind loads on windows and cladding and the types of response to these loads. The overall problem is complex and multi-faceted and in certain respects the present work represents an initial step. The study has been broken into several more clearly defined areas, and a description of each along with the overall objectives are given in this section. Results of the reaserch in each area follow in succeeding chapters.

Figure 1.3-1 diagrams the overall organization of the study and shows the grouping into three areas: (i) field study at a 29-story lightweight clad highrise building; (ii) analytical modelling of a representative window assembly and associated cladding for both static and transient dynamic behavior; and (iii) development of a laboratory facility for full-scale dynamic load simulation and testing. The work in each area proceeded in parallel, but was accompanied by extensive cross-flow of data, results, and insights throughout the course of the study. The objectives of the research are outlined in the figure but can be more generally summarized as:

(i) characterize the spectral and temporal features of the localized cladding pressure loading, especially in relation to building geometry and flow features;

(ii) identify the major window response mechanisms, both experimentally and analytically, and assess the degree of causality between measured forcing function and response (e. g., identify the degree of response attributable to a particular forcing function);

(iii) develop an analytical model that can satisfactorily represent both the static and dynamic behavior of a representative window-cladding assembly;

(iv) develop a capability and methodology for performing full-scale dynamic testing of window or curtain wall assemblies.

The diagrams in Figs. 1.3-2 to -4 show a schematic outline of each of the research areas and define the basic approaches towards accomplishing the objectives. The field study (Fig. 1.3-2) involved at the outset a parallel effort to obtain wind tunnel model data and to develop the instrumentation and measurement techniques for full-scale testing. The model data was used for preliminary identification of "critical" regions or other areas of interest, while the instrument development phase was aimed at constructing the specialized transducers

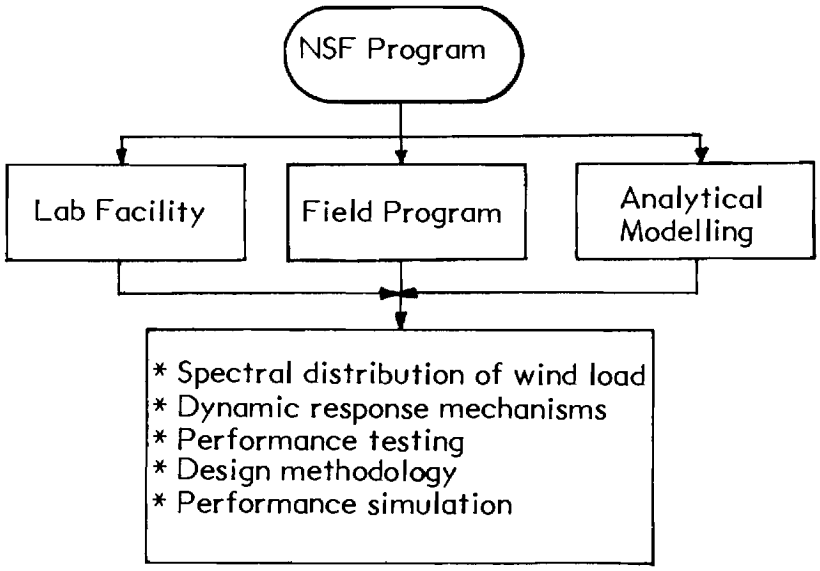

Figure 1.3-1 Program Organization

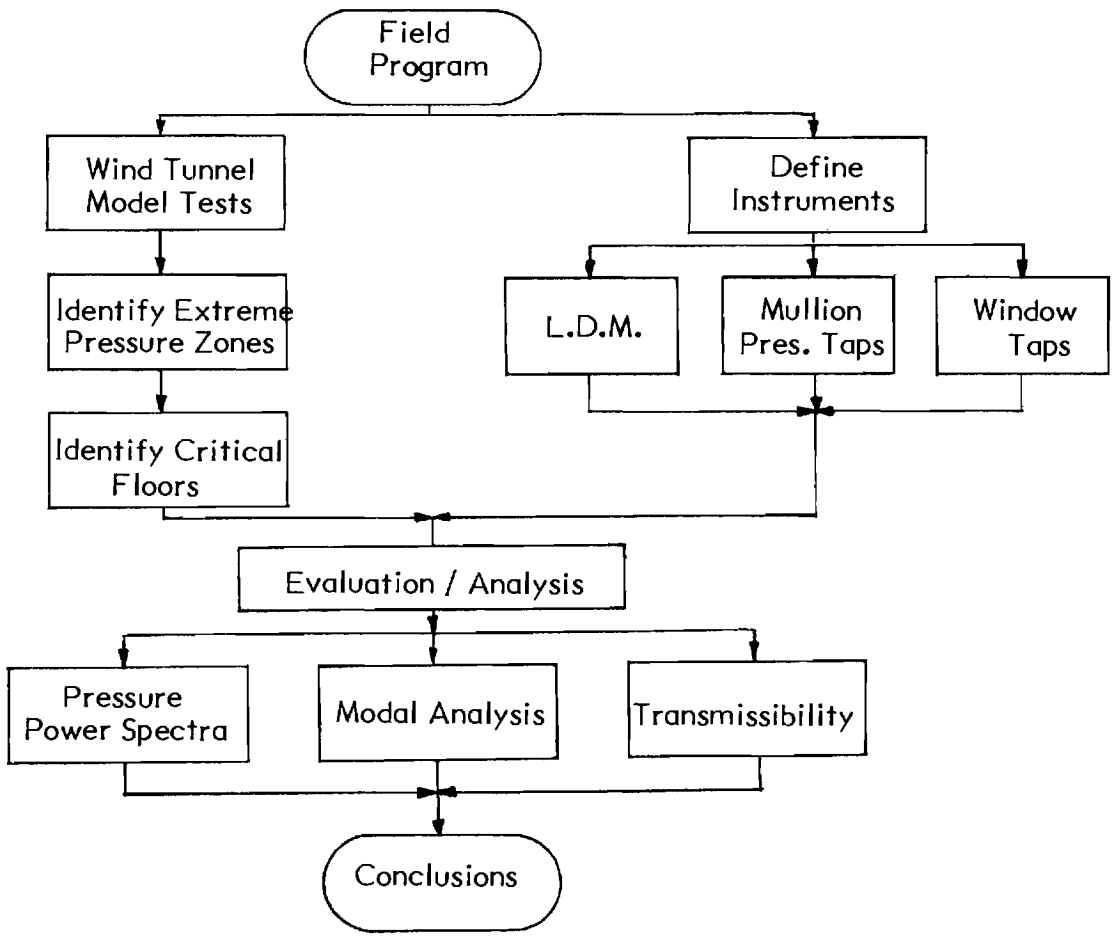

Figure 1.3-2 Field Study Program

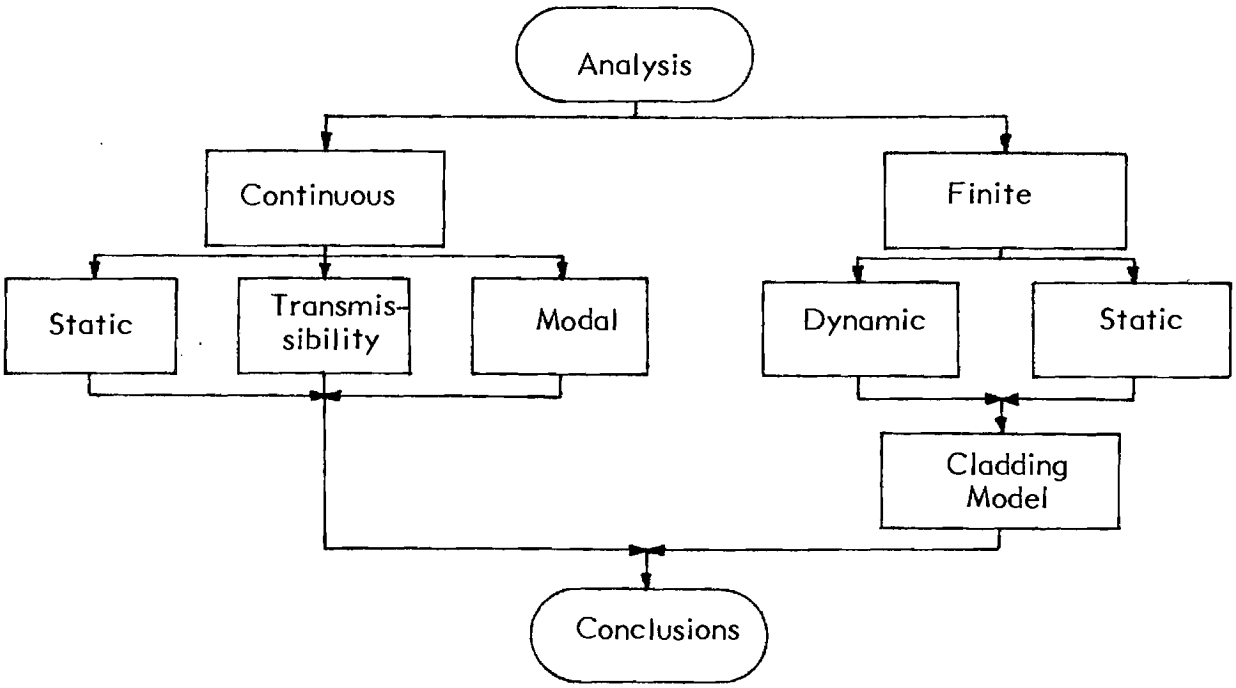

Figure 1.3-3 Analysis and Modelling Program

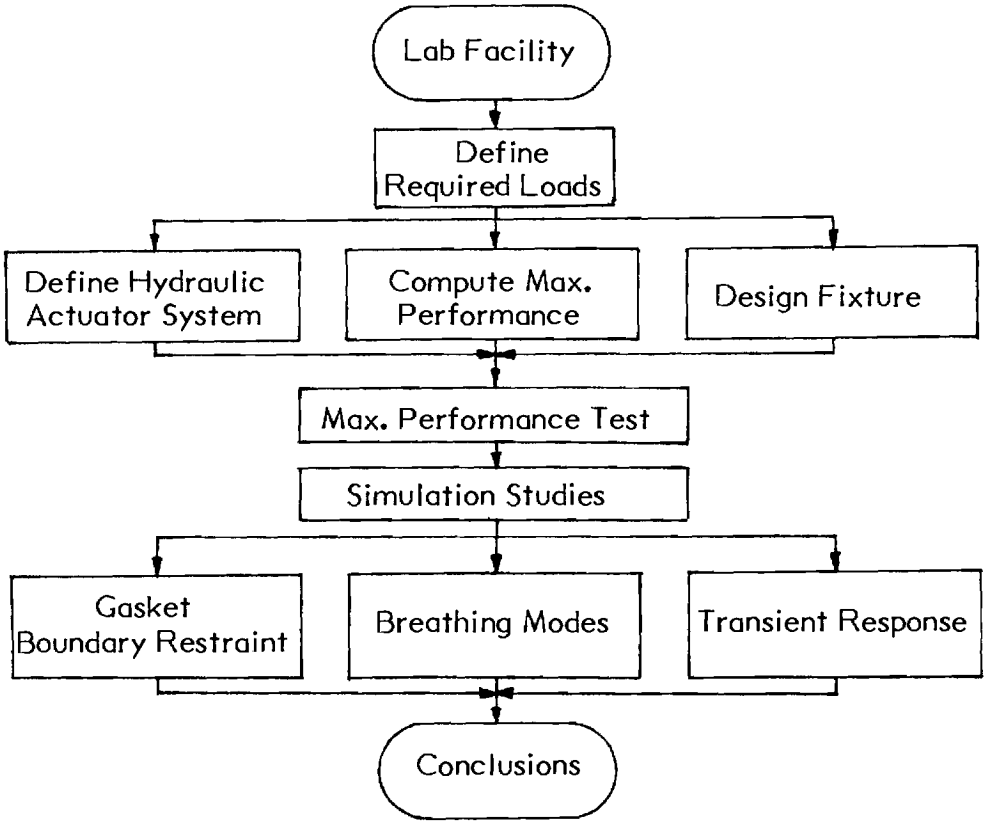

Figure 1.3-4 Laboratory Study Program

and techniques for the subsequent testing. This was followed by development of the measurement analysis techniques for evaluation of the data and finally by the actual testing (40).

The analytical study, Fig. 1.3-3, is intimately related to the other two areas, and for simplicity, can be broken into continuous and finite analyses. The continuous modelling was designed to provide the qualitative, if not quantitative, characterization of both the static and dynamic response to directly support the field and full-scale lab testing. Particular emphasis was on describing the dynamics of a double plate window assembly. The finite modelling, on the other hand, was designed to provide a detailed quantitative description of the window and cladding system that could be "calibrated" against the observations from full-scale and lab measurements. The ultimate objective for utilization of a model of this type is as a design-oriented subsystem model for incorporating cladding effects into more general building models. The basic results are a series of dimensionless parametric performance curves for representative window-framing systems along with a detailed listing of the finite element coding developed for the study.

The laboratory study, Fig. 1.3-4, was aimed at defining the requirements for a full-scale dynamic pressure simulation facility and then building the apparatus. Following a series of performance demonstration tests, the equipment was used to study under laboratory conditions the static and dynamic response characteristics of a window-framing system similar to that employed at the building used for the field study.

2.0 FIELD STUDY

2.1 Background

The nature of wind forces acting on windows is determined not only by the wind characteristics, but also by the wind-structure interaction phenomena. Even though wind forces on buildings have been of concern in the past, the fluid mechanics related to buildings in atmospheric boundary layer winds is not well understood. Unlike the aerodynamics of streamlined bodies which is highly developed for aeronautical applications, the aerodynamics of bluff buildings in turbulent, nonhomogeneous boundary layers is complex and is not well described by either analytical or numerical techniques. Consequently, the available wind force information for buildings and structures has been obtained primarily from measurements on small scale models and in limited instances on actual structures.

Boundary layer wind tunnel measurements on tall buildings have shown that the wind-structure interaction gives rise to fluctuating local wind pressures. It has been recognized that, whereas the temporal and spatial fluctuations of the local wind pressures from the mean may not affect the design of the primary structure, their effect on portions of the building such as windows and cladding panels cannot be ignored. Model tests have also shown that the most severe pressure fluctuations are associated with the following mechanisms:

a. Separation and reattachment of flow around buildings (41).

b. Local vortex formation and the subsequent shedding of these vortices.

Flow separation around buildings can induce locally high suction (outward acting) pressures which often exceed the dynamic pressure of the mean wind. Probability density estimates of pressure fluctuations on tall building models indicate (25) that in regions of separation, negative values of the peak pressure coefficient, $C_{p_{max}}$, can attain magnitudes of 8 - 10 times the rms pressure coefficient, $C_{p_{rms}}$. This is strongly affected by the geometrical features of the building and the most severe pressure fluctuations have been found to occur at reentrant corners where flow separating at one edge of the corner reattached at the opposite edge (41).

Vortex flows may be developed by a particular combination of building shape and wind direction, and are responsible for periodicities in the cladding loads. Model studies of the Bank of America World Headquarters Building (42), show that fluted walls in conjunction with setbacks at various elevations are the main reasons for the appearance of various vortex flows over the entire wall surface. The shedding of these vortices is one of the primary aerodynamic phenomena which develop periodic forces on the building as well as its cladding.

The frequency content of both types of pressure fluctuations is of concern in defining wind loads for window glass and cladding panels, since sufficient energy at frequencies in the vicinity of panel resonance can result in dynamic amplification of deflections and stresses. However, the available spectral data from either model or full-scale tests is rather sparse. Upwind surface pressure fluctuation spectra for a pair of square section towers have been measured on a model (43) and show that most of the pressure fluctuation energy is

concentrated in the low frequency range extending to about 20 Hz. These spectra have been found to be related closely to turbulence spectra of the simulated oncoming wind.

Full-scale tests on existing structures have provided greater insight into the nature and severity of surface pressure fluctuations on tall buildings. Some of the pertinent full-scale tests are surveyed in Table 2.1, partially reproduced from Reference 19. Newberry et al. (44) from their measurements on an 18-story rectangular building conclude that the most severe suction pressures occur under the incidence of glancing winds and large negative excursions are apparent at locations around corners. Dalgliesh (45) in comparing model and full-scale pressure coefficients, points out that large values of $C_{p_{rms}}$, and hence large pressure fulctuations from the mean, occur when the wind is nearly parallel to the building surface on which the tap is located. The data also demonstrate a reduction in wind pressures as the ground level is approached. Full-scale measurements by Dalgliesh (46) have provided valuable information on another aspect of the wind loading mechanism, namely: gust effects. Gust action usually is considered as random turbulent fluctuations superimposed on the mean wind and is generally defined by its time domain characteristics. Statistical analyses of extreme pressure data were used to define static pressure magnification or gust effect factors for various exposure conditions and expected recurrence intervals.

Results of frequency decomposition of surface pressure fluctuations on actual structures have been presented in Refs. 47 - 50. Pressure spectra in Refs. 47 and 48 have been obtained over a range of low

Table 2.1 A Partial Survey of Full Scale Investigations of Wind Effects on Tall Buildings

Investigators	Ref.	Building		Experimental Procedure				Analysis		
		Type	Ht. in ft.	Pressure		Wind		Pressure		
				Ext.	Int.	V	Dir.	Mean	Histo-gram	PSD
C. W. Newberry K. J. Eaton J. R. Mayne	44	R. C.	267	48	3	1	1	x	x	x
W. A. Dalgliesh W. von Tobel H. S. Ward	45, 46	St. Fr.	784	34	1	2	2	x	x	x
W. A. Dalgliesh W. von Tobel H. S. Ward	47	St. Fr.	430	12	0	1	1	x		x
Mario Takeuchi Gengo Matsui Satora Kazama Ryoichi Nagai	48	Comp. St./C	251	20	0	1	1	x	x	x
W. A. Dalgliesh W. von Tobel H. S. Ward	49	St. Fr.	640	12	0	1	1	x	x	x
S. Miyoshi Masahiko Ida T. Terayama	50	St. Fr.	482	6	6	2	2			x

*Abbreviations: St. = Steel; Fr. = Frame; R.C. = Reinforced Concrete;
Comp. = Composite Steel & Concrete

frequencies pertinent to the vibrations of the entire building. Since the fundamental frequencies of window glass and cladding panels are typically in the range of 5 - 50 Hz, the results of Refs. 49 and 50 are significant in that the spectral bandwidth exceeds 10 Hz. Standen et al. (49) have obtained power spectra of pressures at various locations on the surface of a rectangular platform high-rise building, Fig. 2.1-1. rapid roll-off of power density with frequency is evident in most cases. However, the increased power at higher frequencies in (c) with the pressure taps subject to glancing winds shows that some locations on the surface may be susceptible to dynamic loads.

Measurements of Miyoshi, et al. (50), on a tall rectangular building appear to be the first data which provide response information in terms of glass panel strains in addition to pressure spectra. The pressure spectra, measured under typhoon conditions, are reproduced in Fig. 2.1-2. A similar feature to that of Fig. 2.1-1c is apparent in curve, P_E, where the pressure fluctuations for glancing flow contain significant energy at higher frequencies as compared to the sharp roll-off observed in the other spectra.

In the past few years the problem of determining wind loads for cladding design has centered on the assumption of static or quasi-static pressures, and, therefore, on the specification of static loads for cladding panel design against outright fracture. Current building codes, as for example the ANSI Standard, allow for large pressure fluctuations and gusts by augmenting the static loads with gust and terrain factors. The basis for a static pressure assumption is the

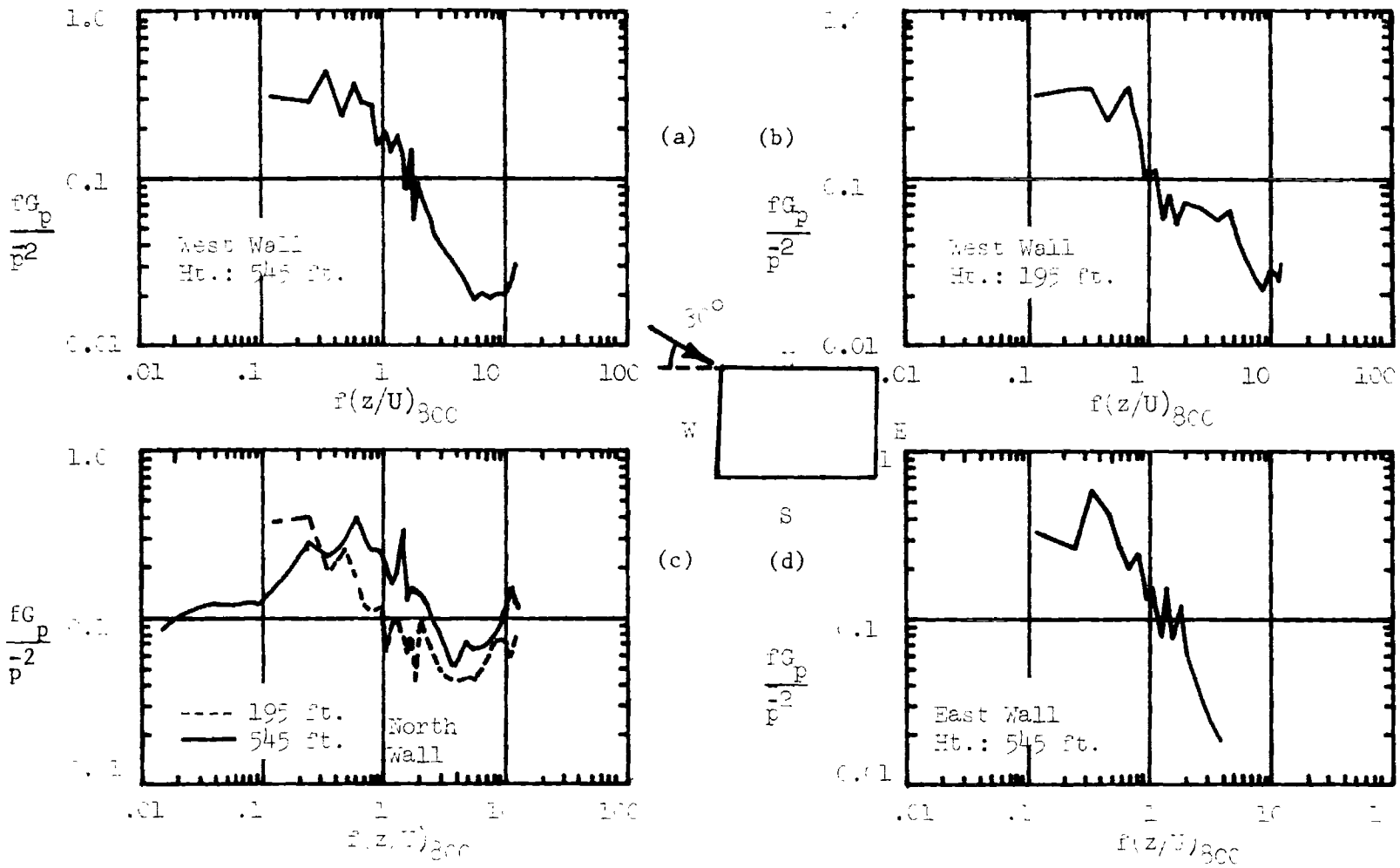

Symbols: f = frequency, $(z/U)_{800}$= Height to velocity ratio at 800 ft., G_p= PSD

$\bar{p}^2$= Mean square value of the pressure, U= 50 ft./sec.

Figure 2.1-1 Power Spectra From Full-Scale Tests of Standen et al. [49]

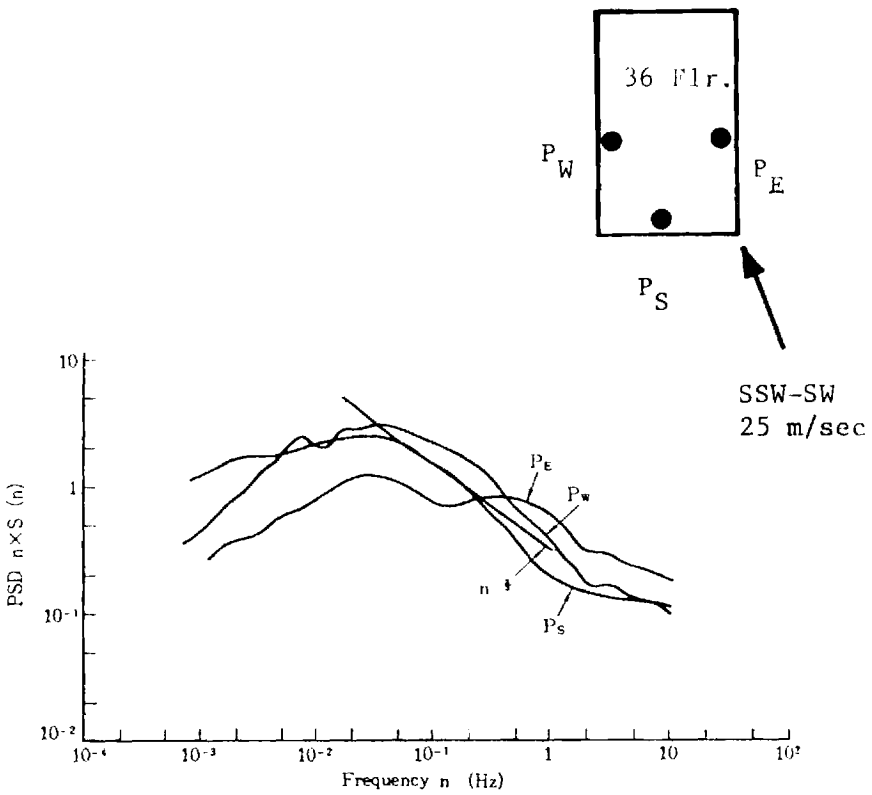

Figure 2.1-2 Power Spectra From Full-Scale Tests of Miyoshi et al. [50].

preliminary pressure fluctuation data for buildings with simple geometries which generally show that the wind pressure energy is concentrated over frequencies considerably lower than the resonance frequencies typical of cladding construction. It has been acknowledged, however, that the nature and severity of local dynamic wind loads on buildings with complicated shapes such as those with fluted walls, reverse setbacks, and surface irregularities may not follow this pattern (51,52).

The results of Refs. 49 and 50 discussed above, hint at the existence of "critical response locations" where intense high frequency pressure fluctuations would necessitate consideration of dynamic loading mechanisms and wind tunnel tests have illustrated that these critical response locations should depend on the nature of the wind-structure interaction. Relatively large windows and cladding panels in these locations would be susceptible to vibration and flutter, and damage in the form of glass panel breakage, cladding panel fatigue failure, and panel anchor failure. Therefore, design of window glass for static loads, in such locations would be inadequate. In addition, design to minimize breakage alone may not in itself be a solution to the window failure problem.

Wind loads for buildings under design can presently be obtained only by measurements on models in wind tunnels. However, to establish a systematic set of simulation criteria and to ensure the predictive quality of model test results, measurements on actual structures and model/full-scale comparisons are essential. Full-scale tests are also of value in understanding the wind loading mechanisms and the

characteristic response. However, since full-scale experiments pertain to particular structures with unique properties and exposure conditions, an ensemble of such measurements need to be examined prior to rational definition of wind loads and formulation of design procedures.

This chapter reports the results of a full-scale study of the characteristics of the localized window and cladding pressure loadings. This approach to the problem of window design has been adopted to understand the dynamic response characteristics of real window installations and the nature of dynamic wind loads, particularly the heretofore unreported dynamic effects under so-called "normal" wind conditions.

The study concerns itself with the problem of dynamic wind load and response identification for doubly glazed windows. Mathematical modelling of the window response, both static and dynamic, is the subject of Chapter 3, and modelling of the wind structure in the strictest sense is not within the scope of this work. The principal objective was to assess the wind loads and window dynamic response with regard to:

(a) Capability of the wind loads to excite window vibrations and the dependence of the wind loads on the building profile.

(b) The degree of dependence of the window response on wind loads from amongst other excitation sources.

(c) Vibration parameters of the window system from measured data.

2.2 Design Considerations

In formulating rational design procedures for the elements of a glass curtain wall, the first step is to translate the wind environment of buildings into a set of numerically-defined loads. The kinds of failures that these loads might cause must then be studied in light

of the different response mechanisms. This process leads to the formulation of a set of failure criteria. Once the loads have been defined and the failure criteria established, the design problem reduces to one of predicting the response of the window system, and evaluating this response in terms of the damage criteria.

In a practical application this reduces to the situation: Given a design wind velocity, one should be able to predict the response of the system in the form of peak stresses, accelerations deflections, etc. This requires mathematical models for the prediction of the forces of interaction of the main structure and the turbulent, gusty wind. Wind-structure interaction forces can be aerodynamic as well as aeroelastic, but insofar as window systems in building structures are concerned, only aerodynamic forces are important. Given the current state-of-the-art, the greatest uncertainty is in defining the wind environment of buildings and translating this into cladding loads.

The American National Standards Institute ANSI 58.1-1972 standard (11) contains a method for determining wind loads applicable to the design of parts and portions of a building. Design wind pressures for window glass are assumed to be static and are defined by:

$$P_1 = .00256\, V_{des}^2 K_z \cdot G(C_p - C_{p_i}) \qquad (2.2\text{-}1)$$

where

P_1 is the design pressure in lbs/ft^2 (Psf);

V_{des} is the fastest mile wind speed with a 50-year recurrence period, in MPH;

K_z is the velocity pressure coefficient which depends on the exposure and the height z above ground;

G is the gust response coefficient;

C_p is the external pressure coefficient; and

C_{p_i} is the internal pressure coefficient.

Minimum values of $C_p - C_{p_i}$ for locations susceptible to large suctions, for example, near corners, are specified. The standard was founded on the available wind research and was prepared for use in conjunction with common building shapes (i.e., rectangular), and is similar to the approach employed by the National Building Code of Canada (53).

Current window design procedures, as for example in the Southern Standard Building Code (54), assume the design pressure as a uniformly-applied static design load. With this load, a factor of safety representing a value which has appeared to give an acceptable probability of breakage in extensive static strength tests conducted by window glass manufacturers (12), is used.

Recent efforts at improving upon the static load specifications have been directed at modifying the gust factor, G. In Ref. 51 it is suggested that G be expressed as:

$$G_1 = 1 + g \cdot \frac{C_{p'}}{\overline{C}_p} \qquad (2.2\text{-}2)$$

where g is a gust effect factor;

$C_{p'}$ is rms value of the pressure coefficient (about the mean); and

$\overline{C}_p$ is mean pressure coefficient.

The gust effect factor, g, from Eq. (2.2-2) has values lying between 3 and 5 for windward faces, as determined experimentally. Allen and Dalgliesh (26) have proposed a gust factor G_2 which incorporates effects of dynamic amplification. These dynamic effects are included in the gust factor as a "gust material" factor, K_m, with the reasoning that the effects are related only to the turbulent component of the wind. The gust factor is then expressed as:

$$G_2 = 1 + g \cdot K_m \cdot \frac{C_{p'}}{\overline{C}_p} \qquad (2.2\text{-}3)$$

Window design requires consideration of the mechanical properties of glass, especially its brittle behavior. The statistical variation in glass strength, due to its sensitivity to surface flaws, is accounted for by designing on the basis of probability of breakage. Design procedures for window glass considering its static fatigue* property have been proposed, where gust factors are replaced by pressure coefficients averaged over a period determined from the strength-load duration curves (55, 56). Consideration of edge supports, clearances and glazing details has been emphasized in a design method (29) based on static pressures defined by the ANSI standard.

The widespread adoption of static design loads is a direct consequence of the available experimental data. The experimental data base

* In the accepted definition "static fatigue" implies decrease in breaking stress with increased duration of load.

has also provided valuable insight into the wind-structure interaction phenomena. However, the model test results are beset by a lack of confidence in their predictive quality. Full-scale tests have been limited in their scope by the emphasis on measurements for validation of wind tunnel test techniques, and have used buildings with simple shapes. The local nature of failure of windows, especially those near the corners of a building, has been recognized, but assessment of factors influential in specification of wind loads for curtain walls is as yet incomplete. It is not unreasonable to suspect that the severe pressure fluctuations in the separation region at a corner of the building could excite the window dynamically as well. Buildings with the following shape characteristics are prime candidates for localized regions of relatively high frequency loading:

(a) Setbacks or reverse setbacks along the height;

(b) Fluted walls presenting a cascade of triangular outsets and reentrant corners to the flow;

(c) Rough surface texture of the building facade as dictated by the architectural details.

These "critical response locations" would also depend upon the directional properties of the wind.

In regions where dynamic wind loads are severe eneough to offset the alleviating effect of glass static fatigue, dynamic response of the glass panels becomes an important consideration. Ejection type failures, where relative motion between the glass and its frame is suspected, accentuate the need to define the response of the entire window assembly. A review of curtain wall damage caused by a hurricane (57) shows that all the components of a window assembly should be included in a design philosophy.

2.3 Site Specification

2.3(a) Test Site Description

The structure selected is a 29-story steel frame medium high-rise building of modern design located some six miles north of the downtown Atlanta area on the crest of a ridge and one-half mile from the nearest comparable building to the northeast. The lightweight exterior curtain wall makes extensive use of aluminum extrusions in its design. The cladding consists of large (100 in x 57 in) doubly-glazed windows incorporating a heat-reflecting exterior light and smaller singly-glazed spandrel panels. A view of the building just after completion is shown in Fig. 2.3-1, and details of the mullion and glazing are shown in Fig. 2.3-2.

The 400-ft-tall structure is essentially prismatic with a plan-form that includes twelve exterior right corners at the base. The geometry is modified for the upper twelve floors to provide twenty and thirty-six corner floor plans, Fig. 2.3-3. In the aerodynamic sense, the building is most interesting with profiles to the wind which change with height. The architectural features contribute to a striking design, and provide the variable geometry so important to the present investigation.

The prevailing wind direction for the Atlanta area is the north-west, and the exposure of the building to prevailing winds can be described as a heavily-forested, relatively flat region of residential construction. The terrain in other directions with respect to the building can be similarly described with surrounding buildings 3 - 4 stories high. The exposure conditions determine the vertical velocity

Figure 2.3-1 Field Site in Atlanta; View from the Southeast Relative to the Building Axes.

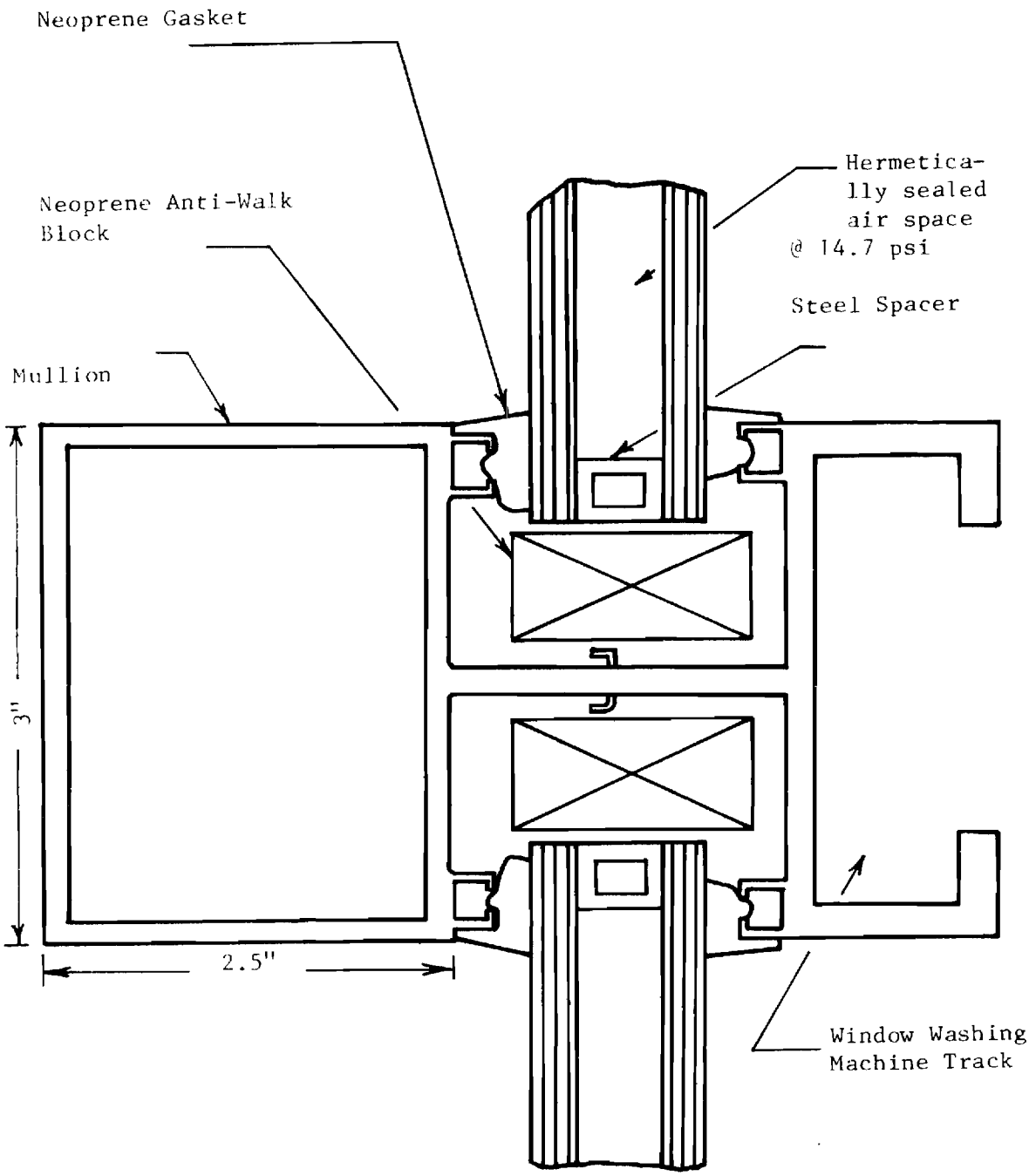

Figure 2.3-2. Mullion and Glazing Detail.

profile of the mean wind boundary layer which can be approximated by the relation

$$\frac{v}{v_o} = \left[\frac{z}{z_o}\right]^{1/n} \qquad (2.3\text{-}1)$$

where v_o is the measured wind speed at height, z_o, and v is the velocity at a height, z. The exponent, n, depends on the aerodynamic roughness of the surrounding terrain and in accordance with Ref. (103) in following relationships apply:

Terrain	1/n
Open Sea	0.1
Flat Open Country	0.16
Wooded Forest	0.28
Urban Area	0.40

The velocity profile for the wooded area surrounding the building can be approximated by:

$$\frac{v}{v_o} = \left[\frac{z}{z_o}\right]^{0.28} \qquad (2.3\text{-}2)$$

2.3(b) Wind Tunnel Study

At the outset of the research program, a scale model wind tunnel investigation of the flow patterns around and the wind-induced pressures on the building was conducted in the 9-ft. low speed wind tunnel facility at Georgia Tech. The purpose of the study was to obtain an overall qualitative view of the flow characteristics around the building for the given terrain and to determine flow directions and response locations that resulted in the most severe pressure loadings. Details of the study have been reported in a GIT-DGSA report (58).

The tests were run using a special flat floor in the tunnel with the 1/160 scale model placed at the center of a 4-ft-diameter turntable. The desired mean wind profile was developed by arranging a series of 1/4-in. wire screens in the throat of the upstream contraction cone and measuring the velocities with a pitot-static rake. Due to the limited upstream space available in the test section, no attempt was made to accurately model the turbulence characteristics. Due to 2-axis symmetry only half the model needed instrumentation, and a total of 88 flush pressure taps were located in horizontal rows at 4 vertical elevations and in 8 positions on the roof. In order to minimize tubing length and thus improve dynamic response, the pressure taps were connected to two 48-port "Scanivalves" and a variable capacitance electronic manometer located inside the model. The stepping valves and pressure transducer were operated under minicomputer control for rapid port-by-port sampling in any specified sequence.

All tests were run at an indicated airspeed of 50 mph as measured at an elevation equal to the building height and the pressure measurements reduced to dimensionless pressure coefficient form. Flow directions of from 0° to 180° were used with increments of 10° or 5° as required. Both tuft and oil flow studies were used to explore an unusual vortex pattern over the roof of certain incidence angles.

The results generally revealed no anomalous behavior or unusually large pressure coefficients. As might be anticipated, the maximum (negative) coefficient was measured on the flat side of the model at the higher elevation (Figure 2.3-3(c)) for a glancing flow. Under the relatively low turbulence level achieved with the screens alone, the

maximum coefficient magnitude was about 1.4 which should, on the basis of additional oscilloscope measurements, be increased to about 2.3 to account for the averaging effect of the integrating voltmeter used. The most extreme pressures occurred over the upper half of the model wither on the flat faces for glancing flows or within the set-back regions for ±45° (to building axes) flow directions. Based on these very simple and basically qualitative measurements, locations in the set-back and flat regions at 3 elevations were identified for testing in the full-scale study.

2.4 Evaluation Methodology

In much of the full-scale test work reported to date the primary emphasis has been placed on the logistics and techniques for acquiring the data. Relatively little study has been given to the test methodology, that is, to the manner in which the data will be handled from acquisition, through processing, and finally to evaluation, in light of current analytical understanding. In full-scale tests, and to a large extent in boundary layer simulation tunnel testing, one must deal with a system in which the loads, or inputs, cannot be defined in a deterministic manner. Consequently, statistical techniques must often be employed. Unfortunately, much of the work has dealt with basic time domain statistics such as means, moments, probability distributions, etc., while the application of the frequency domain has been either overlooked or misapplied.

In the present study, the wind load-cladding response problem is modelled as an input-output system with the dynamic wind loads constituting the input and the measured responses as the output. The loading

and response problem has been purposely cast in this form to allow the application of many of the powerful time series analysis techniques. The following subsections describe the evaluation methodology in general and its unique application to the present loading-response identification problem.

2.4(a) System Description

The window-cladding problem can be represented by the generalized model shown in Fig. 2.4-1. The present concern is with the inverse problem in engineering where the input to the system and the resulting response are measured and are to be used to describe the system dynamics as well as the input characteristics.

The input, i.e., the wind loading, itself can be visualized as the out-put of another system describing the wind flow interaction with the structure. In the present study this wind-structure interaction system identification is not considered. In this context the term load identification implies a study of the measured wind loading with respect to a set of parameters describing the wind characteristics and the building profile.

As is the case in the majority or real-world large systems, the window as a structural system is expected to have nonlinear and time dependent properties. These properties, for example, could be due to the fact that a window unit is an isolated part of an entire curtain wall, and that glass strength is sensitive to surface flaws which are affected by service load duration. The identification problem in this case can be formidable (59). In this investigation, the nonlinearities of the system and its time dependent character are neglected as a first

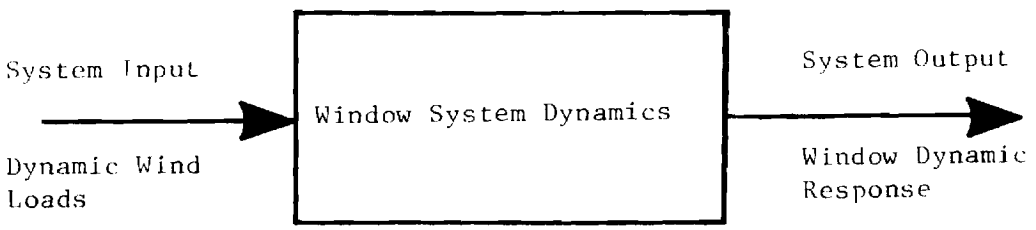

Figure 2.4.1. The Window System as an Input/Output Model.

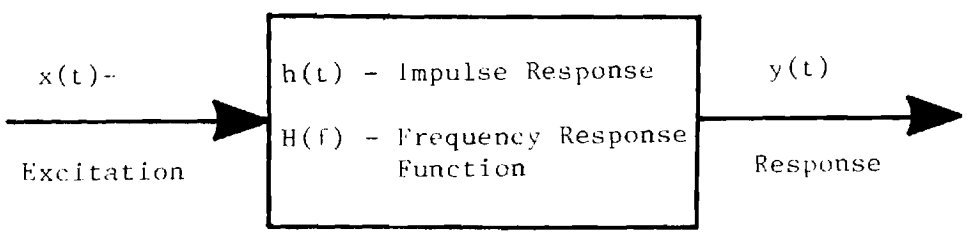

Figure 2.4-2 Single Input/Single Output Linear System.

approximation. The system model is thus simplified so that it can be described by linear constant coefficient differential equations.

Linear system theory is the mainstay of the present data analyses procedures. In this approach the window assembly is assumed to be the linear system and the dynamic wind loads considered as the band-limited random input. The theoretical concepts are not new; however, their present application to large structures is broader in scope, specifically, with respect to the use of the coherence function in assessing the linear dependence of the response on the wind loads.

A linear, time-invariant system also called a constant parameter linear system (CPLS) is one which can be described by linear differential equations with constant coefficients. The dynamic characteristics of a constant parameter linear system can be described by its impulse response function, $h(\tau)$. The input-output relations for such a system, represented by the block diagram of Fig. 2.4-2, can be described by the convolution integral:

$$y(t) = \int_0^\infty h(\tau)\ x\ (t - \tau)d\tau \qquad (2.4\text{-}1)$$

where a physically realizable system, $h(\tau) = 0$, if $\tau < 0$. The system can also be described by a transfer function, $H(s)$, which is the Laplace transform of $h(\tau)$:

$$H(s) = \int_0^\infty h(\tau)e^{-s\tau}d\tau \quad s = a + jb \qquad (2.4\text{-}2)$$

An alternate representation of the transfer function is the frequency response function where $s = \omega = j2\pi f$. The frequency response function is the Fourier transform of $h(\tau)$:

$$H(f) = \int_{0}^{\infty} h(\tau) e^{-j2\pi f\tau} d\tau \qquad (2.4\text{-}3)$$

Taking Fourier transforms of both sides of Eq. (2.4-1) yields the input-output relation in the frequency domain:

$$Y(f) = H(f)\ X(f) \qquad (2.4\text{-}4)$$

where X(f) and Y(f) are Fourier transforms of x(t) and y(t). Equation (2.4-4) can also be obtained as a direct result of the Convolution Theorem which states that convolution in the time domain is equivalent to multiplication in the frequency domain and vice versa.

The frequency response function, H(f), is a complex valued quantity and can be written in polar notation as:

$$H(f) = |H(f)| e^{-j\phi(f)} \qquad (2.4\text{-}5)$$

It follows from Eq. (2.4-3) that:

$$H(-f) = H^*(f)$$

where * denotes complex conjugate, and therefore:

$$|H(-f)| = |H(f)|$$

$$\phi(-f) = \phi(f)$$

If the excitation, x(t), is a sample function of a stationary random process {x(t)}, then the output, y(t) is also a sample function of a stationary random process, {y(t)}, as will be shown. The input-output relations for this case must be described in terms of the expected values of the input and the output. The expected value of any real single-valued continuous function, g(x), of the random variable, x, is given by:

$$E[g(x)] = \int_{-\infty}^{\infty} g(x) p(x) dx \qquad (2.4\text{-}6)$$

where p(X) is the probability density function for x. For stationary random processes, {x(t)} and {y(t)}, the correlation functions are defined as follows:

$$R_{xx}(\tau) = E[x(t)\ x(t+\tau)] \qquad (2.4\text{-}7)$$
$$R_{yy}(\tau) = E[y(t)\ y(t+\tau)]$$
$$R_{xy}(\tau) = E[x(t)\ y(t+\tau)]$$

The first two of Eq. (2.4-7) define the autocorrelation functions of {x(t)} and {y(t)} respectively, while the third defines the cross correlation function between {x(t)} and {y(t)}.

For the single input-single output linear system of Fig. 2.4-2 the output autocorrelation function can be obtained from the input autocorrelation function as follows:

$$y(t)\ y(t+\tau) = \int_{\circ}^{\infty}\int_{\circ}^{\infty} h(t_1)h(t_2)x(t-t_1)x(t+\tau-t_2)dt_1dt_2$$

and taking the expected value, E[ ](30):

$$R_{yy}(\tau) = \int_{\circ}^{\infty}\int_{\circ}^{\infty} h(t_1)h(t_2)R_{xx}(\tau+t_1-t_2)dt_1dt_2 \qquad (2.4\text{-}8)$$

Thus the response of a CPLS to a stationary random input is a stationary random process. Similarly, the stationary cross-correlation function $R_{xy}(\tau)$ between the input, x(t), and the output, $y(t+\tau)$, is:

$$R_{xy}(\tau) = \int_{-\infty}^{\infty} h(t)R_{xx}(\tau-t)dt \qquad (2.4\text{-}9)$$

The transformation of Equations 2.4-8 and 2.4-9 to the frequency domain yields input-output relations in terms of auto and cross-power spectral densities.

$$S_{yy}(f) = |H(f)|^2 S_{xx}(f) \qquad (2.4\text{-}10)$$
$$S_{xy}(f) = H(f)\ S_{xx}(f)$$

where S_{xx}, S_{yy} and S_{xy} are the theoretical two-sided spectral density functions defined over $-\infty \leq f \leq \infty$ as:

$$S_{ij}(f) = \int_{-\infty}^{\infty} R_{ij}(\tau) e^{-j2\pi f\tau} dt \quad \text{(Wiener-Khintchine Relations)}$$

From the symmetry properties of stationary correlation functions, it is seen that S_{xx} and S_{yy} are real, non-negative, and symmetric functions of f, whereas S_{yx} is complex valued.

In practical situations the negative frequencies have no real significance, and it is more convenient to define a practical power density function $G_{ij}(f)$, which exists for positive frequencies only:

$$G_{ij}(f) = 2S_{ij}(f) \text{ for } f \geq 0$$
$$= 0 \text{ otherwise.}$$

Eq. (2.4-10), therefore, can also be written as

$$\begin{aligned} G_{yy}(f) &= |H(f)|^2 G_{xx}(f) \\ G_{xy}(f) &= H(f)\, G_{xx}(f) \end{aligned} \qquad (2.4\text{-}11)$$

The cross power spectral density function, $G_{xy}(f)$, may be shown to satisfy the inequality (60):

$$|G_{xy}(f)|^2 \leq G_{xx}(f)\, G_{yy}(f) \qquad (2.4\text{-}12)$$

Also, from Eq. (2.4-12), a generalized cross-spectral density function, known as the coherence function may be defined,

$$\gamma_{xy}^2(f) = \frac{|G_{xy}(f)|^2}{G_{xx}(f)G_{yy}(f)} = \frac{|S_{xy}(f)|^2}{S_{xx}(f)S_{yy}(f)} \qquad (2.4\text{-}13)$$

where for random processes

$$0 \leq \gamma_{xy}^2(f) \leq 1$$

Eqs. (2.4-11) and (2.4-13) provide the basis for the physical applica-

tion of linear system theory to the problem of dynamic loading and response of window systems. In particular, the coherence function can be used as a powerful tool for assessing causality in systems and its application in the present study is a point of major interest.

The coherence function, also known as mean squared coherence or the coherence coefficient, was introduced by Wiener (61) in 1930. The terminology was motivated by the interference effects of coherent, and incoherent light sources; however, the "coefficient of coherency" was derived as a natural extension of the theory of harmonic analysis of time series. Wiener also pointed out the analog between the coefficient of coherence and the correlation coefficient, ρ_{xy}, between two random variables, x and y, defined as:

$$\rho_{xy} = \frac{C_{xy}}{\sigma_x \sigma_y}$$

where C_{xy} is the covariance of x and y and σ_x and σ_y the standard deviations of x and y, respectively. It was remarked that the correlation coefficient is a tool for the statistical analysis of frequency series, where time does not enter as a parameter; whereas, the coefficient of coherence is a tool in the analysis of time series.

For two stationary time series, x(t) and y(t), the coherence function, Eq. (2.4-13), as a consequence of the Schwarz inequality, Eq. (2.4-12), is restricted to values between 0 and 1. For deterministic signals the coherence function can only take the values 0 or 1. As applied to stationary stochastic processes, the coherence function possesses the properties outlined below, which suggest several of its applications.

Consider the linear system configuration shown in Fig. 2.4-3 (62). It is assumed that $s(t)$, $n_1(t)$, and $n_2(t)$ are sample functions of stationary, uncorrelated random processes. By the application of Eqs. (2.4-11) and the basic relations for multiple input linear systems, (Ref. 60, p. 147), it can be shown that:

$$\gamma^2_{y_1y_2} = \gamma^2_{r_1r_2} = \frac{G^2_{xx}(f)|H_a(f)H^*_b(f)|^2}{G_{xx}(f)|H_a(f)|^2+G_{n_1n_1}(f)\quad G_{xx}(f)|H_b(f)|^2+G_{n_2n_2}(f)} \tag{2.4-14}$$

The properties of the coherence function can now be summarized from Eqs. (2.4-13) and (2.4-14) as follows:

1. The coherence function is a real valued function conveniently normalized to lie between zero and unity.

2. Since $\gamma^2_{y_1y_2}(f)$ is independent of $H_1(f)$ and $H_2(f)$ in Eq. (2.4-14), the coherence function between two time series is not affected by the arbitrary linear processing of these signals. In other words, the coherence function is invariant under linear filtering operations.

3. With $n_1(t) = n_2(t) = 0$, $\gamma^2_{y_1y_2}(f) = 1$. Consequently the coherence function of two signals derived from the linear operations on the same signal is unity. Equivalently, the coherence of two linearly related signals is unity. It can be shown (63) that the coherence function is less than unity for any nonlinearities in the system, and the linear-to-nonlinear ratio (in the absence of noise) is given by $\frac{\gamma_{y_1y_2}}{1-\gamma_{y_1y_2}}$

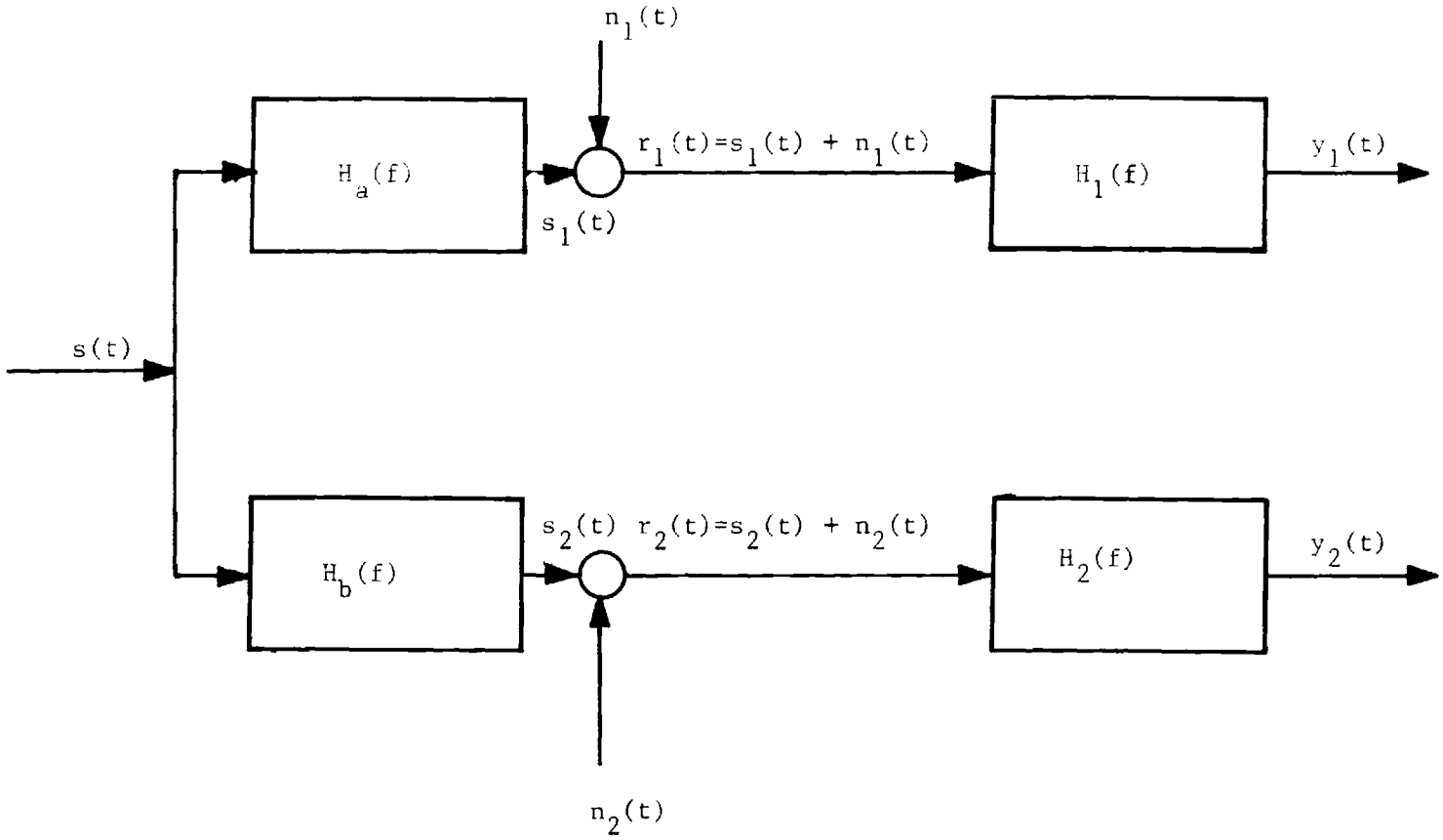

Figure 2.4-3 Configuration for Examining Properties of the Coherence Function.

4. For a linear system, the presence of noise, i.e. $n_1(t)$ and $n_2(t)$, tends to reduce the true value of the coherence function. In such a case

$$\frac{\gamma_{y_1y_2}}{1 - \gamma_{y_1y_2}}$$

is a measure of the signal to noise ratio.

5. An interesting property of the coherence function is obtained from its relation to the error spectrum resulting from a linear prediction, $y(t)$, of $y(t)$ from $x(t)$, described in (60):

$$y(t) = \int_o^\infty h_o(t)x(t-\tau)d\tau$$

where $h_o(t)$ is a weighting function to be determined and $x(t)$, $y(t)$ are sample functions of a stationary stochastic process. When the linear filter is chosen to minimize the mean square value of the error, $e(t)$, i.e., the area under the error spectrum, where,

$$e(t) = E[\{y(t) - \hat{y}(t)\}]^2$$

the error spectrum takes the form (31, 34):

$$G_{ee}(f) = [1-\gamma^2_{xy}(f)]G_{yy}(f)$$

Therefore, the error is small when the coherence function is near unity, indicating that the $y(t)$ series can be predicted very well from the $s(t)$ series data. On the other hand when $\gamma^2_{xy}(f)$ is near zero, the error spectrum very nearly coincides with that of $y(t)$, and the $x(t)$ data contribute almost nothing to the predictability of $y(t)$. This property relates closely with the intuitive meaning of coherence, i.e.

two time series can be described as "coherent" at a frequency, f, when $\gamma^2_{xy}(f) \approx 1$. When $\gamma^2_{xy}(f) \approx 0$, they are referred to as "incoherent". Alternatively, $\gamma^2_{xy}(f)$ is the proportion of $G_{yy}(f)$ contained in the linear component of y(t), and $1 - \gamma^2_{xy}(f)$ is the proportion of $G_{yy}(f)$ contained in the error, or, in the absence of noise, in the nonlinear component of y(t).

Properties (3) and (5) indicate that the coherence function can be used as a measure of linearity. Furthermore, property (5) enables the use of the coherence function in establishing the degree of linear dependence of a system output y(t), on the input x(t). Property (4) indicates that the coherence function can be used in measuring the signal to noise ratio. It is because of these properties that the coherence function has found widespread application in communication systems in estimating the signal/noise ratio and determination of time delay.

The coherence function has numerous other applications, as for example in control systems for system identification (65), and in geophysics (66) to assess the signal to noise gain of an array of sensors. The earliest applications of the coherence function to the structural dynamics of mechanical systems appear to be those of Kaneshige (67) and Barnoski (68). The coherence function, however, was used only to assess the validity of the estimated frequency response functions. A novel application of the coherence function in acoustic noise measurements (69) is based on the capability of $\gamma^2_{xy}(f)$ to determine if two signals that produce a spectral line are correlated. This property enables the detection of noise sources

in a mechanical system.

The above application suggests use of the coherence function in the identification of loading sources that produce vibrations in a structural system. Recalling properties 3 and 5, it is seen that $\gamma^2_{xy}(f)$ can be used to assess the degree of linear dependence of the dynamic response of a structure on a particular loading source. With this point of view, the coherence function can be utilized to assess the causality in a complex system. For example, in the present study the coherence function can be used to evaluate the causality of the wind loads in exciting the dynamic response of window units or other elements of the curtain wall.

Theoretically, a similar assessment can, of course, be made by cross-correlation techniques. In fact, cross-correlation techniques have been applied to isolation of noise sources (70), where the technique was used for the separation of noise at a given point A into components according to the source, the transit time from the source to point A, and the frequency.

The choice of which approach to adopt for a particular problem can only be made when the overall objectives of the study and the methodology to be used have been established. If the problem description is based largely on a frequency domain formulation, for instance, using modal analysis or eigenvalue techniques, a transfer or frequency response function characterization is most appropriate, and use of the coherence function would provide more readily usable information. On the other hand, if a time domain formulation of the problem was made, for example, to study transient response behavior or transit

time effects, then a correlation function approach would likely be preferable. Generally, the type of approach used in any situation will depend on the computational efficiency and the type of information desired, and the choice of using either the coherence or correlation function for source identification purposes must be made accordingly.

2.4(b) Application to Wind Loads and Window Response

General: The window assembly shown in Fig. 2.4-4 which together with smaller spandrel panels formed the exterior curtain wall of the building, is divided into two linear subsystems for the present application, Fig. 2.4-5(a).

Wind loads act on the double plate system formed by the two glass panes and through boundary connections are transmitted to the supports (shear forces in the case of simply-supported boundary conditions). The two systems are assumed to behave linearly under ambient wind loads.* The supports are assumed to be rigid for the evaluation of the transmissibility function defined below.

The input to the interconnected double plate system is the non-deterministic surface pressure due to the wind. The displacement response of the two plates, Fig. 2.4-4, was considered as the output. The input and the response parameters in the transmissibility model of the supporting structure depend on the definition of transmissibility used. From Fig. 2.4-5 the force transmissibility is defined as the magnitude of the ratio of the total force F_1 transmitted to the plate perimeter to the driving force F_o (71). The force F_1 comprises a

*"Ambient Wind Loads" excludes unusually strong meteorological phenomena such as tornadoes and hurricanes. Observations in strong squalls ($v > 65$ mph) indicated that static glass pane deflections comparable to glass thickness occur and linearity may not hold.

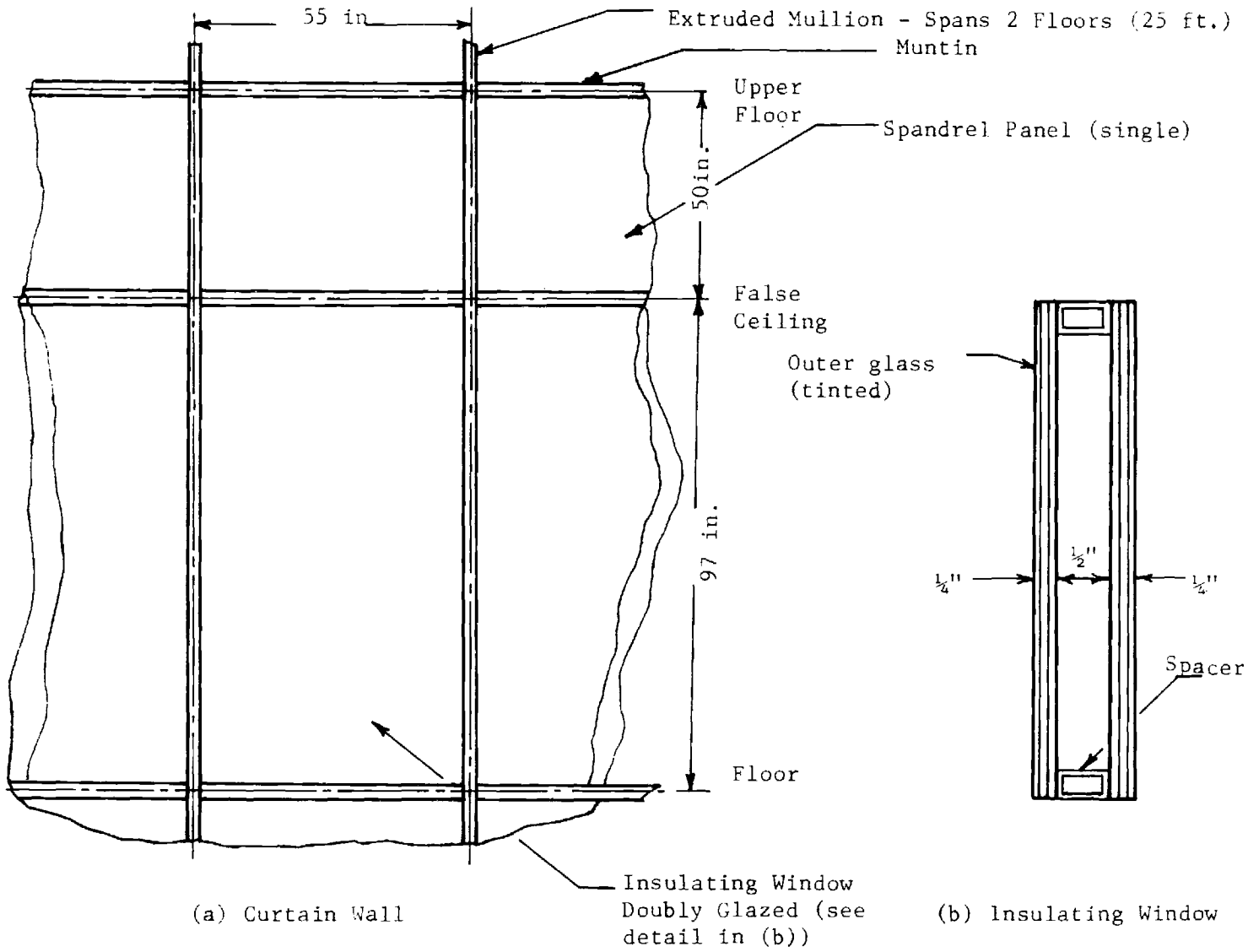

Figure 2.4-4. Components of a Curtain Wall and a Doubly Glazed Window Unit.

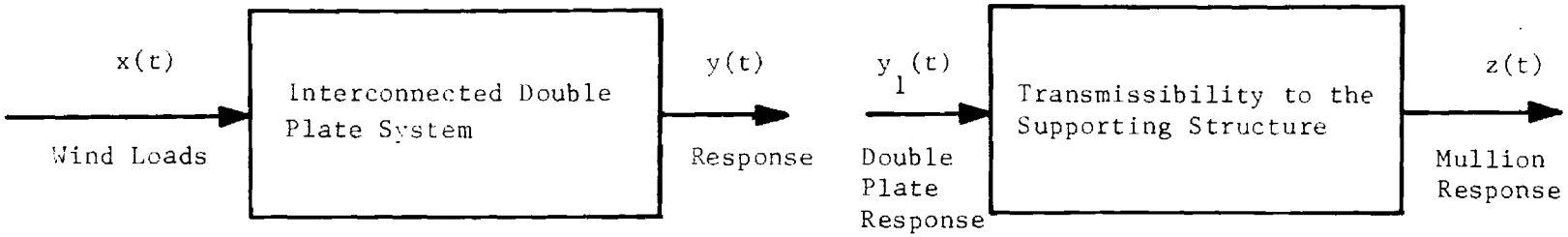

(a) Subdivision of The Window Assembly Into Linear Systems.

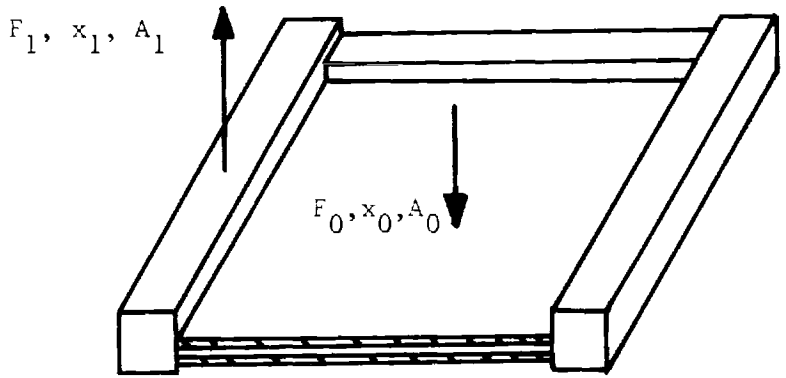

(b) Definition of Transmissibility.

Figure 2.4-5 Window System Models

distributed force around the plate boundaries plus four discrete forces one at each plate corner. The displacement, x_o, of the midpoint of the plate to the displacement, x_1, of its boundary (71). As a result of a general transmissibility theorem (72) the two definitions are identical in the frequency domain. Furthermore, at any given frequency the displacement transmissibility is identical with the corresponding acceleration ratios:

$$|T(f)| = \left|\frac{F_1}{F_o}\right| = \left|\frac{x_o}{x_1}\right| = \left|\frac{A_o}{A_1}\right| \qquad (2.4\text{-}15)$$

Since the rigid body accelerations can be measured with relative ease, in an experimental study, the acceleration ratio is generally measured.

The structural dynamic behavior of the two linear systems shown in Fig. 2.4-5 can be completely characterized by either their impulse response functions, $h(\tau)$ and $s(\tau)$, in the time domain or by their transfer functions, $H(f)$ and $T(f)$, in the frequency domain. The use of the transfer function, i.e., frequency domain characterization, is convenient in an experimental study where, as in the present case, the system characteristics are not known. Among the reasons for the choice are:

(a) the difficulties associated with interpreting the time domain response of a linear structure where several modes have been excited. This situation is aggravated if the modes are closely spaced.

(b) the ease with which background noise in the measured input and response can be minimized in frequency domain analyses.

(c) use of the Fast Fourier Transform (FFT) algorithm permits rapid analysis of voluminous data on a digital processor thereby

providing greater computational efficiency in the estimation of frequency domain functions, e.g., power spectra.

The disadvantage of the frequency-domain viewpoint is that it is not directly applicable to nonlinear systems. In the present application, however, the system behavior is assumed to be linear and only the steady state characteristics are of interest. Therefore, frequency domain representation of the CPLS is used, with Eqs. (2.4-11) and (2.4-13) providing the basis. The most severe restrictions in the use of this formulation are that the system must be linear, time-invariant, and the input must be a stationary random process.

The Input-Wind Loads: The natural wind turbulence together with the roughness effects on the earth's surface features cause the wind pressures on a building facade to be random in nature. Cladding loads, therefore, must be considered as a random process and described in terms of statistical functions. It appears reasonable to assume that over a short period of time the wind loads can be classified as stationary.* The frequency decomposition and distribution characteristics of the process can then be described by its power spectral density function (PSD) and amplitude probability density function (pdf).

The wind-structure interaction modifies the free stream wind properties, i.e., the PSD's and the pdf's. As a result, the surface pressure frequency content and amplitude distribution depend on the following four variables:

1. Surrounding terrain conditions or exposure.
2. Mean wind speed, denoted by $\bar{v}$.

*The classification of cladding loads as stationary in light of the experimental data is discussed in section 2.5.

3. Mean wind direction, $\bar{\theta}$.

4. Building profile, assumed to be described by the parameters ϕ and z, where ϕ denotes the surface orientation at a height z.

These features of the wind flow past a bluff body may combine to produce the following effects related to cladding loads in the time and frequency domain:

1. Time domain - The descriptor in this case is the amplitude pdf.

(a) Variation in the magnitude of rms pressure fluctuations as indicated by the variance of the pdf.

(b) Variation in gust factors, g, as defined by Eq. (2.2-2).

(c) Negative peak C_p excursions as determined from the extreme values in the pdf.

2. Frequency domain - The descriptor in this case is the power spectral density function, and effects of interest in addition to the overall bandwidth relative to the window natural frequencies are:

(a) Periodic forces due to vortex shedding.

(b) Narrow band pressure pulsations.

(c) Modification of the slope of the spectrum from the Kolmogorov inertial subrange spectrum which is proportional to $f^{-5/3}$.

(d) Variation in levels of the spectrum. This variation is related to the severity of dynamic loading.

To assess the dependence of these effects on the four variables mentioned above it is necessary to examine the roles each one of these plays in the present investigation.

(1) Terrain Conditions - The terrain surrounding the building used as the test site shows no characteristic variation and, therefore,

can be eliminated from the list of independent variables.

(2) Wind Speed - Wind speed is converted to the nondimensional Reynolds number, $Re = \frac{\bar{v}d}{\nu}$, where d is a characteristic dimension. The Reynolds number does not explicitly appear as a variable since it affects the surface pressures only with a transition from one Reynolds number range to another.

(3) Wind Direction - The wind direction, θ, is an explicit variable in that it governs the relative pressure distribution on the building facade.

(4) Building Profile - The building geometry is best described in terms of a coordinate system similar to cylindrical. The coordinates, ϕ and z, can be visualized as a polar angle and the height, respectively. For the present study, the angular interpretation for ϕ is discarded and instead ϕ is given discrete labels corresponding to the sites on each floor at which measurements were conducted.

If x(t) is a random variable describing the instantaneous surface pressure, then a realistic functional form of the power spectral density can be hypothesized as:

$$G^{R}_{xx}(\xi) = F_{x}(\phi_{z}, z, \xi, \theta; R_{e}) \qquad (2.4\text{-}16)$$

where,

$G^{R}_{xx}(\xi) = \frac{G_{xx}(\xi)}{\left[\frac{1}{2}\rho\bar{v}^{2}\right]^{2}}$ in units of 1/Hz is the reduced PSD,

and

ξ is the reduced frequency given by $\frac{f \cdot d}{v}$.

Local pressures due to wind may not necessarily follow the Gaussian distribution. Wind tunnel measurements (25) show that for the wind-

ward face of a structure, the local pressures follow the same distribution as expected for velocity fluctuations in the approach flow (usually Gaussian for open exposure). For the leeward side, however, the positive local pressures show a generally Gaussian character whereas the large negative pressures are non-Gaussian. It has been pointed out by Davenport (73) that the strong negative tails are exponential in form. Since the pdf depends on the nature of the wind-structure interaction, the mean and the variance of the pdf of C_p's can be expected to have a functional form as follows:

$$\text{Mean:} \quad \bar{C}_p = C_1[\theta, \phi_z, z; R_e] = \frac{\int_{-\infty}^{\infty} \Delta p \cdot p(\Delta p) \cdot d\Delta p}{\frac{1}{2}\rho \bar{v}^2} \qquad (2.4\text{-}17)$$

$$\text{Standard Deviation:} \quad C'_p = C_2[\theta, \phi_z, z; R_e] = \frac{\int_{-\infty}^{\infty} (\Delta p - \bar{\Delta p})^2 \cdot p(\Delta p) \cdot d\Delta p}{\frac{1}{2}\rho \bar{v}^2}$$

where, $p(\Delta p)$ is the probability density function of the surface pressure, Δp, and $\bar{v}$ is a mean reference velocity. Experimental investigation of the hypothesis of critical response locations, therefore, reduces to a parametric study of the functional forms of Eqs. (2.4-16) and (2.4-17). Load identification consists of examining the effects of the independent variables on the estimated PSD's and pdf's.

Causality of Wind Loads: There are several possible sources of the dynamic loading acting on a window system as mentioned in 2.1. Therefore, the degree of linear dependence of the response on the direct wind loads must be known in order to establish the causality of wind loads in exciting the window response. This can be accomplished by means of the coherence function, Eqs. (2.4-13) and (2.4-14). Although

its meaning in communication theory has been known for several decades, the use of a coherence function for identification of noise and vibration sources has only recently received attention (69, 74).

The theoretical coherence function is basically a measure of the linearity between two processes. In practical applications, however, measurement noise becomes an important consideration and the real-valued coherence function may be simultaneously affected by nonlinearity in the system and measurement noise. When the system between the input and the output is linear, $\gamma^2_{xy}(f)$ assumes the value 1. Low values of the measured coherence function are indicative of:

(i) Extraneous noise present in the measurements;

(ii) The system relating x(t) and y(t) is not linear;

(iii) y(t) is an output due not only to x(t) but also to other unspecified inputs (partial coherence problem).

System linearity for multiple inputs can be estimated from the multiple coherence function. For several correlated inputs the system linearity is determined from the partial coherence functions. In the present application the ordinary coherence is used.

The Response: The frequency response function of the double plate system, H(f), can be represented in a matrix form as:

$$H(f) = \begin{bmatrix} H_{11}(f) & H_{12}(f) \\ H_{21}(f) & H_{22}(f) \end{bmatrix} \qquad (2.4\text{-}18)$$

where $H_{ij}(f)$ is the ratio of the displacement response at plate j to an input force at plate i. The force to displacement transfer function is called the compliance transfer function. The elements of the transfer function matrix of Eq. (2.4-18) may themselves be matrices.

The frequency response function estimated from the measured input and output can be used to determine the vibration properties of the double plate system, namely

(a) Natural Frequency

(b) Damping

(c) Mode Shapes

(d) Modal Mass

(e) Modal Stiffness

An excellent survey of system identification techniques is given in Ref. 59. The particular procedure used in the identification of the modal parameters of the double plate system is detailed in 2.5.

The transmissibility function is used to evaluate the effect of the glazing retaining the double glass plate in the supports. Comparison of theoretical and measured acceleration transmissibilities provides an estimate of the reduction in support acceleration and thus forces caused by the neoprene gasket.

2.4(c) Data Processing

The large quantities of inherently nondeterministic data that result from an experimental study required that data processing techniques be fast and fairly streamlined. In recent years, the advent of high performance low cost minicomputers, and the Fast Fourier Transform algorithm have made digital processing of time series of data attractive. The various frequency domain quantities in the transfer function description of linear system dynamics, can be rapidly computed using digital time series analysis procedures. Digital techniques also offer the advantages of ease of manipulating the processed results,

and greater dynamic range. These considerations, and the availability of a digital system to be described later, dictated use of digital computation of the various auto and cross-power spectra from the experimental data.

The mathematical development in 2.4(a) of the frequency-domain input-output relations for a linear system dealt with exact values of the frequency-domain quantities. This means, in the case of random time series, that the spectra are based on time samples of data that are both infinite and continuous. In practice, of course, the sample lengths are finite and in the case of digital analysis are further limited to discrete data values. The effect of truncating the data is that magnitude and phase information in the frequency domain is obtained only at discrete frequencies. The effect of sampling at discrete time increments is to limit the highest frequency at which valid information is obtained. In addition, to determine the descriptive properties of random time series from finite data, estimators, as for example the sample mean and the sample variance, for the various spectral quantities must be used. This means that only estimates of the properties of a random process can be obtained. Thus, it is necessary to recognize the uncertainty or statistical variation in the estimates and know the techniques to minimize this uncertainty.

Digitation of random analog data and estimation of their descriptive properties from finite samples, therefore, requires consideration of the following:

(a) Sampling at discrete time increments

(b) Effects of truncation of the random time series

(c) The Estimators used

(d) Statistical errors in the estimates

Practical implications of these aspects of digital time series analysis in computing the various frequency-domain quantities are briefly outlined in the following paragraphs.

Digitization of Analog Data: Digitizing analog data of duration, T, by sampling in the time domain with an interval, Δt, requires that the frequency spectrum be band-limited to a frequency, $\frac{1}{2\Delta t}$. This is a consequence of Shannon's sampling theorem which states that it requires slightly more than two samples per period to uniquely define a sinusoid (75). In terms of the time domain and frequency domain interrelationship this can be written as

$$F_{max} < \frac{1}{2\Delta t} \qquad (2.4\text{-}19)$$

where F_{max} is the highest frequency present in the spectrum. The sampling rate, $F_s = \frac{1}{\Delta t}$, determines the Nyquist folding frequency, $f_N = 2F_s$. Frequencies in the spectrum which are greater than f_N are seen as replicas of frequencies in the base band, $(0 - f_N)$, e. g., $f_N + f_i$ will be seen as $f_N - f_i$ (76). This folding back of frequencies is known as aliasing, and the "image" frequencies cannot be distinguished from the true base band spectrum. In practice aliasing can be avoided by low pass filtering the data with a sharp cut-off frequency slightly less than f_N. The total number of samples is given as: $N = T\Delta t$. In digital computation, N is frequently referred to as the block size.

Sampling the data over only a finite duration, T, results in discretization of the frequency domain, i. e., the Fourier transform

of the sample can be calculated only at a finite number of frequencies spaced $\Delta f = \frac{1}{T}$ apart. The frequency resolution, Δf, is related to the Nyquist frequency, f_N, and the total number of discrete values, N, in the time domain as follows:

$$\Delta f = \frac{f_N}{N/2}$$

This is because N discrete values in the time domain allow computation of frequency and phase information in the frequency domain at N/2 points. Theoretically, discretization of the data in the frequency domain at intervals of $\Delta f = \frac{1}{T}$ is equivalent to assuming the data to be periodic, i. e., the sampled segment repeats itself with a period, T.

Truncation of a random time series is mathematically equivalent to multiplication of the data by the boxcar function shown in Fig. 2.4-6, and expressed as:

$$u(t) = 1 \qquad 0 \leq t \leq T$$

$$= 0 \qquad \text{otherwise}$$

The data are then said to have been viewed through a rectangular window of width, T. The Fourier transform of the rectangular window, also known as its line shape function, is:

$$U(f) = \frac{\mathrm{Sin}\pi fT}{\pi f}$$

Computation of Fourier transform of a finite data sample, therefore, is equivalent to taking the Fourier transform of the product of an infinite data record and the time window. The result in the frequency domain is the convolution of the transform of the record of infinite

length with the transform of the time window. For example, if $G_{xx}(f)$ denotes the true power spectrum of a stationary time series x(t) and $\tilde{G}_{xx}(f)$ the net result of convolution with the time window transform, then

$$\tilde{G}_{xx}(f) = \int_{o}^{\infty} G_{xx}(f_o) U_T(f - f_o) df_o$$

Thus, the true spectrum is "smeared" by the window line shape. This convolution is effected before quantization along the frequency axis. Thus, if the original data are periodic such that there is an integer number of periods in the time window, the line shape does not appear in $\tilde{G}_{xx}(f)$ because frequency samples occur only at zero crossings of $U_T(f)$. However, if there is an odd number of half cycles in the time window, frequency samples occur at the peaks of $U_T(f)$, and a single frequency waveform may transform into a broad band of frequencies. This phenomenon is known as frequency leakage and the cure is to reshape the time window to produce a line shape with smaller side lobes (See Figure 2.4-6.). This technique will broaden the main lobe and hence reduce frequency resolution, but it reduces the interference of one frequency with its neighbors.

The selection of a time weighting function to reshape the rectangular window transform and thus suppress leakage reduces to a study of the various windows and their line shapes. A number of weighting functions, also called windows, and their line shapes are described in Refs. 60, 75, 76, and 77. For the present application the Hanning window of Fig. 2.4-7 described by

$$w_H(t) = 0.5 \left(\text{Cos } \frac{2\pi t}{T} - 1\right)$$

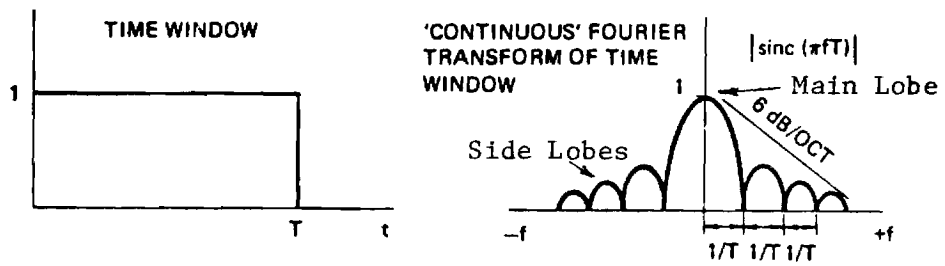

Figure 2.4-6. Boxcar Function and Its Fourier Transform.

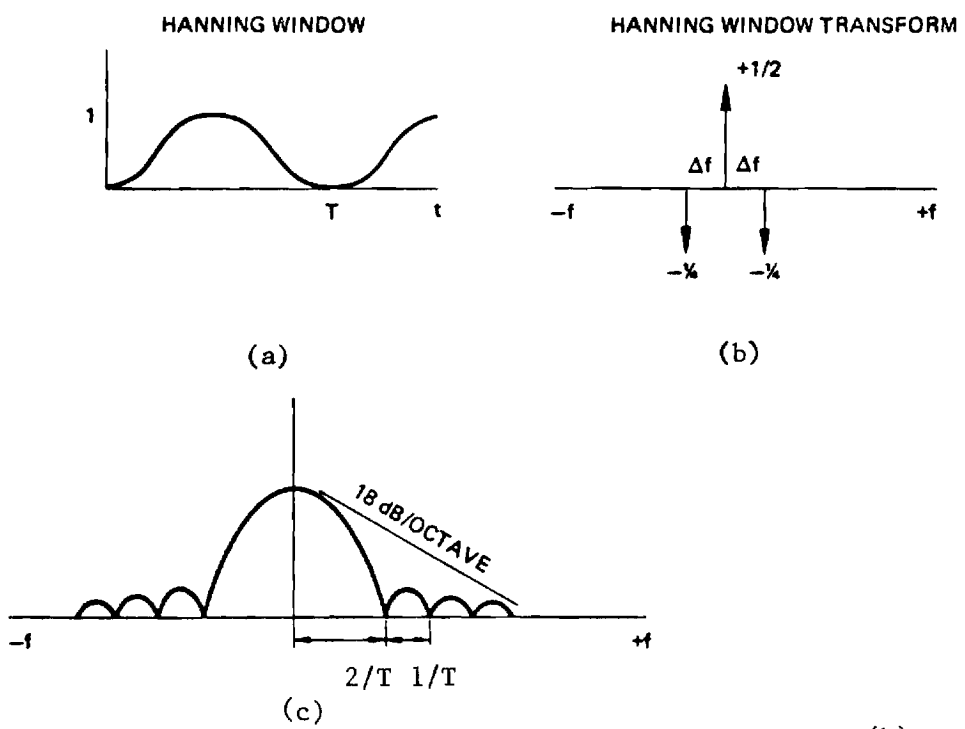

Figure 2.4-7. Hanning Window (a), its Fourier Transform (b), and its Convolution With The Boxcar Function(c).

$$W_H(f) = 0.5\delta(0) - 0.25\delta(\Delta f)$$

was used. The Hanning window is attractive due to its relatively narrow main lobe together with greatly reduced amplitude of the side lobes (78).

Digital Computation Requirements: The descriptive properties of a random process, x(t), cannot be precisely determined from sample data. Therefore, suitably defined estimators have to be used in computing the spectral density, transfer, and coherence functions from finite samples of data. The raw estimates (denoted by superior carets) thus obtained require smoothing operations to reduce the statistical uncertainty in the estimates. The smoothed quantities are denoted by superior tildes.

The accuracy of parameter estimates based on sample values can be described by a mean square error defined as (60):

$$\text{Mean Square Error} = E[(\hat{\phi} - \phi)]^2 \qquad (2.4\text{-}20)$$

where $\hat{\phi}$ is an estimator of ϕ and E is the expectation operator. The root mean square can also be expressed as

$$\text{rms error} = \sqrt{\sigma^2[\hat{\phi}] + b^2[\hat{\phi}]} \qquad (2.4\text{-}21)$$

or, the normalized random error

$$\varepsilon = \sqrt{\varepsilon_r^2 + \varepsilon_b^2} = \frac{\sqrt{\sigma^2[\hat{\phi}] + b^2[\hat{\phi}]}}{\phi}$$

where $b\hat{\phi}$ is the bias error in the estimate and $\sigma[\hat{\phi}]$ is the standard deviation of the estimate and $\varepsilon_r = \frac{\sigma[\hat{\phi}]}{\phi}$ is called the normalized random error and is a measure of the variance of the estimate. $\varepsilon = \frac{b[\hat{\phi}]}{\phi}$, on the other hand, is a measure of the bias of the

estimate and is called the normalized bias error. An estimator with a small random error is said to have high stability and that with a small bias error is said to reproduce the true function with high fidelity.

Estimates of power spectral density functions from digital data can be obtained by one of the following two methods (60):

1. Blackman - Tukey Method: The power spectral density function is computed by first estimating the autocorrelation function and then Fourier transforming it, i. e., by using the Wiener-Khintchine relations.

2. Cooley - Tukey Method: This method is based on computing the discrete finite Fourier transform, via the FFT, of the original data.

Consideration of the computational speed advantage of the direct FFT make the second method more attractive; in fact, the autocorrelation function can often be most easily computed using the inverse FFT and the Blackman-Tukey method in reverse. The Cooley-Tukey method was used in the present study to compute the various spectra. In this method, raw estimates of the spectral density functions are computed as follows:

$$\hat{G}_{xx}(k\Delta f) = \frac{2}{T}\left|X(k\Delta f)\right|^2 = \frac{2}{T}\, X(k\Delta f)\cdot X^*(k\Delta f) \qquad (2.4\text{-}22)$$

$$\hat{G}_{xy}(k\Delta f) = \frac{2}{T}X^*(k\Delta f)Y(k\Delta f)$$

where $X(k\Delta f)$ and $Y(k\Delta f)$ are discrete Fourier transforms of stationary, Gaussian, zero-mean random processes, $\{x(t)\}$ and $\{y(t)\}$, respectively. The index, k, is an integer and * denotes the complex conjugate.

The estimator, $\hat{G}$, of Eq. (2.4-22) can be shown to be a χ^2_2 random variable and has a substantial random error (60). In practice the

random error of an estimate produced by Eq. (2.4-22) is reduced by smoothing over an ensemble (averaging) or by smoothing over frequency. The averaging technique was used in the present application and consists of dividing a record of length, T_S, into n_d disjoint segments such that $T_S = n_d T$ and $T = N\Delta t$, where N is the number of values in each data segment. Individual estimates are computed for each of the n_d disjoint segments and the smoothed estimate, $\tilde{G}$, obtained by averaging these. The normalized (with respect to the expected value) random error for smoothed estimates is given by

$$\varepsilon_r[\tilde{G}(f)] = \sqrt{\frac{1}{n_d}} = \sqrt{\frac{1}{\Delta f \cdot T_S}} \qquad (2.4\text{-}23)$$

The bias error, $b\{G(f)\}$, is proportional to $\Delta f^2 = \left(\frac{1}{T}\right)^2$. Hence, T should be made as large as possible to minimize bias, but at the same time, $n_d = \frac{T_S}{T}$ should be large to reduce the random error. Thus, reduction of bias and random errors imposes conflicting requirements on the data analysis parameters.

The overall level or mean square value estimates can be readily obtained from the power spectra by using Parseval's theorem which can be stated as follows:

Let $\Psi_x^2 = \lim_{T\to\infty} \frac{1}{T} \int_0^T x^2(t)dt$ be the true mean square value of x(t), then Ψ_x^2 can also be expressed as:

$$\Psi_x^2 = \int_0^\infty G_{xx}(f)df$$

The implication of Parseval's theorem is that the mean square value of a signal is the area under its power spectrum. Alternatively, the area under the power spectrum in a frequency band, $(f, f + \Delta f)$, is

the mean square value of the signal in that frequency band. This provides the basis for analog computation of the power spectral density function by filtering and squaring.

The mean square value can be estimated from the spectral density as

$$\hat{\psi}_x^2 = 2\sum_{k=1}^{N/2} \tilde{G}_{xx}(k\Delta f) \qquad (2.4\text{-}24)$$

The errors in the estimate, $\hat{\psi}_x$, depend on the errors in the smoothed estimates, $\tilde{G}_{xx}$. It can be shown (69) that relatively large errors in power spectrum estimates will have relatively small errors for $\hat{\psi}_x^2$ when N is sufficiently large.

Coherence function estimates can be obtained from two sample time history records of {s(t)} and {y(t)}, assuming the sample records to exist over a common time interval T, as:

$$\hat{\gamma}_{xy}^2(f) = \frac{|\tilde{G}_{xy}(f)|^2}{\tilde{G}_{xx}(f)\tilde{G}_{yy}(f)} \qquad (2.4\text{-}25)$$

The statistical accuracy of the estimate $\hat{\gamma}_{xy}^2(f)$ depends on the estimation procedure of Eq. (2.4-25) as well as the accuracy of the power spectral density estimates. Empirical studies of Ref. 79 show that estimates of the coherence function in the range of $0.34 \leq \gamma_{xy}^2 \leq 0.95$ based upon spectral density estimates with $n_d \geq 20$ can be evaluated in terms of the transformation

$$\hat{w}(f) = \tanh^{-1}\hat{\gamma}_{xy}(f)$$

In terms of n_d, the number of disjoint independent segments, the bias and variance errors are given by

$$b[\hat{w}(f)] \simeq \frac{1}{2n_d-2}$$

$$\sigma[\hat{w}(f)] \quad \frac{1}{2n_d-2}$$

The frequency response function estimate for a single input-single output CPLS with transfer function H(f) input x(t) and output y(t) is obtained as

$$\hat{H}(f) = \frac{\hat{G}_{xy}(f)}{\hat{G}_{xx}(f)} = |\hat{H}(f)| \; e^{-j\hat{\phi}(f)} \qquad (2.4\text{-}26)$$

The bias and random errors in this estimate are shown in Ref. 60 to depend on the number of degrees of freedom, $n = 2n_d$, of the spectral density function estimates and the coherence function estimate, $\hat{\gamma}^2_{xy}(f)$. The bias error is generally less than the rendom error for any given combination of n and $\hat{\gamma}^2_{xy}(f)$. The random error in $\hat{H}(f)$ approaches zero as either $n \to \infty$ or $\hat{\gamma}^2_{xy}(f) \to 1$. In interpreting practical measurements, if $\hat{\gamma}^2_{xy}(f) \approx \gamma^2_{xy}(f) = 0$, it follows that no physical system exists between the measurement points and no frequency response function can be defined. On the other hand, if $\gamma^2_{xy}(f)$ has a nonzero value, no matter how small, then a frequency response function can be estimated with any desired degree of accuracy given sufficient data to make n appropriately large. Thus, $\hat{\gamma}^2_{xy}(f)$ is an indicator of the validity of the frequency response function.

The Digital Processor: For computation of power spectra, transfer and coherence functions and amplitude histograms by digital techniques, a minicomputer based Fourier Analyzer (HP5451B) was used. The main features of the Fourier Analyzer are a 2-channel, 12-bit analog-to-digital converter which accepts analog data to 25 kHz, and a dedicated

minicomputer (32k core). Time-domain and frequency domain computations are performed in accordance with instructions from a keyboard. Simultaneous two-channel operations are possible and the results can be recorded on a x-y plotter or punched on paper tape. "Quick Look" data inspection is possible on a CRT display, an integral part of the unit.

2.4(d) Experimental Techniques

The experimental plan called for the measurement, at various locations throughout the building, of cladding loads and the response of the two glass plates and the mullion to these loads. In addition, the reference wind velocity and direction were also required. The inaccessibility of the outdoor light from within the building required that a method for measuring its response without direct contact be devised, and a novel transducer was designed specifically for this purpose. Conventional transducers with suitable performance specifications were chosen for the measurement of the other variables. The instrumentation and its integration into a portable system is described below.

Wind Loading: The pressure loading on a window was assumed at the outset to be uniform over the area. The assumption, although at first seemingly crude, is realistic since the window area is relatively small compared to the building facade and, therefore, sudden spatial variations of pressure over this area are not expected. With this assumption, the wind loading on a window can be measured from the difference in the external and internal pressure provided the internal pressure is known.

Internal pressure variation due to the normal building activity, such as opening and closing of doors, operation of elevators and mechanical services of the building does not permit its use as a reference pressure. The ideal reference pressure would give a zero output for a transducer when the wind speed was zero. In comparing full-scale measurements with wind tunnel tests, various methods of referencing the wind pressure have been proposed, including most recently, the use of absolute pressure transducers (80). However, since the cladding loads are simply the differential pressure between the inside and the outside, no reference pressure is required in the present measurements. The differential pressure transducers used were variable capacitance Datametrics Type 501-11 Barocels with an internal volume of 0.15 cu. in. Datametrics Type 1015 signal conditioners were used with the Barocels. The auto-ranging feature of the Type 1015 was used to ensure that the pressure signals were not clipped in strong squalls, and was useful in providing adequate dynamic range.

With the uniform pressure assumption, a small number of point pressure taps can provide a measure of the loads on a window. Pressure taps through the mullion were planned initially but the channel-shaped mullion exterior appeared in early tests to cause upflow interference effects. The pressure taps were ultimately located on the muntion (horizontal top support) of the window, flush with the exterior surface. One side of the Barocel was connected to the tap and the other was vented inside. The external pressure tap and its location are shown in Fig. 2.4-8.

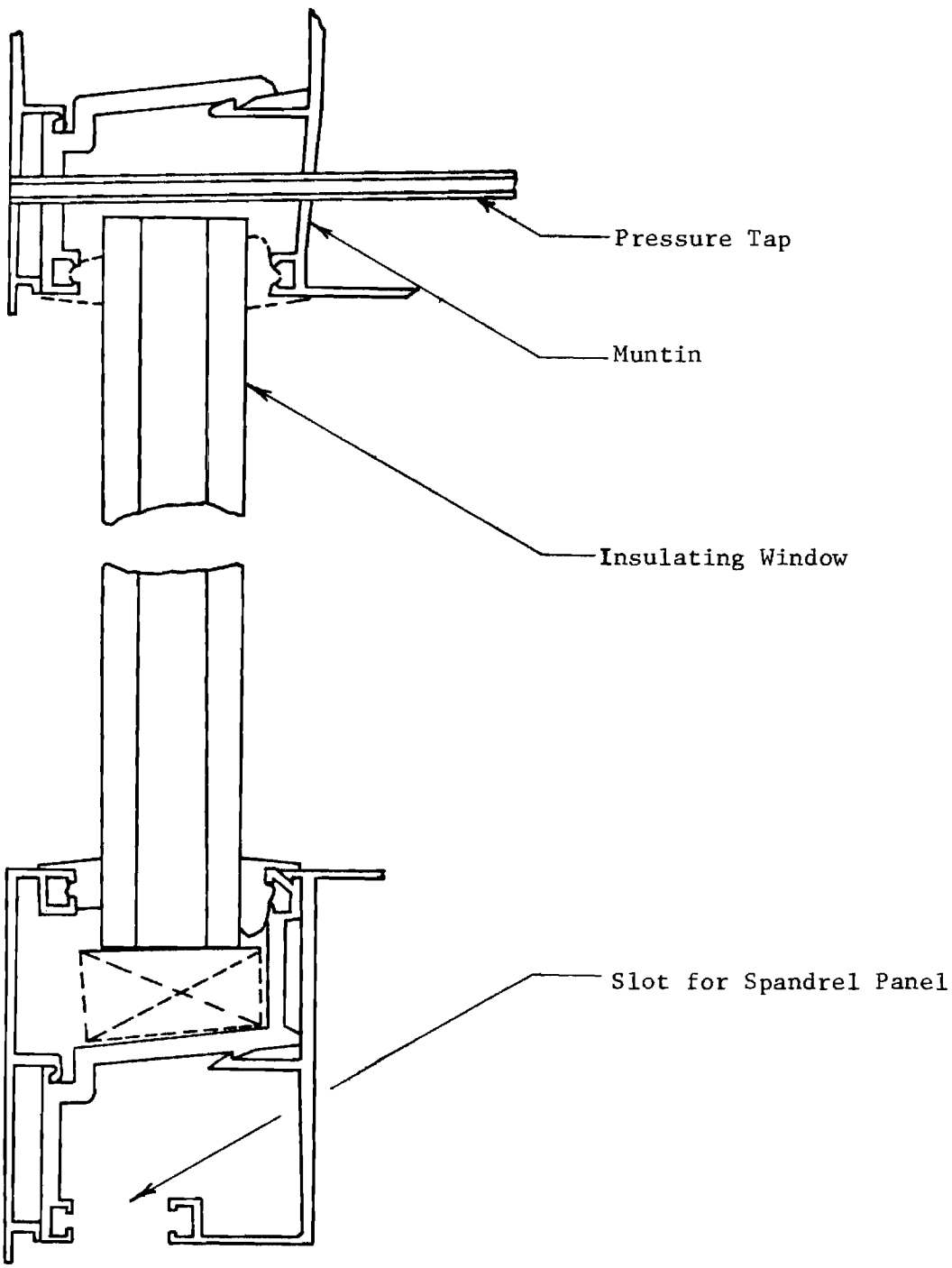

Figure 2.4-8. Pressure Tap and its Location.

The use of the sensor in dynamic pressure measurements required that the length of tubing used for the external pressure tap be selected to ensure adequate dynamic response. A suitable length was chosen after considering the resonance effects and damping in the system, and hardware limitations. Details of the response estimate are given in Ref. 40. A tubing length of 18 in. gave a flat response bandwidth up to 38 Hz with phase linearity up to 22 Hz. The bandwidth was considered suitable for pressure measurements (auto spectra) and the range of phase linearity adequate to span at least two structural response modes.

Reference Wind Velocity and Direction: The reference wind speed and direction were measuerd with an MRI Model 1022 Wind Sensor. The speed sensor has a range of 0.5 - 80 mph. To obtain reasonably undisturbed measurements of wind speed and direction, the anemometer was mounted on an "open" antenna tower at a height of approximately 455 ft above the ground level. Due to the existence of an atmospheric boundary layer compounded by interference effects due to the building, the velocity measured is not truly that of the mean wind. If the building interference effects are ignored, however, velocities at any other height can be obtained by using Eq. (2.3-2) applicable to the terrain conditions in the vicinity of the building. The wind speed and direction were recorded on strip chart recorders and the records used to compute the mean wind speed and direction over a certain length of time.

Response Measurement: The primary response parameters for the window glass were single point transverse surface displacements, w_i

and w_e, of the inner and outer panes, respectively, and mullion acceleration, a_m.

The inner glass displacement, w_i, was measured by a linear variable differential transformer (LVDT) mounted in a fixture referenced to the building structure. The LVDT core was flexure-mounted so as to enable it to accurately follow the dynamic glass displacement. The kHz carrier frequency of the LVDT permitted adequate dynamic response for the present application.

The mullion acceleration was measured using an MB accelerometer. The piezoelectric accelerometer could not be used for frequencies below 5 Hz; however, for transmissibility measurements in the vicinity of resonance ($\sim$10 Hz, 1st mode) the dynamic response posed no serious limitations.

Measurement of w_e for a double glazed window is complicated by the inaccessibility of the outer pane to measurement by conventional transducers located inside the building. Therefore, a method for measuring w_e without direct contact was required. Some common contactless transducer concepts are based on capacitive, inductive or optical effects. Capacitive and inductive methods generally would require treatment of the outer glass. Optical techniques, on the other hand, were judged most promising and a variety of available optical displacement transducers were evaluated with respect to their performance and portability. Most of these required relatively complex processing of the measured signals, while others were found to be unsuitable because of a limited range or were affected by the presence of background illumination. As a result, a unique optical

transducer was designed which provided simplicity of operation, sufficient range and accuracy, and a capability of integration into a portable measurement system.

The sensor operates on geometric optics and utilizes a He-Ne laser beam for a collimated light source. The geometric movement of a beam reflected off the outer glass pane is sensed by an array of linear semi-conductor detectors. The detector output after conditioning by a set of preamplifiers and analog computing circuits produces voltages proportional to the motion and intensity of the beam. The design of the geometrical configuration of the laser-detector system and other details such as elimination of the effect of rotation in the vertical plane, and special signal conditioning electronics are given in Ref. 104. The transducer is capable of measuring both transverse displacements and changes in surface slope of the window. For the particular configuration used in the measurement of w_e, the transverse displacement sensitivity was 6.25 V/in. The usable range of displacements was 0.35 in. before effects of detector differential nonlinearity and violation of small angle assumptions caused the output to deviate from the linear relation.

Physical construction of the transducer is best described by Fig. 2.4-9 where the laser and the detector enclosure box are shown mounted on a 4" x 4" steel beam supported by a torsionally rigid tripod. The laser displacement meter (LDM) support also served as the fixture for the LVDT which is partially visible. The Barocel sensor seen clamped to the beam was located on the top horizontal support during an actual run. Retractable wheels on the tripod

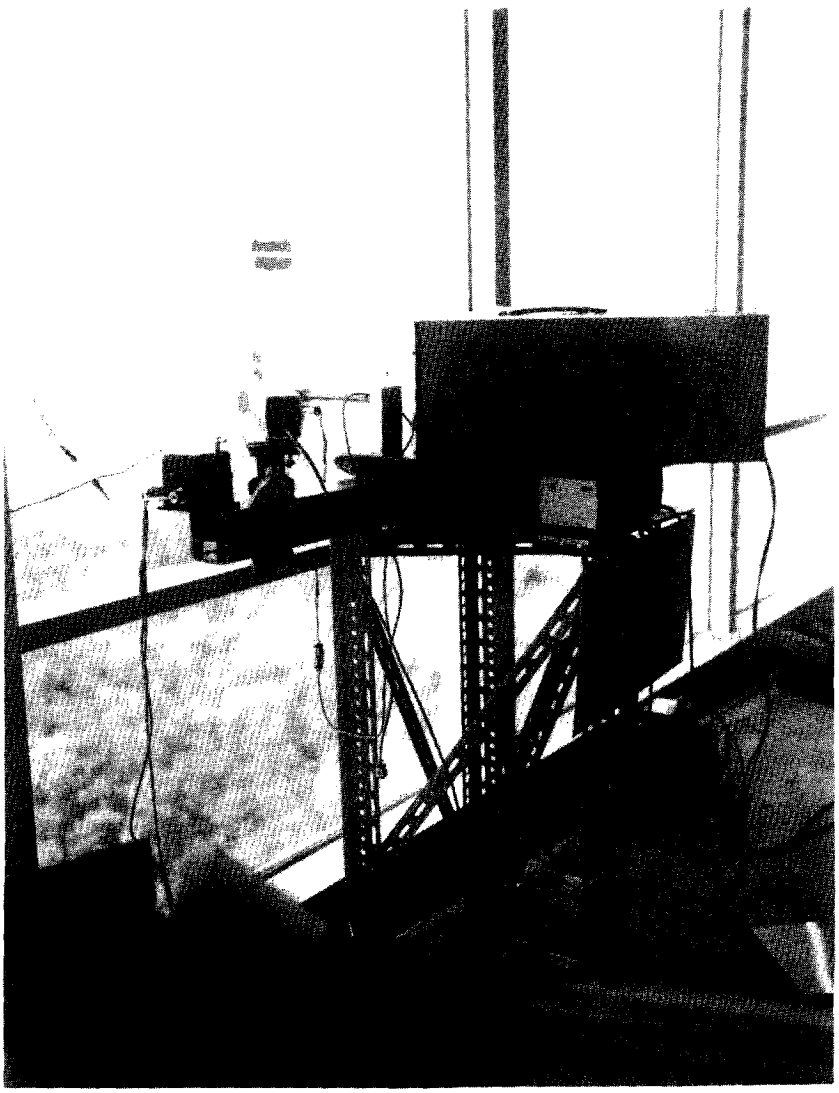

Figure 2.4-9 The Experimental Set-up.

permitted easy transport of the LDM/LVDT combination to various locations throughout the building. The figure also shows the displacement transducers positioned (by means of aluminum "spacer" rods to ensure calibration) opposite a window to record displacement histories.

The LVDT and LDM were positioned to measure the transverse displacements at corresponding points on the two panes. The measurement point was typically at the centroid of the horizontal axis and approximately 5 in. below the centroid of the vertical axis. This arrangement is suitable for detecting motion in any symmetric modes of the window glass. To measure the displacement response of the plates in antisymmetric modes a position closer to the supports is desirable and could be used by repositioning the platform. A schematic of the entire instrumentation is shown in Fig. 2.4-10.

Data Recording: The large quantities of data inherent in full-scale investigations require that careful consideration be given to a data acquisition system. Portability, unattended operation for several hours and compatibility of the system with the transducers is essential. While the use of a total digital recording system would have facilitated digital data analysis, the relatively high cost and lack of portability of such a system led to the choice of analog recording. For the present experiments the analog signals form all the transducers except the remotely located anemometer were recorded on a portable FM tape recorder (HP 3968A). Since the planned data analyses required only a mean wind speed and direction for a set of sample records from the response and load transducers,

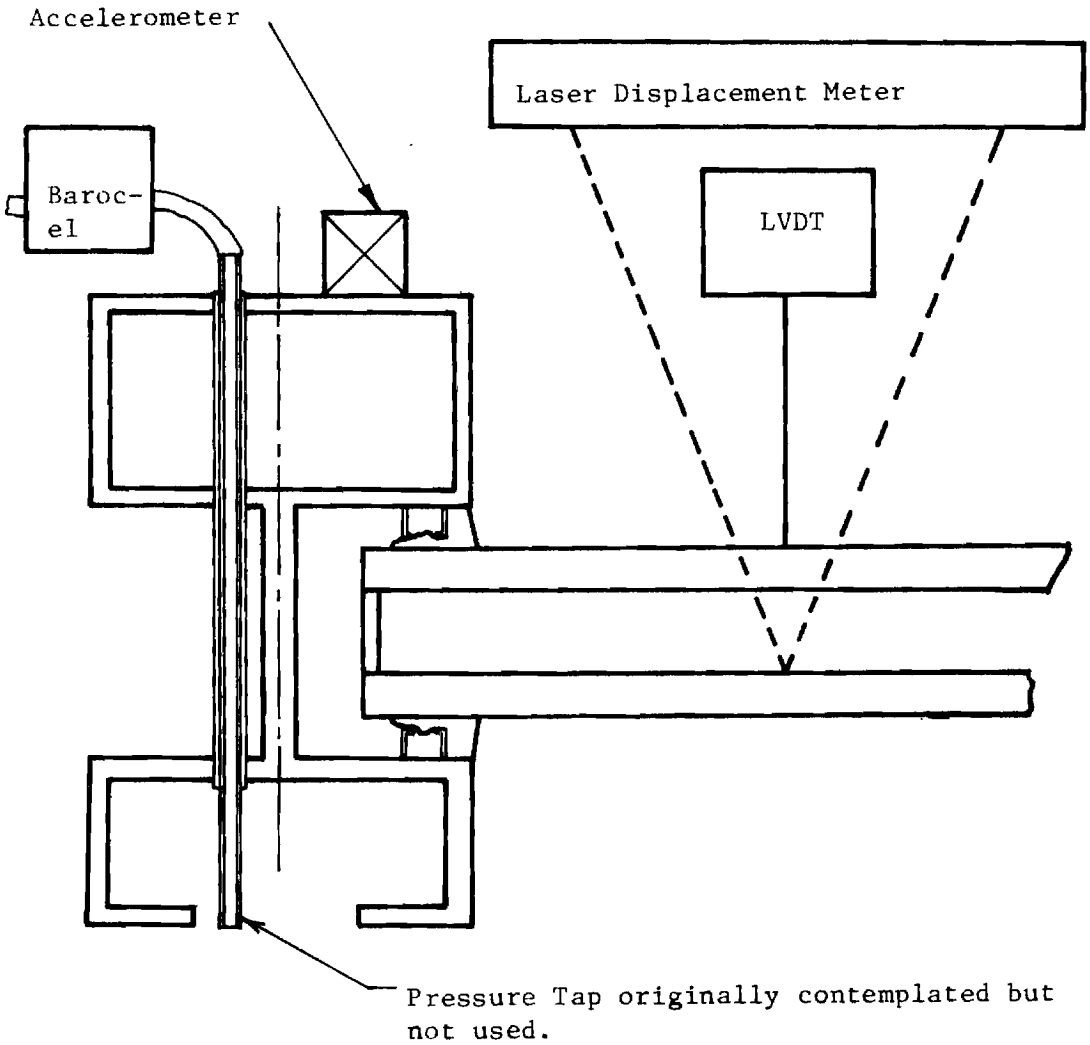

Figure 2.4-10. Schematic of the Instrumentation.

the use of strip chart recorders for the anemometers posed no serious problems. Data recording was continuous for a particular session (up to 16 hours) and the records were sorted for relatively large pressure fluctuations prior to analysis.

Test Methodology: Weather forecasts were used to select days on which the experiments were run. The test sites for the measurements were selected on the basis of available wind tunnel pressure distribution data from an earlier simulation (58). Windows were selected in areas where large negative pressure coefficients occurred in the simulation with the prevailing wind direction as the flow direction. In order to assess the variation of wind loads with height, tests were planned to include three different floors of the building, viz. 9th, 21st, and 28th. The window nomenclature used and the wind directions for which data were recorded are shown in Fig. 2.4-11.

On days when reasonable wind velocities were forecast (about 15 - 20 mph) the portable instrumentation system was set up at a suitable window, depending on the wind direction, and the data recorded. For unexpected storm systems moving into the area data acquisition was not possible due to the time required to get to the test site and make the measurement system operational. A summary of the acquired data is shown in Table 2.4. Recording sessions were usually unattended and on the average were conducted over periods of approximately six hours.

The major problem encountered in the data acquisition process was one of dynamic range of the transducers. The selection of transducer signal conditioner range was dictated by the extremes of adequate

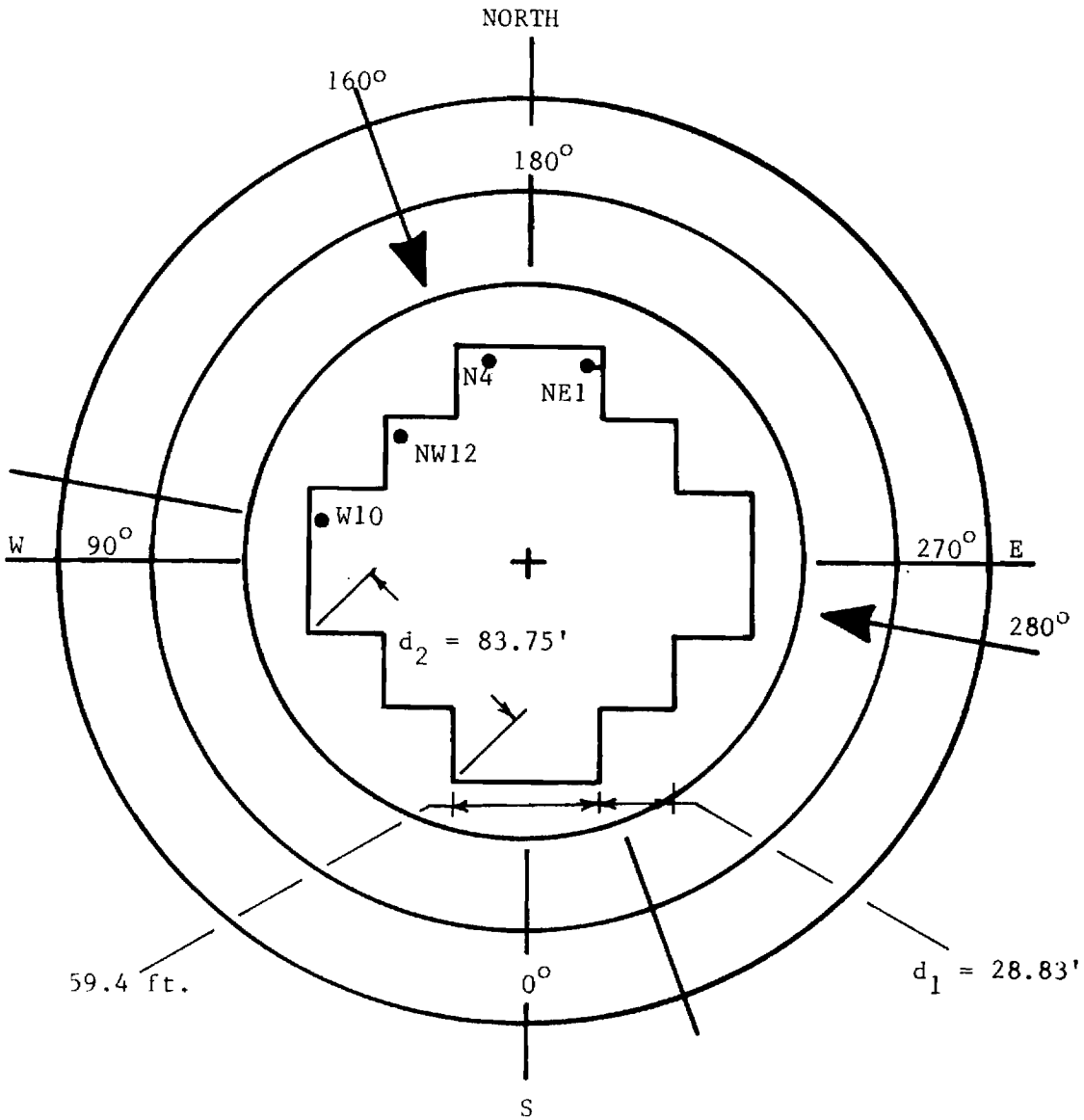

(a) 9th Floor

Figure 2.4-11. Window Nomenclature; Directions With Respect to Building Axis.

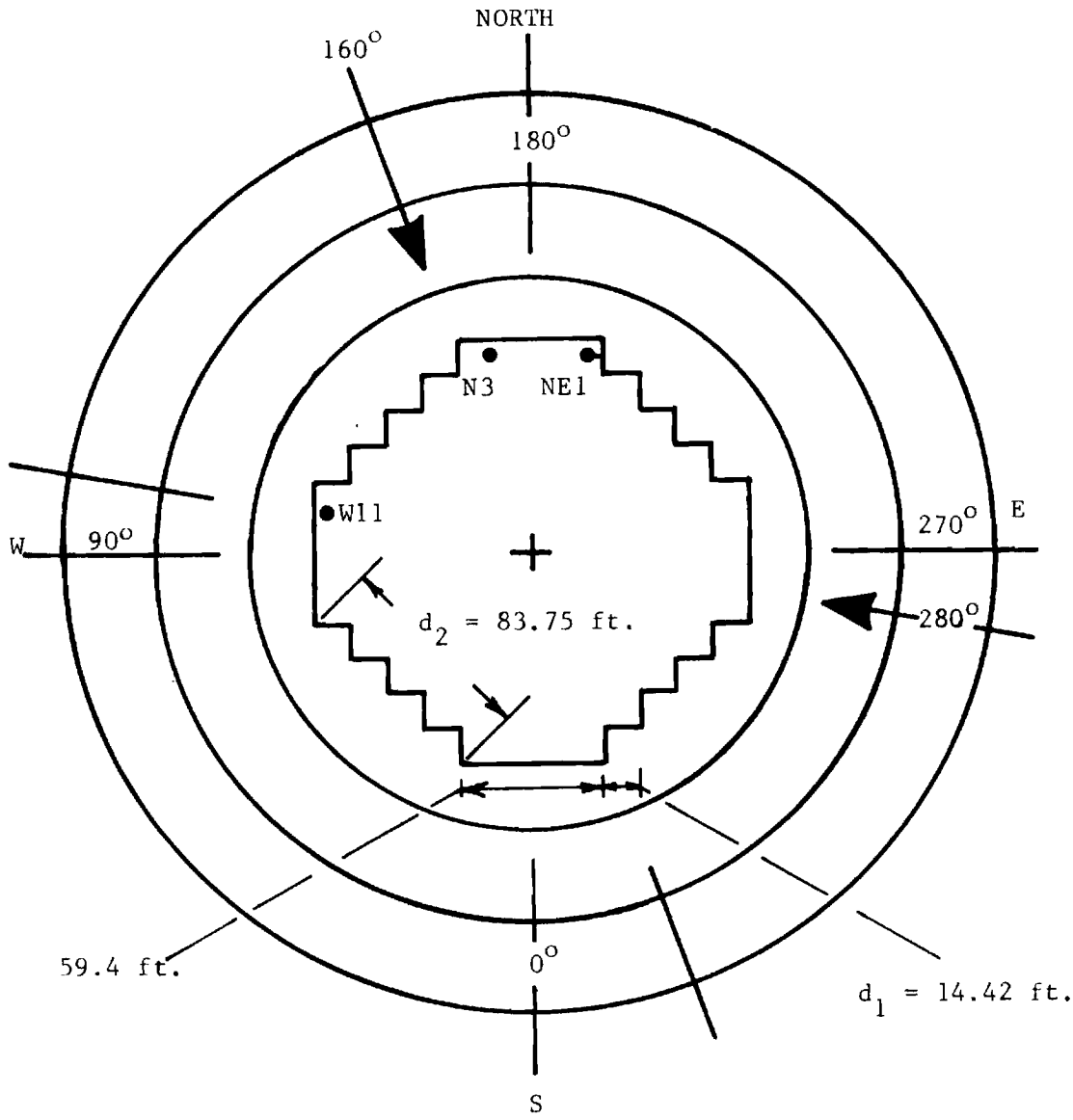

(b) 21st Floor

Figure 2.4-11 (contd.). Window Nomenclature; Directions With Respect To Building Axis.

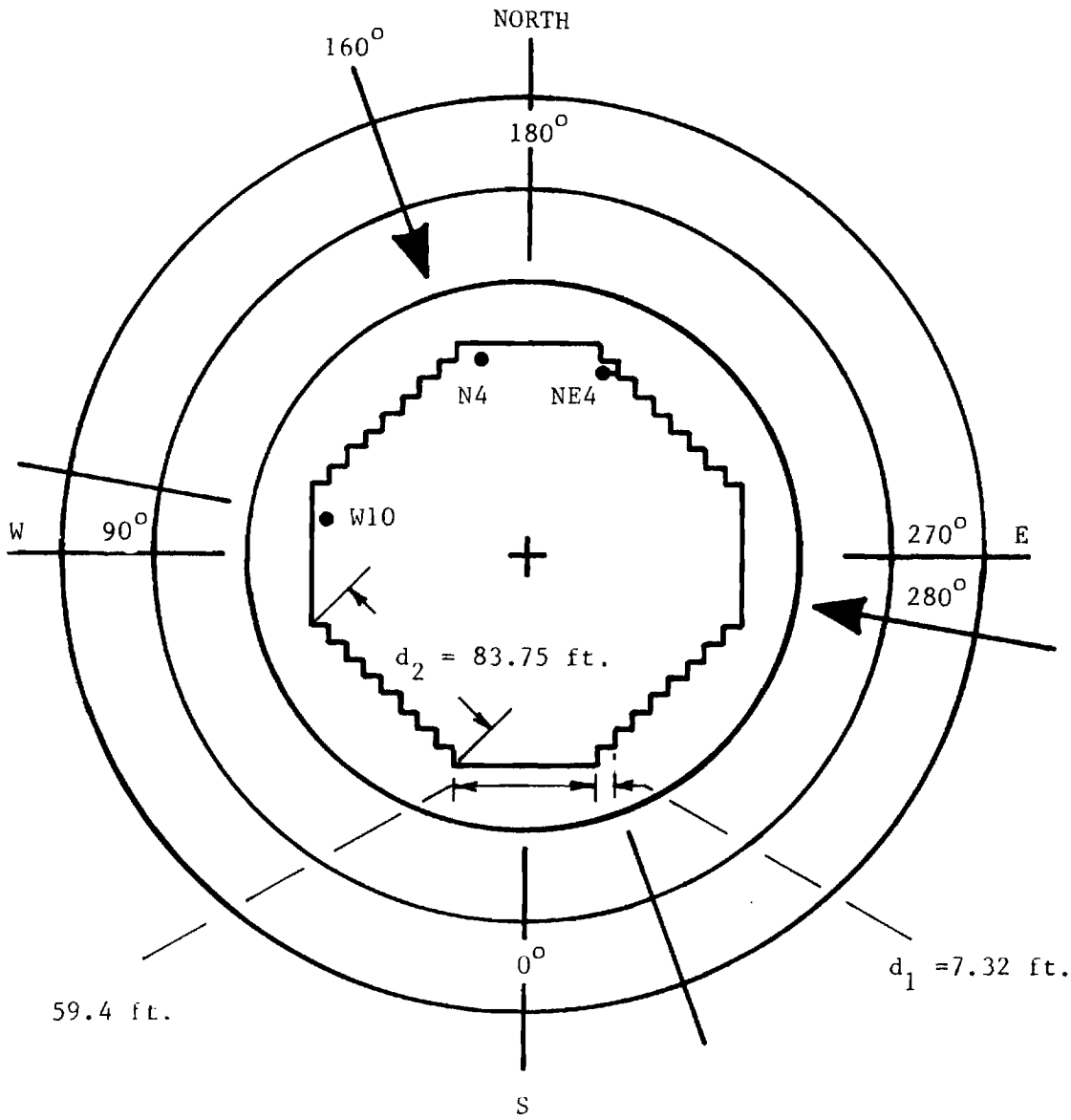

(c) 28th Floor

Figure 2.4-11 (contd). Window Nomenclature; Directions With Respect To Building Axis.

Table 2.4 Summary of the Data Collected

#	Date (1976)	Duration Start/# hrs	Window	fps $\bar{v}$	0^{o} S $\bar{\theta}$	Transducers Used				
						Δp	Wext	Wint	Am	Δp mull
1	6-2	3:52pm/3	F28/W10	23	108^{o}	x	x	x		x
2	6-5	2:35pm/4	F28/NE3	23	290^{o}	x	x	x		x
3	6-6	2:52pm/6	F28/N10	18	270^{o}	x	x	x	x	
4	6-7	5:43pm/3	F28/N4	15	281^{o}	x	x	x	x	
5	6-15	2:45pm/6	F21/NE1	12	324^{o}	x	x	x	x	
6	6-16	3:50pm/8	F21/W11	15	98^{o}	x	x	x	x	
7	6-19	3:58pm/4	F21/NW19	12	72^{o}	x	x	x	x	
8	7-16	12:30pm/5	F21/N3		194^{o}	x	x	x		
9	7-16	8:09pm/6	F21/N3	15	108^{o}	x	x	x		
10	8-2	2:55pm/3	F21/N3			x	x	x		
11	8-3	2:29pm/4	F21/NE1			x	x	x		
12	8-18	4:05pm/4	F21/N3,NE1	23	280^{o}	x	x	x		
13	8-19	1:42pm/5	F9/N4,NE1,NW12	30	270^{o}	x				
14	8-20	2:13pm/8	F9/N10,N4,NE1	15	270^{o}	x	x	x		
15	9-10	1:38pm/5	F9/W10,N4,NE1	30	160^{o}	x	x	x		
16	9-17	5:42pm/3	F21/NE1,N3,W10	18	160^{o}	x				
17	9-21	6:20pm/8	F28/W10,N4,NE4	23	160^{o}	x				
18	10-21	10:30pm/8	F9/N4,NW12,NW4	30	160^{o}	x	x	x	x	

signal-to-noise ratio and avoidance of clipping of the high amplitudes. The range selected in the first hour or so of a run, therefore, in some cases was inadequate for the strong gusts that occurred later in the recording period. To overcome this problem, an autoranging signal conditioner that automatically switched to a higher range when a preset threshold was crossed (accompanied by a switching pulse to indicate the change) was used. In a typical run the starting range and that at the end of the run were recorded. The switching transients in the data were then used to associate the correct scales with the recorded segments.

2.5 Experimental Results

Having defined the site and established the ground work for the data evaluation, it is now possible to present the results of the field study. In the sections that follow, the characteristic features of the localized pressure loads and their relationship to the overall structural geometry will be presented, the causality between the pressure loads and the window assemblies themselves will be determined. In making comparisons with expected behavior, reference will be made to the theoretical descriptions in Chapter 3. Two basic themes underlie the results that follow. The first is, of course, the problem of parametrically analyzing the pressure loads and defining critical combinations of independent variables that could give rise to extreme dynamic loads at a particular site. The second is the uniqueness of applying the particular evaluation methodology to the present problem. While most of the procedures have been previously developed in the area of information theory, their application to problems in mechanics

is quite new.

2.5(a) Parametric Analysis of Wind Loads

In Section 2.4(b) functional forms for the wind load characteristics, namely the reduced power spectral density, the mean, and the rms pressure coefficients, were hypothesized. The differential pressure measurements were conducted to examine the effects of changes in the independent variables. It can be anticipated that determination of the exact functional forms of Eqs. (2.4-16) and (2.4-17) by field tests on an actual structure is a practical impossibility. Rather, in the present case, data from sites preselected on the basis on wind tunnel tests and from the viewpoint of susceptibility to dynamic loads are analyzed. The objective is to assess the severity of dynamic loading and describe in a qualitative fashion the dependence of the load properties at these sites on the various profile and flow parameters.

Before proceeding with the analyses of the data certain preprocessing operations were required. The large volume of data (close to 300 hours, real time) necessitated selection of segments from the analog records where, for example, significant pressure fluctuations were observed. Error considerations in the estimation of the spectra required that the spectral analysis parameters be suitably chosen. In the following sections, the data sorting procedures used and design of the spectral analysis are described.

Data Sorting: The differential pressure and the response in a particular session were recorded over spans of up to 12 hours. During these intervals, periods of calm where the wind speeds are so low as to produce insignificant cladding loads were observed in the

recorded data, as expected, and unless the winds were due to a transient weather system, the periods of calm could be of long duration. Therefore, selection of particular segments of pressure and response signals of interest was required. This sorting process could, of course, have been obviated if the recorder were actuated when, for example, the reference wind velocity exceeded certain threshold. There are, however, several drawbacks to this mode of data acquisition that ruled it out for the present study:

1. The recorder takes time (approximately 10 secs.) to reach the correct recording speed, during which a significant part of the data may be lost.

2. The triggering process may introduce nonstationarity in the mean square value.

3. Due to the 3-dimensional nature of the flow around the building, the wind speed measured at the remotely located anemometer may not indicate the local activity.

Instead, weather forecasts were used to select periods and the recording equipment was operated continuously during that time. The data segments to be analyzed were selected on the basis of the wind speed records and visual inspection of the pressure data. Portions of the analog records with relatively large pressure fluctuations were isolated, and the corresponding wind speed and direction records were then inspected in order to choose those segments where $\overline{v}$ and θ showed a fairly constant mean value over a period of about 15 - 30 min. Records from a given session with $\overline{v}$ greater than 20 fps were analyzed.

In order to assess the dependence of the wind loads on the independent variables of Eqs. (2.4-16) and (2.4-17), the analyses were carried out in accordance with the following:

1. Variation of wind loading with height z. Corresponding window locations were chosen on each of the three floors, 9th, 21st, and 28th. For each of these locations, records corresponding to a constant wind direction $\bar{\theta} = \bar{\theta}_o \pm 10°$ were processed to obtain the PSD and histograms.

2. Dependence of the wind loading on the wind direction $\bar{\theta}$. The variables ϕ_z and z were kept constant by selecting pressure records, for a particular window on a given floor, corresponding to wind directions differing by at least 30°.

3. Variation of wind loading along the building profile. To assess this effect, the variables $\bar{\theta}$ and z had to be kept constant and the local pressure characteristics examined as ϕ_z was varied. Thus for a preselected wind direction (accurate to within 10°) the pressure spectra and histograms for a number of windows on a given floor were obtained. The variation of wind direction form the selected mean for each of these windows was less than 20° with the difference due to the data being recorded in different sessions.

In all, about 96 hours of usable data were processed. The grouping of the sorted data is summarized in Table 2.3.

Spectral Analysis: The formal mathematical basis for power spectrum estimation techniques can be found in the more general topic of estimation theory. However, estimation of power spectra with high stability and fidelity as it is currently practiced has a very

Table 2.3 Data Sorting on the Basis of Wind Direction

Window Location	$\bar{\theta}$	$\bar{v}$ fps	Record #	$\bar{\theta}$	$\bar{v}$ fps	Record #	$\bar{\theta}$	$\bar{v}$	Record #	$\bar{\theta}$	$\bar{v}$	Record #
F28 W10	160°	24	17				108°	24	1	72°	24	1
N4	160°	24	17	280°	15	4						
NE3	160°	24	17									
NE3				280°	24	2						
N10				280°	18	3						
NW4												
F21 W11	160°	18	16				81°	15	6			
N3	160°	18	16	280°	24	12	119°	21	8			
NE1	160°	18	16	280°	24	12	324°	12	5			
NW2												
NW19												
F9 W10	160°	30	15									
N4	160°	30	15	270°	30	13						
NE1	160°	30	15	270°	30	13						
NW4	160°	30	18									
NW12	160°	30	18	270°	30	13						

strong empirical basis. A general agreement on the best combination of analysis parameters is rare prior to data collection. After data acquisition, however, the analysis parameters can be properly chosen by pilot analyses.

Before conducting a pilot spectral analysis of the raw data certain preprocessing decisions must be made that involve:

1. Sampling considerations
2. Trend removal
3. Stationarity check

Sampling considerations require the maximum frequency, F_{max}, present in the data be known and subsequent digitization be in accordance with Shanon's sampling theorem. The maximum frequency in the pressure data was limited to 50 Hz by an analog low-pass filter with a roll-off rate of 48 dB/octave, to minimize aliasing errors; the actual frequency range of interest was about 40 Hz since it was sufficient to include the first few response modes.

A trend in the data is defined as any frequency component whose period is longer than the record length. This means that the lowest frequency in the data should be greater than the frequency resolution, Δf. A low frequency trend is illustrated by curve (a) of Fig. 2.5-1. The trend is generally removed using linear or polynomial regression, but for the present pressure data, considering the physics of the phenomena (significant energy at low frequencies), high-pass analog filtering with a cut-off frequency of approximately $2\Delta f$ was used instead. The advantages were threefold:

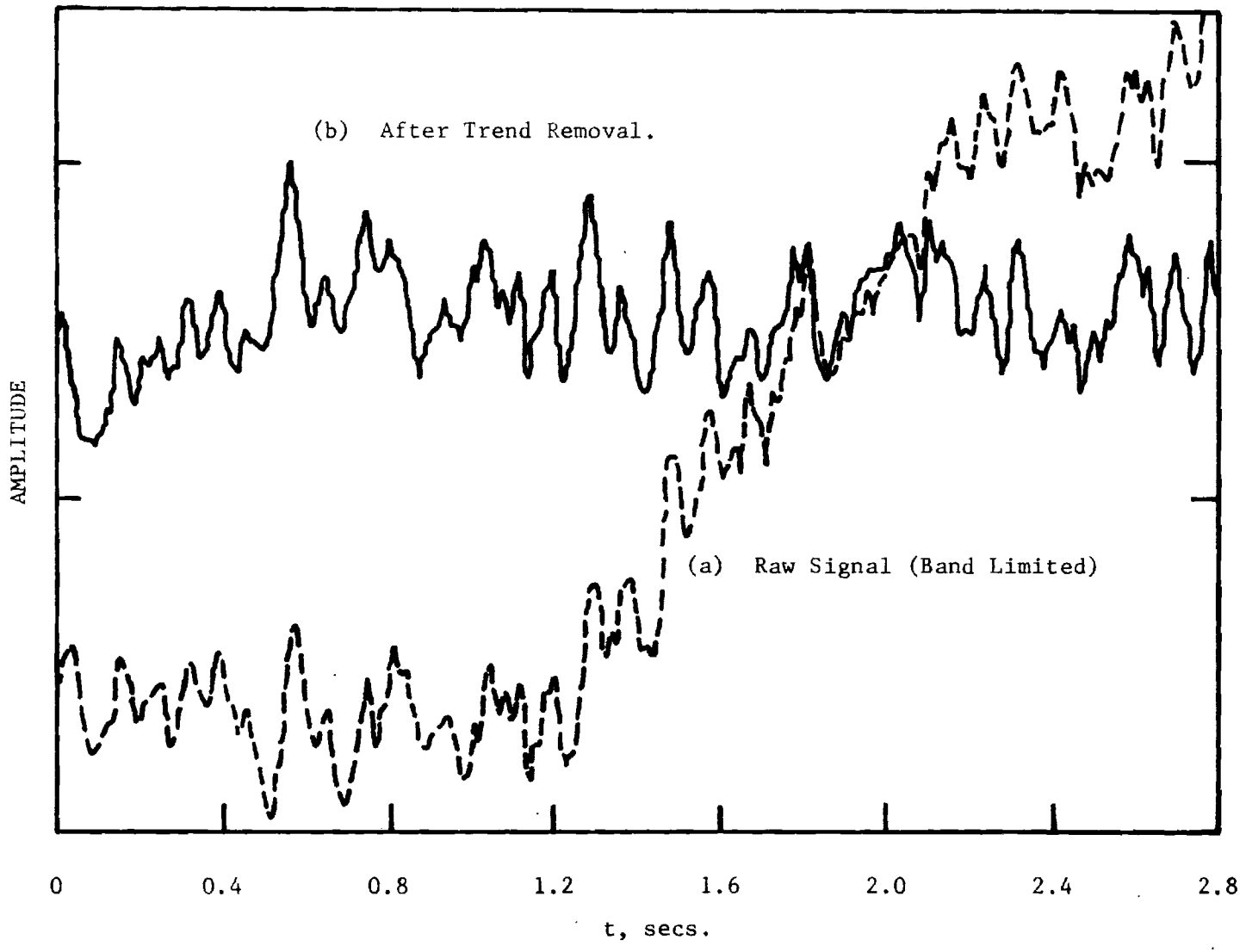

Figure 2.5-1. Trend Removal.

(a) Reduced quantization noise. To keep the quantization noise level low the signal must occupy as much of the input range of the A/D converter as possible (78). High-pass filtering eliminates the large low frequency excursions and permits higher A/D gain for digitization of the small fluctuations about the mean.

(b) Increased dynamic range. Dynamic range can be defined as the ratio of the highest and lowest spectral component that the processor can detect from the roundoff and quantization noise, and for the present processor is about 90 dB (double precision spectra, 32-bit word size). Since a high value of the dc component can often exceed this range, effectively drowning out small values at higher frequencies, high pass filtering thus provides increased dynamic range.

(c) Removal of the low frequency trend (curve (b) Fig. 2.5-1). Trend removal by high-pass filtering required that the pressure spectrum be analyzed in two parts: a high frequency and a low frequency band. The dividing frequency was chosen after analysis parameters had been finalized.

The wind pressures were not expected to be stationary over the entire recording period ($\sim$6 hours) due to diurnal changes and gust variations. However, stationarity over a short period (an hour or so) was checked for representative data in accordance with Ref. 60, and over these periods the data were found to be stationary.

Estimation of the power spectra from the stationary random data requires consideration of the following errors:

1. Frequency leakage
2. Bias errors in the estimate
3. Variance errors in the estimate

With reference to section 2.4, Eqs. (2.4-23) to (2.4-26), these can be minimized to acceptable levels by selection of:

(a) a suitable time window, w(t)

(b) frequency resolution, Δf, or block size, N

(c) number of ensemble averages, n_d

To a large extent, the choice depends on the nature of the data and reduces to a design problem. The single Hanning time window was chosen to reduce leakage for reasons outlined in section 2.4. Figure 2.5-2 illustrates the effect on the bias in the estimate of varying the block size, N, or equivalently, Δf. As N is increased the bias is reduced (the difference between spectra is diminished) at the expense of the variance.

The bias for N = 512 and 1024 shows no significant change, however, since the computation time for N = 1024 is substantially increased, N = 512 was chosen. The variance can be reduced by increasing the number, n_d, of disjoint records that are averaged:

$$\frac{\sigma}{\mu} = \frac{1}{\sqrt{n_d}}$$

The mean power spectrum can thus be estimated within 10% of its true value with 95% confidence (Gaussian distribution) if:

$$0.01 = \frac{1.96\sigma}{\mu} = \frac{1.96}{\sqrt{n_d}}$$

which yields $n_d \simeq 384$. The reduction in variance is apparent from Fig. 2.5-3 and is independent of N or Δf.

The analysis parameters for the high-band portion of the power spectrum can be summarized as follows:

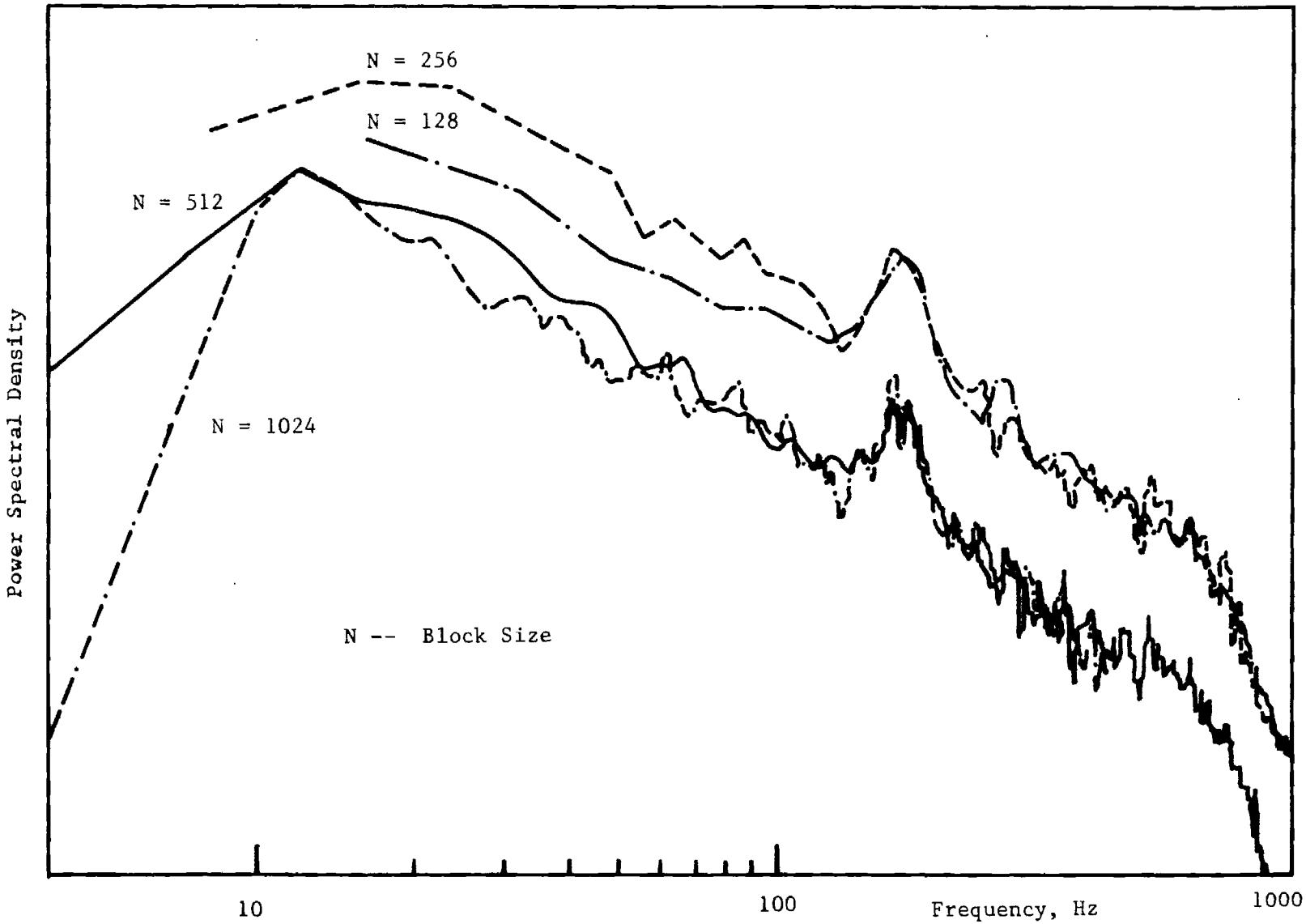

Figure 2.5-2. Effect of Block Size on Spectral Estimates.

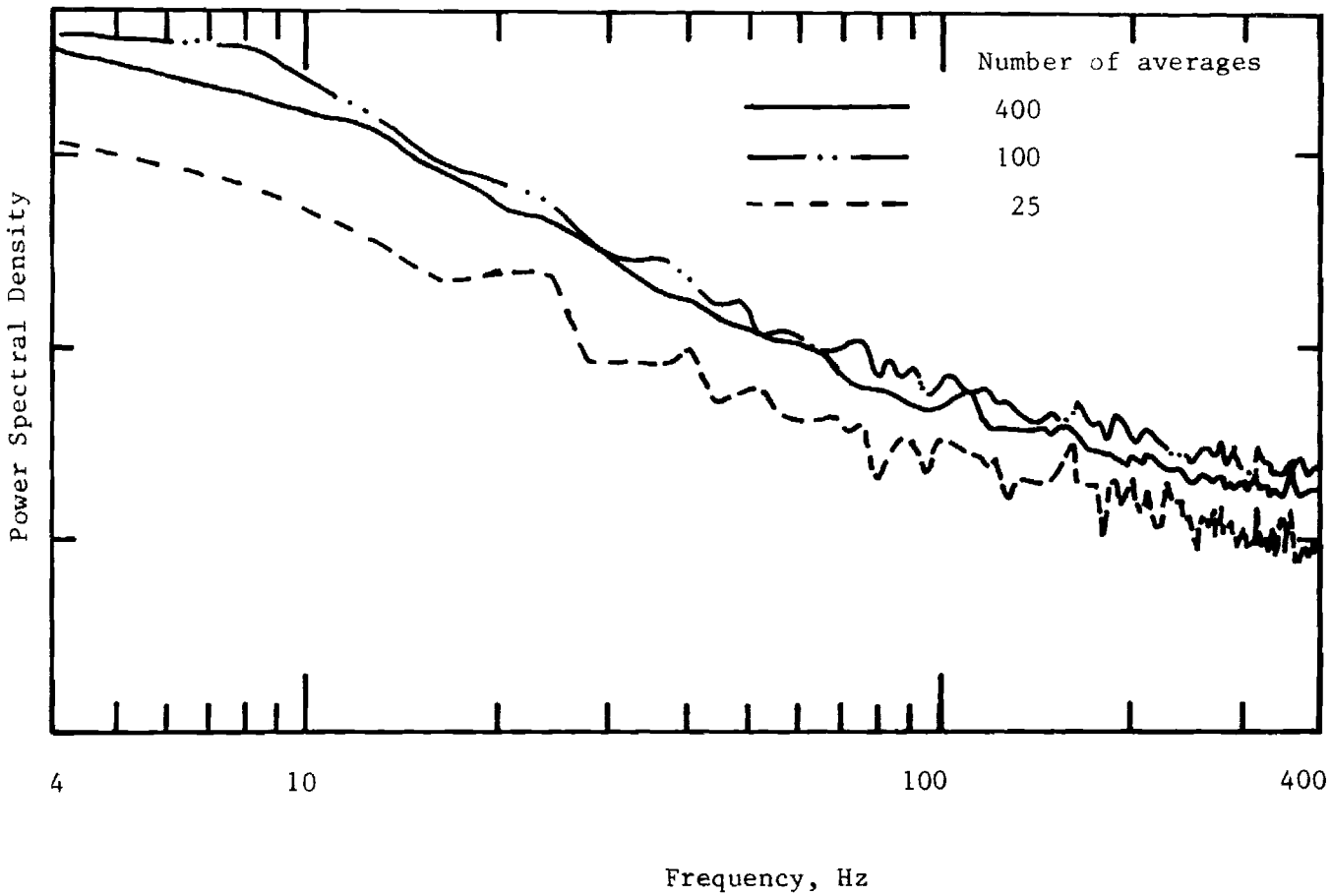

Figure 2.5-3 Effect of Averaging on Spectral Estimates.

1. Maximum Frequency = 50 Hz Block Size = 512

   Anti-Aliasing Filter = 3 Hz High Pass Filter - 0.025 Hz

   Number of Averages = 30

The lowest frequency that can be resolved above is about 0.75 Hz.

The parameters used for the low frequency part of the spectrum were:

2. Maximum frequency = 3.125 Hz High Pass Filter = 0.025 Hz

   Anti-Aliasing Filter = 3 Hz Number of Averages = 30

   Block size = 512

The lowest frequency that could be resolved was 0.025 Hz, corresponding to a period of 40 secs., which is sufficient to include short duration gusts.

Discussion of Results: In order to describe the wind pressure loading as a random process, the data were processed in accordance with the above specifications to obtain the following descriptors:

1. High frequency band power spectral densities (PSD) (0.8 - 40 Hz)
2. Low frequency band power spectral densities (PSD) (0.03 - 3 Hz)
3. Normalized pressure amplitude histograms

After sorting, the available data permit a qualitative assessment of the wind loading with respect to the following values of the independent variables:

1. Wind Direction, $\bar{\theta}$: 160°, 280° (±10°)
2. Height, z: 9th Floor (120 ft.)

   21st Floor (270 ft.)

   28th Floor (357.5 ft.)

   (Total height: 376.15 ft.)
3. Window Locations, ϕ: N4, W10, NE1

Wind Incidence, $\bar{\theta}$ = 160°: Figures 2.5-4a, b, and c show the spectra and normalized histograms for window N4 with the height, z, as a parameter and $\bar{\theta}$ = 160°. The respective floor planforms and wind incidence for the three floors are shown in Fig. 2.4-11.

The window N4 is on the windward side, and therefore the turbulence characteristics of the distant flow are expected to be preserved. If the flow is visualized as 2-dimensional, location N4 is expected to be downstream of the stagnation point and in the reattached region (flow separation at the corner). The pressure fluctuations, therefore, must be due to the wind turbulence and possibly due to roughening caused by the mullions. It appears reasonable to consider the pressure characteristics at N4 as reference, and examine with respect to these, the pressure fulctuations at aerodynamically more complex locations such as W10 and NE1. It is recognized, however, that in reality the flow is 3-dimensional and pressure characteristics at the higher floors may be considerably altered due to upflow.

Magnitudes of the pressure coefficients are seen from Fig. 2.5-4a to be considerably higher at z = 9 than at the upper floors. The positive pressure coefficients at the 9th floor and the mostly negative values at the 21st and 28th suggest the existence of an upflow. At the same time, discrete frequencies are seen in the low frequency band spectra as follows:

1.	28th	f_1 = 0.86 Hz	f_2 = 1.7 Hz
2.	21st	f_1 = 0.86 Hz	
3.	9th	None	

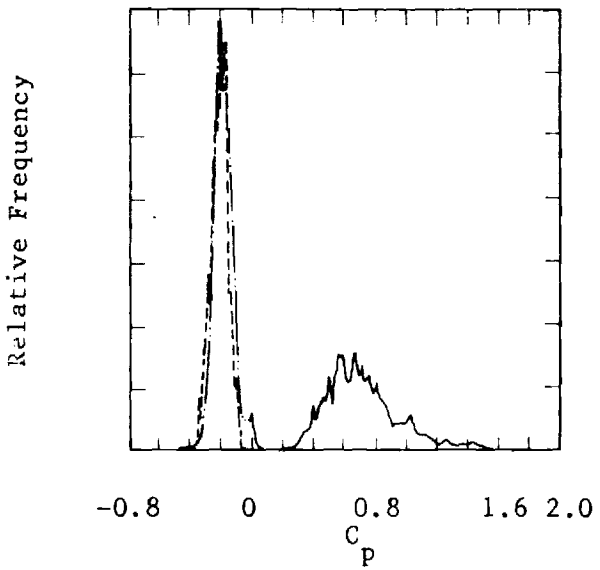

(a) Normalized Histogram

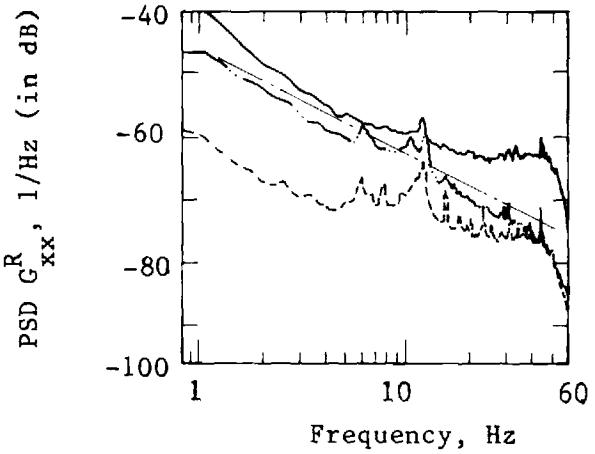

(b) High Frequency Band PSD

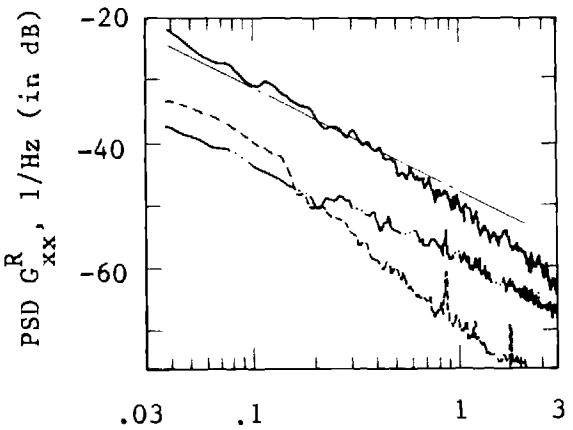

(c) Low Frequency Band PSD

Notes:

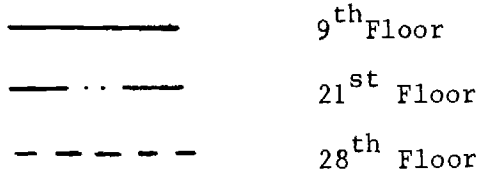

PSD in dB Relative to 1 1/Hz
e.g. -20 dB = 10^{-2}

Figure 2.5-4. Spectra and Normalized Histograms, Window N4, $\bar{\theta} = 160^{\circ}$

These frequencies could be due to vortex shedding from the reverse setbacks at the 19th and the 24th floors, Fig. 2.3-1. In the event that there is some upflow, the pressure fluctuations at z = 21 are affected by a single change in cross-section, whereas at z = 28 the flow has traversed two cross-sectional changes. The fact that f_1 = 0.86 Hz is seen in the PSD for the 21st as well as the 28th and that $f_2 = 2f_1$, serves to reinforce the observation that there is an upward flow component (not necessarily vertical) and periodicities are induced by the setbacks. That f_1 = 0.86 Hz is generated by the characteristic corner dimension, d_{19} = 14.42', and f_2 = 1.7 Hz is generated by the characteristic corner dimension, d_{24} = 7.32', is evident from the Strouhal number, $S = \frac{fd}{\bar{v}} = 0.48$ in both cases. (The Reynolds number based on the corner dimension is of the order of 10^6.

The high frequency band PSD, Fig. 2.5-4b, reveal that the mean square value of the pressure fluctuations decreases with increasing height. The PSD levels in dB are with respect to G^R_{xx} = 1 sec as defined in section 2.4. The histograms in Fig. 2.5-4a show, however, that the variance at the 28th and the 21st floors is approximately the same. This is because of the increased energy (higher PSD level) at the 28th floor for low frequencies. In Fog. 2.5-4b, a discrete frequency component is seen at approximately 12 Hz in all three spectra. The value corresponds to the fundamental frequency of the glass plates and appears in the spectrum due to feedback to the wind support. Association of this frequency with the flow characteristics, therefore, seems tenuous at best, but its appearance does point out the unusual sensitivity of the evaluation method. The narrow-band noise around

6 Hz for z = 21 and 28 could be due to the external architectural features such as the protruding mullions affecting the flow. At z = 9, this component has lost prominence due to higher energy levels. The flattening of the 9th and 28th floor PSD's beyond about 20 Hz (Fig. 2.5-4b) is unusual as regards turbulence spectra, but was also observed in a number of other instances. The most plausible reason is that in these particular runs the combination of transducer range and tape recorder gain served to restrict the dynamic range and thus suppress the low amplitude, high frequency pressure fluctuations into the noise floor. The effect of the anti-aliasing filter is clearly seen as the sharp roll-off beyond 50 Hz.

Figures 2.5-5a, b, and c show the results for the aerodynamically more complex case of window W10 with $\bar{\theta}$ = 160°. The location is downstream of a varying number of corners depending on the height being considered.

The magnitudes of the pressure coefficients are smaller than for N4 at z = 9. The pressure coefficients at z = 9 and z = 28 are predominantly negative, whereas at z = 21 they are distributed such that $\overline{C}_p \simeq 0$ (actually $\overline{C}_p = 0.008$). One explanation for this behavior is the roughening effect provided by the corners. The large corner dimensions and the small number of corner at z = 9 may not dramatically affect the flow at location W10. Hence, the pressure coefficients at W10 are expected to be the same as they would be for flow around a right corner, thus accounting for negative C_p's. However, negative C_p's are also predominant at z = 28. In this case the much smaller corner dimensions and the large number of corners tend to smooth out

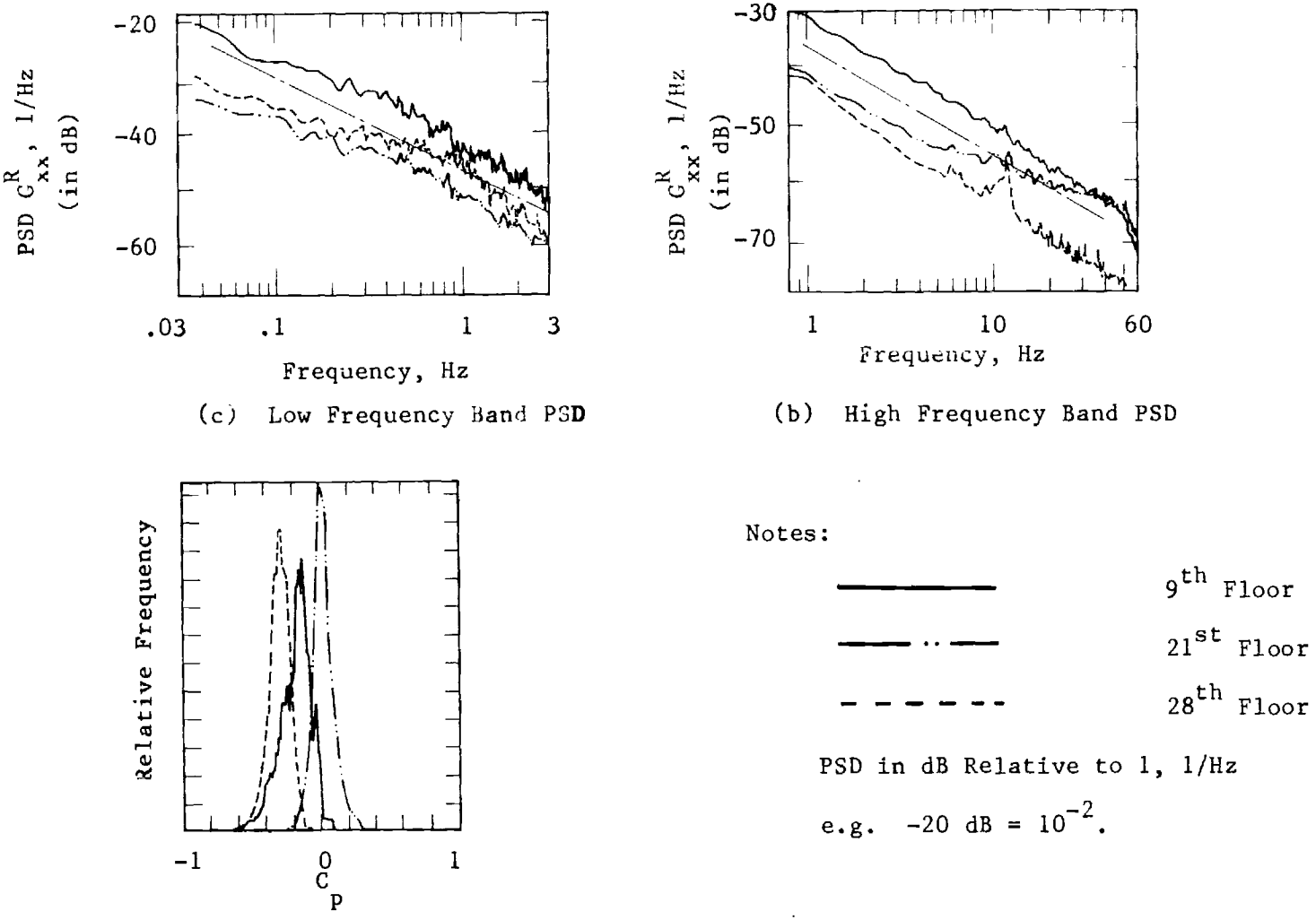

Figure 2.5-5 Spectra and Normalized Histograms, Window W10, $\bar{\theta} = 160^{\circ}$

along the diagonal from face N to face W. Therefore, W1o again happens to be around a corner with respect to the flow, although the corner is not as sharp as at z = 9, and negative C_p's can be expected. At the 21st floor, on the other hand, the corners may be expected to roughen up and thus randomize the flow. This results in negative and positive C_p's occurring equally often. Considering the roughening effect in terms of the ratios $r = \frac{d_1}{d_2}$ (See Fig. 2.4-11 for notation.) it is seen that $r_9 = 0.34$ and $r_{28} = 0.085$ provide the extremes, whereas $r_{21} = 0.17$ tends to alleviate the pressure loads.

The high frequency band spectra are somewhat different from those at N4. The energy levels of the spectra at z = 9 and z = 28 are considerably higher for W10 (of the order of 10dB or by a factor of 3 on the rms values of the pressure) than on N4. However, the spectra for W10 at z = 9 and 28 roll off much faster with frequency. The high frequency flattening in the PSD for z = 9 and 28 is again attributed to the energy levels being in the noise floor for those recording sessions. The trends in PSD levels, however, are similar in that the levels decrease with height. At W10 for z = 21, the PSD levels, Fig. 2.5-5b, are almost the same as in Fig. 2.5-4b for z = 21, although the slopes differ somewhat. These observations suggest that higher levels of PSD, i.e., higher energies in a frequency band, occur in regions of negative pressure insofar as z = 9 and z = 28 are concerned. On the other hand, the small changes in energy levels at z = 21 could be due to flow randomization. The observation that the energy levels decrease with height in the two cases considered, suggest that the lower building regions are affected by the terrain features so as to increase the

band-width of the wind loads. The peaks in the spectra around 12 Hz may again be fictitious as pointed out before. The low frequency band spectra, Fig. 2.5-5c, except for minor differences in levels are similar.

Window NE1 is located at a reentrant corner with respect to the flow direction being considered. The results for this case are shown in Figs. 2.5-6a, b, and c. Referring to (a), it is seen that the pressure coefficients for z = 9 and 21 are predominantly negative, whereas at z = 28 they are more evenly distributed. Table 2.5-2 shows the different C_p values and the factor g from Eq. (2.2-3) for the various window locations considered. The aerodynamic effects are more complex at this location that the previous cases, as is evidenced by the shape of the histograms. Even after taking into account variance in the pdf estimates, the histograms at z = 21 and 28 appear to have periodic components as manifest by the presence of dual peaks. A cross-check with the respective spectra does not reveal any discrete frequency component of comparable amplitude.

The high frequency band spectra are now reversed in energy levels, in that the overall energy levels, and hence the mean square values, increase with height. This suggests that in a region of separation, such as can be expected at NE1, the rms values of the pressure fluctuations increase with height. For z = 21, the PSD contains a discrete frequency peak at 30 Hz and it is suspected that rotating machinery in the building (such as 1800 rpm motors used in the air handling unit) may have caused it to appear in the signal.

The low frequency band spectra of Fig. 2.5-6c show level variations similar to the high frequency band; however, the PSD for the 9th floor

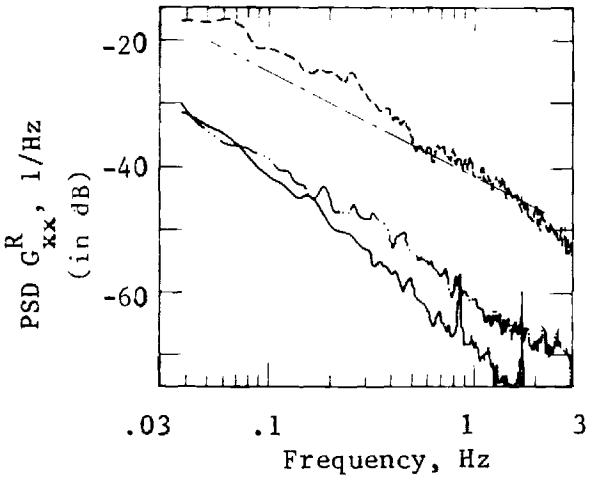

(c) Low Frequency Band PSD

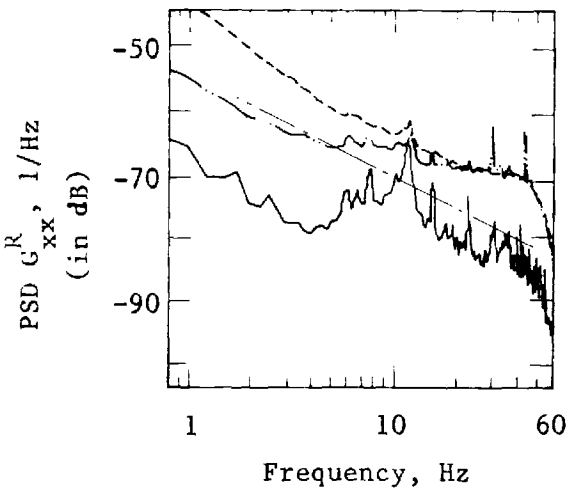

(b) High Frequency Band PSD

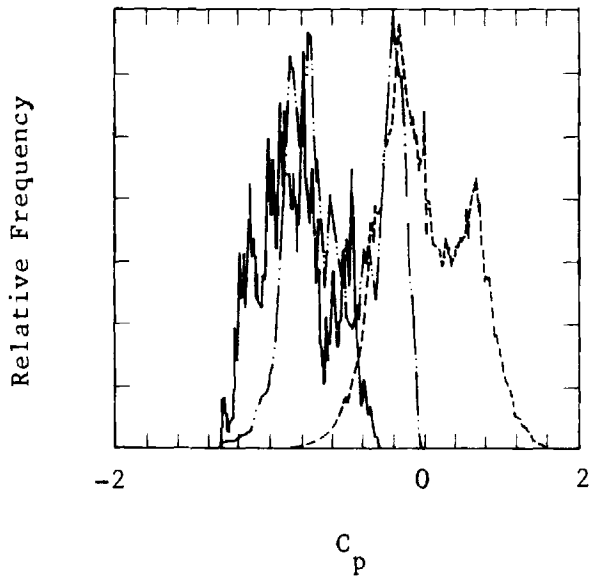

(a) Normalized Histograms

Notes:

——— 9th Floor

— · · — 21st Floor

– – – – 28th Floor

PSD in dB Relative to 1, 1/Hz

e.g. -20 dB = 10^{-2}.

Figure 2.5-6. Spectra and Normalized Histograms, Window NE1, $\bar{\theta} = 160^{\circ}$

Table 2.5-2 Pressure Coefficients and Gust Factors for $\bar{\theta} = 160^{o}$

Floor	Window	$\bar{C}_p$	$C_{p_{rms}}$	C'_p	$C_{p_{max}}$	$g = \frac{C_{p_{max}}}{C'_p/\bar{C}_p}$
28	W10	-.307	.313	.061	-.7	3.52
	N4	-.203	.210	.054	-.38	1.43
	NE4*	+.014	.277	+.277	+.86	.043
21	W11	+.008	.075	.075	+.384	.041
	N3	-.197	.206	.06	-0.53	1.73
	NE1	-.55	.622	.29	-1.36	2.6
9	W10	-.398	.524	.339	-2.64	3.08
	N4	+.46	.472	.106	.84	3.66
	NE1	-.591	.764	.234	-1.77	4.47
	NW12	.539	.753	.526	+2.80**	2.87

*NE4 presents the same profile to the flow as NE1 except for an additional upstream corner.

**Positive C_p greater than +1 since the local velocities may be considerably different from the reference velocity.

reveals the discrete frequencies, 0.86 Hz and 1.7 Hz. The flow effects in this region are extremely complex, and although the characteristic frequencies could have been produced by a downwash, such a description is at best crude conjecture at this time.

Wind Incidence, $\bar{\theta}$ = 280°: Figures 2.5-7a, b, and c show the PSD's and histograms for window NE1 at z = 9 and 21. At z = 9 the windward location of NE1 together with the larger corner dimension results in a C_p histogram which is almost entirely on the positive side.*

The high frequency band spectra, Fig. 2.5-7b, show that the mean square value of the pressure fluctuations is larger at z = 21 that at z = 9. On the other hand, in the low frequency band, (c), the PSD levels at frequencies below 0.5 Hz are greater at z = 9. Considering the negative C_p's at z = 21 and differences in PSD levels, it appears that an upflow component may exist and that the building facade features tend to produce increased higher frequency loading.

Window N4 is downstream of NE1 with respect to the flow and the wind direction is almost parallel to the wall on which the pressure tap is located. From Fig. 2.5-8a the randomization effect of the corners at the 21st floor is apparent in that at a z = 9, the C_p's are mostly positive and at z = 28 large negative C_p excursions occur, whereas at z = 21 the distribution is almost symmetric with respect to a zero mean.

The high frequency band spectra, Fig. 2.5-8b, have almost the same slope and closely follow the $f^{-5/3}$ Kilmogorov inertial subrange spectrum. The PSD level at N4 is reduced from that seen at NE1 for z = 21 whereas for z = 9 it is almost the same. The periodicity at 12 Hz is again asso-

*The erroneous values $C_p > +1.0$ result because of differences in the local speeds and the remote reference velocity of the wind used for normalization.

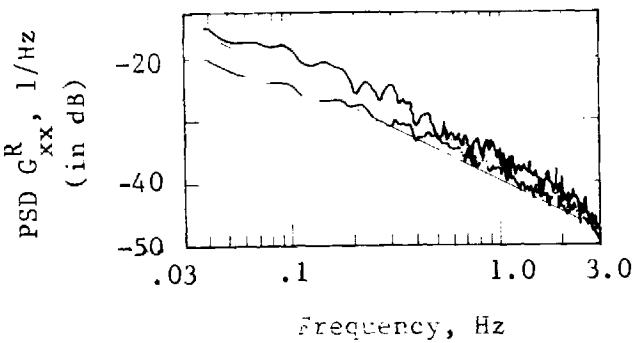

(c) Low Frequency Band PSD

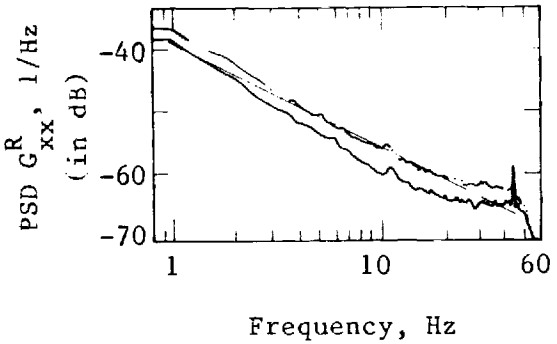

(b) High Frequency Band PSD

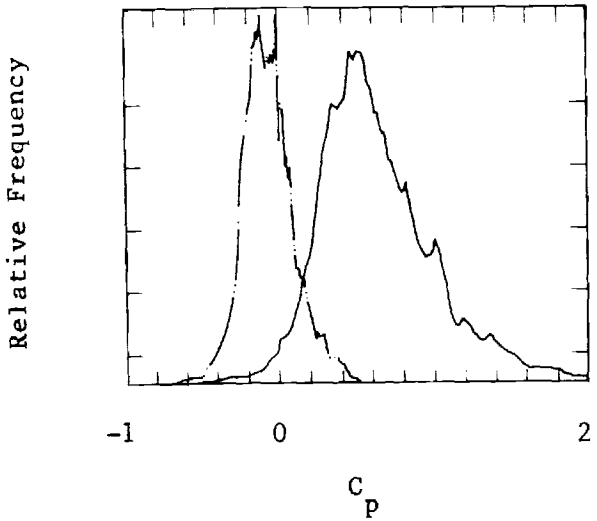

(a) Normalized Histogram

Notes:

——— 9^{th} Floor

——·· ——— 21^{st} Floor

– – – – – 28^{th} Floor

PSD in dB Relative to 1, 1/Hz

e.g. -20 dB = 10^{-2}.

Figure 2.5-7 Spectra and Normalized Histograms, Window NE1, $\bar{\theta} = 280^{o}$

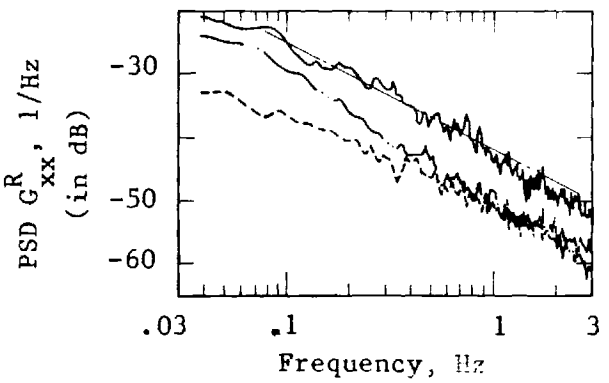

(c) Low Frequency Band PSD

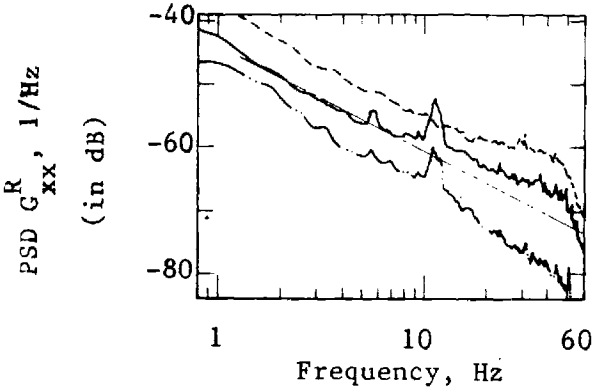

(b) High Frequency Band PSD

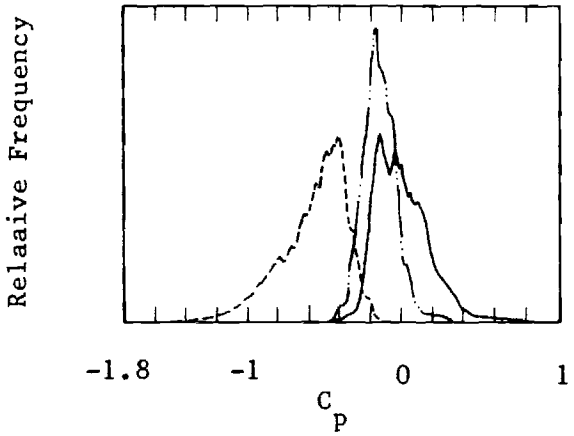

(a) Normalized Histogram

Notes:

——— 9th Floor

——·——·—— 21st Floor

– – – – – 28th Floor

PSD in dB Relative to 1, 1/Hz

e.g. -20 dB = 10^{-2}.

Figure 2.5-8 Spectra and Normalized Histograms, Window N4, $\bar{\theta} = 280^{o}$

ciated with the window response, although the amplitude of this component is higher than those observed in other cases. Discrete flow effects such as peaks are not seen in the low frequency band spectra of Fig. 2.5-8c, although the relative levels are the same as in (b).

In concluding this section, some significant observations about the general character of the pressure spectra are made and the identified features of the cladding loads are summarized. With regard to dynamic cladding loads, the overall PSD levels or the mean square value of the loading are of concern.

Higher spectral levels are seen to occur on faces where the pressure coefficients are predominantly negative. In other words the highest spectral levels can be expected when the bulk of the samples in a pressure histogram lie on the negative C_p side and the magnitude of the negative mean C_p is largest. The variance of the normalized histogram (pdf) and the area under a power spectrum are both equal to the mean square value of the random process (Parseval's theorem). This implies that the higher variance should be associated with the histogram having the larger magnitude of the negative mean pressure coefficient $\overline{C}_p$. That this is indeed the case is manifested by the longer negative tails in the histograms as $\overline{C}_p$ tends to be more negative.

The PSD levels on the windward side increase as the building ground level is approached, which is consistent with the assumption that gusts due to the effects of the surrounding terrain are largely responsible for the increase. The additional observation that in regions of separation, i.e., where the wind effects are not direct, the spectral levels increase with height, serves to reinforce the speculation of the effects of surrounding terrain.

Discrete flow effects such as vortex shedding, narrow band pressure fluctuations (bandwidth approximately 1 Hz), and spikes in the high frequency band spectra, are seen only for some particular combination of ϕ, θ, and z. Exterior architectural features, such as mullions, are suspected to be the prime contributors to spectrum levels by way of narrow band fluctuations in the flow. Existence of an upflow and consequent vortex shedding at the reverse setbacks is responsible for the low frequency spectral lines corresponding to a Strouhal number of 0.48.

The multiple corners in the building planforms appear to act as roughness elements on the building profile. The relatively small number of large dimension corners, described by the nondimensional coefficient value r - 0.34, essentially act as bluff extensions of the building floor plan and are largely unaffected by the other corners. On the other hand, for a relatively large number of smaller dimension corners, described by r = 0.85, the roughening is considerably less. A side with such corners acts essentially as a flat wall, the corners at the ends of which are nearly unaffected by the intermediate corners. A building profile roughness described by r = 0.17, however, serves to randomize the flow effects, resulting in diminished mean and rms values of the pressure fluctuations (small mean and variance in the pdf, and low PSD levels). A preliminary indication, therefore, is that a roughness ratio in the vicinity of r = 0.2 could have an alleviating effect on the cladding loads.

A feature of the low frequency band spectra that deserves mention is that the spectra do not level off or show a peak at the extremely low

frequencies. This behavior is expected because of the finite energy in the pressure signal. The absence of a peak or limiting behavior could be due to the restricted bandwidth of the spectra. At these low frequencies the external wind pressures are no longer distinct from the internal building pressure variations due to normal building operations. The period of the internal pressure fluctuations could be considerably longer, perhaps extending over an entire day. Periods longer than about 30 secs. are not encompassed by the low frequency band spectra. Several attempts were made to explore this point by analyzing the data with ultra-low F_{max} and Δf but were unsuccessful because of the inability to adequately reduce the variance by processing enough sample records over the 1 - 2 hours during which stationarity could be assumed. Also, attempts to measure an absolute internal pressure and compute the resulting PSD with sufficient accuracy and fidelity proved beyond the present transducer limits.

An inspection of the histograms for pressure taps located on a flat face with the flow nearly parallel to the face, shows that the distribution of the instantaneous C_p's moves to the negative side as the height increases. This is not a surprising result, but only an instance substantiating two of the conclusions drawn earlier. Specifically, it was seen that the spectral levels increase with height in regions of separation, and that higher spectral levels are associated with predominantly negative pressure coefficient histograms, i.e., where the bulk of the samples in a pressure histogram lie on the negative C_p side. The above observation, therefore, provides increased confidence in the consistency of the data.

The overall levels of the spectra in the Reynolds number range of $1 - 5 \times 10^6$ are in general quite small and would require considerable dynamic amplification by structural vibration to approach static load levels. For this type of geometry at least, this must be taken as a negative conclusion to the original conjecture that significant wind pressure excitation power could be found at frequencies of concern for local structural dynamics. Finally, the slopes of the spectra differ only slightly from the Kolmogorov spectrum, although for energy levels they tend to be flatter.

2.5(b) Window Response Causality

The sailient features of the localized wind pressure loads, particularly the dynamic aspects, were identified from experimental data in the previous section. It is strikingly apparent from those results that there is an extremely small amount of power in the pressure loading over those frequencies of concern for localized structural dynamic response. However, the present field study, while of a somewhat general nature owing to the variable geometry of the building, cannot be considered as completely representative case insofar as wind loads are concerned. Consequently, it is still essential to identify the window response levels associated with the wind loads, and equally important to ascertain over what frequencies these take place. For example, it is reasonable to expect the static or zero frequency response to depend on factors other than wind (e.g., stack effect, thermal loading, etc.). At the ultra-low frequencies (periods down to about 10 sec.) it is likely that the response is due largely to wind effects, while at frequencies above this point the causality is not clear and is the subject of the present study.

The identification of causality can be accomplished by means of the coherence function, the derivation of which has been previously discussed. In the present applications the coherence function as estimated from the measured wind load and response data serves to establish the causality of the wind loads for the response. In a practical measurement situation the measurement noise also affects the coherence function and can lead to erroneous, low values. These considerations and the evaluation of the coherence function are discussed in the following section in light of the experimental results.

The present implementation of the coherence function is based on the single input/single output problem of Fig. 2.5-9. The true source, or input, of the system is u(t), assumed to be stationary, and the output is v(t). Extraneous noise at the input and output measurement points is represented by n(t) and m(t), respectively, and is assumed to be incoherent with u(t) and v(t). The quantities x(t) and y(t) are the measurement signals and correspond to the wind pressure and window displacement, respectively. Note that $x(t) = u(t) + n(t)$ and $y(t) = v(t) + m(t)$.

Assuming that m and n are uncorrelated* with x and y, it follows:

$$G_{xx}(f) = G_{uu}(f) + G_{nn}(f)$$

$$G_{yy}(f) = G_{vv}(f) + G_{mm}(f)$$

$$G_{xy}(f) = G_{uv}(f)$$

Then using Eq. 2.4-11 for the present case:

$$G_{vv}(f) = |H(f)|^2 G_{uu}(f)$$

$$G_{uv}(f) = H(f) G_{uu}(f)$$

---

*For the effect of correlated noise on the coherence function, See Ref. 51.

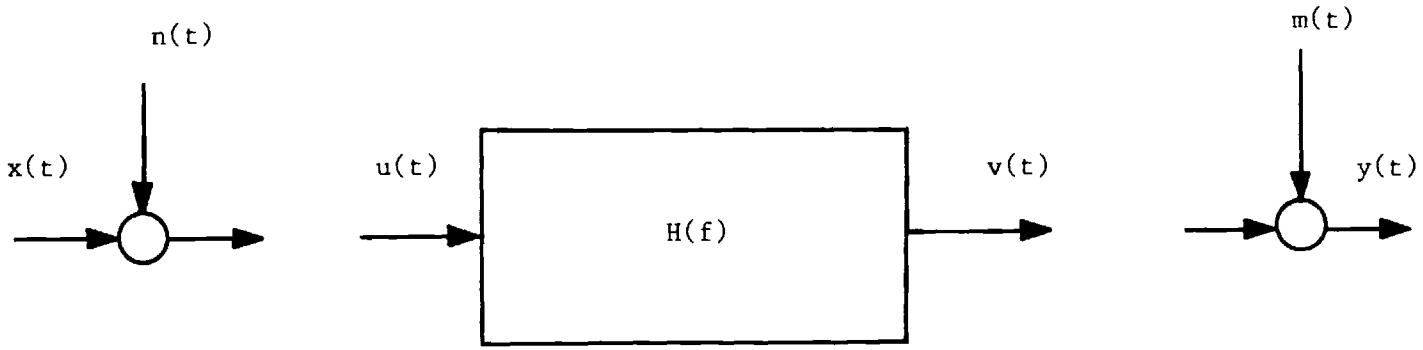

Figure 2.5-9 Ordinary Coherence Function Measurement Model

The true system coherence function $\gamma^2_{uv}(f)$ is defined as:

$$\gamma^2_{uv}(f) = \frac{|G_{uv}(f)|^2}{G_{uu}(f)G_{vv}(f)}$$

and for a CPLS system is identically equal to one for all frequencies. The true coherence is related to the measured coherence function, $\gamma^2_{xy}(f)$, as follows:

$$\gamma^2_{uv}(f) = \frac{|G_{xy}(f)|^2}{G_{xx}(f)G_{yy}(f)}$$

$$= \frac{|G_{uv}(f)|^2}{[G_{uu}(f) + G_{nn}(f)][G_{vv}(f) + G_{mm}(f)}$$

$$= \frac{\gamma^2_{uv}(f)}{[1 + \frac{G_{nn}(f)}{G_{uu}(f)}][1 + \frac{G_{mm}(f)}{G_{vv}(f)}]}$$

Thus, the measured value of the coherence function is diminished from the true value by terms involving the measurement signal-to-noise ratios. Clearly $0 \leq \gamma^2_{xy}(f) \leq 1$. In the absence of any system nonlinearities the ratio $\gamma_{xy}/1-\gamma_{xy}$ can be interpreted as the signal-to-noise ratio at the output. Alternatively, for a noise-free system $\gamma_{xy}/1-\gamma_{xy}$ can be interpreted as the linear-to-nonlinear ratio. In practical measurement systems the various spectra are averaged over a sufficiently large number of samples to remove the uncorrelated noise terms.

In the present experimental study the coherence function was applied to the systems shown in Fig. 2.4-5(a) to determine the degree of linear dependence of the response on the measured differential pressures, Δp. Several preliminary remarks are in order before the computational procedure and the results are detailed.

1. From the physics of the phenomenon it is apparent that sustained vibration of the window system cannot be expected. Hence selected sample records need to be used to compute the coherence function.

2. The sample records should be such that the response signal-to-noise ratio is considerable, i.e., the response amplitude should be above the noise floor of the measurement and data acquisition system.

3. Such a selection can be accomplished by triggering the data input to the Fourier Analyzer using the pressure (or response) signal.

4. Sorting the data as in 3, it was found, restricts the number of sample records that can be extracted from an hour-long data record with stationary wind characteristics. Alternatively, therefore, visual inspection and sorting as described in Section 2.4(c) can be used.

5. For inputs which are not triggered in (This applies to the processing equipment used and other similar analyzers.) overlap processing of the data can be used to reduce the estimation errors in the coherence function(62). This estimation technique consists of applying the FFT operation to overlapped data segments. The result is a reduced variance at the expense of the number of FFT's to be performed, i.e., computational time. Overlap processing is readily implemented on the 5451B Fourier analyzer. The overlap fraction can be varied by the addition of a delay loop to the program.

The coherence function was computed from the measured data for the following cases:

1. Coherence between the differential pressure and the interanl glass plate displacement, i.e., $\gamma^2_{\Delta p, w_i}$

2. $\gamma^2_{\Delta p, w_e}$

3. $\gamma^2_{w_i, w_e}$

The first two of the above determine the fraction of the response power due to Δp. The function $\gamma^2_{w_i, w_e}$ is used to verify the existence of coupling between the two plates.

All of the previously-discussed computational procedures, namely, triggered (without Hanning), free run and overlap processing were utilized to obtain the best possible coherence function estimate for the various signal pairs. Differences in the coherence functions estimated by the four techniques (This includes triggering the input on response.) were insignificant and were attributed to inherent uncertainty in the estimation procedures. Overlap processing did smooth the coherence function to some extent although the difference was not substantial to warrant an increase in computation time.

The coherence functions shown in Figs. 2.5-10 thru 2.5-12 were computed from record segments selected according to the sorting procedures described earlier. The input was free run, the sample records were disjoint and weighted by a single Hanning function. The high frequency band (0.8 - 50 Hz) functions were computed from the respective spectra averaged over 400 disjoint segments. The low frequency band (0.03 - 3 Hz) functions utilized 30 disjoint records. The coherence functions of Figs. 32, 33, are representative of the response dependence on the differential pressure. The actual wind and structural variables shown are for reference purposes only.

Figs. 2.5-10a, b, and c show the coherence functions $\gamma^2_{\Delta p, w_e}$,

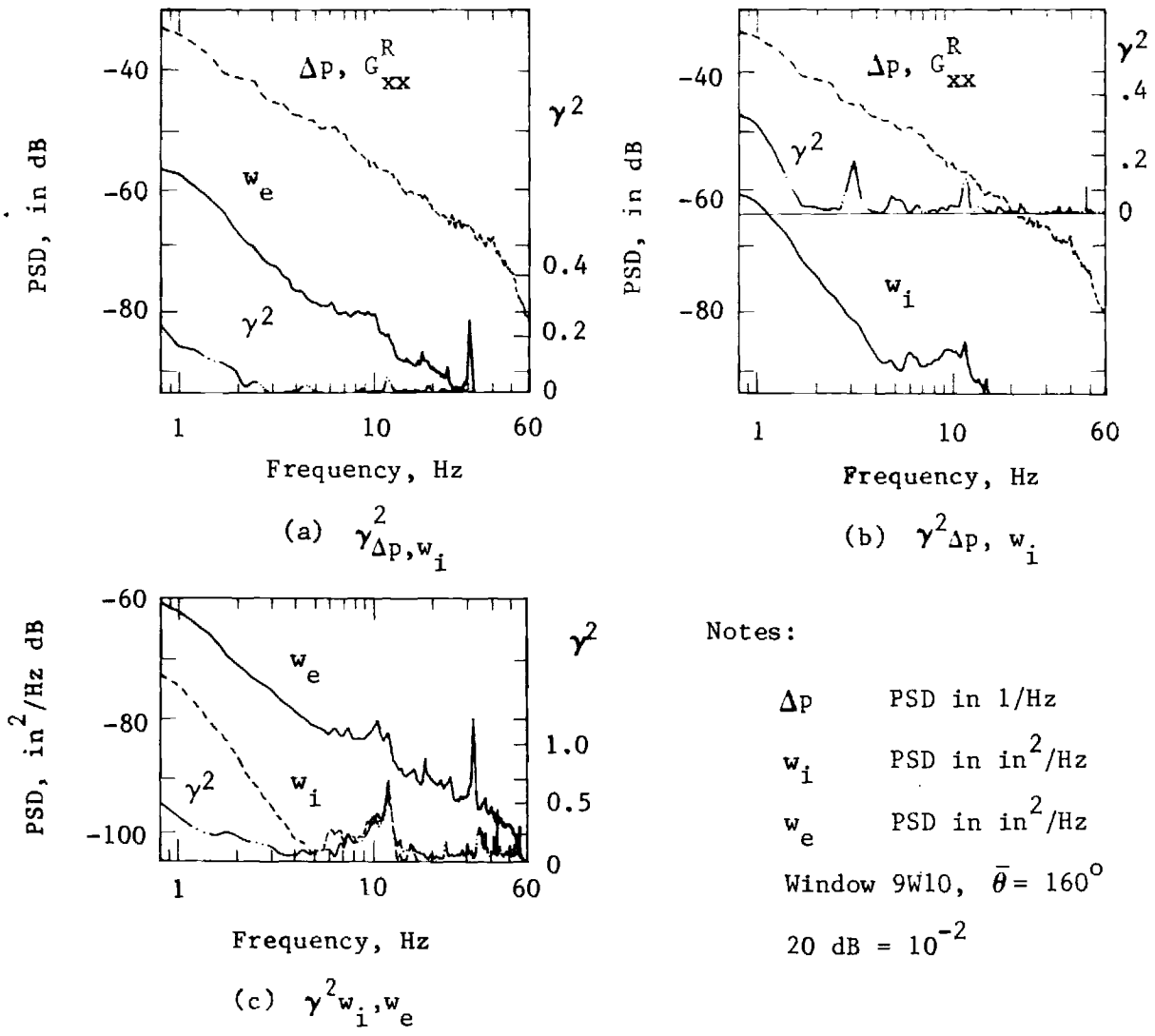

Figure 2.5-10 Measured Coherence Function, High Frequency Band

$\gamma^2_{\Delta p,w_i}$, and $\gamma^2_{w_e,w_i}$, respectively, together with the input and output spectra, for the high frequency band. Significant values of the coherence functions in Figs. 2.5-10a, b, are seen only below 1.7 Hz. The peak values in the two cases of $\gamma^2_{\Delta p,w_e} = 0.26$ and $\gamma^2_{\Delta p,w_i} = 0.35$ at 0.8 Hz differ due to the associated statistical uncertainty. At frequencies above 1.7 Hz there appears to be no causality between the differential pressure and the response. The values of the coherence function between 0.8 - 1.7 Hz are too small compared to 1.0 and majority of the response power is due to sources other than wind loads. Examination of Fig. 2.5-10c reveals similar behavior in $\gamma^2(f)$ up to 3 Hz. From the spectra it can be seen that the root-mean-square value of w_e is higher (at all frequencies) than of w_i. The difference in rms values in the vicinity of 1 Hz is about 6 dB corresponding to a ratio $\frac{w_e}{w_i} = 4$. This difference can be attributed to the compliance of the entrapped air. A high value of the coherence function $\gamma^2 = 0.7$ indicating extremely good causality is seen at 11.5 Hz which is close to the natural frequency for inphase motion of the two plates in the (1,1) mode calculated from the model (Chapter 3). However, Figs. 2.5-10a and b do not show any pressure-to-response causality at this frequency. This implies that the vibratory motion of the window is due to sources other than the wind loading. The internal glass plate response rolls off much faster than the external plate response at frequencies above 1 Hz. A strong peak in w_e is seen at 31 Hz and compares with the calculated (3,1) inphase motion frequency. A corresponding peak in w_i is not so obvious. The coherence function at this frequency is of the order of 0.26. An explanation for the discrepancy at 31 Hz is that the

peak is fictitious and not due to glass plate motion. The frequency could have been introduced in the signal due to floor virations arising from rotating machinery used in building services (generally 1800 rpm motors). The LDM being more sensitive to floor vibrations, the frequency shows up prominently in w_e. The erroneous coherence function value is typical of the false coherence case described in Ref. 31.

Figures 2.5-11a, b, and c show the coherence functions in the low frequency band (0.03 - 3 Hz) corresponding to the data used in Fig. 2.5-10. This low frequency loading can be assumed to be quasi-static. Excellent causality between pressure and response is seen up to 0.6 Hz from Figs. 2.5-11a and b. This leads to the conclusion that the "static" response of the window systems is largely due to pressure loads. It is noted here that since only the differential pressure was measured and the internal pressure contributes to the quasi-static differential, a distinction as to the source of the pressure loads cannot be made from the data collected, in this low frequency range.

The roll-off of w_e and w_i spectra, as seen from Fig. 2.5-11c is almost identical up to 1 Hz and the difference in spectrum levels at 1 Hz is approximately 12 dB corresponding to a ratio $\frac{w_e}{w_i} \simeq 4$.

Figure 2.5-12 shows the high frequency band spectra and coherence functions for a case which differed markedly from the representative response spectra and coherence function. The difference is seen in the frequency band extending from 6 - 16 Hz, where the coherence function is very close to 0.5. Considering the statistical variation in the estimates this is within the 95% confidence limits of true $\gamma^2 = 0.5$.

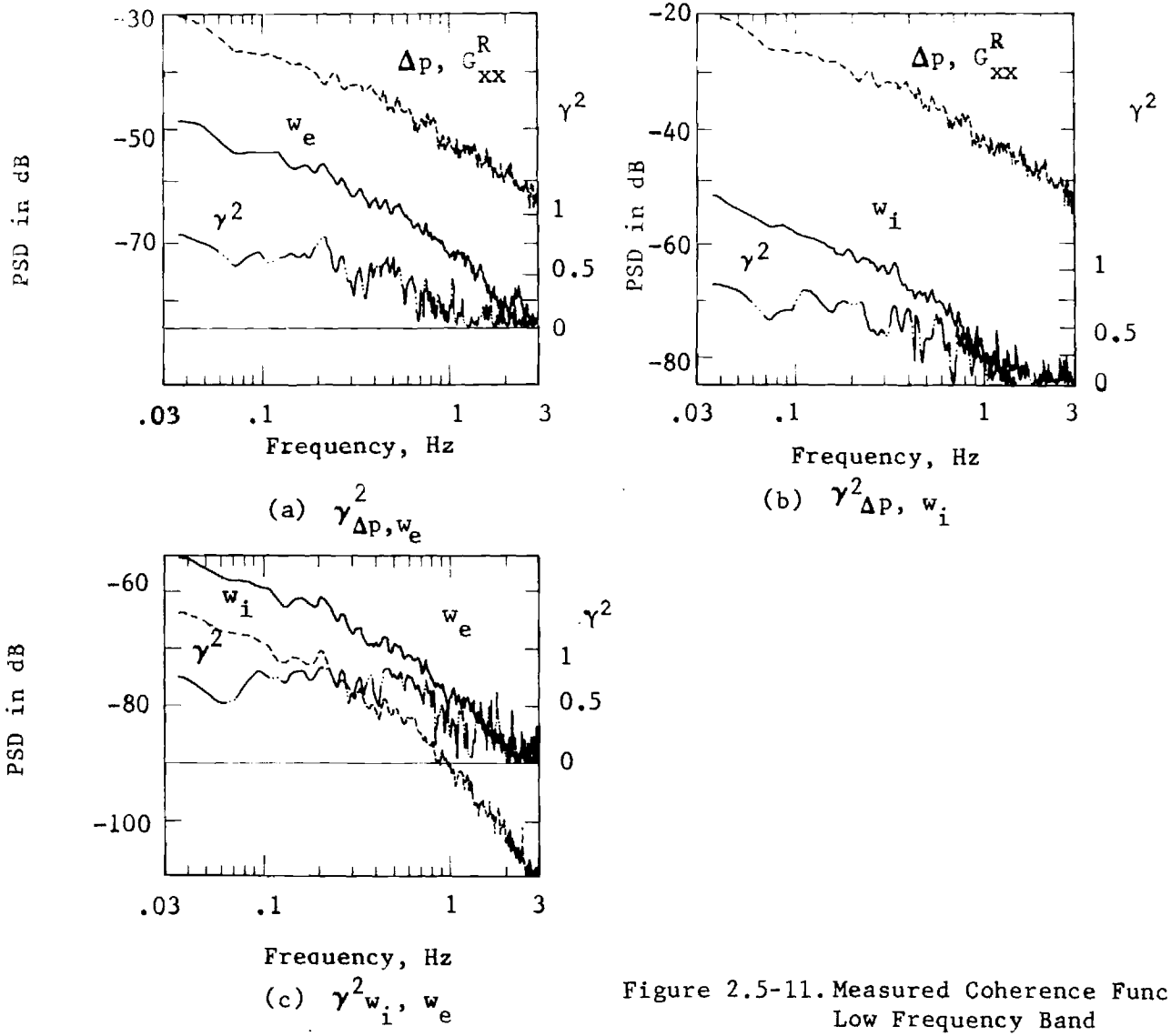

Figure 2.5-11. Measured Coherence Function, Low Frequency Band

Notes:

Δp PSD in 1/Hz

w_i PSD in in^2/Hz

w_e PSD in in^2/Hz

Window 9N4, $\bar{\theta} = 160^\circ$

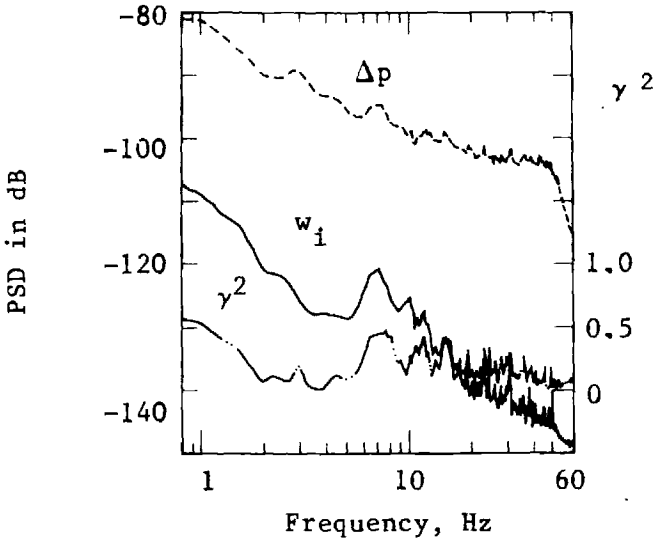

(a) Input Δp, Response w_i, $\gamma^2 \Delta p$, w_i

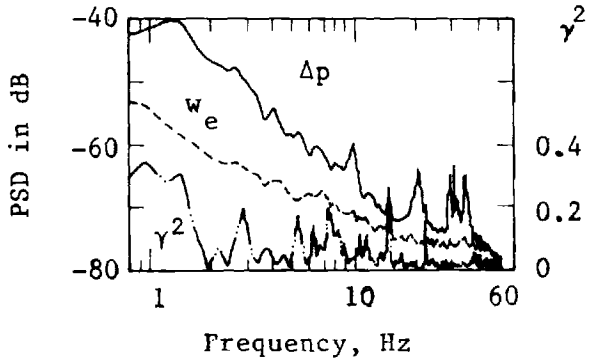

(b) Input Δp, Response w_e, $\gamma^2 \Delta p$, w_e

Figure 2.5-12 Measured Coherence Function, Window 9N4, $\bar{\theta} = 160^\circ$

The pressure spectrum shows a bulge between 6 - 8 Hz indicating that the wind pressure is responsible for the response at these frequencies. Since the window at which these data were measured was on the 9th floor, the relatively high frequency response is possibly due to gust effects.

The coherence function, as has been demonstrated, serves to identify the response levels associated with the wind or pressure loads. Several features of the window response dependence on wind loads are now apparent. High coherence between the input and output up to 1 Hz shows that the "quasi-static" response of the glass plates is primarily due to pressure loading. Beyond 1 Hz the coherence value decreases and becomes insignificant for frequencies less than 1.7 Hz. In the region from 1 to 1.7 Hz the values of the coherence function are in the vicinity of 0.25 implying that pressure loads may no longer be the sole excitation source. Interpretation of the coherence function at resonant peaks requires that care be exercised so as to isolate false coherence which may be due to an extraneous source affecting both the input and the output. At the fundamental frequency of 11.5 Hz (for window W10 on the 9th floor) which appears in the response spectrum the coherence between the pressure and the response is extremely low. Therefore, the fundamental frequency is excited by sources other than the wind loading. In some instances the fundamental was also seen in the pressure spectra yielding a coherence of almost unity (it is noted that for purely sinusoidal signals the coherence function can only be 0 or 1). This was diagnosed as a typical false coherence since the fundamental was strongly excited and appeared, by way of motion of the pressure tap located on the support and/or feedback

of panel vibrations to the flow, in the pressure spectra. False coherence also appears to be the reason for the high coherence function values seen at 31 Hz. This frequency corresponds to the rpm of some rotating machinery in the building.

The isolated case of Fig. 2.5-12 demonstrates that high values of the coherence function in the high frequency band may occur for a particular combination of the building profile and flow characteristics. In this case the wind loads are capable of exciting window dynamic response, in a relatively narrow frequency band extending from 6 - 16 Hz. In view of these observations the hypothesis of "critical response locations" appears more realistic.

2.5(c) Window Dynamic Properties

The previous two subsections have attempted to characterize the localized wind pressure loads on windows and to assess the causality between these loads and the response. This subsection deals with the problem of measuring the transfer function of the window system from which the modal properties of the double plate system and the support transmissibility can, in turn, be estimated. The "inverse" problem thus posed is that of obtaining a mathematical model for the windows system from measured data and is referred to as System Identification (81). There are a variety of time domain and frequency domain techniques that have been employed for system identification, and the application of transfer function-based schemes is dealt with in Refs. 82 - 85.

These types of measurements are usually handled most conveniently in a laboratory and could be performed on either model or full-scale window assemblies. Such a program, including design and construction

of a dynamic pressure loading facility for full-scale testing and response measurements for window assemblies similar to those at the field site, is reported in Chapter 4. However, there still exists a need for measurements of the dynamic response characteristics of window units as they exist in the field under actual service conditions. This can best be argued on the basis of three points:

(a) The dynamic characteristics of the window unit depend on the nature of its installation and the fact that it is affected by adjoining elements of the curtain wall. It would be unrealistic to simulate the entire curtain wall. In addition, any significant resonant frequency variation from one window to another can be treated as indicative of the variation in installation characteristics. A correlation between the frequency variation and the nature of the installation would enable detection of a faulty installation during assembly of the curtain wall or at a later time in its service life when structural degradation might have occurred.

(b) Measured transmissibility functions for a window provides an estimate of the support force attenuation arising from the presence of the rubber gasket. The transmissibility function can, therefore, be used to assess the quality of the gasket and gasket installation.

(c) In=situ dynamic measurements such as resonant frequencies and damping characteristics are needed for comparison with the results of laboratory simulation tests in order to verify the fidelity of those tests or improve the methodology.

In Sections 2.1 and 2.2 it was envisioned that the measured ambient wind pressure loading, at least in certain critical locations

about the building, would contain sufficient power to excite an appreciable dynamic response in windows and cladding components. The full-scale wind pressure and window response measurements reported in Section 2.5(a) and (b) have, however, shown that the dynamic wind loads (pressure loading with power spanning the first few natural frequencies of the plates, say from 5 - 30 Hz) are extremely small in magnitude and do not bear significant causality for the window dynamic response. The low values of the coherence function at higher frequencies have another important implication. As mentioned in Section 2.4(b), the coherence function is a measure of the validity of the transfer function estimates. It is evident, therefore, that at higher frequencies the transfer function of the window system cannot be estimated from ambient data.

An examination of the response levels form the w_i and w_e spectra shown in Figs. 2.5-10 to 2.5-12 reveals that the response of the double plate system is essentially quasi-static.* This characteristic of the measured window response provides an increased confidence in the measured wind load spectra which were also seen to be quasi-static.* It can be concluded, therefore, that at all of the locations where the measurements were conducted, the wind loads do not possess sufficient energy to excite window vibrations. The mullion acceleration response spectra and its coherence function were also computed and are shown in Fig. 2.5-13. As can be anticipated, estimation of the transmissibility function from these data is not possible either.

Considering these factors, the dynamic properties of a window in an actual curtain wall must be determined from some type of forced excitation

*Response period large compared to the period of the fundamental.

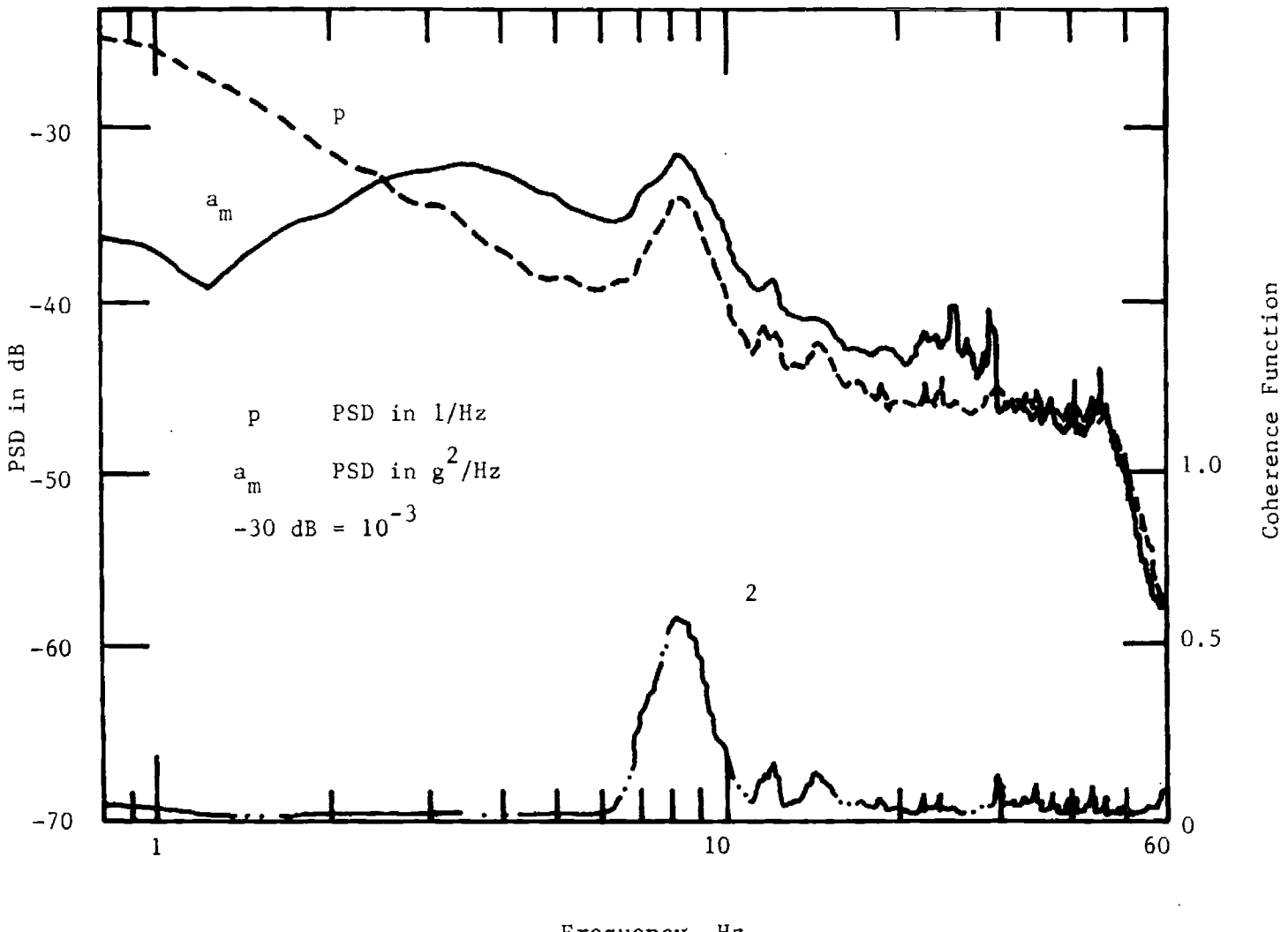

Figure 2.5-13 Mullion Acceleration Response Spectrum and Coherence Function

rather than from ambient loading. A variety of techniques are available for this purpose, but all can be classified as either (i) periodic, (ii) random, or (iii) transient. There is controversy as to which method is the most efficient for a given application (86), since some approaches trade off test simplicity for computational complexity, and vice versa. For the present application where field set-up time and test simplicity are of paramount importance, a transient forcing method was adopted. In conjunction with complex digital processors, such as the Fourier Analyzer used in these tests, this technique is capable of providing faster measurements compared to traditional sinusoidal excitation since the actual testing phase is considerably simplified.

A simple method of performing transient tests is to use a hand-held hammer with a load cell mounted on it to strike the structure and then measure the response to this transient excitation. The impulsive input has a flat frequency spectrum whose bandwidth depends on the "hardness" of the impacting head, a harder head providing a larger bandwidth. The transfer function computed from such an input-response pair can be used to determine the resonant frequencies and the damping coefficients. Multi-point measurement of the transfer function, ie.e, computation of the transfer function between various excitation and response points can be used to determine the mode shapes corresponding to these frequencies. The modal mass and modal stiffness can also be estimated from the transfer function data, although this almost invariably requires some type of data fitting (84).

Measurement of the frequency response functions for the present application to window systems was directed at obtaining the resonant

frequencies, f_n, the viscous damping coefficient, ζ, and the mode shapes of the inner plate. The mode shapes of the outer glass plate were not obtained since multiple point response measurements by the LDM proved time-consuming and inconvenient. However, results of the analytical model of the window system (Chapter 3) are used to obtain some idea of the double plate mode shapes corresponding to measured frequencies. In addition, the transfer function between w_i and w_e provides the vibration phase angle between w_i and w_e at the resonant frequencies and, therefore, the nature of the motion.

The procedures described below for the estimation of the vibration parameters are based on the following assumptions:

(i) The modes of the system are widely spaced in frequency.

(ii) Although modal coupling exists, a lightly-damped multi-degree-of-freedom system can be closely approximated by a single-degree-of-freedom system of appropriate natural frequency and damping near each of the system's natural frequencies.

The measured dynamic properties are:

(i) The resonant frequencies of a single window unit and the damping coefficients for each of the first 6 modes;

(ii) Variation in the resonant frequency (single mode) for a sample of 12 windows;

(iii) The mode shapes for the inner plate of the double pane system.

No attempt has been made to develop computational methods for determining these quantities directly from the raw transfer function data since this is beyond the scope of this research, and in addition, several commercial

software systems have already been developed for this purpose.* Rather, most of the interpretation has been done manually with limited curve-fitting. This provides acceptable accuracy of the lower modes which are relatively widely spaced, but owing to the amount of work involved, only a limited amount of data has been processed.

Modal Parameters: The inner plate of the window was marked at 3 spatial locations as shown in Fig. 2.5-14. The outer plate response was monitored at a single point 2' corresponding to point 2 of the inner plate. An accelerometer was used to measure the response at 2 and its location was fixed. The LDM measured the displacement response at point 2'. An instrumented hammer was used to excite the inner glass plate at each of the 3 points. Transfer functions for these 3 cases were computed from the measured response. The measured transfer function $H_{2i}(f)$, i = 1, 2, 3, are the elements of the second row of a 3 x 3 transfer function matrix. It can be shown (84) that only a single row or column of the transfer function matrix needs to be measured to compute the modal amplitudes at the 3 points. The LDM output provides the natural frequencies of the outer plate.

The compliance of the hammer head was first adjusted to provide a near uniform energy spectrum out to 50 Hz. Then, the hammer was used to repeatedly excite the structure at a designated point, and the resulting ensemble-averaged auto and cross power spectra were used to compute the transfer and coherence functions. The excitation was stopped when an acceptable coherence function was obtained, and the entire process was then repeated for each designated point. Transfer functions for the inner plate of window N4 on the 28th floor are shown

*None of these were available for the present work.

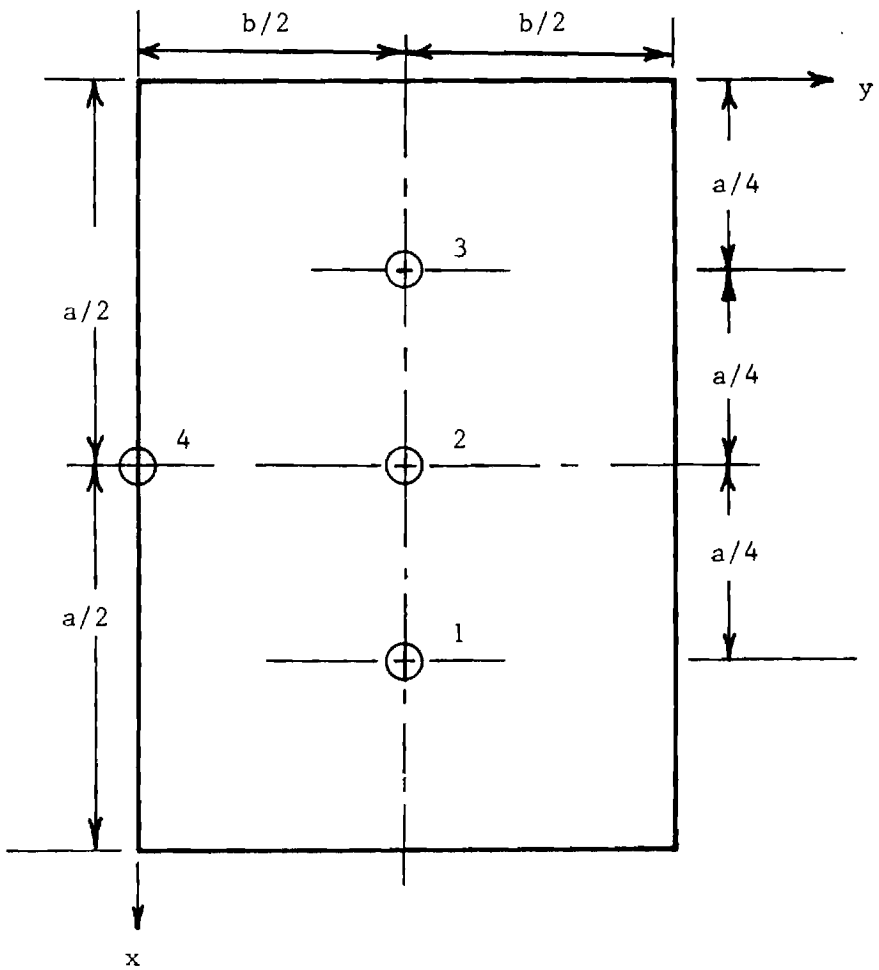

Figure 2.5-14. Location of Accelerometers on the Inner Plate

in Fig. 2.5-15 and Fig. 2.5-16 shows the $H_{2,1}(f)$ transfer function of the outer plate. The modal parameters computed from these transfer functions are as follows:

Resonant Frequencies: The acceleration-to-force transfer function is called inertance whereas the displacement-to-force transfer function is called compliance. In inertance or compliance plots the natural frequency corresponds to the following transfer function characteristics:

(a) Peak of the magnitude of the transfer function

(b) Phase angle of 90°

(c) Zero of Re H(f)

(d) Peak of Im H(f)

In practice, (c) and (d) were used to locate a resonance and the frequency was then determined by examining the imaginary peak.

Damping Coefficient: Several techniques for estimating the damping coefficient from the measured transfer function are available. Nyquist plots of the transfer function, where the real and imaginary parts are plotted in the complex plane, can be used to estimate the modal damping (87); however, in practice, estimation of damping from these plots requires careful curve fitting.

Damping is often measured using the amplification factor, Q, defined as:

$$Q = \frac{1}{2\zeta}$$

Q, in turn, may be measured from the magnitude of the transfer function as follows:

$$Q = f_n/\Delta f_n$$

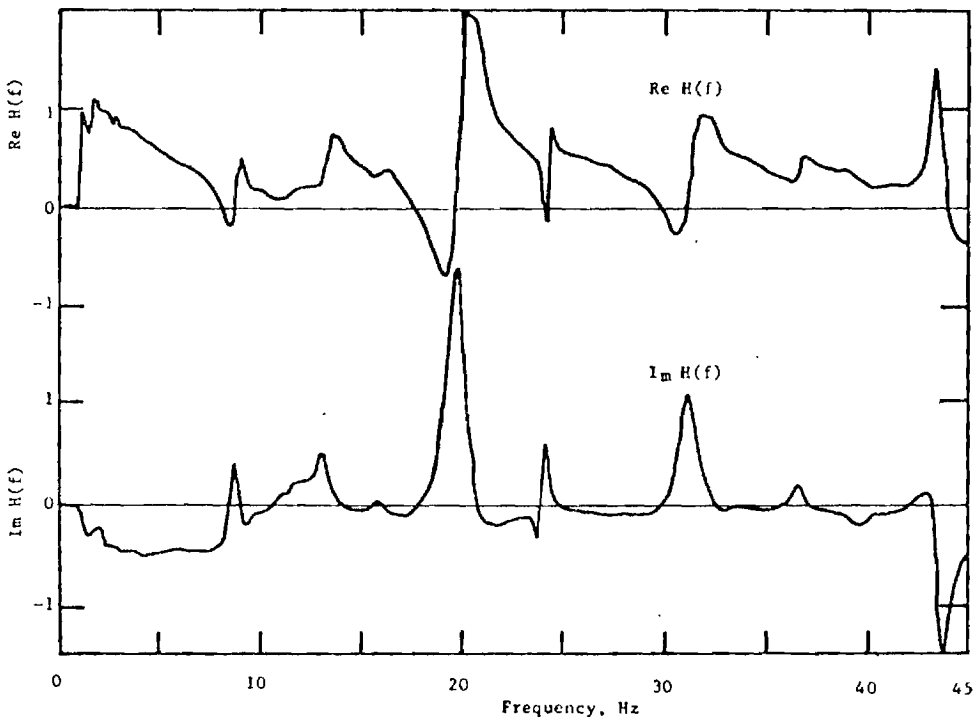

Real and Imaginary

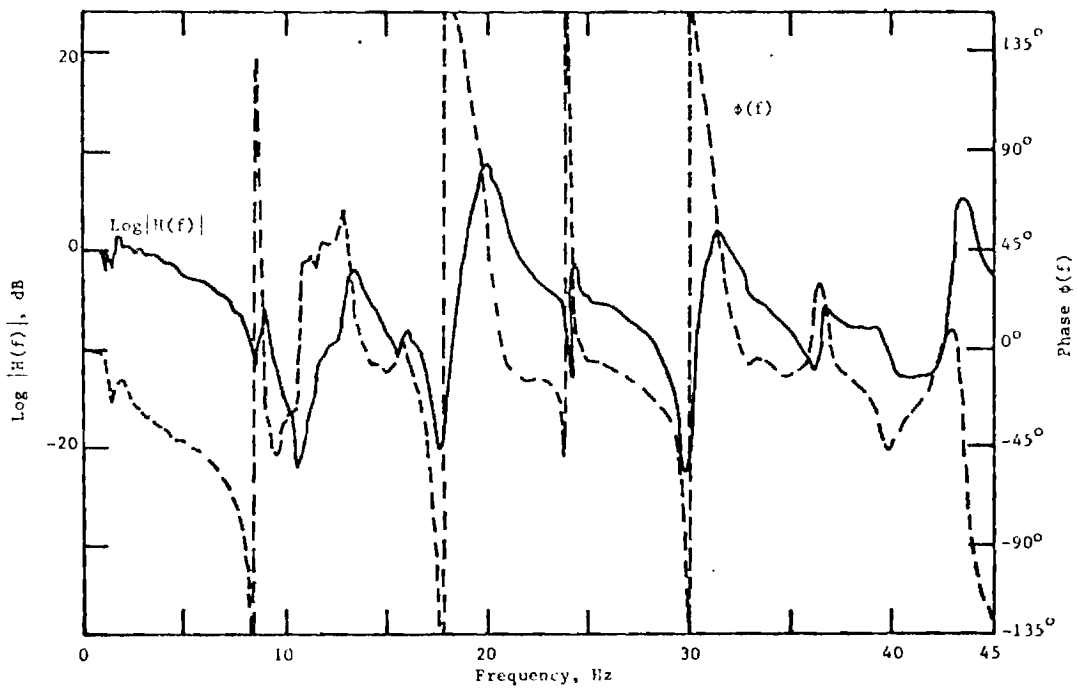

Magnitude and Phase

Figure 2.5-15(a) Frequency Response Function: Impact at 1, Response at 1

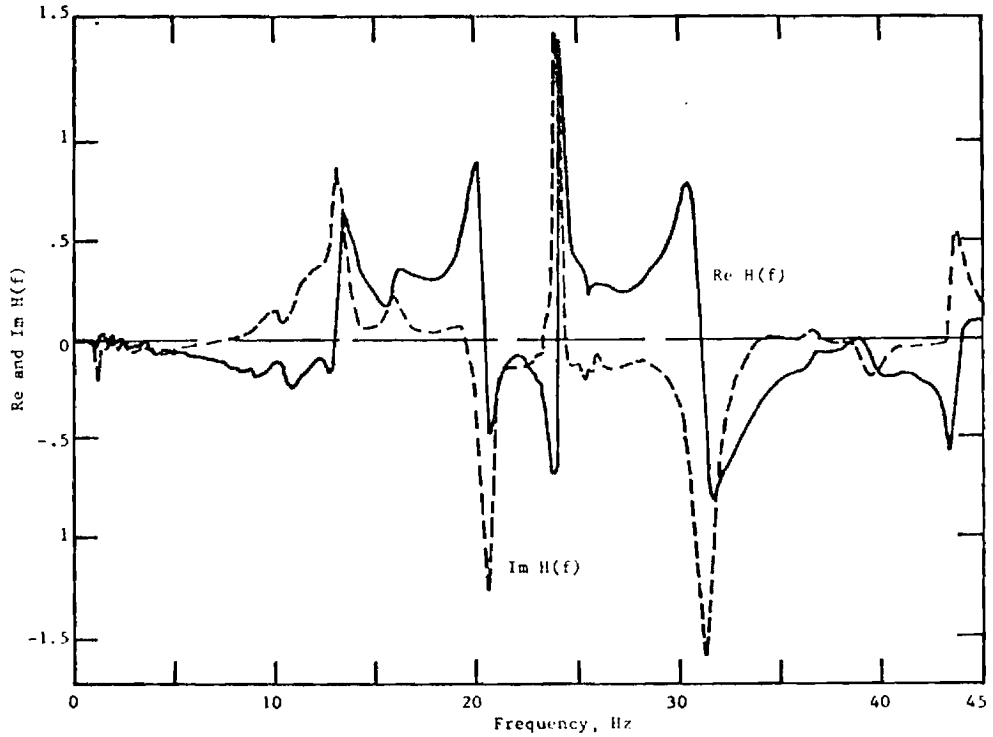

Real and Imaginary

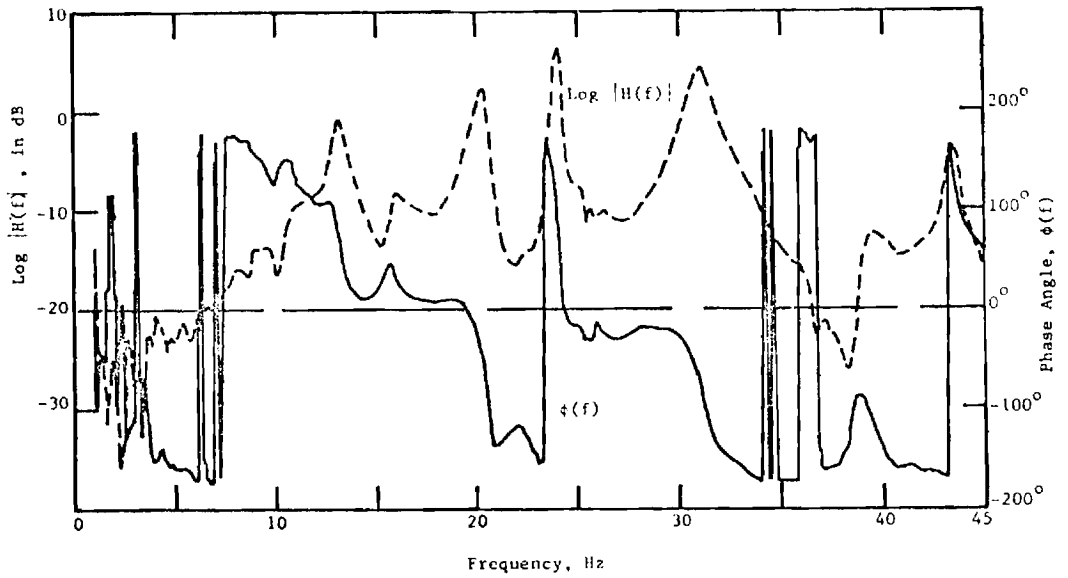

Magnitude and Phase

Figure 2.5-15(b) Frequency Response Function: Impact at 2, Response at 1

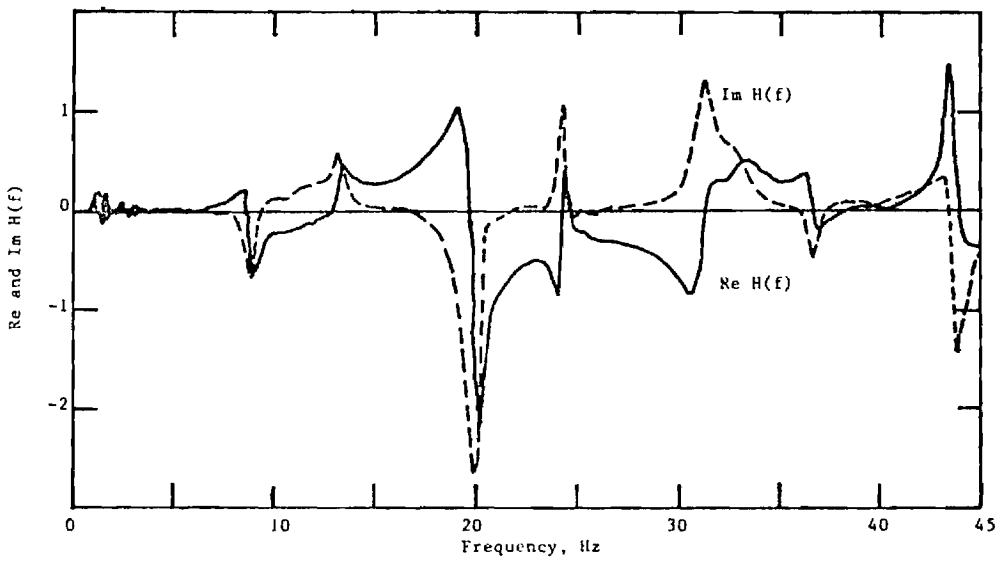

Real and Imaginary

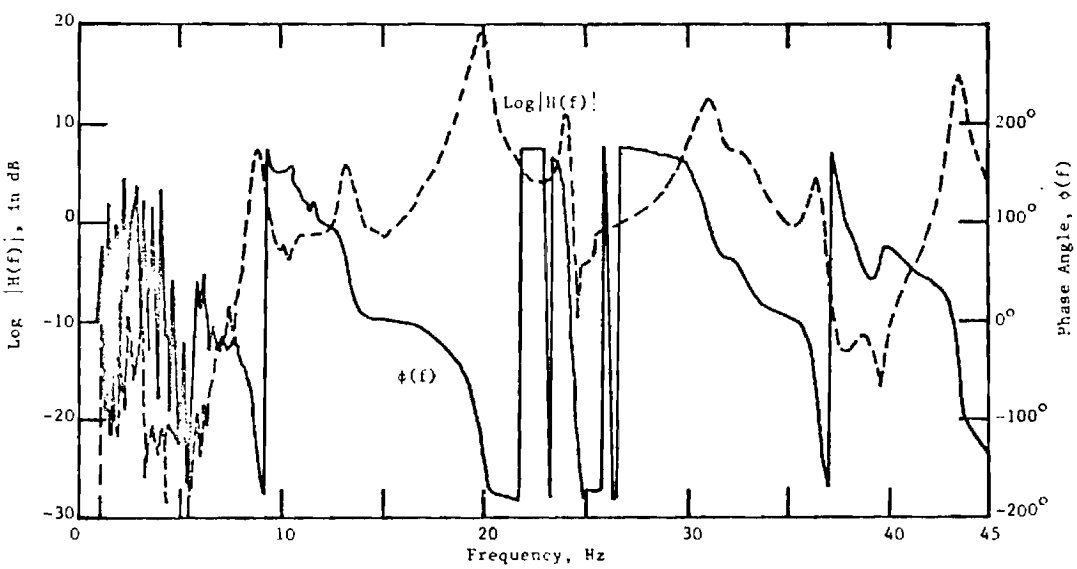

Magnitude and Phase

Figure 2.5-15(c) Frequency Response Function: Impact at 3, Response at 1

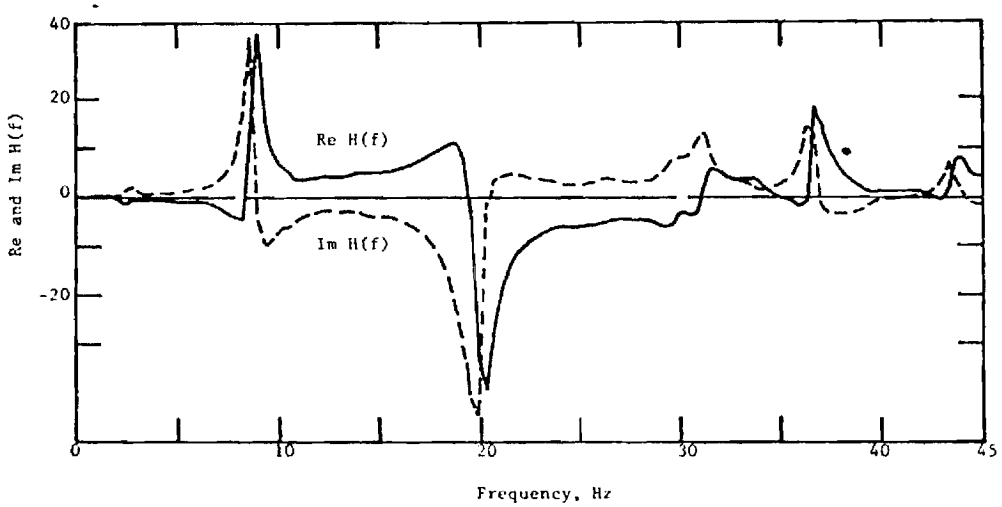

Real and Imaginary

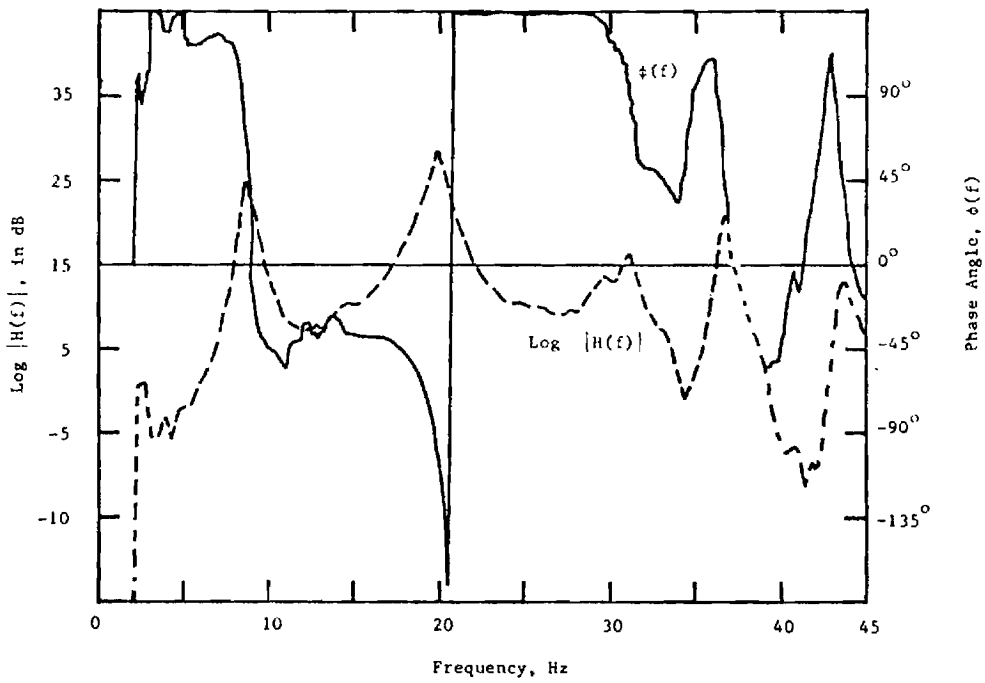

Magnitude and Phase

Figure 2.5-16 Frequency Response Function: Impact at 2, Response at 2'

where Δf_n is the half-power bandwidth of the resonance peak corresponding to f_n.

Alternatively, a method based on features of the real and imaginary response spectra can be used to estimate Q:

$$Q = \frac{(f_a/f_b)^2 + 1}{(f_a/f_b)^2 - 1}$$

where f_a is the frequency above resonance where the real part of compliance or inertance reaches a peak and f_b is the frequency below resonance, where the real part of the compliance or inertance reaches a peak of opposite sign. The latter method has proven most useful for the present transfer functions which are computed in real and imaginary form directly.

Mode Shape: The mode shape is estimated by measuring quadrature (imaginary) response values from all of the measured inertance or compliance functions at each resonant frequency. The N mode shapes are normalized with respect to the maximum value of the quadrature component at each of the N natural frequencies.

These techniques were applied to the transfer functions of Figs. 2.5-15 and 2.5-16 to yield the mode shapes shown in Fig. 2.5-17 at the frequencies tabulated in Table 2.5-3. Since the test points were constrained to lie on the vertical centerline, only the vertical mode shapes are defined, and it is not possible to distinguish between symmetric horizontal mode shapes (odd wave numbers). From Fig. 2.5-17 it is apparent that the first few modes have been detected but the precise shape of higher modes is not clearly defined. Modes 1, 2, and 4 are the (1,1), (2,1), and (3,1) shapes, while modes 3 and 5 involve

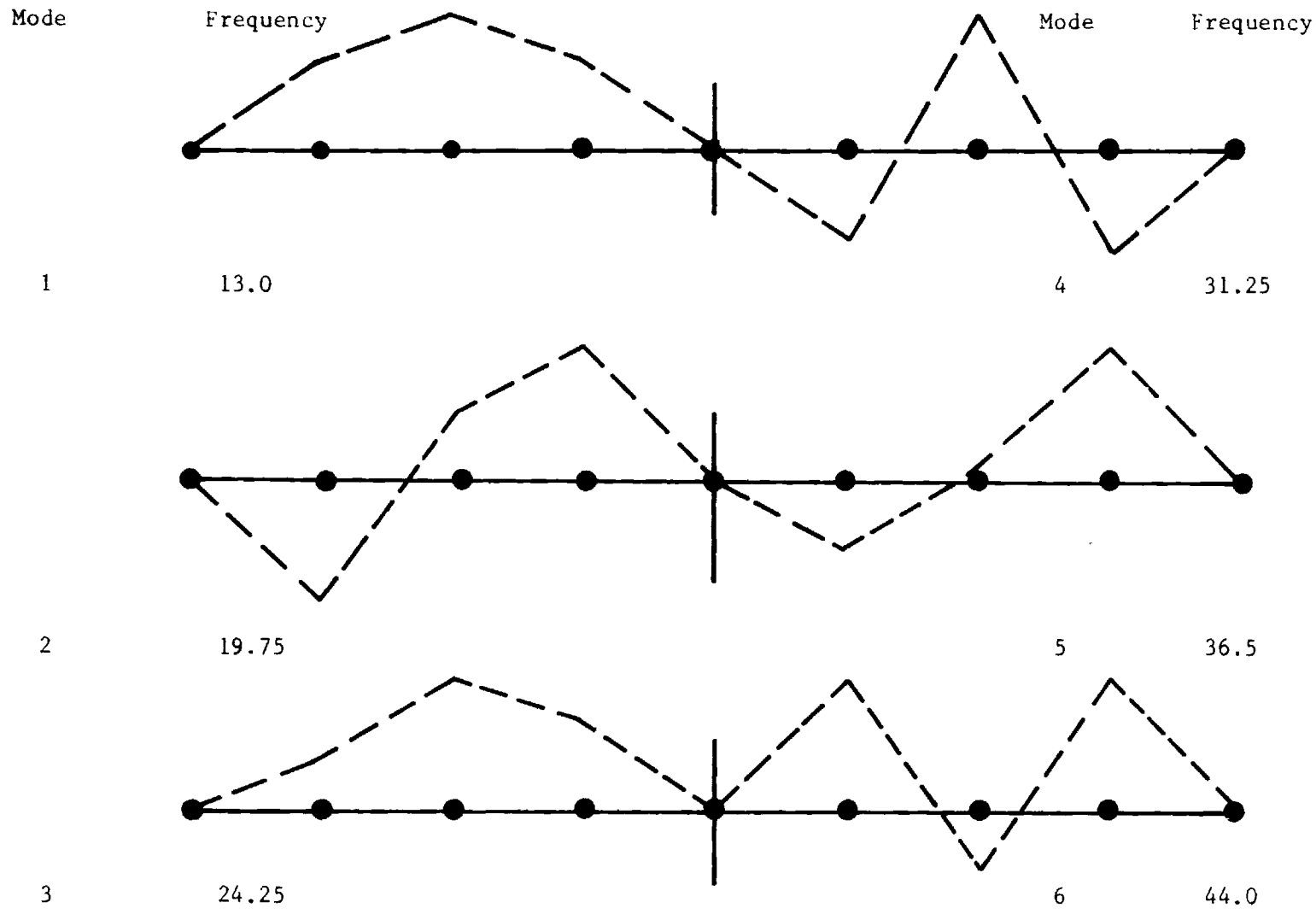

Figure 2.5-17. Mode Shapes

higher but undefined horizontal modes. The data from Table 2.5-3 shows that the natural frequencies of the window system are substantially higher than the bandwidth over which most of the wind power appears. There appears to be some evidence, however, from certain of the wind pressure psd and coherence plots, that in a few critical locations or situations, the (1,1) mode may be mildly excited.

The transfer function data show several other interesting features. There appears to be a strong mode at about 8.5 Hz that would seem at first to be the (1,1) fundamental. Closer study, however, indicates that this mode has a node at the midpoint and appears to be a type of rocking mode associated with the frame and adjoining windows. In addition, there appear to be a number of other unidentified modes with very small amplitudes as evidenced by the minor peaks between the major resonances. These are most likely associated with other elements in the adjoining cladding and were disregarded here. The damping coefficients shown in Table 2.5-3 are somewhat larger than the 0.5 to 1% usually associated with material damping alone. The 2 - 5% values reflect the additional viscoelastic behavior provided by the rubber glazing gaskets at the boundary. The largest values are associated with the lower modes.

The transfer function in Fig. 2.5-16 was obtained for single point (midpoint) on the outer pane by using the LDM displacement signal. As shown in Table 2.5-4, the modal frequencies generally agree with those for the inner pane; however, the corresponding mode 1 is not present. Instead, it is replaced by a strong resonance at the 8.5 Hz value previously associated with a generalized rocking mode.

Table 2.5-3 Longitudinal Modes, Window 28N4, Inner Plate

Mode #	Resonant Freq. H_z	Damping Coeff. ζ	Mode Shape i.e. n =
1	13.0	.045	1
2	19.75	.028	2
3	24.0	.01	1
4	31.25	.02	3
5	36.5	---	2
6	44.0	.01	3

Table 2.5-4 Resonant Frequencies of Outer Glass Plate

Mode #	Frequency, f_n
1	----
2	20.75
3	31.0
4	36.75
5	43.75

Similar results were obtained for other windows examined but with variations in the associated frequencies. This is most clearly shown in Table 2.5-5 which is a tabulation of the (2,1) mode frequencies for 12 adjoining windows on the north side of the 28th floor. The range from 18.25 to 21.25 Hz represents a 15% variation in behavior which from the distribution in the table does not appear to be correlated with location.

In general the field tests to determine the dynamic response were troublesome to perform. The outer pane was accessible to measurement only with the LDM instrument which proved accurate in operation but somewhat difficult to move over the window area. In addition, the windows under study were clearly a part of the overall cladding and the measured response included certain modes associated with more generalized motion. The primary objective of this phase of the work was to ascertain, in general, what the in-situ modes looked like and their relation to the measured wind power. More detailed modal studies are described in the lab tests in Chapter 4.

Table 2.5-5. Variation in Resonant Frequency (2, 1) Mode

Window	Frequency, Hz
N1	18.5
N2	19.25
N3	19.25
N4	19.75
N5	18.25
N6	19.0
N7	18.5
N8	19.25
N9	18.5
N10	18.25
N11	21.25
N12	21.25

3.0 ANALYTICAL INVESTIGATIONS

3.0(a) Need for Discrete Element Model

The laboratory window test facility described in this report can be used to test a number of glass cladding designs to determine their adequacy in carrying actual static and dynamic loads in the field. Naturally, the range of panel sizes and configurations as well as the loading types that can be applied in the laboratory are limited for reasons of economy. For example, the present test rig cannot be used to apply in-plane racking distortions to the frame-panel structure (although such modification to the test rig is possible), and the range of full-scale panels that can be tested is limited by the physical size and performance characteristics of the rig. Therefore, a computer model which was capable of accurately reproducing actual lab tests as well as permitting a broader range of panel sizes and support conditions and loading types to be evaluated was needed. To meet these requirements, a discrete element model of the frame, gasket, and glass panel was constructed using the finite element method. All basic components of the actual window installation are present in the analytical model, and complex static and dynamic loading conditions not possible in the laboratory can be handled with relative ease. In addition, the window model presented herein can be expanded to represent an entire glass curtain wall in a modern high-

rise building. The window model is sufficiently general that it can be directly incorporated into existing three-dimensional analytical models for static and dynamic analysis of multistory buildings. This extension of the present work would permit the determination of the interaction forces between frame and cladding for a wide range of loading conditions. The work described in this chapter constitutes the first step in an analytical study of cladding-structure interaction in highrise buildings.

3.0(b) Objectives

The basic objectives guiding this portion of the overall research program are as follows:

1. To develop a discrete element analytical model which is an accurate representation of the actual frame-panel structure;
2. To develop a FORTRAN computer program which implements the analytical model and permits the performance of a wide range of window designs of varying size, properties, and support conditions, and with static or dynamic applied loadings to be evaluated;
3. And, to conduct sensitivity studies to determine key parameters affecting the static and dynamic response of the total window-frame system.

The basic analytical model developed to satisfy objective 1. above is described in the next section. Model properties and support conditions were adjusted until both static displacements and vibration

frequencies for the analytical model were in good agreement with laboratory findings. The model was then considered to be a reasonably accurate representation of the actual structure which could be used in later sensitivity studies.

A FORTRAN computer program, WINDOW, based upon the finite element displacement method was developed to meet objective 2. above. A macro-flow chart of the program, a detailed user's guide, a listing of the program and several example problems illustrating its use for both static and dynamic loadings are presented in this chapter and in Appendix C.

To meet the final objective, basic properties of the frame-panel model were varied and the structure response computed for a number of representative loadings. Results are presented in the form of nondimensional curves which show the influence of system components on window response.

3.1 Analytical Model

3.1(a) Description of Discrete Element Model

The discrete element model developed for this study employs a combination of two-dimensional plane stress and plate bending finite elements to represent the glass panel, and one-dimensional space frame elements to model the surrounding framework. Translational and rotational linear springs are used to represent the gasket on the panel boundary, and frame and panel are spring-connected at panel node points as shown in Figure 3.1-1. Nonrigid connections at frame corners are also included to account for frame connection rotational flexibility.

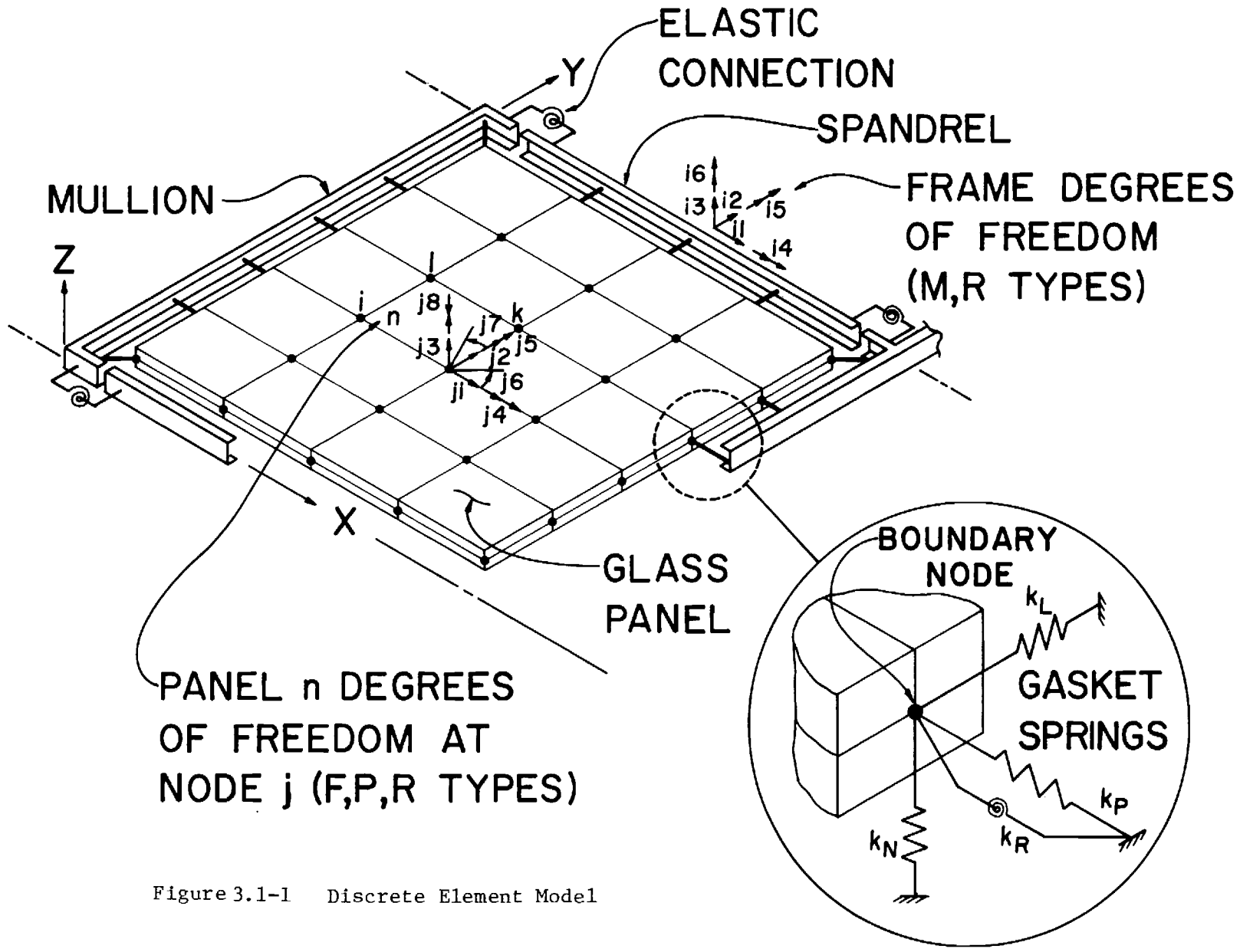

Figure 3.1-1 Discrete Element Model

Both in-plane and out-of-plane effects can be handled with this model, but the two are assumed uncoupled. Applied loads or racking displacements of the frame in the plane of the panel introduce distortions into the panel which are determined from the plane stress finite elements, while loads and frame movements normal to the panel cause bending distortions which activate the plate bending elements in the model. Deterministic planar and normal loadings may be applied simultaneously but coupled bending and stretching are not permitted since the model is assumed to be both geometrically and materially linear.

The stiffness method was used to assemble consistent stiffness and mass descriptions of the structure. Condensation of both stiffness and mass matrices was employed to eliminate extraneous degrees of freedom from the model thereby reducing the number of equations to be solved. A special purpose computer program was written to assemble the model, reduce the number of equations, and print and plot the system response for both static and time-dependent loadings.

Finite Elements: The plane stress and plate bending finite elements are superposed to form a single rectangular finite element, with eight degrees of freedom per node, referred to as the basic element. A refined plane stress element (88) and a conforming plate bending element (89), each having four degrees of freedom per node, were chosen because of their excellent past performance in modeling the static and dynamic behavior of plate-like structures (90). The geometry, nodal numbering scheme, and local coordinate system for the two elements are shown in Figure 3.1-2.

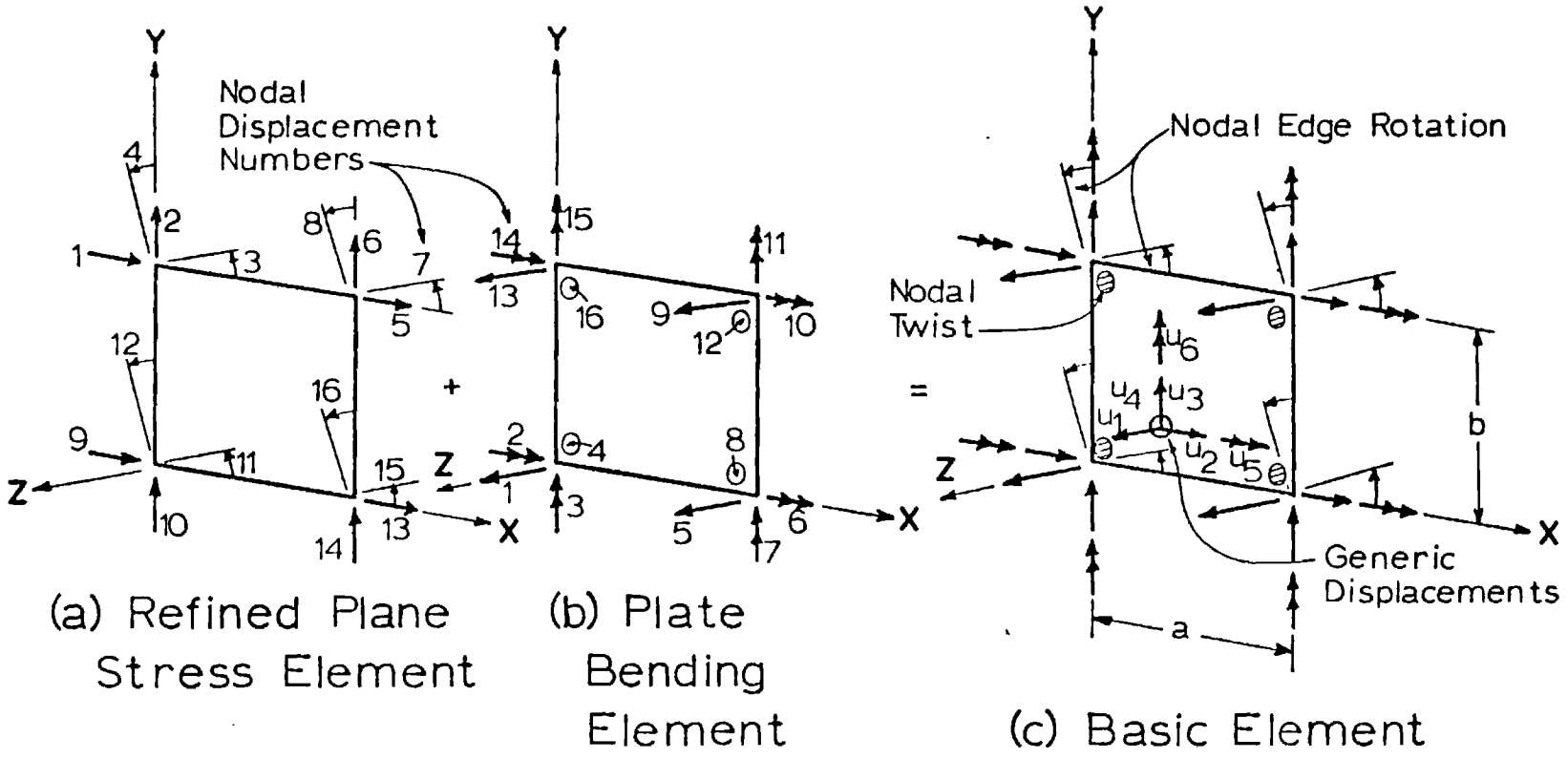

Figure 3.1-2 Formation of Basic Element

The generic displacements $\underset{\sim}{u}$ at any point in the basic element are expressed in terms of the nodal displacements $\underset{\sim}{q}$ for the element by the matrix equation:

$$\underset{\sim}{u} = T_1 \underset{\sim}{q} \tag{3.1-1}$$

where $\underset{\sim}{u}' = \{u_1 \; u_2 \; u_3 \; u_4 \; u_5 \; u_6\}$ 1 x 6

$\underset{\sim}{q}' = \{q_1 \; q_2 \; \cdots \; q_{32}\}$ 1 x 32

and T_1 is the matrix of shape functions for the basic element, assembled from the shape function arrays of the plane stress and plate bending finite elements (90). Generic displacements u_1, u_4, u_5, and u_6 and nodal displacements q_1, ..., q_{16} pertain to the plate bending finite element; while generic displacements u_2 and u_3 and nodal displacements q_{17}, ..., q_{32} are associated with the plane stress element. Generic displacements u_4, u_5, and u_6 are dependent on u_1 as follows:

$$u_4 = -\frac{\partial^2 u_1}{\partial x \partial y}, \quad u_5 = \frac{\partial u_1}{\partial y}, \quad u_6 = -\frac{\partial u_1}{\partial x} \tag{3.1-2}$$

where u_4 represents a twist curvature and u_5 and u_6 represent rotations out of the plane of the plate bending element. For the plane stress element, rotations of the element edges parallel to the x and y axes are expressed as partial derivatives $\frac{\partial u_3}{\partial x}$ and $-\frac{\partial u_2}{\partial y}$, respectively, evaluated at the element corners.

The plate bending element is both complete and conforming. A complete cubic polynomial plus six additional terms are employed in the derivation of the 16 x 16 element stiffness matrix $\underset{\sim}{S}_{PB}$ for this element based on the principle of minimum potential energy. The 16 x 16 element stiffness matrix $\underset{\sim}{S}_{PS}$ for the refined plane stress element

is obtained in the same manner. A linear-cubic displacement function is used, however, and the refined plane stress element is compatible with line elements in bending in frame and shear-wall models (88).

As a final step in the assembly of the basic element, a 32 x 32 element stiffness matrix $\underset{\sim}{S}_E$ is constructed from arrays $\underset{\sim}{S}_{PB}$ and $\underset{\sim}{S}_{PS}$ as follows:

$$\underset{\sim}{S}_E = \begin{bmatrix} \underset{\sim}{S}_{PB} \text{ 16x16} & \underset{\sim}{0} \\ \underset{\sim}{0} & \underset{\sim}{S}_{PS} \text{ 16x16} \end{bmatrix} \quad \text{32x32} \qquad (3.1\text{-}3)$$

Standard matrix operations were used to rearrange $\underset{\sim}{S}_E$ to obtain the counterclockwise ordering of node numbers k, j, k, and ℓ and degree of freedom ordering at any node j as shown in Figure 3.1-1. In particular, a combined element stiffness matrix $\underset{\sim}{S}_C$ for the 32 degree of freedom element in Figure 3.1-2 can be obtained from $\underset{\sim}{S}_E$ as follows:

$$\underset{\sim}{S}_C = \underset{\sim}{T}' \; \underset{\sim}{S}_E \; \underset{\sim}{T} \qquad (3.1\text{-}4)$$

where $\underset{\sim}{T}$ is a matrix which correlates degree of freedom numbers in Figures 3.1-1 and 3.1-2 and $\underset{\sim}{T}'$ is the transpose of $\underset{\sim}{T}$. Arrays $\underset{\sim}{S}_C$ for each element in the panel are assembled to form the panel stiffness matrix.

Frame Elements: The frame surrounding the panel is divided into mullion and spandrel elements each having six degrees of freedom per node. Mullion elements are space frame elements with local member axes parallel to the structure y axis while spandrel elements are space frame elements parallel to the structure x axis (Figure 3.1-3). The same number of frame and panel elements and nodes must be selected along each structure boundary so that frame and panel nodes correspond. However, the actual number of elements used will depend upon the finite element mesh employed.

The rotational connection stiffness of spandrel elements may be selected arbitrarily at the two ends of the member element. Connection stiffnesses at node j are denoted Sy_j and Sz_j for stiffness about the y and z axes, respectively; similarly stiffnesses at node k are Sy_k and Sz_k. Ordinarily, only spandrel element connections at mullion-spandrel junctures would be treated as nonrigid to account for framework flexibility at the joints; connection stiffnesses at all interior spandrel elements, with or without nonrigid connections, can be developed and assembled with mullion elements to form the window framework.

Spring Elements: The neoprene gasket which holds the glass panel in its frame was modeled as a series of discrete linear elastic springs joining adjacent frame and panel nodes along the boundary. Four basic springs are used as shown in Figure 3.1-1. Axial springs model the resistance of the gasket to motions in the plane of the panel, either perpendicular (k_P) or parallel to (k_L) a panel edge. Another axial spring represents the gasket's resistance to boundary displacements normal to the panel (k_N), while a rotational spring (k_R) accounts for

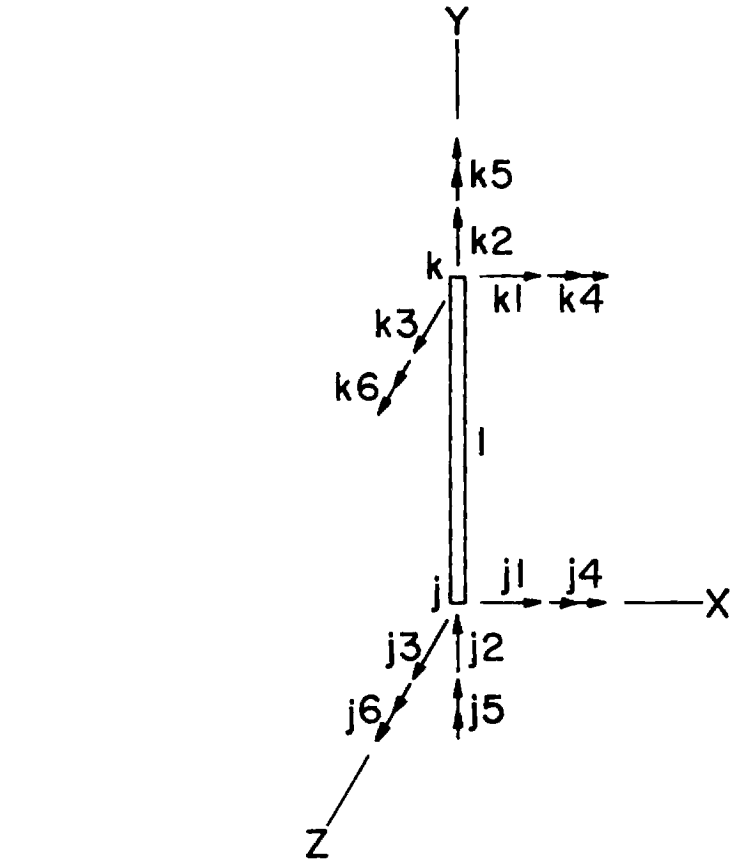

a) MULLION ELEMENT

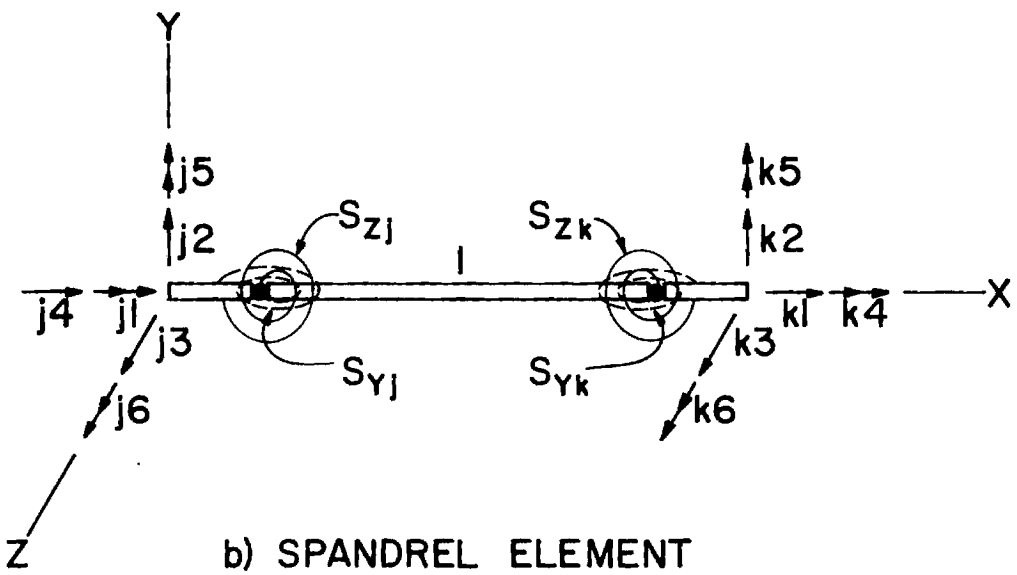

b) SPANDREL ELEMENT

Figure 3.1-3 Frame Elements

gasket resistance to relative rotation between frame and panel on the boundary. All four spring constants are expressed as stiffness per unit length of panel boundary and must be multiplied by the tributary panel length to obtain the actual stiffness terms added to attached panel and frame nodes. Numerical values for unit spring constants k_P, k_L, k_N, and k_R were determined using simple laboratory static tests to be described later.

Mass and Damping Models: If dynamic behavior of the system is of interest, mass and damping properties must be specified for each element of the structure. The formation of a mass model for each element parallels the development of element stiffness matrices discussed above. A mass matrix for the basic finite element is constructed from element mass matrices for the plane stress and plate bending elements as follows:

$$\underset{\sim}{M}_E = \begin{bmatrix} \underset{\sim}{M}_{PB} \text{ 16x16} & \underset{\sim}{0} \\ \underset{\sim}{0} & \underset{\sim}{M}_{PS} \text{ 16x16} \end{bmatrix} \text{ 32x32} \qquad (3.1\text{-}5)$$

If a consistent mass formulation is used, arrays $\underset{\sim}{M}_{PB}$ and $\underset{\sim}{M}_{PS}$ will be filled matrices. An alternative to consistent mass (CM) is assembled lumped mass (ALM) in which the mass of the element is lumped at nodal translational degrees of freedom. With ALM, arrays $\underset{\sim}{M}_{PB}$ and $\underset{\sim}{M}_{PS}$ are diagonal matrices; only entries (1,1), (5,5), (9,9), and (13,13) of $\underset{\sim}{M}_{PB}$ and (1,1), (2,2), (5,5), (6,6), (9,9), (10,10), (13,13), and (14,14) of $\underset{\sim}{M}_{PS}$ are non-zero for ALM, each term having the value 1/4 ρabt where

a, b, t are element dimensions and ρ is the mass density of the material. (See Figure 3.1-4.) The ALM formulation has been shown to be superior to CM in determination of vibration frequencies for certain structures (90). In either case, element mass matrix $\underset{\sim}{M}_E$ must be rearranged to produce $\underset{\sim}{M}_C$ as in equation (3.1-4). Arrays $\underset{\sim}{M}_C$ are then assembled for each panel element to form the panel mass matrix.

Consistent or assembled lumped mass matrices can be developed for frame elements in the same manner as for panel finite elements. However, linear springs representing the gaskets are assumed massless.

Element stiffness and mass matrices for panel finite elements, frame member elements, and spring elements are finally assembled, using procedures described below, to form overall structure stiffness and mass matrices for the entire window-frame structure. A structure damping matrix is not developed in explicit form; rather simple modal viscous damping was used with the fraction of critical viscous damping arbitrarily specified in each normal mode of vibration.

3.1(b) Structural Assemblage and Condensation

Panel, frame, and spring elements are assembled to form stiffness and mass properties of the total structure model. Extraneous degrees of freedom on the panel and frame are eliminated using a two-stage condensation procedure. The primary motivation for this approach was to construct an efficient model for dynamic analysis with as few dynamic degrees of freedom as practicable. In the first stage nonessential panel (or P type) degrees of freedom are condensed out, while in the second stage unnecessary frame (or M type) degrees of freedom are eliminated. Stiffness and mass arrays are partitioned into subarrays to conserve computer storage and to

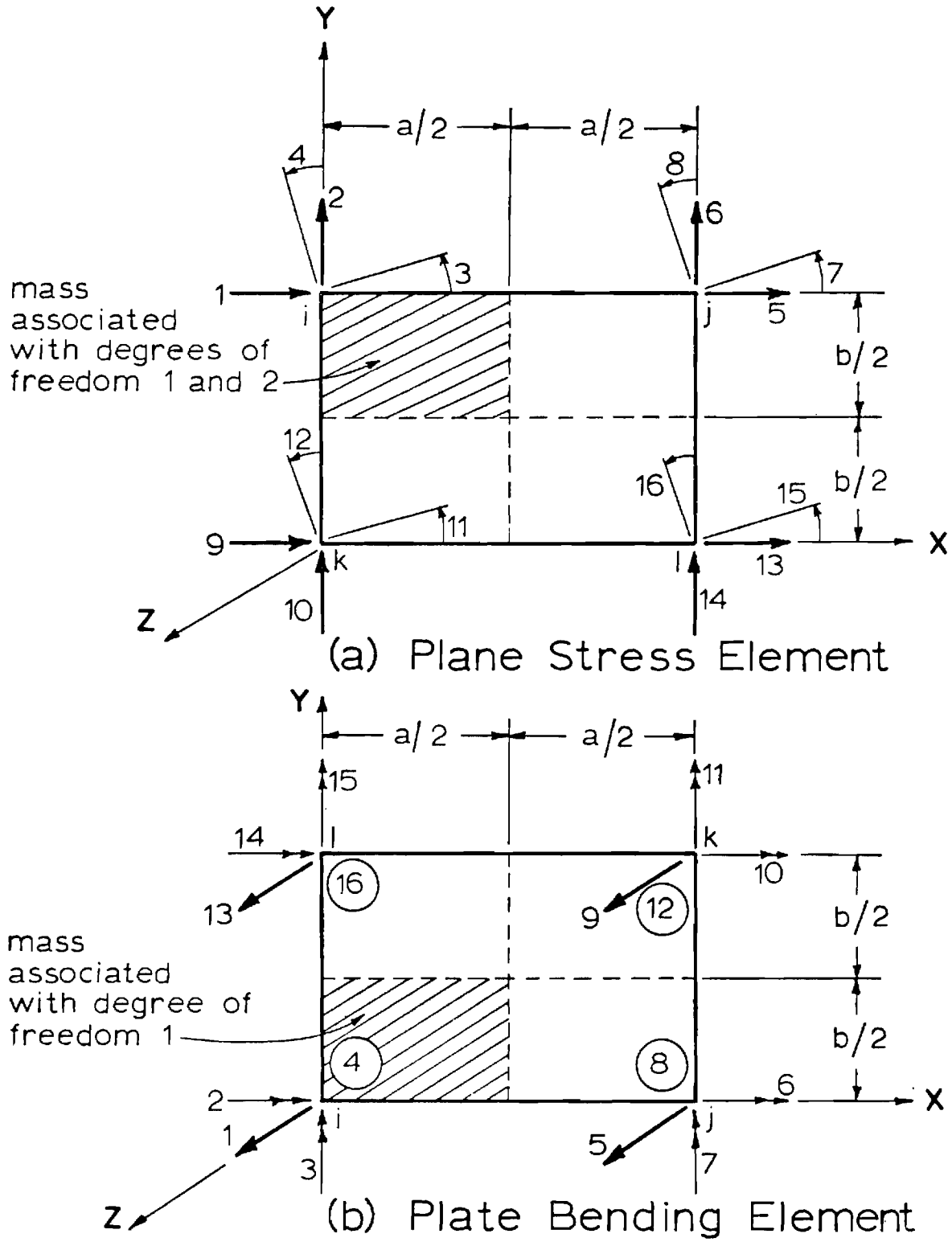

Figure 3.1-4 Assembled Lumped Mass (ALM)

expedite the assembly and condensation procedures.

Displacement Types: Structure degrees of freedom are categorized as F, P, M, and R displacement types as a basis for partitioning stiffness and mass matrices and for orderly elimination of unessential degrees of freedom. F displacement types are those panel degrees of freedom which are to remain at the end of the condensation operations as master degrees of freedom. Any number and distribution of panel displacements may be selected as F types but points of load application or mass concentration should be chosen and corresponding degrees of freedom designated as F types. For example, nodal degrees of freedom of type j3 (Figure 3.1-1) at all unrestrained panel nodes could be selected as F types if the response normal to the plane of the panel were of interest. The remaining unrestrained panel degrees of freedom are designated as P type displacements to be eliminated in the first stage of condensation. All unrestrained frame displacement coordinates called M types are removed in the second condensation operation. Finally, R types refer to all restrained panel and frame displacement coordinates, which together with all F types, remain at the end of the condensations. The F and R types, then, constitute a reduced set of degrees of freedom which can be used to describe the response of particular points of interest on the panel. Applied loadings corresponding to the F degrees of freedom and support displacements at R displacement coordinates are acceptable loading conditions in the reduced structure model. Furthermore, static and dynamic response at eliminated (P,M) displacement coordinates may still be determined through a backsubstitution operation once the response at the master degrees of freedom is known.

The undamped equations of motion for the total window-frame model can be written as follows:

$$\underset{\sim}{M}_J \ddot{\underset{\sim}{D}}_J + \underset{\sim}{S}_J \underset{\sim}{D}_J = \underset{\sim}{A}_J \qquad (3.1\text{-}6)$$

or in partitioned form:

$$\begin{bmatrix} \underset{\sim}{M}_{FF} & \underset{\sim}{M}_{FP} & \underset{\sim}{M}_{FM} & \underset{\sim}{M}_{FR} \\ \underset{\sim}{M}_{PF} & \underset{\sim}{M}_{PP} & \underset{\sim}{M}_{PM} & \underset{\sim}{M}_{PR} \\ \underset{\sim}{M}_{MF} & \underset{\sim}{M}_{MP} & \underset{\sim}{M}_{MM} & \underset{\sim}{M}_{MR} \\ \underset{\sim}{M}_{RF} & \underset{\sim}{M}_{RP} & \underset{\sim}{M}_{RM} & \underset{\sim}{M}_{RR} \end{bmatrix} \begin{Bmatrix} \ddot{\underset{\sim}{D}}_F \\ \ddot{\underset{\sim}{D}}_P \\ \ddot{\underset{\sim}{D}}_M \\ \ddot{\underset{\sim}{D}}_R \end{Bmatrix} + \begin{bmatrix} \underset{\sim}{S}_{FF} & \underset{\sim}{S}_{FP} & \underset{\sim}{S}_{FM} & \underset{\sim}{S}_{FR} \\ \underset{\sim}{S}_{PF} & \underset{\sim}{S}_{PP} & \underset{\sim}{S}_{PM} & \underset{\sim}{S}_{PR} \\ \underset{\sim}{S}_{MF} & \underset{\sim}{S}_{MP} & \underset{\sim}{S}_{MM} & \underset{\sim}{S}_{MR} \\ \underset{\sim}{S}_{RF} & \underset{\sim}{S}_{RP} & \underset{\sim}{S}_{RM} & \underset{\sim}{S}_{RR} \end{bmatrix} \begin{Bmatrix} \underset{\sim}{D}_F \\ \underset{\sim}{D}_P \\ \underset{\sim}{D}_M \\ \underset{\sim}{D}_R \end{Bmatrix} = \begin{Bmatrix} \underset{\sim}{A}_F \\ \underset{\sim}{A}_P \\ \underset{\sim}{A}_M \\ \underset{\sim}{A}_R \end{Bmatrix} \qquad (3.1\text{-}7)$$

where F, P, M, and R subscripts refer to the displacement types described above. Mass and stiffness matrices $\underset{\sim}{M}_J$ and $\underset{\sim}{S}_J$ are symmetric so only those subarrays on and above the diagonals are actually assembled.

Assemblage: Selected submatrices of structure stiffness matrix $\underset{\sim}{S}_J$ are assembled and condensed first, then a similar operation is performed to build and condense mass matrix $\underset{\sim}{M}_J$. To begin the procedure panel finite elements are processed one at a time, element stiffness matrices $\underset{\sim}{S}_C$ (Equation 3.1-4) formed, and contributions of $\underset{\sim}{S}_C$ to submatrices in $\underset{\sim}{S}_J$ recorded. If successive panel elements are identical, $\underset{\sim}{S}_C$ need not be regenerated until an element of different size is encountered. Next, mullion element and spandrel element (with or without nonrigid connections) stiffness matrices are formed for each framing element and are used to augment submatrices of $\underset{\sim}{S}_J$. Finally, spring elements add stiffness terms at panel and frame degrees of freedom along the boundary of the model to complete the assemblage of matrix $\underset{\sim}{S}_J$. Following condensation of $\underset{\sim}{S}_J$, mass matrix $\underset{\sim}{M}_J$ is formed.

Panel element degrees of freedom may be F, P, or R types. Consequently, matrices $\underset{\sim}{S}_C$ and $\underset{\sim}{M}_C$ for each element add stiffness and mass terms

to FF, FP, FR, PP, PR, and RR subarrays in Equation 3.1-7. Frame elements form MM and MR subarrays and augment the RR submatrix. Spring elements tie the panel and frame together to form a stable model; spring stiffness terms are used to form FM and PM stiffness submatrices and to add stiffness terms to FF, PP, MM, RR, FR, PR, and MR subarrays. Springs are assumed massless and do not contribute to $\underset{\sim}{M}_J$. If the consistent mass (CM) formulation is used, all ten of the mass submatrices which are formed will have nonzero entries, while assembled lumped mass (ALM) will result in diagonal FF, PP, MM, and RR subarrays and all remaining entries in $\underset{\sim}{M}_J$ are zeros.

Condensation: Elimination of displacement coordinates which have very little or no mass associated with them or whose response is not of primary interest produces a more efficient model for dynamic analysis. The two-stage reduction procedure employed here begins with static condensation of $\underset{\sim}{S}_J$ to eliminate first P and then M type displacements. The static equilibrium equations,

$$\underset{\sim}{S}_J \, \underset{\sim}{D}_J = \underset{\sim}{A}_J \tag{3.1-8}$$

with the partitioned forms of arrays $\underset{\sim}{S}_J$, $\underset{\sim}{D}_J$, and $\underset{\sim}{A}_J$ shown in Equation (3.1-7), are reduced to

$$\underset{\sim}{S}^*_J \, \underset{\sim}{D}_{J_1} = \underset{\sim}{A}_{J_1} \tag{3.1-9}$$

where

$$\underset{\sim}{S}^*_J = \begin{bmatrix} \underset{\sim}{S}^*_{FF} & \underset{\sim}{S}^*_{FM} & \underset{\sim}{S}^*_{FR} \\ \underset{\sim}{S}^*_{MF} & \underset{\sim}{S}^*_{MM} & \underset{\sim}{S}^*_{MR} \\ \underset{\sim}{S}^*_{RF} & \underset{\sim}{S}^*_{RM} & \underset{\sim}{S}^*_{RR} \end{bmatrix} \tag{3.1-10}$$

and

$$\underset{\sim}{D}_{J_1} = \begin{Bmatrix} \underset{\sim}{D}_F \\ \underset{\sim}{D}_M \\ \underset{\sim}{D}_R \end{Bmatrix}, \quad \underset{\sim}{A}_{J_1} = \begin{Bmatrix} \underset{\sim}{A}_F \\ \underset{\sim}{0} \\ \underset{\sim}{A}_R \end{Bmatrix} \tag{3.1-11}$$

and asterisk superscripts denote condensed arrays. Vectors $\underset{\sim}{A}_P$ and $\underset{\sim}{A}_M$, representing applied forces at P and M displacement coordinates, are assumed zero for simplicity. Condensed matrix $\underset{\sim}{S}^*_J$ is obtained by solving for $\underset{\sim}{D}_P$ in the first of equations (3.1-8) as

$$\underset{\sim}{D}_P = \underset{\sim}{S}^{-1}_{PP} \left(-\underset{\sim}{S}'_{FP}\underset{\sim}{D}_F - \underset{\sim}{S}_{PM}\underset{\sim}{D}_M - \underset{\sim}{S}_{PR}\underset{\sim}{D}_R\right) \tag{3.1-12}$$

and substituting this expression into the remaining equations. Only condensed matrices on and above the diagonal of $\underset{\sim}{S}^*_J$ are actually computed due to symmetry. The form of $\underset{\sim}{S}^*_{FF}$, for example, is

$$\underset{\sim}{S}^*_{FF} = \underset{\sim}{S}_{FF} - \underset{\sim}{S}_{FP}\underset{\sim}{S}^{-1}_{PP}\underset{\sim}{S}'_{FP} \tag{3.1-13}$$

In the next stage of condensation, static equilibrium equations (3.1-9) for F, M, and R degrees of freedom are reduced to final form, retaining only F and R types, yielding

$$\underset{\sim}{S}^{**}_J \underset{\sim}{D}_{J_2} = \underset{\sim}{A}_{J_2} \tag{3.1-14}$$

where

$$\underset{\sim}{S}^{**}_J = \begin{bmatrix} \underset{\sim}{S}^{**}_{FF} & \underset{\sim}{S}^{**}_{FR} \\ \underset{\sim}{S}^{**}_{RF} & \underset{\sim}{S}^{**}_{RR} \end{bmatrix} \tag{3.1-15}$$

and

$$\underset{\sim}{D}_{J_2} = \begin{Bmatrix} \underset{\sim}{D}_F \\ \underset{\sim}{D}_R \end{Bmatrix}, \quad \underset{\sim}{A}_{J_2} = \begin{Bmatrix} \underset{\sim}{A}_F \\ \underset{\sim}{A}_R \end{Bmatrix} \tag{3.1-16}$$

Here, an expression for displacement vector $\underset{\sim}{D}_M$ was obtained by solving the second of equations (3.1-9) with the result

$$\underset{\sim}{D}_M = \underset{\sim}{S}^{*-1}_{MM} \left(-\underset{\sim}{S}^{*\prime}_{FM}\underset{\sim}{D}_F - \underset{\sim}{S}^{*}_{MR}\underset{\sim}{D}_R\right) \tag{3.1-17}$$

Substituting this expression into the remaining equations produced Equation (3.1-14). The forms of the $\underset{\sim}{S}^{**}_J$ submatrices are:

$$\underset{\sim}{S}^{**}_{FF} = \underset{\sim}{S}^{*}_{FF} - \underset{\sim}{S}^{*}_{FM}\underset{\sim}{S}^{*-1}_{MM}\underset{\sim}{S}^{\prime}_{FM} \tag{3.1-18}$$

$$\underset{\sim}{S}^{**}_{FR} = \underset{RF}{S}^{**\prime} = \underset{\sim}{S}^{*}_{FR} - \underset{\sim}{S}^{*}_{FM}\underset{\sim}{S}^{*-1}_{MM}\underset{\sim}{S}^{*}_{MR} \tag{3.1-19}$$

$$\underset{\sim}{S}^{**}_{RR} = \underset{\sim}{S}^{*}_{RR} - \underset{\sim}{S}^{*\prime}_{MR}\underset{\sim}{S}^{*-1}_{MM}\underset{\sim}{S}^{*}_{MR} \tag{3.1-20}$$

where array $\underset{\sim}{S}^{**}_{FF}$, for example, represents holding forces at F degrees of freedom due to unit displacements at F degrees of freedom in a partially restrained structure with P and M displacement types allowed to occur freely.

With the condensation of $\underset{\sim}{S}^{*}_J$ complete, mass matrix $\underset{\sim}{M}_J$ can be reduced to $\underset{\sim}{M}^{*}_J$ and then to $\underset{\sim}{M}^{**}_J$ in parallel fashion, removing first P and then M displacement terms. The equations of motion after elimination of P types have the form

$$\underset{\sim}{M}^{*}_J \ddot{\underset{\sim}{D}}_{J_1} + \underset{\sim}{S}^{*}_J \underset{\sim}{D}_{J_1} = \underset{\sim}{A}_{J_1} \tag{3.1-21}$$

where $\underset{\sim}{M}^{*}_J$ is similar in form to $\underset{\sim}{S}^{*}_J$ above. After elimination of M types, the final reduced set of undamped equations of motion are

$$\underset{\sim}{M}^{**}_J \ddot{\underset{\sim}{D}}_{J_2} + \underset{\sim}{S}^{**}_J \underset{\sim}{D}_{J_2} = \underset{\sim}{A}_{J_2} \tag{3.1-22}$$

where

$$\underset{\sim}{M}^{**}_J = \begin{bmatrix} \underset{\sim}{M}^{**}_{FF} & \underset{\sim}{M}^{**}_{FR} \\ \underset{\sim}{M}^{**}_{RF} & \underset{\sim}{M}^{**}_{RR} \end{bmatrix} \tag{3.1-23}$$

Condensation of $\underset{\sim}{M}_J$ to $\underset{\sim}{M}^*_J$ is accomplished by equating the virtual work of the inertia forces in equations (3.1-6) and (3.1-21), as discussed by Guyan (91), with the result

$$\underset{\sim}{M}^*_J = \underset{\sim}{T}'_P \, \underset{\sim}{M}_J \, \underset{\sim}{T}_P \tag{3.1-24}$$

where

$$\underset{\sim}{T}_P = \begin{bmatrix} \underset{\sim}{I} & \underset{\sim}{0} & \underset{\sim}{0} \\ -\underset{\sim}{S}^{-1}_{PP}\underset{\sim}{S}'_{FP} & -\underset{\sim}{S}^{-1}_{PP}\underset{\sim}{S}_{PM} & -\underset{\sim}{S}^{-1}_{PP}\underset{\sim}{S}_{PR} \\ \underset{\sim}{0} & \underset{\sim}{I} & \underset{\sim}{0} \\ \underset{\sim}{0} & \underset{\sim}{0} & \underset{\sim}{I} \end{bmatrix} \tag{3.1-25}$$

Stiffness array products in $\underset{\sim}{T}_P$ are available from condensation of $\underset{\sim}{S}_J$ to $\underset{\sim}{S}^*_J$, and $\underset{\sim}{I}$ and $\underset{\sim}{0}$ are identity and null matrices, respectively, of appropriate size. In the second condensation stage, inertia terms in equations (3.1-21) and (3.1-22) are made energy equivalent with the result

$$\underset{\sim}{M}^{**}_J = \underset{\sim}{T}'_M \, \underset{\sim}{M}^*_J \, \underset{\sim}{T}_M \tag{3.1-26}$$

where

$$\underset{\sim}{T}_M = \begin{bmatrix} \underset{\sim}{I} & \underset{\sim}{0} \\ -\underset{\sim}{S}^{*-1}_{MM}\underset{\sim}{S}^{*\prime}_{FM} & -\underset{\sim}{S}^{*-1}_{MM}\underset{\sim}{S}^*_{MR} \\ \underset{\sim}{0} & \underset{\sim}{I} \end{bmatrix} \tag{3.1-27}$$

Stiffness array products in $\underset{\sim}{T}_M$ were generated during the reduction of $\underset{\sim}{S}^*_J$ to $\underset{\sim}{S}^{**}_J$ (See equations 3.1-18, 3.1-19.). If the transformation in equation (3.1-26) is carried out, the explicit expression for $\underset{\sim}{M}^{**}_{FF}$, for example, is:

$$\underset{\sim}{M}^{**}_{FF} = \underset{\sim}{M}^*_{FF} + \underset{\sim}{M}^*_{FM}(-\underset{\sim}{S}^{*-1}_{MM}\underset{\sim}{S}^{*\prime}_{FM}) + (-\underset{\sim}{S}^{*-1}_{MM}\underset{\sim}{S}^{*\prime}_{FM})'\underset{\sim}{M}^{*\prime}_{FM} + (-\underset{\sim}{S}^{*-1}_{MM}\underset{\sim}{S}^{*\prime}_{FM})'\underset{\sim}{M}^*_{MM}(-\underset{\sim}{S}^{*-1}_{MM}\underset{\sim}{S}^{*\prime}_{FM}) \tag{3.1-28}$$

At the end of the assembly and condensation procedures, only arrays $\underset{\sim}{S}^{**}_J$ and $\underset{\sim}{M}^{**}_J$ remain reflecting the elastic and inertial force coupling, respectively, among selected master (F type) and restraint (R type) displacement coordinates. Using these arrays, static and dynamic analyses of the reduced structure model may now be performed.

3.1(c) Static Analysis Procedures

The basic static equilibrium equations for the condensed structure model were presented above in equations (3.1-14), (3.1-15) and (3.1-16). If the double asterisk superscripts (denoting two stages of condensation) are dropped to simplify the notation, the equations can be written as

$$\begin{bmatrix} \underset{\sim}{S}_{FF} & \underset{\sim}{S}_{FR} \\ \underset{\sim}{S}'_{FR} & \underset{\sim}{S}_{RR} \end{bmatrix} \begin{Bmatrix} \underset{\sim}{D}_F \\ \underset{\sim}{D}_R \end{Bmatrix} = \begin{Bmatrix} \underset{\sim}{A}_F \\ \underset{\sim}{A}_R \end{Bmatrix} \qquad (3.1\text{-}29)$$

where $\underset{\sim}{D}_F$ = vector of static nodal displacements at master degrees of freedom (F types), $\underset{\sim}{D}_R$ = vector of specified restraint displacements at panel or frame supports, $\underset{\sim}{A}_F$ = vector of applied nodal loads at F types, and $\underset{\sim}{A}_R$ = vector of support reactions. As many master degrees of freedom on the panel as desired can be retained to characterize the load distribution and displaced configuration of the panel. Distributed loadings must be replaced by equivalent concentrated nodal loads $\underset{\sim}{A}_F$ at F type displacement coordinates, and points of application of concentrated loads should have F degrees of freedom associated with them. Support displacements $\underset{\sim}{D}_R$ can be specified if panel response to racking displacements is of interest.

Solution for Nodal Displacements: In the stiffness method of analysis, displacements at structure nodes are the basic unknowns. Displacements at master degrees of freedom $\underset{\sim}{D}_F$ due to applied nodal loads $\underset{\sim}{A}_F$ and specified

support motions $\underset{\sim}{D}_R$ are obtained by solving the first of matrix equations (3.1-29) as follows:

$$\underset{\sim}{D}_F = \underset{\sim}{S}_{FF}^{-1}(\underset{\sim}{A}_F - \underset{\sim}{S}_{FR}\underset{\sim}{D}_R) \qquad (3.1\text{-}30)$$

Then, the second of equations (3.1-29) yields the support reaction forces

$$\underset{\sim}{A}_R = \underset{\sim}{S}_{FR}'\underset{\sim}{D}_F + \underset{\sim}{S}_{RR}\underset{\sim}{D}_R \qquad (3.1\text{-}31)$$

If static frame displacements at M type degrees of freedom are of interest, equation (3.1-17) can be solved to obtain displacement vector $\underset{\sim}{D}_M$ in the backward substitution phase of the analysis. Finally, unknown panel displacements $\underset{\sim}{D}_P$ are found from equation (3.1-12). With all frame and panel displacements known, frame member end forces and panel element stresses can be computed as discussed below.

Solution for Member Forces and Stresses: If the member stiffness matrix for any frame member i is referred to as $\underset{\sim}{S}_i$, the forces $\underset{\sim}{A}_i$ at member ends, corresponding to the member degrees of freedom in Figure (3.1-3), can be computed as

$$\underset{\sim}{A}_i = \underset{\sim}{S}_i\underset{\sim}{D}_i \qquad (3.1\text{-}32)$$

where $\underset{\sim}{D}_i$ = vector of displacements at the j and k ends of member i assembled from vectors $\underset{\sim}{D}_M$ and $\underset{\sim}{D}_R$.

Likewise, stresses may be computed within any panel finite element once nodal displacements are known for that element. Recall that the generic displacements $\underset{\sim}{u}$ at any point within the element depend upon the nodal displacements $\underset{\sim}{q}$ as follows:

$$\underset{\sim}{u} = \underset{\sim}{T}_1\underset{\sim}{q} \qquad (3.1\text{-}1) \text{ repeated}$$

where $\underset{\sim}{T}_1$ is the shape function matrix for the element and $\underset{\sim}{q}$ is assembled

from displacement vectors $\underset{\sim}{D}_F$ and $\underset{\sim}{D}_P$ (equations (3.1-30) and (3.1-12)). Element generic and nodal displacements are related to element strains,

$$\underset{\sim}{\varepsilon} = \underset{\sim}{T}_2\underset{\sim}{u} = \underset{\sim}{T}_2\underset{\sim}{T}_1\underset{\sim}{q} = \underset{\sim}{B}\underset{\sim}{q} \tag{3.1-33}$$

and element strains are related to element stresses,

$$\underset{\sim}{\sigma} = \underset{\sim}{T}_3\underset{\sim}{\varepsilon} = \underset{\sim}{T}_3\underset{\sim}{T}_2\underset{\sim}{T}_1\underset{\sim}{q} = \underset{\sim}{T}_3\underset{\sim}{B}\underset{\sim}{q} \tag{3.1-34}$$

at any point within the element. Vectors $\underset{\sim}{\varepsilon}$ and $\underset{\sim}{\sigma}$ are the strain and stress vectors, respectively, expressed as

$$\underset{\sim}{\sigma} = \begin{Bmatrix} \sigma_x \\ \sigma_y \\ \tau_{xy} \end{Bmatrix}, \quad \underset{\sim}{\varepsilon} = \begin{Bmatrix} \varepsilon_x \\ \varepsilon_y \\ \gamma_{xy} \end{Bmatrix} \tag{3.1-35}$$

where σ and ε represent normal stress and strain components, and τ and γ shear stress and strain components in the x-y plane. If plate bending and plane stress effects are superimposed, strain component ε_x, for example, may be computed in the following manner:

$$\varepsilon_x = \left(\frac{\partial u_2}{\partial x}\right)_{\text{plate bending}} + \left(\frac{\partial u_2}{\partial x}\right)_{\text{plane stress}}$$

$$= -z\,\frac{\partial^2 u_1}{\partial x^2} + \frac{\partial u_2}{\partial x} \tag{3.1-36}$$

where u_1 and u_2 are the element generic displacements shown in Figure 3.1-2.

Matrix $\underset{\sim}{T}_2$ above is a matrix of derivatives and $\underset{\sim}{B}$ is the strain-displacement matrix. Matrix $\underset{\sim}{T}_3$ is the stress-strain matrix expressed as

$$\underset{\sim}{T}_3 = \frac{E}{1-\nu^2}\begin{bmatrix} 1 & & 0 \\ & 1 & 0 \\ 0 & 0 & \frac{1-\nu}{2} \end{bmatrix} \tag{3.1-37}$$

for two-dimensional plane stress problems, where E is the modulus of elasticity and ν is Poisson's ratio for the element.

The basic approach outlined above for obtaining stresses or stress resultants in frame and panel members in a static problem may be used to compute stress-time histories in a dynamics problem. In this case, displacement vectors $\underset{\sim}{D}_F$, $\underset{\sim}{D}_P$, $\underset{\sim}{D}_M$, and $\underset{\sim}{D}_R$ represent the displaced configuration of the structure at any selected time of interest during dynamic response, and are used to assemble vectors $\underset{\sim}{D}_i$ and $\underset{\sim}{q}$ in equations (3.1-32) and (3.1-1) as described in the next section.

3.1(d) Dynamic Analysis Procedures

The undamped equations of motion for master (F) and restrained (R) displacement coordinates in the condensed structure model were presented earlier in equation (3.1-22) which is repeated here in partitioned form

$$\begin{bmatrix} \underset{\sim}{M}_{FF} & \underset{\sim}{M}_{FR} \\ \underset{\sim}{M}'_{FR} & \underset{\sim}{M}_{RR} \end{bmatrix} \begin{Bmatrix} \ddot{\underset{\sim}{D}}_F \\ \ddot{\underset{\sim}{D}}_R \end{Bmatrix} + \begin{bmatrix} \underset{\sim}{S}_{FF} & \underset{\sim}{S}_{FR} \\ \underset{\sim}{S}'_{FR} & \underset{\sim}{S}_{RR} \end{bmatrix} \begin{Bmatrix} \underset{\sim}{D}_F \\ \underset{\sim}{D}_R \end{Bmatrix} = \begin{Bmatrix} \underset{\sim}{A}_F \\ \underset{\sim}{A}_R \end{Bmatrix} \qquad (3.1\text{-}38)$$

with asterisk superscripts omitted for simplicity. If the first of these equations is considered and applied forces $\underset{\sim}{A}_F$ and support motions $\ddot{\underset{\sim}{D}}_R$ and $\underset{\sim}{D}_R$ are assumed to be zero, the equation of motion governing undamped free vibration of the structure results:

$$\underset{\sim}{M}_{FF}\ddot{\underset{\sim}{D}}_F + \underset{\sim}{S}_{FF}\underset{\sim}{D}_F = \underset{\sim}{0} \qquad (3.1\text{-}39)$$

This equation characterizes the free vibration behavior of an ideal elastic structure which, if properly disturbed, will execute harmonic motion in a natural mode of vibration. Each natural mode i has a natural frequency p_i and a characteristic shape $\underset{\sim}{X}_{M_i}$, with the number of frequencies

and mode shapes equal to the number of master degrees of freedom.

The solution of equation (3.1-39) is of the form

$$\underset{\sim}{D}_{F_i} = \underset{\sim}{X}_{M_i} \sin (p_i t + \phi_i) \qquad (3.1\text{-}40)$$

where $\underset{\sim}{D}_{F_i}$ is the nodal displacement vector for master degrees of freedom in the i-th mode and ϕ_i is the i-th mode phase angle. Substitution of equation (3.1-40) into equation (3.1-39) yields

$$\underset{\sim}{S}_{FF} \underset{\sim}{X}_{M_i} = p_i^2 \underset{\sim}{M}_{FF} \underset{\sim}{X}_{M_i} \qquad (3.1\text{-}41)$$

the algebraic eigenvalue problem in nonstandard form in which p_i^2 is the i-th mode eigenvalue and $\underset{\sim}{X}_{M_i}$ the i-th mode eigenvector. Solution of equation (3.1-41) gives frequencies p_i and modal amplitudes $\underset{\sim}{X}_{M_i}$.

Solution of Equations of Motion: The normal mode method is a widely used technique for solution of the equations of motion for linear systems. In this approach, the system displacement ($\underset{\sim}{D}_F$) and acceleration ($\ddot{\underset{\sim}{D}}_F$) response can be determined by transforming to normal coordinates where arrays $\underset{\sim}{M}_{FF}$ and $\underset{\sim}{S}_{FF}$ are diagonal. The multi-degree of freedom system is reduced to a set of equivalent single degree of freedom oscillators whose damped responses are readily determined. The structure response in the original coordinate system is obtained by a back transformation from normal coordinates. Finally, reactions $\underset{\sim}{A}_R$ at supports for all times of interest can be determined from the second set of matrix equations (3.1-38).

It is the orthogonality property of the eigenvectors that permits the transformation of the equations of motion to normal coordinates. Orthogonality with respect to $\underset{\sim}{M}_{FF}$ means that, for any two modes i and j with $i \neq j$,

$$\underset{\sim}{X}'_{M_j} \underset{\sim}{M}_{FF} \underset{\sim}{X}_{M_i} = 0 \qquad (3.1\text{-}42)$$

When i = j,

$$\underset{\sim}{X}'_{M_j} \underset{\sim}{M}_{FF} \underset{\sim}{X}_{N_j} = Q_j \qquad (3.1\text{-}43)$$

where Q_j is an arbitrary constant which can be set to unity by normalizing the eigenvectors with respect to the mass matrix such that

$$\underset{\sim}{X}'_{N_j} \underset{\sim}{M}_{FF} \underset{\sim}{X}_{N_j} = 1 \qquad (3.1\text{-}44)$$

Vector $\underset{\sim}{X}_{N_j}$ denotes the normalized eigenvector for the j-th vibration mode. It follows that

$$\underset{\sim}{X}'_{N} \underset{\sim}{M}_{FF} \underset{\sim}{X}_{N} = \underset{\sim}{I} \qquad (3.1\text{-}45)$$

and

$$\underset{\sim}{X}'_{N} \underset{\sim}{S}_{FF} \underset{\sim}{X}_{N} = \underset{\sim}{p}^2 \qquad (3.1\text{-}46)$$

where $\underset{\sim}{I}$ is the identity matrix and $\underset{\sim}{p}^2$ is the spectral matrix containing terms p_i^2 along its diagonal. Array $\underset{\sim}{X}_N = \{\underset{\sim}{X}_{N_1} \underset{\sim}{X}_{N_2} \ldots \underset{\sim}{X}_{N_j} \ldots \underset{\sim}{X}_{N_n}\}$ is the normalized modal matrix composed of the normalized eigenvectors for all n master degrees of freedom. Now, ignoring support motion terms in the first of equations (3.1-38) for the moment, orthogonality relationships (3.1-45) and (3.1-46) can be used to uncouple the equations of motion as follows:

$$\underset{\sim}{X}'_{N} \underset{\sim}{M}_{FF} \underset{\sim}{X}_{N} \underset{\sim}{X}_{N}^{-1} \ddot{\underset{\sim}{D}}_F + \underset{\sim}{X}'_{N} \underset{\sim}{S}_{FF} \underset{\sim}{X}_{N} \underset{\sim}{X}_{N}^{-1} \underset{\sim}{D}_F = \underset{\sim}{X}'_{N} \underset{\sim}{A}_F \qquad (3.1\text{-}47)$$

or

$$\ddot{\underset{\sim}{D}}_N + \underset{\sim}{p}^2 \underset{\sim}{D}_N = \underset{\sim}{F}_N \qquad (3.1\text{-}48)$$

where

$$\ddot{\underset{\sim}{D}}_N = \underset{\sim}{X}_N^{-1}\ddot{\underset{\sim}{D}}_F = \underset{\sim}{X}_N'\underset{\sim}{M}_{FF}\ddot{\underset{\sim}{D}}_F \tag{3.1-49a}$$

$$\underset{\sim}{D}_N = \underset{\sim}{X}_N^{-1}\underset{\sim}{D}_F = \underset{\sim}{X}_N'\underset{\sim}{M}_{FF}\underset{\sim}{D}_F \tag{3.1-49b}$$

$$\underset{\sim}{F}_N = \underset{\sim}{X}_N'\underset{\sim}{A}_F \tag{3.1-49c}$$

Simple modal damping may now be inserted into equations (3.1-48) to produce the i-th mode damped equation of motion

$$\ddot{D}_{N_i} + 2\gamma_i p_i \dot{D}_{N_i} + p_i^2 D_{N_i} = F_{N_i} \tag{3.1-50}$$

where γ_i is the fraction of critical damping in mode i. Solution of equation (3.1-50) provides the response in normal coordinates for each single degree of freedom oscillator. Finally, the system response in the original coordinates is obtained from equations (3.1-49a) and (3.1-49b) as

$$\ddot{\underset{\sim}{D}}_F = \underset{\sim}{X}_N\ddot{\underset{\sim}{D}}_N \tag{3.1-51a}$$

$$\underset{\sim}{D}_F = \underset{\sim}{X}_N\underset{\sim}{D}_N \tag{3.1-51b}$$

and support reactions $\underset{\sim}{A}_R$ are calculated using equation (3.1-38) in which $\underset{\sim}{D}_R$ and $\ddot{\underset{\sim}{D}}_R$ are either specified or zero. Further details may be found in reference (92).

Types of Loadings: While the basic solution procedure outlined above is quite straightforward, several details regarding various types of system excitations are worthy of specific mention. The most elementary case is concerned with transient response of the system due to initial conditions of displacement and velocity alone with forcing functions $\underset{\sim}{A}_F$ zero. In this case, vectors of initial displacements $\underset{\sim}{D}_0$ and velocities $\dot{\underset{\sim}{D}}_0$ at master

degrees of freedom are specified and are transformed to normal coordinates as follows:

$$\underset{\sim}{D}_{N_O} = \underset{\sim}{X}_N^{-1} \underset{\sim}{D}_O \tag{3.1-52a}$$

$$\dot{\underset{\sim}{D}}_{N_O} = \underset{\sim}{X}_N^{-1} \dot{\underset{\sim}{D}}_O \tag{3.1-52b}$$

where $\underset{\sim}{D}_{N_O}$ and $\dot{\underset{\sim}{D}}_{N_O}$ are the initial displacement and velocity vectors in normal coordinates. Equation (3.1-50), with F_{N_i} taken as zero, can now be solved to obtain the free vibration response in normal coordinates due to initial conditions $D_{N_{Oi}}$ and $\dot{D}_{N_{Oi}}$. Equations (3.1-51) provide acceleration and displacement response at master degrees of freedom in the original coordinate system.

Proportional loading is assumed for the case of applied forcing functions $\underset{\sim}{A}_F$ at master degrees of freedom. Therefore, $\underset{\sim}{A}_F$ can be expressed as the product of a matrix of load factors $\underset{\sim}{F}_M$, containing force amplitudes at master degrees of freedom, and normalized force-time histories $\underset{\sim}{F}(t)$ as follows:

$$\underset{\sim}{A}_F = \underset{\sim}{F}_M \underset{\sim}{F}(t) \tag{3.1-53}$$

where example time-histories for x and y direction forces are shown in Figure (3.1-5). The time-histories are taken to be piecewise-linear functions of time which can be treated as a succession of trapezoidal pulses for computational purposes. Vector $\underset{\sim}{A}_F$ is transformed to normal coordinates as shown in equation (3.1-49c) to produce the following expression for normal coordinate forces:

$$\underset{\sim}{F}_N = \underset{\sim}{X}_N' \underset{\sim}{F}_M \underset{\sim}{F}(t) \tag{3.1-54}$$

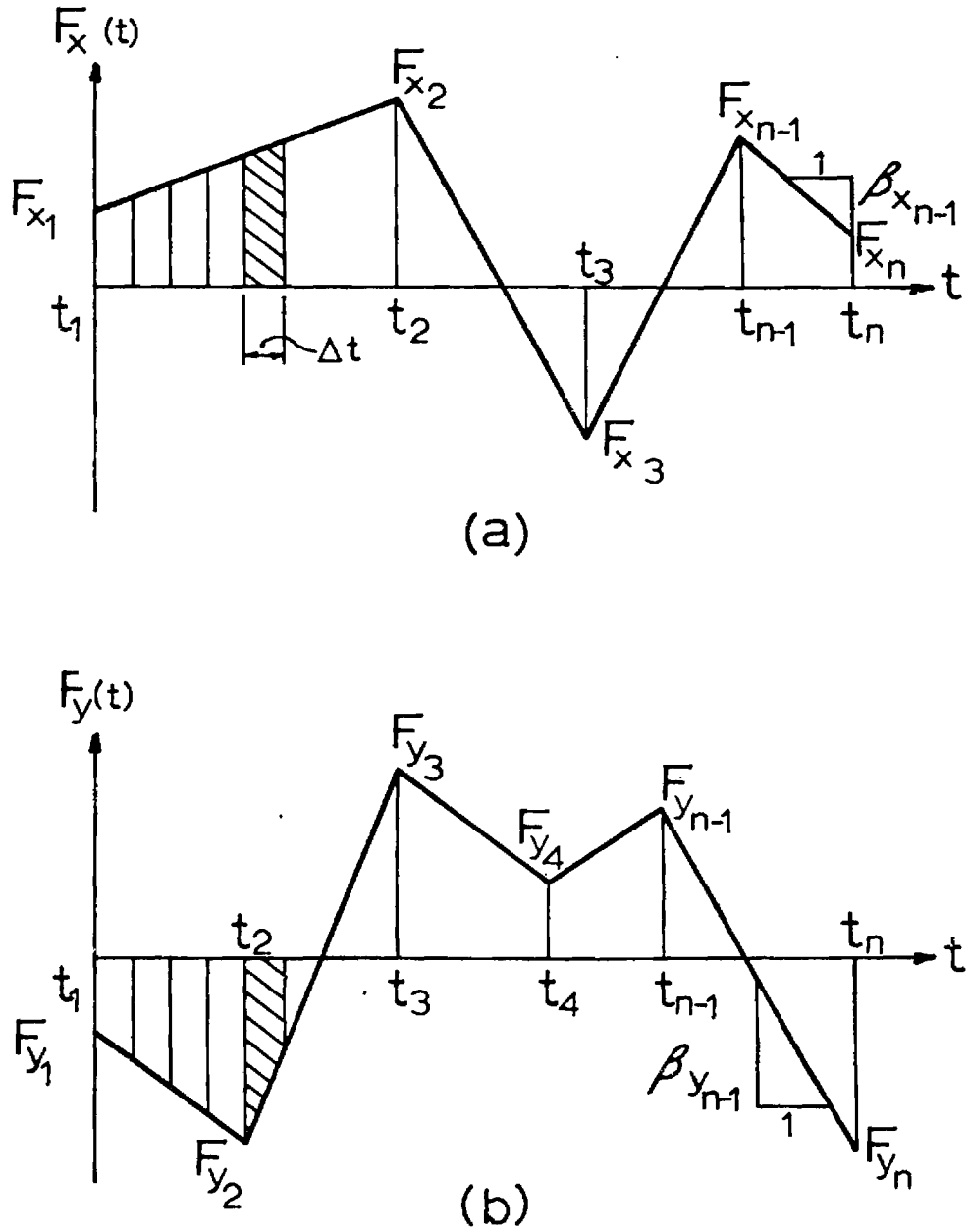

Figure 3.1-5 Piecewise-Linear Forcing Functions

These forces are used in equation (3.1-50) to determine normal mode response and equations (3.1-51) are used to obtain system response in the original coordinate system.

If the response of the structure to the acceleration of a rigid-body support system is sought, a new expression for the normal coordinate forces must be developed for use in the normal mode solution procedure described above. In this case, the vector $\ddot{D}_R$ of independent restraint accelerations degenerates to $\ddot{D}_G$ which describes the accelerations of the rigid body support system as piecewise-linear functions of time. Structure response is calculated relative to the supports and the equations of motion must be expressed in relative coordinates. Let r equal displacements at master degrees of freedom due to unit support motions. Then, from equation (3.1-29),

$$r = -S_{FF}^{-1} S_{FR} \tag{3.1-55}$$

and relative motions of master degrees of freedom can be expressed as

$$D_F^* = D_F - rD_G \tag{3.1-56a}$$

$$\ddot{D}_F^* = \ddot{D}_F - r\ddot{D}_G \tag{3.1-56b}$$

Writing the first of equations (3.1-38), with A_F zero, in relative coordinates gives

$$M_{FF}\ddot{D}_F^* + S_{FF}D_F^* = -(M_{FF}r + M_{FR})\ddot{D}_G \tag{3.1-57}$$

If this equation is transformed to normal coordinates, the appropriate normal coordinate forces are

$$F_N = -X_N'(M_{FF}r + M_{FR})\ddot{D}_G \tag{3.1-58}$$

and the normal mode response analysis may be performed using equation (3.1-50).

The final type of excitation to be considered is the case of arbitrary independent motion of multiple supports. In this case, support racking motions are specified as piecewise-linear functions using vectors $\underset{\sim}{D}_R$ and $\ddot{\underset{\sim}{D}}_R$ and total response at master degrees of freedom is obtained using the first of equations (3.1-38). Rearrangement of this equation gives

$$\underset{\sim}{M}_{FF}\ddot{\underset{\sim}{D}}_F + \underset{\sim}{S}_{FF}\underset{\sim}{D}_F = -\underset{\sim}{M}_{FR}\ddot{\underset{\sim}{D}}_R - \underset{\sim}{S}_{FR}\underset{\sim}{D}_R \qquad (3.1\text{-}59)$$

Transformation to normal coordinates produces normal coordinate forces

$$\underset{\sim}{F}_N = -\underset{\sim}{X}'_N\underset{\sim}{M}_{FR}\ddot{\underset{\sim}{D}}_R - \underset{\sim}{X}'_N\underset{\sim}{S}_{FR}\underset{\sim}{D}_R \qquad (3.1\text{-}60)$$

and normal mode response analysis proceeds with equation (3.1-50).

Backward substitution operations can be used in all of the cases discussed above to determine remaining frame and panel displacements and stresses at selected times of interest in the dynamic analysis. The solution for nodal displacements, member forces and panel stresses then follows the procedures outlined in the static analysis section above.

3.2 Computer Program

3.2(a) Description

A FORTRAN computer program, WINDOW, was developed during the course of this research program to evaluate the static and dynamic response of a wide range of glass panels of varying size and support conditions. This program, containing approximately 4200 source statements, implements the finite element model described earlier. All program development and de-

bugging was performed on Georgia Tech's CDC Cyber 74 digital computer. Disk storage is used extensively to save matrix condensation products for later use in the backsubstitution phase of static and dynamic problem solutions.

Program WINDOW is quite versatile and may perform any of a variety of tasks. The program can be used to:

1. Generate stiffness and mass arrays for a finite element model of a panel alone or of a window-framework assembly supported in an arbitrary manner;

2. Develop the framework model with or without elastic connections to account for joint flexibility;

3. Construct a reduced dynamic model of the structure, with arbitrarily-selected master degrees of freedom on the panel, while retaining the ability to compute all panel displacements and stresses through backsubstitution if desired;

4. Compute displacements, stresses, and reactions for applied static loadings or support movements;

5. Compute displacements, stresses, and reactions for applied dynamic nodal loads, time-dependent support displacements and accelerations, or initial conditions of displacement and velocity;

6. Print and/or plot response quantities of interest.

A macro-flow chart and a data input guide for WINDOW are contained in the following sections. Sample analyses using the program are presented in the discussion of results.

3.2(b) Macro-Flow Chart

Figure 3.2-1 contains a macro-flow chart showing the basic organiza-

Figure 3.2-1 Macro-Flow Chart of Program WINDOW

1. Read in number (NS) of structures to be analyzed.

Initialize structure number

2. Start loop on structural number

3. Read in structure data for structure number SN

Initialize code variable for stiffness and mass assemblage

4. Begin loop for assemblage of stiffness (ISM = 1) and mass (ISM = 2) matrices

Omit mass matrix assemblage for static problems (ISDA = 0)

Omit mass matrix assemblage if lumped mass matrix is input directly (MCODE = 3)

5. Form panel stiffness (ISM = 1) and mass (ISM = 2) submatrices

Test for existence of boundary frame

6. Form frame stiffness (ISM = 1) and mass (ISM = 2) submatrices

Test for existence of elastic spring members

7. Add spring stiffness terms to structure stiffness submatrices

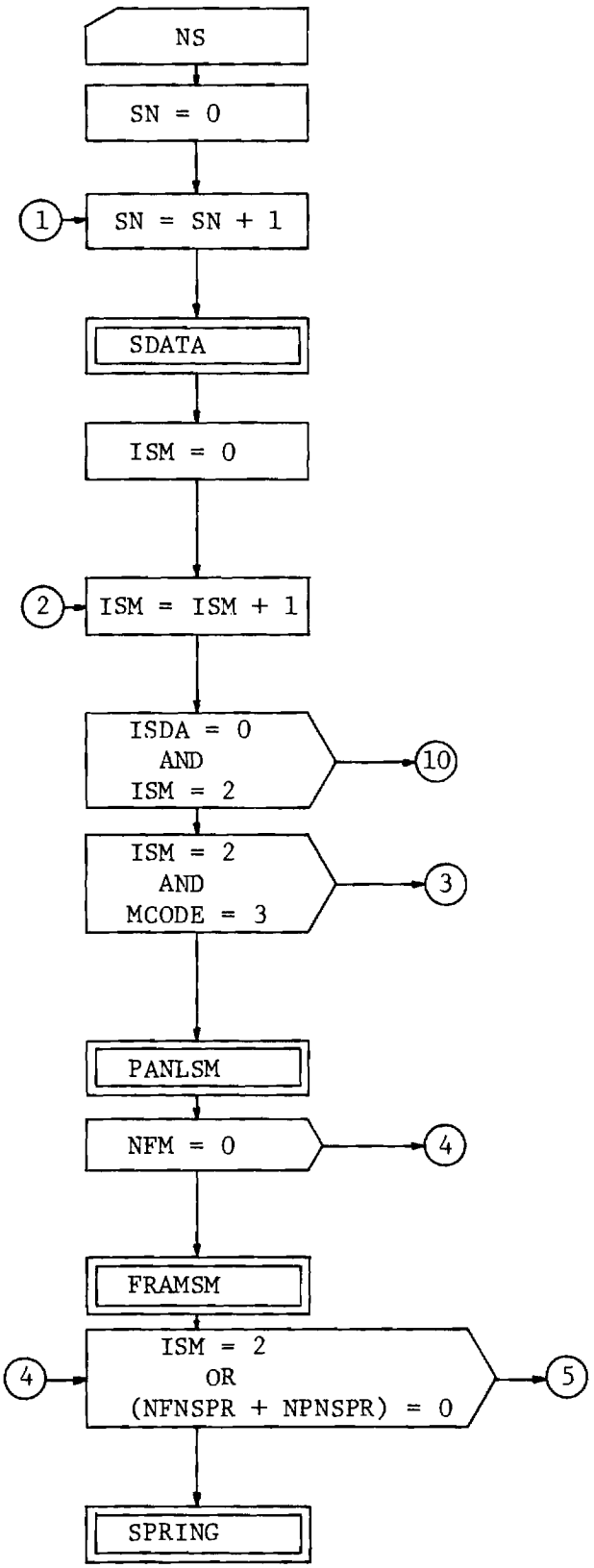

Figure 3.2-1--Cont'd.

8. Condense stiffness (ISM = 1) and mass (ISM = 2) matrices

9. Form mass arrays from direct input data if MCODE = 3

10. Save stiffness subarrays on mass storage prior to mass matrix assemblage

11. Determine structure frequencies, mode shapes, and dynamic response

12. Determine all static nodal displacements and element stresses

13. Test for last structure

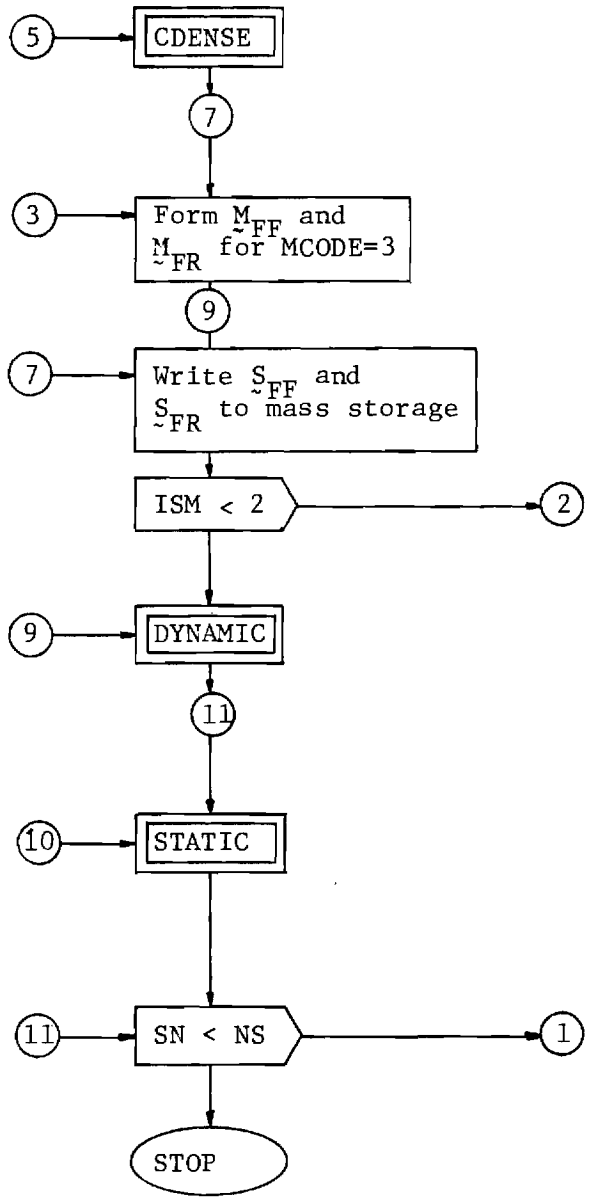

tional layout of the program. Double-lined boxes indicate subprograms and descriptive comments show program operations and flow. A listing of the program is contained in the Appendix.

3.2(c) Notation and Input Guide

Key program variables are defined in Table 3.2-1. A data input user's guide is provided in Table 3.2-2.

3.3 Discussion of Results

The discrete element analytical model and computer program were used to conduct parametric studies of the static and dynamic performance of insulating windows typical of those employed in the field study building. The initial objective of these studies was to construct a model of a single panel, including mullion and spandrel elements, between floor levels and to adjust model properties until a satisfactory comparison was achieved between measured field and laboratory data and computer program results for the analytical model. This task was not viewed as a system identification problem, however, and formal parameter estimation procedures were not used. Rather, each of the model properties, such as gasket spring constant values and framework area moments of inertia, was varied in turn and the response sensitivity of the model recorded. Model properties were then adjusted in steps until displacements and frequencies were reasonably close to measured laboratory values. System properties which had relatively more influence on panel displacement or frequency response were studied further for varying panel aspect ratios. The results of these more in-depth sensitivity studies are presented in the form of nondimensional curves showing panel response versus selected panel, frame, and gasket properties and panel aspect ratios.

Table 3.2-1 Notation for Program WINDOW

Variable	Definition
A( )	frame member cross-sectional area
AF( )	nodal load vector
AX( ), AY( ), AZ( )	x, y, z accelerations
DENSP, DENSF	panel and frame mass densities
DR( )	support displacements
D1	response calculation time interval
EP,EF	elastic moduli for panel and frame
EZJ( ), EZK( ), EYJ( ), EYK( )	elastic connection parameters
FX( ), FY( ), FZ( )	forcing function time histories
G( )	modal damping ratios
I	member number
IAF	forcing function code
ICNTY(,)	counter-clockwise element node numbers
IDTH,IDMAX	codes to print displacement time history and maximum response
IFM( )	frame member type code
IGA	support acceleration code
IND, INV	initial displacement and velocity codes
IREAC, ISTRES	codes for reaction and stress calculations
IREP( )	code for repeated finite elements
ISD	support displacement code
ISDA	indicator for static (0) or dynamic (1) problem
IX( ), IY( ), IZ( )	frame area moments of inertia
J	joint number
JJ( )	joint at j end of frame member
JK( )	joint at k end of frame member
JPN( )	panel node number
JRL( )	frame joint restraint list
K	joint number
KS(,)	spring stiffness constants
LF( )	load factors at nodes

Table 3.2-1--Cont'd.

Variable	Definition
MCODE	mass assemblage type code
MP( ), MF( )	added lumped masses at panel and frame nodes
NDLC	number of dynamic loading conditions
NFJ	number of frame joints
NFJSD	number of frame joints with support displacements
NFM	number of frame members
NFL( )	panel master degree of freedom list
NFNSPR	number of frame nodes with attached springs
NFT	number of F displacement types
NFR	number of frame restraints
NJPLOT	number frame displacement-time history plots
NLN	number of loaded nodes
NMEC	number of frame members with elastic connections
NMODES	number of modes in response analysis
NNIND, NNINV	number of nodes with initial displacements, velocities specified
NNLF	number of nodes with load factors
NNPLOT	number of element displacement-time history plots
NNWFT	number of nodes with F displacement types
NPE	number of panel elements
NPN	number of panel nodes
NPNSD	number of panel nodes with specified support displacements
NPNSPR	number of panel nodes with springs
NPR	number of panel restraints
NRFJ	number of restrained frame joints
NRL( )	nodal restraint list
NRPN	number of restrained panel nodes
NS	number of structures to be analyzed
NSATI	number of static stress analysis times of interest
NSLC	number of static loading conditions
NTX, NTY, NTZ	number of time points in forcing function vectors
PRP, PRF	Poisson's ratio for panel and frame
PLIST( )	degree of freedom plot list

Table 3.2-1--Cont'd.

Variable	Definition
SKPO, SKL, SKN, SKR	elastic spring constants for gaskets
TITLE	descriptive problem title
TP	panel thickness
TX( ), TY( ), TZ( )	times corresponding to data points in FX, FY, FZ
UNITS	active units in problem for calculations
VOP	initial velocity vector
XP( ), YP( )	panel node coordinates
XF( ), YF( )	frame joint coordinates
XOP( )	initial displacement vector

Table 3.2-2 Input Data for Program WINDOW

Data		Restrictions
1.	NS	provide NS sets of data (all data free format)
2.	TITLE	
3.	UNITS	
4.	NPE, NFM, ISDA	
5.	NPN, NRPN, NPR, NNWFT, NFT, EP, PRP, DENSP, TP, MCODE	
6.	N, XP(N), YP(N), MP(N)	NPN cards
7.	K, (ICNTY(K,J)J=1,4), IREP(K)	NPE cards
8.	J, NFL(8J-7),...,NFL(8J)	NNWFT cards
9.	J, NRL(8J-7),...,NRL(8J)	If NRPN>0, NRPN cards
10.	NFJ, NFR, NRFJ, NMEC, EF, PRF, DENSF	If NFM>0
11.	J, XF(J), YF(J), MF(J)	If NFM>0, NFJ cards
12.	I, JJ(I), JK(I), A(I), IX(I), IY(I), IZ(I), IFM(I)	If NFM>0, NFM cards
13.	J, JRL(6J-5),..., JRL(6J)	If NFM>0, NRFJ cards
14.	I, EZJ(I), EZK(I), EYJ(I), EYK(I)	If NFM and NMEC>0, NMEC cards
15.	NFNSPR, NPNSPR	
16.	SKPO, SKL, SKN, SKR	If NFNSPR>0
17.	JPN(I), (KS(I,J),J=1,5)	If NPNSPR>0
	Static Load Data: Items 18 - 22	
18.	NSLC	If ISDA = 0
19.	NLN, NPNSD, NFJSD, IREAC, ISTRES	If ISDA = 0
20.	K, AF(8K-7),...,AF(8K)	If ISDA = 0 and NLN>0, NLN cards
21.	K, DR(6K-5),...,DR(6K)	If ISDA = 0 and NFJSD>0, NFJSD cards
22.	K, DR(8K-7),...,DR(8K)	If ISDA = 0 and NPNSD>0, NPNSD cards
	Dynamic Load Data: Items 23 - 48	
23.	NDLC	If ISDA = 1

Table 3.2-2--Cont'd.

Data		Restrictions
24.	IND, INV, IGA, IAF, ISD	If ISDA = 1 and NDLC > 0
25.	NMODES, NNPLOT, NJPLOT, IDTH, IDMAX	If ISDA = 1 and NDLC > 0
26.	N, PLIST(8N-7),...,PLIST(8N)	If ISDA = 1, NDLC > 0, and NNPLOT > 0, NNPLOT cards
27.	N, PLIST(6N-5),...,PLIST(6N)	If ISDA = 1, NDLC > 0, NJPLOT > 0, and NFM > 0, NJPLOT cards
28.	G( )	If ISDA = 1, and NDLC > 0
29.	NNIND	If ISDA = 1, NDLC > 0, and IND = 1
30.	N, XOP(8N-7),...,XOP(8N)	If ISDA = 1, NDLC > 0, and IND = 1, NNIND cards
31.	NNINV	If ISDA = 1, NDLC > 0, and INV = 1
32.	N, VOP(8N-7),...,VOP(8N)	If ISDA = 1, NDLC > 0, and INV = 1, NNINV cards
33.	NNLF	If ISDA = 1, NDLC > 0, and IAF = 1
34.	N, LF(8N-7),...,LF(8N)	If ISDA = 1, NDLC > 0, and IAF = 1, NNLF cards
35.	K, LF(8K-8),...,LF(8K)	*If ISDA = 1, NDLC > 0, ISD = 1, and NPR > 0, NRPN cards
36.	K, LF(6K-5),...,LF(6K)	*If ISDA = 1, NDLC > 0, ISD = 1, and NFR > 0, NRFJ cards
37.	NTX, NTY, NTZ, D1	If ISDA = 1, NDLC > 0
38.	FX( )	If ISDA = 1, NDLC > 0, NTX points
39.	AX( )	If ISDA = 1, NDLC > 0 and ISD = 1, NTX points
40.	TX( )	If ISDA = 1, NDLC > 0, NTX points
41.	FY( )	If ISDA = 1, NDLC > 0, NTY points
42.	AY( )	If ISDA = 1, NDLC > 0 and ISD = 1, NTY points
43.	TY( )	If ISDA = 1, NDLC > 0, NTY points
44.	FZ( )	If ISDA = 1, NDLC > 0, NTZ points
45.	AZ( )	If ISDA = 1, NDLC > 0 and ISD = 1, NTZ points
46.	TZ( )	If ISDA = 1, NDLC > 0, NTZ points
47.	NSATI, IREAC, ISTRES	If ISDA = 1, NDLC > 0
48.	PLIST( )	If ISDA = 1, NDLC > 0, NSATI points

* translational x, y, and z support motion only

Sample analyses in which model properties were adjusted to calibrate the analytical model are described first. Then, nondimensional ratios are defined and sensitivity analysis results presented for the static and dynamic response studies. Several displacement-time history plots showing the influence of key system parameters on dynamic response of the model are presented next. Finally, panel response to in-plane racking distortions caused by differential motions of adjacent floors is presented.

3.3(a) Sample Analyses

Model Description: Several finite element models of the panel-frame structure with different finite element meshes, properties, and boundary conditions were assembled, but that shown in Figure 3.3-1 produced the best correlation with experimental results and was used for most sensitivity studies. In this model, the x-z and y-z planes are planes of symmetry; therefore, only symmetric loadings, displacement patterns, and modes of vibration are considered. Appropriate symmetry boundary conditions are imposed along the x and y axes. Studies of the in-plane racking behavior of the system, however, employed a model in which symmetry was not considered. This model of the entire panel-frame structure between floor levels is described in Section 3.3(e).

The symmetry model features twelve finite elements, nine frame elements, and eight points of attachment of gasket spring elements at frame joints 1 to 8. Corresponding frame and panel nodes to which gasket springs are attached are assumed to have the same joint coordinates even though they are shown as distinct points in Figure 3.3-1. The frame is simply-supported at frame joint 9 but the length (L_e) of member 9 can be

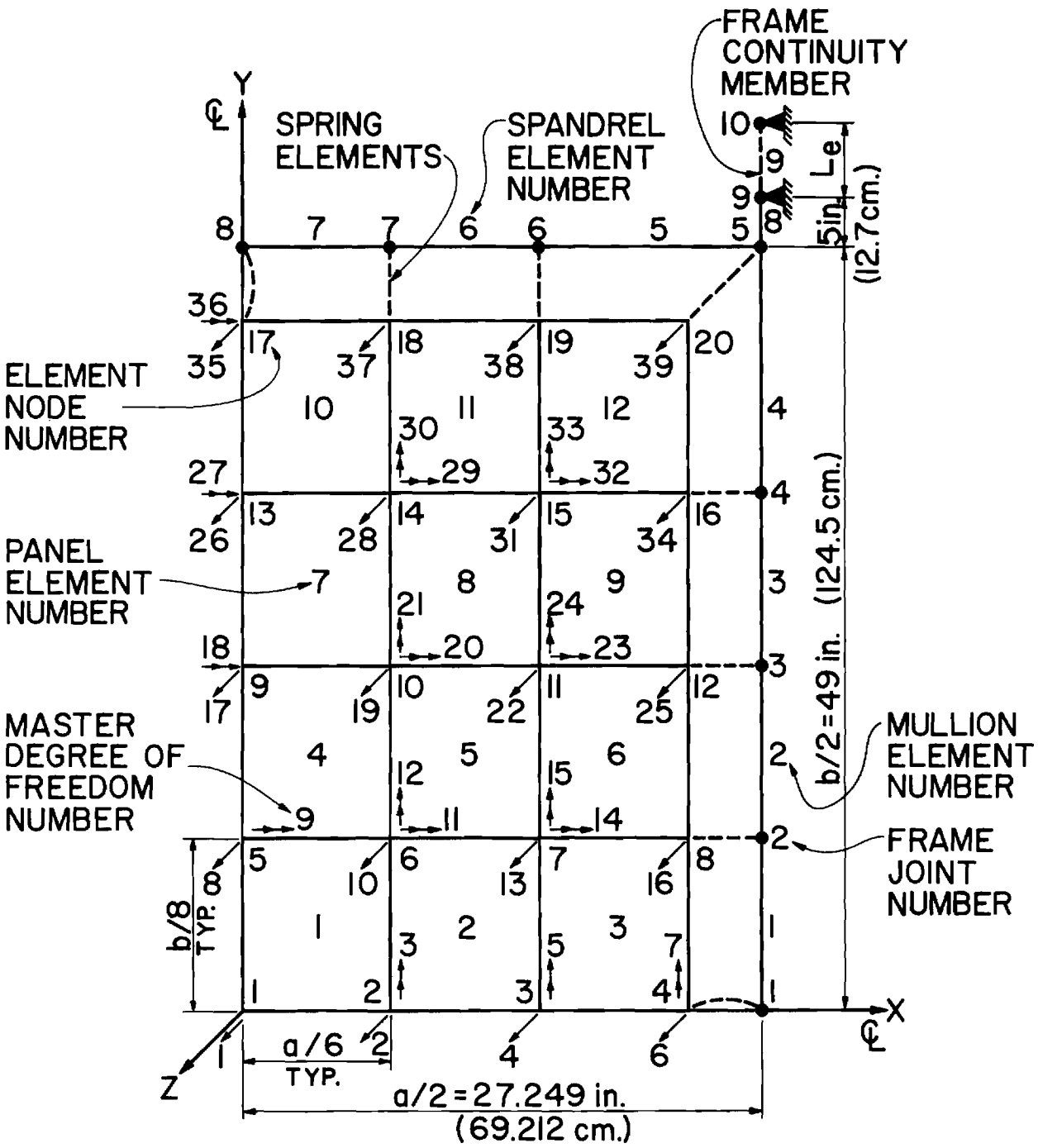

Figure 3.3-1 Finite Element Model of Quarter Panel

selected arbitrarily to provide values of rotational stiffness at joint 9 which lie between the extremes of zero (simple support) and infinity (fixed support). Length L_e is adjusted to simulate the effect of mullion continuity on panel response. If L_e is zero, member 9 is omitted from the frame and continuity is neglected. In addition, an elastic connection for rotation about the global y axis was inserted in frame member 5 at joint 5 to investigate the effect of a nonrigid spandrel-mullion connection on panel response.

Thirty-nine master degrees of freedom were selected from the 160 panel displacements available in the model. Enough master degrees of freedom must be chosen to ensure that distributed loadings, static displacement patterns, and vibration mode shapes are adequately represented.

The panel aspect ratio b/a was varied between 0.5 and 5.0 in the sensitivity studies with 1.8 being the actual ratio for insulating windows in the prototype structure. Discrete values of 0.5, 1.0, 1.8, 2.5, and 5.0 were selected. The area of the quarter panel model was held constant at 1335.2 in^2 (8614.2 cm^2) so that total load for distributed static pressure loadings and total panel mass would remain constant for static and dynamic sensitivity studies.

Model Properties: Elastic constants, mass densities, cross-sectional areas and area moments of inertia of frame members, and gasket spring constants are summarized in Table 3.3-1. Area moments of inertia are taken with respect to x-y-z axes in the member cross-section which are parallel to the coordinate axes in Figure 3.3-1. Gasket spring constant values are expressed as spring constant per unit length of boundary and are arranged as shown in Figure 3.1-1. These values were determined from simple laboratory experiments described in Chapter 4.

Table 3.3-1 Model Properties

Glass Panel:	
Elastic Modulus (E)	1×10^7 psi (6.9×10^7 kN/m^2)
Poisson's Ratio (ν)	0.23
Mass Density (ρ)	5 slugs/ft^3 (2575 kg/m^3)
Frame:	
Elastic Modulus (E)	1×10^7 psi (6.9×10^7 kN/m^2)
Poisson's Ratio (ν)	0.25
Mass Density (ρ)	5.37 slugs/ft^3 (2766 kg/m^3)
Area Moments of Inertia	
Mullion Elements	
Ix	8.321 in^4 (346.3 cm^4)
Iy	11.390 in^4 (474.1 cm^4)
Iz	3.069 in^4 (127.7 cm^4)
Spandrel Elements	
Ix	3.452 in^4 (143.7 cm^4)
Iy	2.481 in^4 (103.3 cm^4)
Iz	0.971 in^4 (40.4 cm^4)
Cross-sectional Areas	
Mullion (A)	2.613 in^2 (1686 mm^2)
Spandrel (A)	1.404 in^2 (906 mm^2)
Gasket Equivalent Spring Constants:	
k_L	318.0 lb/in/in (2194 kN/m/m)
k_P	81.1 lb/in/in (560 kN/m/m)
k_N	556.9 lb/in/in (3843 kN/m/m)
k_R	305.3 in-lb/radian/in (1358 N·m/radian/m)

The one inch (2.54 cm) thick insulating windows in the prototype structure consist of two 0.25 in. (0.64 cm) thick glass panels separated by a sealed 0.50 in. (1.27 cm) thick air space with metal spacer bars on the periphery of the panel. For simplicity, the double plate system was replaced by an equivalent single panel which could be represented by a single-layer finite element model. This model assumes that both plates act together and vibrate in phase. (A double plate continuum model and a parallel-plate finite element model were also developed to study out-of-phase motions of the double panel system and are discussed in Section 3.4.).

The thickness of the equivalent single panel was determined by assuming that the flexural rigidity of the single plate is equal to the flexural rigidity of the double plate system. Using the plate properties in Table 3.3-1, a thickness of 0.315 in. (0.8 cm) is computed for the equivalent single panel. However, measured glass thicknesses were somewhat less for the window tested in the laboratory pressure test assembly, having a measured total thickness of 0.9803 in. (2.49 cm) and a glass panel thickness of 0.237 in. (0.60 cm). If these thicknesses are used, a value of 0.298 in. (0.76 cm) results for the equivalent single panel thickness. This lower value was used in the panel sensitivity studies rather than the value of 0.315 in. (0.80 cm) based on nominal panel dimensions.

Results: Initial studies employed a finite element model of the panel only and were used to check program WINDOW output against classical plate theory results. Static displacement and vibration frequency comparisons are not presented here for brevity but finite element results were within one or two percent of continuum theory values.

Other calibration studies using the frame-panel model shown in Figure 3.3-1 investigated the effect of changes in panel thickness and density and in frame continuity member length (L_e) on panel frequencies. Results of these studies are presented in Tables 3.3-2, 3.3-3, and 3.3-4. A consistent mass formulation was used for both frame and panel elements and the cross-sectional area of the continuity member was set to a very small value so that its mass would not affect panel vibrations.

Results presented in Table 3.3-2 show that increased panel thickness results in increased structure fundamental frequency for all cases except that of panel aspect ratio equal to 5. In this case increased panel thickness adds more mass than stiffness effect resulting in a reduction in panel frequency with thickness for the range of panel thicknesses and aspect ratios considered. Table 3.3-3 shows that panel frequencies decrease somewhat uniformly with increasing mass density for all panel aspect ratio cases as expected. Table 3.3-4 displays the variation in structure fundamental frequency with the length L_e of the continuity member. This member provides variable rotational stiffness at joint 9 equal to $3EI/L_e$ where I is the area moment of inertia of the continuity member about the x axis in Figure 3.3-1. Results in Table 3.3-4 show that added rotational stiffness at joint 9 changes structure frequency by less than 4% for the range of values of length L_e considered. Similar results were obtained when the effect of a nonrigid mullion-spandrel connection at joint 5 (Figure 3.3-1) was investigated. In this case the effect of the elastic connection on static displacement and vibration frequency results was negligible.

Figures 3.3-2, 3.3-3, and 3.3-4 show the frequencies and mode shapes of the first three symmetric structure modes for model properties in Table

Table 3.3-2 Fundamental Frequency of Framed Panels of Varying Thickness and Aspect Ratio

Equivalent Single Panel Thickness, in inches (mm) (1)	Fundamental Frequency, in Hertz, for Varying Panel Aspect Ratios, R				
	R = 0.5 (2)	R = 1.0 (3)	R = 1.8 (4)	R = 2.5 (5)	R = 5.0 (6)
0.150 (3.81)	8.82	7.25	8.64	10.41	12.04
0.200 (5.08)	9.82	8.46	9.90	11.58	11.58
0.250 (6.35)	10.63	9.64	11.12	12.57	11.12
0.298 (7.57)	11.23 (13.23)[a]	10.77 (10.59)[a]	12.24 (12.46)[a]	13.31 (15.35)[a]	10.70 (27.53)[a]
0.350 (8.89)	11.64	11.94	13.31	13.81	10.28
0.400 (10.2)	11.83	12.97	14.14	14.04	9.90
0.450 (11.4)	11.90	13.86	14.75	14.08	9.56

NOTE: See Figure 3.3-1 and Table 3.3-1 for panel dimensions and properties; panel density = 5 slugs/ft^3 (2575 kg/m^3); no continuity member in frame.

[a]Classical plate theory frequency for simply-supported plate with same dimensions and properties.

Table 3.3-3 Fundamental Frequency of Framed Panels of Varying Density and Aspect Ratio

Mass Density of Panel, in slugs/ft^3 (kg/m^3) (1)	Fundamental Frequency, in Hertz, for Varying Panel Aspect Ratios, R				
	R = 0.5 (2)	R = 1.0 (3)	R = 1.8 (4)	R = 2.5 (5)	R = 5.0 (6)
4.0 (2060)	12.50	12.04	13.66	14.77	11.52
4.5 (2318)	11.81	11.35	12.89	13.98	11.09
5.0 (2575)	11.23	10.77	12.24	13.31	10.70
5.5 (2833)	10.72	10.27	11.68	12.72	10.35
6.0 (3090)	10.28	9.83	11.18	12.20	10.03
6.5 (3348)	9.89	9.45	10.75	11.74	9.74
7.0 (3605)	9.54	9.11	10.36	11.33	9.47

NOTE: See Figure 3.3-1 and Table 3.3-1 for panel dimensions and properties; panel thickness = o.298 in. (7.57 mm); no continuity member in frame

Table 3.3-4 Fundamental Frequency of Framed Panel with Continuity Member of Varying Length

Continuity Member Length, Le, in inches (cm) (1)	Fundamental Frequency, Hertz (2)
0.0[a]	12.24
1000 (2540)	12.35
500 (1270)	12.44
324 (823)	12.52
270 (686)	12.55
252 (640)	12.57
234 (594)	12.58

[a] No continuity member in frame

NOTE: See Figure 3.3-1 and Table 3.3-1 for dimensions and properties of panel and frame; panel thickness = 0.298 in (7.57 mm); panel aspect ration R = 1.8.

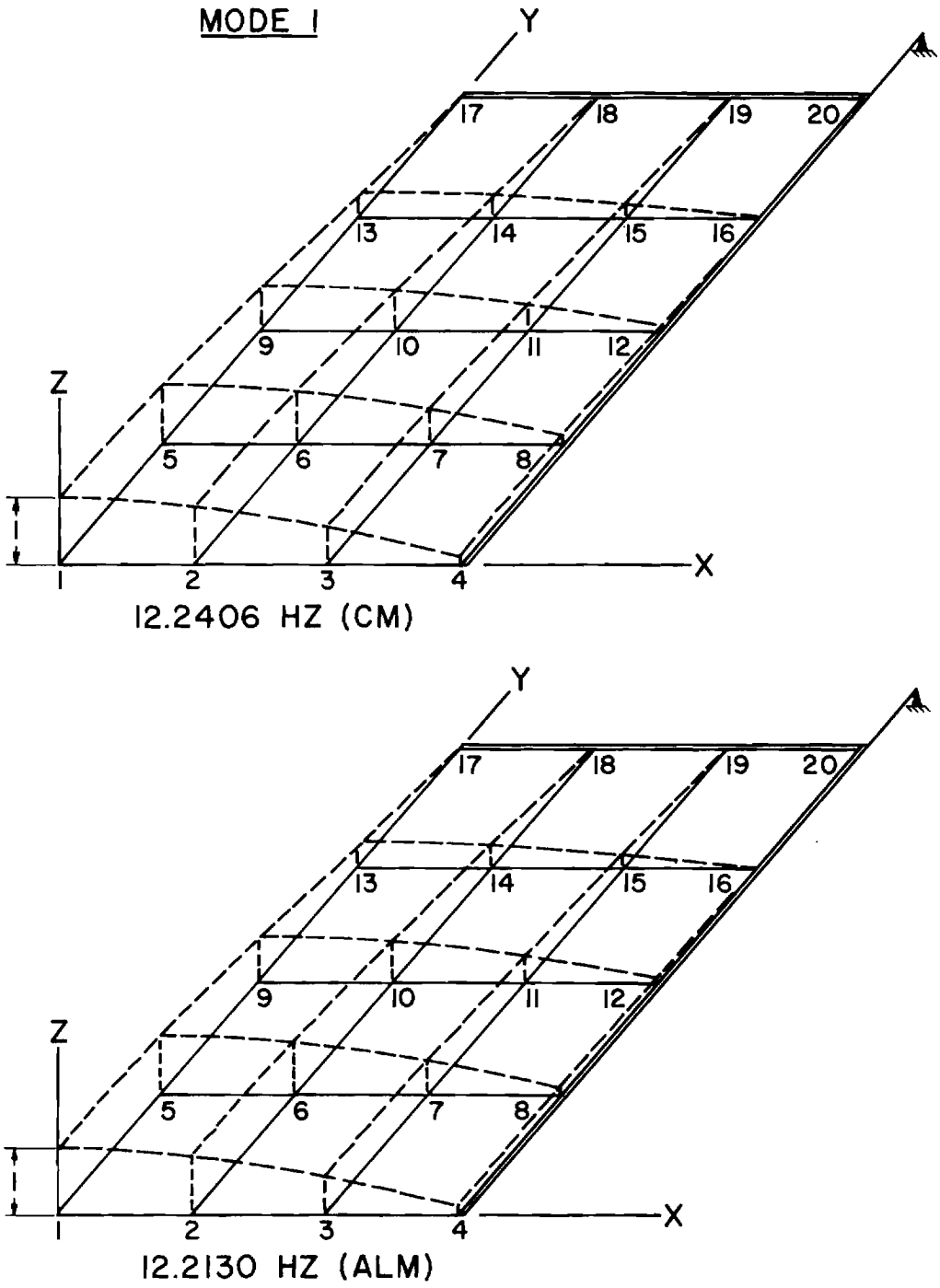

Figure 3.3-2 Plate Bending Frequencies and Mode Shapes, Mode 1

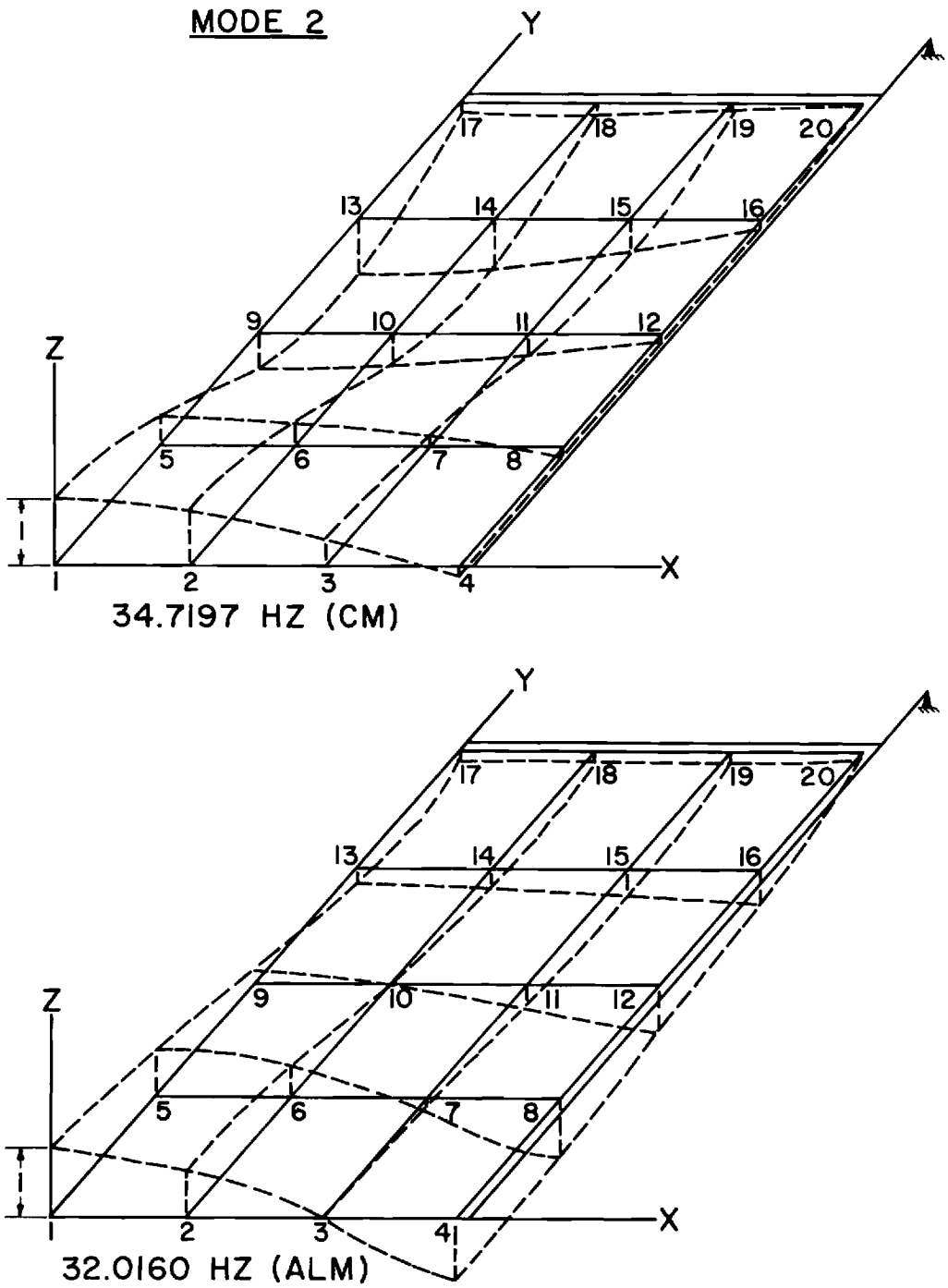

Figure 3.3-3 Plate Bending Frequencies and Mode Shapes, Mode 2

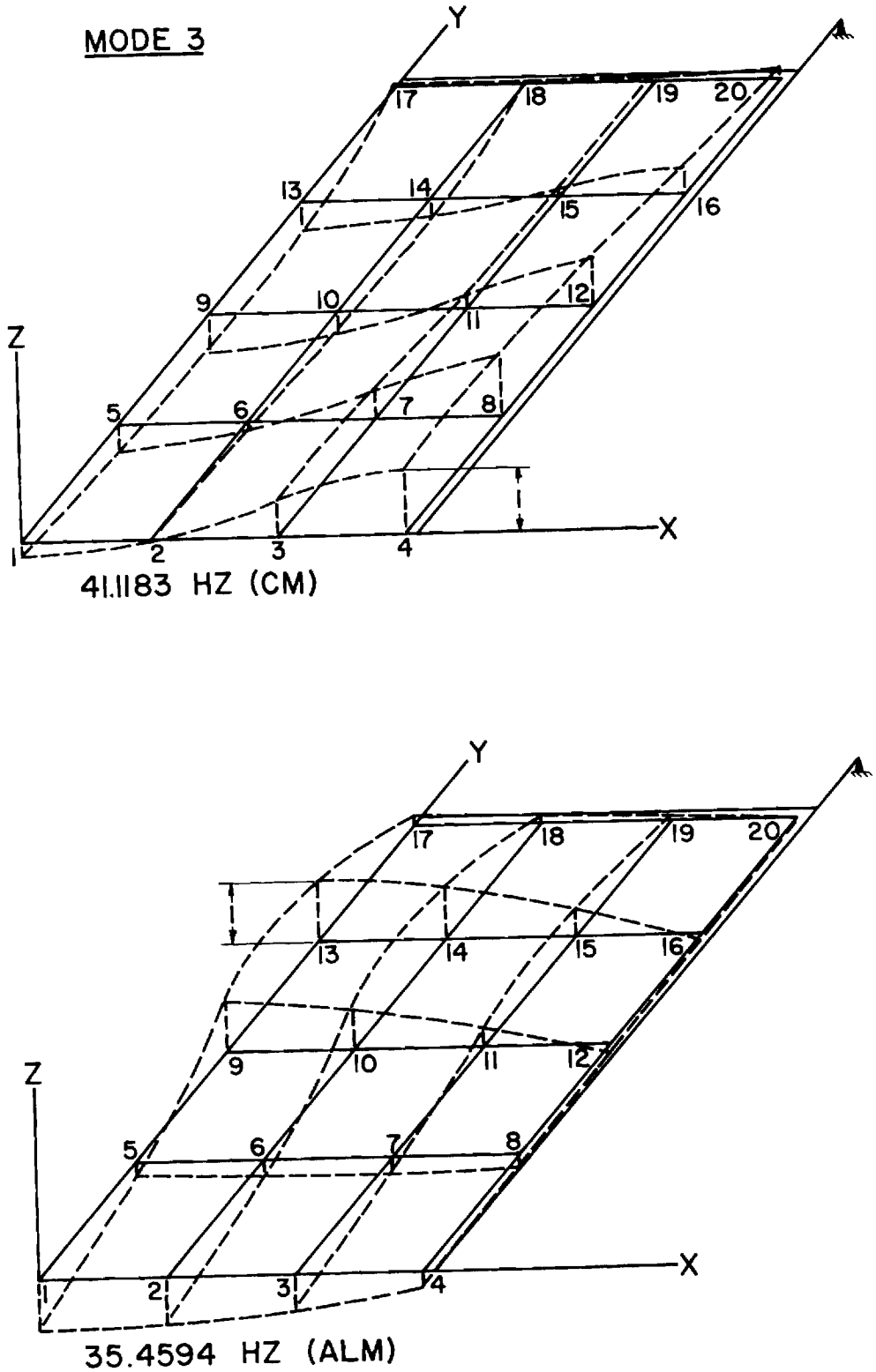

Figure 3.3-4 Plate Bending Frequencies and Mode Shapes, Mode 3

3.3-1 and panel thickness of 0.298 in. (7.57 mm) and $L_e = 0$. The consistent mass (CM) and assembled lumped mass (ALM) formulations are compared and show excellent agreement in frequency and mode shape for mode 1. The CM formulation has mass terms associated with all thirty-nine master degrees of freedom in Figure 3.3-1 while the ALM model assigns mass to the twenty nodal translations in the Z direction only. Mode 2 and 3 frequency values for CM and ALM differ by 8% and 14%, respectively. In addition, mode 2 for ALM contains significantly more boundary displacement than the CM shape, and mode 3 shapes are quite dissimilar. Because the CM model contains more master degrees of freedom with mass terms associated with both translational and rotational displacements, the CM mode shapes were assumed to be more accurate and the CM model was used in all sensitivity and dynamic response studies.

The effect of change in stiffness constant k_N for the boundary spring normal to the panel on mode shapes for mode 1 was also studied for panels of varying aspect ratio but of constant surface area. Model properties in Table 3.3-1 were used, with panel thickness equal to 0.298 in. (0.76 cm) and L_e equal to zero, but k_N took on values between 10 lb/in/in (69 kN/m/m)(soft spring) and 1×10^6 lb/in/in (6.9×10^6 kN/m/m) (hard spring) with rotational spring constant k_R held fixed at 305.3 in-lb/radian/in (1358 N·m/radian/m). Mode 1 displacements along x and y symmetry axes are plotted in Figures 3.3-5 and 3.3-6 and corresponding frequencies are recorded in Table 3.3-5. The percent increase in frequency with change in k_N is also shown in Table 3.3-5. Figure 3.3-6 shows that the value of k_N has negligible effect on the first mode shape of the panel with aspect ratio of 5.0.

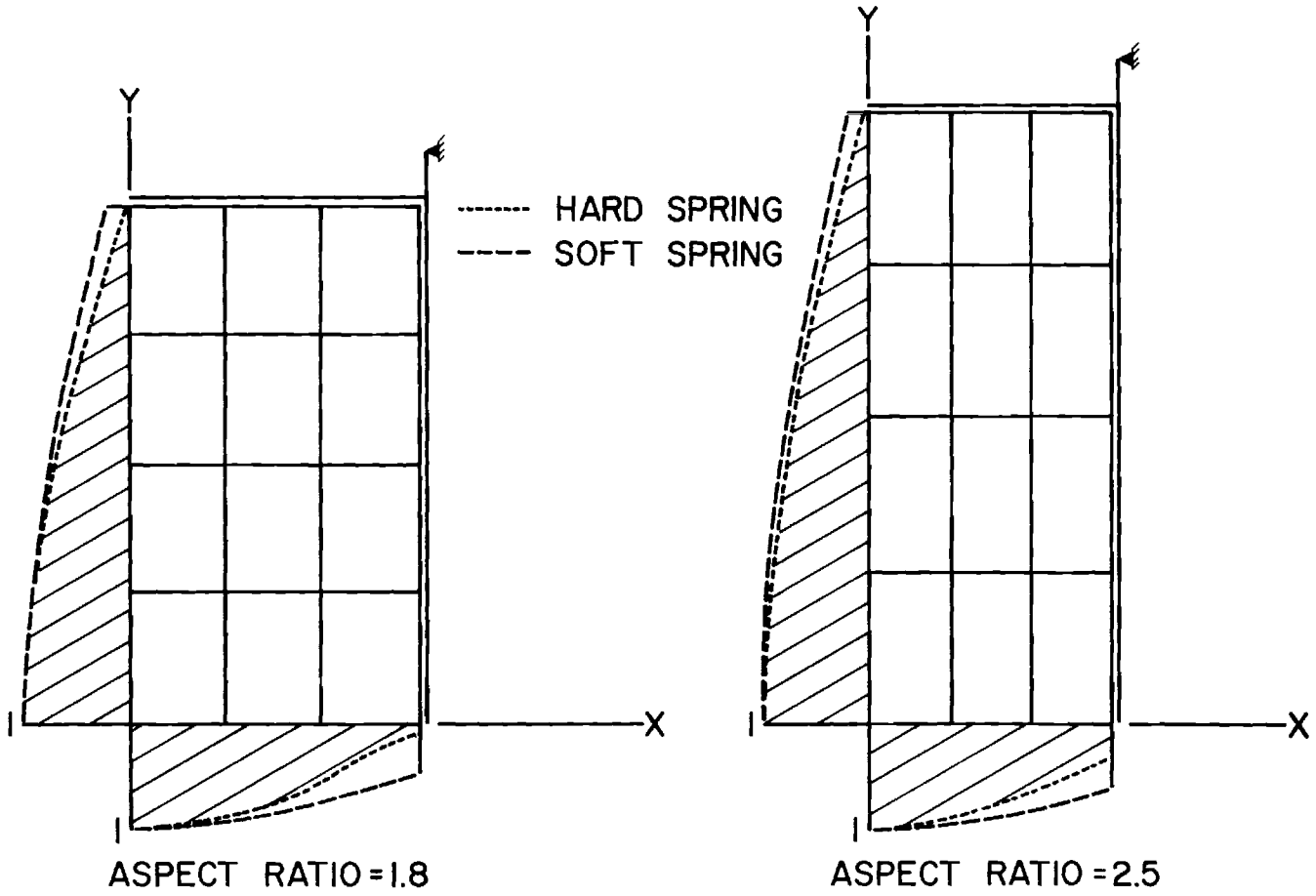

Figure 3.3-5 Effect of Normal Spring on Mode Shape 1, R = 1.8 and 2.5

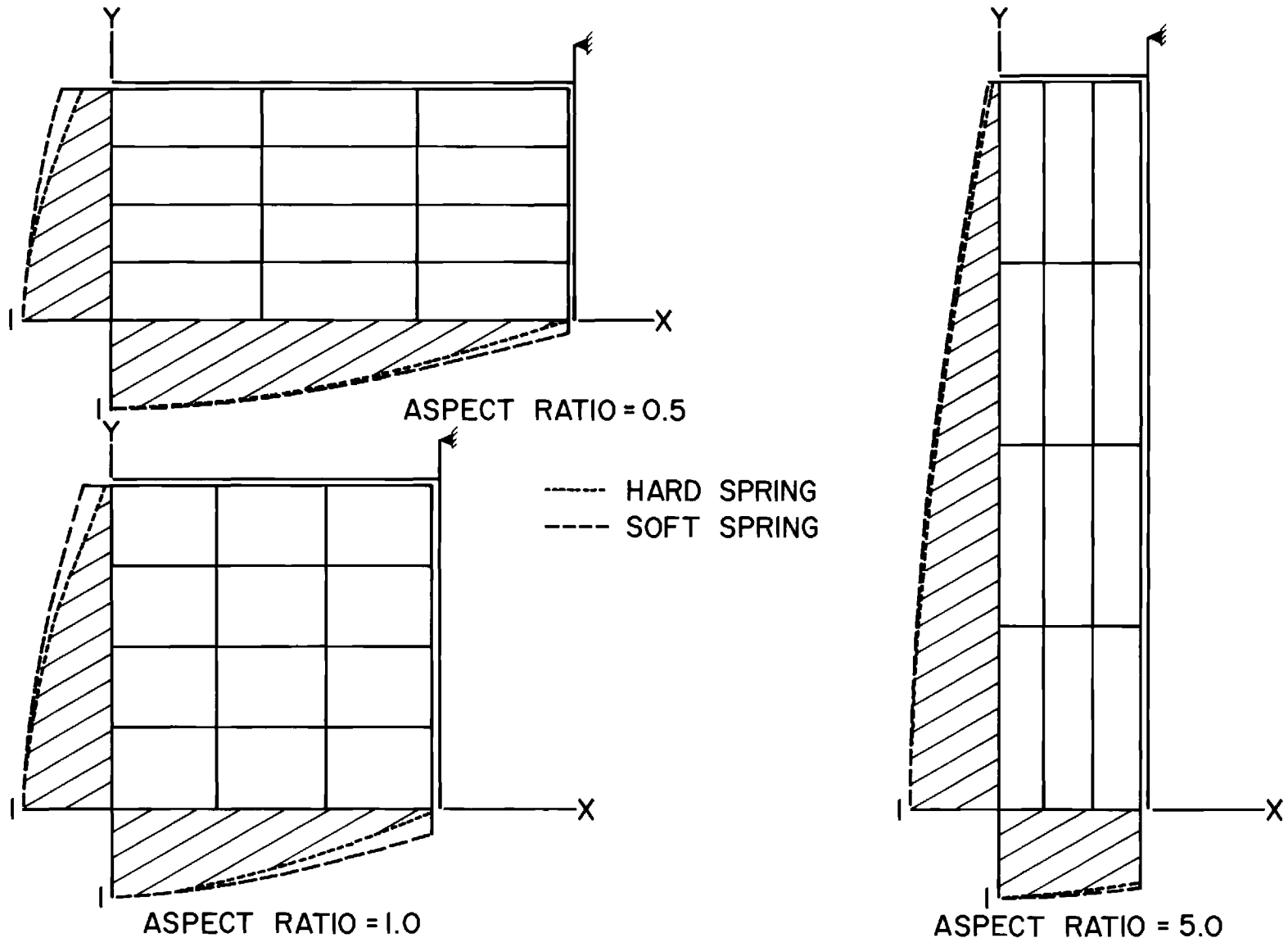

Figure 3.3-6 Effect of Normal Spring on Mode Shape 1, R = 0.5, 1, and 5

Table 3.3-5 Fundamental Frequencies of Framed Panels of Varying Normal Spring Constant and Aspect Ratio

Aspect Ratio, R (1)	Fundamental Frequency, in Hertz		Frequency Increase (%) (4)
	Soft Spring[a] (2)	Hard Spring[b] (3)	
0.5	8.74	11.31	29
1.0	8.51	10.87	28
1.8	9.19	12.24[c]	33
2.5	9.73	13.43	38
5.0	9.20	10.73	17

[a] Normal spring constant k_N = 10 lb/in/in (69 kN/m/m)

[b] Normal spring constant k_N = 1 x 10^6 lb/in/in (6.9 x 10^6 kN/m/m)

[c] Classical plate theory, simply-supported plate: 12.46 Hz

NOTE: See Table 3.3-1 for other model properties.

If the value of the boundary rotational spring constant k_R is varied between 50 in-lb/radian/in (222 N·m/radian/m)(soft spring) and 1×10^6 in-lb/radian/in (4.45×10^6 N·m/radian/m), the range of frequencies shown in Table 3.3-6 is obtained. Comparison of percent frequency increase with increase in k_N or k_R in Tables 3.3-5 and 3.3-6 shows that a change in k_R affects the fundamental frequency of structures with aspect ratios of 1.0 and 1.8 most, while aspect ratio 0.5, 2.5, and 5.0 panels are more heavily influenced by a change in k_N for the range of values considered.

Further model sensitivity results are presented below in the form of nondimensional plots of static and dynamic structure response versus variation in selected system parameters.

3.3(b) Nondimensional Ratios

Static and dynamic sensitivity studies employ the nondimensional ratios in Table 3.3-7 in plots showing variation of system parameters versus system response. Table 3.3-1 should be consulted for specific values of terms in the ratios except that panel thickness t_p equals 0.298 in. (0.76 cm) and $L_e = 0$ for all figures. The symmetry model in Figure 3.3-1 was used throughout.

Parameters K_1 through K_4 are nondimensional forms of normal and rotational spring constants k_N and k_R. If system response is plotted for varying k_N or k_R and varying aspect ratio R, terms K_3 and K_4 containing constant panel area A_p are used. If results are presented for one aspect ratio only, variables K_1 and K_2 are used.

Parameters I_1 through I_8 are dimensionless ratios for variation of mullion and spandrel area moments of inertia. I_1 and I_2 are flexural

Table 3.3-6 Fundamental Frequencies of Framed Panels of Varying Rotational Spring Constant and Aspect Ratio

Aspect Ratio, R (1)	Fundamental Frequency, in Hertz		Frequency Increase (%) (4)
	Soft Spring[a] (2)	Hard Spring[b] (3)	
0.5	10.83	13.47	24
1.0	10.19	15.28	50
1.8	11.61	17.07[c]	47
2.5	12.80	16.43	28
5.0	10.66	10.94	3

[a]Rotational spring constant k_R = 50 in-lb/radian/in (222 N·m/radian/m)

[b]Rotational spring constant k_R = 1 x 10^6 in-lb/radian/in (4.45 x 10^6 N·m/radian/m)

[c]Classical plate theory, clamped plate: 24.42 Hz

Table 3.3-7 Nondimensional Parameters

Parameter	Definition
R	Aspect Ratio, b/a
K_1	$k_n \bar{b}^3/D$, $\bar{b} = b/2$
K_2	$k_R \bar{b}/D$
K_3	$k_N A_p t_p/D$, $A_p = ab/4 = \bar{a}\,\bar{b}$, $\bar{a} = a/2$
K_4	$k_R A_p/t_p D$
I_1	$EI_x/\bar{b}D$, mullion
I_2	$EI_x t_p/A_p D$, mullion
I_3	$EI_y/\bar{b}D$, mullion
I_4	$EI_y t_p/A_p D$, mullion
I_5	$EI_y/\bar{a}D$, spandrel
I_6	$EI_y t_p/A_p D$, spandrel
I_7	$EI_x/\bar{a}D$, spandrel
I_8	$EI_x t_p/A_p D$, spandrel
W_1	$w_{max}/w^*_{max,ss}$, static displacement
f	$f_{11}/f^*_{11,ss}$, fundamental frequency
W_2	$w_{max}/w^*_{max,ss}$, dynamic displacement

* Simply-supported plate with R = 1.8

inertias for mullion elements and I_5 and I_6 for spandrel elements. Terms I_3 and I_4 are nondimensional torsion constants for mullion elements and I_7 and I_8 for spandrel elements. Quantities I_2, I_4, I_6, and I_8 are used in plots containing system response for more than one aspect ratio; response plots using I_1, I_3. I_5, and I_7 are for aspect ratio R = 1.8 only.

Symbols W_1, f, and W_2 refer to the nondimensional static displacement, frequency, and dynamic displacement response of the system in Figure 3.3-1 for fixed or varying panel aspect ratio, R. W_1 is the ratio of static displacement at node 1 (center of panel) for panels of fixed or varying R to the maximum static displacement of a simply-supported plate with R = 1.8 and identical properties and loading. Parameter f is the fundamental structure frequency divided by the fundamental frequency of a simply-supported plate with R = 1.8 from classical plate theory. Finally, W_2 is the ratio of the maximum dynamic response of the structure to a specified pressure loading to the maximum dynamic response of a simply-supported plate (R = 1.8) subjected to the same loading.

3.3(c) Static Analysis Results

Static displacement response to uniform pressure loading over the entire quarter panel versus variation in spring and frame properties for selected aspect ratios are presented in Figures 3.3-7 through 3.3-10. Data points on all plots were generated using program WINDOW and then connected by smooth curves. Numerical values of parameters defined in Table 3.3-7 which were held fixed are recorded on each figure.

Figure 3.3-7 displays panel center displacement W_1 versus normal spring constant K_3. W_1 is seen to be relatively insensitive to normal

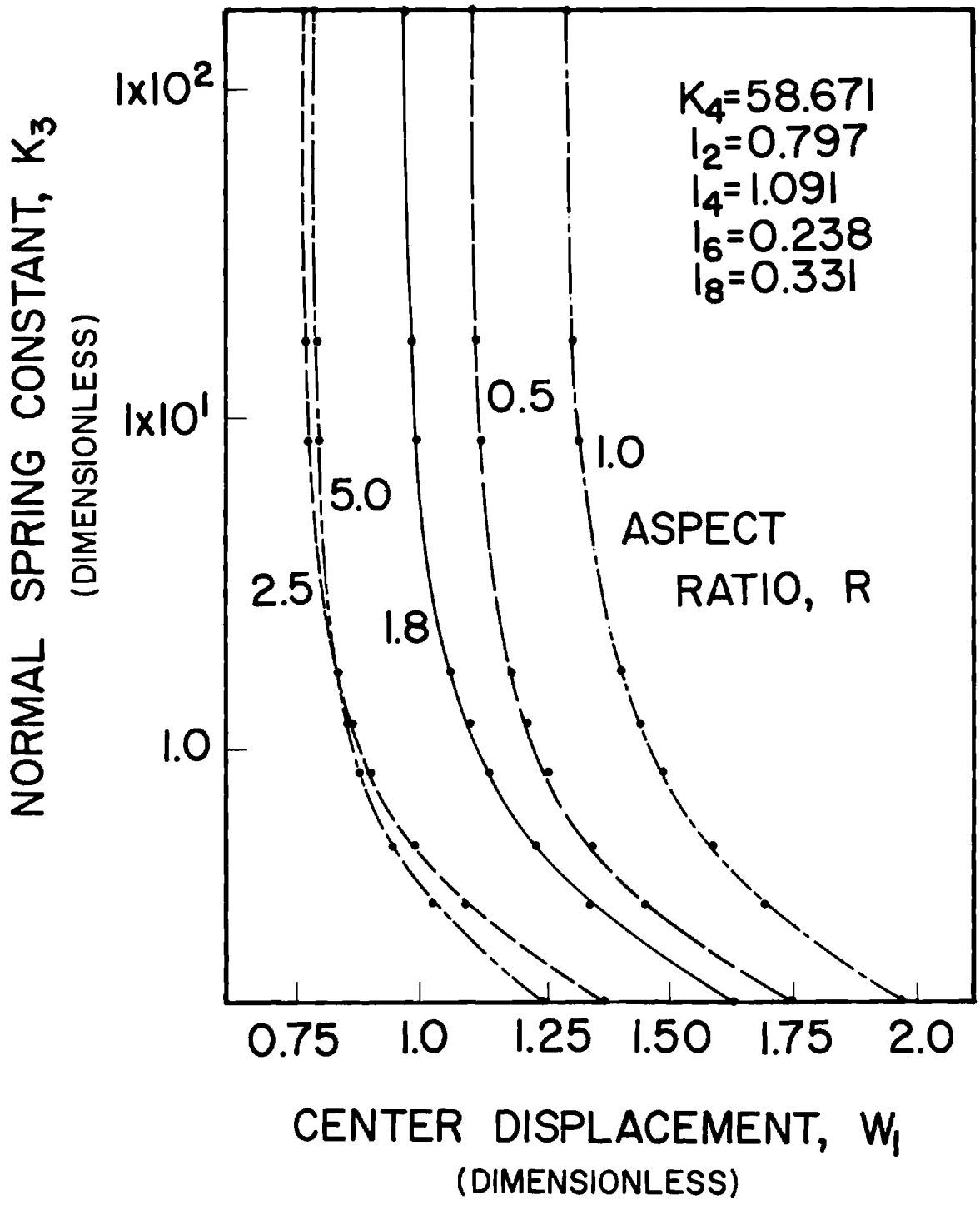

Figure 3.3-7 Static Displacement of Panels with Uniform Loading Versus Normal Spring Constant on Boundary

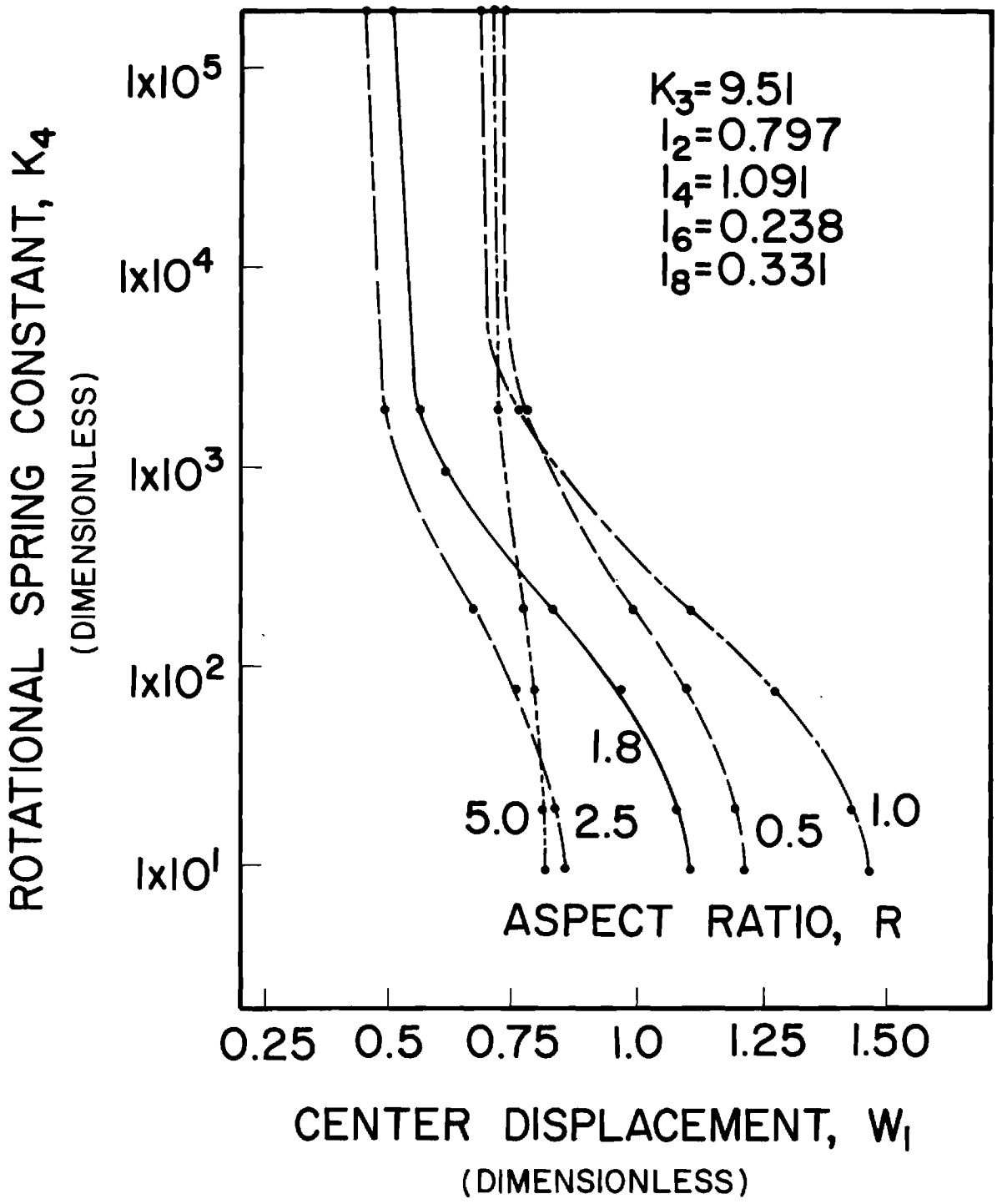

Figure 3.3-8 Static Displacement of Panels with Uniform Loading Versus Rotational Spring Constant on Boundary

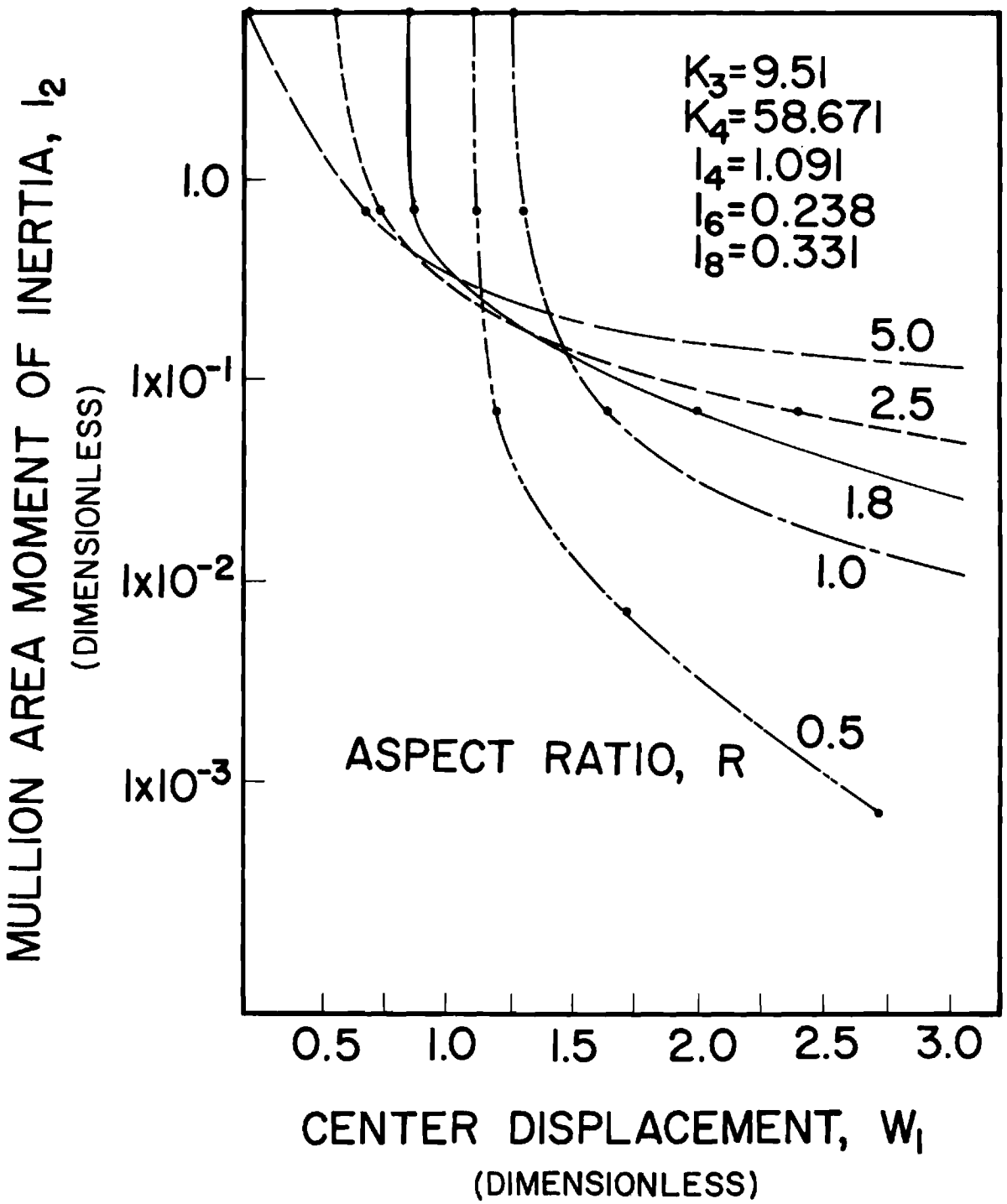

Figure 3.3-9 Static Displacement of Panels with Uniform Loading Versus Mullion Moment of Inertia

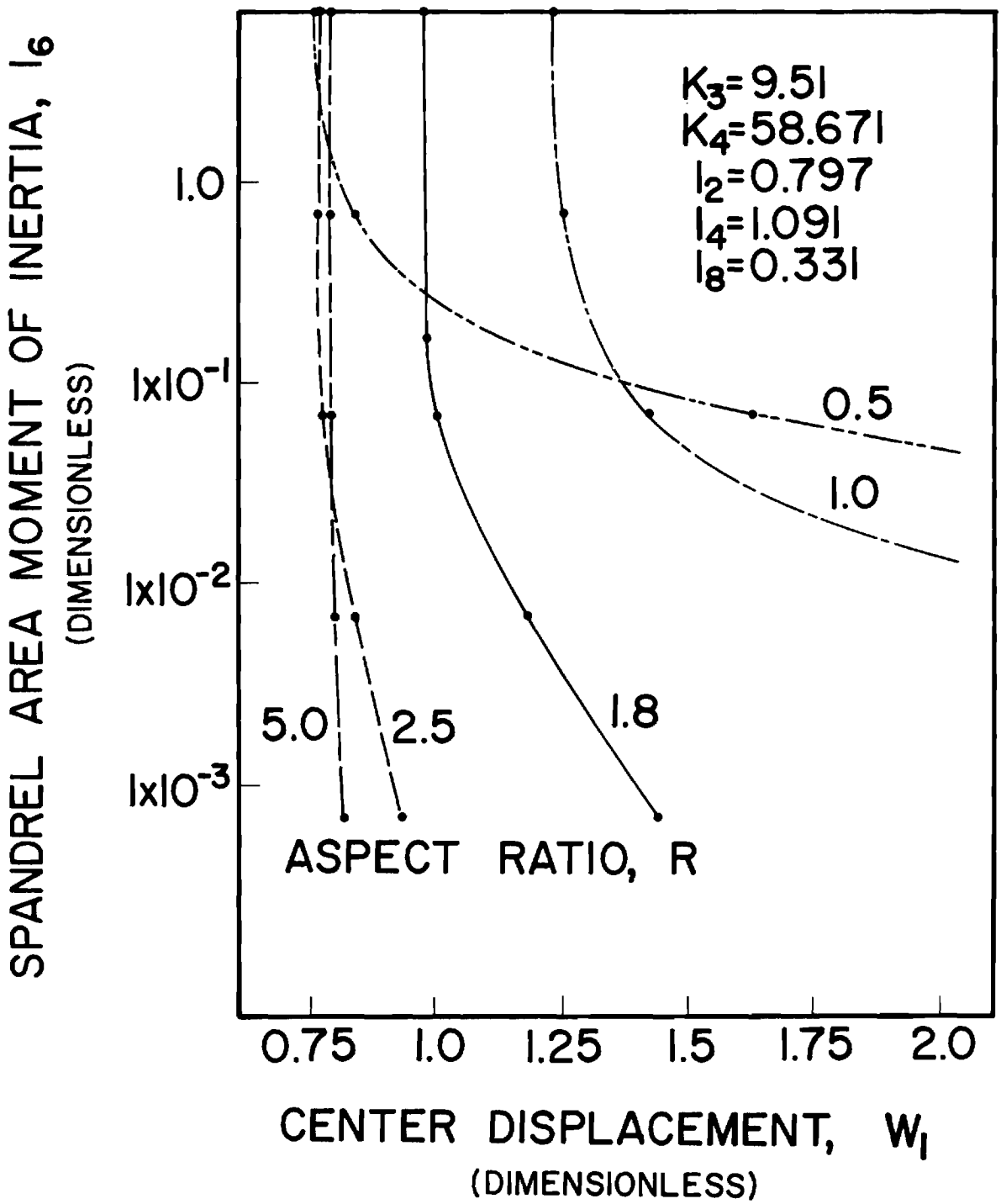

Figure 3.3-10 Static Displacement of Panels with Uniform Loading Versus Spandrel Moment of Inertia

spring stiffness in the range between 1.0 and 10.0 in which K_3 was measured for the prototype structure. Panel response does vary with panel aspect ratio, however, with the largest displacement ratio W_1 recorded for square windows (R = 1.0).

All structures except those of aspect ratio 5.0 are sensitive to change in rotational spring constant K_4 as shown in Figure 3.3-8. As the boundary rotational spring stiffness increases, the static displacement at the center of the window decreases. An increase in K_4 is most effective for square (R = 1.0) and nearly square (R = 0.5, 1.8) structures. When K_4 approaches 1000, panel displacement drops below that of a simply-supported equivalent plate for all aspect ratios.

Figures 3.3-9 and 3.3-10 show structure displacement versus area moment of inertia for mullion and spandrel elements, respectively. Mullion elements which are stiff in flexure reduce static displacements of high aspect ratio panels most effectively since mullion elements are parallel to the long side of the panel (Figure 3.3-9). Figure 3.3-10 demonstrates that spandrel elements are most effective on low aspect ratio windows for the same reason. In both cases, square window-frame structures experience the largest center displacement relative to a simply-supported plate with the same properties, dimensions, and loading.

3.3(d) Dynamic Analysis Results

Dynamic sensitivity of the model is displayed in Figures 3.3-11 through 3.3-18 in which the effect of variation of model properties on fundamental frequency is recorded. Figure 3.3-11 demonstrates that fundamental frequency is insensitive to change in normal spring stiffness except for very low values of K_3. At the same time, an increase in rotational spring

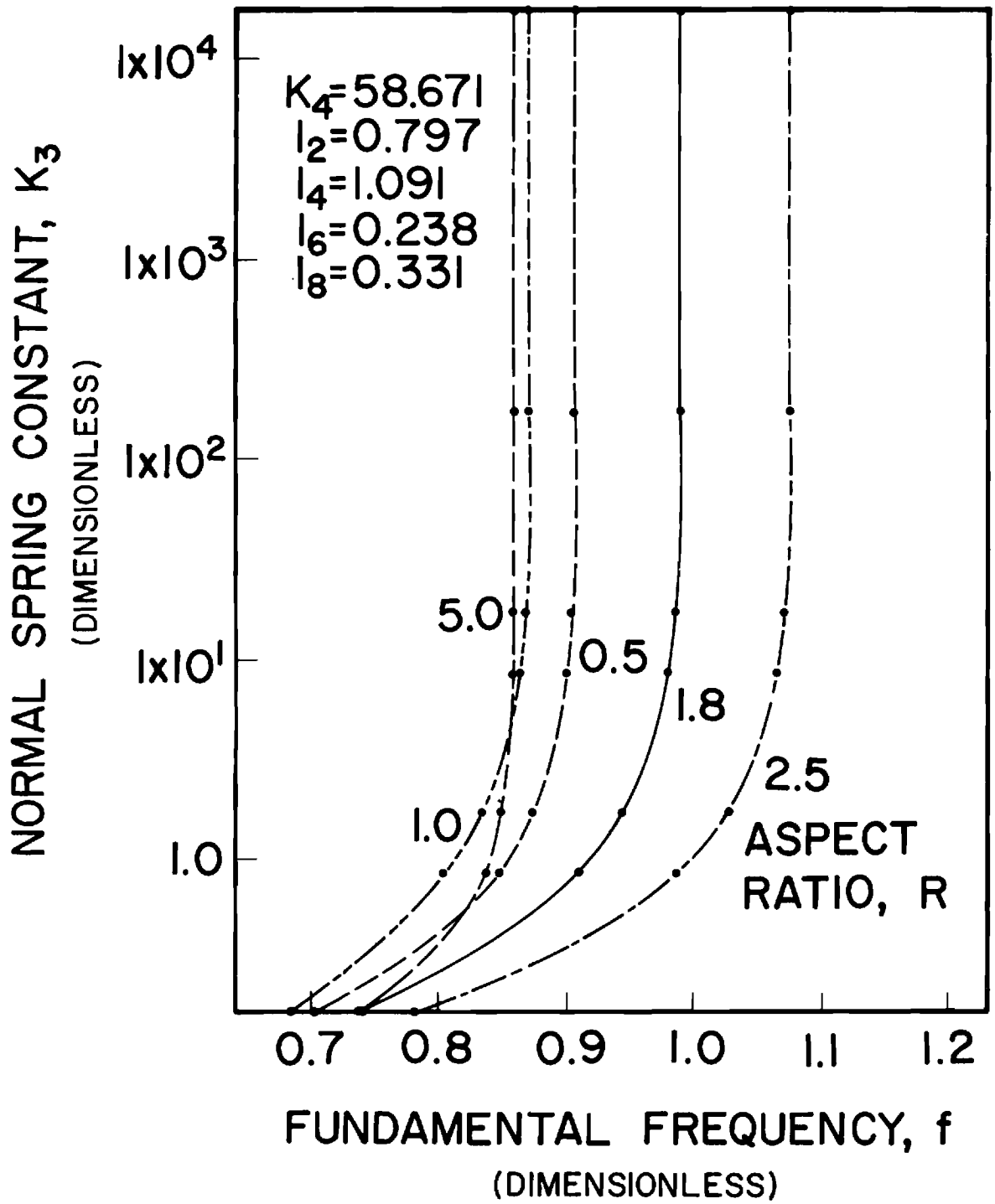

Figure 3.3-11 Panel Fundamental Frequency Versus Normal Spring Constant K_3 on Boundary

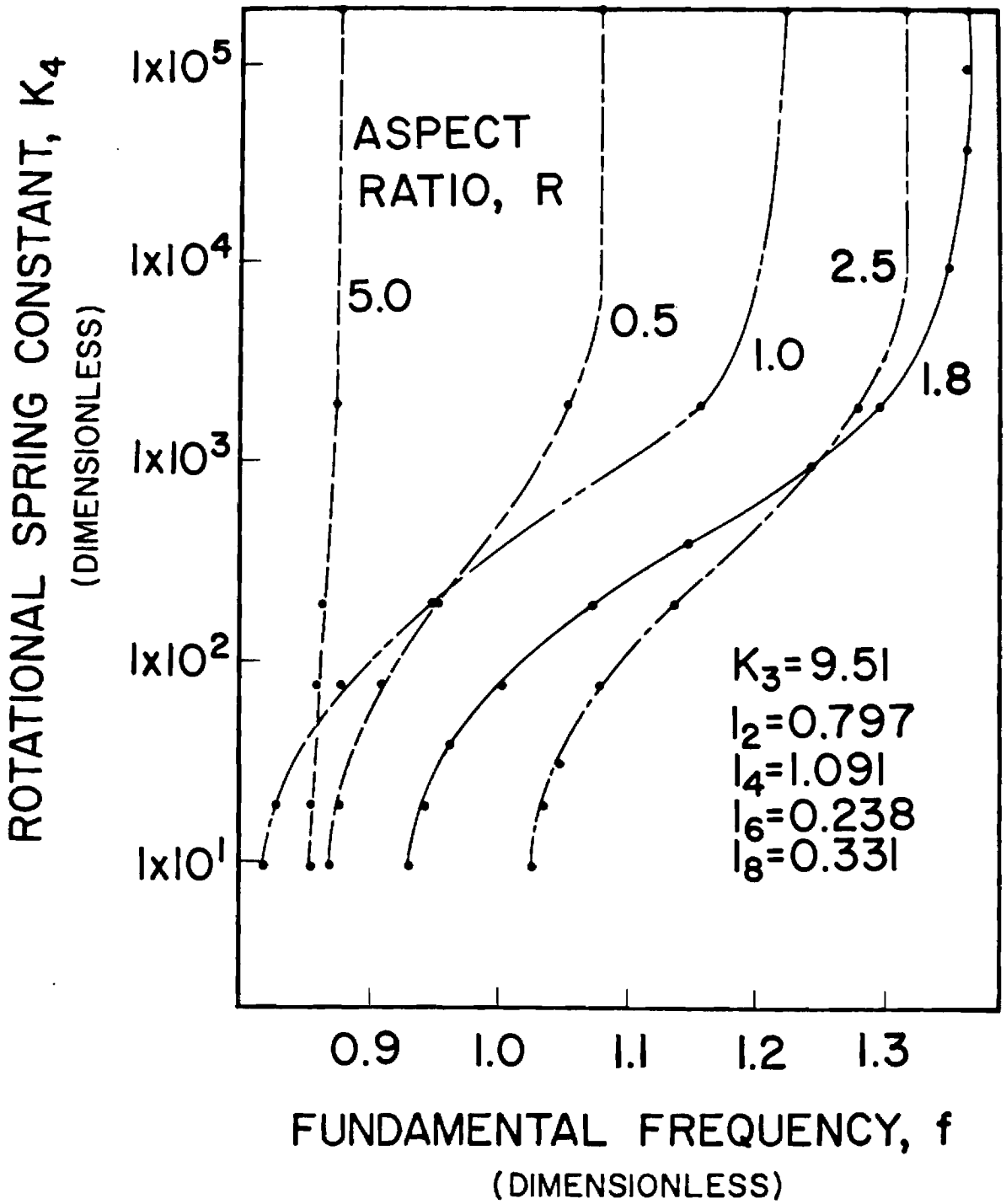

Figure 3.3-12 Panel Fundamental Frequency Versus Rotational Spring Constant K_4 on Boundary

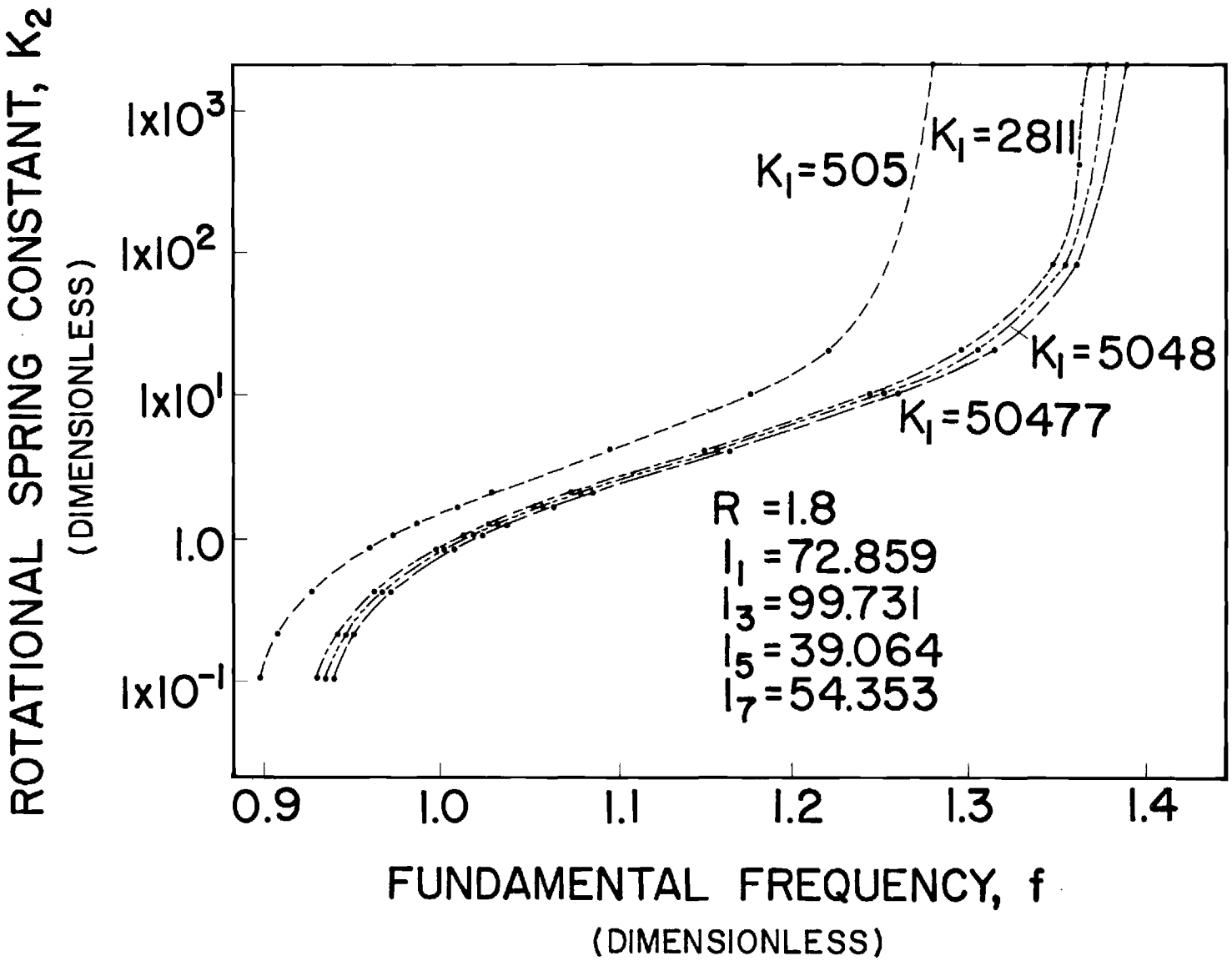

Figure 3.3-13 Panel Fundamental Frequency Versus Rotational Spring Constant K_2 on Boundary

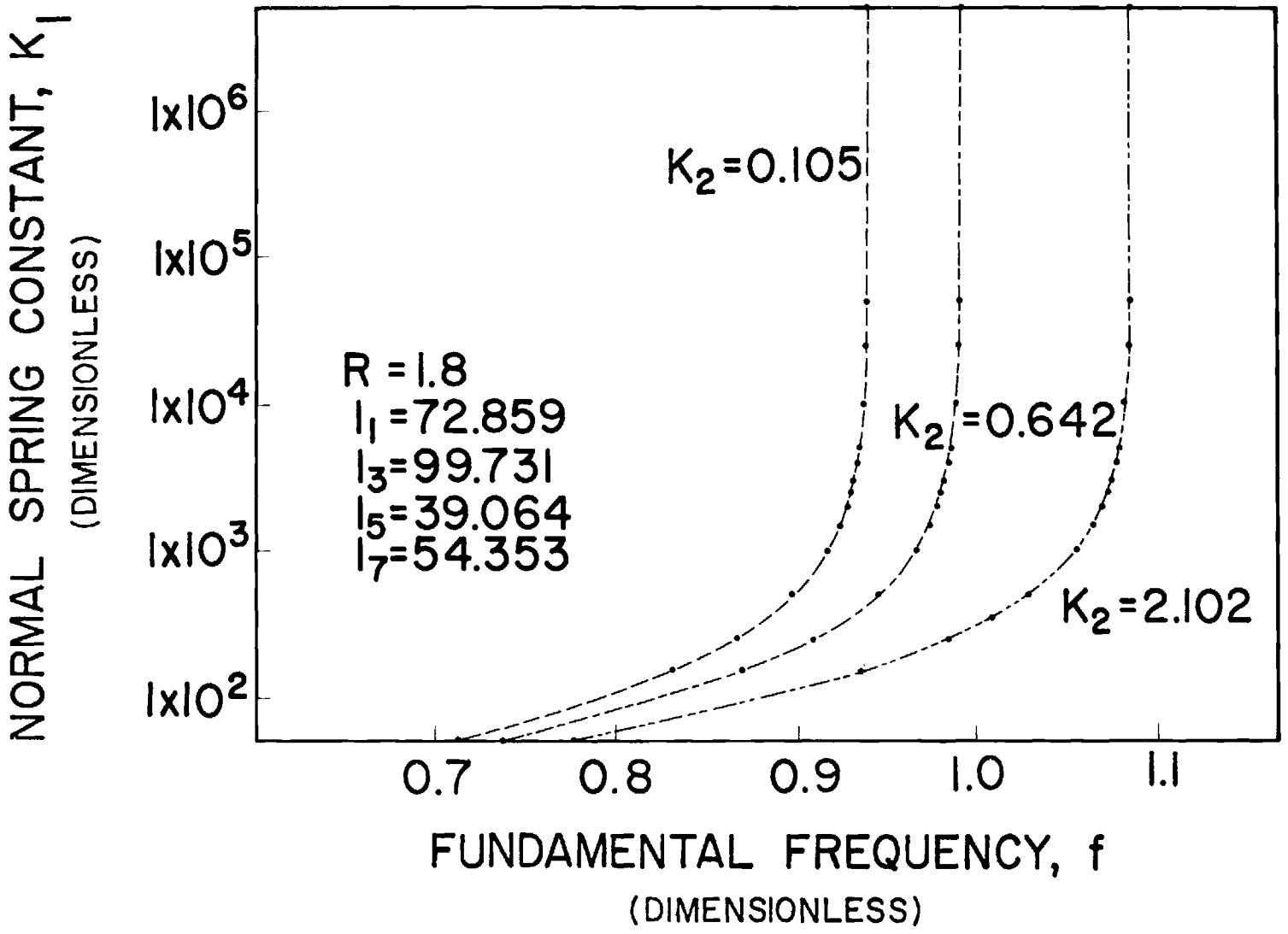

Figure 3.3-14 Panel Fundamental Frequency Versus Normal Spring Constant K_1 on Boundary

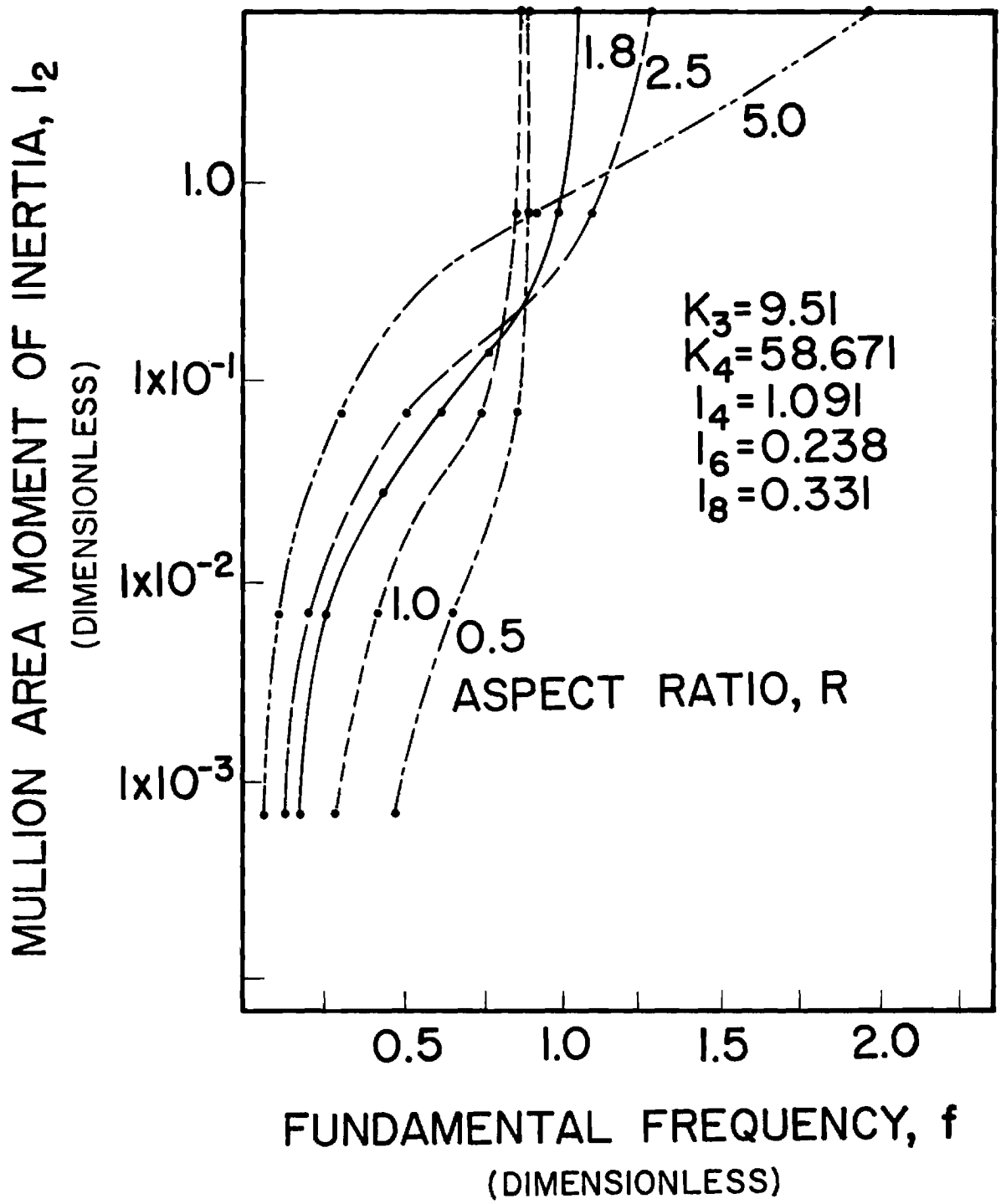

Figure 3.3-15 Panel Fundamental Frequency Versus Mullion Moment of Inertia

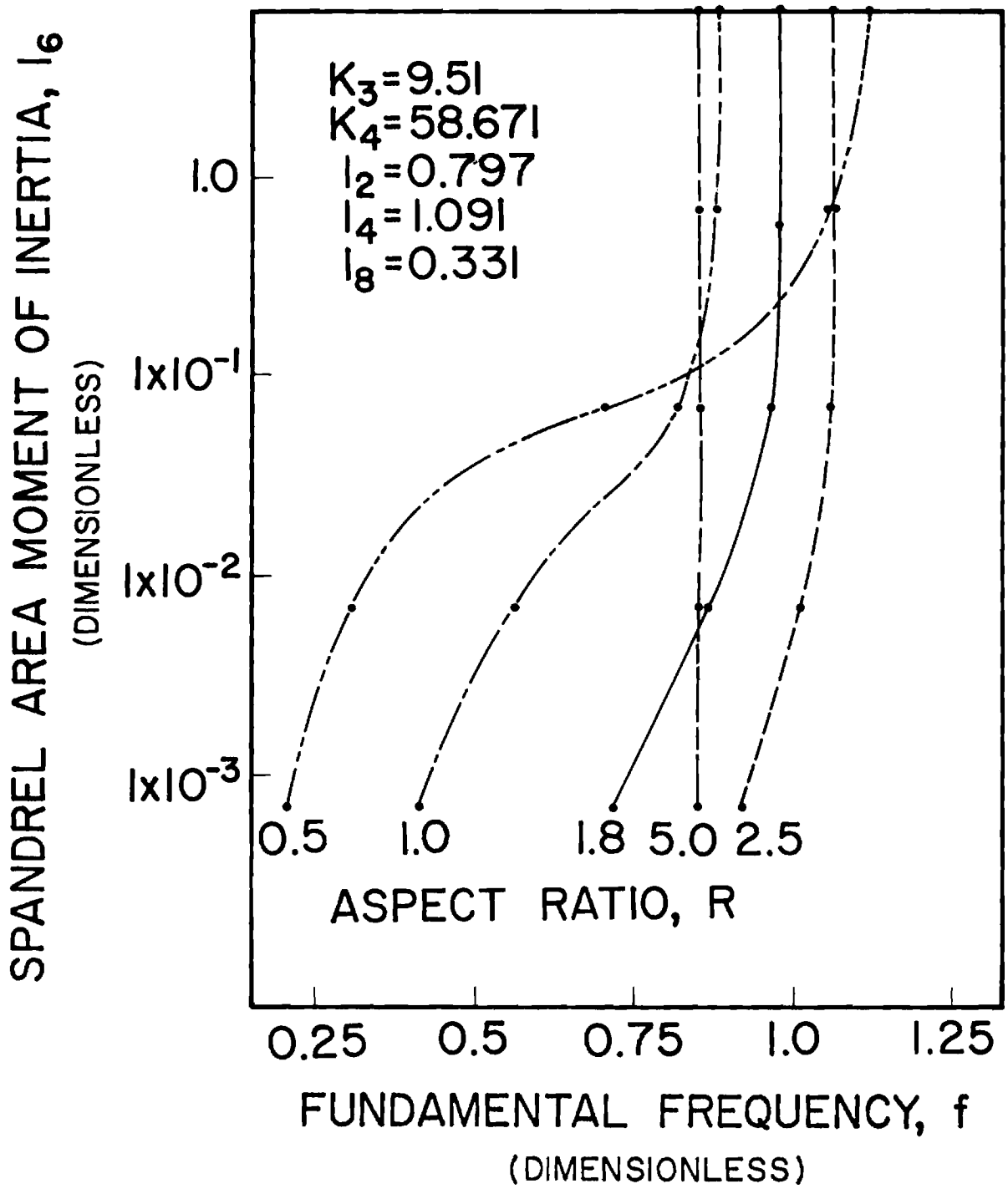

Figure 3.3-16 Panel Fundamental Frequency Versus Spandrel Moment of Inertia

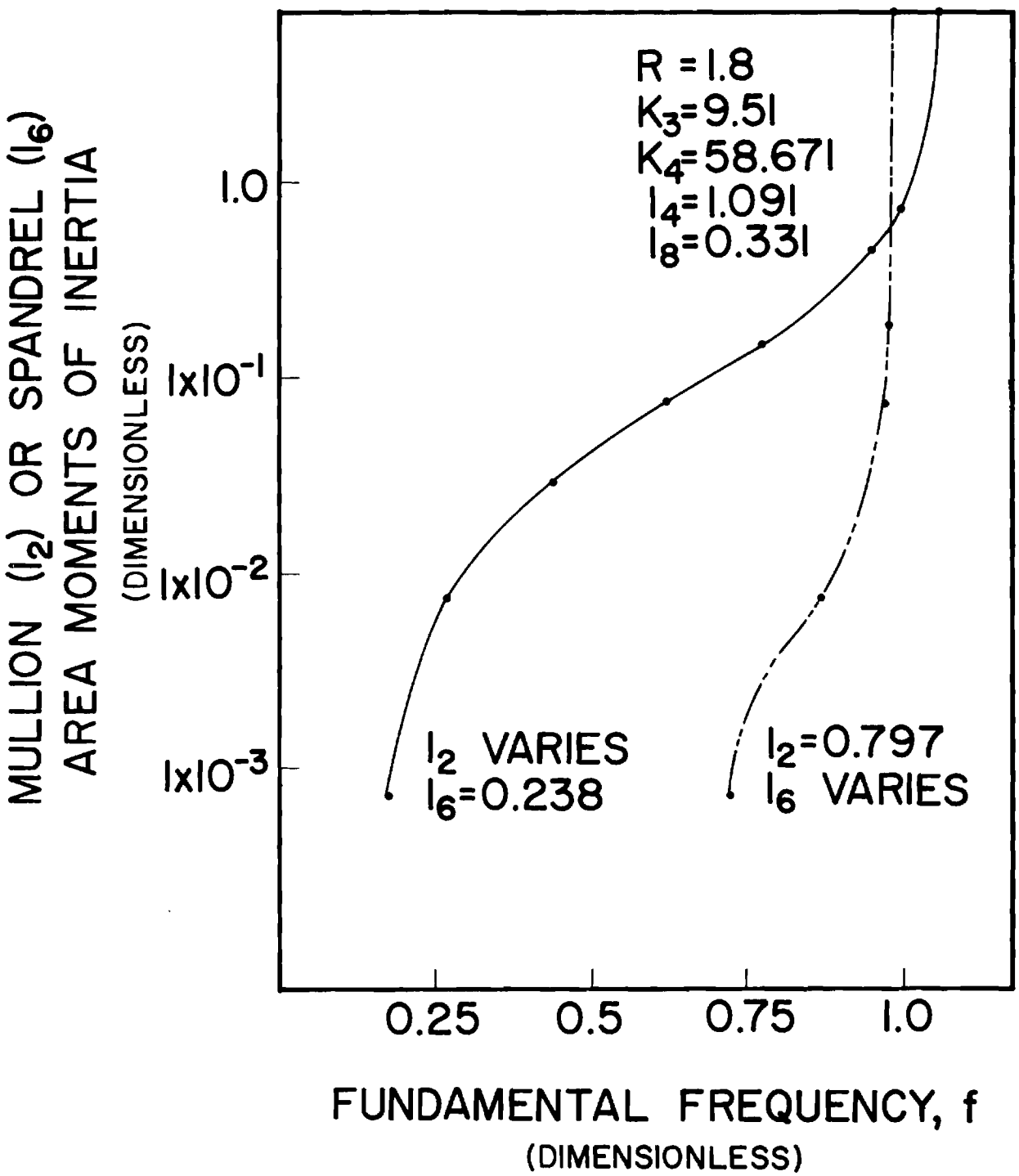

Figure 3.3-17 Panel Fundamental Frequency Versus Mullion and Spandrel Moments of Inertia

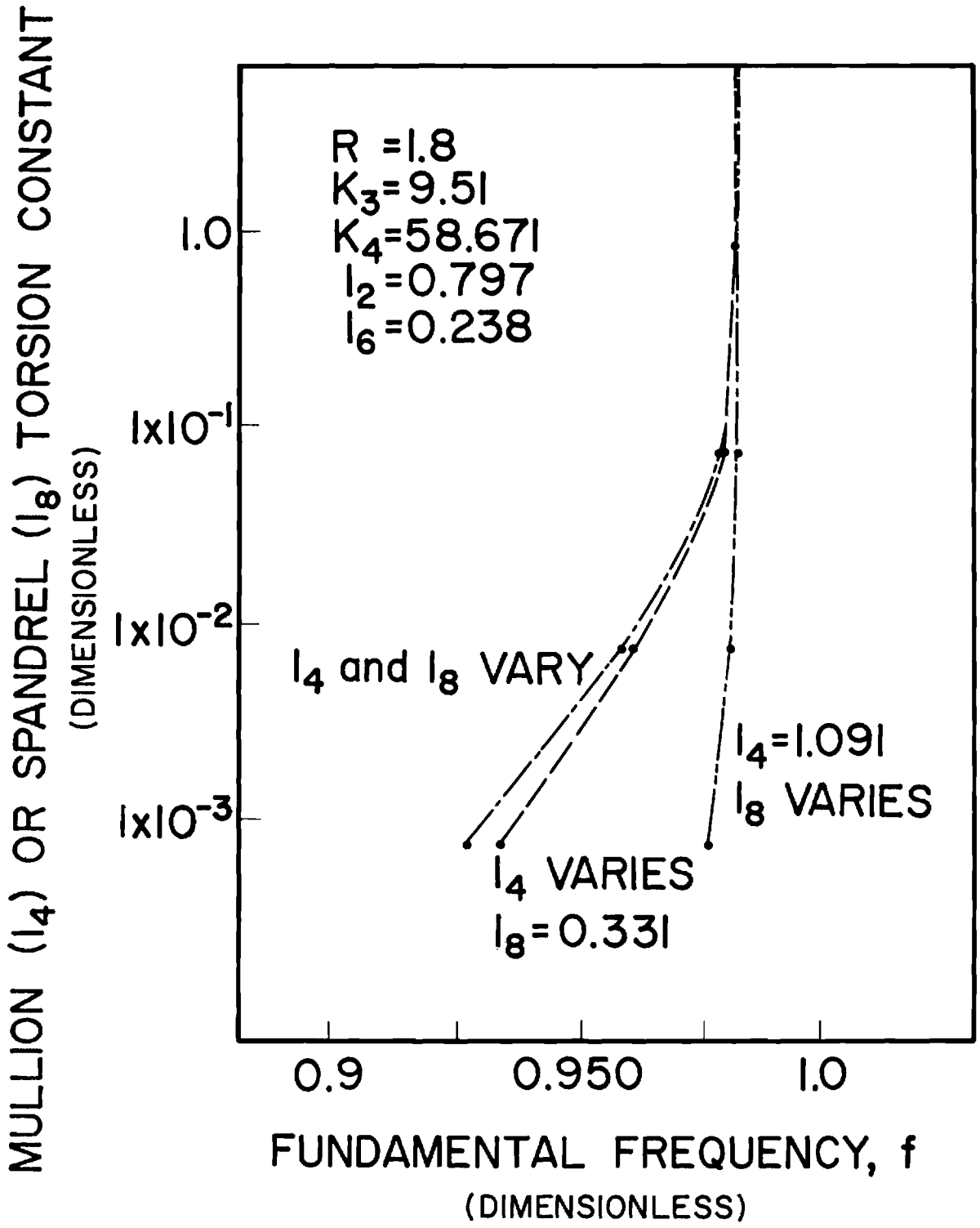

Figure 3.3-18 Panel Fundamental Frequency Versus Mullion or Spandrel Torsion Constant

stiffness produces a notable increase in fundamental frequency with R = 1.8 panels experiencing the greatest variation as shown in Figure 3.3-12. However, as observed earlier in Figure 3.3-8 for the static case, R = 5.0 panels are virtually unaffected by a change in K_4. The greater sensitivity of frequency to rotational rather than normal spring stiffness is also shown in Figure 3.3-13 for the R = 1.8 case. Variation in K_2 is much more effective in changing f than a similar change in K_1 and the influence of K_1 diminishes rapidly at higher values. However, Figure 3.3-14 shows that increasing normal spring stiffness parameter K_1 in the region below $K_1 = 1 \times 10^4$ results in greater increase in frequency for larger values of rotational spring constant K_2. Figure 3.3-14 applies to the R = 1.8 case only, for the numerical values of frame inertia parameters defined in the figure.

Figures 3.3-15 and 3.3-16 display change in fundamental frequency versus mullion and spandrel area moments of inertia, respectively. Mullion flexural stiffness which increases with value of I_2 especially augments frequencies for high aspect ratio panels where the mullion borders the long side of the panel. In Figure 3.3-16, stiff spandrel elements increase the frequency of low aspect ratio panels for the same reason. Finally, in Figure 3.3-17, the effect of change in either mullion (I_2) or spandrel (I_6) area moment of inertia on fundamental frequency of R = 1.8 panels are shown on the same plot. For this aspect ratio and the particular window-frame model used (see Figure 3.3-1), variation in I_2 is much more effective in changing structure frequency than variation in I_6.

Figure 3.3-18 displays the effect of mullion and spandrel torsional stiffness on fundamental frequency of vibration for R = 1.8 structures.

While torsional stiffness of frame elements has very little effect on frequency, mullion stiffness (I_4) is relatively more important than spandrel stiffness (I_8) for this aspect ratio.

Dynamic Response: The dynamic response of the window-frame symmetry model in Figure 3.3-1 was computed for a number of forcing functions, one of which is presented here. An exhaustive study encompassing many different types of excitations was not made although a wide range of loading types can be handled by the analytical model. As an example, panel response to in-plane racking distortions was determined and is presented in the next section. In general, the limited number of cases studied served to confirm results presented in the dimensionless plots above; for example, the model's sensitivity to gasket rotational stiffness was evident in the dynamic response studies.

The pressure signal in Figure 3.3-19 was recorded in the laboratory during dynamic testing and was assumed to be a representative pressure fluctuation-time history which could be used to investigate the dynamic sensitivity of the system. The pressure was assumed to be uniformly distributed over the surface of the panel. Attention was confined to equivalent single plate models with properties listed in Table 3.3-1, thickness of 0.298 in. (0.76 cm), R = 1.8, and $L_e = 0$.

As stated above, the model proved to be more sensitive to rotational spring stiffness than to normal spring stiffness as Figures 3.3-20 and 3.3-21 show. In these figures, dimensionless normal spring constant K_1 and rotational spring constant K_2 are plotted versus dimensionless maximum dynamic response W_2 at the center of the panel due to the excitation in Figure 3.3-19. The maximum dynamic response of a twelve-finite element

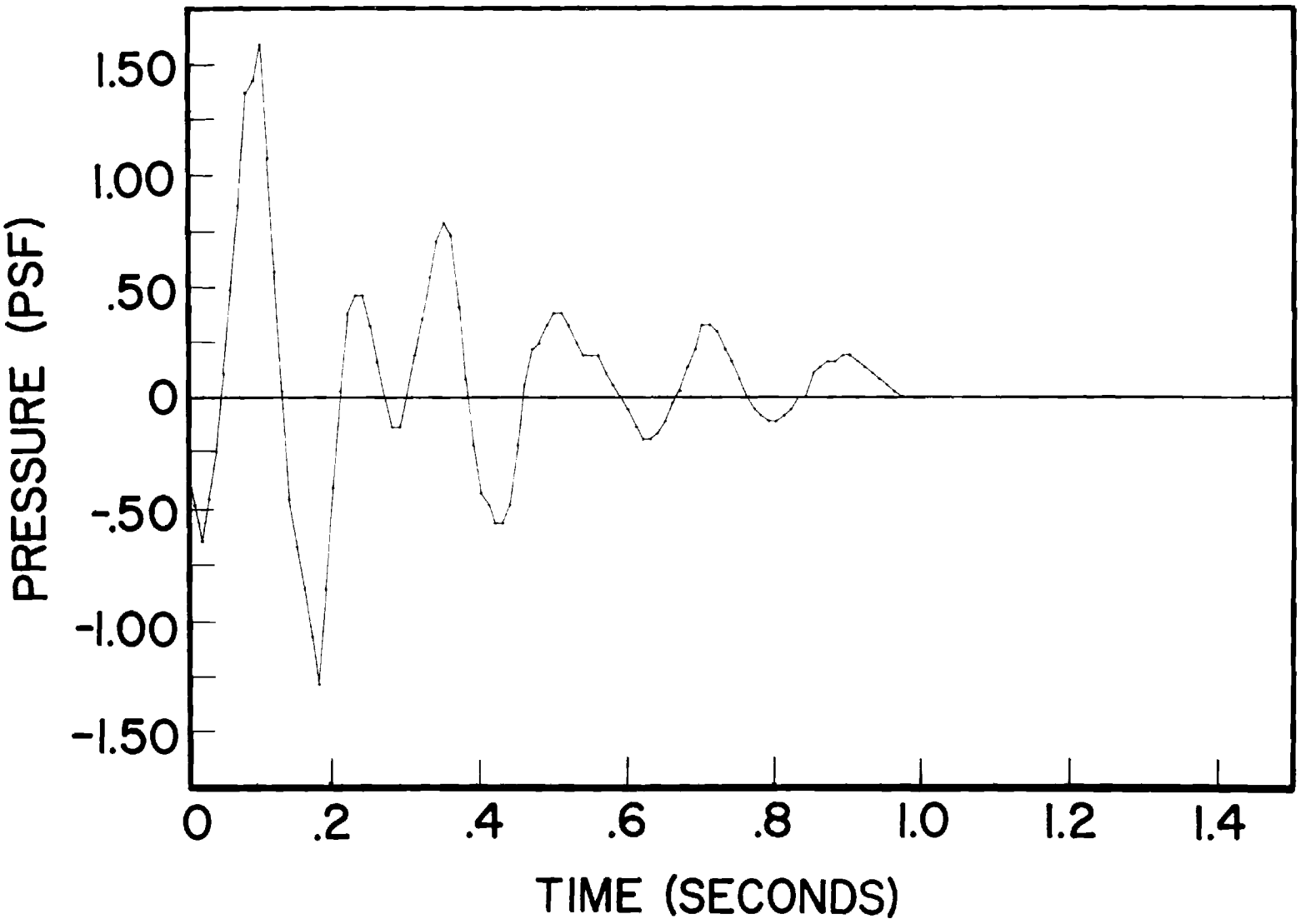

Figure 3.3-19 Uniform Pressure Excitation

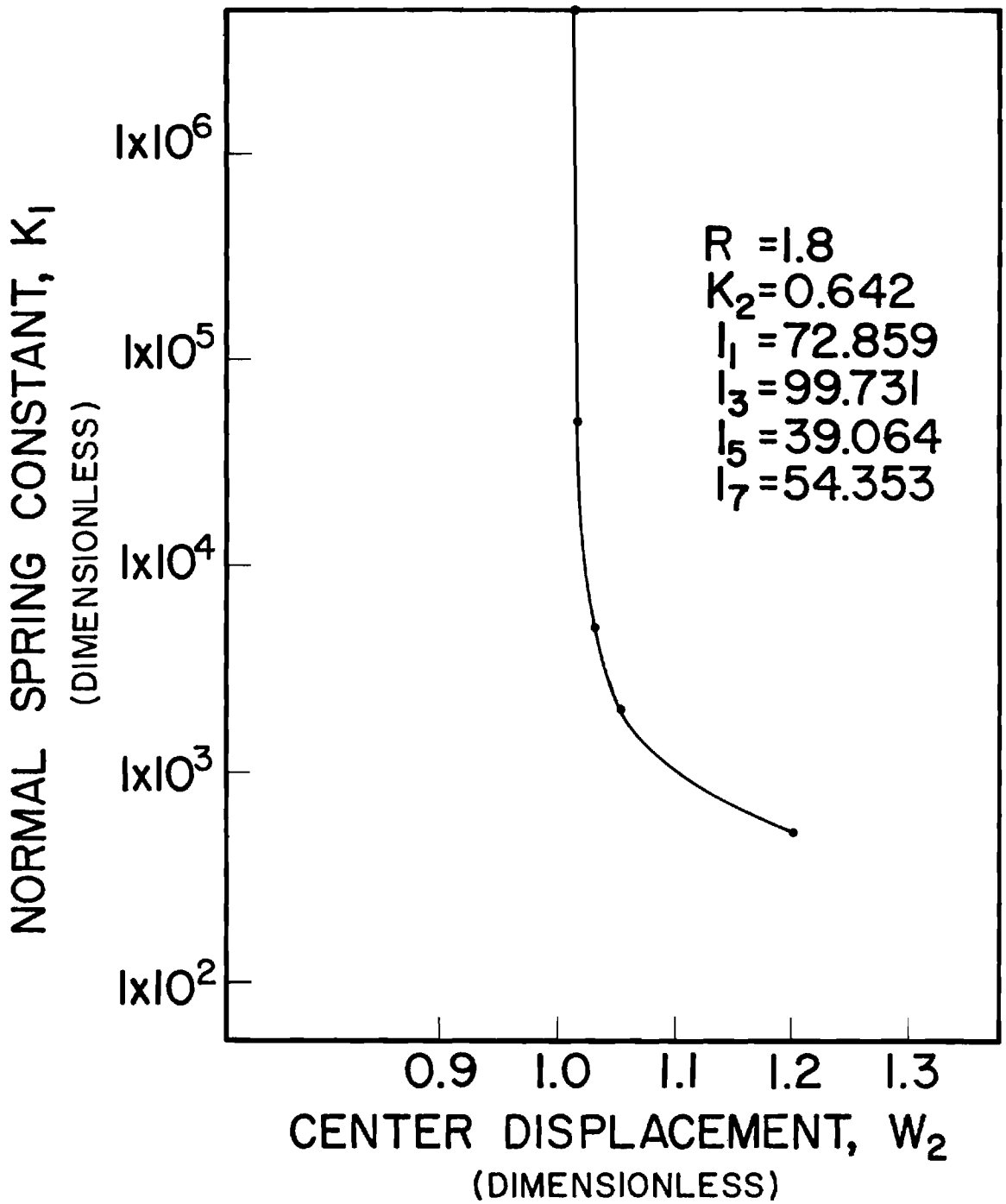

Figure 3.3-20 Maximum Dynamic Response to Pressure Excitation Versus Normal Spring Constant on Boundary

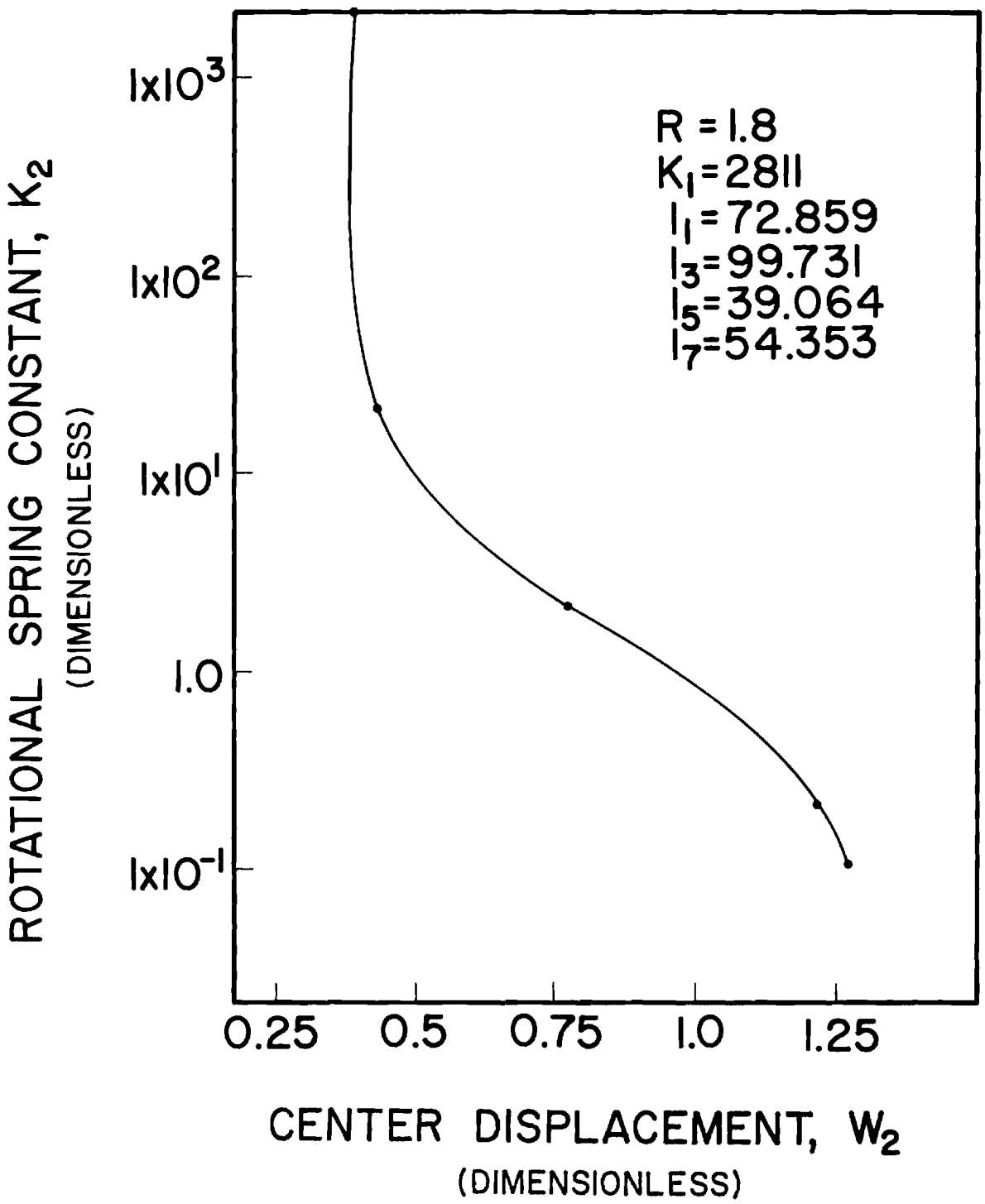

Figure 3.3-21 Maximum Dynamic Response to Pressure Excitation Versus Rotational Spring Constant on Boundary

model of a simply-supported quarter plate (similar to Figure 3.3-1) to this excitation was used to nondimensionalize these plots; its response-time history is recorded in Figure 3.3-22.

The effectiveness of soft (k_R = 50 in-lb/radian/in = 222 N·m/radian/m) and hard (k_R = 1 x 10^6 in-lb/radian/in = 4.45 x 10^6 N·m/radian/m) rotational springs in reducing panel response at the center is also shown in time history plots, Figures 3.3-23 and 3.3-24. Figures 3.3-25 and 3.3-26, however, show that soft (k_N = 100 lb/in/in = 690 kN/m/m) and hard (k_N = 1 x 10^6 lb/in/in = 6.9 x 10^6 kN/m/m) normal springs result in response-time histories which differ only slightly in comparison.

3.3(e) Panel Racking Studies

Differential motions of adjacent floors in a highrise building induced by wind or earthquake introduce in-plane racking distortions into the window-framework structure. The analytical model presented in this report can be used to study the linear small displacement behavior of the system. The finite element model of the full panel and frame between floor levels shown in Figure 3.3-27 was developed to study displacement response but a finer mesh would be needed for detailed stress investigations. The support boundary conditions are modified slightly compared to the symmetry model of Figure 3.3-1 to more closely represent actual points of support in the prototype structure. The frame is simply-supported at lower corner points and at the end of mullion element extensions of length Y_m. Two values of Y_m are considered to provide a range of natural frequencies of vibration for in-plane motion: Y_m = 5 in. (127 mm) represents the laboratory test rig support conditions and Y_m = 50 in. (1270 mm) approximates the support conditions in the field study building.

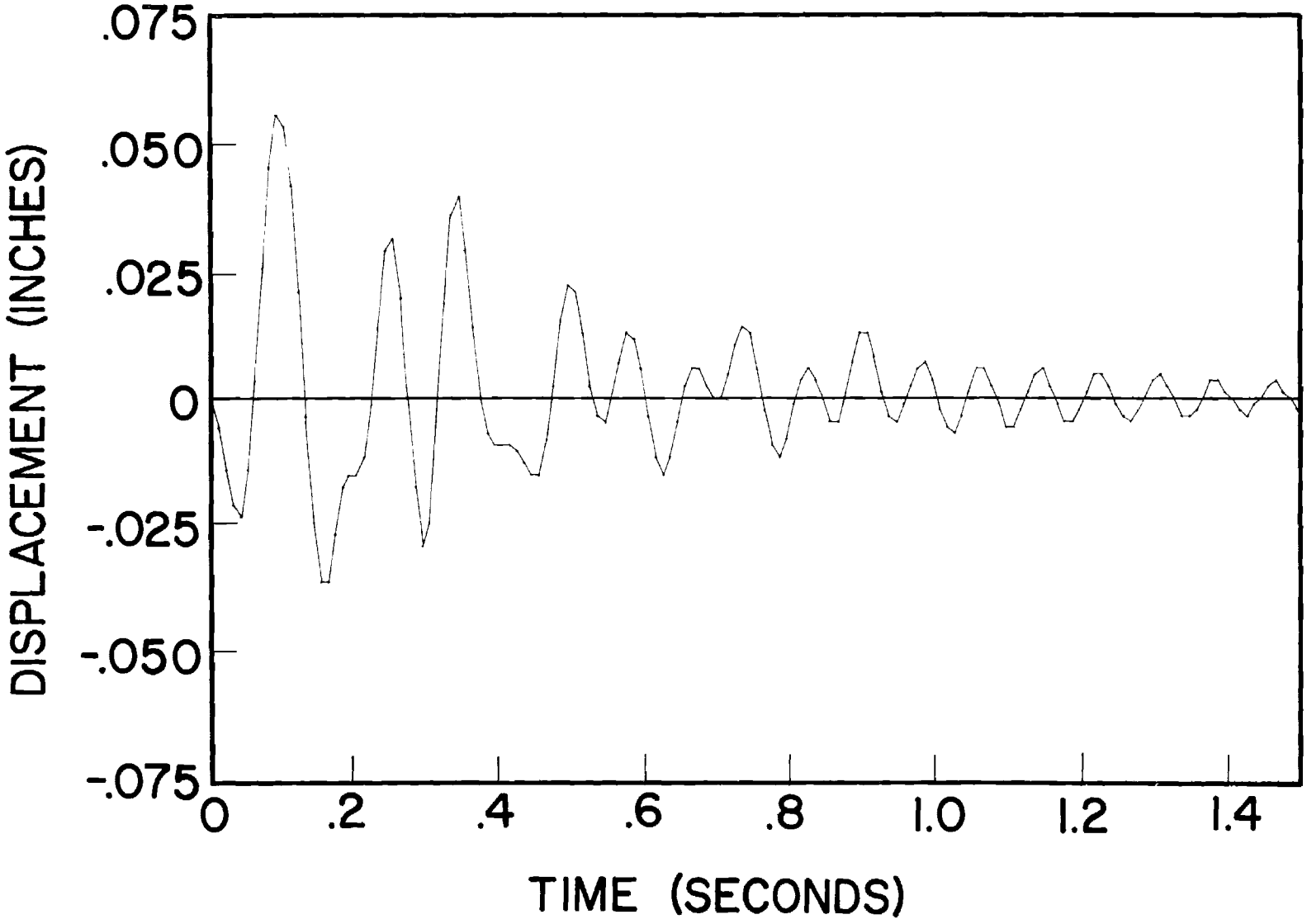

Figure 3.3-22 Dynamic Response of Simply-Supported Plate to Uniform Pressure Excitation

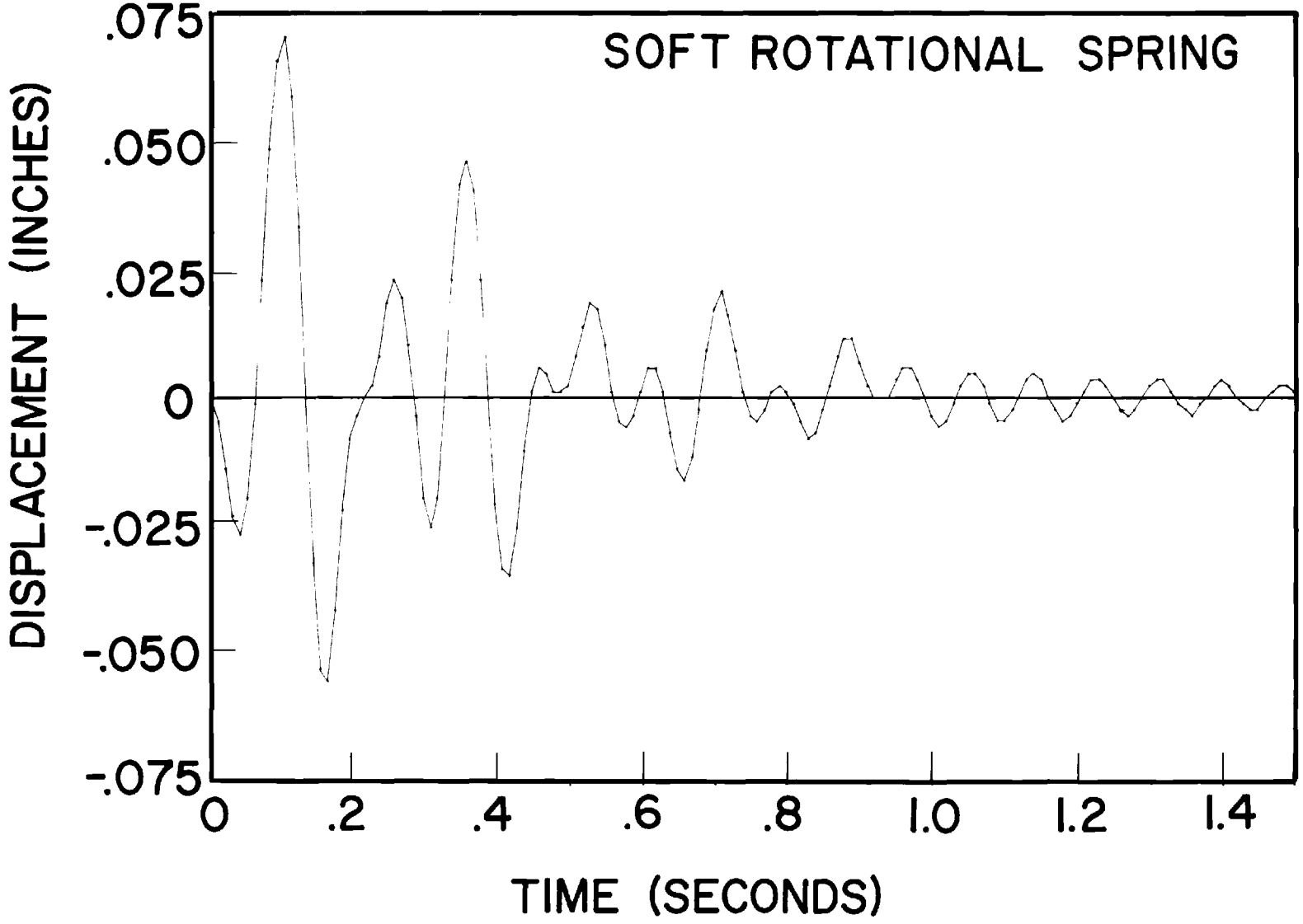

Figure 3.3-23 Dynamic Response of Panel to Uniform Pressure Excitation with Soft Rotational Spring on Boundary

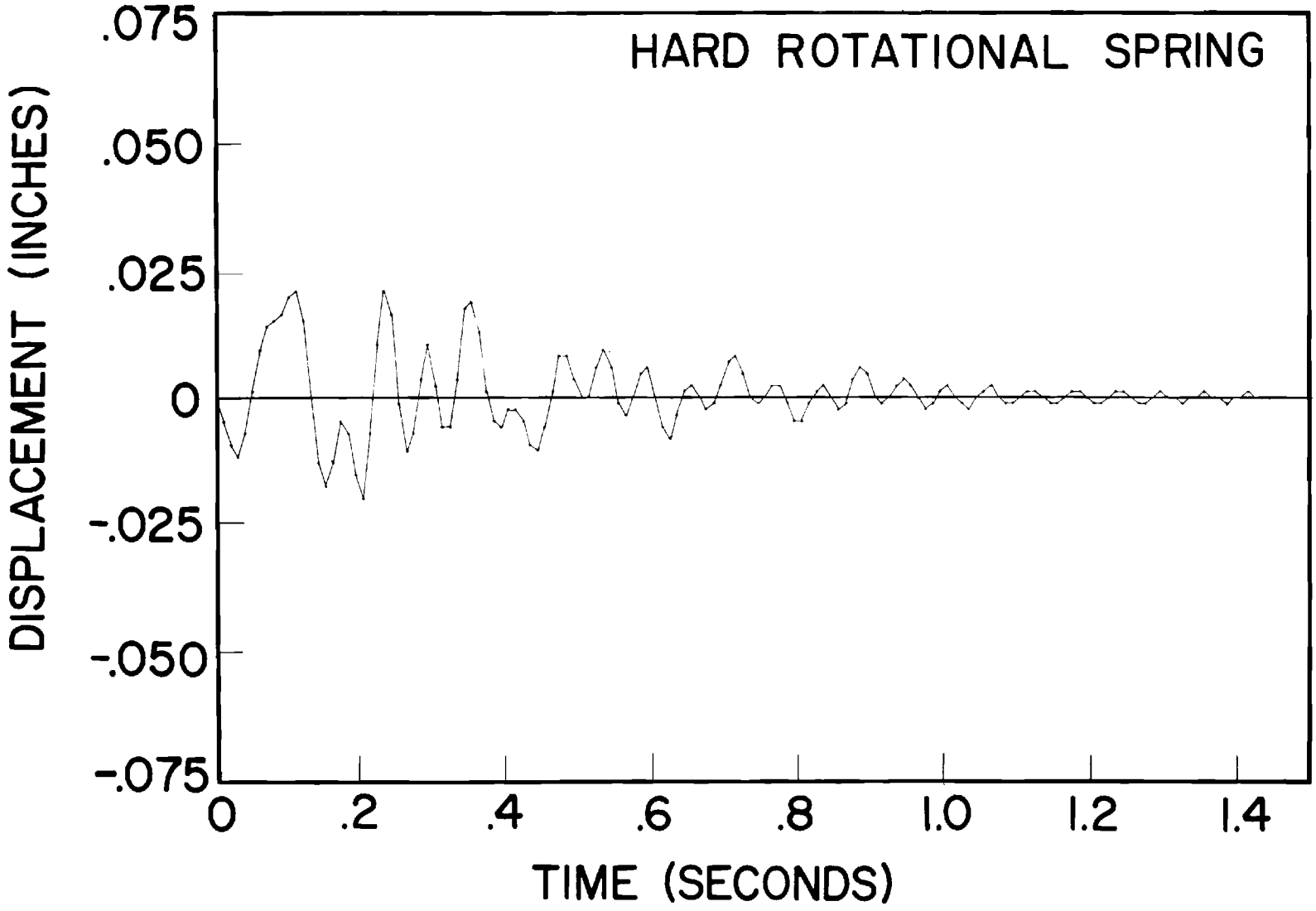

Figure 3.3-24 Dynamic Response of Panel to Uniform Pressure Excitation with Hard Rotational Spring on Boundary

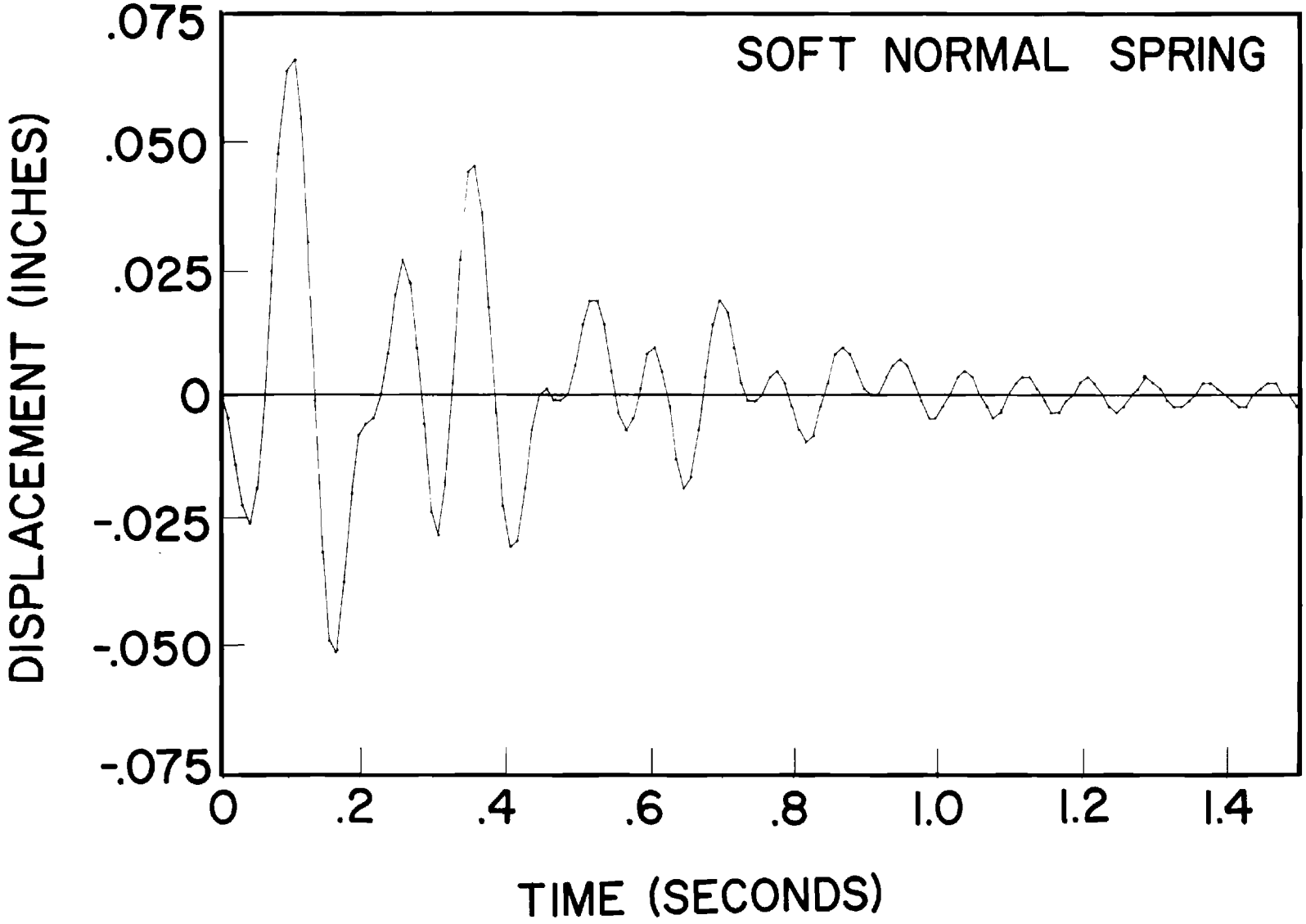

Figure 3.3-25 Dynamic Response of Panel to Uniform Pressure Excitation with Soft Normal Spring on Boundary

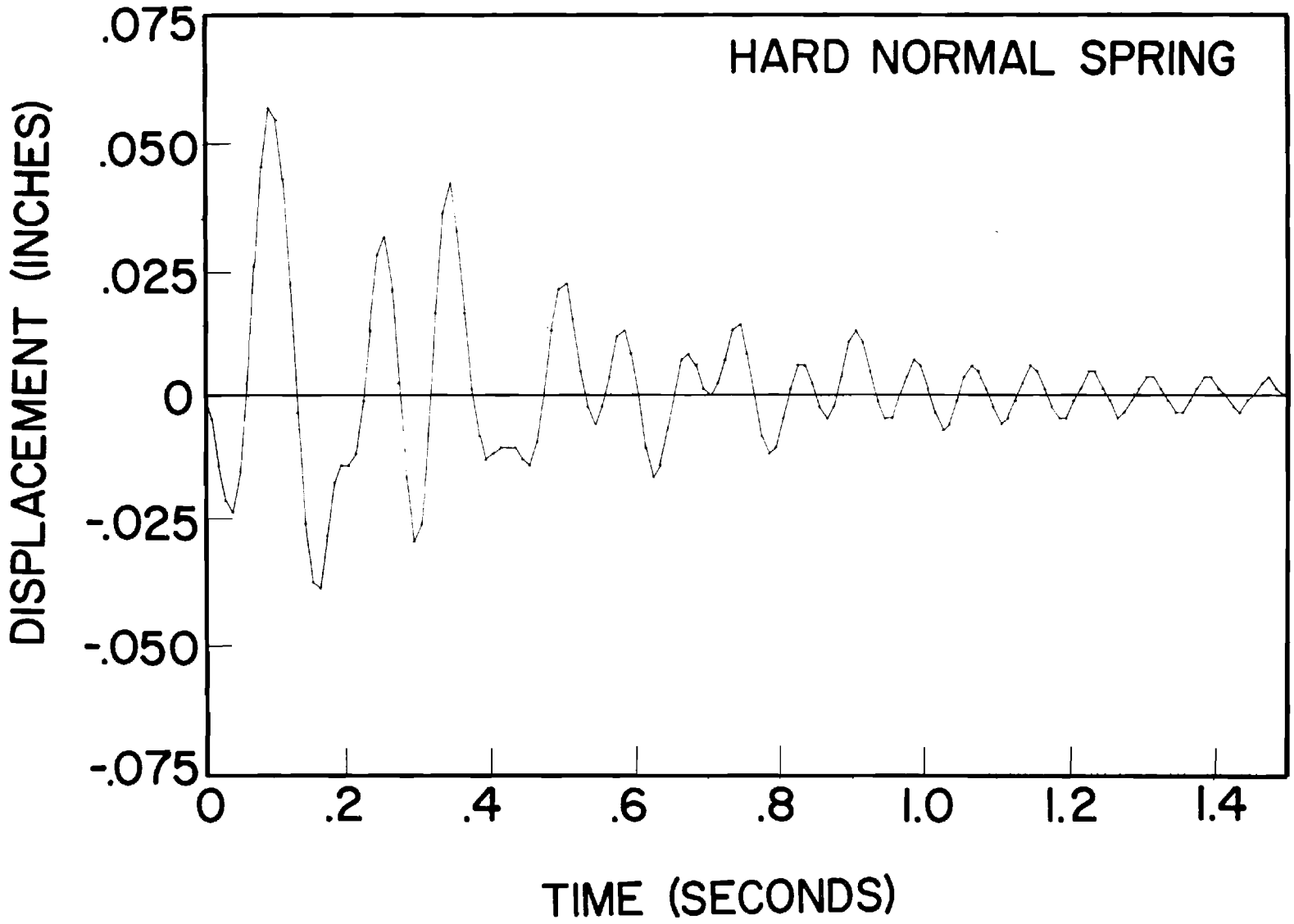

Figure 3.3-26 Dynamic Response of Panel to Uniform Pressure Excitation with Hard Normal Spring on Boundary

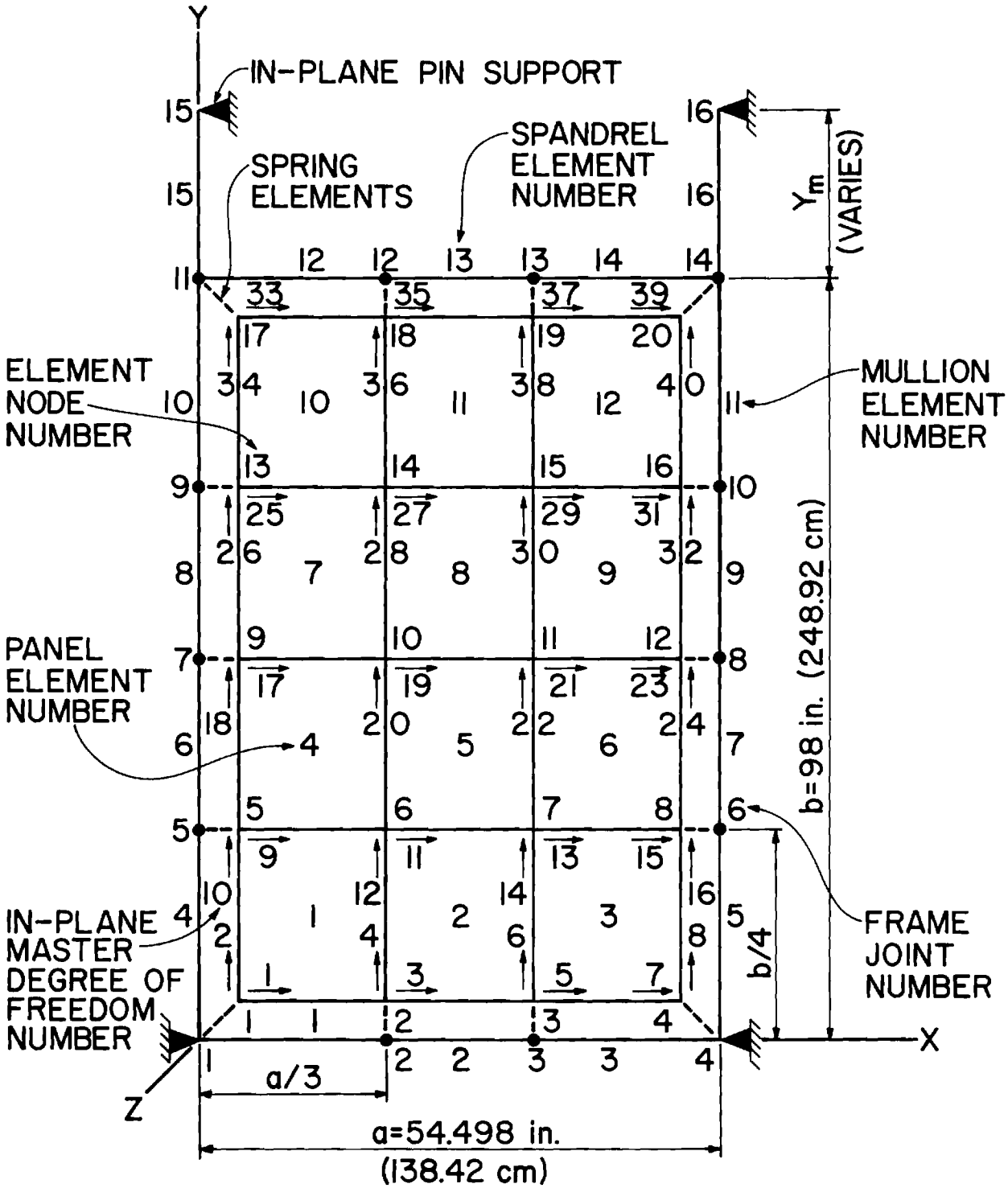

Figure 3.3-27 Finite Element Model of Full Panel and Frame with In-plane Master Degrees of Freedom

An equivalent single panel of thickness 0.298 in. (0.76 cm) and the remaining frame and panel properties in Table 3.3-1 were used for all studies. A consistent mass formulation of the structure mass matrix was chosen and frequencies of vibration determined for the two values of Y_m listed above. Frequencies and mode shapes for the first three modes are summarized in Figures 3.3-28, 3.3-29, and 3.3-30. First and third mode frequencies and vibration shapes are seen to depend on the value of mullion extension length Y_m while second mode results are unaffected by Y_m. All three modes are boundary spring and frame deformation modes and involve very little panel deformation.

To demonstrate the capabilities of the analytical model and to provide some indication of the level and type of response to be expected during racking motions, building response recorded in a moderate earthquake was used to excite the model. The supports at the upper floor level only of the model with Y_m = 50 in. (1270 mm) were assumed to move in accordance with the horizontal displacement and acceleration traces (Figure 3.3-31) recorded on the sixteenth floor of the Alexander Building in the S81W direction during the 1957 San Francisco, California, earthquake. This earthquake of Richter magnitude 5.3 produced a peak floor acceleration of 0.04 g and peak floor displacement of 0.61 in. (1.55 cm). Direct integration of equation (3.1-59) was used to determine the total response of the model assuming simple modal viscous damping at 2% of critical in all modes.

Thirty seconds of displacement response at model degrees of freedom 1, 17, 18, 24, and 33 (see Figure 3.3-27) are shown in Figure 3.3-32. Peak response of 0.107 inches (0.271 cm) is seen to occur at degree of freedom 33 at the top corner of the panel. Comparison of response at

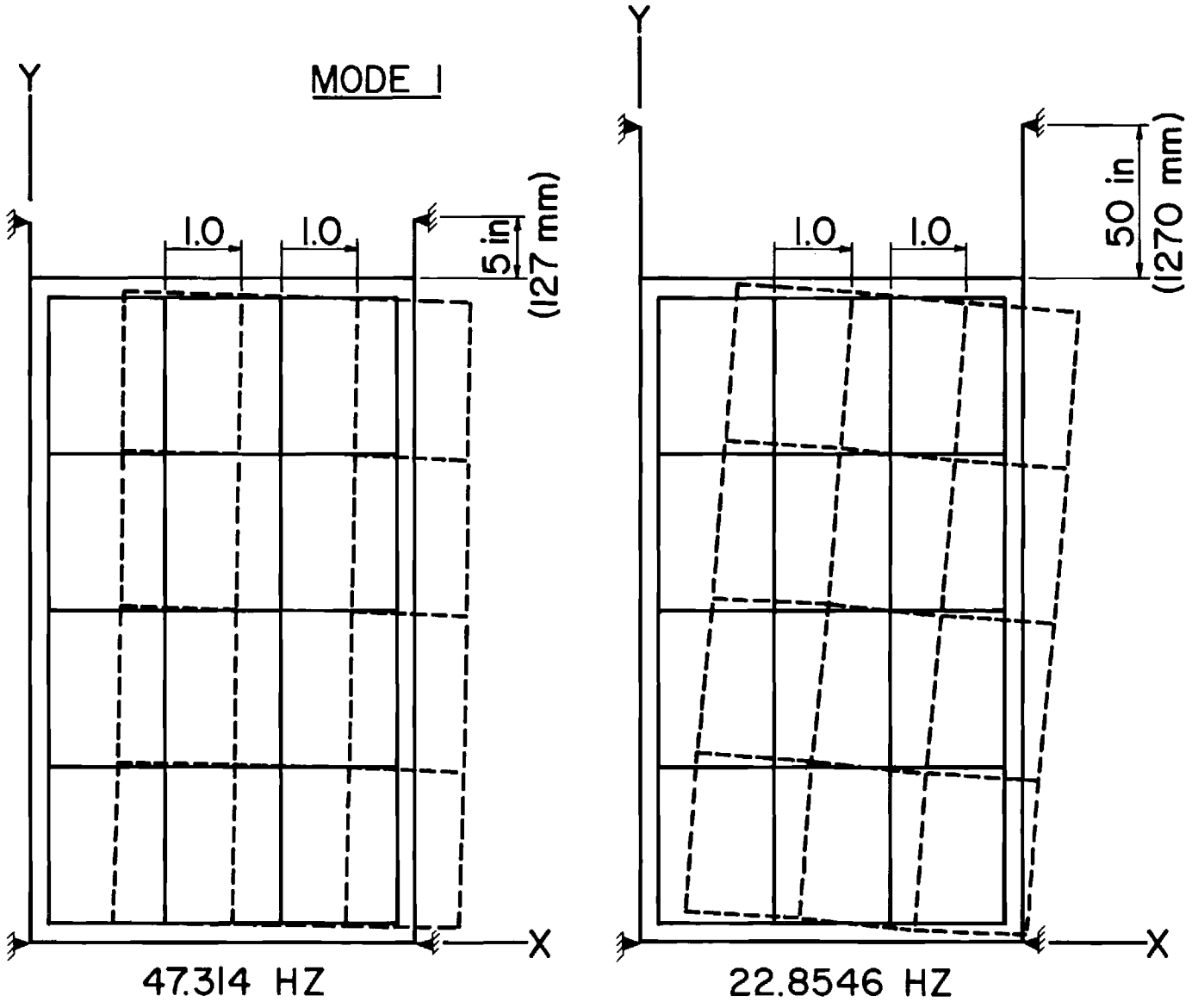

Figure 3.3-28 In-plane Model Frequencies and Mode Shapes, Mode 1

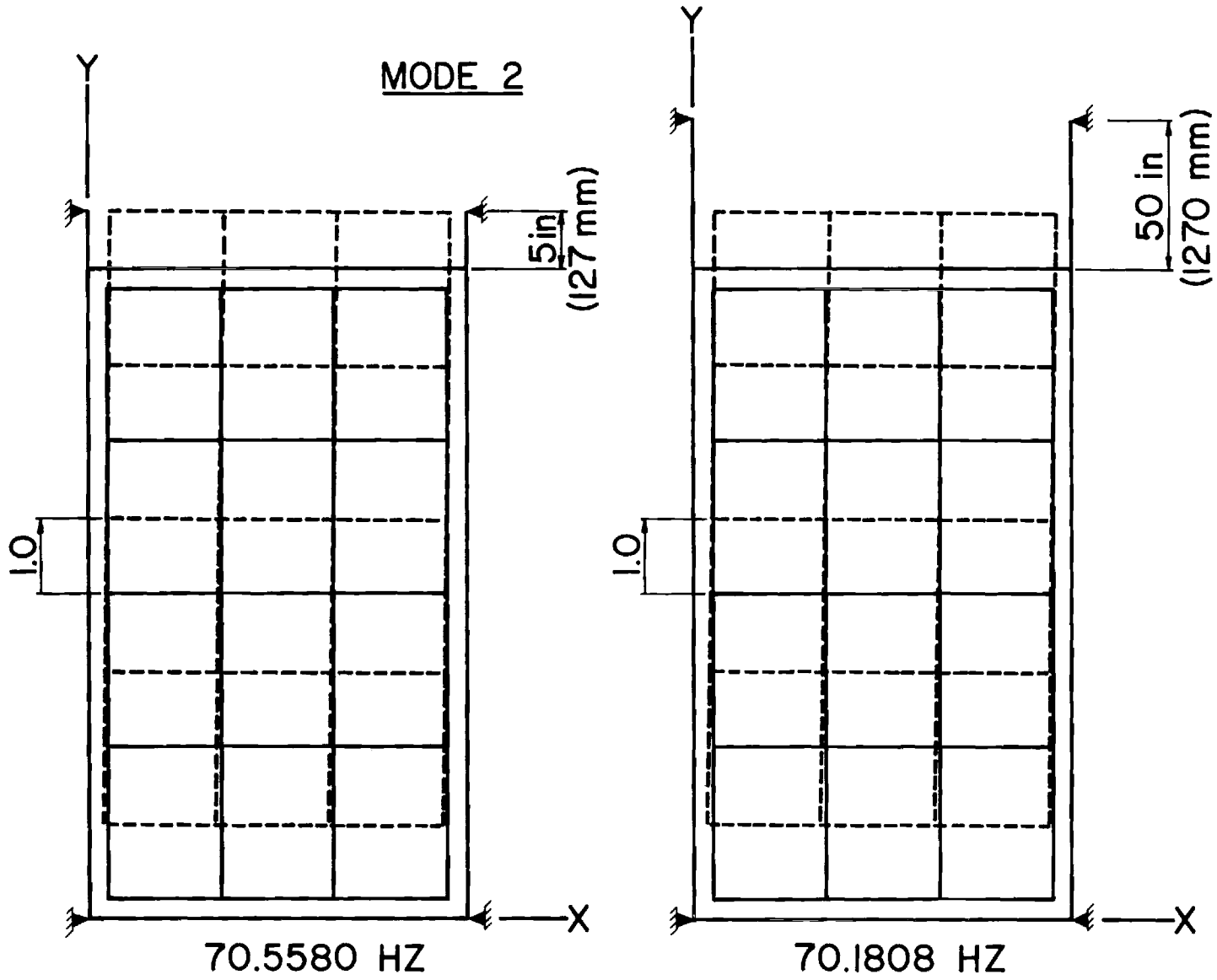

Figure 3.3-29 In-plane Model Frequencies and Mode Shapes, Mode 2

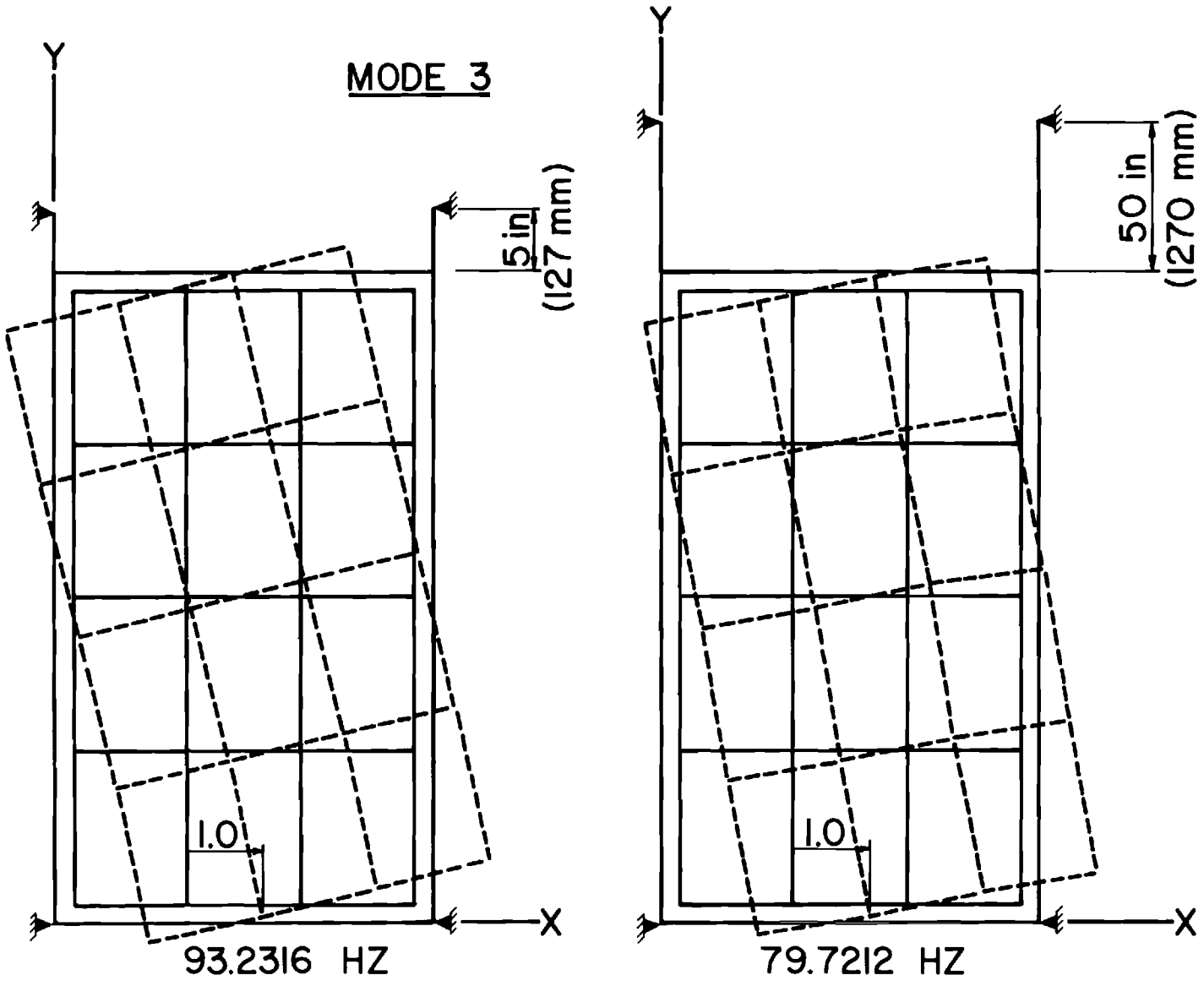

Figure 3.3-30 In-plane Model Frequencies and Mode Shapes, Mode 3

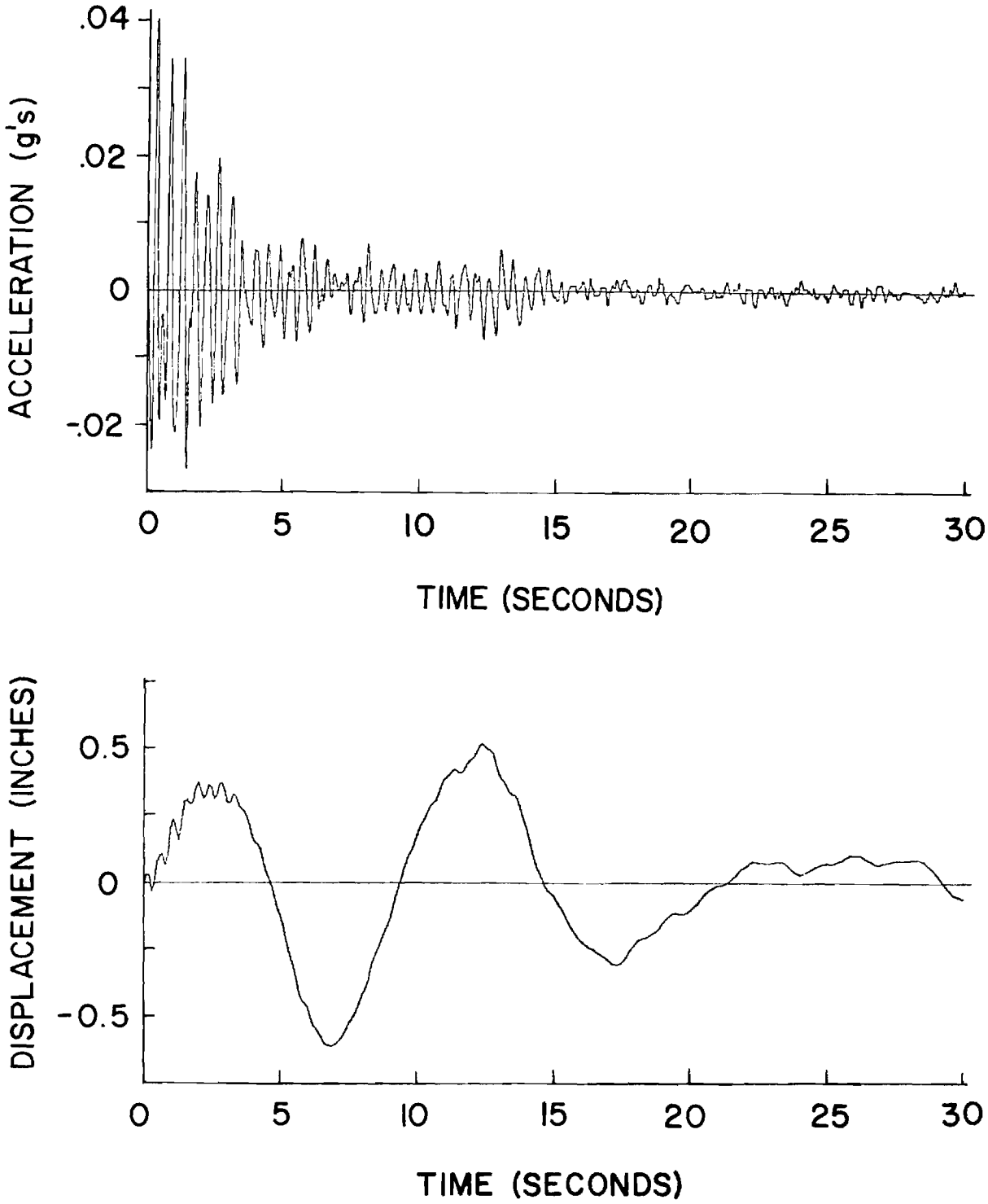

Figure 3.3-31 Acceleration and Displacement Records on 16th Floor of Alexander Building in S81W Direction, 1957 San Francisco, California, Earthquake

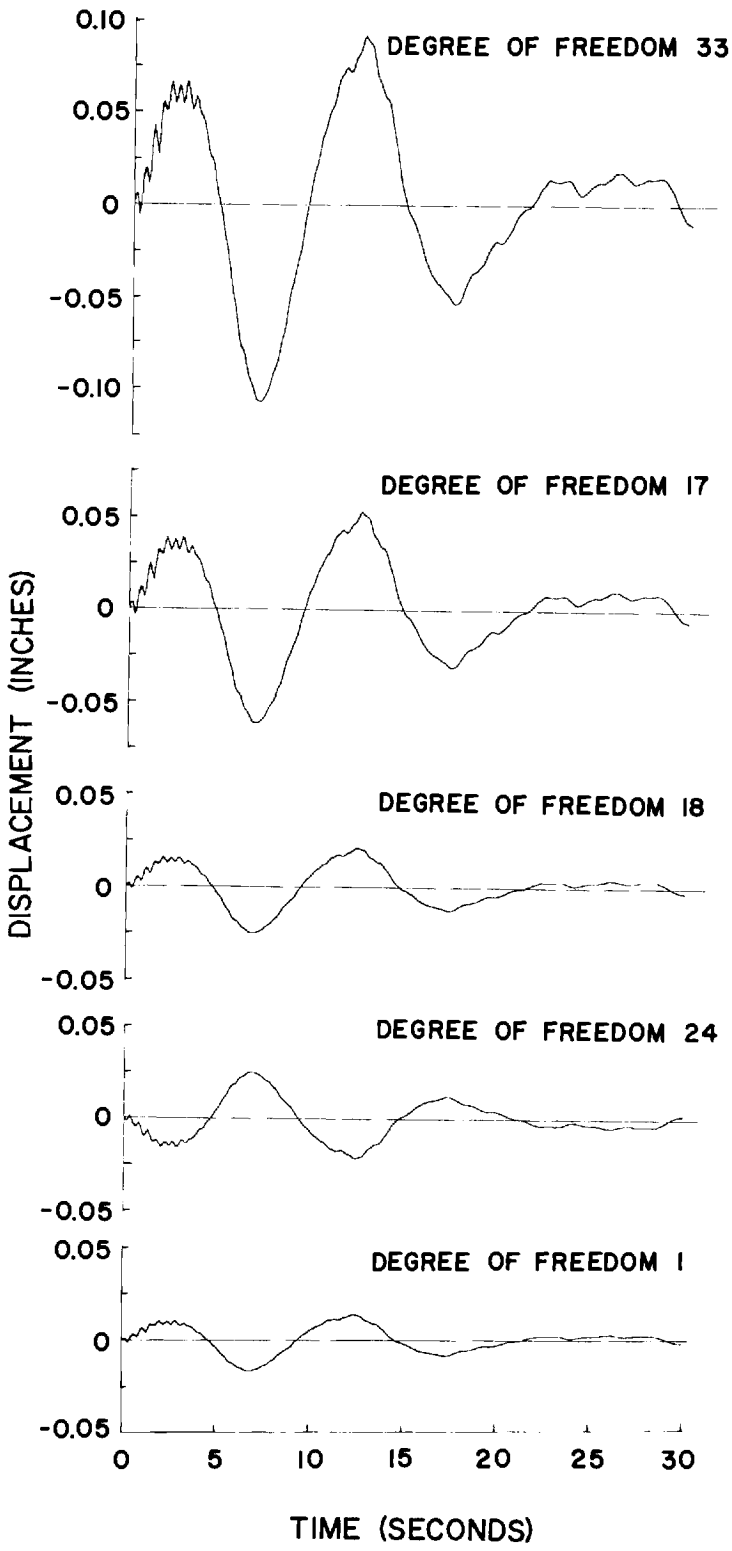

Figure 3.3-32 In-plane Model Displacement Response at Master Degrees of Freedom 1, 17, 18, 24, and 33

degrees of freedom 18 and 24 demonstrates that panel rocking within the frame and gasket assembly is the primary mode of behavior. Panel stress-time histories were not computed.

3.4 Double Panel Models

An equivalent single plate model was developed for the static and dynamic sensitivity studies reported in section 3.3. Actual insulating windows in the prototype structure however are composed of two panes of glass separated by a 0.5 inch (1.27 cm) sealed air space. A double plate continuum model and a parallel-plate finite element model were developed to investigate the out-of-phase dynamic properties of the double panel system.

3.4(a) Continuum Model

The double plate continuum model shown in Figure 3.4-1 is based on the assumption that the glass unit is simply-supported within the boundary frame. The metal spacer bars on the periphery of the panel are assumed to introduce rotational coupling between the plates represented by a distributed rotational spring with spring constant K_θ in units of lb-in/radian/in (N·m/radian/m). A detail of the boundary connection is presented in Figure 3.4-2. A range of values of K_θ, expressed in terms of nondimensional parameters

$$\xi_B = 2K_\theta b/D, \quad \xi_A = \xi_B a/b \tag{3.4-1}$$

was used to approximate varying degrees of interplate connection on the boundary.

In modes of vibration in which volume change occurs, the air gap was modeled as a distributed linear spring with spring constant K_δ expressed in units of lb/in/in^2 (N/m/m^2), i.e. spring stiffness per unit

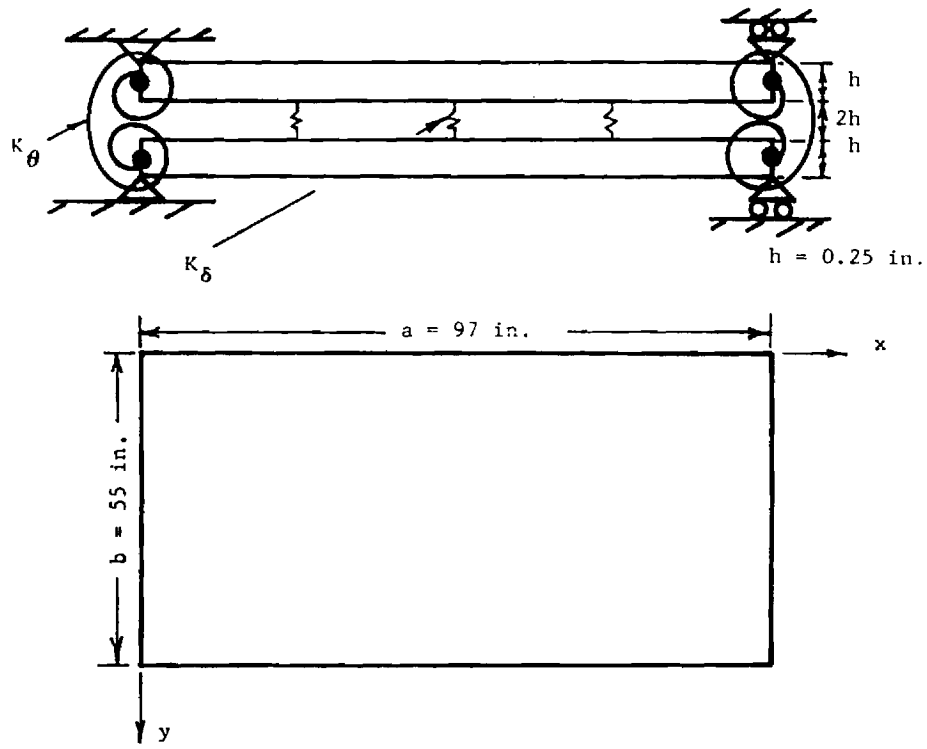

Figure 3.4-1 Continuum Model of the Double Plate System

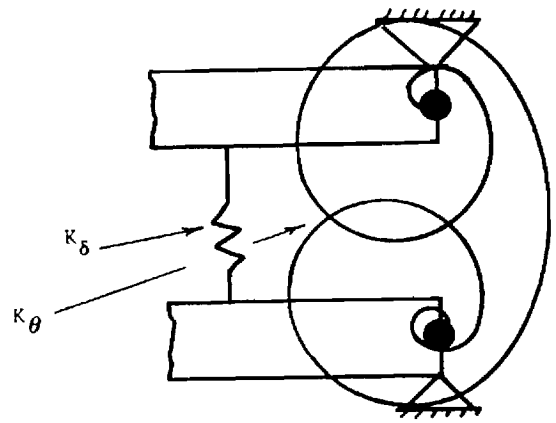

Figure 3.4-2 Details of End Connection

area. To obtain estimates of the natural frequencies, the distributed spring stiffness was taken to be a different constant in each mode of vibration. The stiffness K_δ for the entrapped air was determined by assuming adiabatic compression of the volume and by neglecting resonances of the air mass. A linear relationship between volume change and pressure change was assumed to evaluate K_δ. The linearized pressure-volume relationship for an adiabatic process can be written as:

$$\frac{\Delta p}{p_o} = -\frac{\gamma \Delta V}{V_o}, \quad \gamma = 1.4 \tag{3.4-2}$$

where Δp is the pressure change, p_o = 14.7 psi (101.4 kPa), γ is the adiabatic exponent, ΔV is the volume change, and V_o is the initial volume of the air space which is equal to 2661 in^3 (4.36 x $10^{-2} m^3$). Constant $K_{\delta mn}$ was then computed for the mn^{th} mode as the pressure change per unit modal amplitude, namely,

$$K_{\delta mn} = \frac{\Delta p_{mn}}{a_{mn}} = \frac{\gamma p_o}{V_o} \frac{\Delta V_{mn}}{a_{mn}} \tag{3.4-3}$$

where a_{mn} is the amplitude in the mn^{th} mode. For the (1,1) mode, for example, $K_{\delta 1,1}$ is equal to 19.88 lb/in/in^2 (4328 N/m/m^2). This value applies to a rotationally restrained system with K_θ equal to 256.2 lb-in/radian/in (1140 N·m/radian/m) which corresponds to ξ_B = 2 in equation 3.4-1.

With K_θ and K_δ defined, the governing differential equations for the double plate model of Figure 3.4-1 can be written as follows, assuming the two plates are identical:

$$D\nabla^4 w_1 + \rho h \ddot{w}_1 = -K_\delta (w_1 - w_2)$$
$$D\nabla^4 w_2 + \rho h \ddot{w}_2 = -K_\delta (w_2 - w_1) \qquad (3.4\text{-}4)$$

where w_1 and w_2 are the displacement functions of the upper and lower plate, respectively.

After separation of variables

$$D\nabla^4 W_1 - \omega^2 \rho h W_1 = -K_\delta (W_1 - W_2) \qquad (3.4\text{-}5a)$$

$$D\nabla^4 W_2 - \omega^2 \rho h W_2 = -K_\delta (W_2 - W_1) \qquad (3.4\text{-}5b)$$

where

$$W_i = W_i\,(x,y), \quad i = 1,2$$

The appropriate boundary conditions are:

$$\begin{aligned}
y = 0 \quad & W_1 = 0 \quad D\frac{\partial^2 W_1}{\partial y^2} = K_\theta \frac{\partial (W_1 - W_2)}{\partial y} \\
& W_2 = 0 \quad D\frac{\partial^2 W_2}{\partial y^2} = K_\theta \frac{\partial (W_2 - W_1)}{\partial y} \\
y = b \quad & W_1 = 0 \quad -D\frac{\partial^2 W_1}{\partial y^2} = K_\theta \frac{\partial (W_1 - W_2)}{\partial y} \\
& W_2 = 0 \quad -D\frac{\partial^2 W_2}{\partial y^2} = K_\theta \frac{\partial (W_2 - W_1)}{\partial y} \\
x = 0 \quad & W_1 = 0 \quad D\frac{\partial^2 W_1}{\partial x^2} = K_\theta \frac{\partial (W_1 - W_2)}{\partial x} \\
& W_2 = 0 \quad D\frac{\partial^2 W_2}{\partial x^2} = K_\theta \frac{\partial (W_2 - W_1)}{\partial x} \\
x = a \quad & W_1 = 0 \quad -D\frac{\partial^2 W_1}{\partial x^2} = K_\theta \frac{\partial (W_1 - W_2)}{\partial x} \\
& W_2 = 0 \quad -D\frac{\partial^2 W_2}{\partial x^2} = K_\theta \frac{\partial (W_2 - W_1)}{\partial x}
\end{aligned} \qquad (3.4\text{-}6)$$

The solution of equations 3.4-5 satisfying equations 3.4-6 can be simplified if in-phase and out-of-phase vibration modes are considered separately. For in-phase motions, no volume change occurs and equations 3.4-5 reduce to

$$D\nabla^4 W_S - \omega^2 \rho h W_S = 0 \tag{3.4-7}$$

where

$$W_S(x,y) = W_1(x,y) + W_2(x,y) \tag{3.4-8}$$

and boundary conditions in equation 3.4-6 become

$$\begin{aligned} y = 0,\ b \quad & W_S = 0 \quad \frac{\partial^2 W_S}{\partial y^2} = 0 \\ x = 0,\ a \quad & W_S = 0 \quad \frac{\partial^2 W_S}{\partial x^2} = 0 \end{aligned} \tag{3.4-9}$$

The eigenvalues and eigenvectors of equation 3.4-7 are

$$\omega_{mn} = \pi^2 \sqrt{\frac{D}{\rho h}} \left\{ \left(\frac{m}{a}\right)^2 + \left(\frac{n}{b}\right)^2 \right\} \tag{3.4-10a}$$

$$W_{S_{mn}} = \frac{2}{\sqrt{\rho a b}} \operatorname{Sin} \frac{m\pi x}{a} \operatorname{Sin} \frac{n\pi y}{b} \tag{3.4-10b}$$

where

$$\rho \int\int W_{S_{mn}}^2 \, dxdy = 1 \tag{3.4-10c}$$

For out-of-phase motions, the equations of motion 3.4-5 reduce to

$$D\nabla^4 W_o - (\omega^2 \rho h - 2K_\delta) W_o = 0 \tag{3.4-11}$$

where

$$W_o = W_1(x,y) - W_2(x,y) \tag{3.4-12}$$

If

$$\Omega^2 = \omega^2 \rho h - 2K_\delta \tag{3.4-13}$$

then equation 3.4-11 becomes

$$D\nabla^4 W_o - \Omega^2 W_o = 0 \tag{3.4-14}$$

The boundary conditions governing out-of-phase vibrations are

$$y = 0,\ b \quad W_o = 0 \quad \frac{\partial^2 W_o}{\partial y^2} = \pm\frac{\xi_B}{b}\frac{\partial W_o}{\partial y}$$

$$x = 0,\ a \quad W_o = 0 \quad \frac{\partial^2 W_o}{\partial x^2} = \pm\frac{\xi_A}{a}\frac{\partial W_o}{\partial x} \qquad (3.4\text{-}15)$$

where

$$\xi_B = \frac{2K_\theta b}{D}\ ,\ \xi_A = \xi_B\, a/b \qquad (3.4\text{-}1)\ \text{repeated}$$

Using assumed eigenfunctions of the form

$$W_o = \sum_m^M \sum_n^N a_{mn} X_m(x) Y_n(y) \qquad (3.4\text{-}16)$$

the resulting eigenvalue for the mn^{th} mode is shown to be

$$\Omega_{mn}^2 = \frac{1}{b^2}\sqrt{\frac{D}{\rho h}}\left[\left(\frac{b}{a}\right)^4 \alpha_m^{\,4} + \alpha_n^{\,4} + 2\left(\frac{b}{a}\right)^2 \phi_{mm}\phi_{nn}\right]^{1/2} \qquad (3.4\text{-}17)$$

where

$$\phi_{mn} = \frac{\alpha_m^2\left[\alpha_m(B^2_m + 1) + 2A_m(B_m - 1)\right]}{\alpha_m\left[2A_m^2 - B_m^2 + 1\right] + 2A_m(B_m + 1)} \qquad (3.4\text{-}18a)$$

$$\phi_{nn} = \frac{\alpha_n^2\left[\alpha_n(B_n^2 + 1) + 2A_n(B_n - 1)\right]}{\alpha_n\left[2A_n^2 - B_n^2 + 1\right] + 2A_n(B_n + 1)} \qquad (3.4\text{-}18b)$$

Further details are provided in reference 40.

Calculated values of the natural frequencies of in-phase motion up to 55 Hz, and corresponding values for out-of-phase motion are shown in Table 3.4-1. Equations 3.4-10a and 3.4-17 were evaluated to obtain in-phase and out-of-phase values respectively. The natural frequencies for out-of-phase motions are evaluated at extreme and intermediate values of ξ_B where $\xi_B = 0$ implies no plate interconnection at the boundaries and $\xi_B = \infty$ indicates that the plates are rigidly connected.

Table 3.4-1. Natural Frequencies of the Double Plate System, Continuum Model

Mode Shape		Natural Frequency, f_n in Hz			
m(x-ax)	n	In Phase	Out of Phase, K_θ & K_δ included		
		S. S. BC's	$\xi_B = 1 \times 10^{-10}$	$\xi_B = 2.0$	$\xi_B = 1 \times 10^{10}$
(1)	(2)	(3)	(4)	(5)	(6)
1	1	10.46	120.02	129.35	160.14
2	1	18.09	18.09	20.04	28.44
3	1	30.81	75.60	81.98	112.46
1	2	34.21	34.21	36.86	52.10
2	2	41.84	41.84	44.32	59.80
4	1	48.61	48.61	50.41	62.03
3	2	54.56	54.56	56.85	72.80

3.4(b) Discrete Element Model

A parallel-plate finite element model was developed for comparison with the continuum model described above. The model shown in Figure 3.4-3 includes the entire frame and panel but only the upper plate is represented due to symmetry. The boundary frame is simply-supported at all frame joints and the panel is permitted to vibrate freely within the framework. Discrete springs with spring constant k_N equal to twice $K_{\delta 1,1}$ (due to symmetry) times tributary panel area are attached to interior panel nodes to account for air gap stiffness in the first breathing mode. The value of $K_{\delta 1,1}$ of 19.88 lb/in/in^2 (4328 N/m/m^2) reported earlier is used to compute k_N. Normal springs on the panel boundary, representing the normal stiffness of the spacer bar between the glass plates, have a spring constant k_{NB} which varies between soft (8.85×10^3 lb/in = 1.55×10^3kN/m) and hard (5×10^7 lb/in = 8.76×10^6 Kn/m) values so that a range of breathing mode frequencies could be determined. The rotational spring on the panel boundary representing the rotational stiffness of the spacer bar has spring constant k_R equal to twice K_θ (due to symmetry) times tributary boundary length. The value of K_θ was set at 256.2 lb-in/radian/in (1140 N·m/radian/m) as in the continuum model.

Discrete model results were generated for the first breathing mode only but for soft and hard springs k_{NB} and for soft, intermediate, and hard springs K_θ (expressed in terms of ξ_B in equation3.4-1). Frequencies of vibration are tabulated in Table 3.4-2. The flexible spring boundary used in the discrete model results in first mode frequencies which are up to 10% lower than continuum model values, but hard spring results are within 5% of continuum model frequencies.

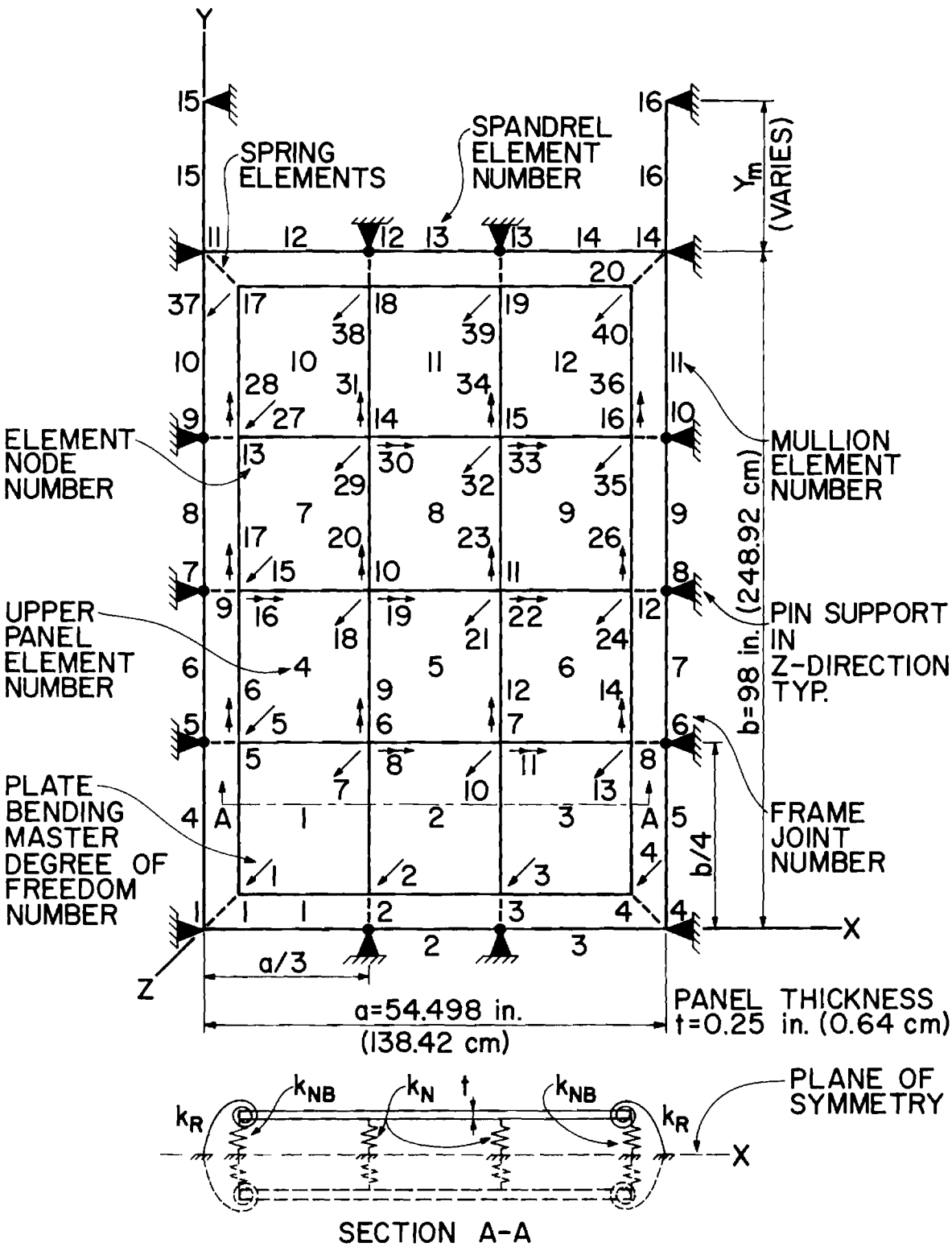

Figure 3.4-3 Finite Element Model of Double Plate System

Table 3.4-2 Natural Frequencies of Double Plate System, First Breathing Mode

Model	Natural Frequency in Hertz		
	$\xi_B = 1 \times 10^{-10}$	$\xi_B = 2$	$\xi_B = 1 \times 10^{10}$
(1)	(2)	(3)	(4)
Continuum[a]	120.02	129.35	160.14
Discrete			
--soft spring[b]	116.93	119.91	144.68
--hard spring[c]	118.44	122.28	156.89

[a] See Table 3.4-1.

[b] $k_{NB} = 8.85 \times 10^3$ lb/in (1.55×10^3 kN/m)

[c] $k_{NB} = 5.0 \times 10^7$ lb/in (8.76×10^6 kN/m)

3.5 Overall Structure Cladding Model

The laboratory, field, and computer studies described in this report have sought to provide information on dynamic loadings and response mechanisms which affect the structural integrity of individual window-frame units such as those found in the prototype structure. Attention has been focused on a small part of the structure's curtain wall and factors affecting interaction of the exterior cladding with the structural frame have not been considered in these initial studies. However, a number of recent failures particularly of lightweight cladding elements demonstrate that the building curtain wall forms a first line of defense for the structure. In fact the overall cladding system may actually provide a considerable amount of resistance to low level excitations and help to control interstory drift and building motion affecting occupant comfort.

The stiffness of expensive cladding elements can, and should, be used to advantage by the structural designer. In the past, the exterior curtain wall has been treated as nonstructural and isolated from the motions of the primary structure. However, analytical models of the total structure including both the basic frame and exterior curtain wall can be developed using a multistory building model, such as the tier building substructure model (93,94,95), and an appropriate cladding model of the type described in this report. For example, a finite element representation of a portion of the curtain wall can be assembled and inserted into the framing substructure between floor levels A and B as shown in Figure 3.5-1. In this way, all elements contributing stiffness to the overall structure can be accounted for in a rational manner and cladding-structure interaction forces determined for use in design of the curtain wall. Follow-on studies of this kind are currently underway.

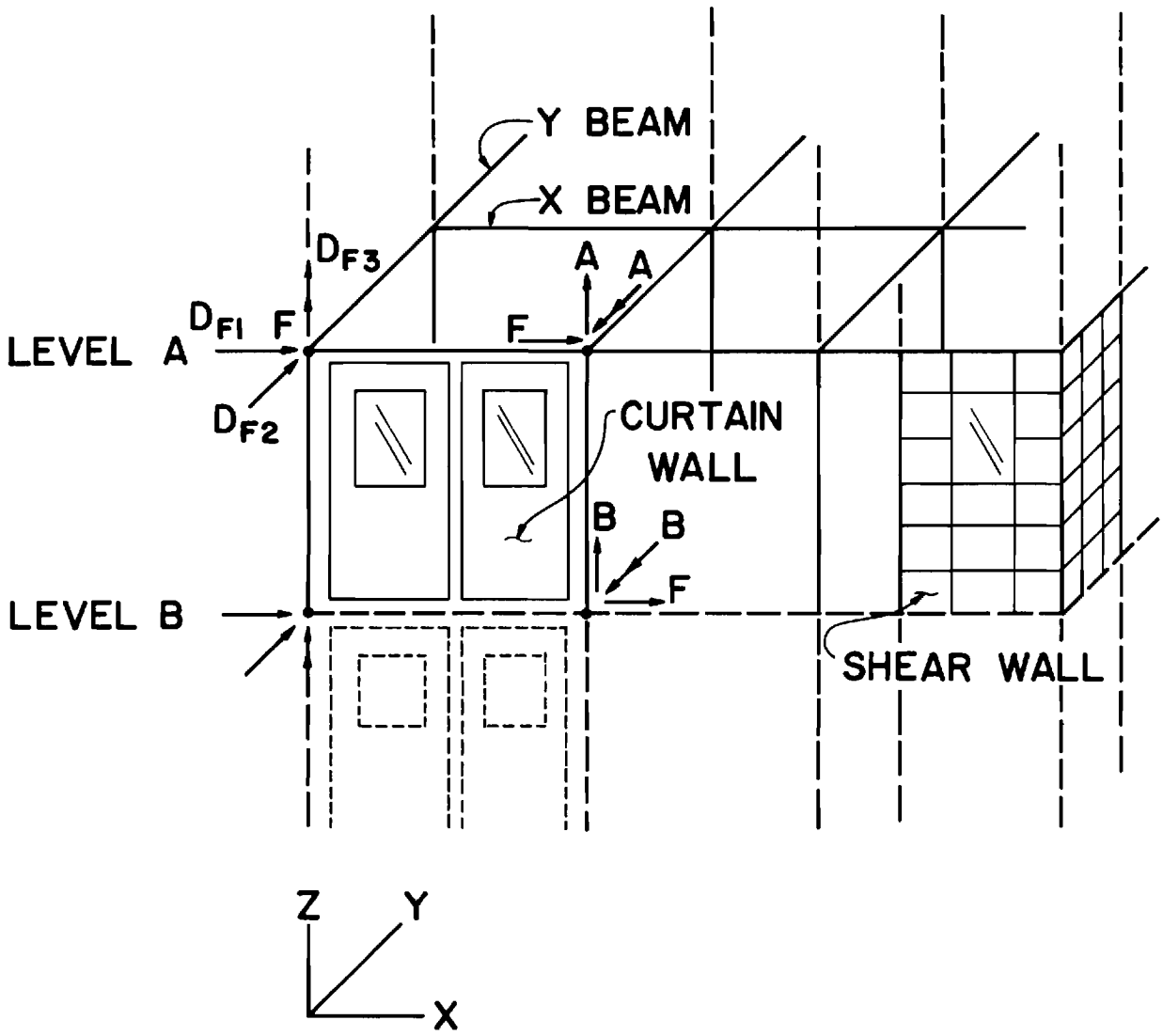

Figure 3.5-1 Tier Building Substructure with Curtain Wall Model

3.6 Summary

The initial analytical studies of the static and dynamic response of glass curtain wall systems described in this chapter have focused attention on the properties and behavior of a small segment of the exterior curtain wall encompassing the frame, gaskets, and a single glass panel. A frame-finite element model and computer program were developed to represent the cladding system and model properties adjusted until a good correlation between laboratory and computer response was established. The analytical model is general in scope and permits a wide range of cladding configurations and loading types to be considered. Panel response to static and dynamic pressure loadings and racking distortions introduced by differential motion of adjacent floors were some of the loadings considered.

Sensitivity studies were conducted to determine the influence of model properties on the static and dynamic response of the panel-frame assembly. Response was shown to be sensitive to gasket rotational stiffness and frame flexural stiffness for selected panel aspect ratios. Results of the analytical studies are presented in a series of nondimensional plots of selected properties versus normalized panel displacement or natural frequency of vibration.

The analytical cladding model is compatible with existing three-dimensional multi-story building models and is currently being used to study cladding-structure interaction in highrise buildings.

4.0 LABORATORY FACILITY

4.1 Background

A comprehensive review of the cladding loads and response problem was presented in Chapter 1, and a field study to both qualitatively and quantitatively explore the problem in a uniquely shaped highrise building was then described in Chapter 2. The data collected from the field study consisted largely of differential pressure measurements taken across the cladding at numerous locations and for various wind conditions. These data were used to construct a probabilistic description of the time and frequency domain aspects of the localized pressure, and by comparison to measured window response data, to determine the causality between dynamic wind pressure loading and response over a range of frequencies. While the measurements provided invaluable data under service conditions, a number of problems were encountered in both refining and generalizing this information. First, it was not possible to control the manner of loading or the test conditions; for example, a 15-20% variation in dynamic properties as a result of mounting, support framing, etc., was observed over 12 windows. In addition even though sophisticated remote sensing transducers and portable instrumentation were used, it was not practical to make extensive measurements of the outer pane response. For obvious reasons, as well, it was not possible to geometrically or structurally alter the windows and associated cladding.

The full scale, laboratory grade dynamic loading facility described in this chapter provides the means for resolving many of the problems encountered in the field study, and in addition, for the first time

offers the general capability for simulating a variety of dynamic loading conditions under controlled conditions. The facility was designed and built under the present research project and is currently in operation in the School of Civil Engineering (96).

Present design procedures for windows consider an essentially static pressure load and rely upon full scale laboratory or on-site tests to verify performance. In this case, static retention of the lights and resistance to water penetration are the prime considerations. As a result, most of the tests have involved extremely simple arrangements for providing a static pressure while at the same time spraying intense streams of water at the test assembly. Dynamic response mechanisms have not generally been considered in the experimental work, and the reason can be traced to two problems: (a) the dearth of information as to the precise nature of the dynamic loads themselves, and (b) the lack of adequate test facilities for producing dynamic loads. Chapter 2 addressed the first point; this chapter deals with the latter.

The concept of a full scale wind load simulation facility is not new. The fixture described by Frownfelter (97) was in operation in 1959 and is capable of producing pressure loads of up to 40 psf.(1.9 kPa) It can accomodate a 16 ft by 16 ft (4.9m by 4.9m) specimen, thus making it possible to test several sections of a curtain wall and anchor system as installed on a real structure. The specimen wall forms one side of a sealed chamber which can be partially evacuated using a high volume blower. Suction was controlled with a valve on the blower exhaust and measured with a direct reading pressure gage. Deflection of the system under load was measured with dial

indicators and stresses were measured with resistance wire strain gages. Although the importance of dynamic loading was recognized and the test apparatus could produce pulsating pressures, no details were given on the method used to drive the system and no dynamic load data or dynamic performance data were included in the publication.

A more elaborate Japanese test facility was completed in 1965 and can produce time varying pressure loads representative of a typhoon or other severe weather (98). The typical specimen size is approximately 10 ft by 11.5 ft high (3m by 3.5m) As with the apparatus described by Frownfelter, the specimen forms one side of a pressurized chamber, but two blowers are used, one to create positive pressure and the other for suction. The two separate supply pipes used to connect the blowers to the pressure chamber each contain a butterfly damper valve. The butterfly dampers are linked together and operate 90^{o} out of phase so that one is fully opened while the other is closed. The apparatus was designed to produce peak pressures of approximately $\pm$100 psf ($\pm$4.8kPa) with a flat frequency response up to 0.3 Hz. An analog computer was used to control the butterfly servo mechanism with feedback signals obtained from a potentiometer on the damper linkage and a secondary feedback transducer monitoring chamber pressure. An optical curve tracer converted the desired pressure excursions from analog paper charts to voltage which was then used as primary input to the computer. Except for some leakage problems that were discussed, the equipment appeared to perform as designed.

The British Standards Institute at Hemel Hempstead has constructed a wind load test facility which was reported on in 1974 (99). The apparatus is similar in concept to the equipment previously discussed.

It consists of a double chamber arrangement driven by an air blower whose output is boosted by a compressed air reservoir. A typical test cycle consists of raising the internal pressure on one side of the chamber to a maximum in approximately 7 seconds holding at this level for 3 seconds, and finally bleeding down to ambient over 6 seconds, to complete a 16 sec. cycle. The cycle can be immediately repeated, and the proposed test sequence calls for 5 such cycles at each test pressure, to be followed by similar treatment in the opposite direction. The general emphasis in this facility is more towards standards testing than experimental research. The Paisley Institute of Technology boasts a similar facility and photographs of the Paisley equipment appear in (104).

All of the above facilities were designed primarily to check the integrity of windows or curtain wall structures when subjected to severe steady state or low frequency (< 1 Hz) wind loads. In addition, some have the capability of spraying the specimen with water to check for resistance to rain leaks. The facility described here has been designed to extend the simulation capabilities to a higher frequency range more representative of sharp, short duration transient loads such as might be produced by severe localized flow separation or perhaps by sonic booms. No provision has been made for water injection.

4.2 Design of the Facility

A peak static pressure capability of 75 psf (3.6kPa) was chosen as being a conservative maximum based upon the existing body of experimental data on wind pressure loads. The maximum dynamic component is not so readily specified, since relatively few studies have been

directly concerned with the frequency content of localized wind pressures, or have employed pressure transducer systems with flat response above about 5 or 10 Hz. The desire to simulate sharp-edged transient pressures coupled with mechanical compliance and driving power limitations above about 20 Hz combined to fix the dynamic specification at ±25 psf (±1.2 kPa) at a 20 Hz. cyclic rate. This figure is consistent with wind tunnel measurements of fluctuating pressures (101), recent full-scale measurements (102), and the results of the present field study presented in Chapter 2. The range is adequate to provide significant driving poewr for the lower vibration modes of many components of typical cladding systems, particularly windows with areas greater than about 20 sq. ft.($2m^2$).

The principle of mounting the cladding specimen to the side of an airtight box which can be pressurized has been amply justified by previous experiments and was chosen as the basis of this design. Further, the existence of a robust hardback structure of suitable dimensions fixed the maximum specimen size to be 8 ft. by 15 ft. high (2.5m by 4.5m). The main frame was constructed of heavy structural steel tubing, and as no water spraying or other bulky equipment is required and response of the apparatus is important, the chamber depth was limited to the dimension of the steel section. This minimizes the chamber volume for best dynamic performance as will be shown later.

Two system concepts were considered for producing the time-varying pressures in the test volume: (a) a flow control design similar to that in (98), and (b) a positive displacement design in which

moving "pistons" are used to produce volume changes and hence pressure fluctuations. The positive displacement approach was ultimately adopted, primarily for its better frequency response above 5 Hz, and because of the ready availability of high pressure hydraulic servo components with low moving mass and high force capability.

In order to estimate the volume change required to produce the design pressure levels and frequency response, several assumptions were made:

(1) Chamber volume would be approximately 80 cu. ft ($2.3m^3$).

(2) Test panel compliance would provide a maximum volume change equivalent to the volume under the deflected shape of a 3/4 in. (19.1mm) glass (or aluminum) plate covering the entire fixture.

(3) The effect of chamber leaks on the dynamic response is equivalent to increasing the fixture compliance.

(4) The chamber pressure varies isothermally.

The maximum test panel compliance when considered over the design pressure change will produce a 3 cu. ft. (85 1.) change in the chamber volume. An additional 3 cu. ft. (85 1.) displacement is used to account for the effects of leaks; the figure represents roughly 40% of the total displaced volume and is reasonable based upon the results of leak tests carried out in (98). Finally, assuming an otherwise rigid test chamber, the isothermal volume charge that is required to produce the design limit psf pressure change can be readily calculated at approximately 2 cu. ft. (57 1). Thus, the positive displacement system must be capable of producing a gross dynamic volume change of 8 cu. ft. ($0.23m^2$) at a 20 Hz rate. This amounts to a 10% volume

change in 0.05 seconds.

The geometry of the final positive displacement type design is shown in Fig. 4.2-1. The design consists of an upright welded steel test fixture approximately 15 ft. by 8 ft. (2.5 by 4.5 m) which supports the hydraulically driven positive displacement actuators mounted behind the test panel. The test panel(s) are attached over the front of the fixture and enclose the 80 cu. ft. ($2.3m^3$) chamber volume. The displacement system consists of 6 large "doors" hinged at their top edge and pneumatically sealed on all edges to the test chamber by means of a flexible seal. The doors are each 15 sq. ft. ($1.4m^2$) in area and cover the entire rear surface of the chamber. Each door is driven at its center by a servo-controlled hydraulic actuator which receives electronic command signals from a feedback control system. The actuators are supported by a steel framewrok structure which forms part of the rear of the test fixture and which is capable of handling both the static as well as the dynamic actuator reactions. Static loads are obtained by either pressurizing or evacuating the chamber using a blower system, and the door diplacements produce the prescribed dynamic component of loading. The fixture is fitted with a large capacity pressure relief valve (actually, a simple weighted poppet valve 6 in. (15cm) in diameter) to prevent inadvertent static or dynamic over-pressures.

Major design considerations which ultimately led to this system configuration can be summarized as:

(1) Components necessary for a one moving piece displacement system were too large to handle and prohibitively expensive.

(2) Off-peak conditions are more readily handled by six smaller

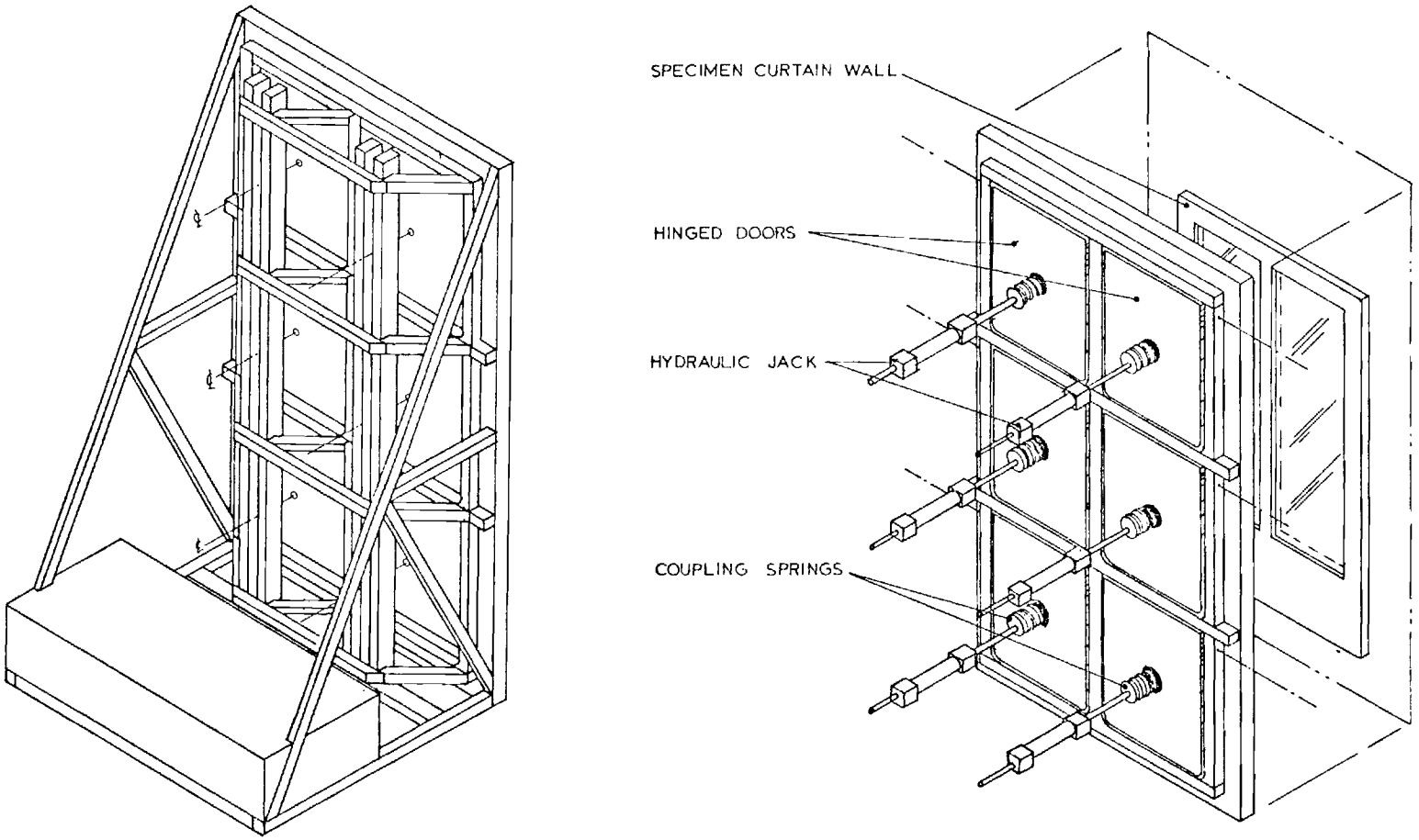

(a) Structure

(b) Geometry

Figure 4.2-1 Test Fixture Structure and Geometry

components; it is not necessary to drive all six doors all the time.

(3) Future simulation of pressures with spatial variation is possible with a split system.

(4) Hydraulic servo valves of suitable size were immediately available.

The completed fixture with two of the six doors installed and operational is shown in Fig. 4.2-2 and 4.2-3. A large double glazed window (approximately 40 sq. ft. ($3.7m^2$)) is installed in the test area. The servo-control electronics and minicomputer data acquisition are also shown. The rear view shows a more detailed picture of the high pressure hydraulic components required to operate the doors.

4.3 Performance Evaluation

The number of active doors, their mass and area, the hydraulic actuator size, and the hydraulic flow rates are all related and a particular combination is required to meet the specified performance. The principle constraints were the available hydraulic driving power and the maximum hydraulic flow rate to each door limited by the available servovalves). Increasing the number of doors decreases the flow rate to each, while increasing the door area reduces the required actuator stroke and hence the flow rate as well. The effective piston area of the hydraulic jack fixes the maximum force output and is thus related to the mass of the moving doors and the design frequency and pressure objectives. The door is by far the most critical component in the system design because of the mass and strength considerations. After several studies, the concept of ultra-lightweight doors was deemed technically feasible but was rejected because of the large

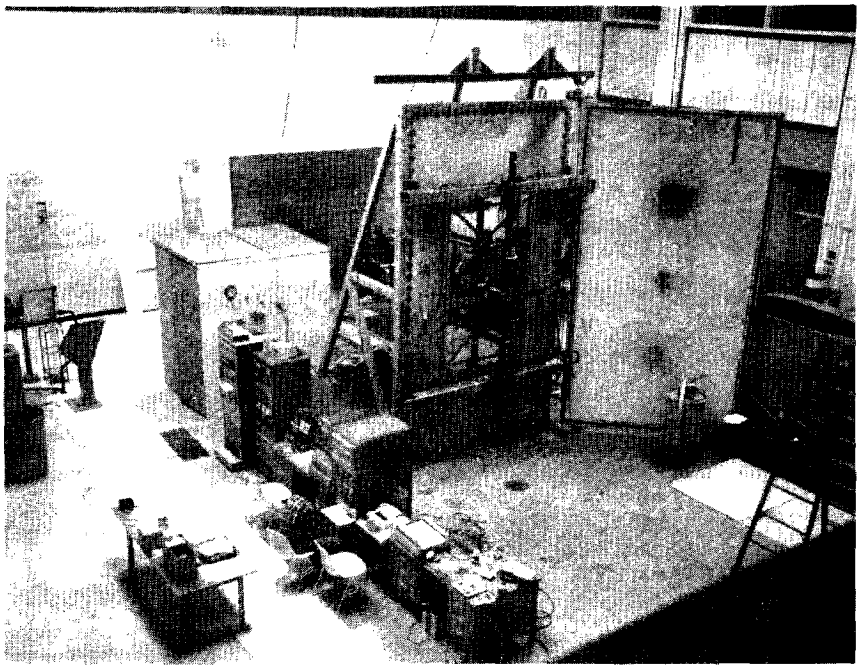

Figure 4.2-2 Test Fixture and Instrumentation.

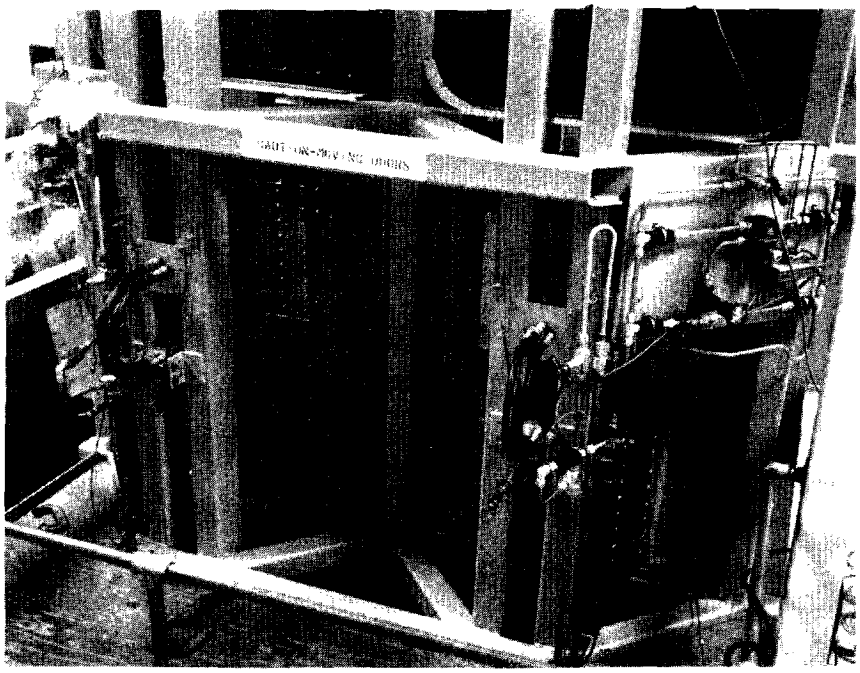

Figure 4.2-3 Moving Doors and Hydraulic Controls.

expense and the time required to build them. The present doors were designed primarily to be rugged and easily assembled, and secondarily, to be as light as possible.

The doors are driven through adjustable coupling springs by small, 1 1/8 in. (28.6 mm) bore hydraulic actuators mounted to the support structure. The role of the coupling springs will be described later. The hydraulic flow to the actuator is modulated by an electronically controlled high-response servovalve manifolded directly to the actuator.

A schematic of the driving system and the feedback control required to operate it is shown in Figure 4.3-1. The springs are lumped parameter models for the specimen compliance (k_w), the chamber compressibility including leaks (k_a), and the coupling spring (k_s), while the door is represented by a lumped mass. It is necessary to use a feedback type control system as shown in order to accurately produce the time-varying pressure load. Mean pressures are supplied statically but the dynamic component is produced entirely by door movement. Primary control of the door motion in response to a forcing function, p(t), is therefore required. However, direct control of the actuator in response to a prescribed pressure forcing function is not desirable because this places a resonant mechanical system (m, k_s, k_a, k_w, m_w) in the loop and requires extensive compensation for stable operation. Rather, the actuator is operated under direct stroke control with stability compensation provided by a ΔP transducer and rate control in A_2. The setpoint for this inner loop is provided by a second loop consisting of a door motion transducer and controller, A_1. The command signal, p(t), can be furnished by a signal generator, a noise generator, or from a tape recording of actual wind pressures.

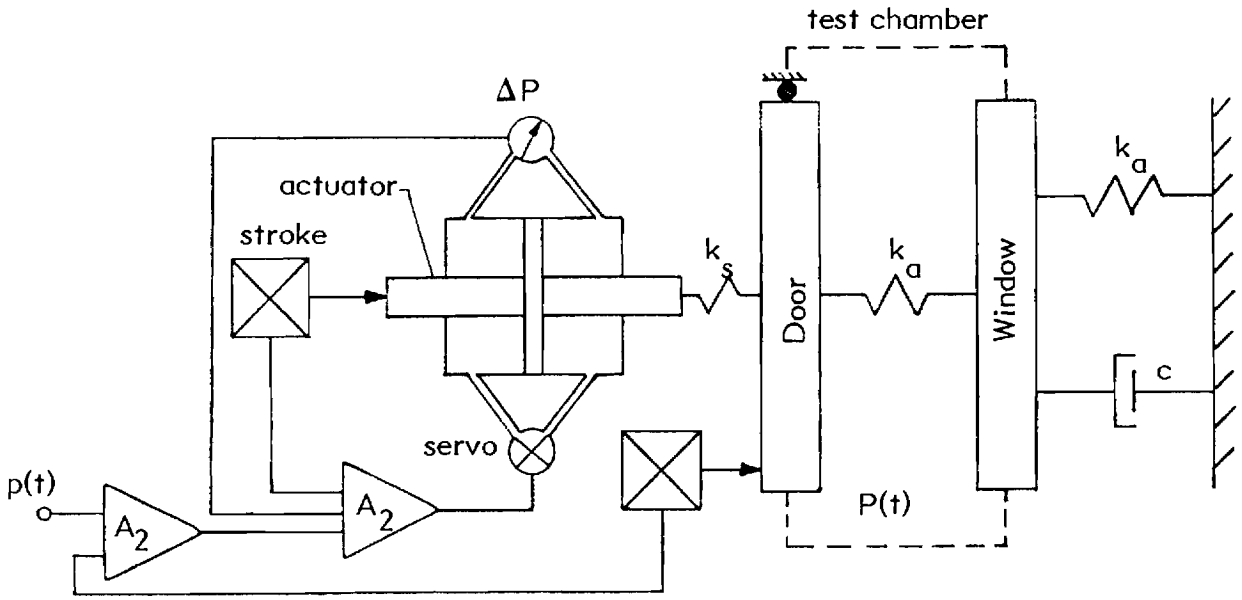

Figure 4.3-1 Feedback Control System

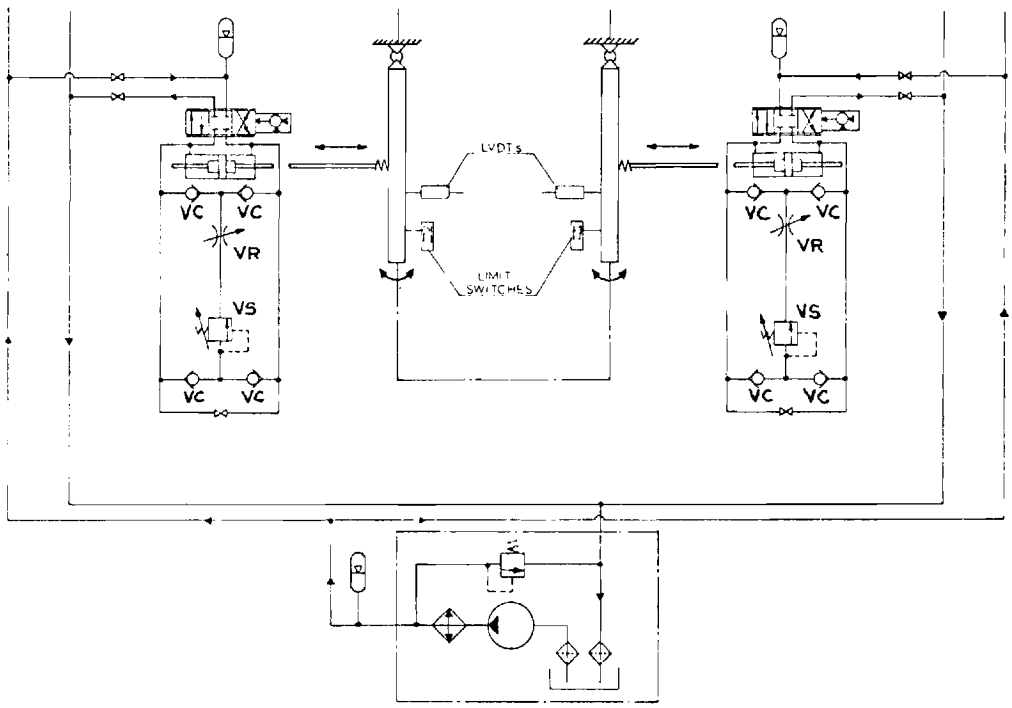

Figure 4.3-2 Hydraulic Schematic Showing Actuator Overpressure Circuits (2 doors)

The lumped parameter values and component sizes are fixed by the dynamic response requirements. For example, to a first approximation, the compressibility effects in the chamber as felt by a single door can be represented by a linear spring with stiffness:

$$k_a = k_o A_d^2 N$$

where $k_o = \Delta P / \Delta V$ is the ratio of pressure change to the isothermal volume change required to produce it, A_d is the door area, and N is the number of doors operating together. The effect of specimen compliance and leakage can be considered similarily as a series stiffness:

$$k_w = k_e A_d^2 N$$

where $k_e = \Delta P / \Delta V_e$ is the ratio of pressure change to chamber volume change due to test panel flexure and fixture leakage. The overall fixture stiffness as seen by each door is, then, the series combination of k_a and k_w, and given the door masses, the system natural frequencies can be determined from this. An interesting feature is that the stiffness, and hence natural frequencies, are dependent upon the numbers of driven doors, so that system dynamics may be readily adjusted by varying this value. For example, with the present door weight of 64 lbs (29 kg), when all six doors are driven the natural frequency is 14 Hz, but when only two doors are used this drops to 6 Hz.

If the system were driven directly by a prescribed actuator force, large and uncontrollable door motions and pressure amplitudes would result from the resonant behavior. However, when driven with servo-displacement control of the door and actuator stroke, a properly tuned feedback controller will suppress the resonance and provide uniform response. Two limitations exist that reduce the ultimate performance:

(1) Hydraulic flow restrictions (10gpm (69 l/m)) in the servovalve and actuator effectively limit the maximum piston velocity and hence stroke at a given frequency.

(2) Actuator force is limited by the maximum hydraulic pressure available (3000 psi (20.7 MPa)) and the total opposing static chamber pressure on each door.

The limitations are all the more severe because they are self-conflicting; that is, piston velocity can be increased by reducing the bore, but this then reduces the maximum force available.

The performance can, however, be improved within these restrictions by two methods:

(1) By decreasing the door mass or increasing the number of driven doors the natural frequency is raised; this reduces the required force at higher frequencies, especially near natural resonance,

(2) By adding a coupling spring, k_s, (Fig. 4.3-1) the door is partially uncoupled from the actuator stroke restriction so that large motion is possible at high frequencies; the system thus oeprates in a controlled-resonance mode.

For typical windows of less than about 40 sq ft ($3.7m^2$), the latter method is not required and adequate performance can be obtained simply by increasing the number of driven doors.

When operating under feedback control near resonant conditions, there is always the risk that failure of a control circuit or transducer will result in loss of control and possibly catastrophic instability of the system. A simple pressure relief valve described earlier will automatically limit the maximum test pressures. Hydraulic pressures can, however, exceed allowable levels independently so that additional protection circuits are required. A special hydraulic damping circuit as shown in Fig. 4.3-2 (showing circuits for two doors) is connected across the actuator to provide protection to the equipment in the event of loss of power or control near resonance. The circuit uses an adjustable sequence valve, VS, and four check valves, VC, arranged so that when hydraulic pressure across the actuator piston exceeds a preset value, the sequence valve will open and shunt the actuator parts together through a flow-restricting needle valve, VR. The sequence valve automatically resets at lower pressures and normal operation is restored. In combination with the relief valve, this feature can be used to mechanically limit the maximum allowable test pressures.

In order to verify operation of the facility at design levels,

the system was configured with two driven doors and fixed panels in place of the other four doors. The test area was enclosed with a stiff reinforced steel plate and the chamber volume carefully sealed. A single door, and later both doors together, were driven sinusoidally at fixed amplitudes over the 20 Hz operating range. Actual door motion and the fluctuating chamber pressures were then recorded for several static pressure levels. Control loop compensation was adjusted, first to identify stability limits beyond which large, uncontrollable oscillations occurred, and finally to tune the system for maximum stable dynamic response. The measured single door natural frequencies agreed well with the calculated value of 6.8 Hz for a well-sealed chamber.

Figure 4.3-3 shows the performance envelopes for the two-door system for several different mean pressure levels and fixture compliances. Flow restrictions limit the stroke inversely with frequency, and this can be translated into a maximum cycle pressure limitation which depends, as shown by the two curves, on chamber compliance. The envelop curves fall off at a 6dB/octave rate.

The performance is also limited by the maximum actuator force available to drive the inertial loads (door mass). This restriction depends directly upon the mean chamber pressure since a static hydraulic pressure level must be applied to maintain the door at rest. The maximum available force, and hence chamber pressure, depend inversely on the square of frequency and consequently roll off at a 12 dB/octave rate. At low peak pressures (or stroke) the maximum cyclic rate is alternately limited by inertial loads while at higher pressures the limit is due to flow capacity.

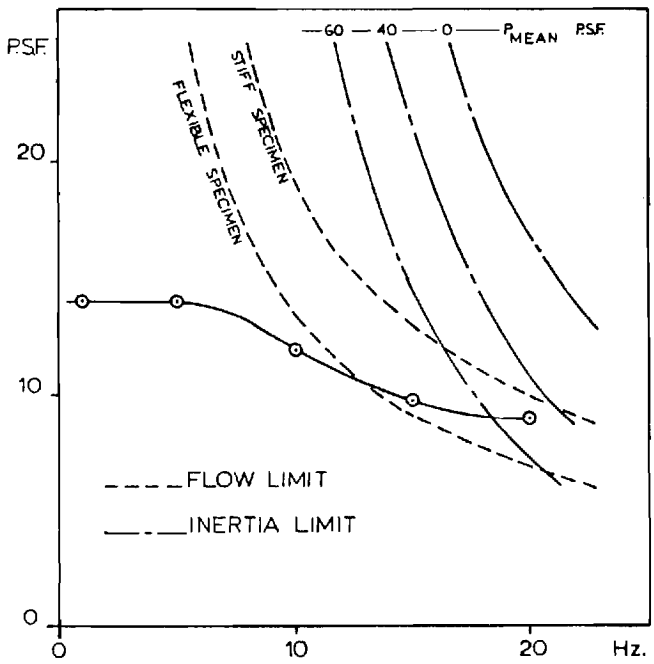

Figure 4.3-3 Performance Envelopes and Maximum System Performance Results for Two Doors

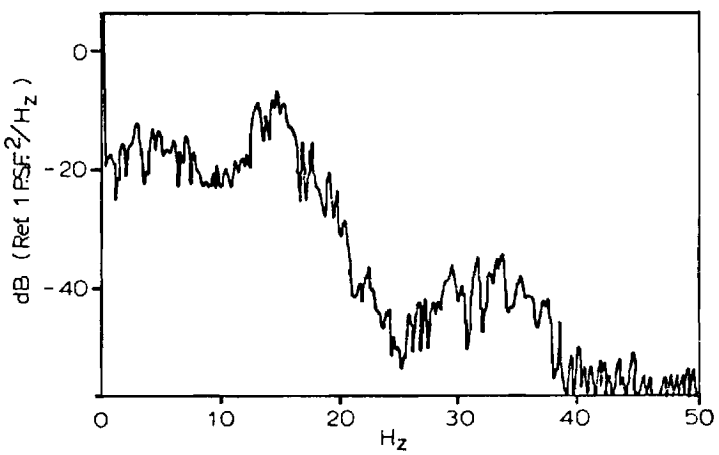

Figure 4.3-4 Typical Simulated Pressure Power Spectral Density

The performance is also limited by the maximum actuator force available to drive the inertial loads (door mass). This restriction depends directly upon the mean chamber pressure since a static hydraulic pressure level must be applied to maintain the door at rest. The maximum available force, and hence chamber pressure, depend inversely on the square of frequency and consequently roll off at a 12 dB/octave rate. At low peak pressures (or stroke) the maximum cyclic rate is alternately limited by inertial loads while at higher pressures the limit is due to flow capacity.

Actual performance values are shown in Figure 4.3-3 for a 14 psf (670 Pa) cyclic load produced with a 15 psf (720 Pa) mean pressure. The curve is essentially flat with frequency until the flow limitation is met. However, it can be seen that this limit is exceeded at 20 Hz. The explanation lies in the use of a finite coupling spring, k_s, which in this case consisted of a heavy rubber bushing attaching the actuator to the door.

A typical simulated wind pressure power spectrum obtained using an ensemble of 20 pressure records is shown in Fig. 4.3-4. The forcing function in this case was a pseudo-random binary sequence signal generator with a Gaussian amplitude distribution. Low pass filters were used to shape the rolloff to approximate wind pressure characteristics.

4.4 Static Testing

The full scale test fixture described in Section 4.3 was used for the present work to conduct static and dynamic tests on a section of cladding from the same high rise building used in the field study (Section 2). A single storey section of the cladding, including mullions, muntions, spandrel framing, glazing materials and 4 double

pane vision lights, was obtained from the fabricator and installed in the test fixture as shown in Fig. 4.4 1. In actual service, the 24 ft. (731 cm) mullion sections are pinned to the floor slabs at a 12 ft. (366 cm) spacing with a splice every 2 storeys, but in the present case, only two 12 ft. (366 cm) sections were available so a single storey spliced configuration was constructed. The overall layout along with typical sections are shown in Fig. 4.4-2. The vision light was a 99 x 57 x 1 in. (251.5 x 144.8 x 2.5 cm) insulated silver reflective glass unit composed of two 0.24 in (6.4 mm) thick panes bonded along their edges to a 0.5 in. (12.7 mm) thick square steel spacer. Plywood panels were installed around the window in the same manner to simulate the effect of spandrel sections (single glazing in the field site) and adjacent windows. With the exception of the light itself, the entire test section was sealed internally with a plastic membrane so that internal pressurization could be produced with minimum leakage. The window assembly was oriented with the normal "outside" surfaces facing outward so that building external suction (negative) pressures could be produced. It should be noted, however, that the test fixture is capable of handling negative internal pressures and was limited in these tests to positive pressures only for convenience of sealing. Details of the design of the window assembly and the static test program along with results and a static analysis are given in Ref. 104.

4.4(a) Boundary Properties

A major step in understanding and modelling the behavior of a window must begin with a thorough and precise evaluation of the

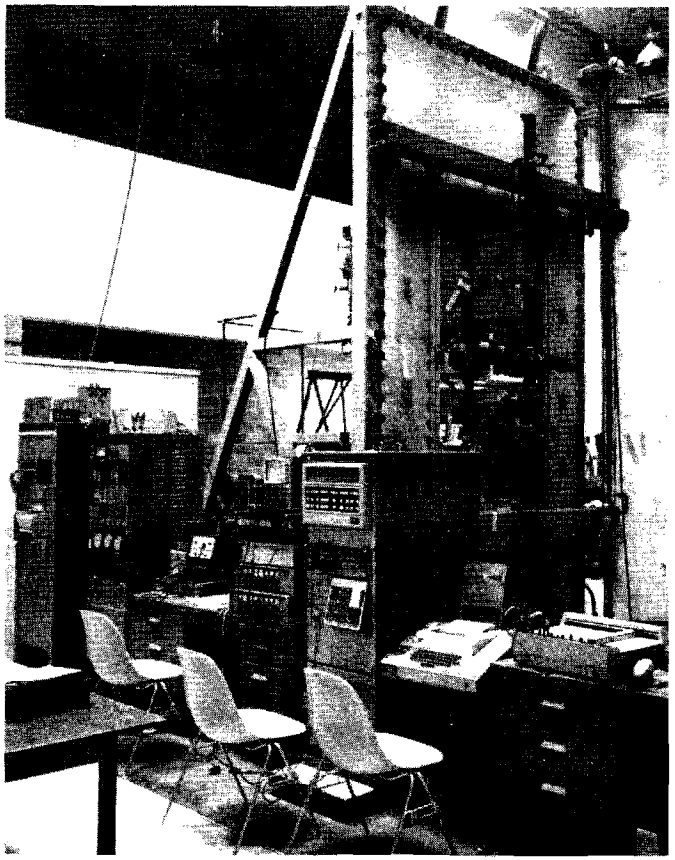

General View

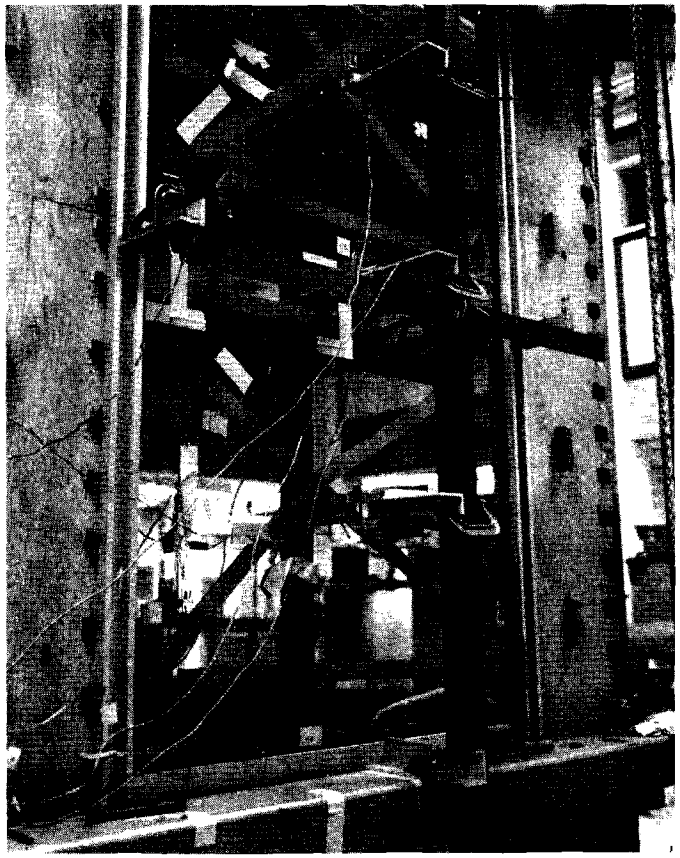

Instrumentation Detail

Figure 4.4-1 Test Window Installed in Fixture.

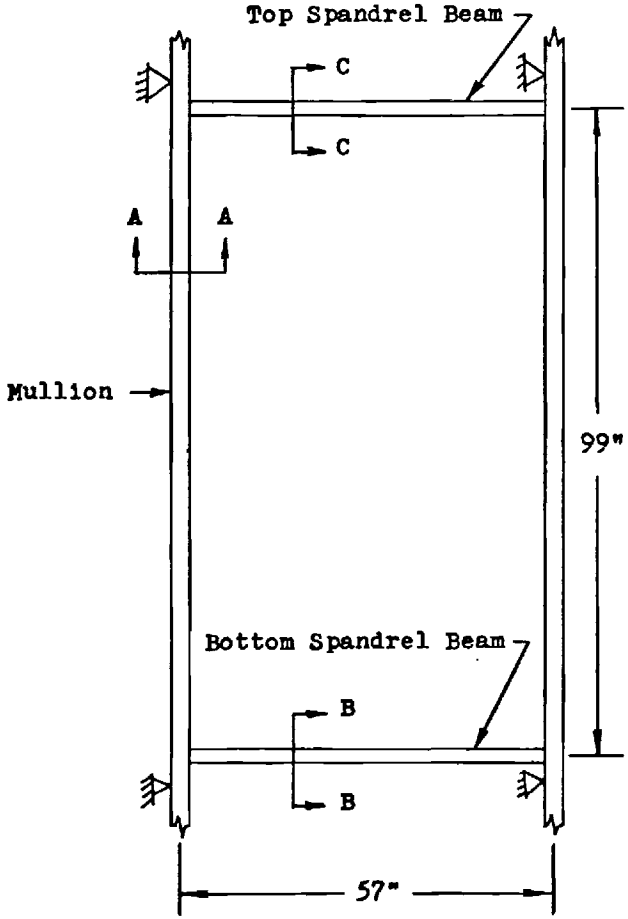

(a) Window Geometry

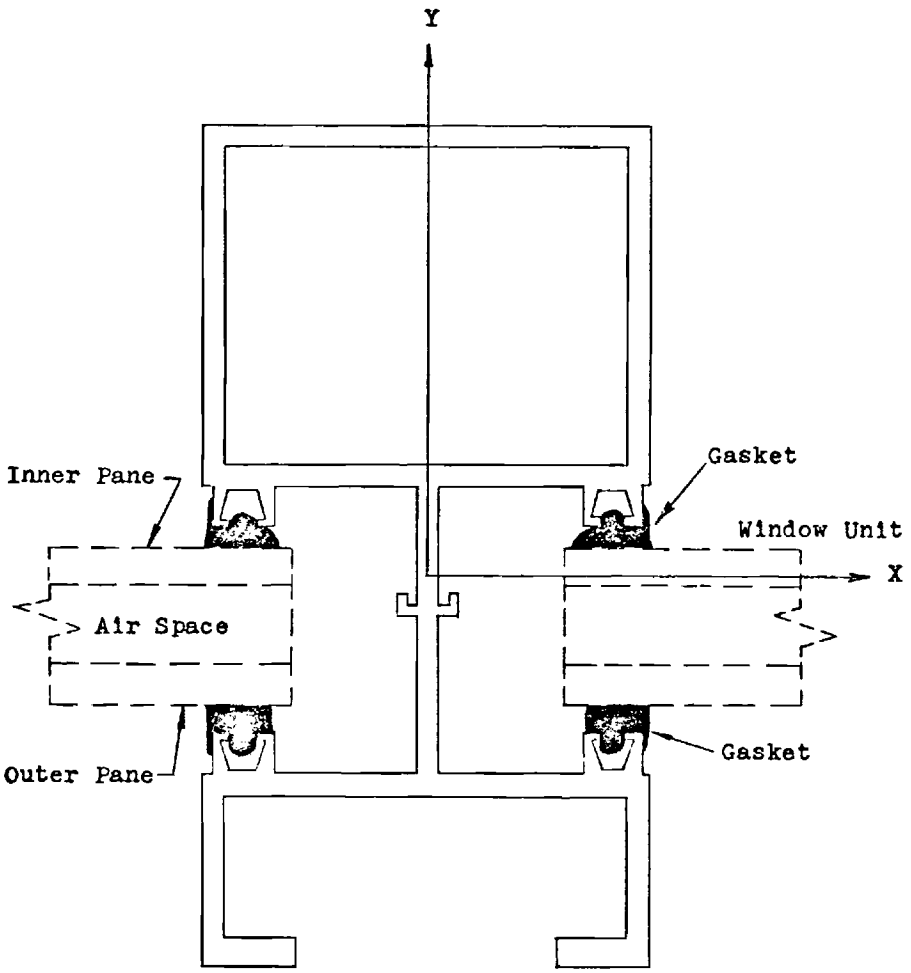

(b) Section A-A

Figure 4.4-2 Test Window Geometry with Framing Section Details

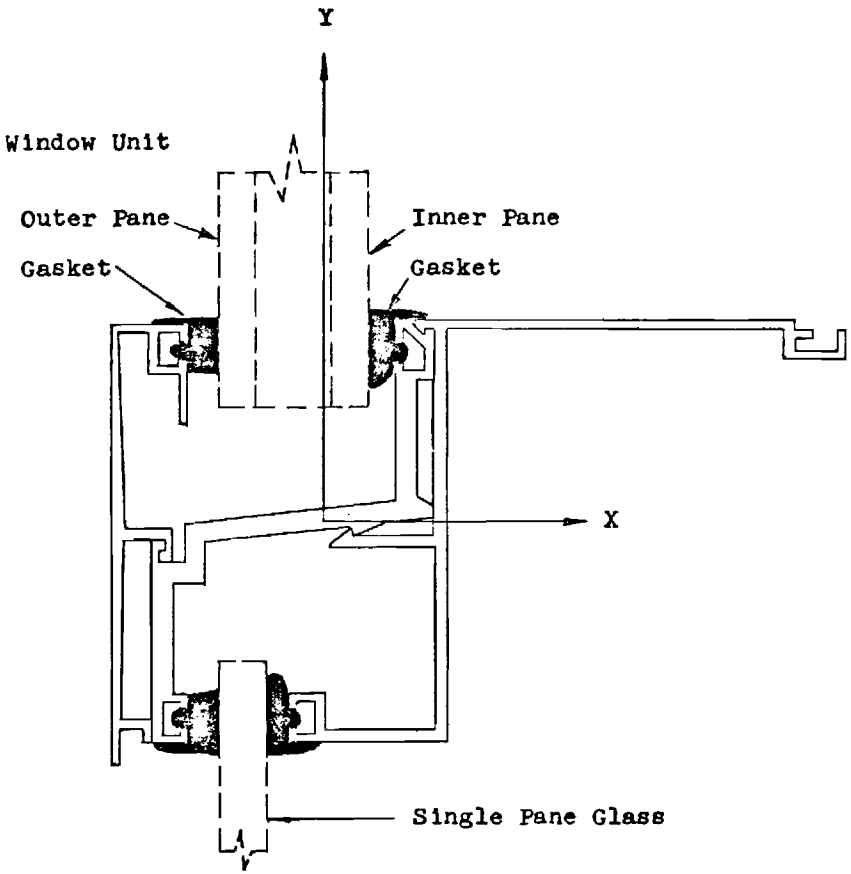

(c) Section B-B

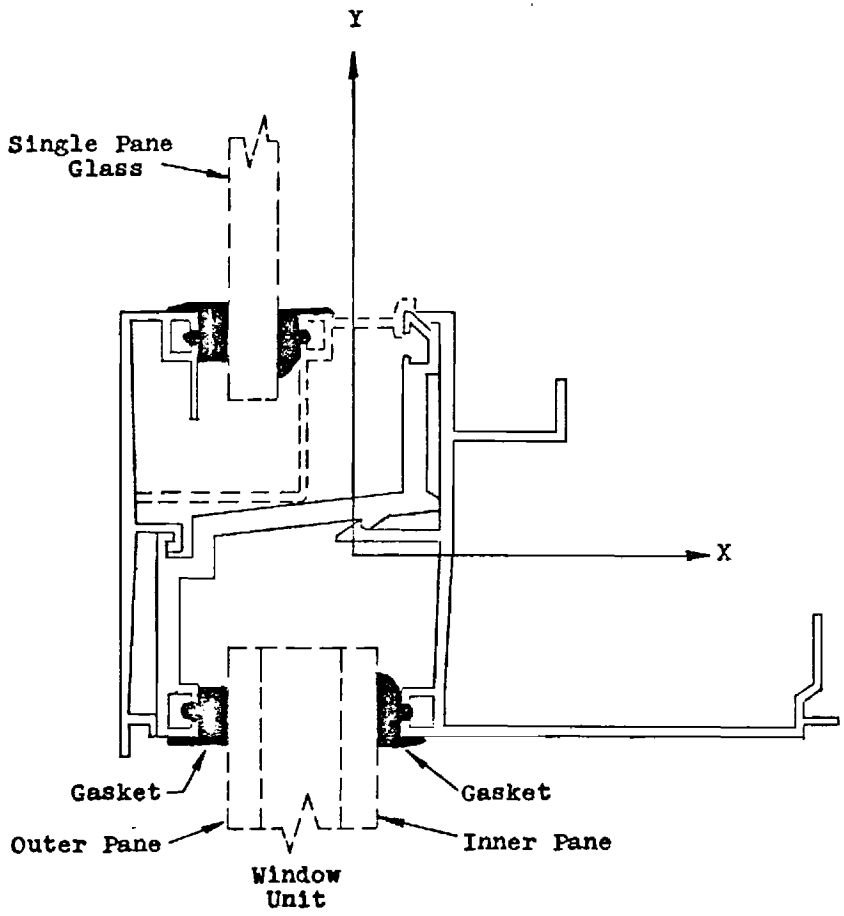

(d) Section D-D

Figure 4.4-2 (continued)

supporting structure, its configuration, dimensions, and material properties. The window/cladding system employed in the present tests is representative of a large class of glazing systems using metal mullion-spandrel sections with neoprene sealing gaskets. As a result, while the reported properties and performance are for a specific configuration, the general behavior is representative of a larger class.

The glazing support structure is a built-up framework consisting of several interlocking aluminum extrusions as shown in Fig. 4.4-2. The glazing gaskets which actually support the glass within the framework are made from special neoprene rubber arranged as shown in Fig. 4.4-3. The "outer" gasket is made from a closed-cell neoprene sponge of medium density while the "inner" gasket is a 75-duro solid neoprene. The outer gasket is located in the frame first, the window is next installed and positioned on two or more glazing blocks, and finally, the inner gasket is wedged into position using a special tool and some force. This latter step can result in differences in support conditions from window to window since invariably the inner gasket installation is accompanied by some longitudinal extension or compression. If the gasket is wedged in with a roller-type of tool moving from corner to corner with any excess cut off, the gasket may be stretched by as much as 10%, but if the gasket is precut and worked in from each corner to the middle of an edge, no stretching will result. In the event that the gasket is precut to a slightly longer length and forced into position, a net compression results. This might be done in an attempt to "strengthen" the glazing, but

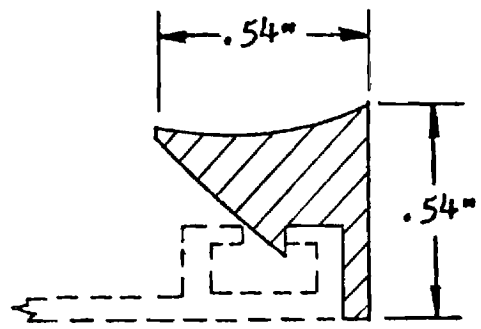

75 Duro-neoprene Gasket

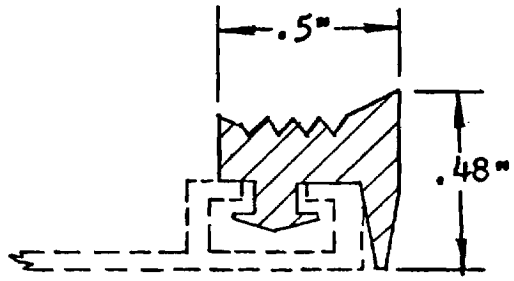

Neoprene Sponge Gasket

Figure 4.4-3 Neoprene Gasket Cross-sections

if exercise forces are used may produce a failure of either the glass or the spacer or both.

In order to characterize the gasket support, a series of tests were devised to determine the elastic properties for four modes of motion at the glass plate boundary. Specifically stiffnesses are:

1. Out-of-plane or normal stiffness which is due directly to the compressive gasket stiffness.
2. In-plane-normal or pull-out stiffness which is due to the shear stiffness of the gasket in a direction perpendicular to a boundary edge.
3. In-plane-longitudinal stiffness which is also due to the gasket shear stiffness but in a direction parallel to a boundary edge.
4. Rotational stiffness or the moment restraint about an axis parallel to the edge which is due to a combination of shear and compression in the gasket.

In general, of course, there are 6 degrees of freedom at the edge and 6 corresponding restraint stiffnesses can be defined. The above 4 are the predominant ones for static deflection or dynamic out-of-plane response. Along with the edge restraints, additional constraint forces are produced between the two glass plates in the window as a result of the spacer. Unfortunately, short of disassembling the vision light itself, there is no simple means for experimentally measuring the associated stiffnesses so that in all analytical work, extreme values have been arbitrarily assumed.

Wey (104) in his thesis described a series of tests to determine the above four stiffnesses and then using both continuous and discrete models for the window and framework compared the measured deflections with the predicted for static pressures up to 20 psf (958 Pa). This section presents a summary of the boundary stiffness results along with several observations on the behavior. The measurements were performed using a small 1 ft. by 1 ft. (30.5 cm by 30.5 cm) architectural evaluation sample of the actual window which, other than its area, was of identical construction. An edge of the test sample was glazed in the actual test fixture for the inplane and rotational stiffness tests. Loads were supplied by weights using cables and pulleys, and deflections were measured with precision dial gages. The gasket compression tests were performed in a Universal Test Machine, again using the glass window sample and a short piece of the mullion section.

Out-of-Plane Stiffness:

The out-of-plane gasket stiffnesses were measured by applying a direct compressive load to the gasket and measuring the resulting deformation. The gasket was mounted in a section of mullion to duplicate installed conditions. Figures 4.4-4 and 4.4-5 show typical results for the neoprene sponge and 75 duro-neoprene. In both cases the behavior is nonlinear and hardening although the effect is much less severe than expected. The most significant result is the observation that the sponge material is apparently stiffer as evidenced by the steeper average slope:

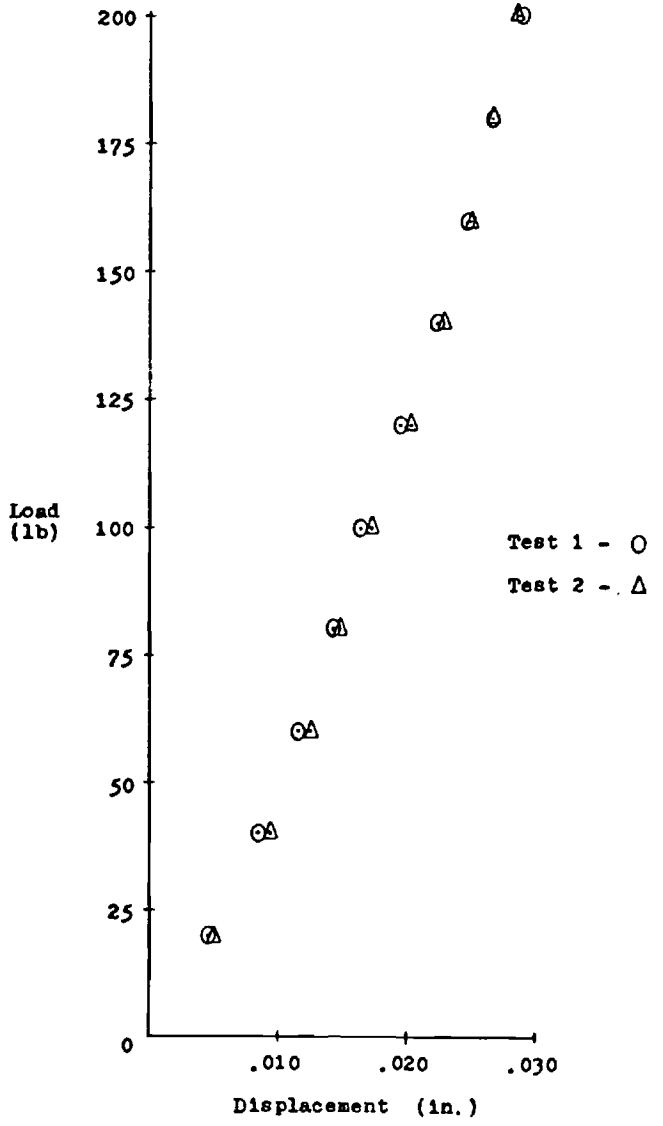

Figure 4.4-4 Gasket Compression Test for Neoprene Sponge Gasket Material

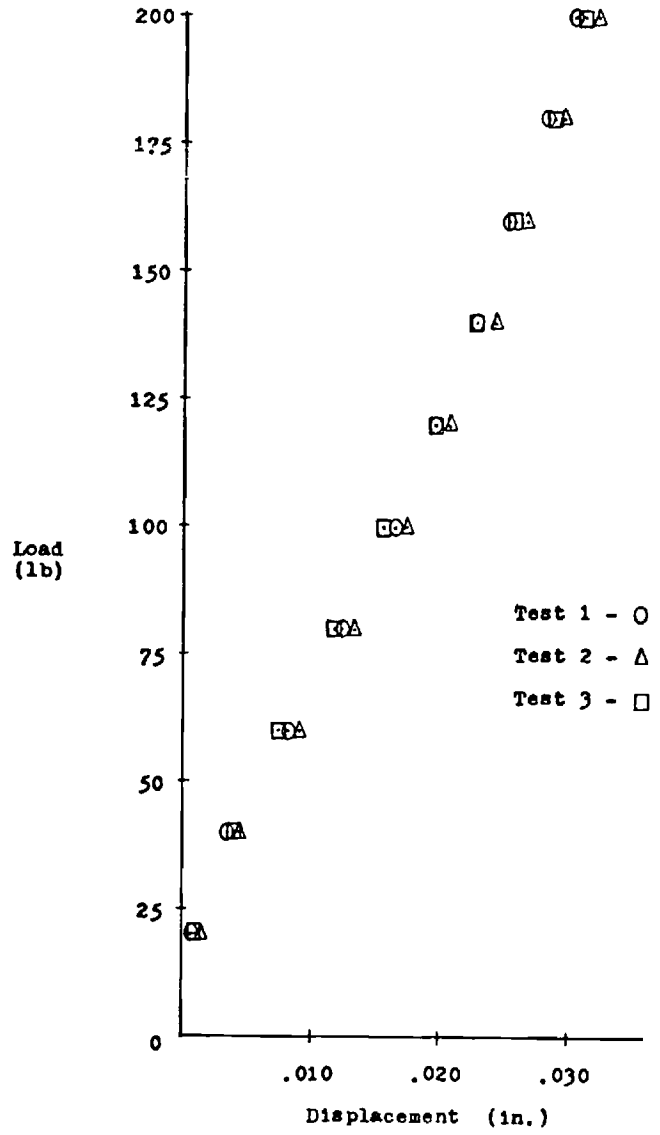

Figure 4.4-5 Gasket Compression Test for 75-duro Neoprene Gasket

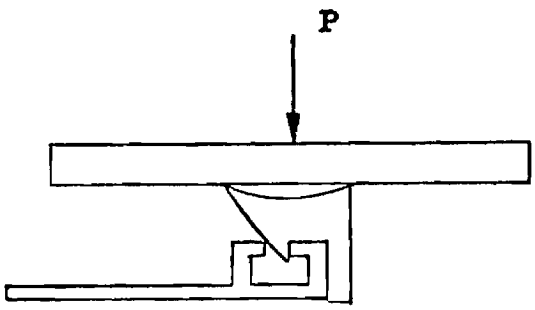

75 Duro-neoprene Gasket Under Load

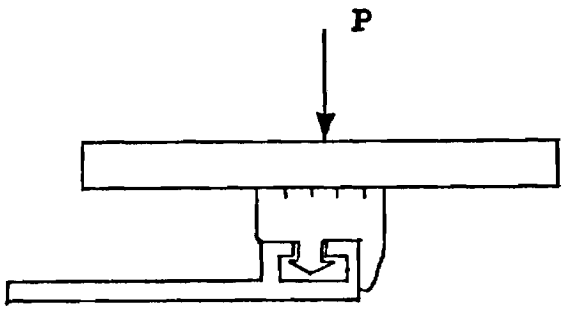

Neoprene Sponge Gasket Under Load

Figure 4.4-6 Detail of Gaskets Under Normal Compression Load Showing Different Contact Areas

Material	Average Slope, lb/in/in, (kN/m/m)
Neoprene Sponge	335 (2310)
Solid Neoprene (75 duro)	222 (1530)

The explanation for this seemingly contradictory behavior lies in the manner of deformation for each gasket. As shown in Figure 4.4-6, the two gaskets behave quite differently under load. The sponge material is in full contact with the glass at all times so the stress is fairly uniform. The solid neoprene because of its shape is in contact with the glass along two lips and considerable localized bending occurs. Even at a compressive load equivalent to three times the expected service load, a significant cup shape remained. When the material was loaded until full contact was established the expected sharp increase in stiffness was observed, however, this condition was not judged typical.

Normal In-Plane Stiffness: The in-plane stiffness normal to a glazing edge was measured using a small specimen light mounted in the full-scale test rig to simulate actual glazing conditions. As might be anticipated, after the load was increased beyond a certain value the light began to slip and, if the load was maintained, would pull out of the glazing. The pull-out load was found to depend on several parameters that were difficult to control, e.g., installation technique, load history. Experience with actual field installations generally reveals that after a window has been installed for a few months, the glazing gasket becomes tightly stuck to the glass. To simulate this condition, a cyano-acrylate adhesive was used to adhere the glass to the gasket and prevent slipping during the tests. Figure 4.4-7 shows results from several tests. As a result of the initial gasket

configuration after gluing and localized gasket tip behavior a measurable deflection does not occur until a threshold load has been reached. The average stiffness for loads above the threshold is 342 lb/in/in (2360 kN/m/m) although as before a noticeable hardening behavior is evident.

In Plane Longitudinal Stiffness: The gasket stiffness parallel to the window edge was determined in a manner similar to that above. Figure 4.4-8 shows typical results which, in contrast to the normal in-plane case, do not exhibit the threshold feature. In this case the gasket tip distortion phenomenon is not present since the load is acting along the edge. The curves show an initial softening followed ultimately by slippage of a maximum load. It is apparent that the inherent hardening characteristic of the rubber is overcome by slippage. The average stiffness for shear loads above 1 lb/in (0.2 kN/m) is 318 lb/in/in (2190 kN/m/m).

Rotational-Stiffness: Boundary rotational stiffness was determined in a manner similar to the above two cases, but in this case the loading was applied so as to produce a known edge moment and the resultant rotations were measured. The gasket loading involves a combination of compression and shearing normal to the edge, and as for the in-plane stiffness normal to an edge, the effect of gasket-window slippage is evident with and without slippage. In this case, when the gasket is free to slip, localized lip slippage increases the contact surface and a higher rotational stiffness results. When the gasket is glued, the primary deformation mode involves localized bending of the gasket lips and a considerably lower rotational stiffness results. Figure 4.4-9 shows the measured behavior.

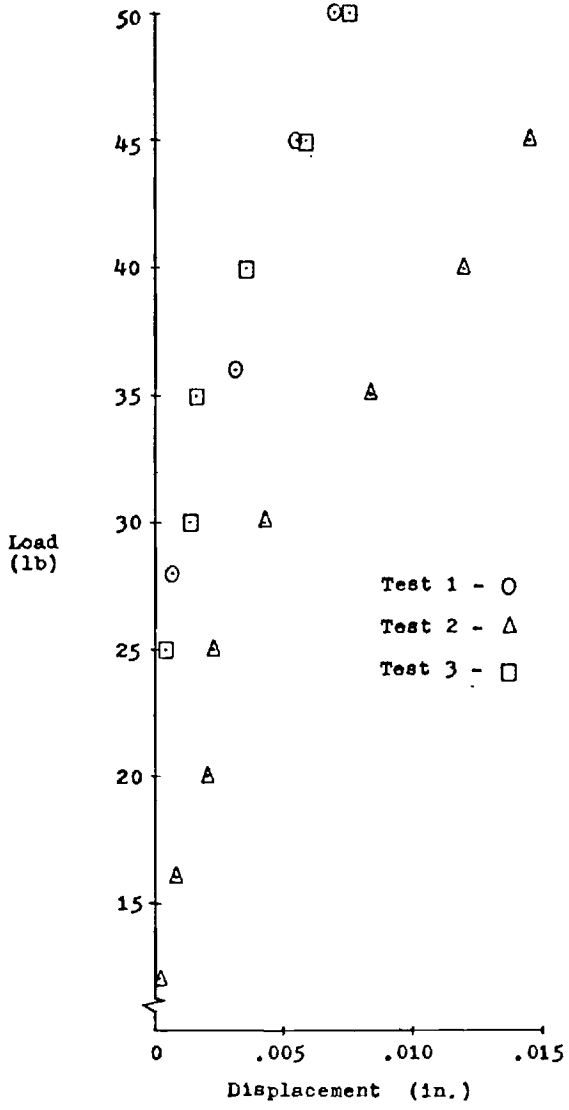

Figure 4.4-7 In-plane Stiffness Normal to the Edge - No Gasket Slippage

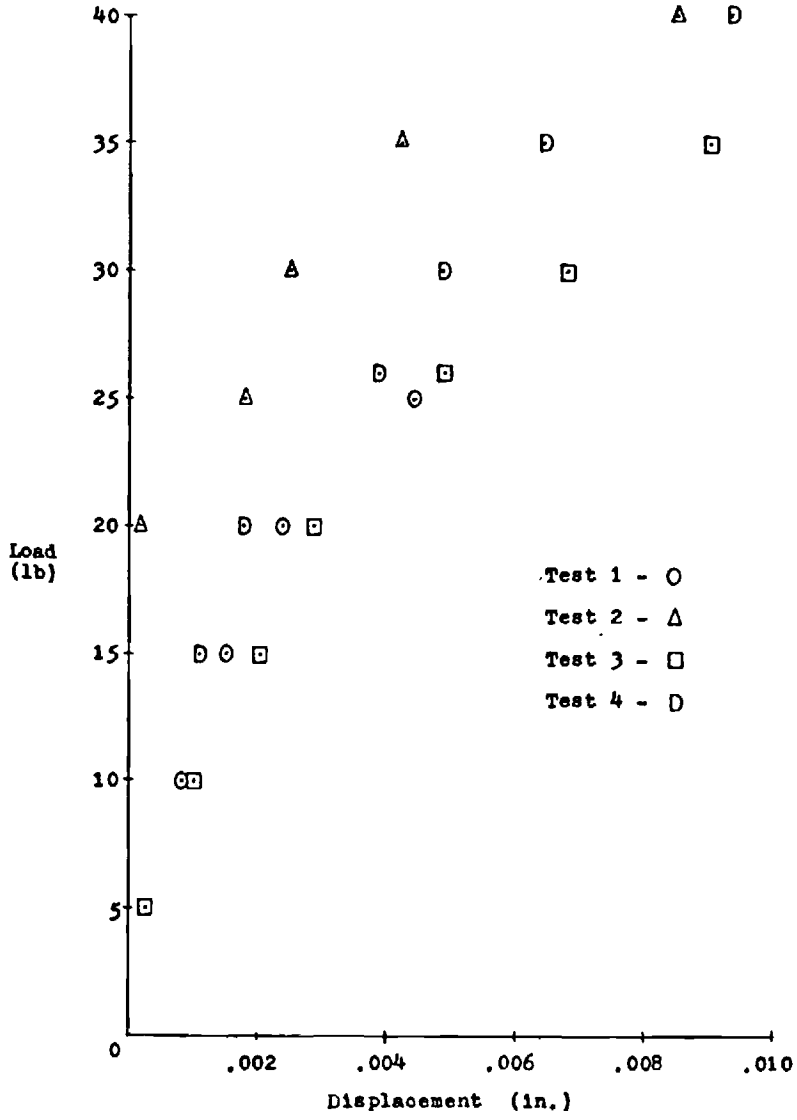

Figure 4.4-8 In-plane Stiffness Parallel to the Edge - No Gasket Slippage

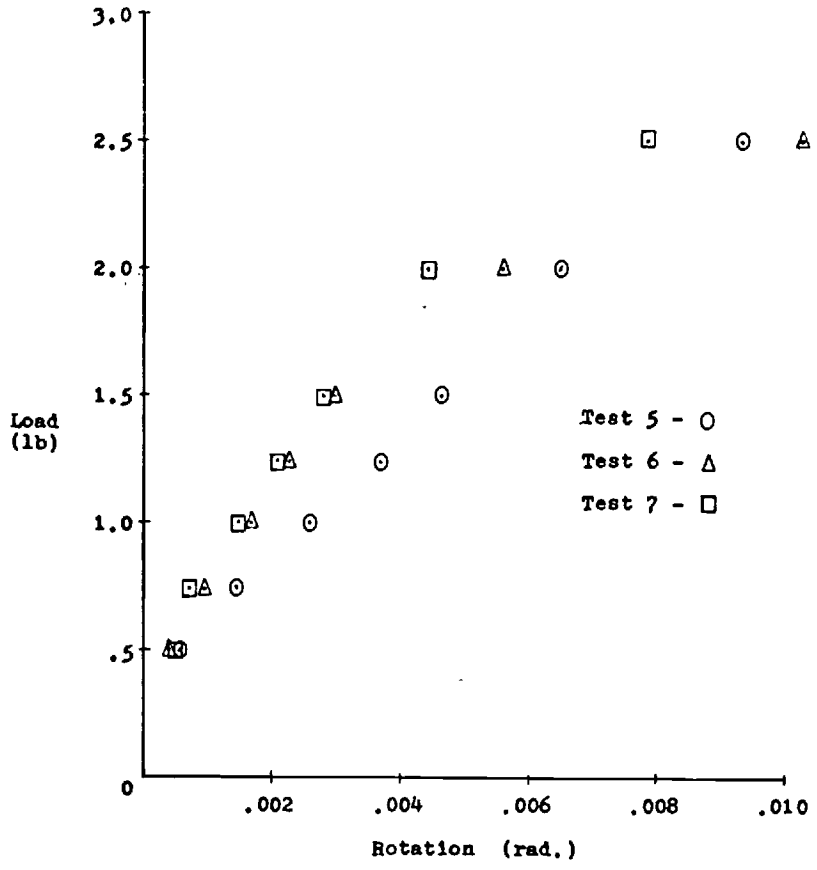

(a) Gasket Free to Slip

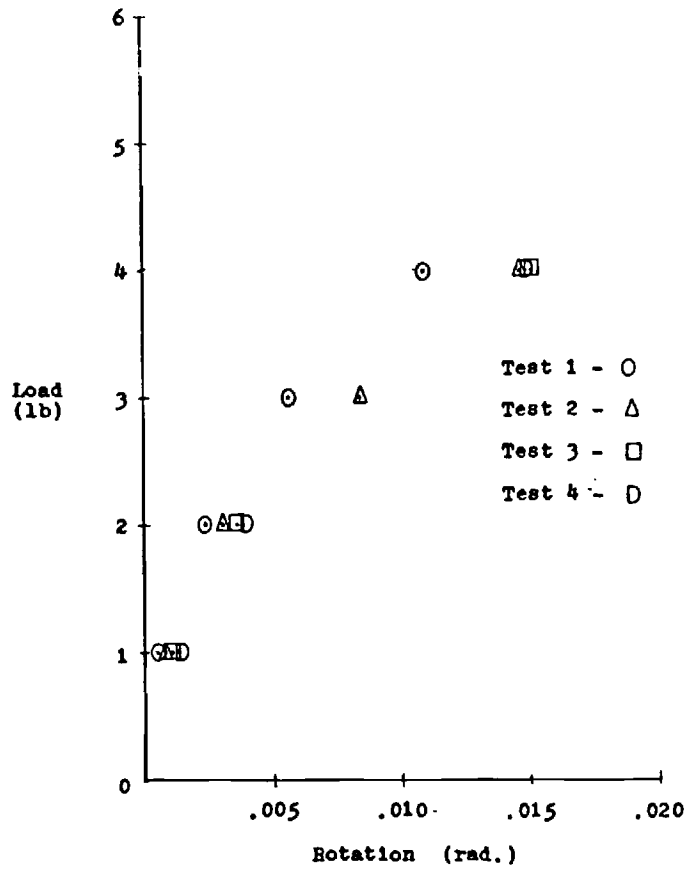

(b) Gasket Not Slipping

Figure 4.4-9 Edge Moment Restraint Stiffnesses

The gasket properties as found above were used in the analytical modelling in Chapter 3. They are summarized below:

Mode	Stiffness, lb/in/in, (kN/m/m)
Out-of-Plane	
Neoprene sponge	335 (2310)
Neoprene, 75-duro	222 (1530)
In-Plane, Normal (no slip)	342 (2360)
In-Plane, Longitudinal	318 (2190)
Rotational	
Slip	305 (2100)
No slip	159 (1100)

Of these, the out-of-Plane and Rotational stiffnesses are the most important in their effect on static and dynamic window behavior. The inplane stiffnesses are so small compared to the inplane window stiffness as to be insignificant (as they are supposed to be by design in order to avoid introduction of detrimental inplane loading).

4.4(b) Static Test Results

Static pressure tests were conducted on the basic window unit described in 4.4(a) while it was mounted in the full scale test fixture. As noted, the support conditions were arranged to closely duplicate a typical mounting configuration. The instrumentation consisted of an array of linear variable differential transformers (LVDT's) for the measurement of deflection and numerous electrical resistance foil strain gages bonded directly to the glass and framing

surfaces. The LVDT's were Hewlett-Packard DCDT-series transduers which are dc powered and provide a dc output with from 6 to 30 V/in (15-75V/cm) sensistivity. The units were used on both sides of the window and for reference purposes were mounted to stiff support bars firmly anchored to the test fixture frame. As many as 8 units were used simultaneously. The strain gages were 350 ohm metal foil types with a large gage area selected so as to minimize self-heating at the 6V excitation level used. Sixteen gages were typically used in the tests. The displacement and straingage layout is shown in Fig. 4.4-10.

An HP9825A calculator-based data acquisition system using an HP3490 voltmeter and HP3495 reed scanner was used to acquire, process and output the test data. Strain readings were computed directly from the microvolt-level Wheatstone bridge outputs and bridge balance was accounted for simply by subtracting the initially measured unbalance voltage at zero load using the calculator program. In this way, a typical test required no more than 15 sec. measurement time at each pressure load.

Test Configurations: The static tests were designed to determine as much as possible about the behavior of a typical insulating glass window when supported in a manner typical of that found in lightweight cladding designs. For reasons of economy, both of time and effort, the reported test program was limited to a particular window and mounting configuration, but extensive measurements were made to ascertain the behavior mechanisms under so-called "standard" installation conditions as well as under "abnormal" conditions. While this approach is not

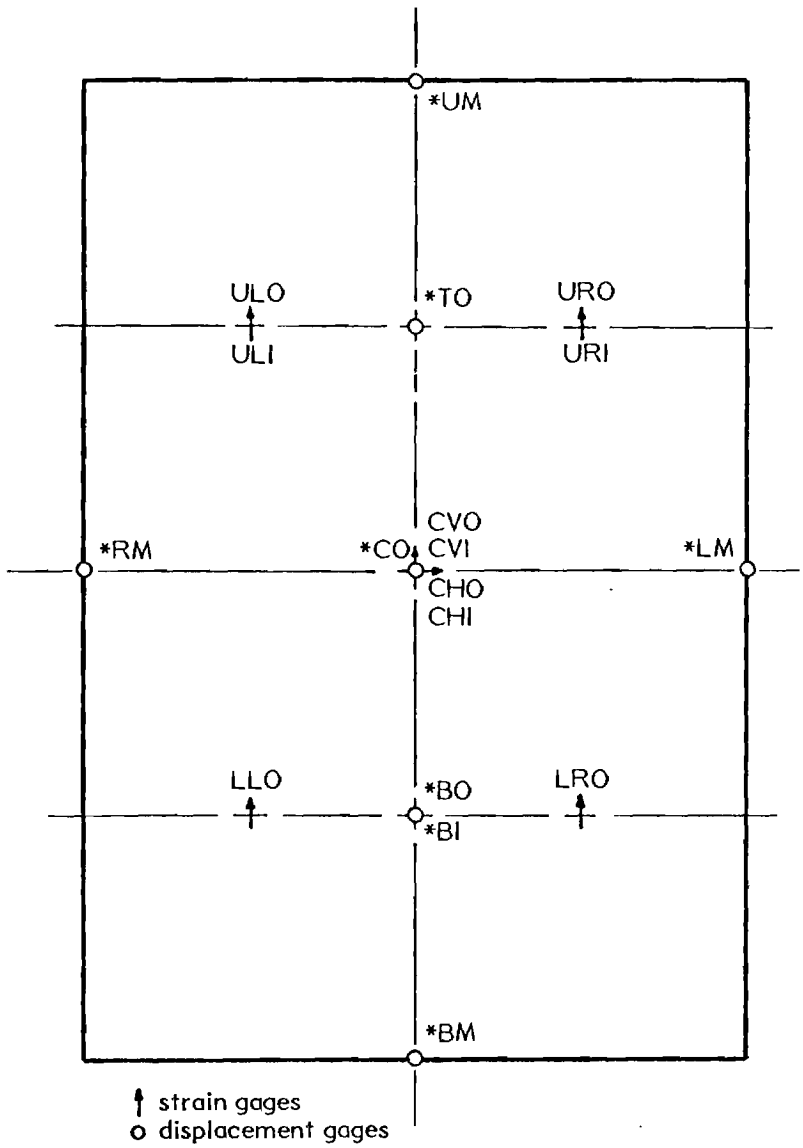

Figure 4.4-10 LVDT Deflection and Strain Gage Transducer Locations on the Test Specimen

as general as might be desired, it does provide certain design sensitivity information for variations in conditions from the standard or nominal configuration. In the present study two major parameters were considered:

(1) Glazing support conditions - in particular, the effect of increased or decreased glazing support due to precompression of the neoprene glazing gasket.

(2) Window integrity - the effect on deformation and stresses of maintaining a hermetically sealed volume (or gap) of gas between the two glass panes in an insulating window.

The first case is directly concerned with the effect of gasket support conditions on static response. Rather than consider the more complex case of variable structural geometry (which has been extensively explored in the analytical developments in Chapter 3), the present tests were concerned with the effect on static performance when more or less gasket material is forced in the glazing thus providing varying degrees of gasket precompression. This is typically the result of differences in glazing techniques and for certain designs the effect on performance may be substantial. The second case deals with the case of window performance when the seal between window panes is broken, either through aging or mechanical failure of the spacer and sealant.

The first case was simulated by using a standard galzing configuration in which the gasket length was cut exactly equal to the window perimeter. Then configurations with 10% less and 5% more gasket lengths were used. These values were the practical limits of the

amounts of gasket that could be removed without leaving gaps or the extra length that could be forced into the glazing.

The second case was simulated by boring four 3/8 in (9.5mm) holes through the insulating window spacer and into the internal volume. These were located near each corner and were fitted with removable rubber plugs to allow simulation of either a "vented" or "sealed" configuration. One plug was fitted with a pressure tap to allow measurement of the internal pressure under "sealed" conditions.

The test window with strain gages attached was mounted in the framing and glazed with the specified amount of gasket material. The window was supported on glazing blocks and carefully centered with a uniform penetration in the mullion and spandrel sections of approximately 0.5in (13mm). A period of 48 hours was allowed before testing to provide time for the gasket material to relax and conform to the support framing.

Standard Gasket Length-Sealed Spacer: This represents the nominal design configuration to which the balance of the tests are referenced Figure 4.4-11 shows the deflections measured at the center of the outer (*CO) and inner (*CI) panes as well as a the mid-height of the right mullion (*RM). Two results are immediately clear:

(1) The inner and outer panes deflect almost equal amounts,

(2) The deflection is almost linear with pressure with only a slight hardening evident.

The difference between the inner and outer pane movement is less than 3% when the window spacer seals the enclosed volume. The relative

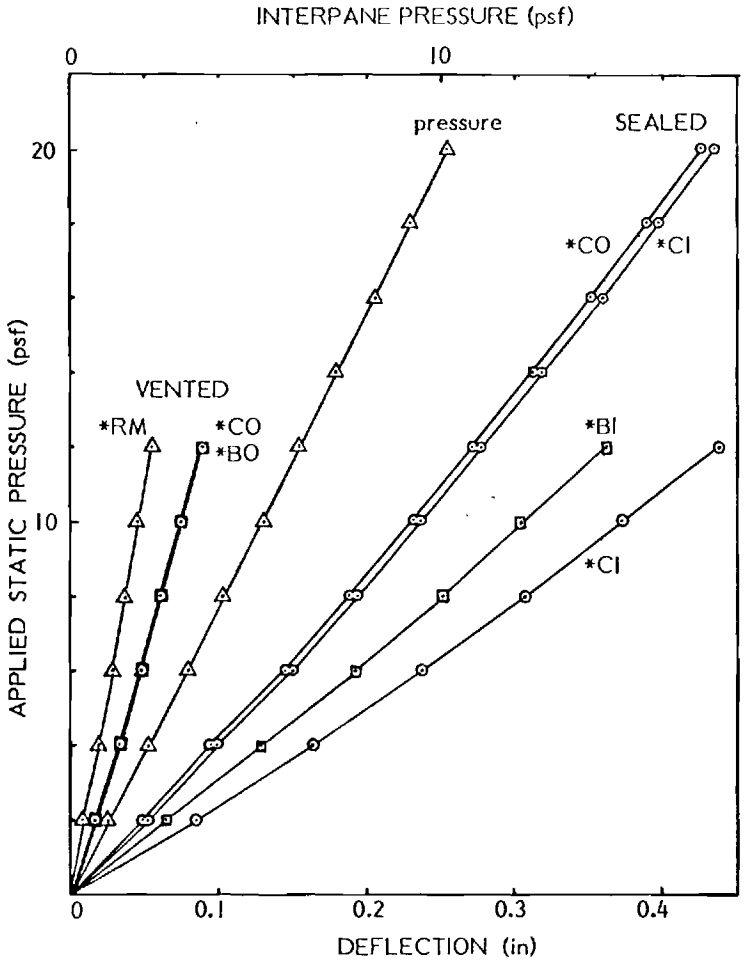

Figure 4.4-11 Deflection and Interpane Pressure Versus Static Pressure Applied Across the Window

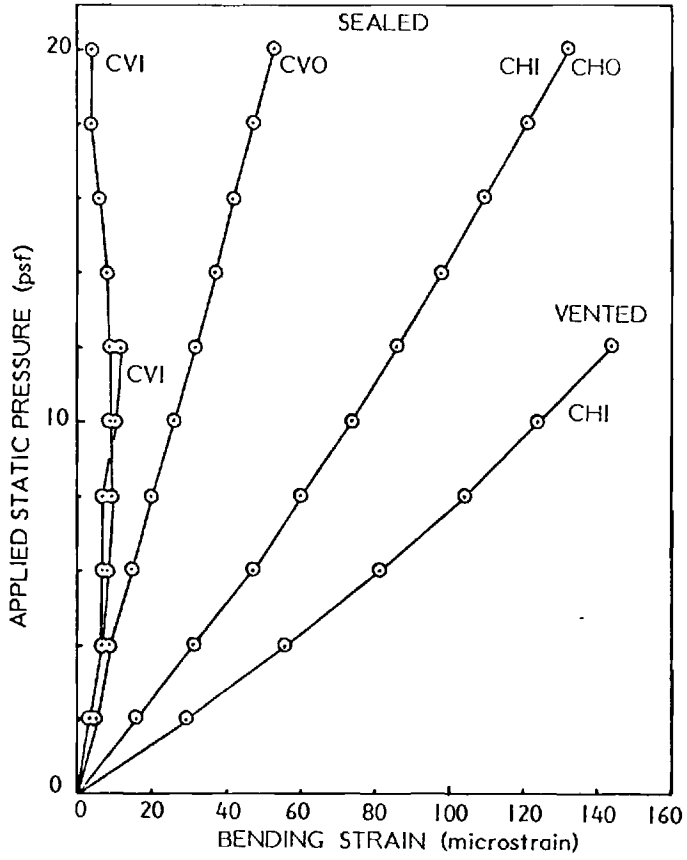

Figure 4.4-12 Glass Strain Versus Applied Pressure for the Standard Gasket Configuration

midpoint deflection (difference between *CI or *CO and *RM) is approximately linear with pressure over a range of deflection that is on the order of the equivalent double-plate thickness, 0.32in (8.1mm), obtained by assuming the two panes act together in bending with the neutral surface located halfway between. Figure 4.4-11 also shows the interpane pressure reference to outside pressure as a function of the applied differential pressure across the complete window. The values are almost exactly one half the total differential pressures which, like the deflection data, indicates that the load is almost equally divided between the two panes.

Figure 4.4-12 shows the variation in strain with static pressure for selected locations. Again as for displacements the same two features are evident in the strain from gages located at the center with horizontal orientation (CHI, CHO). In addition, the data show that the strains in the vertical direction at the center (CVI, CVO) are much smaller. Thus, the deflected shape primarily involves curvature in the horizontal direction as would be expected for a plate of that aspect ratio. The table below which lists the strain for each location bears this out.

Strain Levels at 20 psf (958Pa) - Sealed Spacer

Location	Microstrain	Location	Microstrain	Location	Microstrain
CVO	53	URO	37	LRO	36
CHO	127	URI	-37	LRI	-30
CVI	-3	ULO	36	LLO	36
CHI	-132	ULI	-32	LLI	-32

The peak strains are clearly well below the ultimate values for glass.

Standard Gasket Length - Vented Spacer: This configuration represents the situation where the spacer seal has been compromised so that the pressure load is developed across one pane only. Figure 4.4-11 shows the deflections at the midpoint of the window as well as the quarter-height location (*BO, *BI). Pressures were limited to 12 psf (575 Pa) in order to maintain deflections within the linear range (less than about one equivalent plate thickness). It is clear from the plot that the deflection occurs almost entirely in the inner plate across which the pressure is developed, while the outer pane deflection is about that of the mullion midopint. Similar curves in Figure 4.4-12 show the same behavior for the midpoint strains. The strain levels at 12 psf (575Pa) are shown below:

Strain Levels at 12 psf (975 Pa) -Vented Spacer

Location	Microstrain	Location	Microstrain	Location	Microstrain
CVO	4	URO	3	LRO	6
CHO	12	URI	-39	LRI	-34
CVI	-1	ULO	2	LLO	4
CHI	-144	ULI	-37	LLI	-37

It is apparent that the outer pane deformation is due to a combination of mullion deflection and edge moment transmitted through the spacer.

Deflected Shape: The measured deflections presented above and reported in detail in (104) show that when either in a sealed or vented configuration, the window behaves like a flat plate of equivalent thickness with its edges supported by boundary frame members.

The analytical representation presented in Chapter 3 when used with member properties for the test setup, predict the behavior with high accuracy. In addition, a classical solution developed in (103) for a more simplified model also agrees well with the measured data.

Comparison of Predicted and Measured Deflection at a Pressure Load of 20 psf (958 Pa) - Sealed

Location	Discrete Model (Chapt. 3)	Continuous Model (Ref. 103)	Measured Results
Midpoint	0.460 (11.7)	0.436 (11.1)	0.430 (10.9)
Mullion	0.054 (1.4)	0.049 (1.2)	0.086 (2.2)

Note: deflections are: in(mm)

The above summary shows excellent agreement for midpoint deflections and moderate agreement at the boundary frame.

Gasket Effects: For both the sealed and vented spacer conditions, static tests were run for three different gasket configurations:

(1) Standard Length Gasket - both the inner and outer gaskets were cut to the exact glazing dimensions and installed accordingly.

(2) 10% Less Gasket - the 75 duro neoprene gasket was cut 10% under length and during installation was stretched to complete the glazing.

(3) 5% Extra Gasket - the 75 duro neoprene gasket was cut 5% over length and during installation was compressed to fit the glazing.

These configurations represent the nominal and the extreme conditions likely to be encountered. For (2) the stretching reduces the cross

section dimensions and thus the pressure exerted by the gasket on the window. This reduces the effective moment restraint along the edge. In (3) the axial compression of the gasket that occurs as the extra length is forced in the glazing increases the cross section dimensions and increases the gasket pressure on the window, thus increasing the edge restraint.

The static deformation results for the Standard Length Gasket are shown in Fig. 4.4-13 for both sealed and vented conditions. The data are similar to those in Fig. 4.4-11 and show the same features. Fig. 4.4-14 shows the deformation for 10% Less Gasket and it is apparent that the behavior is close to the same as for the sealed configuration. On the other hand there is a definite increase in the inner pane deflection for the vented configuration. While not shown, a decrease in deflection occurs for the 5% Extra Gasket - vented configuration.

The plots in Fig. 4.4-15 show the effects of gasket properties on the static response more clearly. As noted earlier, the inner and outer pane displacements are essentially the same for the standard gasket configuration when the interpane space is sealed. The same behavior was observed for both the 10% Less Gasket and 5% Extra Gasket. Fig. 4.4-15(a) shows a comparison between the inner pane center displacement for the different gasket configurations when compared to the standard configuration. The abcissa is the difference between the particular inner-pane deflection and the value for the Standard Gasket configuration. It is clear that there is no significant variation with gasket properties over the pressure range tested (the

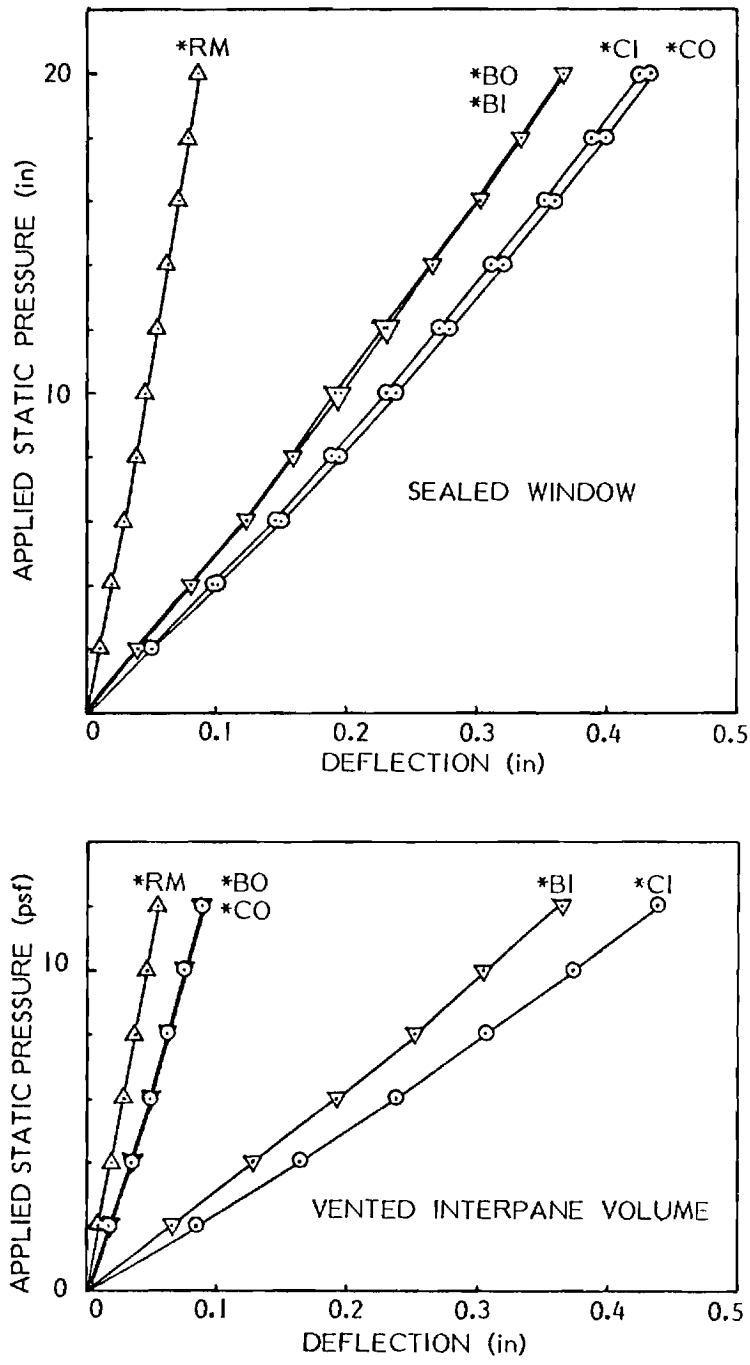

Figure 4.4-13 Static Deformation with Applied Pressure for the Standard Gasket Configuration

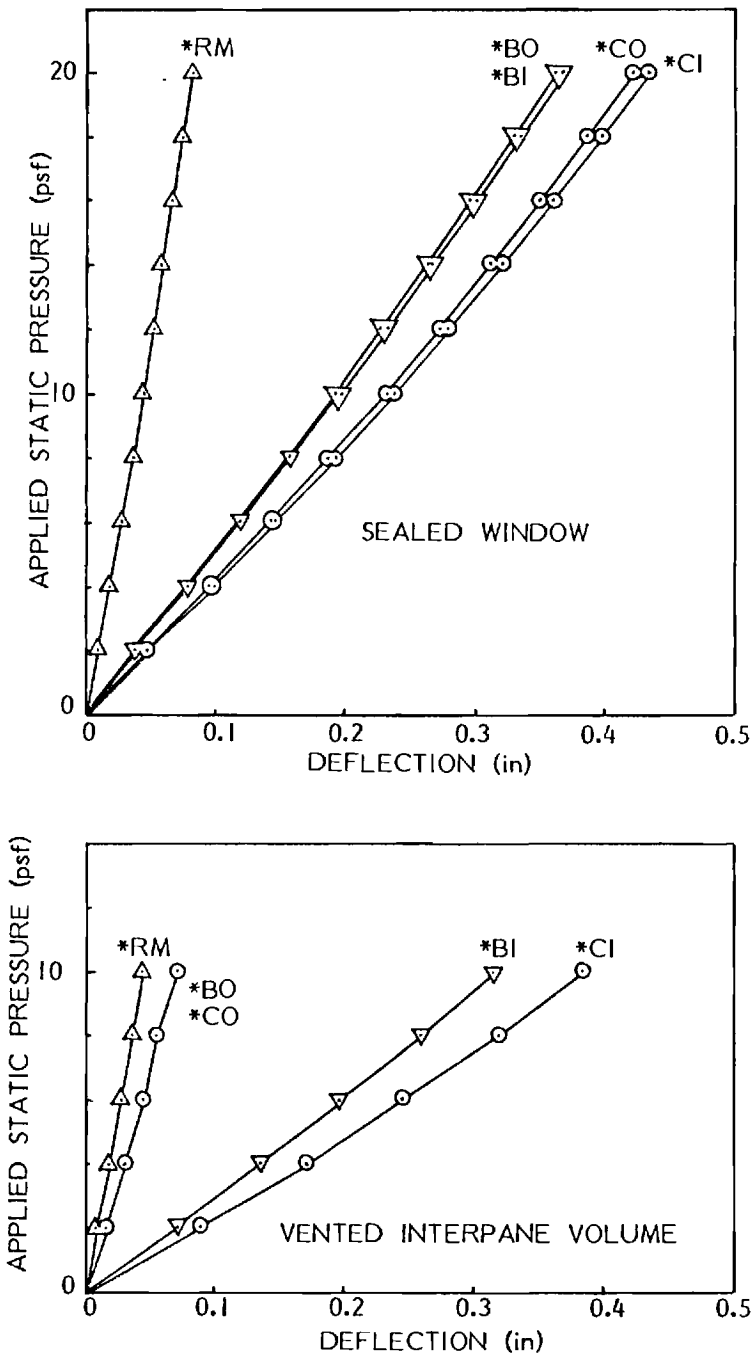

Figure 4.4-14 Static Deformation with Applied Pressure for the 10% Less Gasket Configuration

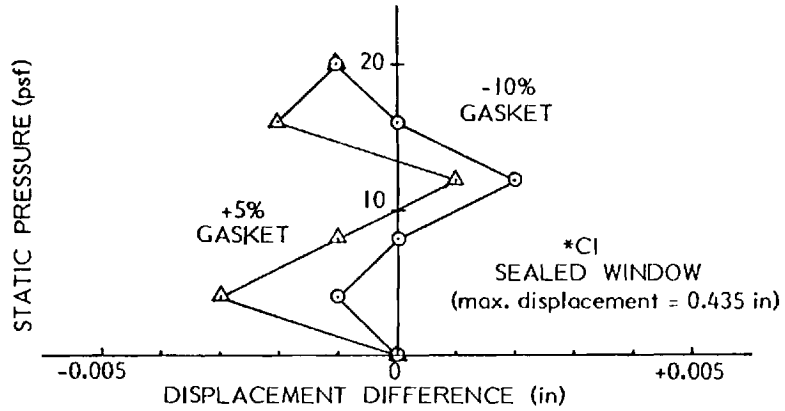

(a) Inner Pane Deflection Referenced to Standard Gasket - Sealed

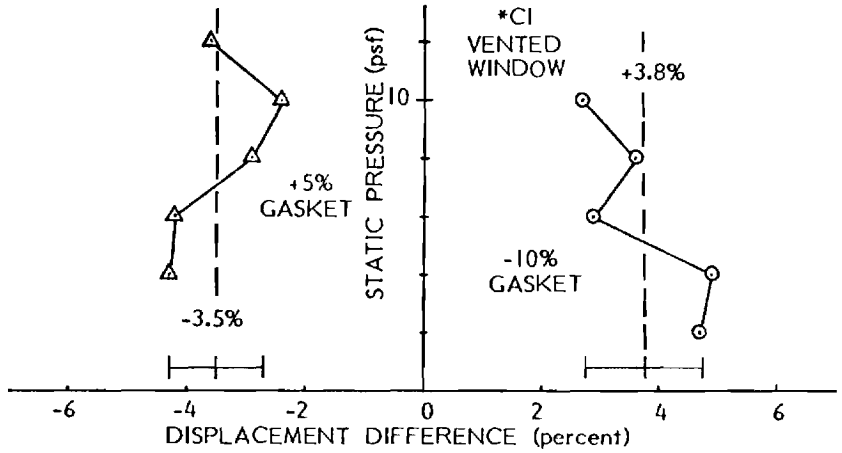

(b) Inner Pane Deflection Referenced to Standard Gasket - Vented

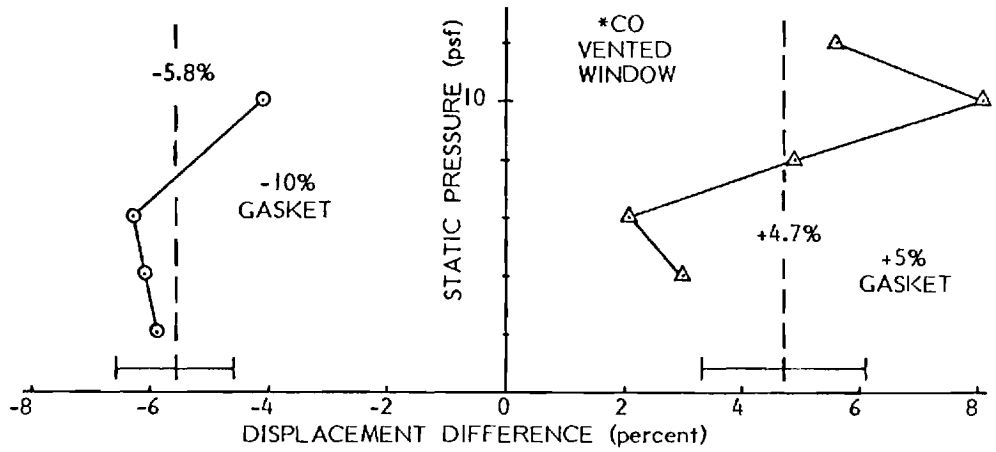

(c) Outer Pane Deflection Referenced to Standard Gasket - Vented

Figure 4.4-15 Effect of Gasket Properties on the Static Deflection

variation is less than 0.5% at the maximum pressure). When a similar plot is made for the window with the interpane space vented as shown in Fig 4.4-15(b), a distinct difference in behavior is evidient for both gasket configurations. With the reduced gasket the inner pane deflection is increased by an average of 3.8% over the standard configuration, while a 3.5% reduction is shown for the extra gasket case. Fig. 4.4-15(c) shows the same type of plot for the deflection at the midpoint of the outer pane, but now the behavior is just the opposite with the increased deflection associated with the extra gasket.

The most obvious conclusion from these data is that the effect of the glazing gasket on the static response is not significant for the nominal case of a sealed interpane space. Even when the seal is compromised, the effect on deflections and strains is not pronounced.

The particular reversal of the effect between the inner and the outer pane noted above can be explained by reference to the test configuration. The inner pane is supported directly by the neoprene foam gasket of higher "effective" stiffness while the 75 duro gasket with somewhat lower "effective" stiffness is used to make the outer glazing. Thus as more (or less) compression of the inner gasket with a consequent increase (or decrease) in the rotational restraint for the inner pane edge. Since the two panes are still bonded together, an increase in the inner gasket restraint force will reduce the corresponding inner glass deformation and shift more load to the outer pane which exhibits increased deformation. The reverse holds for a reduction in gasket restraint levels.

4.5 Dynamic Testing

Following completion of the static tests, a series of dynamic response measurements were carried out using the same window unit and mounting arrangement. The simple static pressurization procedure used for the static testing was replaced with dynamic excitation. The same strain gage and LVDT instrumentation was employed, but the essentially static-level logging instrumentation was replaced by a minicomputer-based dynamic response analysis system. The test procedure and measurement methodology are described in the first subsection, and the results obtained from the tests are presented in the second.

4.5(a) Measurement and Analysis Methodology

The strain gage and LVDT instrumentation used for the static tests and shown schematically in Fig. 4.4-10 was also used for the dynamic response measurements. The LVDT's were equipped with light weight cores and were preloaded with small springs to keep them in contact with the glass plate over the range of frequencies and accelerations encountered in the tests. Thus, the output from these transducers is proportional to the transverse displacement of the glass at that point. The strain gage outputs, on the other hand, are due to glass strain at the measurement point. For the range of deflections and loads used for the tests, the strain is due primarily to the plate curvature, and hence the gage output can be directly related to the plate deflection (this is not true when a substantial fraction of the strain is due to midplane stretching or to nonlinear effects). Strain gages are relatively inexpensive and simple to use and since in contrast to the LVDT's require no special reference mounting, they have been employed as the primary dynamic

response transducers. The LVDT's were used as a secondary source of information to resolve ambiguities in the strain signals. It should be noted that inertial accelerometers were not used because of their relatively high cost and the somewhat inaccessibility of the rear surface of the glass inside the test chamber.

The strain gage and LVDT signals were amplified and low-pass filtered and then were digitized using the HP5451B Fourier Analyzer described in Chapter 2. The analog-to-digital converter could accept only two signals simultaneously so that only pairs of transducers could be handled at a time. While substantially increasing the testing time, this restriction did not alter the basic measurement and analysis plan described below.

Modal Analysis: The primary objective of the dynamic response testing was to determine the basic modal characteristics of the window assembly when mounted in a manner similar to that in practice and when subjected to similar loading. In addition, the effect of systematic variations in the boundary restraint was evaluated. The classical approach to this type of problem has been to provide a means for dynamically exciting the structure and then to measure and identify the response at each of the natural modes of vibration within the frequency range of interest. Typically, a harmonic excitation is used and the frequency swept slowly over a range while the phase and amplitude measurements at selected points are used to identify normal mode response. In this connection various methods have been used to provide excitation of selected normal modes.

More recently, additional signal processing and analysis techniques

have become available that reduce the measurement time and allow a greater variety of excitation methods to be used. These are based on the "fast Fourier transform" or FFT algorithm and as such are implemented using digital time series realizations of the excitation and response signals. The methodology has been described in Chapter 2 in connection with the full scale building measurements and will not be repeated here. As before, the present work is based largely around the capabilities and features of the HP5451B Fourier Analyzer system which was used for the acquisition and processing of the dynamic response time series.

The measurement procedure was based on the linear response model for the system so that an influence or a transfer function could be measured which would relate the response at one point to a unit impulse applied at another. If sufficient points on the structure are chosen and a matrix of transfer functions are measured relating input at one point to output at another, it can be shown (84) that this is sufficient information to identify the modal response characteristics for most cases. Furthermore, it is possible to accomplish this using only a single row or column of the matrix, that is, using transfer functions obtained for a single input point and multiple response locations or for a single response measurement point and multiple input locations. The modal frequencies, and damping as well as the mode shapes can be obtained from the transfer functions by a variety of techniques based on certain features of the real and imaginary or magnitude and phase components as described in Chapter 2.

In the field studies reported in Chapter 2 and initially in the

present lab work, the modal identification process was carried out by examination of each of the transfer functions manually. Since these processes require relatively widely separated modal frequencies for accuracy, the results were limited in these studies to only the first two or three modes. After acquisition of the transfer functions and completion of the laboratory test program, access became available to a powerful and sophisticated analytically-based modal identification system that could be incorporated directly in the HP5451B Fourier Analyzer. This system (basically the HP Modal Analysis software package) is capable of mathematically fitting multiple degree of freedom analytical transfer functions to the measured data and adjusting the modal characteristics until the best match is made in a least squares sense. This ability has allowed more careful examination of the transfer function data than was possible manually, especially in situations where the modes are somewhat closely spaced. Unfortunately, since the system became available well after completion of the actual laboratory measurements, it has not been possible to go back and obtain improved quality data when the original data was found lacking for purposes of the modal analysis. It should be noted that this type of activity is now underway outside the scope of the present grant and will be reported on shortly.

Input Excitation: The full-scale test facility described in Section 4.2 was used to produce the dynamic excitation required for a response analysis of the window system. Two different procedures were employed depending which aspects of the response were being analyzed. The first procedure consisted of using the closed-loop servo-controlled hydraulic

system to produce time varying pneumatic pressures across the test window. As described in Section 4.3, a time varying electrical signal was applied to the control system which in turn caused the hydraulic actuators to displace the two large doors or pneumatic pistons located on the rear side of the test fixture. The door motion produced corresponding time varying pressure fluctuations in the test facility and thus provided the desired fluctuating differential pressure across the test window.

A variety of signal sources could be used including actual recorded cladding pressure waveforms. For purposed of the present modal analysis, however, it was desirable to provide simultaneous excitation over a band of frequencies encompassing the first several modes for the window assembly. Consequently, a band-limited stationary random signal with "white" spectral characteristics and a Gaussian amplitude distribution was used as the excitation source. When coupled with the digital time series analysis capability described above this allowed simultaneous measurement and analysis over a band of frequencies rather than at a single frequency as with the swept-sine approach. Appropriate ensemble averaging was used to provide input and output response measurements with a minimum acceptable level of variance. A single transducer (strain gage or LVDT) was defined as the input reference and the corresponding transfer function matrix row was determined by successively measuring the transfer functions between this and all other transducers (taken two at a time because of signal digitizing limitations noted earlier).

While this manner of excitation closely resembled the actual service conditions in character, the symmetric placement of the window in the

fixture coupled with the symmetric arrangement of the driving doors combined to strongly favor excitation of symmetric modes only. One of the modes of most interest, namely the 1'-2' mode in which the panes can move in opposite directions to each other, is not a symmetric mode and it was not possible to clearly excite this type of response using the uniform random pressure method. As a result, an alternate method was developed and used along with the random excitation. This method was basically an impulse excitation applied unsymmetrically at a point on the window. Again, a single transducer near the application point for the impulse was defined as the input reference and the corresponding transfer function matrix row was determined as above. Due to the relative inaccessibility of the window surface on the test chamber inside, a single input point was chosen and multiple response points were used. The impulse was applied by hand using a large mallet with a suitably cushioned head to provide the necessary impulse energy over the frequency range of interest. Ensemble averaging was also used to insure an acceptable level of variance in the data.

4.5(b) Dynamic Response Results

Test Method: As described earlier, the same strain and displacement transducers (shown in Fig.4.4-10) were used for static and dynamic tests. In contrast to the static tests, dynamic analysis requires considerably more data be acquired from each transducer in order to adequately define the time-frequency behavior. For example, in order to obtain a frequency resolution of Δf, one must analyze a sample record roughly $1/\Delta f$ long (see Chapter 2) which for the desired resolution of 0.1 H_z in the present tests resulted in collection of data typically over periods of 10 sec or

more. While this was readily done using the HP5451B analyzer, the off-line storage of this data for future analysis proved especially burdensome since the system was not originally equipped with any mass storage devices; the only medium available was 1" punched paper tape. As a result, a compact (from the standpoint of amount of data) test method was developed as follows. With reference to Fig. 4. 4-10, the 2 center and 4 lower quarter point strain gage locations (CHx, LLx, LRx) and the 5 LVDT locations on the midline (*xx) were taken as the primary measurement sensors and only data from these were saved on paper tape. In this way, by comparing the phase between pairs of sensors it is possible to detect modes with up to 3 node points in the vertical and up to 2 in the transverse directions (up to the 3-2 mode):

Next, using either the random pressure or the point impulse excitation methods, a single sensor (LRO strain or * BO LVDT) was selected as the input reference and the transfer function between that and the other locations (output points) were computed digitally in the HP5451B. For the strain gages this required 5 transfer functions which in turn defined a row in the transfer function matrix. Four transfer functions were computed in a similar manner for the LVDT's. For each test, ensemble averaging was performed to reduce the variance and the data were rejected if the computed coherence function was of poor quality (e.g. substantially below about 0.85).

Finally, the transfer functions were analyzed, first by hand and much later using the HP Modal Analysis software, to determine

the modal response characteristics. As described in 2.5(c) the modal frequencies and damping can be identified by certain features of the real and imaginary components of the transfer function, and for a given modal frequency, the phase between the input and each output point can be computed. This latter information is particularly critical for it effectively defines the mode shape. For example, in a pure (normal) mode, the frequency is identified by zero real and maximum imaginary components. Accordingly, the phase will be either 0° or 180° and the modal amplitude will be determined solely by the imaginary value. In reality, however, perfect 0° or 180° phase is seldom observed due to the effects of high or nonideal damping, close modal spacing, nonlinear effects, or analysis limitations. Such has been the case in the present study where the primary difficulty has been the tendency for each of the two plates to exhibit slight but noticeably different modal properties. The behavior was not constant and tended to be more pronounced with some modes than others.

Test-Configurations: The dynamic response tests were carried out for the same three different gasket configurations employed for the static tests (the same actual test set-ups were used) and for both a sealed and "vented" interpane void. The test glazings are described in section 4.4 and are referred to as: (i) nominal gasket installation, (ii) 10% less gasket (lineal basis), and (iii) 5% more gasket (lineal basis). Interpane venting involved drilling 4 3/8 inch diameter holes (one near each corner) through the interpane spacer. These were either sealed mechanically or

left clear and open as required. For clarity, the results are discussed below in two categories, first the general behavior for a given configuration and second the effects of variations in gasket properties and venting of the interpane void.

Nominal Gasket: Table 4.5-1 shows the modal frequencies and damping for the nominal gasket configuration as obtained using the transfer function curve-fitting algorithms incorporated in the Modal Analysis software on the HP5451B Analyzer. Each mode was identified by the phase relations at the measurement points. The results are shown for both the sealed and vented interpane void tests, and for comparison, the continuous and discrete analytical predictions are also listed. Several points are noteworthy.
(1) - The experimental results identify not only the first 4 "classical" plate modes but also the 1'-2' and possibly the 2'-1' modes. In the classical modes, the two plates move together and the window behaves like an equivalent single plate, while for the primed modes, the two plates move in opposite directions. As noted in Chapter 3, the latter behavior may or may not involve a net interpane compression or breathing action, depending on the mode shape. The primed modes above are of the even-odd type and hence do not involve a net void volume change (breathing), but they do depend on the interplate rotational coupling at the edge. This coupling stiffness was not quantitatively assessed (since it would involve destruction of a specimen) but from the continuous model results (section 3.4) the 1'-2' freqeuncy could range from 18.09-22.44 Hz as the rotational stiffness varies from 0 to ∞. The observed

frequencies indicate that this type of coupling is not particularily strong for the present type of window. (2) - The measured damping is in excess of 5% for most modes which is somewhat large for metal or glass structures alone. This behavior is largely due to the viscoelastic properties of the boundary gasket, especially for the classical plate modes. The damping values for the primed modes are considerably smaller and reflect the reduced participation of the gasket in this type of response. From a design point of view, this suggests that glazing properties, through their viscoelastic behavior, might be used to control peak dynamic response in the classical plate modes. On the other hand, this will likely have little effect on the primed modes which could lead to the possibility of interplate contact, especially for very large panes with strong non-uniform pressure loadings. (3) - The effect of interpane venting is essentially neglegible, for the present conditions. This is basically in agreement with the analysis since for the lower modes there should be no net interpane volume change. The effect would be a factor only for the breathing modes, the lowest of which is near 100 Hz, and at that frequency, the present holes would be of insignificant size. In contrast, the static response is highly affected. (4) - While not evident in Table 4.5-1, the presence of other modes at similar frequencies which involve substantial boundary participation was not initially anticipated and proved difficult to interpret. These modes are predicted by the discrete model in section 3.3 but due to test scheduling, appropriate boundary response instrumentation was not installed. (5) - A clear normal

mode response was not observed for some of the modes. This can be attributed in part to the high damping, but was largely due to the tendancy of the two plates comprising the window to behave slightly differently for different modes. This effectively resulted in two very closely spaced modes which proved impossible to detect by hand and difficult at best to handle with the modal analysis software.

Boundary Gasket Effects: The effect of variation in the boundary gasket support stiffness is shown in Table 4.5-2. The data cover the first two modes for both vented and sealed interpane conditions. As before, these data were obtained at first in rough form by visual inspection of the transfer functions and later in the present form using the analytical curve-fitting software. Several features are noteworthy. (1) - There is little difference between the vented and sealed interpane void data. As was anticipated and observed in the previous results. For clarity, these two cases have been averaged together and listed in the lower lines as the "Average" modal values. (2) - There is a consistent trend for the frequencies to increase as the boundary support is stiffened. This is seen most clearly in the "average" values and is most pronounced for the higher mode. This type of behavior is fully consistent with the analytical predictions developed in Chapter 3. In the present tests the major effort has been to simulate the field conditions as closely as possible, using for example the actual cladding components (mullions, spandrells, etc.). Unfortunately, this approach while yielding results representative

TABLE 4.5-1

MEASURED MODAL FREQUENCIES AND DAMPING

FOR NOMINAL GASKET AND SEALED INTERPANE VOID

Source	Parameter	Mode					
		1-1	1-2	1'-2'	1-3	2-1	2'-1'
Measured	Freq. (Hz)	10.2	19.4	19.6	28.6	32.8	42.3
	Damping (%)	6.0	3.3	1.8	10.9	7.6	1.1
Theory	Freq. (Hz)	12.2[1]	18.1[2]	18.1[3] 28.4	34.7[1]	34.2[2]	36.9 52.1

Notes:

1. Discrete element model with measured properties.
2. Continuum model for simple support.
3. Continuum model for interplate restraint from 0 to infinity (these are out-of-phase modes involving opposing movement).

TABLE 4.5-2

DEPENDENCE OF MODAL VALUES ON GASKET RESTRAINT

Configuration	1-1 MODE		1-2 MODE	
	Frequency (Hz)	Damping (%)	Frequency (Hz)	Damping (%)
Sealed				
-10%	10.18	5.7	17.54	3.5
0%	10.23	6.0	19.31	3.5
+5%	10.01	3.5	19.70	2.6
Vented				
-10%	9.95	5.7	17.49	3.1
0%	10.16	7.6	19.40	-
5%	10.48	7.8	19.67	2.9
Average				
-10%	10.06	5.7	17.52	3.3
0%	10.20	7.8	19.36	3.3
5%	10.25	5.8	19.68	2.8

of field conditions, does not readily allow for quantitative variations in these conditions. (For this purpose a special adjustable test frame would be required). Thus, it has not been possible to quantitatively assess the range of boundary restraint conditions (-10%, + 5% gasket material) used. Rather, the nominal configuration was carefully evaluated in a series of tests described in section 4.4 and two other configurations were then selected to represent the practical extremes of support for the present glazing system. (3) - The damping is not appreciably affected by alteration of the glazing gasket as presently accomplished. However, as observed earlier, there is a substantial change in the damping from mode to mode.

Summary: The modal tests using either impulse or uniform random pressure have yielded frequencies, damping and mode shapes for the double glazed window when supported in a manner closely duplicating the actual service conditions. The measured frequencies agree reasonably well with analytical predictions, Although sufficient experimental measurements were not made to adequately define those modes involving significant boundary movement. Damping values tended to be rather large for glass or metal structures as a result of the viscoelastic boundary restraint provided by the glazing gaskets. However, variations in the amount of gasket material used in the glazing produced insignificant changes in damping. The most significant result of the tests was the detection of the primed modes in which the two panes move in opposite directions. Since the damping was found to be relatively low in the lab tests,

the possibility exists that these modes could be excited at relatively high amplitudes, especially in large windows where non-uniform pressure loading may occur. Several problems were encountered, however. For certain modes, there was a measurable difference in the dynamics of each plate which appeared in the measured transfer functions as two extremely closely spaced modes and greatly complicated the analysis. Finally, the major effort was made to closely simulate actual conditions and while this yielded results in close agreement with field and analytical studies, (and provided confidence in the analysis validity), it did not allow enough time to carry out a parametric analysis for design purposes.

5.0 Conclusions

The study reported here has attempted to more precisely characterize the nature of the local cladding pressure loads and to identify the degree of causality for the dynamic response of the cladding--in particular, large insulating glass windows. This has involved a combination of field measurements, analytical modelling of the cladding, and laboratory simulation and testing.

The field measurement results are generally in agreement with the limited amount of other reported work. The chosen site exhibited a range of building geometries because of its unique shape, and consequently, it has been possible to measure the behavior of similar cladding components for a variety of flow conditions. Generally it was found that the differential cladding pressure contained relatively little power over frequency ranges encompassing the first few cladding natural frequencies and the causality (or coherence function value) was very low as well. Taken together this implies that substantial dynamic response is not likely due to pressure loading. On the other hand, for certain locations and under specific conditions, relative large pressure power levels were observed over frequency ranges including the cladding fundamental frequency. For these critical locations, a significant causality existed between the input pressure and the dynamic response.

The analytical studies centered around development of a general cladding model and computer program which would permit a wide range of cladding configurations and loading types to be considered. Panel response to static and dynamic pressure loading and racking

distortions introduced by differential motions of adjacent floors, both treated as deterministic functions of time, were the principal loadings considered. Sensitivity studies were conducted to determine the influence of system properties on the response of the panel-frame assembly. Response was shown to be sensitive to gasket rotational stiffness and frame flexural stiffness for selected panel aspect ratios. In general, the finite element model produced frequency and displacement results which were in good agreement with laboratory and field test values. Out-of-phase double panel modes were predicted both at relatively low frequencies and at frequencies beyond the range of practical interest.

Subsequent analytical studies of glass cladding should consider large displacement response of the lights. Viscoelastic properties of the gasket, damping mechanisms, and treatment of wind excitation as a random process are also worthy extensions to this study. The present discrete element model can be modified to include these effects. Finally, the interaction of the entire glass curtain wall with the structural frame should be investigated in future studies. Claddings of various types are likely to provide measurable in-plane stiffness which could be used to advantage by the structural designer to help control interstory drift and building motion affecting occupant comfort.

The laboratory phase of the study centered around development of a full-scale pressure simulation facility and subsequent use of this equipment with cladding components from the field site. The facility has generally met or exceeded its design objectives

and has been found of great value in simulating both steady state and transient test conditions. Extensive laboratory measurements were carried out to precisely define the local structural characteristics of the cladding system under study (which is representative of a number of common designs). Subsequent static and dynamic response measurements produced results that were in good agreement with the predictions of the analytical model and thus confirmed its validity and appropriateness. The dynamic response measurements using a point impulse forced excitation method revealed the presence as predicted, of double plate modes in which the plates move out of phase with respect to each other. One of these, modes involving no net interpane volume change, was found to occur at a low enough frequency (20 Hz) to pose potential problems in large windows where significant pressure non-uniformity (which is required to excite this mode) might occur. This type of motion, if severe enough, could obviously lead to plate-to-plate impact with the risk of consequent failure.

The lab studies were unfortunately somewhat limited in breadth since the primary requirement was to characterize a typical cladding system and validate the analysis for it. Future work with this facility should attempt to apply the model to and determine the characteristics of a variety of cladding systems. This approach will directly furnish design-oriented information so critical for efficient, sound and economical design.

6.0 REFERENCES

1. Minor, J. E., and Beason, W. L., "Window Glass Failure in Windstorms," ASCE National Structural Engineering Convention, April 14-18, 1975, New Orleans, La. Meeting Preprint 2486.

2. Eaton, K. J., "Cladding and the Wind," ASCE National Structural Engineering Convention, April 14-18, 1975, New Orleans, La. Meeting Preprint 2436.

3. Gannon, Robert, "Wind Engineering," Popular Science, October, 1975, pp.84.

4. Minor, J. E., Mehta, K. C., and McDonald, J. R., "Failures of Structures Due to Extreme Winds," Journal of the Structural Division, ASCE, Vol.98, No. ST11, Proc. Paper 9324, November, 1972, pp. 2455-2471.

5. "Hancock Glass breakage: A Combination of Errors?," Engineering News-Record, May 13, 1976, p.9.

6. Engineering-News Record, Vol. 187, December 23, 1971, p. 15; Vol. 188, January 6, 1972, p. 12.

7. Engineering-News Record, Vol. 189, August 10, 1972, p.11.

8. Engineering-News Record, Vol. 189, October 12, 1972, p. 46-47.

9. Engineering-News Record, Vol. 188, February 3, 1972, p. 14.

10. Engineering-News Record, Vol. 187, December 9, 1971, p. 13.

11. American National Standard Building Code Requirements for Minimum Design Loads in Buildings and Other Structures, ANSI A58.1-1972, American National Standards Institute, New York.

12. Glass Product Recommendations, Technical Service Report No. 101, PPG Industries, 1972, 26 pages.

13. Robertson,L. E., and Chen, P. W., "Glass Design and Code Implications for Extremely Tall Buildings," Building Research, Vol. 4, May-June, 1967,pp.6-11

14. Gwyn, J. D., "Factors Affecting Structural Performance of Glass," Building Research, Vol. 4, May-June, 1967, pp. 36-38.

15. Khan, F. R., "Optimum Design of Glass in Buildings," Building Research, Vol. 4, May-June, 1967, pp. 45.48.

16. Proceedings of the Seminar on Wind Loads on Structures, University of Hawaii, October, 1970.

17. International Research Seminar on Wind Effects on Buildings and Structures, Ottawa, Canada, September 11-15, 1967.

18. Proceedings of the Third International Conference on Wind Effects on Buildings and Structures, Tokyo, 1971.

19. Symposium on Full-Scale Measurements of Wind Effects on Tall Buildings and Other Structures, University of Western Ontario, London, Canada, June 23-29, 1974 (also Journal Industrial Aero., 1 (1975), Appendix Z)

20. Proceedings of Second U. S. National Conference on Wind Engineering Research, Colorado State University, Ft. Collins, Colorado, June 1975.

21. Proceedings of the Chicago Design Symposium, Northwestern University, Evanston, Ill., March 23, 1970.

22. Engineering-News Record, Vol. 188, February 3, 1972, p. 15.

23. Engineering-News Record, Vol. 189, December 21, 1972, p. 27.

24. Sadeh, W. Z., and Cermak, J.E., "Turbulence Effect of Wall Pressure Fluctuations." Journal of the Engineering Mechanics Division, ASCE, Vol.98 No. EM6, Proc. Paper 9445, December, 1972, pp. 1365-1379.

25. Peterka, Jon A., and Cermak, J. E., "Wind Pressures on Buildings-Probability Densities," Transactions ASCE Structures Division, June 1975 Proc. Paper 11373.

26. Allen, D. E., and Dalgliesh, W. A., "Dynamic Wind Loads and Cladding Design," The Preliminary Publication of the International Association of Bridge and Structural Engineering Symposium held in Lisbon, 1973, pp. 279-285.

27. Ida, M., Terayama, T., and Miyoshi, S., "Measurement of Natural Wind Pressure Acting on Glass Panels of Kasumigaseki High Rise Building in High Wind," Report Research Laboratory Asahi Glass Company, Vol. 20, No. 2, 1970, pp. 79-92.

28. Miyoshi, S., and Miura, T., "Study of the Wind Resistance of Glass Panels (Part 2). Breaking Tests of Large Glass Panels by Means of Oscillatory Pressure," Asahi Glass Company Lab., Research Report, Vol. 14, (2), 1964, pp. 82-92 (B.G.I.R.A. Translation No. 660).

29. Khan, F. R., "A Rational Method for the Design of Curtain Walls," Wind Effects on Buildings, Proceedings, Design Symposium, Evanston, Illinois, March 23, 1970, pp. 145-147.

30. Nassetta, A. F., "L'Enfant Plaza Project," Building Research, Vol. 4, May-June, 1967, pp. 49-51.

31. Chang, F. K., "Human Response to Motions in Tall Buildings," Presented at ASCE National Environmental Engineering Meeting, Houston, Texas, October 16-22, 1972, Preprint 1785.

32. Pretlove, A. J., and Bowler, J. F., "An Estimate of Sonic Boom Damage to Large Windows," Journal of Sound and Vibration, Vol. 22, 1972, pp. 107-112.

33. Bowles, R., and Sugarman, B., "The Strength and Deflection Characteristics of Large Rectangular Glass Panels under Uniform Pressure," Glass Technology, Vol. 3, No. 5, 1962, pp. 156-170.

34. Orr, L., "Engineering Properties of Glass - Windows and Glass in the Exterior of Buildings," Publication 478, Building Research Unit, U. S. National Academy of Sciences, 1957, pp. 51-62.

35. Rousseau, P. E., "Evolution of Conception of Curtain Walls in Relation with Flexibility of Structures," Proceedings of the International Conference on Planning and Design of Tall Buildings, ASCE-IABSE Joint Committee, Bethlehem, Pa., Vol. Ia-12, pp. 1153-1154.

36. Newby, F., "Stiffness Related to Nonstructural Elements," Proceedings of the International Conference on Planning and Design of Tall Buildings and Structures, National Bureau of Standards, Building Science Series 30, Jan., 1969, pp. 9-18.

37. Raggett, J. D., "Influence of Nonstructural Partitions on the Dynamic Response Characteristics of Structures," Report No. JAB-99-94, John A. Blume and Associates Research Division, San Francisco, Calif., July, 1972.

38. Oppenheim, I., "Dynamic Behavior of Tall Buildings with Cladding," Proceedings, Fifth World Conference on Earthquake Engineering, Rome, Italy, June, 1973, pp. 2769-2773.

39. Sharpe, R. L., "Seismic Design of Nonstructural Elements," Proceedings of the International Conference on Planning and Design of Tall Buildings, ASCE-IABSE Joint Committee, Bethlehem, Pa., Vol. Ia-12, pp. 1143-1148.

40. Deo, R., "An Experimental Investigation of the Performance of Insulating Windows - Wind Loads and Dynamic Response," Ph.D. Dissertation, Georgia Institute of Technology, School of Aerospace Engineering, June 1977.

41. Cermak, J. E., "Separation-Induced Pressure Fluctuations on Buildings," Proceedings of the Seminar on Wind Loads on Structures, University of Hawaii, October 1970, pp. 55.

42. Ostrowski, J. S., Marshall, R. D. and Cermak, J. E., "Vortex Formation and Pressure Fluctuations on Buildings," International Research Seminar on Wind Effects on Buildings and Structures, Ottawa, Canada, 11-15 September, 1967, Vol 1.

43. Cermak, J. E., and Sadeh, W. Z., "Pressure Fluctuations on Buildings," Proceedings of the Third International Conference on Wind Effects on Buildings and Structures, Tokyo, 1971, pp. 189-198.

44. Newberry, C. W., et. al., "The Nature of Gust Loading on Tall Buildings," Loc. Cit. Ref. 7.

45. Dalgliesh, S. A., "Comparison of Model/Full Scale Wind Pressures on a High Rise Building," J. Ind. Aerod. 1 (1975) 55-66.

46. Dalgliesh, W. A., "Statistical Treatment of Peak Gust on Cladding," J. ASCE Structural ST9, Vol. 97, Sept. 1971, p. 2173.

47. Dalgliesh, W. A., et.al., "Wind Pressure Measurements on a Full-Scale High Rise Office Building," Loc. Cit. Ref. 7.

48. Takeuchi, M., et. al., "Actual Fluctuating Wind Pressures on a Tall Building and its Response," Loc, Cit. Ref. 8, pp. 285.

49. Standen, N. M., Dalgliesh, W. A., and Templin, R. J., "A Wind Tunnel and Full Scale Study of Turbulent Wind Pressures on a Tall Building," Loc. Cit. Ref. 8.

50. Miyoshi, S., et. al., "Wind Pressure Coefficients on Exterior Wall Elements of Tall Buildings," Loc. Cit. Ref. 8, pp. 273.

51. Davenport, A. G., and Dalgliesh, W. A., "A Preliminary Appraisal of Wind Loading Concepts of the 1970 Canadian National Building Code," Loc. Cit. Ref. 8, pp. 441.

52. Cohen, E., and Vellozzi, J., "Proposed American Standard Building Code Requirements for Minimum Design Wind Loads," Wind Effects on High Rise Buildings, Proceedings of the Chicago Design Symposium March 23, 1970, Northwestern University, Evanston, Ill.

53. National Building Code of Canada 1970, Issued by the Associate Committee on the NBC, NRC Ottawa, Canada.

54. Southern Standard Building Code, Southern Building Code Congress, Birmingham, Alabama, 1969.

55. Ishizaki, H., "On the Wind Resistant Design of Exterior Cladding," National Conference on Planning and Design of Tall Buildings, Proc. Pap. Tokyo, Japan, Aug. 28-30, 1973.

56. Ishizaki, H., "On the Design of Glass Pane Against Wind Loading," Ind. Aerod. Abstracts 2.273A7.

57. Saffir, H. S., "Hurricane Camille: Data on Storm and Structural Damage," Loc. Cit. Ref.8, pp. 457.

58. Palfery, J. G. and Harper, J. J., "Wind Tunnel Investigation of Wind Induced Pressures on a 1/158.4 Scale Model of Tower Place," Georgia Institute of Technology, School of Aerospace Engineering, DGSA Report No. E15-300-ZAA, August 1974.

59. Sage, A. P., "System Identification History, Methodology, Future Prospects,: in System Identification of Vibrating Structures, ASME, Ed. W. D. Pilkey and R. Cohen, 1972.

60. Bendat, J. S. and Piersol, A. G., Random Data: Analysis and Measurement Procedures, 1971, Wiley-Interscience.

61. Wiener, N., "Generalized Harmonic Analysis," Acta Mathematica 1930, Vol. 55, pp. 117-258.

62. Carter, G. C., et. al., "Estimation of the Magnitude-Squared Coherence Function via Overlapped Fast Fourier Transform Processing," IEEE Trans. on Audio and Electroacustics, Vol. Au-21, No. 4, August 1973.

63. Carter, G. C. et. al., "Coherence and its Estimation via the Partitioned Modified Chirp-Z Transform," IEEE Transactions on Acoustics, Speech, and Signal Processing, June 1975.

64. Shapiro, A., "Estimation of Coherence Between Signal and Signal Plus Echoes," Bell Telephone Labs. Tech. Man., Whippany, N. J., 1963.

65. Akaike, H., "Statistical Measurement of Frequency Response Functions," Annals of the Institute of Statistical Mathematics, Supplement III, 1964, pp. 5-17.

66. Dean, W. C., Enochson, L. D., and Shumway, R. H., "The Coherency Analysis of Seismic Noise," SDLR 155, Air Force Technical Applications Center, Washington, D. C., July 1966.

67. Kaneshige, I., "Frequency Response of an Automobile Engine Mounting," Annals of the Institute of Statistical Mathematics, Supplement III, 1964, pp. 49-57.

68. Barnoski, R. L., "Ordinary Coherence Functions and Mechanical Systems," J. Aircraft, Vol. 6, No. 4, April 1969, pp. 372.

69. Bendat, J. S. and Halvorsen, W. G., "Noise Source Identification Using Coherent Output Power Spectra," Sound and Vibration, Aug. 1975.

70. Goff, K. W., "The Application of Correlation Techniques to Some Acoustic Measurements," Journal of the Acoustical Society of America, Vol. 27, No. 2, March 1955.

71. Snowdon, J. C., "Forced Vibration of Internally Damped Rectangular and Square Plates with Simply Supported Boundaries," Journal of the Acoustical Society of America, Vol. 56, No. 4, pp. 1177, October 1974.

72. Snowdon, J. C., "Mechanical Four-Pole Parameters and Their Applications," Journal of Sound and Vibration, Vol. 15, No. 3, pp. 307-323, April 1971.

73. Davenport, A. G., Discussion of Ref. 6, Journal of the Structural Division, ASCE, Vol. 102, No. ST11, Nov. 1976, pp. 2235.

74. Roth, Peter, Hewlett-Packard Application Note 140-1.

75. Otnes, R. K., and Enochson, L. D., Digital Time Series Analysis, 1972, Wiley-Interscience.

76. Jenkins, G. M., and Watts, D. G., Spectral Analysis and Its Applications, 1968, Holden Day, San Francisco.

77. Potter, R. W., "Compilation of Time Windows and Line Shapes for Fourier Analysis," Hewlett-Packard Company., Publication 1970.

78. Oliver, B. M., and Cage, John M., Electronic Measurements and Instrumentation, 1971, McGraw-Hill, New York.

79. Enochson, L. D., and Goodman, N. R., "Gaussian Approximation to the Distribution of Sample Coherence," Measurement Analysis Corp., Los Angeles, Ca., Contract Report AFFDL TR-65-57, June 1965.

80. Schiff, A. J., "Evaluation of Pressure Transducers for Full Scale Testing," in Proceedings ASCE-EMD Specialty Conf., UCLA, March 30-31, 1976.

81. Hart, G. C., et. al., "System Identification in Structural Dynamics," Loc. Cit. Ref. 42.

82. Schiff, A. J., "Identification of Large Structures Using Data From Ambient and Low Level Excitations," Loc. Cit. Ref. 29.

83. Ramsey, K. A., "Effective Measurements for Structural Dynamics Testing," Sound and Vibration, April 1976, Vol. 10, No. 4, pp.18.

84. Richardson, M., and Potter, R. W., "Identification of the Modal Properties of an Elastic Structure from Measured Transfer Function Data," presented at the 20th ISA Symposium, May 21-23, 1974, Albuquerque, N. M.

85. Richardson, M., "Modal Analysis Using Digital Test Systems," Presented at Seminar on Understanding Digital Control and Analysis in Vibration Test Systems, Goddard Space Flight Center, Md.

86. Hamma, G. A., Smith, S. and Stroud, R. C., "An Evaluation of Excitation and Analysis Methods for Modal Testing," SAE Aerospace Engineering and Manufacturing Meeting, San Diego, November 1976, Paper 760872.

87. Kennedy, C. C., and Pancu, C. D. P., "Use of Vectors in Vibration Measurement and Analysis," J. Aero. Sci., Vol. 14, No. 11, Nov. 1947.

88. Oakberg, R. G., and Weaver, W., Jr., "Analysis of Frames with Shear Walls by Finite Elements,: Proceedings, Symposium on Application of Finite Element Methods in Civil Engineering, Vanderbilt University, Nashville, Tennessee, November, 1969.

89. Bogner, F. K., Fox, R. L., and Schmit, L. A., "The Generation of Inter-element-compatible Stiffness and Mass Matrices by the Use of Interpolation Formulas," Proceedings of the Conference on Matrix Methods in Structural Mechanics, Wright-Patterson Air Force Base, Ohio, October 26 - 28, 1965, AFFDL TR 66-80, 1966.

90. Goodno, B. J., and Gere, J. M., "Analysis of Shear Cores Using Super-Elements," Journal of the Structural Division, ASCE, Vol. 102, No. ST1, Proc. Paper 11837, Jan., 1976, pp. 267 - 283.

91. Guyan, R. J., "Reduction of Stiffness and Mass Matrices," AIAA Journal, Vol. 3, No. 2, 1965, p. 380.

92. Timoshenko, S. P., Young, D. H., and Weaver, W., Jr., Vibration Problems in Engineering, 4th ed., John Wiley and Sons, Inc., New York, N. Y., 1974, pp. 279 - 355.

93. Weaver, W., Jr., and Nelson, M. F., "Three-Dimensional Analysis of Tier Buildings," Journal of the Structural Division, ASCE, Vol. 92, No. ST6, Proc. Paper 5019, Dec., 1966, pp. 385 - 404.

94. Weaver, W., Jr., Nelson, M. F., and Manning, T. A., Jr., "Dynamics of Tier Buildings," Journal of the Engineering Mechanics Division, ASCE, Vol. 94, No. EM6, Proc. Paper 6293, Dec., 1968, pp. 1455 - 1474.

95. Weaver. W., Jr., Brandow, G. E., and Manning, T. A., Jr., "Tier Buildings with Shear Cores, Bracing and Setbacks," Computers and Structures, Vol. 1, Pergamon Press, 1971, pp. 57 - 83.

96. Palfery, J. G. and Craig, J. I., "Full-Scale Wind Pressure Simulation For Windows and Curtain Wall Structures," ASCE/EMD Specialty Conference, Dynamic Response of Structures, UCLA, March, 1976, pp. 380-390.

97. Frownfelter, C. R., "Structural Testing of Large Glass Installations," ASTM Special Technical Publication, STP 251, Feb. 1959, p. 19.

98. Saito, S. and Tsutsui, K., "Behaviors of Window and Curtain Wall Construction Under Typhoon Conditions," Trans. Arch. Inst. of Japan, N. 111, May 1965, p. 19. and N.116, Oct. 1965, p.27.

99. Attryde, A. G. and Dawe, P. S., "Testing Facilities for Windows at the Hemel Hempstead Centre," presented at the Int'l. Symp. on Window Performance, Paisley, U.K., April 1971.

100. Beckett, H. E. and Godfrey, J. A., Windows - Performance, Design and Installation, Van Nostrand Reinhold, New York, Chapt. 7.

101. Peterka, J. A., "Fluctuating-Pressure Tests for Cladding Design," ASCE Nat'l. Structural Engr. Conv., New Orleans, April 1975, preprint 2457.

102. Mukai, H. and Hisataku, T., "An Experimental Study of the Wind Pressure Distribution on a High-Rise Building in Osaka," Proceedings of the 2nd U. S. National Conference on Wind Engineering Research, Ft. Collins, June 1975, p. II-21.

103. Davenport, A. G., "A Rationale for Determination of Design Wind Velocities," Proceedings ASCE, J. Structural Div., Vol. 86, 1960, pp. 39-60.

104. Deo, R. B., and Craig, J. I.,"An Optical Technique for the Measurement of Time-Dependent Displacements," Proceedings of the 24th Int'l. Instrumentation Symposium, Instrument Society of America, Albuquerque, NM, May, 1978.

APPENDIX

Listing of FORTRAN Computer Program WINDOW

```
*DECK MAIN                                                              MAI00000
      PROGRAM WINDOW(INPUT,OUTPUT,TEMPS,SFFMFF,REACS,TAPE5=INPUT,       MAI00010
     #               TAPE6=OUTPUT,TAPE10=TEMPS,TAPE33=SFFMFF,           MAI00020
     #               TAPE11=REACS)                                      MAI00030
C                                                                       MAI00040
C                                                                       MAI00050
C-----PROGRAM WINDOW                                                    MAI00060
C                                                                       MAI00070
C-----PROGRAMMER:  DR. BARRY J. GOODNO                    1975,-6       MAI00080
C                  SCHOOL OF CIVIL ENGINEERING                          MAI00090
C                  GEORGIA INSTITUTE OF TECHNOLOGY                      MAI00100
C                  ATLANTA, GEORGIA  30332                              MAI00110
C                  (404)894-2227                                        MAI00120
C                                                                       MAI00130
C-----DESCRIPTION:                                                      MAI00140
C WINDOW - PROGRAM FOR THE LINEAR STATIC AND DYNAMIC ANALYSIS           MAI00150
C          OF FRAMED PANELS WITH ARBITRARY SUPPORT CONDITIONS AND       MAI00160
C          ARBITRARY SELECTION OF STRUCTURE DEGREES OF FREEDOM.         MAI00170
C                                                                       MAI00180
C IN THIS PROGRAM PANELS ARE REPRESENTED BY A COMBINATION OF THE        MAI00190
C BARBER-OAKBERG-WEAVER (BOW) REFINED PLANE STRESS RECTANGULAR          MAI00200
C FINITE ELEMENT AND THE BOGNER-FOX-SCHMIT (BFS) RECTANGULAR PLATE      MAI00210
C BENDING ELEMENT.  THE EXTERIOR FRAMING (IF PRESENT) CONSISTS OF       MAI00220
C BEAM AND COLUMN ELEMENTS AND THE BEAM ELEMENTS MAY HAVE NONRIGID      MAI00230
C CONNECTIONS.  BOUNDARY NODES ON THE PANEL AND ADJACENT FRAME NODES    MAI00240
C MAY BE JOINED BY THREE TRANSLATIONAL AND ONE ROTATIONAL SPRING        MAI00250
C (PARALLEL TO THE PANEL EDGE); THUS THE MODEL CAN BE USED TO           MAI00260
C REPRESENT A WINDOW-GASKET-MULLION ASSEMBLAGE.  IN ADDITION, LINEAR    MAI00270
C ELASTIC SPRINGS MAY BE ATTACHED TO ANY PANEL NODE IF DESIRED.         MAI00280
C                                                                       MAI00290
C THE BASIC CHARACTER OF THE MODEL DEPENDS UPON THE VALUE OF THE VARIABLMAI00300
C                                                                     E MAI00310
C "NFM" (=NUMBER OF BOUNDARY FRAME MEMBERS).  IF NFM>0, A PANEL-        MAI00320
C FRAME ASSEMBLAGE IS IMPLIED; IF NFM=0, AN ARBITRARILY-SUPPORTED       MAI00330
C PANEL WITH NO FRAME IS IMPLIED.  BOTH PANEL AND FRAME DOF'S MAY       MAI00340
C BE RESTRAINED AS DESIRED AND SUPPORT DISPLACEMENTS SPECIFIED AS       MAI00350
C A LOADING CONDITION.  PANEL AND FRAME ARE NUMBERED INDEPENDENTLY.     MAI00360
C                                                                       MAI00370
C AN ARBITRARY NUMBER AND DISTRIBUTION OF  PANEL NODE DEGREES OF FREEDOMMAI00380
C MAY BE DESIGNATED AS THE STRUCTURE DEGREES OF FREEDOM (CALLED F       MAI00390
C DISPLACEMENT TYPES) AND EXTRANEOUS PANEL AND MULLION DEGREES OF       MAI00400
C FREEDOM ARE ELIMINATED THROUGH MATRIX CONDENSATION (GUYAN REDUCTION). MAI00410
C AT THE END OF THE ANALYSIS, STRUCTURE STIFFNESS AND MASS MATRICES     MAI00420
C COUPLING THE DEGREES OF FREEDOM WITH EACH OTHER AND WITH THE SUPPORT  MAI00430
C RESTRAINTS (R DISPLACEMENT TYPES) ARE LEFT, AND STRUCTURE FREQUENCIES MAI00440
C AND MODE SHAPES MAY BE DETERMINED.  THE STRUCTURE MASS MATRIX MAY BE  MAI00450
C FORMED USING CONSISTENT MASS(CM), ASSEMBLED-LUMPED MASS(ALM), OR      MAI00460
C INPUT-LUMPED MASS(ILM).                                               MAI00470
C                                                                       MAI00480
C TIME DEPENDENT NODAL LOADS, ACCELERATIONS OF THE RIGID SUPPORT SYSTEM MAI00490
C OR ARBITRARY INDEPENDENT DISPLACEMENTS OF SUPPORTS,                   MAI00500
C ALL TREATED AS PIECEWISE-LINEAR FUNCTIONS OF TIME IN THE STRUCTURE X, MAI00510
C Y, AND Z DIRECTIONS, ARE ACCEPTABLE LOADING CONDITIONS.  THE NORMAL   MAI00520
C MODE METHOD IS USED TO DETERMINE THE DISPLACEMENT RESPONSE OF THE     MAI00530
C SYSTEM.  DISPLACEMENT-TIME HISTORIES ARE PRINTED AND/OR PLOTTED FOR   MAI00540
C DEGREES OF FREEDOM (F TYPES) SELECTED BY THE ANALYST,                 MAI00550
C IN ADDITION, STATIC DISPLACEMENTS, PANEL STRESSES, AND SUPPORT        MAI00560
C REACTIONS MAY BE DETERMINED IF STATIC BEHAVIOR IS OF INTEREST         MAI00570
C (I.E., ISDA=0).                                                       MAI00580
C                                                                       MAI00590
C-----SUBPROGRAMS IN PROGRAM WINDOW:                                    MAI00600
C                                                                       MAI00610
C  1) PRIMARY SUBPROGRAMS                                               MAI00620
C    SDATA - READS AND PRINTS STRUCTURE DATA AND CONTROL PARAMETERS     MAI00630
C    PANLSM - FORMS STIFFNESS AND MASS SUBMATRICES FOR PANEL            MAI00640
C    FRAMSM - FORMS STIFFNESS AND MASS SUBMATRICES FOR FRAME            MAI00650
C    SPRING - FORMS STIFFNESS SUBMATRICES FOR PANEL AND FRAME DEGREES   MAI00660
C             OF FREEDOM COUPLED BY ELASTIC SPRINGS                     MAI00670
C    CDENSE - CONDENSATION OF STIFFNESS AND MASS MATRICES               MAI00680
C    EIGENV - DETERMINES FREQUENCIES AND MODE SHAPES FOR STRUCTURE DOFS  MAI00690
C    STATIC - COMPUTES STATIC DISPLACEMENTS, STRESSES, REACTIONS        MAI00700
C    DYNAMIC - FREQUENCIES, MODE SHAPES, AND DYNAMIC RESPONSE           MAI00710
C    DYDATA - READS AND PRINTS DATA FOR DYNAMIC ANALYSIS                MAI00720
C    RESPON - COMPUTES AND PRINTS DISPLACEMENT RESPONSE OF STRUCTURE    MAI00730
C                                                                       MAI00740
C  2) SECONDARY SUBPROGRAMS                                             MAI00750
C    AXLBX, TRED2, TQL2 - EIGENVALUE PROBLEM SOLUTION ROUTINES (CALLED  MAI00760
C                         BY EIGENV)                                    MAI00770
C    MATPRT - PRINTS MATRICES                                           MAI00780
C    DCOMP - CHOLESKY DECOMPOSITION OF A MATRIX (CALLED BY CDENSE)      MAI00790
C    SOLVE - SOLVES SIMULTANEOUS EQUATIONS (CALLED BY CDENSE)           MAI00800
C    GRAPH - PRINTER PLOT OF SYSTEM RESPONSE (CALLED BY RESPON)         MAI00810
C    TSET - FORMS PERMUTATION VECTOR FOR FORMATION OF ELEMENT           MAI00820
C           STIFFNESS AND MASS MATRICES (CALLED BY PANLSM)              MAI00830
C    RCALC - DYNAMIC RESPONSE CALCULATIONS (CALLED BY RESPON)           MAI00840
C    SBOG - STIFFNESS MATRIX FOR BFS ELEMENT (CALLED BY PANLSM)         MAI00850
C    SBOW - ELEMENT STIFFNESS MATRIX FOR REFINED PLANE STRESS ELEMENT   MAI00860
C           (CALLED BY PANLSM)                                          MAI00870
C    BOGCM - CONSISTENT MASS MATRIX FOR BFS ELEMENT (CALLED BY PANLSM)  MAI00880
C    BOWCM - CONSISTENT MASS MATRIX FOR BOW ELEMENT (CALLED BY PANLSM)  MAI00890
C    BFSSTR - STRESS CALCULATIONS FOR BFS ELEMENT (CALLED BY STATIC)    MAI00900
C    BOWSTR - STRESS CALCULATIONS FOR BOW ELEMENT (CALLED BY STATIC)    MAI00910
C                                                                       MAI00920
C                                                                       MAI00930
C-----------------------------------------------------------------------MAI00940
C                                                                       MAI00950
C-----MAIN PROGRAM OF WINDOW                                            MAI00960
C                                                                       MAI00970
C                                                                       MAI00980
      REAL MFF,MFR,L,MP,MF,IX,IY,IZ,KS1,KS2                             MAI00990
      INTEGER SN,JKJ(3),PPV,FPV,PLIST                                   MAI01000
C                                                                       MAI01010
      COMMON                                                            MAI01020
     1/CBNPN/XP(25),YP(25),MP(25),KS1(25,5),JFN(25,2),JPN(25),INTYP(25),MAI01030
     #       IREP(16),ICNTY(16,4),KS2(25,5)                             MAI01040
     2/CBNFJ/XF(16),YF(16),MF(16),IX(16),IY(16),IZ(16),A(16),L(16),     MAI01050
     #       EZJ(16),EZK(16),EYJ(16),EYK(16),IFM(16),JJ(16),JK(16)      MAI01060
     3/CBNPFD/PPV(200),FPV(96),NFL(200),NRL(200),JRL(96)                MAI01070
     4/CBSTIF/SFF( 40, 40),SFP( 40, 120),MFF( 40, 45),SFR( 40, 56),     MAI01080
     #                     SPP(120,120),SPM(120,45),MFR(120, 56),       MAI01090
     #                                  SMM( 45, 45),SMR( 45, 56),      MAI01100
     #                                               SRR( 56, 56)       MAI01110
     5/CBTSTOR/TS1(120,45),TS2(120, 56),TS3( 45, 120)                   MAI01120
     6/CBMISC/SW(32,32),SMD(12,12),DUM(20)                              MAI01130
     7/CBDATA/EP,TP,PEP,DENSP,EF,GF,TF,DENSF,NS,SN,MODOE,ISM,           MAI01140
     #        NRPN,NFT,NPT,NMT,NPT,NF,NP,NM,NR,NPN,NPE,NPD,NPDOF,       MAI01150
     #        NFJ,NFM,NJ6,NFNSPR,NPNSPP,ISDA,NPR,NFR,NRFJ,              MAI01160
     #        NFRT,IREAC,ISTRES,ISTAT,IL,IKKK,TIME                      MAI01170
     8/CBDYNO/PLIST(300),IND,IAV,IAF,IGA,ISD,NDLC,LN,NPTS,NMODES,       MAI01180
     #        IOMAX,IDTH,ND,D1,D2,FX0,FY0,FZ0,AX0,AY0,AZ0,SX,SY,SZ,     MAI01190
```

```
      #        SXA,SYA,SZA,NTX,NTY,NTZ                                        MAI01200
C                                                                             MAI01210
C-----ARRAY DIMENSIONS IN COMMON (TS1: NPXNM; TS2: NPXNR; TS3: NMXNP)         MAI01220
C                                                                             MAI01230
      NF=40                                                                   MAI01240
      NP=120                                                                  MAI01250
      NM=45                                                                   MAI01260
      NR=56                                                                   MAI01270
C                                                                             MAI01280
C-----READ IN NUMBER OF STRUCTURES TO BE PROCESSED (NS);                      MAI01290
C     ALSO, READ IN PARAMETER 'ISOA' (ISOA=0, STATIC ANALYSIS; ISOA=1,        MAI01300
C     DYNAMIC ANALYSIS)                                                       MAI01310
C                                                                             MAI01320
      READ(5,*) NS                                                            MAI01330
C                                                                             MAI01340
      SN=0                                                                    MAI01350
    1 SN=SN+1                                                                 MAI01360
C                                                                             MAI01370
C-----READ IN STRUCTURE DATA FOR STRUCTURE NUMBER SN                          MAI01380
C                                                                             MAI01390
      CALL SDATA                                                              MAI01400
C                                                                             MAI01410
C-----GENERATE STIFFNESS (ISM=1) AND MASS (ISM=2) MATRICES FOR STRUCTURE      MAI01420
C                                                                             MAI01430
      ISM=0                                                                   MAI01440
    2 ISM=ISM+1                                                               MAI01450
C                                                                             MAI01460
      IF((ISOA.EQ.0).AND.(ISM.EC.2))GO TO 10                                  MAI01470
      IF((ISM.EQ.2).AND.(MCODE.EQ.3))GO TO 3                                  MAI01480
C                                                                             MAI01490
C-----FORM PANEL STIFFNESS (ISM=1) AND MASS (ISM=2) SUBMATRICES               MAI01500
C                                                                             MAI01510
      CALL PANLSM                                                             MAI01520
C                                                                             MAI01530
C-----FORM FRAME STIFFNESS (ISM=1) AND MASS (ISM=2) SUBMATRICES (UNLESS       MAI01540
C                                                              NFM=0)         MAI01550
C                                                                             MAI01560
      IF(NFM.EQ.0)GO TO 4                                                     MAI01570
C                                                                             MAI01580
      CALL FRAMSM                                                             MAI01590
C                                                                             MAI01600
C-----ADD BOUNDARY SPRING CONSTANTS TO STIFFNESS SUBMATRICES                  MAI01610
C                                                                             MAI01620
    4 IF((ISM.EQ.2).OR.((NFNSPR+NPNSPR).EQ.0))GO TO 5                         MAI01630
C                                                                             MAI01640
      CALL SPRING                                                             MAI01650
C                                                                             MAI01660
    5 CONTINUE                                                                MAI01670
C                                                                             MAI01680
C-----CONDENSE STIFFNESS (ISM=1) AND MASS (ISM=2) MATRICES BY ELIMINATIN      MAI01690
C                                                                  G          MAI01700
C     P (NFM=0), OR P AND M (NFM>0), DISPLACEMENT TYPES                       MAI01710
C                                                                             MAI01720
      CALL CDENSE                                                             MAI01730
C                                                                             MAI01740
      GO TO 7                                                                 MAI01750
C                                                                             MAI01760
C-----FORM MASS SUBMATRICES FOR MCODE=3 CASE                                  MAI01770
C                                                                             MAI01780
    3 DO 102 I=1,NFT                                                          MAI01790
      DO 103 J=1,NFT                                                          MAI01800
  103 MFF(I,J)=0.                                                             MAI01810
      DO 102 K=1,NRT                                                          MAI01820
  102 MFR(I,K)=0.                                                             MAI01830
C                                                                             MAI01840
      DO 104 I=1,NPN                                                          MAI01850
      JKJ(1)=6*I-7                                                            MAI01860
      JKJ(2)=JKJ(1)+1                                                         MAI01870
      JKJ(3)=JKJ(1)+2                                                         MAI01880
      DO 105 K=1,3                                                            MAI01890
      J=PPV(JKJ(K))                                                           MAI01900
      IF(J.GT.NFT)GO TO 105                                                   MAI01910
      MFF(J,J)=MFF(J,J)+MP(I)                                                 MAI01920
  105 CONTINUE                                                                MAI01930
  104 CONTINUE                                                                MAI01940
      WRITE(33) ((MFF(I,J),J=1,NFT),I=1,NFT)                                  MAI01950
      WRITE(33) ((MFR(I,J),J=1,NRT),I=1,NFT)                                  MAI01960
      GO TO 9                                                                 MAI01970
C                                                                             MAI01980
C-----SAVE CONDENSED MATRICES SFF AND SFR (ISM=1) AND MFF AND MFR (ISM=2      MAI01990
C     AND MCODE.NE.3) ON MASS STORAGE                                         MAI02000
C                                                                             MAI02010
    7 IF(ISM.EQ.1)REWIND 33                                                   MAI02020
      WRITE(33) ((SFF(I,J),J=1,NFT),I=1,NFT)                                  MAI02030
      WRITE(33) ((SFR(I,J),J=1,NRT),I=1,NFT)                                  MAI02040
C                                                                             MAI02050
      IF(ISM.LT.2)GO TO 2                                                     MAI02060
C                                                                             MAI02070
      DO 100 I=1,NFT                                                          MAI02080
      DO 101 J=1,NFT                                                          MAI02090
  101 MFF(I,J)=SFF(I,J)                                                       MAI02100
      DO 100 K=1,NRT                                                          MAI02110
  100 MFR(I,J)=SFR(I,J)                                                       MAI02120
C                                                                             MAI02130
      REWIND 33                                                               MAI02140
      READ(33) ((SFF(I,J),J=1,NFT),I=1,NFT)                                   MAI02150
      READ(33) ((SFR(I,J),J=1,NRT),I=1,NFT)                                   MAI02160
C                                                                             MAI02170
C-----DETERMINE FREQUENCIES, MODE SHAPES, AND DYNAMIC RESPONSE                MAI02180
C                                                                             MAI02190
    9 CALL DYNAMIC                                                            MAI02200
      GO TO 11                                                                MAI02210
C                                                                             MAI02220
C-----STATIC ANALYSIS                                                         MAI02230
C                                                                             MAI02240
   10 CALL STATIC                                                             MAI02250
C                                                                             MAI02260
C-----TEST FOR FINAL STRUCTURE                                                MAI02270
C                                                                             MAI02280
   11 IF(SN.LT.NS)GO TO 1                                                     MAI02290
C                                                                             MAI02300
      STOP                                                                    MAI02310
      END                                                                     MAI02320
```

```
*DECK SDATA                                                              SDAL0000
      SUBROUTINE SDATA                                                   SDAL0010
C                                                                        SDAL0020
C-----SUBPROGRAM TO READ IN STRUCTURE DATA FOR PANEL, FRAME, AND         SDAL0030
C     BOUNDARY SPRINGS; CONTROL PARAMETERS, MATERIAL PROPERTIES,         SDAL0040
C     NODAL COORDINATES, MASS DATA, AND CONNECTIVITY AND RESTRAINT       SDAL0050
C     INFORMATION.                                                       SDAL0060
C                                                                        SDAL0070
      REAL IX,IY,IZ,L,MF,MP,KS1,KS2,TITLE(8),UNITS(8)                    SDAL0080
      INTEGER SN,PPV,FPV                                                 SDAL0090
C                                                                        SDAL0100
      COMMON                                                             SDAL0110
     1/CBNPN/XP(25),YP(25),MP(25),KS1(25,5),JFN(25,2),JPN(25),INTYP(25), SDAL0120
     #       IREP(16),ICNTY(16,4),KS2(25,5)                             SDAL0130
     2/CBNFJ/XF(16),YF(16),MF(16),IX(16),IY(16),IZ(16),A(16),L(16),      SDAL0140
     #       EZJ(16),EZK(16),EYJ(16),EYK(16),IFM(16),JJ(16),JK(16)      SDAL0150
     3/CBNPFD/PPV(200),FPV(96),NFL(200),NRL(200),JRL(96)                SDAL0160
     7/CBDATA/EP,TP,PRP,DENSP,EF,GF,TF,DENSF,NS,SN,MCODE,ISM,           SDAL0170
     #        NRPN,NFT,NPT,NMT,NRT,NF,NP,NM,NR,NPN,NPE,NPD,NPDOF,       SDAL0180
     #        NFJ,NFM,NJ6,NFNSPR,NPNSPR,ISDA,NPR,NFR,NRFJ,              SDAL0190
     #        NFRT,IREAC,ISTRES,ISTAT,IL,IKKK,TIME                      SDAL0200
C                                                                        SDAL0210
  99  FORMAT(*1    STATIC/DYNAMIC ANALYSIS OF AN ARBITRARILY-SUPPORTED*, SDAL0220
     # * PLATE STRUCTURE*,//)                                           SDAL0230
 100 FORMAT(*1    STATIC/DYNAMIC ANALYSIS OF FRAMED PANELS*,//)         SDAL0240
      READ(5,101) TITLE                                                  SDAL0250
      READ(5,101) UNITS                                                  SDAL0260
 101 FORMAT(8A10)                                                        SDAL0270
      READ(5,*) NPE,NFM,ISDA                                             SDAL0280
      NFR=NPR=NRT=0                                                      SDAL0290
C                                                                        SDAL0300
C---I.  PANEL DATA; CONTROL PARAMETERS, MATERIAL PROPERTIES, NODAL       SDAL0310
C       COORDINATES, LUMPED MASSES , CONNECTIVITY                        SDAL0320
C       DATA, AND RESTRAINT INFORMATION (IF NRPN > 0)                    SDAL0330
C       NOTE; PANEL NODES ARE NUMBERED 1,...,NPN                         SDAL0340
C                                                                        SDAL0350
C-----A. CONTROL PARAMETERS, MATERIAL PROPERTIES                         SDAL0360
C                                                                        SDAL0370
  103 FORMAT(*0PANEL DATA*,/,* ----------*,/,* NPE  NPN  NRPN*,          SDAL0380
     # *  NNWFT      EP          PRP         DENSP          TP*)         SDAL0390
C-----MCODE; 1=CM(+ILM); 2=ALM(+ILM); 3=ILM ONLY                         SDAL0400
      READ(5,*) NPN,NRPN,NPR,NNWFT,NFT,EP,PRP,DENSP,TP,MCODE             SDAL0410
      IF(NFM.EQ.0)PRINT 99                                               SDAL0420
      IF(NFM.GT.0)PRINT 100                                              SDAL0430
      PRINT 102,TITLE,UNITS                                              SDAL0440
  102 FORMAT(*0TITLE;  *,8A10,/,*0UNITS;  *,8A10)                        SDAL0450
      PRINT 500,SN,NS,ISDA                                               SDAL0460
  500 FORMAT(/,*0STRUCTURE NUMBER*,I3,* OF*,I3,/,                        SDAL0470
     # * ISDA =*,I2,/)                                                  SDAL0480
      PRINT 103                                                          SDAL0490
      PRINT 104,NPE,NPN,NRPN,NNWFT,EP,PRP,DENSP,TP                       SDAL0500
  104 FORMAT(I4,2I5,I7,1P4E13.5)                                         SDAL0510
      NPD=8*NPN                                                          SDAL0520
      NPDOF=NPD-NPR                                                      SDAL0530
      NPT=NPDOF-NFT                                                      SDAL0540
      NRT=NPR                                                            SDAL0550
      PRINT 105                                                          SDAL0560
  105 FORMAT(*0 NPD  NPDOF  NFT  NPT  NPR  MCODE*)                       SDAL0570
      PRINT 106,NPD,NPDOF,NFT,NPT,NPR,MCODE                              SDAL0580
  106 FORMAT(I5,2I6,3I5)                                                 SDAL0590
      DO 1061 I=1,NPD                                                    SDAL0600
 1061 NFL(I)=NRL(I)=0                                                    SDAL0610
C                                                                        SDAL0620
C-----B.  NODAL COORDINATES; LUMPED MASSES                               SDAL0630
C                                                                        SDAL0640
      PRINT 107                                                          SDAL0650
  107 FORMAT(*0NODAL COORDINATES*,/* NODE  X COORD.      Y COORD.*,      SDAL0660
     # *       ADDED MASS*)                                              SDAL0670
      DO 108 I=1,NPN                                                     SDAL0680
      READ(5,*) N,XP(N),YP(N),MP(N)                                      SDAL0690
  108 PRINT 109,N,XP(N),YP(N),MP(N)                                      SDAL0700
  109 FORMAT(I4,1P3E13.5)                                                SDAL0710
C                                                                        SDAL0720
C-----C. CONNECTIVITY, DEGREE-OF-FREEDOM (F TYPES), AND RESTRAINT DATA   SDAL0730
C                                                                        SDAL0740
      PRINT 110                                                          SDAL0750
  110 FORMAT(*0ELEMENT CONNECTIVITY DATA*,/,* ELEMENT       NODE *,      SDAL0760
     # *NUMBERS       REPETITION*,/,14X,*I   J   K   L          CODE*)  SDAL0770
C                                                                        SDAL0780
C-----ICNTY(K,J) = CCW NODE NOS. FOR ELEMENT #K; J=1 TO 4 FOR RECT.      SDAL0790
C                  ELEMENT; START NODE NOS. AT LOWER LEFT NODE           SDAL0800
C-----IREP(K) = REPETITION CODE FOR ELEMENT #K (0 = DIFFERENT;           SDAL0810
C               1 = SAME MATERIAL AND DIMENSIONS AS ELEMENT #(K-1))      SDAL0820
C                                                                        SDAL0830
      DO 111 I=1,NPE                                                     SDAL0840
      READ(5,*) K,(ICNTY(K,J),J=1,4),IREP(K)                             SDAL0850
  111 PRINT 112,K,(ICNTY(K,J),J=1,4),IREP(K)                             SDAL0860
  112 FORMAT(I6,I9,3I4,I12)                                              SDAL0870
C-----READ IN NODAL F-TYPE LIST (NFL) FOR NODE #J (1=F TYPE, 0=OTHER)    SDAL0880
      PRINT 113                                                          SDAL0890
  113 FORMAT(*0NODAL F DISPL. TYPES*,/,* NODE  J1  J2  J3  J4  J5*,      SDAL0900
     # *  J6  J7  J8*)                                                  SDAL0910
      DO 114 K=1,NNWFT                                                   SDAL0920
      READ(5,*) J,NFL(8*J-7),NFL(8*J-6),NFL(8*J-5),NFL(8*J-4),           SDAL0930
     # NFL(8*J-3),NFL(8*J-2),NFL(8*J-1),NFL(8*J)                         SDAL0940
      J1=8*J-7                                                           SDAL0950
      J8=8*J                                                             SDAL0960
  114 PRINT 115,J,(NFL(I),I=J1,J8)                                       SDAL0970
  115 FORMAT(I4,I5,7I4)                                                  SDAL0980
C-----READ IN RESTRAINT LIST (NRL) FOR PANEL (IF NRPN>0)                 SDAL0990
C     (NRL; 0 = NO RESTRAINT, 1 = RESTRAINT EXISTS)                      SDAL1000
C     OTHERWISE (IF NRPN = 0) READ IN BOUNDARY FRAME DATA                SDAL1010
      IF(NRPN.EQ.0) GO TO 200                                            SDAL1020
      PRINT 116                                                          SDAL1030
  116 FORMAT(*0NODAL RESTRAINT LIST*,/,* NODE  J1  J2  J3  J4  J5*,      SDAL1040
     # *  J6  J7  J8*)                                                  SDAL1050
      DO 117 K=1,NRPN                                                    SDAL1060
      READ(5,*) J,NRL(8*J-7),NRL(8*J-6),NRL(8*J-5),NRL(8*J-4),           SDAL1070
     # NRL(8*J-3),NRL(8*J-2),NRL(8*J-1),NRL(8*J)                         SDAL1080
      J1=8*J-7                                                           SDAL1090
      J8=8*J                                                             SDAL1100
  117 PRINT 115,J,(NRL(I),I=J1,J8)                                       SDAL1110
      IF(NFM.EQ.0)GO TO 300                                              SDAL1120
C                                                                        SDAL1130
C---II.  FRAME DATA; CONTROL PARAMETERS, JOINT COORDINATES, MEMBER       SDAL1140
C        AND MATERIAL PROPERTIES, RESTRAINT INFORMATION, AND             SDAL1150
C        ELASTIC CONNECTION DATA                                         SDAL1160
C       NOTE; FRAME JOINTS ARE NUMBERED 1,...,NFJ (I.E., NUMBER FRAME    SDAL1170
C             JOINTS INDEPENDENTLY OF PANEL NODES)                       SDAL1180
C                                                                        SDAL1190
```

```
C-----A. CONTROL PARAMETERS                                                    SDAL1200
C                                                                              SDA01210
  200 PRINT 201                                                                SDAL1220
  201 FORMAT(*0FRAME DATA*,/,* ----------*,/,* NFM  NFJ  NFR  NRFJ*,           SDAC1230
     # *  NMEC        EF          PRF         DENSF*)                         SDAC1240
      READ(5,*) NFJ,NFR,NRFJ,NMEC,EF,PRF,DENSF                                 SDAC1250
      PRINT 202,NFM,NFJ,NFR,NRFJ,NMEC,EF,PRF,DENSF                             SDAC1260
  202 FORMAT(I4,3I5,I6,1P3E13.5)                                               SDAJ1270
      GF=EF/(2*(1+PRF))                                                        SDA01280
      NRT=NRT+NFR                                                              SDA01290
      NJ6=6*NFJ                                                                SDAC1300
      NMT=NJ6-NFR                                                              SDAJ1310
C                                                                              SDAG1320
C-----B.  JOINT COORDINATES, MEMBER AND MATERIAL PROPERTIES, LUMPED MASS       SDAG1330
C                                                                        ES    SDAC1340
C                                                                              SDAG1350
      PRINT 206                                                                SDA01360
  206 FORMAT(*0JOINT COORDINATES*,/,* JOINT X COORD.       Y COORD.*,          SDAL1370
     # *    ADDED MASS*)                                                      SDAC1380
      DO 207 I=1,NFJ                                                           SDAG1390
      READ(5,*) J,XF(J),YF(J),MF(J)                                            SDA01400
  207 PRINT 208,J,XF(J),YF(J),MF(J)                                            SDAC1410
  208 FORMAT(I5,1P3E13.5)                                                      SDAC1420
      PRINT 203                                                                SDA01430
  203 FORMAT(*0MEMBER PROPERTIES*,/,* MEMBER  JJ  JK*,9X,*A*,7X,               SDAG1440
     # *LENGTH*,11X,*IX*,11X,*IY*,11X,*IZ      TYPE*)                        SDAG1450
      DO 204 II=1,NFM                                                          SDAG1460
C-----IFM(I) = INDICATOR FOR FRAME MEMBER TYPE (0=COLUMN, 1=BEAM)              SDAC1470
      READ(5,*) I,JJ(I),JK(I),A(I),IX(I),IY(I),IZ(I),IFM(I)                   SDAC1480
      IF(IFM(I).EQ.0) GO TO 220                                                SDAG1490
      TYPE=6HBEAM                                                              SDA01500
      L(I)=ABS(XF(JK(I))-XF(JJ(I)))                                            SDAC1510
      GO TO 204                                                                SDAC1520
  220 TYPE=6HCOLUMN                                                            SDAC1530
      L(I)=ABS(YF(JK(I))-YF(JJ(I)))                                            SDAC1540
  204 PRINT 205,I,JJ(I),JK(I),A(I),L(I),IX(I),IY(I),IZ(I),TYPE                 SDA01550
  205 FORMAT(I5,I6,I4,1P5E13.5,2X,A6)                                          SDAJ1560
C                                                                              SDAG1570
C-----C. RESTRAINT INFORMATION (1 = RESTRAINT EXISTS, 0 = NO RESTRAINT)        SDA01580
C                                                                              SDA01590
      PRINT 209                                                                SDAC1600
  209 FORMAT(*0JOINT RESTRAINT LIST*,/,* JOINT  J1  J2  J3  J4*,               SDAG1610
     # *  J5  J6*)                                                           SDAG1620
      DO 210 I=1,NJ6                                                           SDAG1630
  210 JRL(I)=0                                                                 SDAG1640
      DO 211 I=1,NRFJ                                                          SDAJ1650
      READ(5,*) J,JRL(6*J-5),JRL(6*J-4),JRL(6*J-3),JRL(6*J-2),                 SDAC1660
     # JRL(6*J-1),JRL(6*J)                                                    SDAC1670
      J1=6*J-5                                                                 SDAL1680
      J6=6*J                                                                   SDAG1690
  211 PRINT 212,J,(JRL(K),K=J1,J6)                                             SDAC1700
  212 FORMAT(2I5,5I4)                                                          SDAJ1710
C                                                                              SDAL1720
C-----D. ELASTIC CONNECTION DATA (FOR BEAM MEMBERS ONLY)                       SDAC1730
C                                                                              SDAC1740
      DO 216 I=1,NFM                                                           SDAG1750
  216 EZJ(I)=EZK(I)=EYJ(I)=EYK(I)=0.                                           SDA01760
      IF(NMEC.EQ.0) GO TO 300                                                  SDAC1770
      PRINT 215                                                                SDAG1780
  215 FORMAT(*0ELASTIC CONNECTION DATA*,/,* MEMBER*,8X,*EZJ*,10X,              SDAL1790
     # *EZK*,10X,*EYJ*,10X,*EYK*)                                             SDAG1800
      DO 217 II=1,NMEC                                                         SDAG1810
      READ(5,*) I,EZJ(I),EZK(I),EYJ(I),EYK(I)                                 SDAG1820
  217 PRINT 218,I,EZJ(I),EZK(I),EYJ(I),EYK(I)                                 SDAG1830
  218 FORMAT(I5,2X,1P4E13.5)                                                   SDAG1840
C                                                                              SDA01850
C---III.  ELASTIC SPRING DATA (NFNSPR = NO. OF FRAME NODES WITH SPRINGS        SDAC1860
C          ATTACHED;  NPNSPR = NO. OF PANEL NODES WITH SPRINGS ATTACHED)       SDAG1870
C                                                                              SDAC1880
  300 READ(5,*) NFNSPR,NPNSPR                                                  SDAG1890
      DO 320 I=1,NPN                                                           SDAC1900
      DO 320 J=1,5                                                             SDA01910
  320 KS1(I,J)=KS2(I,J)=0.                                                     SDA01920
      PRINT 301,NFNSPR,NPNSPR                                                  SDAL1930
  301 FORMAT("0SPRING DATA",/," ------------",/," NFNSPR =",I3,                SDAG1940
     #  "  NPNSPR =",I3,/)                                                    SDAC1950
      IF(NFNSPR.EQ.0) GO TO 310                                                SDAG1960
C-----A.  FRAME-PANEL BOUNDARY SPRINGS                                         SDAC1970
C                                                                              SDAG1980
C-----THE FOLLOWING SECTION PERTAINS TO THE 12 ELEMENT 1/4 MODEL ONLY          SDA01990
C-----AND INVOLVES THE DETERMINATION OF KS1,KS2.... BY FORMULAS                SDA02000
C                                                                              SDA02010
      READ(5,*) SKPO,SKL,SKN,SKR                                               SDAC2020
      PRINT 400,SKPO,SKL,SKR,SKN                                               SDAL2030
  400 FORMAT(/," BASIC BOUNDARY SPRING CONSTANTS",/," PULL-OUT =",             SDA02040
     # F8.2,",   LONGITUDINAL =",F8.2,/," ROTATIONAL =",F8.2,                 SDAG2050
     # ",   NORMAL =",F8.2)                                                   SDA02060
      AAS=XF(5)                                                                SDA02070
      BBS=YF(5)                                                                SDAC2080
C-----FIND KS1,KS2,KS3,KS4,KS5 FOR BOUNDARY NODES                              SDAG2090
      DO 410 I=1,8                                                             SDAC2100
C-----I=FRAME NODE NO.                                                         SDA02110
      JFN(I,1)=I                                                               SDAC2120
      IF(I.LE.5)JFN(I,2)=4*I                                                   SDAG2130
      IF(I.GT.5)JFN(I,2)=25-(                                                  SDAC2140
      GO TO(401,402,402,402,405,406,406,408),I                                 SDAC2150
  401 KS1(I,1)=SKPO*BBS/8.                                                     SDAC2160
      KS1(I,2)=SKL*BBS/8.                                                      SDAG2170
      KS1(I,3)=SKN*BBS/8.                                                      SDAC2180
      KS1(I,4)=2.5E7                                                           SDAC2190
      KS1(I,5)=SKR*BBS/8.                                                      SDAC2200
      GO TO 410                                                                SDAG2210
  402 KS1(I,1)=SKPO*BBS/4.                                                     SDAC2220
      KS1(I,2)=SKL*BBS/4.                                                      SDA02230
      KS1(I,3)=SKN*BBS/4.                                                      SDAL2240
      KS1(I,4)=5.E7                                                            SDA02250
      KS1(I,5)=SKR*BBS/4.                                                      SDAG2260
      GO TO 410                                                                SDAG2270
  405 KS1(I,1)=(SKPO*BBS/8.)+(SKL*AAS/6.)                                      SDAC2280
      KS1(I,2)=(SKPO*AAS/6.)+(SKL*BBS/8.)                                      SDAC2290
      KS1(I,3)=SKN*((BBS/8.)+(AAS/6.))                                         SDAG2300
      KS1(I,4)=SKR*(AAS/6.)                                                    SDA02310
      KS1(I,5)=SKR*BBS/8.                                                      SDAC2320
      GO TO 410                                                                SDAC2330
  406 KS1(I,1)=SKL*AAS/3.                                                      SDAL2340
      KS1(I,2)=SKPO*AAS/3.                                                     SDAG2350
      KS1(I,3)=SKN*AAS/3.                                                      SDAG2360
      KS1(I,4)=SKR*AAS/3.                                                      SDAG2370
      KS1(I,5)=5.E7                                                            SDAG2380
      GO TO 410                                                                SDAL2390
```

```
  408 KS1(I,1)=SKL*AAS/6.                                                SDA02400
      KS1(I,2)=SKP0*AAS/6.                                               SDA02410
      KS1(I,3)=SKN*AAS/6.                                                SDA02420
      KS1(I,4)=SKR*AAS/6.                                                SDA02430
      KS1(I,5)=2.5E7                                                     SDA02440
  410 CONTINUE                                                           SDA02450
C                                                                        SDA02460
      PRINT 302                                                          SDA02470
  302 FORMAT(*0NODES AND SPRING CONSTANTS*,/,* FRAME NODE  PANEL NODE*,  SDA02480
     # 8X,*KS1*,10X,*KS2*,10X,*KS3*,10X,*KS4*,10X,*KS5*)                 SDA02490
C-----KS1(I,J) = SPRING CONSTANT FOR ELASTIC SPRING CONNECTING NODES     SDA02500
C     JFN(I,1) AND JFN(I,2) (I.E., FRAME AND CORRESPONDING PANEL NODE)   SDA02510
C     AND CORRESPONDING TO NODAL DOF J                                   SDA02520
      DO 303 I=1,NFNSPR                                                  SDA02530
  303 PRINT 304,JFN(I,1),JFN(I,2),(KS1(I,J),J=1,5)                       SDA02540
  304 FORMAT(I6,I13,4X,1P5E13.5)                                         SDA02550
C-----8.  PANEL NODE SPRINGS                                             SDA02560
  310 IF(NPNSPR.EQ.0)RETURN                                              SDA02570
      PRINT 311                                                          SDA02580
  311 FORMAT(* PANEL NODE*,8X,*KS1*,10X,*KS2*,10X,*KS3*,10X,*KS4*,       SDA02590
     # 10X,*KS5*)                                                        SDA02600
C-----KS2(I,J) = SPRING CONSIANT FOR SPRING AITACHED TO PANEL NODE       SDA02610
C     JPN(I) AND CORRESPONDING TO NODAL DOF J                            SDA02620
      DO 312 I=1,NPNSPR                                                  SDA02630
      READ(5,*) JPN(I),(KS2(I,J),J=1,5)                                  SDA02640
  312 PRINT 313,JPN(I),(KS2(I,J),J=1,5)                                  SDA02650
  313 FORMAT(I7,4X,1P5E13.5)                                             SDA02660
C                                                                        SDA02670
      RETURN                                                             SDA02680
      END                                                                SDA02690
```

```
*DECK PANLSM                                                             PAN00000
      SUBROUTINE PANLSM                                                  PAN00010
C                                                                        PAN00020
C-----SUBPROGRAM TO FORM PANEL STIFFNESS (ISM=1) AND MASS (ISM=2 AND     PAN00030
C     NCODE DOES NOT EQUAL 3) SUBMATRICES SFF, SFP, SFR, SPP, SPR,       PAN00040
C     SRR (OR MASS ARRAYS MFF,...,MRR)                                   PAN00050
C                                                                        PAN00060
      REAL MP,KS1,KS2,SB(144)                                            PAN00070
      INTEGER SN,PPV,FPV,EPV(32),KL(16)                                  PAN00080
      COMMON                                                             PAN00090
     1/C8NPN/XP(25),YP(25),MP(25),KS1(25,5),JFN(25,2),JPN(25),INTYP(25),PAN00100
     #       IREP(16),ICNTY(16,4),KS2(25,5)                              PAN00110
     3/C8NPFD/PPV(200),FPV(96),NFL(200),NRL(200),JFL(96)                 PAN00120
     4/C8STIF/SFF( 40, 40),SFP( 40, 120),SFM( 40, 45),SFR( 40, 56),      PAN00130
     #                     SPP(120,120),SPM(120,45),SPR(120, 56),        PAN00140
     #                                  SMM( 45, 45),SMR( 45, 56),       PAN00150
     #                                               SRR( 56, 56)        PAN00160
     6/C8MISC/SM(32,32),SMD(12,12),DUM(20)                               PAN00170
     7/C8DATA/EP,IP,PRP,DENSP,EF,GF,TF,DENSF,NS,SN,MCODE,ISM,            PAN00180
     #        NRPN,NFT,NPT,NMT,NRT,NF,NP,NM,NR,NPN,NPE,NPD,NPDOF,       PAN00190
     #        NFJ,NFM,NJ6,NFNSPR,NPNSPR,ISOA,NPR,NFR,NRFJ,              PAN00200
     #        NFRI,IREAC,ISTRES,ISTAT,IL,IKKK,TIME                      PAN00210
C                                                                        PAN00220
      EQUIVALENCE (SB,SPD)                                               PAN00230
C                                                                        PAN00240
C-----CLEAR ARRAYS                                                       PAN00250
C                                                                        PAN00260
      DO 192 I=1,NFT                                                     PAN00270
      DO 193 J1=1,NFT                                                    PAN00280
  193 SFF(I,J1)=0.                                                       PAN00290
      DO 194 J2=1,NPT                                                    PAN00300
  194 SFP(I,J2)=0.                                                       PAN00310
      DO 195 J3=1,NRT                                                    PAN00320
  195 SFR(I,J3)=0.                                                       PAN00330
  192 CONTINUE                                                           PAN00340
      DO 196 I=1,NPT                                                     PAN00350
      DO 197 J1=1,NPT                                                    PAN00360
  197 SPP(I,J1)=0.                                                       PAN00370
      DO 198 J2=1,NRT                                                    PAN00380
  198 SPR(I,J2)=0.                                                       PAN00390
  196 CONTINUE                                                           PAN00400
      DO 199 I=1,NRT                                                     PAN00410
      DO 199 J=1,NRT                                                     PAN00420
  199 SRR(I,J)=0.                                                        PAN00430
C                                                                        PAN00440
C-----CONSTRUCT THE PANEL PERMUTAIION VECTOR (PPV())                     PAN00450
C                                                                        PAN00460
      IF(ISM.GE.2)GO TO 103                                              PAN00470
      I1=0                                                               PAN00480
      I2=NFT                                                             PAN00490
      I3=NPDOF                                                           PAN00500
      DO 100 I=1,NPD                                                     PAN00510
      IF(NRL(I).EQ.1)GO TO 101                                           PAN00520
      IF(NFL(I).EQ.1)GO TO 102                                           PAN00530
C-----P TYPE DEGREE OF FREEDOM (DOF)                                     PAN00540
      I2=I2+1                                                            PAN00550
      PPV(I)=I2                                                          PAN00560
      GO TO 100                                                          PAN00570
C-----F TYPE DOF                                                         PAN00580
  102 I1=I1+1                                                            PAN00590
```

```
      PPV(I)=I1                                                          PAN00600
      GO TO 100                                                          PANC0610
C-----R TYPE DOF                                                         PANC0620
  101 I3=I3+1                                                            PANC0630
      PPV(I)=I3                                                          PANC0640
  100 CONTINUE                                                           PAN00650
C                                                                        PAN00660
C                                                                        PANC0670
C-----NOW CYCLE THROUGH PANEL ELEMENTS TO FORM STIFFNESS (OR MASS FOR    PAN00680
C     ISM=2) SUBMATRICES (SFF, EFC)                                      PAN00690
C                                                                        PANL0700
  103 IREP(1)=0                                                          PAN00710
C                                                                        PANL0720
      DO 110 IE=1,NPE                                                    PANC0730
C                                                                        PANC0740
C-----SKIP GENERATION OF SE AND SM IF CURRENT ELEMENT (#IE) IS IDENTICALPAN00750
C     (IN SIZE AND MATERIAL) TO #(IE-1)                                  PAN00760
C                                                                        PAN00770
      IF(IREP(IE).EQ.1) GO TO 111                                        PAN00780
      DO 191 I=1,32                                                      PAN00790
      DO 191 J=1,32                                                      PAN00800
  191 SM(I,J)=0.                                                         PANL0810
C                                                                        PANL0820
C-----FORM PERMUTATION VECTOR FOR ORDERING OF BOGNER AND A-D-W ELEMENTS PAN00830
C     DOF INDICES                                                        PANC0840
C                                                                        PAN00850
      CALL TSET(EPV)                                                     PAN00860
C                                                                        PAN00870
      J1=ICNTV(IE,1)                                                     PAN00880
      J2=ICNTV(IE,2)                                                     PAN00890
      J3=ICNTV(IE,3)                                                     PANC0900
      A1=XP(J2)-XP(J1)                                                   PAN00910
      B1=YP(J3)-YP(J2)                                                   PANC0920
C-----GENERATE ELEMENT STIFFNESS (OR MASS) ARRAY FOR BOGNER ELEMENT      PAN00930
      IF(ISM.EQ.1)GO TO 112                                              PAN00940
      IF(MCODE.EQ.2)GO TO 113                                            PAN00950
C                                                                        PAN00960
      CALL BOGCM(DENSP,A1,B1,TP,SB)                                      PANC0970
C                                                                        PANC0980
      GO TO 114                                                          PAN00990
  113 XM=DENSP*A1*B1*TP/4.                                               PANC1000
      SM(3,3)=SM(11,11)=SM(19,19)=SM(27,27)=XM                           PAN01010
      GO TO 150                                                          PANC1020
C                                                                        PANC1030
  112 CALL SBOG(A1,B1,TP,EP,PRP,SB)                                      PANC1040
C                                                                        PANC1050
  114 KL(1)=1                                                            PANC1060
      DO 115 I=2,16                                                      PANC1070
  115 KL(I)=KL(I-1)+18-I                                                 PANC1080
      DO 116 I=1,16                                                      PANC1090
      KLT=KL(I)                                                          PANC1100
      DO 116 J=I,16                                                      PANC1110
  116 SM(EPV(I),EPV(J))=SM(EPV(J),EPV(I))=SB(KLT-I+J)                    PANC1120
C-----GENERATE ELEMENT STIFFNESS (OR MASS) ARRAY FOR REFINED PLANE STRESPANC1130
C                                                                    S   PANC1140
C     ELEMENT                                                            PANC1150
  150 IF(ISM.EQ.1)GO TO 149                                              PANC1160
      IF(MCODE.EQ.2)GO TO 151                                            PANC1170
C                                                                        PANC1180
      CALL BONCM(DENSP,A1,B1,TP,SB)                                      PANC1190
C                                                                        PANC1200
      GO TO 152                                                          PANC1210
  151 SM(1,1)=SM(2,2)=SM(9,9)=SM(10,10)=XM                               PANC1220
      SM(17,17)=SM(18,18)=SM(25,25)=SM(26,26)=XM                         PANC1230
      GO TO 111                                                          PANC1240
C                                                                        PANC1250
  149 CALL S90M(A1,B1,TP,EP,PRP,SB)                                      PANC1260
C                                                                        PANC1270
  152 DO 153 I=1,16                                                      PANC1280
      KLT=KL(I)                                                          PANC1290
      II=I+16                                                            PANC1300
      DO 153 J=I,16                                                      PANC1310
      JJ=J+16                                                            PANC1320
  153 SM(EPV(II),EPV(JJ))=SM(EPV(JJ),EPV(II))=SB(KLT-I+J)                PANC1330
C                                                                        PANC1340
C-----FORM THE ELEMENT PERMUTATION VECTOR (EPV) FROM THE PANEL PERMUTATIPANC1350
C                                                                    ON  PANC1360
C     VECTOR (PPV) FOR ELEMENT NUMBER IE                                 PANC1370
  111 JJ=0                                                               PANC1380
      DO 160 I=1,4                                                       PANC1390
      JP=ICNTV(IE,I)                                                     PANC1400
      JP=6*JP-6                                                          PANC1410
      DO 160 J=1,6                                                       PANC1420
      JP=JP+1                                                            PANC1430
      JJ=JJ+1                                                            PANC1440
  160 EPV(JJ)=PPV(JP)                                                    PANC1450
C                                                                        PANC1460
C-----USE THE EPV() TO ADD CONTRIBUTION OF CURRENT PANEL ELEMENT (#IE)  PANC1470
C     TO ARRAYS SFF, SFP, SFR, SPP, SPR, SRR (OR MFF,...,MRF FOR ISM=2   PANC1480
C     AND MCODE NOT EQUAL 3)( NOTE THAT ARRAYS SFR, SPR, AND SRR DO NOT  PANC1490
C     RECEIVE ANY PANEL CONTRIBUTIONS WHEN NRPN=0                        PANC1500
C                                                                        PANC1510
      DO 170 I=1,32                                                      PANC1520
      KR=EPV(I(                                                          PANC1530
      IF(KR.LE.NFT)GO TO 171                                             PANC1540
      IF((KR.GT.NFT).AND.(KR.LE.NPDOF))GO TO 172                         PANC1550
C-----R DISPLACEMENT TYPES (NO R TYPES ON PANEL FOR NRPN=0)               PANC1560
      KR=KR-NPDOF                                                        PANC1570
      DO 183 J=1,32                                                      PANC1580
      KC=EPV(J)-NPDOF                                                    PANC1590
      IF(KC.LE.0)GO TO 183                                               PANC1600
      SRR(KR,KC)=SRR(KR,KC)+SM(I,J)                                      PANC1610
  183 CONTINUE                                                           PANC1620
      GO TO 170                                                          PANC1630
C-----F DISPLACEMENT TYPES                                               PANC1640
  171 DO 181 J=1,32                                                      PANC1650
      KC=EPV(J)                                                          PANC1660
      K1=KC-NFT                                                          PANC1670
      K2=KC-NPDOF                                                        PANC1680
      IF(KC.LE.NFT)SFF(KR,KC)=SFF(KR,KC)+SM(I,J)                         PANC1690
      IF((KC.GT.NFT).AND.(KC.LE.NPDOF))SFP(KR,K1)=SFP(KR,K1)+SM(I,J)     PANC1700
      IF(KC.GT.NPDOF)SFR(KR,K2)=SFR(KR,K2)+SM(I,J)                       PANC1710
  181 CONTINUE                                                           PANC1720
      GO TO 170                                                          PANC1730
C-----P DISPLACEMENT TYPES                                               PANC1740
  172 KR=KR-NFT                                                          PANC1750
      DO 182 J=1,32                                                      PANC1760
      KC=EPV(J)                                                          PANC1770
      IF(KC.LE.NFT)GO TO 182                                             PANC1780
      K1=KC-NFT                                                          PANC1790
```

```
      K2=KC-NPDOF                                                       PANC1800
      IF(KC.LE.NPDOF)SPP(KR,K1)=SPP(KR,K1)+SW(I,J)                      PANC1810
      IF(KC.GT.NPDOF)SPR(KR,K2)=SPR(KR,K2)+SW(I,J)                      PANC1820
  102 CONTINUE                                                          PANC1830
  170 CONTINUE                                                          PANC1840
  110 CONTINUE                                                          PANC1850
C                                                                       PANC1860
      IF(ISM.EQ.1)RETURN                                                PANC1870
C                                                                       PANC1880
C-----ADD LUMPED MASSES TO PANEL FOR MCODE=1,2 CASES                    PANC1890
C                                                                       PANC1900
      DO 200 I=1,NPN                                                    PANC1910
      KL(1)=8*I-7                                                       PANC1920
      KL(2)=KL(1)+1                                                     PANC1930
      KL(3)=KL(1)+2                                                     PANC1940
      DO 201 K=1,3                                                      PANC1950
      J=PPV(KL(K))                                                      PANC1960
      IF(J.LE.NFT)SFF(J,J)=SFF(J,J)+MP(I)                               PANC1970
      IF((J.GT.NFT).AND.(J.LE.NPDOF))SPP(J,J)=SPP(J,J)+MP(I)            PANC1980
      IF(J.GT.NPDOF)SRR(J,J)=SRR(J,J)+MP(I)                             PANC1990
  201 CONTINUE                                                          PANC2000
  200 CONTINUE                                                          PANC2010
C                                                                       PANC2020
      RETURN                                                            PANC2030
      END                                                               PANC2040
```

```
*DECK FRAMSM                                                           FRAL0000
      SUBROUTINE FRAMSM                                                 FRAC0010
C                                                                       FRA00020
C-----SUBPROGRAM TO FORM THE FRAME STIFFNESS (ISM=1) AND MASS (ISM=2 AN0FRAC0030
C     MCODE NOT EQUAL TO 3) SUBMATRICES SMM, SMR, SRR, AND MMM, MMR, MRRFRAC0040
C     *** UNLESS *** NFM=0 (I.E., STRUCTURE = APRIIFARILY-SUPPORTED     FRAC0050
C     PANEL ONLY)                                                       FRA00060
C                                                                       FRA00070
      REAL MF,L,IX1,IX,IY,IZ                                            FRAC0080
      INTEGER SN,PPV,FPV,EPV(12)                                        FRAC0090
C                                                                       FRA00100
      COMMON                                                            FRA00110
     2/CBNFJ/XF(16),YF(16),MF(16),IX(16),IY(16),IZ(16),A(16),L(16),     FRA00120
     #       EZJ(16),EZK(16),EYJ(16),EYK(16),IFM(16),JJ(16),JK(16)      FRA00130
     3/CBNPFD/PPV(200),FPV(96),NFL(200),NRL(200),JRL(96)                FRA00140
     4/CBSTIF/SFF( 40, 40),SFP( 40, 120),SFM( 40, 45),SFR( 40, 56),     FRA00150
     #                    SPP(120,120),SPM(120,45),SPR(120, 56),       FRA00160
     #                                 SMM( 45, 45),SMR( 45, 56),       FRA00170
     #                                              SRR( 56, 56)        FRA00180
     6/CBMISC/SW(32,32),SMD(12,12),DUM(20)                              FRA00190
     7/CBDATA/EP,TP,PRP,DENSP,EF,GF,TF,DENSF,NS,SN,MCODE,ISM,           FRA00200
     #        NRPN,NFT,NPT,NMT,NRT,NF,NP,NM,NR,NPN,NPE,NPD,NPDOF,       FRA00210
     #        NFJ,NFM,NJ6,NFNSPR,NPNSPR,ISDA,NPR,NFR,NRFJ,              FRA00220
     #        NFRT,IREAC,ISTRES,ISTAT,IL,IKKK,TIME                      FRA00230
C                                                                       FRA00240
C                                                                       FRA00250
C-----CLEAR ARRAYS                                                      FRA00260
C                                                                       FRA00270
      DO 100 I=1,NMT                                                    FRA00280
      DO 101 J1=1,NMT                                                   FRA00290
  101 SMM(I,J1)=0.                                                      FRA00300
      DO 102 J2=1,NRT                                                   FRA00310
  102 SMR(I,J2)=0.                                                      FRA00320
      DO 1041 J3=1,NPT                                                  FRA00330
 1041 SPM(J3,I)=0.                                                      FRA00340
      DO 1051 J4=1,NFT                                                  FRA00350
 1051 SFM(J4,I)=0.                                                      FRA00360
  100 CONTINUE                                                          FRA00370
      IF(NRPN.GT.0)GO TO 1031                                           FRA00380
      DO 103 I=1,NRT                                                    FRA00390
      DO 103 J=1,NRT                                                    FRA00400
  103 SRR(I,J)=0.                                                       FRA00410
C                                                                       FRA00420
C-----FORM FRAME PERMUTATION VECTOR                                     FRA00430
C                                                                       FRA00440
 1031 I1=0                                                              FRA00450
      I2=NMT+NPR                                                        FRA00460
      DO 104 I=1,NJ6                                                    FRA00470
      IF(JRL(I).EQ.0)GO TO 105                                          FRA00480
C-----R TYPE DOF                                                        FRA00490
      I2=I2+1                                                           FRA00500
      FPV(I)=I2                                                         FRA00510
      GO TO 104                                                         FRA00520
C-----M TYPE DOF                                                        FRA00530
  105 I1=I1+1                                                           FRA00540
      FPV(I)=I1                                                         FRA00550
  104 CONTINUE                                                          FRA00560
C                                                                       FRA00570
C-----FORM STIFFNESS SUBMATRICES SMM, SMR, AND SRR                      FRA00580
C                                                                       FRA00590
```

```
      DO 106 I=1,NFM                                                    FRA00600
      DO 107 I1=1,12                                                    FRA00610
      DO 107 J1=1,12                                                    FRA00620
  107 SMD(I1,J1)=0.                                                     FRA00630
      IF(ISM.EQ.2)GO TO 150                                             FRA00640
      IF(IFM(I).EQ.0)GO TO 108                                          FRA00650
C-----FORM BEAM ELEMENT STIFFNESS MATRIX (INCLUDES NONRIGID CONNECTIONS)FRA00660
      EZ2J=2*EZJ(I)+1                                                   FRA00670
      EZ2K=2*EZK(I)+1                                                   FRA00680
      EZ3J=3*EZJ(I)+1                                                   FRA00690
      EZ3K=3*EZK(I)+1                                                   FRA00700
      EZ1S=EZJ(I)+EZK(I)+1                                              FRA00710
      EZS=12*EZJ(I)*EZK(I)+4*(EZJ(I)+EZK(I))+1                          FRA00720
      EY2J=2*EYJ(I)+1                                                   FRA00730
      EY2K=2*EYK(I)+1                                                   FRA00740
      EY3J=3*EYJ(I)+1                                                   FRA00750
      EY3K=3*EYK(I)+1                                                   FRA00760
      EY1S=EYJ(I)+EYK(I)+1                                              FRA00770
      EYS=12*EYJ(I)*EYK(I)+4*(EYJ(I)+EYK(I))+1                          FRA00780
      XL=(12*EF)/(L(I)*L(I)*L(I))                                       FRA00790
      B1=EF*A(I)/L(I)                                                   FRA00800
      B2=(EZ1S/EZS)*XL*IZ(I)                                            FRA00810
      B3=(EY1S/EYS)*XL*IY(I)                                            FRA00820
      B4=(XL*L(I)/2)*IZ(I)*(EZ2J/EZS)                                   FRA00830
      B5=(XL*L(I)/2)*IY(I)*(EY2J/EYS)                                   FRA00840
      B6=GF*IX(I)/L(I)                                                  FRA00850
      B7=(2*EF*IZ(I))/(L(I)*EZS)                                        FRA00860
      B8=(2*EF*IY(I))/(L(I)*EYS)                                        FRA00870
      SMD(1,1)=SMD(7,7)=B1                                              FRA00880
      SMD(7,1)=SMD(1,7)=-B1                                             FRA00890
      SMD(2,2)=SMD(8,8)=B2                                              FRA00900
      SMD(8,2)=SMD(2,8)=-B2                                             FRA00910
      SMD(3,3)=SMD(9,9)=B3                                              FRA00920
      SMD(3,9)=SMD(9,3)=-B3                                             FRA00930
      SMD(12,2)=SMD(2,12)=B4                                            FRA00940
      SMD(12,8)=SMD(8,12)=-B4                                           FRA00950
      SMD(6,2)=SMD(2,6)=B4*EZ2K/EZ2J                                    FRA00960
      SMD(8,6)=SMD(6,8)=-B4*EZ2K/EZ2J                                   FRA00970
      SMD(11,9)=SMD(9,11)=B5                                            FRA00980
      SMD(11,3)=SMD(3,11)=-B5                                           FRA00990
      SMD(5,3)=SMD(3,5)=-B5*EY2K/EY2J                                   FRA01000
      SMD(5,9)=SMD(9,5)=B5*EY2K/EY2J                                    FRA01010
      SMD(4,4)=SMD(10,10)=B6                                            FRA01020
      SMD(4,10)=SMD(10,4)=-B6                                           FRA01030
      SMD(5,5)=SMD(11,11)=2*B8*EY3K                                     FRA01040
      SMD(11,5)=SMD(5,11)=B8                                            FRA01050
      SMD(6,6)=SMD(12,12)=2*B7*EZ3K                                     FRA01060
      SMD(12,6)=SMD(6,12)=B7                                            FRA01070
      GO TO 109                                                         FRA01080
C-----FORM COLUMN ELEMENT STIFFNESS MATRIX (WITHOUT NONRIGID CONNECTIONSFRA01090
C                                                          )            FRA01100
  108 C1=12*EF/(L(I)*L(I)*L(I))                                         FRA01110
      C2=C1*L(I)/2                                                      FRA01120
      C3=EF*A(I)/L(I)                                                   FRA01130
      C4=GF*IY(I)/L(I)                                                  FRA01140
      C5=4*EF/L(I)                                                      FRA01150
      SMD(1,1)=SMD(7,7)=C1*IZ(I)                                        FRA01160
      SMD(1,7)=SMD(7,1)=-SMD(1,1)                                       FRA01170
      SMD(12,7)=SMD(7,12)=SMD(6,7)=SMD(7,6)=C2*IZ(I)                    FRA01180
      SMD(6,1)=SMD(1,6)=SMD(1,12)=SMD(12,1)=-SMD(12,7)                  FRA01190
      SMD(2,2)=SMD(8,8)=C3                                              FRA 1200
      SMD(2,8)=SMD(8,2)=-C3                                             FRA01210
      SMD(3,3)=SMD(9,9)=C1*IX(I)                                        FRA01220
      SMD(3,9)=SMD(9,3)=-SMD(3,3)                                       FRA01230
      SMD(4,3)=SMD(3,4)=SMD(3,10)=SMD(10,3)=C2*IX(I)                    FRA01240
      SMD(10,9)=SMD(9,10)=SMD(4,9)=SMD(9,4)=-SMD(4,3)                   FRA01250
      SMD(4,4)=SMD(10,10)=C5*IX(I)                                      FRA01260
      SMD(4,10)=SMD(10,4)=SMD(4,4)/2                                    FRA01270
      SMD(5,5)=SMD(11,11)=C4                                            FRA01280
      SMD(5,11)=SMD(11,5)=-C4                                           FRA01290
      SMD(6,6)=SMD(12,12)=C5*IZ(I)                                      FRA01300
      SMD(6,12)=SMD(12,6)=SMD(6,6)/2                                    FRA01310
      GO TO 109                                                         FRA01320
C                                                                       FRA01330
C-----ASSEMBLE MASS SUBMATRICES MMM, MMR, MRR; REUSE STORAGE AND ARRAY  FRA01340
C     NAMES OF STIFFNESS COMPUTATIONS                                   FRA01350
C                                                                       FRA01360
  150 IF(MCODE.EQ.1) GO TO 151                                          FRA01370
C-----ASSEMBLED LUMPED MASS (ALM) FORMULATION                           FRA01380
      XM=DENSF*A(I)*L(I)                                                FRA01390
      SMD(1,1)=SMD(2,2)=SMD(3,3)=SMD(7,7)=SMD(8,8)=SMD(9,9)=XM          FRA01400
      GO TO 109                                                         FRA01410
C-----CONSISTENT MASS (CM) FORMULATION                                  FRA01420
  151 A1=DENSF*A(I)*L(I)/3                                              FRA01430
      IX1=IY(I)+IZ(I)                                                   FRA01440
      IF(IFM(I).EQ.0)IX1=IX(I)+IZ(I)                                    FRA01450
      A2=A1*IX1/A(I)                                                    FRA01460
      A3=A1*39./35.                                                     FRA01470
      A4=A1*27./70.                                                     FRA01480
      A5=(A1*L(I)*L(I))/35.                                             FRA01490
      A6=(A1*L(I)*33.)/210.                                             FRA01500
      A7=-A5*0.75                                                       FRA01510
      A8=(A6*13.)/22.                                                   FRA01520
      IF(IFM(I).EQ.1)GO TO 152                                          FRA01530
C-----COLUMNS--CONSISTENT MASS (CM)                                     FRA01540
      SMD(2,2)=SMD(8,8)=A1                                              FRA01550
      SMD(1,1)=SMD(3,3)=SMD(7,7)=SMD(9,9)=A3                            FRA01560
      SMD(5,5)=SMD(11,11)=A2                                            FRA01570
      SMD(5,11)=SMD(11,5)=A2/2.                                         FRA01580
      SMD(2,8)=SMD(8,2)=A1/2.                                           FRA01590
      SMD(4,4)=SMD(10,10)=SMD(6,6)=SMD(12,12)=A5                        FRA01600
      SMD(4,10)=SMD(10,4)=SMD(6,12)=SMD(12,6)=A7                        FRA01610
      SMD(7,12)=SMD(12,7)=SMD(3,4)=SMD(4,3)=A6                          FRA01620
      SMD(9,10)=SMD(10,9)=SMD(1,6)=SMD(6,1)=-A6                         FRA01630
      SMD(7,1)=SMD(1,7)=SMD(9,3)=SMD(3,9)=A4                            FRA01640
      SMD(12,1)=SMD(1,12)=SMD(4,9)=SMD(9,4)=A8                          FRA01650
      SMD(12,3)=SMD(3,10)=SMD(6,7)=SMD(7,6)=-A8                         FRA01660
      GO TO 109                                                         FRA01670
C-----BEAMS--CONSISTENT MASS (CM)                                       FRA01680
  152 SMD(4,4)=SMD(10,10)=A2                                            FRA01690
      SMD(4,10)=SMD(10,4)=A2/2.                                         FRA01700
      SMD(1,1)=SMD(7,7)=A1                                              FRA01710
      SMD(12,2)=SMD(8,8)=SMD(3,3)=SMD(9,9)=A3                           FRA01720
      SMD(1,7)=SMD(7,1)=A1/2.                                           FRA01730
      SMD(5,5)=SMD(11,11)=SMD(6,6)=SMD(12,12)=A5                        FRA01740
      SMD(5,11)=SMD(11,5)=SMD(6,12)=SMD(12,6)=A7                        FRA01750
      SMD(6,2)=SMD(2,6)=SMD(9,11)=SMD(11,9)=A6                          FRA01760
      SMD(5,3)=SMD(3,5)=SMD(8,12)=SMD(12,8)=-A6                         FRA01770
      SMD(2,8)=SMD(8,2)=SMD(3,9)=SMD(9,3)=A4                            FRA01780
      SMD(6,8)=SMD(8,6)=SMD(11,3)=SMD(3,11)=A8                          FRA01790
```

```
      SMD(5,9)=SMD(9,5)=SMD(12,2)=SMD(2,12)=-A8                          FRA01800
C                                                                        FRA01810
C-----ASSEMBLE ELEMENT PERMUTATION VECTOR (EPV) FROM FRAME PERMUTATION   FRA01820
C     VECTOR (FPV)                                                       FRA01830
C                                                                        FRA01840
  109 JJ1=0                                                              FRA01850
      JA=6*JJ(I)-6                                                       FRA01860
      DO 110 J=1,6                                                       FRA01870
      JA=JA+1                                                            FRA01880
      JJ1=JJ1+1                                                          FRA01890
  110 EPV(JJ1)=FPV(JA)                                                   FRA01900
      J8=6*JK(I)-6                                                       FRA01910
      DO 111 J=1,6                                                       FRA01920
      J8=J8+1                                                            FRA01930
      JJ1=JJ1+1                                                          FRA01940
  111 EPV(JJ1)=FPV(J8)                                                   FRA01950
C                                                                        FRA01960
C-----USE EPV() TO ADD CONTRIBUTION OF CURRENT FRAME MEMBER (#I) TO      FRA01970
C     STIFFNESS ARRAYS SMM, SMR, SRR (OR CORRESPONDING MASS ARRAYS FOR   FRA01980
C     ISM=2)                                                             FRA01990
C                                                                        FRA02000
      DO 112 K=1,12                                                      FRA02010
      KR=EPV(K)                                                          FRA02020
      IF(KR.LE.NMT)GO TO 113                                             FRA02030
C-----R DISPLACEMENT TYPES                                               FRA02040
      KR=KR-NMT                                                          FRA02050
      DO 114 J=1,12                                                      FRA02060
      KC=EPV(J)-NMT                                                      FRA02070
      IF(KC.LE.0)GO TO 114                                               FRA02080
      SRR(KR,KC)=SRR(KR,KC)+SMD(K,J)                                     FRA02090
  114 CONTINUE                                                           FRA02100
      GO TO 112                                                          FRA02110
C-----M DISPLACEMENT TYPES                                               FRA02120
  113 DO 115 J=1,12                                                      FRA02130
      KC=EPV(J)                                                          FRA02140
      K1=KC-NMT                                                          FRA02150
      IF(KC.LE.NMT)GO TO 116                                             FRA02160
      SMR(KR,K1)=SMR(KR,K1)+SMD(K,J)                                     FRA02170
      GO TO 115                                                          FRA02180
  116 SMM(KR,KC)=SMM(KR,KC)+SMD(K,J)                                     FRA02190
  115 CONTINUE                                                           FRA02200
  112 CONTINUE                                                           FRA02210
C                                                                        FRA02220
  106 CONTINUE                                                           FRA02230
C                                                                        FRA02240
      IF(ISM.EQ.1)RETURN                                                 FRA02250
C                                                                        FRA02260
C-----ADD LUMPED MASSES TO FRAME FOR MODE=1,2 CASES                      FRA02270
C                                                                        FRA02280
      DO 200 I=1,NFJ                                                     FRA02290
      EPV(1)=6*I-5                                                       FRA02300
      EPV(2)=EPV(1)+1                                                    FRA02310
      EPV(3)=EPV(1)+2                                                    FRA02320
      DO 201 K=1,3                                                       FRA02330
      J=FPV(EPV(K))                                                      FRA02340
      IF(J.LE.NMT)SMM(J,J)=SMM(J,J)+MF(I)                                FRA02350
      IF(J.GT.NMT)SRR(J,J)=SRR(J,J)+MF(I)                                FRA02360
  201 CONTINUE                                                           FRA02370
  200 CONTINUE                                                           FRA02380
C                                                                        FRA02390
      RETURN                                                             FRA02400
      END                                                                FRA02410
```

```
*DECK SPRING                                                            SPR00000
      SUBROUTINE SPRING                                                 SPR00010
C                                                                       SPR00020
C-----SUBPROGRAM TO ADD BOUNDARY STIFFNESS TERMS (MODELLED AS LINEARLY- SPR00030
C     ELASTIC SPRINGS) TO STIFFNESS SUBMATRICES FOR FRAME-PANEL         SPR00040
C     ASSEMBLAGE (NFM>0) OR FOR PANEL-ONLY CASE (NFM=0).                SPR00050
C                                                                       SPR00060
C     BOUNDARY SPRINGS:  FORM SFM, SPM AND AUGMENT SFF, SPP, SMM, SRR,  SPR00070
C                        SFR, SPR, AND SMR                              SPR00080
C                                                                       SPR00090
C     PANEL SPRINGS:  AUGMENT SFF, SPP, AND SRR FOR ARBITRARY NUMBER    SPR00100
C                     AND LOCATION OF NODAL SPRINGS                     SPR00110
C                                                                       SPR00120
C                                                                       SPR00130
      INTEGER F1,P1,F2,P2,P3,PPV,FPV,SN,PNPV(8),FNPV(6)                 SPR00140
      REAL KS1,KS2,MP                                                   SPR00150
C                                                                       SPR00160
      COMMON                                                            SPR00170
     1/CBNPN/XP(25),YP(25),MP(25),KS1(25,5),JFN(25,2),JPN(25),INTYP(25),SPR00180
     #       IREP(16),ICNTY(16,4),KS2(25,5)                             SPR00190
     3/CBNPFD/PPV(200),FPV(96),NFL(200),NRL(200),JRL(96)                SPR00200
     4/CBSTIF/SFF( 40, 40),SFP( 40, 120),SFM( 40, 45),SFR( 40, 56),     SPR00210
     #                     SPP(120,120),SPM(120,45),SPR(120, 56),       SPR00220
     #                                  SMM( 45, 45),SMR( 45, 56),      SPR00230
     #                                               SRR( 56, 56)       SPR00240
     7/CBDATA/EP,TP,PRP,DENSP,EF,GF,TF,DENSF,NS,SN,MCODE,ISM,           SPR00250
     #        NRPN,NFT,NPT,NMT,NRT,NF,NP,NM,NR,NPN,NPE,NPO,NPDOF,       SPR00260
     #        NFJ,NFM,NJ6,NFNSPR,NPNSPR,ISOA,NPR,NFR,NRFJ,              SPR00270
     #        NFRT,IREAC,ISTRES,ISTAT,IL,IKKK,TIME                      SPR00280
C                                                                       SPR00290
C                                                                       SPR00300
C-----CLEAR ARRAYS                                                      SPR00310
C                                                                       SPR00320
      DO 90 I=1,NMT                                                     SPR00330
      DO 91 J1=1,NFT                                                    SPR00340
   91 SFM(J1,I)=0.                                                      SPR00350
      DO 92 J2=1,NPT                                                    SPR00360
   92 SPM(J2,I)=0.                                                      SPR00370
   90 CONTINUE                                                          SPR00380
C                                                                       SPR00390
      IF(NRPN.GT.0)GO TO 151                                            SPR00400
C                                                                       SPR00410
      DO 93 I=1,NRT                                                     SPR00420
      DO 94 J1=1,NFT                                                    SPR00430
   94 SFR(J1,I)=0.                                                      SPR00440
      DO 95 J2=1,NPT                                                    SPR00450
   95 SPR(J2,I)=0.                                                      SPR00460
   93 CONTINUE                                                          SPR00470
C                                                                       SPR00480
C-----FRAME-PANEL ASSEMBLY BOUNDARY SPRINGS (NFM>0)                     SPR00490
C                                                                       SPR00500
  151 IF(NFNSPR.EQ.0)GO TO 150                                          SPR00510
      DO 50 I=1,NFNSPR                                                  SPR00520
C                                                                       SPR00530
C     JFN(I,1) AND JFN(I,2) = FRAME AND CORRESPONDING PANEL NODES       SPR00540
C     (RESPECTIVELY) WHERE BOUNDARY SPRINGS ARE ATTACHED                SPR00550
C                                                                       SPR00560
      JF1=6*JFN(I,1)-6                                                  SPR00570
      JP1=8*JFN(I,2)-8                                                  SPR00580
C                                                                       SPR00590
C     FORM FRAME NODE PERMUTATION VECTOR (FNPV) FOR NODE JFN(I,1) FROM  SPR00600
C     FPV()                                                             SPR00610
C                                                                       SPR00620
      DO 51 J=1,6                                                       SPR00630
      JF1=JF1+1                                                         SPR00640
   51 FNPV(J)=FPV(JF1)                                                  SPR00650
C                                                                       SPR00660
C     FORM PANEL NODE PERMUTATION VECTOR (PNPV) FOR NODE JFN(I,2) FROM  SPR00670
C     PPV()                                                             SPR00680
C                                                                       SPR00690
      DO 52 J=1,8                                                       SPR00700
      JP1=JP1+1                                                         SPR00710
   52 PNPV(J)=PPV(JP1)                                                  SPR00720
C                                                                       SPR00730
C-----FORM ARRAYS SFM,SPM; AUGMENT ARRAYS SFF,SPP,SMM,SRR,SFR,SPR,SMR   SPR00740
C     WITH SPRING STIFFNESSES KS1(I,J)  (FOR DOFS 1,...,5 ONLY)         SPR00750
C                                                                       SPR00760
      DO 53 J=1,5                                                       SPR00770
C                                                                       SPR00780
C     F: 1...NFT; P: 1...NPT; M: 1...NMT; R: 1...NRT                    SPR00790
C                                                                       SPR00800
      P1=PNPV(J)                                                        SPR00810
      F1=FNPV(J)                                                        SPR00820
      P2=P1-NFT                                                         SPR00830
      F2=F1-NMT                                                         SPR00840
      P3=P2-NPT                                                         SPR00850
      IF(P2)55,55,561                                                   SPR00860
  561 IF(P3)56,56,562                                                   SPR00870
C-----F, M, R TYPE DOF'S: FORM SFM, AUGMENT SFF, SMM, SRR, SFR          SPR00880
   55 SFF(P1,P1)=SFF(P1,P1)+KS1(I,J)                                    SPR00890
      IF (F2)57,57,58                                                   SPR00900
   57 SFM(P1,F1)=-KS1(I,J)                                              SPR00910
      SMM(F1,F1)=SMM(F1,F1)+KS1(I,J)                                    SPR00920
      GO TO 53                                                          SPR00930
   58 SFR(P1,F2)=-KS1(I,J)                                              SPR00940
      SRR(F2,F2)=SRR(F2,F2)+KS1(I,J)                                    SPR00950
      GO TO 53                                                          SPR00960
C                                                                       SPR00970
C-----P, M, R TYPE DOF'S: FORM SPM, AUGMENT SPP, SMM, SRR, SPR          SPR00980
C                                                                       SPR00990
   56 SPP(P2,P2)=SPP(P2,P2)+KS1(I,J)                                    SPR01000
      IF(F2)59,59,60                                                    SPR01010
   59 SPM(P2,F1)=-KS1(I,J)                                              SPR01020
      SMM(F1,F1)=SMM(F1,F1)+KS1(I,J)                                    SPR01030
      GO TO 53                                                          SPR01040
   60 SPR(P2,F2)=-KS1(I,J)                                              SPR01050
      SRR(F2,F2)=SRR(F2,F2)+KS1(I,J)                                    SPR01060
C                                                                       SPR01070
      GO TO 53                                                          SPR01080
  562 SRR(P3,P3)=SRR(P3,P3)+KS1(I,J)                                    SPR01090
      IF(F2)563,563,564                                                 SPR01100
  563 SMR(F2,P3)=-KS1(I,J)                                              SPR01110
      SMM(F2,F2)=SMM(F2,F2)+KS1(I,J)                                    SPR01120
      GO TO 53                                                          SPR01130
  564 SRR(P3,F2)=SRR(P3,F2)-KS1(I,J)                                    SPR01140
      SRR(F2,P3)=SRR(P3,F2)                                             SPR01150
   53 CONTINUE                                                          SPR01160
   50 CONTINUE                                                          SPR01170
C                                                                       SPR01180
C-----SPRINGS AT PANEL NODES (NOT CONNECTED TO FRAME)                   SPR01190
```

```
C
  150 IF(NPNSPR.EQ.0)RETURN
      DO 100 I=1,NPNSPR
C
C     JPN(I) = NODE NUMBER OF PANEL WITH SPRINGS ATTACHED
C
      JP1=6*JPN(I)-5
C
C      FORM PANEL NODE PERMUTATION VECTOR (PNPV) FOR PANEL NODE JP
C      FROM PPV()
C
      DO 101 J=1,6
      JP1=JP1+1
  101 PNPV(J)=PPV(JP1)
C
C-----AUGMENT ARRAYS SFF,SPP,SRR WITH NODE JPN(I) SPRING STIFFNESSES
C
      DO 102 J=1,5
      K1=PNPV(J)
      K2=K1-NFT
      K3=K2-NPT
      IF(K1.GT.NFT)GO TO 1031
      SFF(K1,K1)=SFF(K1,K1)+KS2(I,J)
      GO TO 102
 1031 IF(K3)103,103,1032
  103 SPP(K2,K2)=SPP(K2,K2)+KS2(I,J)
      GO TO 102
 1032 SRR(K3,K3)=SRR(K3,K3)+KS2(I,J)
  102 CONTINUE
  100 CONTINUE
C
      RETURN
      END
```

```
*DECK CDENSE
      SUBROUTINE CDENSE
C
C-----SUBPROGRAM TO ELIMINATE P AND H TYPES (P TYPES ONLY FOR
C     NFM=6 CASE) FROM STIFFNESS (ISM=1) AND MASS (ISM=2) MATRICES
C     USING GUYAN REDUCTION
C
      REAL TPF(120,45),TPM(120,45),TMFS(120,45),TPR(120,56),TMRS(120,56)
      INTEGER SN
C
      COMMON
     4/CBSTIF/SFF( 40, 40),SFP( 40, 120),SFM( 40, 45),SFR( 40, 56),
     #                     SPP(120,120),SPM(120,45),SPR(120, 56),
     #                                  SMM( 45, 45),SMR( 45, 56),
     #                                               SRR( 56, 56)
     5/CBTSTOR/TS1(120,45),TS2(120, 56),TS3( 45, 120)
     7/CBDATA/EP,TP,PRP,DENSP,EF,GF,TF,DENSF,NS,SN,MCDOE,ISM,
     #        NRPN,NFT,NPT,NMT,NRT,NF,NP,NM,NR,NPN,NPE,NPO,NPOOF,
     #        NFJ,NFM,NJ6,NFNSPR,NPNSPR,ISDA,NPR,NFR,NRFJ,
     #        NFRT,IREAC,ISTRES,ISTAT,IL,IKKK,TIME
C
      EQUIVALENCE (TPF,TPM,TMFS,TS1),(TPR,TMRS,TS2)
C
      IF(ISM.EQ.2)GO TO 150
C
C-----SAVE SFR AND SPR (ALSO SMR FOR NFM>0 CASE) FOR REACTION CALCULATIONS
C                                                                     NS
C
      REWIND 11
      WRITE(11) ((SFR(I,J),J=1,NRT),I=1,NFT)
      WRITE(11) ((SPR(I,J),J=1,NRT),I=1,NPT)
      WRITE(11) ((SRR(I,J),J=1,NRT),I=1,NRT)
      IF(NFM.EQ.0)GO TO 200
      WRITE(11) ((SMR(I,J),J=1,NRT),I=1,NMT)
  200 CONTINUE
C
C-----STIFFNESS CONDENSATION: COMPUTE SFF* AND SFR* (ALSO SFM*,
C     SMM*, AND SMR* IF NFM>0)
C
      REWIND 10
      CALL DCOMP(NPT,SPP,NP,NP(,RETURNS(100)
      GO TO 101
  100 PRINT 102
  102 FORMAT(///,' DECOMPOSITION OF SPP FAILS IN CDENSE',///)
      RETURN
  101 DO 103 I=1,NFT
  103 CALL SOLVE(NPT,SPP,SFP,TPF,I,2,NFT,NP,NP,NF,NP,NP,NM)
C
      IF(MCDOE.NE.3) WRITE(10( ((TPF(I,J),J=1,NFT(,I=1,NPT)
C
      DO 106 I=1,NFT
      DO 106 J=1,NFT
      TEMP=SFF(I,J)
      DO 107 JJ=1,NPT
  107 TEMP=TEMP-SFP(I,JJ(*TPF(JJ,J)
  106 SFF(I,J)=TEMP
C
      DO 108 I=1,NFT
      DO 108 J=1,NRT
      TEMP=SFR(I,J)
```

```
      DO 109 JJ=1,NPT
  109 TEMP=TEMP-TPF(JJ,I)*SPR(JJ,J)
  108 SFR(I,J)=TEMP
C
      IF(MCODE.EQ.3)GO TO 149
C
      DO 130 I=1,NRT
  130 CALL SOLVE(NPT,SPP,SPR,TPR,I,1,NRT,NP,NP,NP,NK,NP,NR)
      WRITE(10) ((TPR(I,J),J=1,NRT),I=1,NPT)
C
  149 IF(NFM.EQ.0)RETURN
C
C-----NOW COMPUTE SFM*, SMM*, AND SMR* FOR NFM>0 CASE
C
      DO 131 I=1,NMT
  131 CALL SOLVE(NPT,SPP,SPM,TPM,I,1,NMT,NP,NP,NP,NM,NP,NM)
      IF(MCODE.NE.3) WRITE(10) ((TPM(I,J),J=1,NMT),I=1,NPT)
C
      DO 111 I=1,NFT
      DO 111 J=1,NMT
      TEMP=SFM(I,J)
      DO 112 JJ=1,NPT
  112 TEMP=TEMP-SFP(I,JJ)*TPM(JJ,J)
  111 SFM(I,J)=TEMP
C
      DO 113 I=1,NMT
      DO 113 J=1,NMT
      TEMP=SMM(I,J)
      DO 114 JJ=1,NPT
  114 TEMP=TEMP-SPM(JJ,I)*TPM(JJ,J)
  113 SMM(I,J)=TEMP
C
      DO 123 I=1,NMT
      DO 123 J=1,NRT
      TEMP=SMR(I,J)
      DO 124 JJ=1,NPT
  124 TEMP=TEMP-TPM(JJ,I)*SPR(JJ,J)
  123 SMR(I,J)=TEMP
C
C-----NOW COMPUTE SFF** AND SFR**
C
      CALL OCOMP(NMT,SMM,NM,NM),RETURNS(115)
      GO TO 116
  115 PRINT 117
  117 FORMAT(///,38H DECOMPOSITION OF SMM* FAILS IN COENSE,///)
      RETURN
  116 DO 118 I=1,NFT
  118 CALL SOLVE(NMT,SMM,SFM,TFFS,I,2,NFT,NM,NM,NF,NM,NP,NM)
      IF(MCODE.NE.3) WRITE(10) ((TMFS(I,J),J=1,NFT),I=1,NMT)
C
      DO 119 I=1,NFT
      DO 119 J=1,NFT
      TEMP=SFF(I,J)
      DO 120 JJ=1,NMT
  120 TEMP=TEMP-SFM(I,JJ)*TMFS(JJ,J)
  119 SFF(I,J)=TEMP
C
      DO 121 I=1,NFT
      DO 121 J=1,NRT
      TEMP=SFR(I,J)
      DO 122 JJ=1,NMT
  122 TEMP=TEMP-TMFS(JJ,I)*SMR(JJ,J)
  121 SFR(I,J)=TEMP
C
      IF(MCODE.EQ.3)RETURN
C
      DO 125 I=1,NRT
  125 CALL SOLVE(NMT,SMM,SMR,TMRS,I,1,NRT,NM,NM,NM,NR,NP,NR)
      WRITE(10) ((TMRS(I,J),J=1,NRT),I=1,NMT)
C
      RETURN
C
C-----MASS CONDENSATION
C
  150 IF(MCODE.EQ.3)RETURN
      REWIND 10
C
C-----COMPUTE MFF* = MFF - MFPXTPF - (MFPXTPF)' + TPF'XMPPXTPF
C     AND     MFR* = MFR - MFPXTPR - TPF'XMPR + TPF'XMPPXTPR
C     LET TS3 = TPF'XMPP
C
      READ(10) ((TPF(I,J),J=1,NFT),I=1,NPT)
      READ(10) ((TPR(I,J),J=1,NRT),I=1,NPT)
C
      DO 151 I=1,NFT
      DO 151 J=1,NPT
      TEMP=0.
      DO 152 JJ=1,NPT
  152 TEMP=TEMP+TPF(JJ,I)*SPP(JJ,J)
  151 TS3(I,J)=TEMP
C
      DO 153 I=1,NFT
      DO 153 J=1,NFT
      QP=SFF(I,J)
      DO 154 JJ=1,NPT
  154 QP=QP-SFP(I,JJ)*TPF(JJ,J)-TPF(JJ,I)*SFP(J,JJ)+TS3(I,JJ)*TPF(JJ,J)
  153 SFF(I,J)=QP
C
      DO 155 I=1,NFT
      DO 155 J=1,NRT
      QP=SFR(I,J)
      DO 156 JJ=1,NPT
  156 QP=QP-SFP(I,JJ)*TPR(JJ,J)-TPF(JJ,I)*SPR(JJ,J)+TS3(I,JJ)*TPR(JJ,J)
  155 SFR(I,J)=QP
C
C
      IF(NFM.EQ.0)RETURN
C
C-----NOW COMPUTE MFM*, MMM*, AND MMR* FOR NFM>0 CASE (PANEL-FRAME ASSEMBLY)
C
C     MFM*=MFM-MFPXTPM-TPF'XMPM+TS3XTPM WHERE TS3=TPF'XMPP
C     MMM*=MMM-MPM'XTPM-TPM'XMFM+TPM'XMPPXTPM  (NOW LET TS3=TPM'XMPP)
C     MMR*=MMR-MPM'XTPR-TPM'XMPR+TPM'XMPPXTPR (SAME TS3 AS FOR MMM*)
C
      DO 157 I=1,NFT
      DO 157 J=1,NMT
      QP=SFM(I,J)
      DO 158 JJ=1,NPT
  158 QP=QP-TPF(JJ,I)*SPM(JJ,J)
```

```
  157 SFM(I,J)=QP                                                       CDEL1800
C                                                                       CDEL1810
C-----REPLACE TPF WITH TPM (SHARE SAME STORAGE)                         CDEL1820
C                                                                       CDEL1830
      READ(10) ((TPM(I,J),J=1,NMT),I=1,NPT)                             CDEL1840
      DO 159 I=1,NFT                                                    CDEL1850
      DO 159 J=1,NMT                                                    CDEL1860
      QP=SFM(I,J(                                                       CDEL1870
      DO 160 JJ=1,NPT                                                   CDEL1880
  160 QP=QP-SFP(I,JJ)*TPM(JJ,J(+TS3(I,JJ)*TPM(JJ,J)                     CDEL1890
  159 SFM(I,J(=QP                                                       CDEL1900
C                                                                       CDEL1910
C-----REDEFINE TS3 FOR DETERMINATION OF MMM* AND MMR*                   CDEL1920
C                                                                       CDEL1930
      DO 161 I=1,NMT                                                    CDEL1940
      DO 161 J=1,NPT                                                    CDEL1950
      TEMP=0.                                                           CDEL1960
      DO 162 JJ=1,NPT                                                   CDEL1970
  162 TEMP=TEMP+TPM(JJ,I)*SPP(JJ,J)                                     CDEL1980
  161 TS3(I,J)=TEMP                                                     CDEL1990
C                                                                       CDEL2000
      DO 163 I=1,NMT                                                    CDEL2010
      DO 163 J=1,NMT                                                    CDEL2020
      QP=SMM(I,J(                                                       CDEL2030
      DO 164 JJ=1,NPT                                                   CDEL2040
  164 QP=QP-SPM(JJ,I)*TPM(JJ,J)-TPM(JJ,I)*SPM(JJ,J)+TS3(I,JJ(*TPM(JJ,J) CDEL2050
  163 SMM(I,J)=QP                                                       CDEL2060
C                                                                       CDEL2070
      DO 165 I=1,NMT                                                    CDEL2080
      DO 165 J=1,NRT                                                    CDEL2090
      QP=SMR(I,J)                                                       CDEL2100
      DO 166 JJ=1,NPT                                                   CDEL2110
  166 QP=QP-SPM(JJ,I)*TPR(JJ,J)-TPM(JJ,I)*SPR(JJ,J)+TS3(I,JJ)*TPR(JJ,J) CDEL2120
  165 SMR(I,J)=QP                                                       CDEL2130
C                                                                       CDEL2140
C-----FINALLY COMPUTE MFF** AND MFP**                                   CDEL2150
C     WHERE                                                             CDEL2160
C             MFF**=MFF*-MFM*XTMF*-TMF*'XMFM*'+TS3XTMF*,  TS3=TMF*'XMMM* CDEL2170
C             MFR**=MFR*-MFM*XTMR*-TMF*'XMMR*+TS3XTMP*                  CDEL2180
C                                                                       CDEL2190
C-----REPLACE TPM AND TPR WITH TMFS AND TMRS, RESPECTIVELY              CDEL2200
C                                                                       CDEL2210
      READ(10) ((TMFS(I,J),J=1,NFT),I=1,NMT)                            CDEL2220
      READ(10) ((TMRS(I,J),J=1,NRT),I=1,NMT)                            CDEL2230
C                                                                       CDEL2240
      DO 167 I=1,NFT                                                    CDEL2250
      DO 167 J=1,NMT                                                    CDEL2260
      TEMP=J.                                                           CDEL2270
      DO 168 JJ=1,NMT                                                   CDEL2280
  168 TEMP=TEMP+TMFS(JJ,I)*SMM(JJ,J)                                    CDEL2290
  167 TS3(I,J)=TEMP                                                     CDEL2300
C                                                                       CDEL2310
      DO 169 I=1,NFT                                                    CDEL2320
      DO 169 J=1,NFT                                                    CDEL2330
      QP=SFF(I,J)                                                       CDEL2340
      DO 170 JJ=1,NMT                                                   CDEL2350
  170 QP=QP-SFM(I,JJ)*TMFS(JJ,J)-TMFS(JJ,I)*SFM(J,JJ)+TS3(I,JJ)*TMFS(JJ, CDEL2360
     * J)                                                               CDEL2370
  169 SFF(I,J)=QP                                                       CDEL2380
C                                                                       CDEL2390
      DO 171 I=1,NFT                                                    CDEL2400
      DO 171 J=1,NRT                                                    CDEL2410
      QP=SFR(I,J)                                                       CDEL2420
      DO 172 JJ=1,NMT                                                   CDEL2430
  172 QP=QP-SFM(I,JJ)*TMRS(JJ,J)-TMFS(JJ,I)*SMP(JJ,J)+TS3(I,JJ)*TMRS(JJ, CDEL2440
     * J)                                                               CDEL2450
  171 SFP(I,J)=QP                                                       CDEL2460
C                                                                       CDEL2470
      RETURN                                                            CDEL2480
      END                                                               CDEL2490
```

```
*DECK EIGENV                                                          EIG00000
      SUBROUTINE EIGENV                                               EIG00010
C                                                                     EIG00020
C-----SUBPROGRAM TO SOLVE THE NON-STANDARD FORM OF THE EIGENVALUE      EIG00030
C     PROBLEM:                                                        EIG00040
C               M*X = (1/P**2)*S*X                                    EIG00050
C                                                                     EIG00060
C     OR        A*X = LAMBDA*B*X                                      EIG00070
C                                                                     EIG00080
C     PARAMETERS:                                                     EIG00090
C       ON INPUT -    N=NO. OF                                        EIG00100
C                     A=MASS MATRIX                                   EIG00110
C                     B=STIFFNESS MATRIX                              EIG00120
C       ON OUTPUT -   SA=PSQ (SQUARES OF NAT. CIRC. FREQUENCIES)      EIG00130
C                     A=MASS MATRIX                                   EIG00140
C                     S=STIFFNESS MATRIX                              EIG00150
C                     X=XN1 (INVERSE OF XN)                           EIG00160
C                     B=XN (MODAL MATRIX NORMALIZED WRT MASS MATRIX)  EIG00170
C                                                                     EIG00180
C                                                                     EIG00190
      REAL LAMBDA,MFR                                                 EIG00200
      INTEGER SN                                                      EIG00210
C                                                                     EIG00220
      COMMON                                                          EIG00230
     4/CBSTIF/  B( 60, 60),S( 60, 120),A( 60, 45),SFR( 60, 56),       EIG00240
     @                          SPP(120,120),SPM(120,45),MFR(120, 56),EIG00250
     @                                       SMM( 45, 45),SMR( 45, 56),EIG00260
     @                                                    SRR( 56, 56)EIG00270
     5/CBTSTOR/X(60,60),FREQ(1000,3),SA(4060),LAMBDA(4060)            EIG00280
     7/C00ATA/EP,TP,PRP,OENSP,EF,GF,TF,OENSF,NS,SN,MCODE,ISM,         EIG00290
     @         NRPN,NFT,NPT,NMT,NRT,NF,NP,NM,NR,NPN,NPE,NPO,NPOOF,    EIG00300
     @         NFJ,NFN,NJ6,NFNSPR,NPNSPR,ISOA,NPR,NFR,NRFJ,           EIG00310
     @         NFRT,IREAC,ISTRES,ISTAT,IL,IKKK,TIME                   EIG00320
C                                                                     EIG00330
      N=NFT                                                           EIG00340
      NA=NF                                                           EIG00350
      NB=NF                                                           EIG00360
      NL=4060                                                         EIG00370
      NX=60                                                           EIG00380
C                                                                     EIG00390
  101 FORMAT(*1FREQUENCIES AND MODE SHAPES*,/,                        EIG00400
     @ * --------------------------*)                                 EIG00410
  102  FORMAT(*0*,* SYSTEM MASS MATRIX*)                              EIG00420
  108  FORMAT(*0*,* SYSTEM STIFFNESS MATRIX*)                         EIG00430
  110  FORMAT(*0*,* CIRCULAR FREQUENCIES (RADIANS/SEC,)*)             EIG00440
  111  FORMAT(*0*,* NATURAL FREQUENCIES (HERTZ)*)                     EIG00450
  112  FORMAT(*0*,* NATURAL PERIODS (SECONDS)*)                       EIG00460
  113  FORMAT(*0*,* MODAL MATRIX XM (SCALED TO MAKE LARGEST ENTRY 1.0)*)EIG00470
  104  FORMAT(1P9E13.5)                                               EIG00480
  105  FORMAT(*   ERROR IN AXLBX  *)                                  EIG00490
       PRINT 101                                                      EIG00500
       DO 114 I=1,N                                                   EIG00510
       SA(I)=A(I,I)                                                   EIG00520
       DO 114 J=1,N                                                   EIG00530
  114 S(I,J)=B(I,J)                                                   EIG00540
       PRINT 102                                                      EIG00550
       CALL MATPRT(N,N,A,NA,NM)                                       EIG00560
       PRINT 108                                                      EIG00570
       CALL MATPRT(N,N,B,NB,NB)                                       EIG00580
       CALL AXLBX(N,NA,NB,NL,NX,A,B,LAMBDA,X),RETURNS(106)            EIG00590
C-----NOW RESTORE MATRIX A, THE MASS MATRIX                           EIG00600
       N1=N-1                                                         EIG00610
       A(N,N)=SA(N)                                                   EIG00620
       DO 115 I=1,N1                                                  EIG00630
       A(I,I)=SA(I)                                                   EIG00640
       J1=I+1                                                         EIG00650
       DO 115 J=J1,N                                                  EIG00660
  115  A(J,I)=A(I,J)                                                  EIG00670
       GO TO 107                                                      EIG00680
  106  PRINT 105                                                      EIG00690
  107  CONTINUE                                                       EIG00700
       DO 103 I=1,N                                                   EIG00710
       FREQ(I,1)=SQRT(1/LAMBDA(I))                                    EIG00720
       FREQ(I,2)=FREQ(I,1)/6.283185308                                EIG00730
  103  FREQ(I,3)=1./FREQ(I,2)                                         EIG00740
       PRINT 110                                                      EIG00750
       PRINT 104,(FREQ(I,1),I=1,N)                                    EIG00760
       PRINT 111                                                      EIG00770
       PRINT 104,(FREQ(I,2),I=1,N)                                    EIG00780
       PRINT 112                                                      EIG00790
       PRINT 104,(FREQ(I,3),I=1,N)                                    EIG00800
       PRINT 113                                                      EIG00810
       CALL MATPRT(N,N,X,NX,NX)                                       EIG00820
C-----NORMALIZE THE MODAL MATRIX (XM) WRT THE MASS MATRIX TO OBTAIN XN EIG00830
       DO 118 I=1,N                                                   EIG00840
       DO 119 J=1,N                                                   EIG00850
       SA(J)=0.                                                       EIG00860
       DO 119 K=1,N                                                   EIG00870
  119 SA(J)=SA(J)+A(J,K)*X(K,I)                                       EIG00880
       SUM=0.                                                         EIG00890
       DO 120 JJ=1,N                                                  EIG00900
  120 SUM=SUM+X(JJ,I)*SA(JJ)                                          EIG00910
       TEMP=SQRT(SUM)                                                 EIG00920
       DO 121 KK=1,N                                                  EIG00930
  121 B(KK,I)=X(KK,I)/TEMP                                            EIG00940
  118 CONTINUE                                                        EIG00950
C-----COMPUTE (XN)**-1 = XN' X M                                      EIG00960
       DO 122 I=1,N                                                   EIG00970
       DO 122 J=1,N                                                   EIG00980
       SUM=0.                                                         EIG00990
       DO 123 K=1,N                                                   EIG01000
  123 SUM=SUM+B(K,I)*A(K,J)                                           EIG01010
  122 X(I,J)=SUM                                                      EIG01020
C-----FINALLY, STORE SQUARES OF NATURAL CIRCULAR FREQUENCIES IN SA()   EIG01030
       DO 124 I=1,N                                                   EIG01040
  124 SA(I)=FREQ(I,1)*FREQ(I,1)                                       EIG01050
C                                                                     EIG01060
       RETURN                                                         EIG01070
       END                                                            EIG01080
```

```
*DECK AXLBX                                                              AXL00000
      SUBROUTINE AXLBX(N,NA,NB,NL,NX,A,B,LAMBDA,X),RETURNS(JJ)           AXL00010
C                                                                        AXL00020
C-----SOLVES EIGENPROBLEM A*X = LAMBDA*B*X                               AXL00030
C     A SYMMETRIC, B SYMMETRIC POSITIVE DEFINITE                         AXL00040
C     INPUT: A AND B (ONLY DIAGONAL AND UPPER TRIANGLE NEEDED)           AXL00050
C     OUTPUT: LAMBDA AND X                                               AXL00060
C     ALTERED: DIAGONAL AND LOWER TRIANGLE OF A AND B                    AXL00070
C     ERROR RETURN: B IS NOT POSITIVE DEFINITE OR TQL2 DID NOT CONVERGE  AXL00080
C     REFERENCES: NUMERERISCHE MATHEMATIK, VOL. 11, PP. 99, 181 AND 293. AXL00090
C                                                                        AXL00100
C*****NOTE: NA,...,NX ARE THE DIMENSIONS OF ARRAYS A, B, LAMBDA, AND X   AXL00110
C     IN THE CALLING PROGRAM.                                            AXL00120
C                                                                        AXL00130
C-----CALLED BY MAIN PROGRAM                                             AXL00140
C                                                                        AXL00150
C-----REQUIRES SUBPROGRAMS TRED2 AND TQL2                                AXL00160
C                                                                        AXL00170
C                                                                        AXL00180
      REAL LAMBDA(NL),A(NA,NA),B(NB,NB),X(NX,NX),E(256)                  AXL00190
C                                                                        AXL00200
      DO 4 I=1,N                                                         AXL00210
      DO 4 J=I,N                                                         AXL00220
      S=B(I,J)                                                           AXL00230
        IF(I.EQ.1) GO TO 2                                               AXL00240
        I1=I-1                                                           AXL00250
        DO 1 K=1,I1                                                      AXL00260
    1     S=S-B(I,K)*B(J,K)                                              AXL00270
    2   IF(J.NE.I) GO TO 3                                               AXL00280
        IF(S.LE.0. ) GO TO 13                                            AXL00290
        T=SQRT(S)                                                        AXL00300
        B(I,I)=T                                                         AXL00310
        GO TO 4                                                          AXL00320
    3   B(J,I)=S/T                                                       AXL00330
    4 CONTINUE                                                           AXL00340
      DO 6 I=1,N                                                         AXL00350
      DO 6 J=I,N                                                         AXL00360
        S=A(I,J)                                                         AXL00370
        IF(I.EQ.1) GO TO 6                                               AXL00380
        I1=I-1                                                           AXL00390
        DO 5 K=1,I1                                                      AXL00400
    5     S=S-B(I,K)*A(J,K)                                              AXL00410
    6 A(J,I)=S/B(I,I)                                                    AXL00420
      DO 10 J=1,N                                                        AXL00430
      DO 10 I=J,N                                                        AXL00440
        S=A(I,J)                                                         AXL00450
        IF(I.EQ.J) GO TO 8                                               AXL00460
        I1=I-1                                                           AXL00470
        DO 7 K=J,I1                                                      AXL00480
    7     S=S-A(K,J)*B(I,K)                                              AXL00490
    8   IF(J.EQ.1) GO TO 10                                              AXL00500
        J1=J-1                                                           AXL00510
        DO 9 K=1,J1                                                      AXL00520
    9     S=S-A(J,K)*B(I,K)                                              AXL00530
   10 A(I,J)=S/B(I,I)                                                    AXL00540
C                                                                        AXL00550
      CALL TRED2(NA,NX,N,2.44E-63,A,LAMBDA,E,X)                          AXL00560
      CALL TQL2(NX,N,2.22E-13,LAMBDA,E,X,IERR)                           AXL00570
      IF(IERR.NE.0) GO TO 13                                             AXL00580
C                                                                        AXL00590
      DO 12 J=1,N                                                        AXL00600
      DO 12 IBACK=1,N                                                    AXL00610
      I=N+1-IBACK                                                        AXL00620
        S=X(I,J)                                                         AXL00630
        IF(I.EQ.N) GO TO 12                                              AXL00640
        I1=I+1                                                           AXL00650
        DO 11 K=I1,N                                                     AXL00660
   11     S=S-B(K,I)*X(K,J)                                              AXL00670
   12 X(I,J)=S/B(I,I)                                                    AXL00680
C-----SCALE EIGENVECTORS TO MAKE LARGEST ENTRY = 1.0                     AXL00690
      DO 301 J=1,N                                                       AXL00700
      BIG=X(1,J)                                                         AXL00710
      DO 302 I=2,N                                                       AXL00720
      IF(ABS(X(I,J)).LE.ABS(BIG))GO TO 302                               AXL00730
      BIG=X(I,J)                                                         AXL00740
  302 CONTINUE                                                           AXL00750
      DO 303 I=1,N                                                       AXL00760
  303 X(I,J)=X(I,J)/BIG                                                  AXL00770
  301 CONTINUE                                                           AXL00780
      RETURN                                                             AXL00790
   13 RETURN JJ                                                          AXL00800
      END                                                                AXL00810
C                                                                        AXL00820
C                                                                        AXL00830
```

```
*DECK TQL2                                                              TQL00000
      SUBROUTINE TQL2 (NM,N,MACHEP,D,E,Z,ERROR)                         TQL00010
C                                                                       TQL00020
      REAL MACHEP,D(N),E(N),Z(NM,N)                                     TQL00030
      INTEGER ERROR                                                     TQL00040
C                                                                       TQL00050
C-----THIS SUBPROGRAM IS A TRANSLATION OF THE ALGOL PROCEDURE TQL2,     TQL00060
C     NUM.MATH.11, 293-306(1968) BY BOWDLER, MARTIN, REINSCH, AND       TQL00070
C     WILKINSON.                                                        TQL00080
C                                                                       TQL00090
C     THIS SUBPROGRAM USES QL TRANSFORMATIONS TO FIND THE               TQL00100
C     EIGENVALUES AND EIGENVECTORS OF A TRIDIAGONAL MATRIX,             TQL00110
C     GIVEN WITH ITS DIAGONAL ELEMENTS IN THE ARRAY D(N)                TQL00120
C     AND ITS SUBDIAGONAL ELEMENTS IN THE LAST N-1 ELEMENTS             TQL00130
C     OF THE ARRAY E(N).                                                TQL00140
C                                                                       TQL00150
C     THE EIGENVALUES ARE OVERWRITTEN ON THE DIAGONAL ELEMENTS          TQL00160
C     IN THE ARRAY D IN ASCENDING ORDER.                                TQL00170
C                                                                       TQL00180
C     THE EIGENVECTORS ARE FORMED IN THE ARRAY Z(N,N), OVERWRITING      TQL00190
C     THE ACCUMULATED TRANSFORMATIONS AS SUPPLIED BY TRED2.             TQL00200
C                                                                       TQL00210
C     IF THE TRIDIAGONAL MATRIX IS PRIMARY DATA (THUS, TRED2            TQL00220
C     HAS NOT BEEN USED), Z SHOULD BE PRESET TO THE IDENTITY            TQL00230
C     MATRIX.                                                           TQL00240
C                                                                       TQL00250
C     MACHEP IS THE RELATIVE MACHINE PRECISION.  MACHEP SHOULD          TQL00260
C     BE SET TO 2**(-52) FOR LONG FORM ARITHMETIC ON S/360.             TQL00270
C                                                                       TQL00280
C     THE PROCEDURE FAILS (ERROR IS SET TO THE INDEX OF THE             TQL00290
C     EIGENVALUE FOR WHICH FAILURE OCCURRED) IF ANY EIGENVALUE          TQL00300
C     TAKES MORE THAN 30 ITERATIONS.                                    TQL00310
C                                                                       TQL00320
C     NM MUST BE SET TO THE ROW DIMENSION OF TWO-DIMENSIONAL ARRAY      TQL00330
C     PARAMETERS AS DECLARED IN THE CALLING PROGRAM DIMENSION STATEMENT.TQL00340
C                                                                       TQL00350
C     TRANSLATED BY V. KLEMA, ARGONNE NATIONAL LABORATORY, NOV., 1968.  TQL00360
C     MODIFIED BY B. GARBOW, JAN. 1971.                                 TQL00370
C                                                                       TQL00380
C-----CALLED BY SUBPROGRAM "AXLBX"                                      TQL00390
C                                                                       TQL00400
C                                                                       TQL00410
C     ------------------------------------------------------------------TQL00420
C                                                                       TQL00430
      ERROR = 0                                                         TQL00440
      IF (N .EQ. 1) GO TO 1001                                          TQL00450
C                                                                       TQL00460
      DO 100 I = 2, N                                                   TQL00470
  100 E(I-1) = E(I)                                                     TQL00480
C                                                                       TQL00490
      F = 0.0                                                           TQL00500
      B = 0.0                                                           TQL00510
      E(N) = 0.0                                                        TQL00520
C                                                                       TQL00530
      DO 240 L = 1, N                                                   TQL00540
         J = 0                                                          TQL00550
         H = MACHEP * (ABS(D(L)) + ABS(E(L)))                           TQL00560
         IF (B .LT. H) B = H                                            TQL00570
C                                                                       TQL00580
C C:C  LOOK FOR SMALL SUB-DIAGONAL ELEMENT                              TQL00590
C                                                                       TQL00600
         DO 110 M = L, N                                                TQL00610
         IF (ABS(E(M)) .LE. B) GO TO 120                                TQL00620
  110  CONTINUE                                                         TQL00630
C                                                                       TQL00640
  120    IF (M .EQ. L) GO TO 220                                        TQL00650
  130    IF (J .EQ. 30) GO TO 1000                                      TQL00660
         J = J + 1                                                      TQL00670
C                                                                       TQL00680
CCCCC: FORM SHIFT                                                       TQL00690
CCC:CCC:                                                                TQL00700
         P = (D(L+1) - D(L)) / (2.0  * E(L))                            TQL00710
         R = SQRT(P * P + 1.0 )                                         TQL00720
         H = D(L) - E(L) / (P + SIGN(R,P))                              TQL00730
C                                                                       TQL00740
         DO 140 I = L, N                                                TQL00750
  140    D(I) = D(I) - H                                                TQL00760
C                                                                       TQL00770
         F = F + H                                                      TQL00780
C                                                                       TQL00790
CCCCC: QL TRANSFORMATION                                                TQL00800
CCCCC                                                                   TQL00810
         P = D(M)                                                       TQL00820
         C = 1.0                                                        TQL00830
         S = 0.0                                                        TQL00840
         MML = M - L                                                    TQL00850
C                                                                       TQL00860
CCCCC: FOR I=M-1 STEP -1 UNTIL L DO -- CCC:CCCCC:                       TQL00870
         DO 200 II = 1, MML                                             TQL00880
            I = M - II                                                  TQL00890
            G = C * E(I)                                                TQL00900
            H = C * P                                                   TQL00910
            IF (ABS(P) .LT. ABS(E(I))) GO TO 150                        TQL00920
            C = E(I) / P                                                TQL00930
            R = SQRT(C * C +1.0 )                                       TQL00940
            E(I+1) = S * P * R                                          TQL00950
            S = C / R                                                   TQL00960
            C = 1.0  / R                                                TQL00970
            GO TO 160                                                   TQL00980
  150       C = P / E(I)                                                TQL00990
            R = SQRT(C * C + 1.0  )                                     TQL01000
            E(I+1) = S * E(I) * R                                       TQL01010
            S = 1.0  / R                                                TQL01020
            C = C / R                                                   TQL01030
  160       P = C * D(I) - S * G                                        TQL01040
            D(I+1) = H + S*(C*G + S*D(I))                               TQL01050
C                                                                       TQL01060
CCCCC: FORM VECTOR CCC:CCCCC:                                           TQL01070
            DO 180 K = 1, N                                             TQL01080
               H = Z(K,I+1)                                             TQL01090
               Z(K,I+1) = S * Z(K,I) + C *  H                           TQL01100
               Z(K,I) = C * Z(K,I) - S * H                              TQL01110
  180       CONTINUE                                                    TQL01120
C                                                                       TQL01130
  200    CONTINUE                                                       TQL01140
C                                                                       TQL01150
         E(L) = S * P                                                   TQL01160
         D(L) = C * P                                                   TQL01170
         IF (ABS(E(L)) .GT. B) GO TO 130                                TQL01180
  220    D(L) = D(L) + F                                                TQL01190
```

```
  240 CONTINUE                                                          TQL01200
C                                                                       TQL01210
CCCCC# ORDER EIGENVALUES AND EIGENVECTORS                               TQL01220
CC                                                                      TQL01230
      NM1 = N - 1                                                       TQL01240
      DO 300 I = 1, NM1                                                 TQL01250
         K = I                                                          TQL01260
         P = D(I)                                                       TQL01270
         IP1 = I + 1                                                    TQL01280
C                                                                       TQL01290
         DO 260 J = IP1, N                                              TQL01300
            IF (D(J) .LE. P) GO TO 260                                  TQL01310
            K = J                                                       TQL01320
            P = D(J)                                                    TQL01330
  260    CONTINUE                                                       TQL01340
C                                                                       TQL01350
         IF (K .EQ. I) GO TO 300                                        TQL01360
         D(K) = D(I)                                                    TQL01370
         D(I) = P                                                       TQL01380
C                                                                       TDL01390
         DO 280 J = 1, N                                                TQL01400
            P = Z (J,I)                                                 TQL01410
            Z(J,I) = Z(J,K)                                             TQL01420
            Z (J,K) = P                                                 TQL01430
  280    CONTINUE                                                       TQL01440
C                                                                       TQL01450
  300 CONTINUE                                                          TQL01460
C                                                                       TQL01470
      GO TO 1001                                                        TQL01480
C                                                                       TQL01490
CCCCC# FAIL EXIT STATEMENT IS 1000                                      TQL01500
CCCCC                                                                   TDL01510
 1000 ERROR = L                                                         TQL01520
 1001 RETURN                                                            TQL01530
C                                                                       TQL01540
CCCCC# LAST CARD OF TQL2                                                TQL01550
CCCCC                                                                   TQL01560
      END                                                               TQL01570
C                                                                       TQL01580
C                                                                       TQL01590
```

```
*DECK TRED2                                                            TREC0000
      SUBROUTINE TRED2  (NM1,NM2,N,TOL,A,D,E,Z)                         TRE00010
C                                                                       TREC0020
      REAL A(NM1,N),D(N),E(N),Z(NM2,N)                                  TREC0030
C                                                                       TRE00040
C-----THIS SUBPROGRAM REDUCES THE GIVEN LOWER TRIANGLE OF A             TREC0050
C     SYMMETRIC MATRIX   STORED IN THE ARRAY A(N,N) TO                  TREC0060
C     TRIDIAGONAL FORM USING HOUSEHOLDER"S REDUCTION.                   TRE00070
C     THE DIAGONAL OF THE RESULT IS STORED IN THE ARRAY D(N)            TRE00080
C     AND THE SUB-DIAGONAL IN THE LAST N-1 ELEMENTS OF THE ARRAY        TRE00090
C     E(N)  (WITH THE ADDITIONAL ELEMENT E(1)=0).                       TREC0100
C     THE TRANSFORMATION MATRICES ARE ACCUMULATED IN THE ARRAY Z(N,N).  TRE00110
C     TOL IS A TOLERANCE FOR CHECKING IF THE TRANSFORMATION IS VALID.   TRE00120
C     TOL SHOULD BE SET TO 10.**(-60) FOR LONG FORM ARITHMETIC ON S360. TRE00130
C     NM1 AND NM2 ARE THE ROW DIMENSIONS OF THE TWO DIMENSIONAL ARRAYS  TRE00140
C     "A" AND "Z" AS DECLARED IN THE CALLING PROGRAM DIMENSION STATEMENTTRE00150
C                                                                       TRE00160
C     THE ARRAY A IS LEFT UNALTERED UNLESS THE ACTUAL PARAMETERS        TREC0170
C     CORRESPONDING TO A AND Z ARE IDENTICAL.                           TREC0180
C     THIS SUBPROGRAM IS A TRANSLATION OF THE ALGOL PROCEDURE TRED2,    TRE00190
C     NUM. MATH. 11.181-195(1968) BY MARTIN, REINSCH, AND WILKINSON.    TRE00200
C                                                                       TREC0210
C                                                                       TREC0220
C-----CALLED BY SUBPROGRAM "AXLBX"                                      TREC0230
C                                                                       TREC0240
      DO 108 I=1,N                                                      TREC0250
      DO 100 J=1,I                                                      TREC0260
  100 Z(I,J)=A(I,J)                                                     TRE00270
      IF (N.EQ.1) GO TO 1015                                            TREC0280
C     FOR I= N STEP -1 UNTIL 2 DO --                                    TRE00290
      DO 1011 II=2,N                                                    TREC0300
      I = N+2 - II                                                      TRE00310
      L=I-2                                                             TREC0320
      F =Z(I,I-1)                                                       TREC0330
      G=0.0                                                             TREC0340
      IF(L.LT.1) GO TO 103                                              TREC0350
      DO 102 K = 1,L                                                    TREC0360
  102 G= G + Z(I,K)*Z(I,K)                                              TREC0370
  103 H = G + F*F                                                       TREC0380
C     IF G IS TOO SMALL FOR ORTHOGONALITY TO BE GUARANTEED, THE         TREC0390
C     TRANSFORMATION IS SKIPPED.                                        TRE00400
      IF (G.GT. TOL) GO TO 104                                          TRE00410
      E(I)= F                                                           TREC0420
      H = 0.0                                                           TREC0430
      GOTO 101                                                          TRE00440
  104 L=L+1                                                             TRE00450
      G=SQRT (H)                                                        TRE00460
      IF (F.GE.0.0 ) G=-G                                               TRE00470
      E(I) = G                                                          TREC0480
      H = H-F*G                                                         TREC0490
      Z(I,I-1) = F-G                                                    TREC0500
      F = 0.0                                                           TRE00510
      DO 105 J= 1,L                                                     TREC0520
      Z(J,I) = Z(I,J)/H                                                 TREC0530
      G=0.0                                                             TREC0540
C     FORM ELEMENT OF A*U                                               TRE00550
      DO 106 K = 1,J                                                    TREC0560
  106 G = G + Z(J,K) * Z(I,K)                                           TREC0570
      JP1 = J+1                                                         TREC0580
      IF (L .LT. JP1) GOTO 9106                                         TREC0590
```

```
      DO 108 K = JP1,L
  108 G = G + Z(K,J) * Z(I,K)
C     FORM ELEMENT OF P
 9108 E(J) = G/H
      F = F + G*Z(J,I)
  105 CONTINUE
C     FORM K -- SEE ALGOL TRED2
      HH = F/(H+H)
C     FORM REDUCED A
      DO 109 J = 1,L
      F = Z (I,J)
      E(J) = E (J) - HH * F
      G = E(J)
      DO 109 K = 1,J
  109 Z(J,K) = Z(J,K)- F * E(K) - G * Z(I,K)
C     101 CORRESPONDS TO SKIP
  101 D(I) = H
 1011 CONTINUE
 1015 D(1) = 0.0
      E(1) = 0.0
C     ACCUMULATION OF TRANSFORMATION MATRICES
      DO 201 I = 1,N
      L = I - 1
      IF (D(I) .EQ. 0.0 ) GO TO 202
      DO 203 J = 1,L
      G = 0.0
      DO 204 K = 1,L
  204 G = G + Z(I,K)*Z(K,J)
      DO 203 K = 1,L
  203 Z(K,J) = Z (K,J) - G*Z (K,I)
  202 D(I) = Z(I,I)
      Z(I,I) = 1.0
      IF (L .LT. 1) GOTO 201
      DO 205 J = 1,L
      Z(I,J) = 0.0
  205 Z(J,I) = 0.0
  201 CONTINUE
      RETURN
      END
```

```
TPEC0600
TREC0610
TPEC0620
TREC0630
TREC0640
TREC0650
TREC0660
TREC0670
TREC0680
TREC0690
TREC0700
TREC0710
TPEC0720
TREC0730
TREC0740
TREC0750
TREC0760
TREC0770
TREC0780
TREC0790
TREC0800
TREC0810
TREC0820
TREC0830
TPEC0840
TREC0850
TREC0860
TREC0870
TREC0880
TREC0890
TREC0900
TREC0910
TREC0920
TREC0930
TREC0940
TREC0950
TREC0960
TREC0970
TREC0980
```

```
*DECK STATIC                                                          STAC0000
      SUBROUTINE STATIC                                               STAC0010
C                                                                     STAC0020
C-----SUBPROGRAM FOR STATIC DISPLACEMENT ANALYSIS OF PANEL (NFM=0) OR STAC0030
C     FRAMED PANEL (NFM>0) STRUCTURES FOR 'NSLC' STATIC LOADINGS.     STAC0040
C     ACCEPTABLE LOADINGS INCLUDE CONCENTRATED LOADS 'AF' (FORCES,    STAC0050
C     MOMENTS) CORRESPONDING TO STRUCTURE F DISPLACEMENT TYPES AND/OR STAC0060
C     STATIC MOVEMENTS 'DR' OF SUPPORT RESTRAINTS.  RESULTS OF THE    STAC0070
C     ANALYSIS ARE THE DISPLACEMENTS 'OF' OF THE STRUCTURE DOF'S WHERE STAC0080
C                                                                     STAC0090
C                OF = (SFF)**-1 (AF - SFR * DR)                       STAC0100
C                                                                     STAC0110
C     ALL PANEL AND FRAME NODE DISPLACEMENTS ARE DETERMINED BY BACK-  STAC0120
C     SUBSTITUTION IF (IREAC+ISTRES)>=1.  SUPPORT REACTIONS ARE COMPUTEDSTAC0130
C     IF IREAC=1 AND PANEL STRESSES ARE COMPUTED IF ISTRES=1.         STAC0140
C***** NOTE: SEE EQUIVALENCE STATEMENT BELOW FOR PROPER DIMENSIONS OF STAC0150
C           THE FOLLOWING ARRAYS                                      STAC0160
C                                                                     STAC0170
C                                                                     STAC0180
      REAL TPF(120,45),TPM(120,45),TMFS(120,45),TPR(120,56),TMRS(120,56)STAC0190
      REAL DPL(810),DFR(810),AR(810),TEMP(810),RXP(100,198)           STAC0200
      REAL MX,MY,MXY                                                  STAC0210
      INTEGER SN,PPV,FPV                                              STAC0220
C                                                                     STAC0230
      COMMON                                                          STAC0240
     1/CBNPN/XP(25),YP(25),DBDW(25),DBFS(125),JFN(25,2),              STAC0250
     #       JPN(25),INTYP(25),IREP(16),ICNTY(16,4),KS2(25,5)         STAC0260
     3/CBNPFO/PPV(200),FPV(96),NFL(200),NRL(200),JPL(96)              STAC0270
     4/CBSTIF/SFF( 40, 40),SFP( 40, 120),SFM( 40, 45),SFR( 40, 56),   STAC0280
     #                     SPP(120,120),SPM(120,45),SPR(120, 56),     STAC0290
     #                                  SMM( 45, 45),SMR( 45, 56),    STAC0300
     #                                               SRR( 56, 56)     STAC0310
     5/CBTSTOR/TS1(120,45),TS2(120, 56),TS3( 45, 120)                 STAC0320
     6/CBMISC/AF(256),DR(256),DF(256),DP(256),DM(144),DUM(20)         STAC0330
     7/CBDATA/EP,TP,PRP,DENSP,EF,GF,TF,DENSF,NS,SN,MCODE,ISM,         STAC0340
     #        NRPN,NFT,NPT,NMT,NRT,NF,NP,NM,NR,NPN,NPE,NPD,NPOOF,     STAC0350
     #        NFJ,NFM,NJ6,NFNSPR,NPNSPR,ISDA,NPR,NFR,NRFJ,            STAC0360
     #        NFRT,IREAC,ISTRES,ISTAT,IL,IKKK,TIME                    STAC0370
     8/CBOYNO/PLIST(300),INO,INV,IAF,IGA,ISO,NDLC,LN,NPTS,NMDOES,     STAC0380
     #        IOMAX,IOTM,NO,D1,D2,FXO,FYO,FZO,AXO,AYO,AZO,SX,SY,S2,   STAC0390
     #        SXA,SYA,SZA,NTX,NTY,NTZ                                 STAC0400
      EQUIVALENCE (TPF,TPM,TMFS,TS1),(TPR,TMRS,TS2),(RXP,SPP)         STAC0410
      EQUIVALENCE (DPL,TS3(1,1)),(DFR,TS3(1,19)),(AR,TS3(1,37)),      STAC0420
     # (TEMP,TS3(1,55))                                               STAC0430
C                                                                     STAC0440
      IOOL=813                                                        STAC0450
C                                                                     STAC0460
C-----NSLC = NO. OF STATIC LOADING CONDITIONS                         STAC0470
C                                                                     STAC0480
C********** FOR DYNAMIC RESPONSE CALCULATIONS, GO TO 7031            STAC0490
      IF(ISOA.EQ.1)GO TO 7031                                         STAC0500
C**********                                                           STAC0510
      READ(5,*) NSLC                                                  STAC0520
      IF(NSLC.EQ.0)RETURN                                             STAC0530
C                                                                     STAC0540
      PRINT 950                                                       STAC0550
  950 FORMAT("0STRUCTURE STIFFNESS MATRIX",/," ------------------",   STAC0560
     # "----------",/)                                                STAC0570
      CALL MATPRT(NFT,NFT,SFF,NF,NF)                                  STAC0580
C                                                                     STAC0590
```

```
C                                                                       STAC0600
      IL=LN=0                                                           STA00610
  703 IL=IL+1                                                           STA00620
C                                                                       STA00630
C-----CLEAR ARRAYS                                                      STA00640
C                                                                       STA00650
      DO 951 I=1,256                                                    STA00660
  951 AF(I)=OR(I)=DF(I)=OP(I)=0.                                        STA00670
      DO 952 I=1,144                                                    STA00680
  952 DM(I)=0.                                                          STA00690
      DO 953 I=1,IDOL                                                   STA00700
  953 DPL(I)=DFR(I)=AR(I)=TEMP(I)=0.                                    STA00710
C                                                                       STA00720
C-----NLN = NO. OF LOADED NODES( NPNSO = NO. OF PANEL NODES WITH SUPPORTSTA00730
C     DISPLACEMENTS SPECIFIED; NFJSO = NO. OF FRAME JOINTS WITH SUPPORT STA00740
C     DISPL. SPECIFIED; IREAC (=0, DO NOT COMPUTE SUPPORT REACTIONS; =1 STA00750
C     COMPUTE REACTIONS); ISTRES (=0, DO NOT COMPUTE STRESSES; =1, COMPUSTA00760
C                                                              TE       STA00770
C     STRESSES)                                                         STA00780
C                                                                       STA00790
      READ(5,*) NLN,NPNSO,NFJSO,IREAC,ISTRES                            STA00800
      PRINT 702,NSLC                                                    STA00810
  702 FORMAT("0STATIC DISPLACEMENT ANALYSIS",/," --------------------",  STA00820
     # "----------",//," NSLC =",I3)                                    STA00830
      PRINT 7021,IL,NLN,NPNSO,NFJSO,IREAC,ISTRES                        STA00840
 7021 FORMAT("0LOADING CONDITION NUMBER",I3,/,"  NLN =",I3,             STA00850
     # "  NPNSO =",I3,"  NFJSO =",I3,"  IREAC =",I3,"  ISTRES =",I3)    STA00860
C                                                                       STA00870
C-----NODAL LOADS                                                       STA00880
C                                                                       STA00890
      IF(NLN.EQ.0)GO TO 704                                             STA00900
      PRINT 708                                                         STA00910
  708 FORMAT("0NODAL LOADS",/,"  NODE       AF1           AF2       ",  STA00920
     # "     AF3           AF4           AF5           AF6           ",  STA00930
     # "AF7           AF8")                                            STA00940
      DO 705 I=1,NLN                                                    STA00950
      READ(5,*) K,TEMP(8*K-7),TEMP(8*K-6),TEMP(8*K-5),TEMP(8*K-4),      STA00960
     # TEMP(8*K-3),TEMP(8*K-2),TEMP(8*K-1),TEMP(8*K)                    STA00970
  705 PRINT 706,K,TEMP(8*K-7),TEMP(8*K-6),TEMP(8*K-5),TEMP(8*K-4),      STA00980
     # TEMP(8*K-3),TEMP(8*K-2),TEMP(8*K-1),TEMP(8*K)                    STA00990
  706 FORMAT(I4,1X,1P8E13.5)                                            STA01000
C                                                                       STA01010
      DO 707 I=1,NPO                                                    STA01020
  707 AF(PPV(I))=TEMP(I)                                                STA01030
C                                                                       STA01040
C-----SUPPORT DISPLACEMENTS                                             STA01050
C                                                                       STA01060
  704 IF((NPNSO+NFJSO).EQ.0)GO TO 709                                   STA01070
      IF(IL.EQ.1)GO TO 7101                                             STA01080
C     REPLACE SFR* (NFM=0) OR SFR** (NFM>0) FOR LOADINGS 2,...,NSLC     STA01090
      BACKSPACE 33                                                      STA01100
      READ(33) ((SFR(I,J),J=1,NRT),I=1,NFT)                             STA01110
 7101 DO 710 I=1,IDOL                                                   STA01120
  710 TEMP(I)=0.                                                        STA01130
C                                                                       STA01140
      PRINT 711                                                         STA01150
  711 FORMAT("0APPLIED SUPPORT DISPLACEMENTS")                          STA01160
  712 FORMAT(" JOINT       DR1           DR2           DR3           ",  STA01170
     # "DR4           DR5           DR6           DR7           DR8")   STA01180
  713 FORMAT("0NODE       DR1           DR2           DR3           DR4", STA01190
     # "           DR5           DR6           DR7           DR8")      STA01200
C                                                                       STA01210
      IF(NFJSO.EQ.0)GO TO 7141                                          STA01220
      PRINT 712                                                         STA01230
      DO 714 I=1,NFJSO                                                  STA01240
      READ(5,*) K,TEMP(6*K-5),TEMP(6*K-4),TEMP(6*K-3),TEMP(6*K-2),      STA01250
     # TEMP(6*K-1),TEMP(6*K)                                            STA01260
      PRINT 716,K,TEMP(6*K-5),TEMP(6*K-4),TEMP(6*K-3),TEMP(6*K-2),      STA01270
     # TEMP(6*K-1),TEMP(6*K)                                            STA01280
  716 FORMAT(I5,1X,1P6E13.5)                                            STA01290
  714 CONTINUE                                                          STA01300
C                                                                       STA01310
      I1=NPR                                                            STA01320
      DO 720 I=1,NJ6                                                    STA01330
      IF(JRL(I).EQ.0)GO TO 720                                          STA01340
      I1=I1+1                                                           STA01350
      DR(I1)=TEMP(I)                                                    STA01360
  720 CONTINUE                                                          STA01370
C                                                                       STA01380
 7141 IF(NPNSO.EQ.0)GO TO 719                                           STA01390
      PRINT 713                                                         STA01400
      DO 717 I=1,IDOL                                                   STA01410
  717 TEMP(I)=0.                                                        STA01420
      DO 715 I=1,NPNSO                                                  STA01430
      READ(5,*) K,TEMP(8*K-7),TEMP(8*K-6),TEMP(8*K-5),TEMP(8*K-4),      STA01440
     # TEMP(8*K-3),TEMP(8*K-2),TEMP(8*K-1),TEMP(8*K)                    STA01450
      PRINT 706,K,TEMP(8*K-7),TEMP(8*K-6),TEMP(8*K-5),TEMP(8*K-4),      STA01460
     # TEMP(8*K-3),TEMP(8*K-2),TEMP(8*K-1),TEMP(8*K)                    STA01470
  715 CONTINUE                                                          STA01480
C                                                                       STA01490
      I1=0                                                              STA01500
      DO 718 I=1,NPO                                                    STA01510
      IF(NRL(I).EQ.0)GO TO 718                                          STA01520
      I1=I1+1                                                           STA01530
      DR(I1)=TEMP(I)                                                    STA01540
  718 CONTINUE                                                          STA01550
C                                                                       STA01560
C-----COMPUTE AF=SFR*DR                                                 STA01570
C                                                                       STA01580
  719 DO 721 I=1,NFT                                                    STA01590
      SUM=AF(I)                                                         STA01600
      DO 722 J=1,NRT                                                    STA01610
  722 SUM=SUM-SFR(I,J)*DR(J)                                            STA01620
  721 AF(I)=SUM                                                         STA01630
C                                                                       STA01640
C-----COMPUTE DF = (SFF)**-1 (AF - SFR * DR)                            STA01650
C                                                                       STA01660
  709 DO 723 I=1,NFT                                                    STA01670
      SFP(I,1)=AF(I)                                                    STA01680
      DO 723 J=1,NFT                                                    STA01690
  723 SPP(I,J)=SFF(I,J)                                                 STA01700
C                                                                       STA01710
      CALL DCOMP(NFT,SPP,NP,NP),RETURNS(724)                            STA01720
      GO TO 726                                                         STA01730
  724 PRINT 725                                                         STA01740
  725 FORMAT("0 DECOMPOSITION OF SFF FAILS IN STATIC")                  STA01750
      RETURN                                                            STA01760
C                                                                       STA01770
  726 CALL SOLVE(NFT,SPP,SFP,SFM,1,1,1,NP,NP,NF,NP,NF,NM)               STA01780
C                                                                       STA01790
```

```
      DO 727 I=1,NFT                                                    STA01800
  727 DF(I)=SFM(I,1)                                                    STA01810
C                                                                       STA01820
C-----PRINT STATIC DISPLACEMENTS FOR STRUCTURE DOF'S                    STA01830
C***** FOR DYN. RESPONSE CALCS., COMPUTE PANEL STRESSES AND REACS. (ISOASTA01840
C                                                                =1)    STA01850
C                                                                       STA01860
      IF(ISOA.EQ.0)GO TO 7032                                           STA01870
 7031 DO 7033 I=1,NFT                                                   STA01880
 7033 DF(I)=RXP(I,ISTAT)                                                STA01890
      LL1=NFT+1                                                         STA01900
      I1=0                                                              STA01910
      DO 7034 I=LL1,NFRT                                                STA01920
      I1=I1+1                                                           STA01930
 7034 DR(I1)=RXP(I,ISTAT)                                               STA01940
      IF(IL.EQ.1)GO TO 7035                                             STA01950
      REWIND 33                                                         STA01960
      READ(33)                                                          STA01970
      READ(33) ((SFR(I,J),J=1,NRT),I=1,NFT)                             STA01980
      GO TO 7035                                                        STA01990
C                                                                       STA02000
 7032 IC=0                                                              STA02010
      PRINT 7271                                                        STA02020
 7271 FORMAT("0STATIC DISPLACEMENTS - STRUCTURE DOF'S ONLY",/,          STA02030
     # " NODE        01            02            03            04",    STA02040
     # "            05            06            07            08")     STA02050
      DO 726 I=1,NPN                                                    STA02060
      PRINT 730,I                                                       STA02070
  730 FORMAT(I4)                                                        STA02080
      I1=6*I-7                                                          STA02090
      I0=I1+7                                                           STA02100
      KC=-12+4                                                          STA02110
      DO 729 J=I1,I0                                                    STA02120
      KC=KC+13                                                          STA02130
      IF(NFL(J).EQ.0)GO TO 729                                          STA02140
      IC=IC+1                                                           STA02150
      PRINT 731,KC,DF(IC)                                               STA02160
  731 FORMAT("+",=X,1PE13.5)                                            STA02170
  729 CONTINUE                                                          STA02180
  726 CONTINUE                                                          STA02190
C                                                                       STA02200
 7035 IF((IREAC.EQ.0).AND.(ISTRES.EQ.0))GO TO 955                       STA02210
C                                                                       STA02220
C-----COMPUTE FRAME AND PANEL DISPLACEMENTS                             STA02230
C                                                                       STA02240
      IF(NFM.GT.0)GO TO 600                                             STA02250
C     COMPUTE DP() FOR NFM=0 CASE                                       STA02260
      REWIND 10                                                         STA02270
      READ(10) ((TPF(I,J),J=1,NFT),I=1,NPT)                             STA02280
      READ(10) ((TPR(I,J),J=1,NRT),I=1,NPT)                             STA02290
C                                                                       STA02300
      DO 601 I=1,NPT                                                    STA02310
      SUM=0.                                                            STA02320
      DO 602 J=1,NFT                                                    STA02330
  602 SUM=SUM-TPF(I,J)*DF(J)                                            STA02340
      DO 603 K=1,NRT                                                    STA02350
  603 SUM=SUM-TPR(I,K)*DR(K)                                            STA02360
  601 DP(I)=SUM                                                         STA02370
      GO TO 607                                                         STA02380
C     COMPUTE DM() AND DP() FOR NFM>0 CASE                              STA02390
  600 IF((IL.GT.1).OR.(LN.GT.1))GO TO 6033                              STA02400
      BACKSPACE 10                                                      STA02410
      BACKSPACE 10                                                      STA02420
 6033 READ(10) ((TMFS(I,J),J=1,NFT),I=1,NMT)                            STA02430
      READ(10) ((TMRS(I,J),J=1,NRT),I=1,NMT)                            STA02440
      DO 610 I=1,NMT                                                    STA02450
      SUM=0.                                                            STA02460
      DO 611 J=1,NFT                                                    STA02470
  611 SUM=SUM-TMFS(I,J)*DF(J)                                           STA02480
      DO 612 K=1,NRT                                                    STA02490
  612 SUM=SUM-TMRS(I,K)*DR(K)                                           STA02500
  610 DM(I)=SUM                                                         STA02510
C                                                                       STA02520
      REWIND 10                                                         STA02530
      READ(10) ((TPF(I,J),J=1,NFT),I=1,NPT)                             STA02540
      READ(10) ((TPR(I,J),J=1,NRT),I=1,NPT)                             STA02550
C                                                                       STA02560
      DO 613 I=1,NPT                                                    STA02570
      SUM=0.                                                            STA02580
      DO 614 J=1,NFT                                                    STA02590
  614 SUM=SUM-TPF(I,J)*DF(J)                                            STA02600
      DO 615 K=1,NRT                                                    STA02610
  615 SUM=SUM-TPR(I,K)*DR(K)                                            STA02620
  613 DP(I)=SUM                                                         STA02630
      READ(10) ((TPM(I,J),J=1,NMT),I=1,NPT)                             STA02640
      DO 616 I=1,NPT                                                    STA02650
      SUM=DP(I)                                                         STA02660
      DO 617 J=1,NMT                                                    STA02670
  617 SUM=SUM-TPM(I,J)*DM(J)                                            STA02680
  616 DP(I)=SUM                                                         STA02690
C                                                                       STA02700
C      FORM DISPLACEMENT VECTOR FOR PANEL FROM DF, DP, AND DR           STA02710
C                                                                       STA02720
C                                                                       STA02730
  607 IF=IP=IR=0                                                        STA02740
      DO 604 I=1,NPO                                                    STA02750
      IF(NRL(I).EQ.1)GO TO 605                                          STA02760
      IF(NFL(I).EQ.1)GO TO 606                                          STA02770
      IP=IP+1                                                           STA02780
      DPL(I)=DP(IP)                                                     STA02790
      GO TO 604                                                         STA02800
  605 IR=IR+1                                                           STA02810
      DPL(I)=DR(IR)                                                     STA02820
      GO TO 604                                                         STA02830
  606 IF=IF+1                                                           STA02840
      DPL(I)=DF(IF)                                                     STA02850
  604 CONTINUE                                                          STA02860
C                                                                       STA02870
      PRINT 608                                                         STA02880
  608 FORMAT("0PANEL DISPLACEMENTS - SUMMARY",/," NODE        01",      STA02890
     # "            02            03            04            05",    STA02900
     # "            06            07            08")                  STA02910
      PRINT 609,(I,(DPL(J+8*(I-1)),J=1,8),I=1,NPN)                      STA02920
  609 FORMAT(I4,1X,1P8E13.5)                                            STA02930
C                                                                       STA02940
      IF(NFM.EQ.0)GO TO 500                                             STA02950
C                                                                       STA02960
C     FORM DISPLACEMENT VECTOR OFR FOR FRAME USING DM, DR (FOR NFM>0)   STA02970
C                                                                       STA02980
      IM=0                                                              STA02990
```

```
      IR=NPR                                                            STAC3000
      DO 618 I=1,NJ6                                                    STAC3010
      IF(JRL(I).EQ.1)GO TO 619                                          STAC3020
      IM=IM+1                                                           STAC3030
      OFR(I)=OM(IM)                                                     STAC3040
      GO TO 618                                                         STAC3050
  619 IR=IR+1                                                           STAC3060
      OFR(I)=OR(IR)                                                     STAC3070
  618 CONTINUE                                                          STAC3080
C                                                                       STAC3090
      PRINT 620                                                         STAC3100
  620 FORMAT("0FRAME DISPLACEMENTS",/," JOINT       D1            D2",  STAC3110
     # "          D3            D4            D5            D6")      STAC3120
      PRINT 621,(I,(OFR(J+6*(I-1)),J=1,6),I=1,NFJ)                      STAC3130
  621 FORMAT(I5,1X,1P6E13.5)                                            STAC3140
C                                                                       STAC3150
C-----COMPUTE SUPPORT REACTIONS (IF IREAC > 0)                          STAC3160
C                                                                       STAC3170
  500 IF(IREAC.EQ.0)GO TO 900                                           STAC3180
C     READ IN UNCONDENSED ARRAYS FOR SUPPORT COUPLING (NOTE THAT SFR*   STAC3190
C     (NFM=0) OR SFR** (NFM>0) IS DESTROYED)                            STAC3200
C                                                                       STAC3210
      IKKK=1                                                            STAC3220
      REWIND 11                                                         STAC3230
      READ(11) ((SFR(I,J),J=1,NRT),I=1,NFT)                             STAC3240
      READ(11) ((SPR(I,J),J=1,NRT),I=1,NPT)                             STAC3250
      READ(11) ((SRR(I,J),J=1,NRT),I=1,NRT)                             STAC3260
      DO 501 I=1,NRT                                                    STAC3270
      SUM=0.                                                            STAC3280
      DO 502 J1=1,NRT                                                   STAC3290
  502 SUM=SUM+SRR(I,J1)*OR(J1)                                          STAC3300
      DO 503 J2=1,NFT                                                   STAC3310
  503 SUM=SUM+SFR(J2,I)*OF(J2)                                          STAC3320
      DO 504 J3=1,NPT                                                   STAC3330
  504 SUM=SUM+SPR(J3,I)*OP(J3)                                          STAC3340
  501 AR(I)=SUM                                                         STAC3350
C                                                                       STAC3360
      IF(NFM.EQ.0)GO TO 505                                             STAC3370
C                                                                       STAC3380
      READ(11) ((SMR(I,J),J=1,NRT),I=1,NMT)                             STAC3390
      DO 506 I=1,NRT                                                    STAC3400
      SUM=AR(I)                                                         STAC3410
      DO 507 J=1,NMT                                                    STAC3420
  507 SUM=SUM+SMR(J,I)*OM(J)                                            STAC3430
  506 AR(I)=SUM                                                         STAC3440
C                                                                       STAC3450
  505 IF(ISDA.EQ.1)PRINT 5051                                           STAC3460
 5051 FORMAT("0NOTE - REACTIONS PRESENTED BELOW DO NOT INCLUDE",        STAC3470
     #  " INERTIA EFFECTS")                                            STAC3480
      IF(NRPN.EQ.0)GO TO 520                                            STAC3490
      PRINT 508                                                         STAC3500
  508 FORMAT("0PANEL SUPPORT REACTIONS",/," NODE       AR1           ", STAC3510
     # "AR2           AR3           AR4           AR5           AR6",  STAC3520
     # "           AR7           AR8")                                  STAC3530
      IC=0                                                              STAC3540
      DO 509 I=1,NPN                                                    STAC3550
      PRINT 73C,I                                                       STAC3560
      I1=6*I-7                                                          STAC3570
      I8=I1+7                                                           STAC3580
      KC=-12+4                                                          STAC3590
      DO 510 J=I1,I8                                                    STAC3600
      KC=KC+13                                                          STAC3610
      IF(NRL(J).EQ.0)GO TO 51)                                          STAC3620
      IC=IC+1                                                           STAC3630
      PRINT 731,KC,AR(IC)                                               STAC3640
  510 CONTINUE                                                          STAC3650
  509 CONTINUE                                                          STAC3660
C                                                                       STAC3670
C                                                                       STAC3680
  520 IF(NFR.EQ.0)GO TO 900                                             STAC3690
      PRINT 521                                                         STAC3700
  521 FORMAT("0FRAME SUPPORT REACTIONS",/," JOINT       AR1           ", STAC3710
     # "  AR2           AR3           AR4           AR5           AR6") STAC3720
      IC=NPR                                                            STAC3730
      DO 522 I=1,NFJ                                                    STAC3740
      PRINT 523,I                                                       STAC3750
  523 FORMAT(I5)                                                        STAC3760
      I1=6*I-5                                                          STAC3770
      I6=I1+5                                                           STAC3780
      KC=-12+5                                                          STAC3790
      DO 524 J=I1,I6                                                    STAC3800
      KC=KC+13                                                          STAC3810
      IF(JRL(J).EQ.0)GO TO 524                                          STAC3820
      IC=IC+1                                                           STAC3830
      PRINT 731,KC,AR(IC)                                               STAC3840
  524 CONTINUE                                                          STAC3850
  522 CONTINUE                                                          STAC3860
C                                                                       STAC3870
C-----COMPUTE PANEL STRESSES (IF ISTRES >0)                             STAC3880
C                                                                       STAC3890
  900 IF(ISTRES.EQ.0)GO TO 955                                          STAC3900
C                                                                       STAC3910
      PRINT 957                                                         STAC3920
  957 FORMAT("0ELEMENT STRESSES AND STRESS RESULTANTS",/,               STAC3930
     #       " ------------------------------------")                  STAC3940
C                                                                       STAC3950
      DO 958 IE=1,NPE                                                   STAC3960
C                                                                       STAC3970
      PRINT 959,IE                                                      STAC3980
  959 FORMAT("0ELEMENT NO.",I3,/," NODE        SX            ",        STAC3990
     #  "SY            SXY           MX            MY            MXY") STAC4000
C                                                                       STAC4010
C---  STRESSES SX, SY, SXY FOR REFINED PLANE STRESS (BOW) ELEMENT AND   STAC4020
C     STRESS RESULTANTS MX, MY, MXY FOR PLATE BENDING (BFS) ELEMENT     STAC4030
C                                                                       STAC4040
      A1=XP(ICNTY(IE,2))-XP(ICNTY(IE,1))                                STAC4050
      B1=YP(ICNTY(IE,3))-YP(ICNTY(IE,2))                                STAC4060
      A2=A1/2.                                                          STAC4070
      B2=B1/2.                                                          STAC4080
C                                                                       STAC4090
C---  FORM DISPL. VECTORS (DBOW, DBFS) FOR DOF'S AT CCW NODES OF ELEM. *STAC4100
C                                                              IE       STAC4110
C                                                                       STAC4120
      I1=-4                                                             STAC4130
      DO 960 J=1,4                                                      STAC4140
      I1=I1+4                                                           STAC4150
      J1=6*ICNTY(IE,J)-7                                                STAC4160
      DBOW(I1+1)=DPL(J1)                                                STAC4170
      DBOW(I1+2)=DPL(J1+1)                                              STAC4180
      DBOW(I1+3)=DPL(J1+5)                                              STAC4190
```

```
      DBDW(I1+4)=DPL(J1+6)
      DBFS(I1+1)=DPL(J1+2)
      DBFS(I1+2)=DPL(J1+3)
      DBFS(I1+3)=DPL(J1+4)
  960 DBFS(I1+4)=DPL(J1+7)
C
      CALL BDWSTR(EP,TP,PRP,A1,B1,0.,0.,DBDW,SX,SY,SXY)
      CALL BFSSTR(EP,TP,PRP,A1,B1,0.,0.,DBFS,MX,MY,MXY)
      PRINT 961,ICNTY(IE,1),SX,SY,SXY,MX,MY,MXY
  961 FORMAT(I4,1X,1P6E13.5)
      CALL BDWSTR(EP,TP,PRP,A1,B1,A1,0.,DBDW,SX,SY,SXY)
      CALL BFSSTR(EP,TP,PRP,A1,B1,A1,0.,DBFS,MX,MY,MXY)
      PRINT 961,ICNTY(IE,2),SX,SY,SXY,MX,MY,MXY
      CALL BDWSTR(EP,TP,PRP,A1,B1,A1,B1,DBDW,SX,SY,SXY)
      CALL BFSSTR(EP,TP,PRP,A1,B1,A1,B1,DBFS,MX,MY,MXY)
      PRINT 961,ICNTY(IE,3),SX,SY,SXY,MX,MY,MXY
      CALL BDWSTR(EP,TP,PRP,A1,B1,0.,B1,DBDW,SX,SY,SXY)
      CALL BFSSTR(EP,TP,PRP,A1,B1,0.,B1,DBFS,MX,MY,MXY)
      PRINT 961,ICNTY(IE,4),SX,SY,SXY,MX,MY,MXY
      CALL BDWSTR(EP,TP,PRP,A1,B1,A2,B2,DBDW,SX,SY,SXY)
      CALL BFSSTR(EP,TP,PRP,A1,B1,A2,B2,DBFS,MX,MY,MXY)
      PRINT 962,SX,SY,SXY,MX,MY,MXY
  962 FORMAT(" CNTR",1P6E13.5)
C
  958 CONTINUE
C
C
  955 IF(ISDA.EQ.1)RETURN
C
      IF(IL.LT.NSLC)GO TO 703
      RETURN
      END
```

```
STAL4200
STAD4210
STAL4220
STAL4230
STAL4240
STAL4250
STAL4260
STAL4270
STAL4280
STAD4290
STAL4300
STAL4310
STAC4320
STAG4330
STAD4340
STAL4350
STAD4360
STAG4370
STAG4380
STAD4390
STAD4400
STAG4410
STAG4420
STAD4430
STAD4440
STAD4450
STAC4460
STAD4470
STAC4480
STAD4490
STAC4500
STAD4510
```

```
*DECK MATPRT                                                          MAT 0000
      SUBROUTINE MATPRT(M,N,A,MAX1,MAX2)                              MAT00010
C                                                                     MAT00020
C-----THIS SUBPROGRAM PRINTS AN M BY N MATRIX 9 COLUMNS AT A TIME     MAT00030
C                                                                     MAT00040
C*****MAX1 AND MAX2 ARE THE DIMENSIONS OF THE ARRAY "A" IN THE CALLING PMAT00050
C                                                              PROGRAM. MAT00060
C                                                                     MAT00070
C-----CALLED BY MAIN PROGRAM                                          MAT00080
C                                                                     MAT00090
C                                                                     MAT00100
      REAL A(MAX1,MAX2)                                               MAT00110
      INTEGER RTCOL                                                   MAT00120
C                                                                     MAT00130
  601 FORMAT (" ",I3,1X,1P9E13.5)                                     MAT00140
  602 FORMAT ("0COLUMN#",I4,3X,9(I10,3X))                             MAT00150
  603 FORMAT(" ------",/,"  ROW")                                     MAT00160
      NPAGES = (N-1)/9 + 1                                            MAT00170
      DO 101 I=1,NPAGES                                               MAT00180
      LTCOL = 9*(I-1) + 1                                             MAT00190
      RTCOL = 9*I                                                     MAT00200
      IF (RTCOL.GT.N) RTCOL=N                                         MAT00210
      PRINT 602,(K,K=LTCOL,RTCOL)                                     MAT00220
      PRINT 603                                                       MAT00230
      DO 101 J=1,M                                                    MAT00240
  101 PRINT 601,J,(A(J,K),K=LTCOL,RTCOL)                              MAT00250
      RETURN                                                          MAT00260
      END                                                             MAT00270
```

```
*DECK DCOMP                                                          DCOL0000
      SUBROUTINE DCOMP (N,A,MAX1,MAX2),RETURNS(JBJ)                  DCOL0010
C                                                                    DCOL0020
C-----THIS SUBPROGRAM DECOMPOSES THE SYMMETRIC, POSITIVE-DEFINITE MATRIXDCOL0030
C     A USING THE CHOLESKY SQUARE ROOT METHOD AS DISCUSSED ON PAGE 56 OFDCOL0040
C     'COMPUTER PROGRAMS FOR STRUCTURAL ANALYSIS,' (1967) BY WM. WEAVER,DCOL0050
C     JR.,  MATRIX A IS NXN, BUT MAY BE DIMENSIONED FOR MAX1 X MAX2 IN TDCOL0060
C                                                                 HE     DCOL0070
C     CALLING PROGRAM.                                               DCOL0080
C                                                                    DCOL0090
C                                                                    DCOL0100
      DIMENSION A(MAX1,MAX2)                                         DCOL0110
C                                                                    DCOL0120
      DO 101 I=1,N                                                   DCOL0130
      DO 101 J=I,N                                                   DCOL0140
      SUM=A(I,J)                                                     DCOL0150
      K1=I-1                                                         DCOL0160
      IF(I.EQ.1) GO TO 1                                             DCOL0170
      DO 102 K=1,K1                                                  DCOL0180
  102 SUM=SUM-A(K,I)*A(K,J)                                          DCOL0190
    1 IF(J.NE.I) GO TO 2                                             DCOL0200
      IF(SUM.LE.0.) RETURN JBJ                                       DCOL0210
      TEMP=1.0/SQRT(SUM)                                             DCOL0220
      A(I,J)=TEMP                                                    DCOL0230
      GO TO 101                                                      DCOL0240
    2 A(I,J)=SUM*TEMP                                                DCOL0250
  101 CONTINUE                                                       DCOL0260
C                                                                    DCOL0270
      RETURN                                                         DCOL0280
      END                                                            DCOL0290
```

```
*DECK SOLVE                                                          SOL00000
      SUBROUTINE SOLVE (N,U,B,X,II,IC,NN,MU1,MU2,MB1,MB2,MX1,MX2)    SOL00010
C                                                                    SOL00020
C-----THIS SUBPROGRAM SOLVES THE SYSTEM OF SIMULTANEOUS EQUATIONS,   SOL00030
C     A * X = B, IN A TWO-STEP PROCESS AS DISCUSSED ON PAGE 57 OF    SOL00040
C     'COMPUTER PROGRAMS FOR STRUCTURAL ANALYSIS' BY WM. WEAVER, JR. SOL00050
C     (1967).  SUBPROGRAM 'DCOMP' PROVIDES THE DECOMPOSED VERSION OF SOL00060
C     MATRIX A (STORED IN UPPER TRIANGULAR MATRIX U) NEEDED IN THE   SOL00070
C     SOLUTION PROCESS.  X IS THE VECTOR (OR MATRIX) OF UNKNOWNS AND SOL00080
C     B IS THE VECTOR (OR MATRIX) OF KNOWN QUANTITIES.               SOL00090
C          SUBPROGRAM 'SOLVE' IS MODIFIED HERE SO THAT IT CAN BE USED SOL00100
C     AS THE OBJECT OF A DO STATEMENT WHERE II IS THE DO VARIABLE.   SOL00110
C     THUS, THE MATRIX OF UNKNOWNS, X(N,NN), CAN BE OBTAINED BY CALLING SOL00120
C     'SOLVE' NN TIMES.                                              SOL00130
C     NOTE: IF IC=1, MATRIX B IS USED AS IS; IF IC=2, THE TRANSPOSE  SOL00140
C           OF MATRIX B IS USED.                                     SOL00150
C                                                                    SOL00160
C-----ARRAY SIZES:  U(N X N), B(N X NN), X(N X NN)                   SOL00170
C                                                                    SOL00180
C*****MU1,....,MX2 ARE THE DIMENSIONS OF ARRAYS U, B, AND X          SOL00190
C     IN THE CALLING PROGRAM.                                        SOL00200
C                                                                    SOL00210
C                                                                    SOL00220
      DIMENSION U(MU1,MU2),B(MB1,MB2),X(MX1,MX2)                     SOL00230
C                                                                    SOL00240
      DO 101 I=1,N                                                   SOL00250
      SUM=B(I,II)                                                    SOL00260
      IF(IC.EQ.2) SUM=B(II,I)                                        SOL00270
      K1=I-1                                                         SOL00280
      IF(I.EQ.1) GO TO 101                                           SOL00290
      DO 102 K=1,K1                                                  SOL00300
  102 SUM=SUM-U(K,I)*X(K,II)                                         SOL00310
  101 X(I,II)=SUM*U(I,I)                                             SOL00320
C                                                                    SOL00330
      DO 103 I1=1,N                                                  SOL00340
      I=N-I1+1                                                       SOL00350
      SUM=X(I,II)                                                    SOL00360
      K2=I+1                                                         SOL00370
      IF(I.EQ.N) GO TO 103                                           SOL00380
      DO 104 K=K2,N                                                  SOL00390
  104 SUM=SUM-U(I,K)*X(K,II)                                         SOL00400
  103 X(I,II)=SUM*U(I,I)                                             SOL00410
C                                                                    SOL00420
      RETURN                                                         SOL00430
      END                                                            SOL00440
```

```
*DECK SBOG                                                              SB000000
      SUBROUTINE SBOG (A1, B1, TT, E, U, SB)                            SB000010
C                                                                       SB000020
C-----THIS SUBPROGRAM GENERATES THE ELEMENT STIFFNESS MATRIX FOR        SB000030
C     THE 16 DEGREE-OF-FREEDOM BOGNER-FOX-SCHMIT RECTANGULAR PLATE-     SB000040
C     BENDING ELEMENT (REFERRED TO AS THE BOGNER RECTANGLE ).           SB000050
C         HOWEVER, THE SIGN CONVENTION AND NODAL NUMBERING              SB000060
C     SEQUENCE HAS BEEN CHANGED FROM THAT USED BY BOGNER, ET AL.        SB000070
C                                                                       SB000080
C-----CALLED BY SUBPROGRAM PANLSM                                       SB000090
C                                                                       SB000100
C                                                                       SB000110
      REAL SB(136)                                                      SB000120
C                                                                       SB000130
      D = E*TT**3/(12.0*(1.0 - U*U))                                    SB000140
      O = D/(A1*B1)                                                     SB000150
      A2 = A1*A1                                                        SB000160
      B2 = B1*B1                                                        SB000170
      A = A2/B2                                                         SB000180
      B = B2/A2                                                         SB000190
      SB(  1)=O*(+156./ 35.*B+156./ 35.*A+ 72./ 25.                )    SB000200
      SB(  2)=O*(  22./ 35.*B+ 78./ 35.*A+  6./ 25.+  6./  5.*U)*B1     SB000210
      SB(  3)=O*(- 78./ 35.*B- 22./ 35.*A-  6./ 25.-  6./  5.*U)*A1     SB000220
      SB(  4)=O*(- 11./ 35.*B- 11./ 35.*A-  1./ 50.-  1./  5.*U)*A1*B1  SB000230
      SB(  5)=O*(-156./ 35.*B+ 54./ 35.*A- 72./ 25.                )    SB000240
      SB(  6)=O*(- 22./ 35.*B+ 27./ 35.*A-  6./ 25.-  6./  5.*U)*B1     SB000250
      SB(  7)=O*(- 78./ 35.*B+ 13./ 35.*A-  6./ 25.                )*A1  SB000260
      SB(  8)=O*(- 11./ 35.*B+ 13./ 70.*A-  1./ 50.-  1./ 10.*U)*A1*B1  SB000270
      SB(  9)=O*(- 54./ 35.*B- 54./ 35.*A+ 72./ 25.                )    SB000280
      SB( 10)=O*(  13./ 35.*B+ 27./ 35.*A-  6./ 25.                )*B1  SB000290
      SB( 11)=O*(- 27./ 35.*B- 13./ 35.*A+  6./ 25.                )*A1  SB000300
      SB( 12)=O*(+ 13./ 70.*B+ 13./ 70.*A-  1./ 50.                )*A1*B1 SB000310
      SB( 13)=O*(  54./ 35.*B-156./ 35.*A- 72./ 25.                )    SB000320
      SB( 14)=O*(- 13./ 35.*B+ 78./ 35.*A+  6./ 25.                )*B1  SB000330
      SB( 15)=O*(- 27./ 35.*B+ 22./ 35.*A+  6./ 25.+  6./  5.*U)*A1     SB000340
      SB( 16)=O*(+ 13./ 70.*B- 11./ 35.*A-  1./ 50.-  1./ 10.*U)*A1*B1  SB000350
      SB( 17)=O*(   4./ 35.*B+ 52./ 35.*A+  8./ 25.                )*B2  SB000360
      SB( 18)=O*(- 11./ 35.*B- 11./ 35.*A-  1./ 50.-  6./  5.*U)*A1*B1  SB000370
      SB( 19)=O*(-  2./ 35.*B- 22./105.*A-  2./ 75.-  2./ 15.*U)*A1*B2  SB000380
      SB( 20)=O*(- 22./ 35.*B+ 27./ 35.*A-  6./ 25.-  6./  5.*U)*B1     SB000390
      SB( 21)=O*(-  4./ 35.*B+ 18./ 35.*A-  8./ 25.                )*B2  SB000400
      SB( 22)=O*(- 11./ 35.*B+ 13./ 70.*A-  1./ 50.-  1./ 10.*U)*A1*B1  SB000410
      SB( 23)=O*(-  2./ 35.*B+ 13./105.*A-  2./ 75.                )*A1*B2 SB000420
      SB( 24)=O*(- 13./ 35.*B- 27./ 35.*A+  6./ 25.                )*B1  SB000430
      SB( 25)=O*(   3./ 35.*B+  9./ 35.*A+  2./ 25.                )*B2  SB000440
      SB( 26)=O*(- 13./ 70.*B- 13./ 70.*A+  1./ 50.                )*A1*B1 SB000450
      SB( 27)=O*(+  3./ 70.*B+ 13./210.*A+  1./150.                )*A1*B2 SB000460
      SB( 28)=O*(  13./ 35.*B- 78./ 35.*A-  6./ 25.                )*B1  SB000470
      SB( 29)=O*(-  3./ 35.*B+ 26./ 35.*A-  2./ 25.                )*B2  SB000480
      SB( 30)=O*(- 13./ 70.*B+ 11./ 35.*A+  1./ 50.+  1./ 10.*U)*A1*B1  SB000490
      SB( 31)=O*(+  3./ 70.*B- 11./105.*A+  1./150.+  1./ 30.*U)*A1*B2  SB000500
      SB( 32)=O*(+ 52./ 35.*B+  4./ 35.*A+  8./ 25.                )*A2  SB000510
      SB( 33)=O*(+ 22./105.*B+  2./ 35.*A+  2./ 75.+  2./ 15.*U)*A2*B1  SB000520
      SB( 34)=O*(+ 78./ 35.*B- 13./ 35.*A+  6./ 25.                )*A1  SB000530
      SB( 35)=O*(+ 11./ 35.*B- 13./ 70.*A+  1./ 50.+  1./ 10.*U)*A1*B1  SB000540
      SB( 36)=O*(  26./ 35.*B-  3./ 35.*A-  2./ 25.                )*A2  SB000550
      SB( 37)=O*(+ 11./105.*B-  3./ 70.*A-  1./150.-  1./ 30.*U)*A2*B1  SB000560
      SB( 38)=O*(+ 27./ 35.*B+ 13./ 35.*A-  6./ 25.                )*A1  SB000570
      SB( 39)=O*(- 13./ 70.*B- 13./ 70.*A+  1./ 50.                )*A1*B1 SB000580
      SB( 40)=O*(+  9./ 35.*B-  3./ 35.*A+  2./ 25.                )*A2  SB000590
      SB( 41)=O*(- 13./210.*B-  3./ 70.*A-  1./150.                )*A2*B1  SB000600
      SB( 42)=O*(- 27./ 35.*B+ 22./ 35.*A+  6./ 25.+  6./  5.*U)*A1     SB000610
      SB( 43)=O*(+ 13./ 70.*B- 11./ 35.*A-  1./ 50.-  1./ 10.*U)*A1*B1  SB000620
      SB( 44)=O*(  18./ 35.*B-  4./ 35.*A-  8./ 25.                )*A2  SB000630
      SB( 45)=O*(- 13./105.*B+  2./ 35.*A+  2./ 75.                )*A2*B1  SB000640
      SB( 46)=O*(   4./105.*B+  4./105.*A+  8./225.                )*A2*B2  SB000650
      SB( 47)=O*(+ 11./ 35.*B- 13./ 70.*A+  1./ 50.+  1./ 10.*U)*A1*B1  SB000660
      SB( 48)=O*(+  2./ 35.*B- 13./105.*A+  2./ 75.                )*A1*B2  SB000670
      SB( 49)=O*(+ 11./105.*B-  3./ 70.*A-  1./150.-  1./ 30.*U)*A2*B1  SB000680
      SB( 50)=O*(+  2./105.*B-  1./ 35.*A-  2./225.                )*A2*B2  SB000690
      SB( 51)=O*(+ 13./ 70.*B+ 13./ 70.*A-  1./ 50.                )*A1*B1  SB000700
      SB( 52)=O*(-  3./ 70.*B- 13./210.*A-  1./150.                )*A1*B2  SB000710
      SB( 53)=O*(+ 13./210.*B+  3./ 70.*A+  1./150.                )*A2*B1  SB000720
      SB( 54)=O*(-  1./ 70.*B-  1./ 70.*A+  1./450.                )*A2*B2  SB000730
      SB( 55)=O*(- 13./ 70.*B+ 11./ 35.*A+  1./ 50.+  1./ 10.*U)*A1*B1  SB000740
      SB( 56)=O*(+  3./ 70.*B- 11./105.*A+  1./150.+  1./ 30.*U)*A1*B2  SB000750
      SB( 57)=O*(+ 13./105.*B-  2./ 35.*A-  2./ 75.                )*A2*B1  SB000760
      SB( 58)=O*(-  1./ 35.*B+  2./105.*A-  2./225.                )*A2*B2  SB000770
      SB( 59)=O*( 156./ 35.*B+156./ 35.*A+ 72./ 25.                )    SB000780
      SB( 60)=O*(+ 22./ 35.*B+ 78./ 35.*A+  6./ 25.+  6./  5.*U)*B1     SB000790
      SB( 61)=O*(+ 78./ 35.*B+ 22./ 35.*A+  6./ 25.+  6./  5.*U)*A1     SB000800
      SB( 62)=O*(+ 11./ 35.*B+ 11./ 35.*A+  1./ 50.+  1./  5.*U)*A1*B1  SB000810
      SB( 63)=O*(+ 54./ 35.*B-156./ 35.*A- 72./ 25.                )    SB000820
      SB( 64)=O*(- 13./ 35.*B+ 78./ 35.*A+  6./ 25.                )*B1  SB000830
      SB( 65)=O*(+ 27./ 35.*B- 22./ 35.*A-  6./ 25.-  6./  5.*U)*A1     SB000840
      SB( 66)=O*(- 13./ 70.*B+ 11./ 35.*A+  1./ 50.+  1./ 10.*U)*A1*B1  SB000850
      SB( 67)=O*(- 54./ 35.*B- 54./ 35.*A+ 72./ 25.                )    SB000860
      SB( 68)=O*(  13./ 35.*B+ 27./ 35.*A-  6./ 25.                )*B1  SB000870
      SB( 69)=O*(+ 27./ 35.*B+ 13./ 35.*A-  6./ 25.                )*A1  SB000880
      SB( 70)=O*(- 13./ 70.*B- 13./ 70.*A+  1./ 50.                )*A1*B1  SB000890
      SB( 71)=O*(+  4./ 35.*B+ 52./ 35.*A+  8./ 25.                )*B2  SB000900
      SB( 72)=O*(+ 11./ 35.*B+ 11./ 35.*A+  1./ 50.+  6./  5.*U)*A1*B1  SB000910
      SB( 73)=O*(+  2./ 35.*B+ 22./105.*A+  2./ 75.+  2./ 15.*U)*A1*B2  SB000920
      SB( 74)=O*(+ 13./ 35.*B- 78./ 35.*A-  6./ 25.                )*B1  SB000930
      SB( 75)=O*(-  3./ 35.*B+ 26./ 35.*A-  2./ 25.                )*B2  SB000940
      SB( 76)=O*(+ 13./ 70.*B- 11./ 35.*A-  1./ 50.-  1./ 10.*U)*A1*B1  SB000950
      SB( 77)=O*(-  3./ 70.*B+ 11./105.*A-  1./150.-  1./ 30.*U)*A1*B2  SB000960
      SB( 78)=O*(- 13./ 35.*B- 27./ 35.*A+  6./ 25.                )*B1  SB000970
      SB( 79)=O*(+  3./ 35.*B+  9./ 35.*A+  2./ 25.                )*B2  SB000980
      SB( 80)=O*(+ 13./ 70.*B+ 13./ 70.*A-  1./ 50.                )*A1*B1  SB000990
      SB( 81)=O*(-  3./ 70.*B- 13./210.*A-  1./150.                )*A1*B2  SB001000
      SB( 82)=O*(+ 52./ 35.*B+  4./ 35.*A+  8./ 25.                )*A2  SB001010
      SB( 83)=O*(+ 22./105.*B+  2./ 35.*A+  2./ 75.+  2./ 15.*U)*A2*B1  SB001020
      SB( 84)=O*(+ 27./ 35.*B- 22./ 35.*A-  6./ 25.-  6./  5.*U)*A1     SB001030
      SB( 85)=O*(- 13./ 70.*B+ 11./ 35.*A+  1./ 50.+  1./ 10.*U)*A1*B1  SB001040
      SB( 86)=O*(+ 18./ 35.*B-  4./ 35.*A-  8./ 25.                )*A2  SB001050
      SB( 87)=O*(- 13./105.*B+  2./ 35.*A+  2./ 75.                )*A2*B1  SB001060
      SB( 88)=O*(- 27./ 35.*B- 13./ 35.*A+  6./ 25.                )*A1  SB001070
      SB( 89)=O*(+ 13./ 70.*B+ 13./ 70.*A-  1./ 50.                )*A1*B1  SB001080
      SB( 90)=O*(+  9./ 35.*B-  3./ 35.*A+  2./ 25.                )*A2  SB001090
      SB( 91)=O*(- 13./210.*B-  3./ 70.*A-  1./150.                )*A2*B1  SB001100
      SB( 92)=O*(+  4./105.*B+  4./105.*A+  8./225.                )*A2*B2  SB001110
      SB( 93)=O*(+ 13./ 70.*B- 11./ 35.*A-  1./ 50.-  1./ 10.*U)*A1*B1  SB001120
      SB( 94)=O*(-  3./ 70.*B+ 11./105.*A-  1./150.-  1./ 30.*U)*A1*B2  SB001130
      SB( 95)=O*(+ 13./105.*B-  2./ 35.*A-  2./ 75.                )*A2*B1  SB001140
      SB( 96)=O*(-  1./ 35.*B+  2./105.*A-  2./225.                )*A2*B2  SB001150
      SB( 97)=O*(- 13./ 70.*B- 13./ 70.*A+  1./ 50.                )*A1*B1  SB001160
      SB( 98)=O*(+  3./ 70.*B+ 13./210.*A+  1./150.                )*A1*B2  SB001170
      SB( 99)=O*(+ 13./210.*B+  3./ 70.*A+  1./150.                )*A2*B1  SB001180
      SB(100)=O*(-  1./ 70.*B-  1./ 70.*A+  1./450.                )*A2*B2  SB001190
```

```
SB(101)=D*(+156./ 35.*B+156./ 35.*A+ 72./ 25.                    )        SB001200
SB(102)=D*(- 22./ 35.*B- 78./ 35.*A-  6./ 25.-  6./  5.*U)*B1     SB001210
SB(103)=D*(  78./ 35.*B+ 22./ 35.*A+  6./ 25.+  6./  5.*U)*A1     SB001220
SB(104)=D*(- 11./ 35.*B- 11./ 35.*A-  1./ 50.-  1./  5.*U)*A1*B1  SB001230
SB(105)=D*(-156./ 35.*B+ 54./ 35.*A- 72./ 25.                    )        SB001240
SB(106)=D*(  22./ 35.*B- 27./ 35.*A+  6./ 25.+  6./  5.*U)*B1     SB001250
SB(107)=D*(+ 78./ 35.*B- 13./ 35.*A+  6./ 25.                    )*A1     SB001260
SB(108)=D*(- 11./ 35.*B+ 13./ 70.*A-  1./ 50.-  1./ 10.*U)*A1*B1  SB001270
SB(109)=D*(+  4./ 35.*B+ 52./ 35.*A+  8./ 25.                    )*B2     SB001280
SB(110)=D*(- 11./ 35.*B- 11./ 35.*A-  1./ 50.-  6./  5.*U)*A1*B1  SB001290
SB(111)=D*(+  2./ 35.*B+ 22./105.*A+  2./ 75.+  2./ 15.*U)*A1*B2  SB001300
SB(112)=D*(+ 22./ 35.*B- 27./ 35.*A+  6./ 25.+  6./  5.*U)*B1     SB001310
SB(113)=D*(-  4./ 35.*B+ 18./ 35.*A-  8./ 25.                    )*B2     SB001320
SB(114)=D*(- 11./ 35.*B+ 13./ 70.*A-  1./ 50.-  1./ 10.*U)*A1*B1  SB001330
SB(115)=D*(+  2./ 35.*B- 13./105.*A+  2./ 75.                    )*A1*B2  SB001340
SB(116)=D*(+ 52./ 35.*B+  4./ 35.*A+  8./ 25.                    )*A2     SB001350
SB(117)=D*(- 22./105.*B-  2./ 35.*A-  2./ 75.-  2./ 15.*U)*A2*B1  SB001360
SB(118)=D*(- 78./ 35.*B+ 13./ 35.*A-  6./ 25.                    )*A1     SB001370
SB(119)=D*(+ 11./ 35.*B- 13./ 70.*A+  1./ 50.+  1./ 10.*U)*A1*B1  SB001380
SB(120)=D*(  26./ 35.*B-  3./ 35.*A-  2./ 25.                    )*A2     SB001390
SB(121)=D*(- 11./105.*B+  3./ 70.*A+  1./150.+  1./ 30.*U)*A2*B1  SB001400
SB(122)=D*(+  4./105.*B+  4./105.*A+  8./225.                    (*A2*B2  SB001410
SB(123)=D*(+ 11./ 35.*B- 13./ 70.*A+  1./ 50.+  1./ 10.*U)*A1*B1  SB001420
SB(124)=D*(-  2./ 35.*B+ 13./105.*A-  2./ 75.                    )*A1*B2  SB001430
SB(125)=D*(- 11./105.*B+  3./ 70.*A+  1./150.+  1./ 30.*U)*A2*B1  SB001440
SB(126)=D*(+  2./105.*B-  1./ 35.*A-  2./225.                    )*A2*B2  SB001450
SB(127)=D*( 156./ 35.*B+156./ 35.*A+ 72./ 25.                    )        SB001460
SB(128)=D*(- 22./ 35.*B- 78./ 35.*A-  6./ 25.-  6./  5.*U)*B1     SB001470
SB(129)=D*(+ 78./ 35.*B- 22./ 35.*A-  6./ 25.-  6./  5.*U)*A1     SB001480
SB(130)=D*(+ 11./ 35.*B+ 11./ 35.*A+  1./ 50.+  1./  5.*U)*A1*B1  SB001490
SB(131)=D*(+  4./ 35.*B+ 52./ 35.*A+  8./ 25.                    )*B2     SB001500
SB(132)=D*(+ 11./ 35.*B+ 11./ 35.*A+  1./ 50.+  6./  5.*U)*A1*B1  SB001510
SB(133)=D*(-  2./ 35.*B- 22./105.*A-  2./ 75.-  2./ 15.*U)*A1*B2  SB001520
SB(134)=D*(+ 52./ 35.*B+  4./ 35.*A+  8./ 25.                    )*A2     SB001530
SB(135)=D*(- 22./105.*B-  2./ 35.*A-  2./ 75.-  2./ 15.*U)*A2*B1  SB001540
SB(136)=D*(+  4./105.*B+  4./105.*A+  8./225.                    )*A2*B2  SB001550
RETURN                                                                    SB001560
END                                                                       SB001570
```

```
*DECK SBOM                                                                SB000010
      SUBROUTINE SBOM (XA,YB,TT,E,PR,SOM)                                 SB000020
C                                                                         SB000030
C-----THIS SUBPROGRAM GENERATES THE ELEMENT STIFFNESS MATRIX FOR THE      SB000040
C     16 DEGREE-OF-FREEDOM REFINED RECTANGULAR PLANE STRESS ELEMENT.      SB000050
C                                                                         SB000060
C*****MAX1 AND MAX2 ARE THE DIMENSIONS OF ARRAY 'SOM'                     SB000070
C     IN THE CALLING PROGRAM.                                             SB000080
C                                                                         SB000090
C-----CALLED BY SUBPROGRAM PANLSM                                         SB000100
C                                                                         SB000110
C                                                                         SB000120
      REAL SOM(136)                                                       SB000130
C                                                                         SB000140
      E1=(TT*E)/(1.-PR**2)                                                SB000150
      E2=1.-PR                                                            SB000160
      SOM(1)=E1*(13.*YB/(35.*XA)+E2*XA/(5.*YB))                           SB000170
      SOM(2)=E1*(-.125-.125*PR)                                           SB000180
      SOM(3)=E1*(XA/48.-PR*XA/16.)                                        SB000190
      SOM(4)=E1*(11.*YB*YB/(210.*XA)+E2*XA/60.)                           SB000200
      SOM(5)=E1*(-13.*YB/(35.*XA)+E2*XA/(10.*YB))                         SB000210
      SOM(6)=E1*(.125-.375*PR)                                            SB000220
      SOM(7)=E1*(-XA/48.+PR*XA/16.)                                       SB000230
      SOM(8)=E1*(-11.*YB*YB/(210.*XA)+E2*XA/120.)                         SB000240
      SOM(9)=E1*(9.*YB/(70.*XA)-E2*XA/(5.*YB))                            SB000250
      SOM(10)=E1*(-.125+.375*PR)                                          SB000260
      SOM(11)=E1*(XA/48.+PR*XA/48.)                                       SB000270
      SOM(12)=E1*(-13.*YB*YB/(420.*XA)+E2*XA/60.)                         SB000280
      SOM(13)=E1*(-9.*YB/(70.*XA)-E2*XA/(10.*YB))                         SB000290
      SOM(14)=E1*(.125+PR*.125)                                           SB000300
      SOM(15)=E1*(-XA/48.-PR*XA/48.)                                      SB000310
      SOM(16)=E1*(13.*YB*YB/(420.*XA)+E2*XA/120.)                         SB000320
      SOM(17) =E1*(13.*XA/(35.*YB)+E2*YB/(5.*XA))                         SB000330
      SOM(18) =E1*(11.*XA*XA/(210.*YB)+E2*YB/60.)                         SB000340
      SOM(19) =E1*(YB/48.-PR*YB/16.)                                      SB000350
      SOM(20) =E1*(.375*PR-.125)                                          SB000360
      SOM(21) =E1*(9.*XA/(70.*YB)-E2*YB/(5.*XA))                          SB000370
      SOM(22( =E1*(-13.*XA*XA/(420.*YB)+E2*YB/60.)                        SB000380
      SOM(23) =E1*(YB/48.+PR*YB/48.)                                      SB000390
      SOM(24( =E1*(.125-PR*.375)                                          SB000400
      SOM(25)=E1*(-13.*XA/(35.*YB)+E2*YB/(10.*XA))                        SB000410
      SOM(26)=E1*(-11.*XA*XA/(210.*YB)+E2*YB/120.)                        SB000420
      SOM(27)=E1*(-YB/48.+PR*YB/16.)                                      SB000430
      SOM(28)=E1*(.125+PR*.125)                                           SB000440
      SOM(29)=E1*(-9.*XA/(70.*YB)-E2*YB/(10.*XA))                         SB000450
      SOM(30)=E1*(13.*XA*XA/(420.*YB)+E2*YB/120.)                         SB000460
      SOM(31)=E1*(-YB/48.-PR*YB/48.)                                      SB000470
      SOM(32( =E1*(XA*XA*XA/(105.*YB)+E2*XA*YB/45.)                       SB000480
      SOM(33( =E1*(-XA*YB/288.-PR*XA*YB/288.)                             SB000490
      SOM(34) =E1*(-XA/48.+PR*XA/16.)                                     SB000500
      SOM(35) =E1*(13.*XA*XA/(420.*YB)-E2*YB/60.)                         SB000510
      SOM(36) =E1*(-XA*XA*XA/(140.*YB)-E2*XA*YB/180.(                     SB000520
      SOM(37) =E1*(XA*YB/288.+PR*XA*YB/288.)                              SB000530
      SOM(38) =E1*(-XA/48.-PR*XA/48.)                                     SB000540
      SOM(39)=E1*(-11.*XA*XA/(210.*YB)+E2*YB/120.)                        SB000550
      SOM(40)=E1*(-XA*XA*XA/(105.*YB)+E2*XA*YB/90.)                       SB000560
      SOM(41)=E1*(XA*YB/288.+PR*XA*YB/288.)                               SB000570
      SOM(42)=E1*(XA/48.+PR*XA/48.)                                       SB000580
      SOM(43)=E1*(-13.*XA*XA/(420.*YB)-E2*YB/120.)                        SB000590
      SOM(44)=E1*(XA*XA*XA/(140.*YB)-E2*XA*YB/360.)                       SB000600
```

```
SOW(45)=E1*(-XA*YB/288.-PR*XA*YB/288.)                                  SA0C0640
SOW(46) =E1*(YB*YB*YB/(105.*XA)+E2*XA*YB/45.)                           SA0C0610
SOW(47) =E1*(-11.*YB*YB/(210.*XA)+E2*XA/120.)                           SA0C0620
SOW(48) =E1*(-YB/48.-PR*YB/48.)                                         SA0C0630
SOW(49) =E1*( XA*YB/288.+PR*XA*YB/288.)                                 SA0C0640
SOW(50) =E1*(-YB*YB*YB/(105.*XA)+E2*XA*YB/90.)                          SA0^0650
SOW(51( =E1*(13.*YB*YB/(420.*XA)-E2*XA/60.)                             SA0C0660
SOW(52)=E1*(-YB/48.+PR*YB/16.)                                          SA0C0670
SOW(53)=E1*(XA*YB/288.+PR*XA*YB/288.)                                   SA0L0680
SOW(54)=E1*(-YB*YB*YB/(140.*XA)-E2*XA*YB/180.)                          SA0C0690
SOW(55(=E1*(-13.*YB*YB/(420.*XA)-E2*XA/120.)                            SA0C0700
SOW(56)=E1*(YB/48.+PR*YB/48.)                                           SA0C0710
SOW(57)=E1*(-XA*YB/288.-PR*XA*YB/288.)                                  SA0C0720
SOW(58)=E1*(YB*YB*YB/(140.*XA)-E2*XA*YB/360.)                           SA0C0730
SOW(59) =E1*(13.*YB/(35.*XA)+E2*XA/(5.*YB))                             SA0C0740
SOW(60( =E1*(.125+PR*.125)                                              SA0C0750
SOW(61) =E1*(XA/48.-PR*XA/16.)                                          SA0C0760
SOW(62) =E1*(11.*YB*YB/(210.*XA)+E2*XA/60.)                             SA0C3770
SOW(63) =E1*(-9.*YB/(70.*XA)-E2*XA/(10.*YB))                            SA0C3780
SOW(64)=E1*(-.125-.125*PR)                                              SA0C0790
SOW(65)=E1*(-XA/48.-PR*XA/48.)                                          SA0C0800
SOW(66)=E1*(13.*YB*YB/(420.*XA)+E2*XA/120.)                             SA0C0810
SOW(67)=E1*(9.*YB/(70.*XA)-E2*XA/(5.*YB))                               SA0C0820
SOW(68)=E1*(.125-3.*PR/8.)                                              SA0C0830
SOW(69)=E1*(XA/48+PR*XA/48.)                                            SA0C0840
SOW(70)=E1*(-13.*YB*YB/(420.*XA)+E2*XA/60.)                             SA0C0850
SOW(71( =E1*(13.*XA/(35.*YB)+E2*YB/(5.*XA))                             SA0C0860
SOW(72) =E1*(-11.*XA*XA/(210.*YB)-E2*YB/60.)                            SA0C0870
SOW(73) =E1*(-YB/48.+PR*YB/16.)                                         SA0C0880
SOW(74) =E1*(-.125-PR*.125)                                             SA0C0890
SOW(75)=E1*(-9.*XA/(70.*YB)-E2*YB/(10.*XA))                             SA0C0900
SOW(76)=E1*(-13.*XA*XA/(420.*YB)-E2*YB/120.)                            SA0C0910
SOW(77)=E1*(YB/48.+PR*YB/48.)                                           SA0C0920
SOW(78)=E1*(-.125+3.*PR/8.)                                             SA0C0930
SOW(79)=E1*(-13.*XA/(35.*YB)+E2*YB/(10.*XA))                            SA0C0940
SOW(80)=E1*(11.*XA*XA/(210.*YB)-E2*YB/120.)                             SA0C0950
SOW(81)=E1*(YB/48.-PR*YB/16.)                                           SA0L0960
SOW(82) =E1*(XA*XA*XA/(105.*YB)+E2*XA*YB/45.)                           SA0C0970
SOW(83) =E1*(-XA*YB/288.-PR*XA*YB/288.)                                 SA0C0980
SOW(84) =E1*(XA/48.+PR*XA/48.)                                          SA0C0990
SOW(85)=E1*(13.*XA*XA/(420.*YB)+E2*YB/120.)                             SA0C1000
SOW(86(=E1*(XA*XA*XA/(140.*YB)-E2*XA*YB/360.)                           SA0C1010
SOW(87(=E1*(-XA*YB/288.-PR*XA*YB/288.)                                  SA0C1020
SOW(88)=E1*(-XA/48.-PR*XA/48.)                                          SA0C1030
SOW(89)=E1*(11.*XA*XA/(210.*YB)-E2*YB/120.)                             SA0C1040
SOW(90)=E1*(-XA*XA*XA/(105.*YB)+E2*XA*YB/90.)                           SA0C1050
SOW(91)=E1*(XA*YB/288.+PR*XA*YB/288.)                                   SA0C1060
SOW(92) =E1*(YB*YB*YB/(105.*XA)+E2*XA*YB/45.)                           SA0C1070
SOW(93) =E1*(-13.*YB*YB/(420.*XA)-E2*XA/120.)                           SA0C1080
SOW(94)=E1*(-YB/48.-PR*YB/48.)                                          SA0C1090
SOW(95)=E1*(-YB*XA/288.-PR*XA*YB/288.)                                  SA0C1100
SOW(96)=E1*(YB*YB*YB/(140.*XA)-E2*XA*YB/360.)                           SA0C1110
SOW(97)=E1*(13.*YB*YB/(420.*XA)-E2*XA/60.)                              SA0C1120
SOW(98)=E1*(YB/48.-PR*YB/16.)                                           SA0C1130
SOW(99)=E1*(XA*YB/288.+PR*XA*YB/288.)                                   SA0C1140
SOW(100)=E1*(-YB*YB*YB/(140.*XA)-E2*XA*YB/180.)                         SA0C1150
SOW(1C1) =E1*(13.*YB/(35.*XA)+E2*XA/(5.*YB))                            SA0C1160
SOW(1J2)=E1*(.125+PR*.125)                                              SA0C1170
SOW(103)=E1*(-XA/48.+PR*XA/16.)                                         SA0C1180
SOW(104)=E1*(-11.*YB*YB/(210.*XA)-E2*XA/60.)                            SA0C1190

SOW(105)=E1*(-13.*YB/(35.*XA)+E2*XA/(10.*YB))                           SA0C1200
SOW(106)=E1*(-.125+3.*PR/8.)                                            SA0C1210
SOW(107)=E1*(XA/48.-PR*XA/16.)                                          SA0C1220
SOW(108)=E1*(11.*YB*YB/(210.*XA)-E2*XA/120.)                            SA0C1230
SOW(109)=E1*(13.*XA/(35.*YB)+E2*YB/(5.*XA))                             SA0C1240
SOW(110)=E1*(11.*XA*XA/(210.*YB)+E2*YB/60.)                             SA0C1250
SOW(111)=E1*(YB/48.-PR*YB/16.)                                          SA0C1260
SOW(112)=E1*(.125-3.*PR/8.)                                             SA0C1270
SOW(113)=E1*(9.*XA/(70.*YB)-E2*YB/(5.*XA))                              SA0C1280
SOW(114)=E1*(-13.*XA*XA/(420.*YB)+E2*YB/60.)                            SA0C1290
SOW(115)=E1*(YB/48.+PR*YB/48.)                                          SA0C1300
SOW(116)=E1*(XA*XA*XA/(105.*YB)+E2*XA*YB/45.)                           SA0C1310
SOW(117)=E1*(-XA*YB/288.-PR*XA*YB/288.)                                 SA0C1320
SOW(118)=E1*(XA/48.-PR*XA/16.)                                          SA0C1330
SOW(119)=E1*(13.*XA*XA/(420.*YB)-E2*YB/60.)                             SA0C1340
SOW(120)=E1*(-XA*XA*XA/(140.*YB)-E2*XA*YB/180.)                         SA0C1350
SOW(121)=E1*(XA*YB/288+PR*XA*YB/288.)                                   SA0C1360
SOW(122)=E1*(YB*YB*YB/(105.*XA)+E2*XA*YB/45.)                           SA0C1370
SOW(123)=E1*(11.*YB*YB/(210.*XA)-E2*XA/120.)                            SA0C1380
SOW(124)=E1*(-YB/48.-PR*YB/48.)                                         SA0C1390
SOW(125)=E1*(XA*YB/288.+PR*XA*YB/288.)                                  SA0C1400
SOW(126)=E1*(-YB*YB*YB/(105.*XA)+E2*XA*YB/90.)                          SA0C1410
SOW(127)=E1*(13.*YB/(35.*XA)+E2*XA/(5.*YB))                             SA0C1420
SOW(128)=E1*(-.125-.125*PR)                                             SA0C1430
SOW(129)=E1*(-XA/48.+PR*XA/16.)                                         SA0C1440
SOW(130)=E1*(-11.*YB*YB/(210.*XA)-E2*XA/60.)                            SA0C1450
SOW(131)=E1*(13.*XA/(35.*YB)+E2*YB/(5.*XA))                             SA0C1460
SOW(132)=E1*(-11.*XA*XA/(210.*YB)-E2*YB/60.)                            SA0C1470
SOW(133)=E1*(-YB/48.+PR*YB/16.)                                         SA0C1480
SOW(134)=E1*(XA*XA*XA/(105.*YB)+E2*XA*YB/45.)                           SA0C1490
SOW(135)=E1*(-XA*YB/288.-PR*XA*YB/288.)                                 SA0C1500
SOW(136)=E1*(YB*YB*YB/(105.*XA)+E2*XA*YB/45.)                           SA0C1510
RETURN                                                                  SA0C1520
END                                                                     SA0C1530
```

```
*DECK BOGCM                                                           BOGC0000
      SUBROUTINE  BOGCM (XMD,A1,B1,T,CM)                              BOGC0010
C                                                                     BOGC0020
C-----THIS SUBPROGRAM GENERATES THE CONSISTENT MASS MATRIX FOR THE 16  BOGC0030
C     DEGREE-OF-FREEDOM PLATE BENDING ELEMENT KNOWN AS THE BOGNEP      BOGC0040
C     RECTANGLE.                                                      BOGC0050
C                                                                     BOGC0060
C-----NOTATION:                                                       BOGC0070
C        XMD = MASS DENSITY (KIPS OR LBS-SEC**2/INCHES**4)            BOGC0080
C        A1,B1 = WIDTH AND HEIGHT OF ELEMENT (INCHES)                 BOGC0090
C        T     = ELEMENT THICKNESS (INCHES)                           BOGC0100
C        CM    = VECTOR USED TO STORE THE UPPER TRIANGLE OF THE       BOGC0110
C                    CONSISTENT MASS MATRIX                           BOGC0120
C                                                                     BOGC0130
C-----CALLED BY SUBPROGRAM PANLSM                                     BOGC0140
C                                                                     BOGC0150
      REAL  CM(136)                                                   BOGC0160
C                                                                     BOGC0170
      C1 = XMD*T*A1*B1/1225.0                                         BOGC0180
      A2 = A1*A1                                                      BOGC0190
      B2 = B1*B1                                                      BOGC0200
C                                                                     BOGC0210
      CM(  1) =  169.0/  1.0*C1                                       BOGC0220
      CM(  2) =  143.0/  6.0*C1*B1                                    BOGC0230
      CM(  3) = -143.0/  6.0*C1*A1                                    BOGC0240
      CM(  4) = -121.0/ 36.0*C1*A1*B1                                 BOGC0250
      CM(  5) =  117.0/  2.0*C1                                       BOGC0260
      CM(  6) =   33.0/  4.0*C1*B1                                    BOGC0270
      CM(  7) = +169.0/ 12.0*C1*A1                                    BOGC0280
      CM(  8) =  143.0/ 72.0*C1*A1*B1                                 BOGC0290
      CM(  9) =   81.0/  4.0*C1                                       BOGC0300
      CM( 10) = - 39.0/  8.0*C1*B1                                    BOGC0310
      CM( 11) = + 39.0/  8.0*C1*A1                                    BOGC0320
      CM( 12) = -169.0/144.0*C1*A1*B1                                 BOGC0330
      CM( 13) =  117.0/  2.0*C1                                       BOGC0340
      CM( 14) = -169.0/ 12.0*C1*B1                                    BOGC0350
      CM( 15) = - 33.0/  4.0*C1*A1                                    BOGC0360
      CM( 16) =  143.0/ 72.0*C1*A1*B1                                 BOGC0370
      CM( 17) =   13.0/  3.0*C1*B2                                    BOGC0380
      CM( 18) = -121.0/ 36.0*C1*A1*B1                                 BOGC0390
      CM( 19) = - 11.0/ 18.0*C1*A1*B2                                 BOGC0400
      CM( 20) =   33.0/  4.0*C1*B1                                    BOGC0410
      CM( 21) =    3.0/  2.0*C1*B2                                    BOGC0420
      CM( 22) = +143.0/ 72.0*C1*A1*B1                                 BOGC0430
      CM( 23) =   13.0/ 36.0*C1*A1*B2                                 BOGC0440
      CM( 24) =   39.0/  8.0*C1*B1                                    BOGC0450
      CM( 25) = -  9.0/  8.0*C1*B2                                    BOGC0460
      CM( 26) = +169.0/144.0*C1*A1*B1                                 BOGC0470
      CM( 27) = - 13.0/ 48.0*C1*A1*B2                                 BOGC0480
      CM( 28) =  169.0/ 12.0*C1*B1                                    BOGC0490
      CM( 29) = - 13.0/  4.0*C1*B2                                    BOGC0500
      CM( 30) = -143.0/ 72.0*C1*A1*B1                                 BOGC0510
      CM( 31) =   11.0/ 24.0*C1*A1*B2                                 BOGC0520
      CM( 32) =   13.0/  3.0*C1*A2                                    BOGC0530
      CM( 33) =   11.0/ 18.0*C1*A2*B1                                 BOGC0540
      CM( 34) = -169.0/ 12.0*C1*A1                                    BOGC0550
      CM( 35) = -143.0/ 72.0*C1*A1*B1                                 BOGC0560
      CM( 36) = - 13.0/  4.0*C1*A2                                    BOGC0570
      CM( 37) = - 11.0/ 24.0*C1*A2*B1                                 BOGC0580
      CM( 38) = - 39.0/  8.0*C1*A1                                    BOGC0590
      CM( 39) = +169.0/144.0*C1*A1*B1                                 BOGC0600
      CM( 40) = -  9.0/  8.0*C1*A2                                    BOGC0610
      CM( 41) =   13.0/ 48.0*C1*A2*B1                                 BOGC0620
      CM( 42) = - 33.0/  4.0*C1*A1                                    BOGC0630
      CM( 43) = +143.0/ 72.0*C1*A1*B1                                 BOGC0640
      CM( 44) =    3.0/  2.0*C1*A2                                    BOGC0650
      CM( 45) = - 13.0/ 36.0*C1*A2*B1                                 BOGC0660
      CM( 46) =    1.0/  9.0*C1*A2*B2                                 BOGC0670
      CM( 47) = -143.0/ 72.0*C1*A1*B1                                 BOGC0680
      CM( 48) = - 13.0/ 36.0*C1*A1*B2                                 BOGC0690
      CM( 49) = - 11.0/ 24.0*C1*A2*B1                                 BOGC0700
      CM( 50) = -  1.0/ 12.0*C1*A2*B2                                 BOGC0710
      CM( 51) = -169.0/144.0*C1*A1*B1                                 BOGC0720
      CM( 52) =   13.0/ 48.0*C1*A1*B2                                 BOGC0730
      CM( 53) = - 13.0/ 48.0*C1*A2*B1                                 BOGC0740
      CM( 54) =    1.0/ 16.0*C1*A2*B2                                 BOGC0750
      CM( 55) = -143.0/ 72.0*C1*A1*B1                                 BOGC0760
      CM( 56) =   11.0/ 24.0*C1*A1*B2                                 BOGC0770
      CM( 57) =   13.0/ 36.0*C1*A2*B1                                 BOGC0780
      CM( 58) = -  1.0/ 12.0*C1*A2*B2                                 BOGC0790
      CM( 59) =  169.0/  1.0*C1                                       BOGC0800
      CM( 60) =  143.0/  6.0*C1*B1                                    BOGC0810
      CM( 61) = +143.0/  6.0*C1*A1                                    BOGC0820
      CM( 62) =  121.0/ 36.0*C1*A1*B1                                 BOGC0830
      CM( 63) =  117.0/  2.0*C1                                       BOGC0840
      CM( 64) = -169.0/ 12.0*C1*B1                                    BOGC0850
      CM( 65) = + 33.0/  4.0*C1*A1                                    BOGC0860
      CM( 66) = -143.0/ 72.0*C1*A1*B1                                 BOGC0870
      CM( 67) =   81.0/  4.0*C1                                       BOGC0880
      CM( 68) = - 39.0/  8.0*C1*B1                                    BOGC0890
      CM( 69) = - 39.0/  8.0*C1*A1                                    BOGC0900
      CM( 70) = +169.0/144.0*C1*A1*B1                                 BOGC0910
      CM( 71) =   13.0/  3.0*C1*B2                                    BOGC0920
      CM( 72) = +121.0/ 36.0*C1*A1*B1                                 BOGC0930
      CM( 73) =   11.0/ 18.0*C1*A1*B2                                 BOGC0940
      CM( 74) =  169.0/ 12.0*C1*B1                                    BOGC0950
      CM( 75) = - 13.0/  4.0*C1*B2                                    BOGC0960
      CM( 76) = +143.0/ 72.0*C1*A1*B1                                 BOGC0970
      CM( 77) = - 11.0/ 24.0*C1*A1*B2                                 BOGC0980
      CM( 78) =   39.0/  8.0*C1*B1                                    BOGC0990
      CM( 79) = -  9.0/  8.0*C1*B2                                    BOGC1000
      CM( 80) = -169.0/144.0*C1*A1*B1                                 BOGC1010
      CM( 81) =   13.0/ 48.0*C1*A1*B2                                 BOGC1020
      CM( 82) =   13.0/  3.0*C1*A2                                    BOGC1030
      CM( 83) =   11.0/ 18.0*C1*A2*B1                                 BOGC1040
      CM( 84) = + 33.0/  4.0*C1*A1                                    BOGC1050
      CM( 85) = -143.0/ 72.0*C1*A1*B1                                 BOGC1060
      CM( 86) =    3.0/  2.0*C1*A2                                    BOGC1070
      CM( 87) = - 13.0/ 36.0*C1*A2*B1                                 BOGC1080
      CM( 88) = + 39.0/  8.0*C1*A1                                    BOGC1090
      CM( 89) = -169.0/144.0*C1*A1*B1                                 BOGC1100
      CM( 90) = -  9.0/  8.0*C1*A2                                    BOGC1110
      CM( 91) =   13.0/ 48.0*C1*A2*B1                                 BOGC1120
      CM( 92) =    1.0/  9.0*C1*A2*B2                                 BOGC1130
      CM( 93) =  143.0/ 72.0*C1*A1*B1                                 BOGC1140
      CM( 94) = - 11.0/ 24.0*C1*A1*B2                                 BOGC1150
      CM( 95) = + 13.0/ 36.0*C1*A2*B1                                 BOGC1160
      CM( 96) = -  1.0/ 12.0*C1*A2*B2                                 BOGC1170
      CM( 97) = +169.0/144.0*C1*A1*B1                                 BOGC1180
      CM( 98) = - 13.0/ 48.0*C1*A1*B2                                 BOGC1190
```

```
      CM( 99) = - 13.0/ 48.0*C1*A2*B1
      CM(100) =    1.0/ 16.0*C1*A2*B2
      CM(101) =  169.0/  1.0*C1
      CM(102) = -143.0/  6.0*C1*B1
      CM(103) =  143.0/  6.0*C1*A1
      CM(104) = -121.0/ 36.0*C1*A1*B1
      CM(105) =  117.0/  2.0*C1
      CM(106) = - 33.0/  4.0*C1*B1
      CM(107) = -169.0/ 12.0*C1*A1
      CM(108) =  143.0/ 72.0*C1*A1*B1
      CM(109) =   13.0/  3.0*C1*B2
      CM(110) = -121.0/ 36.0*C1*A1*B1
      CM(111) =   11.0/ 18.0*C1*A1*B2
      CM(112) = - 33.0/  4.0*C1*B1
      CM(113) =    3.0/  2.0*C1*B2
      CM(114) = +143.0/ 72.0*C1*A1*B1
      CM(115) = - 13.0/ 36.0*C1*A1*B2
      CM(116) =   13.0/  3.0*C1*A2
      CM(117) = - 11.0/ 18.0*C1*A2*B1
      CM(118) = +169.0/ 12.0*C1*A1
      CM(119) = -143.0/ 72.0*C1*A1*B1
      CM(120) = - 13.0/  4.0*C1*A2
      CM(121) =   11.0/ 24.0*C1*A2*B1
      CM(122) =    1.0/  9.0*C1*A2*B2
      CM(123) = -143.0/ 72.0*C1*A1*B1
      CM(124) =   13.0/ 36.0*C1*A1*B2
      CM(125) =   11.0/ 24.0*C1*A2*B1
      CM(126) =   -1.0/ 12.0*C1*A2*B2
      CM(127) =  169.0/  1.0*C1
      CM(128) = -143.0/  6.0*C1*B1
      CM(129) = -143.0/  6.0*C1*A1
      CM(130) =  121.0/ 36.0*C1*A1*B1
      CM(131) =   13.0/  3.0*C1*B2
      CM(132) = +121.0/ 36.0*C1*A1*B1
      CM(133) = - 11.0/ 18.0*C1*A1*B2
      CM(134) =   13.0/  3.0*C1*A2
      CM(135) = - 11.0/ 18.0*C1*A2*B1
      CM(136) =    1.0/  9.0*C1*A2*B2
C
      RETURN
      END
```

```
*DECK BOWCM                                                            BOWL0001
      SUBROUTINE BOWCM (XMO,A,B,TT,CM)                                 BOW00010
C                                                                      BOW00020
C-----THIS SUBPROGRAM GENERATES THE CONSISTENT MASS MATRIX FOR THE 16   BOW00030
C     DEGREE-OF-FREEDOM REFINED RECTANGULAR PLANE STRESS ELEMENT (REFER BOW00040
C     TO R. BARBER'S PH.D. THESIS, 'COMPONENT MODE DYNAMIC ANALYSIS OF  BOW00050
C     MULTISTORY FRAMES WITH SHEAR WALLS', UTAH STATE UNIVERSITY, LOGAN,BOW00060
C     UTAH, 1973, FOR DERIVATION).                                     BOW00070
C                                                                      BOW00080
C-----NOTATION:                                                        BOW00090
C       XMO = MASS DENSITY (KIPS OR LBS-SEC**2/INCHES**4)              BOW00100
C       A,B = WIDTH AND HEIGHT OF ELEMENT (INCHES)                     BOW00110
C       TT  = ELEMENT THICKNESS (INCHES)                               BOW00120
C       CM  = ARRAY USED TO STORE THE UPPER TRIANGLE OF THE CONSISTENT  BOW00130
C             MASS MATRIX                                              BOW00140
C       MAX1,MAX2 = DIMENSIONS OF ARRAY 'CM' IN THE CALLING PROGRAM    BOW00150
C                                                                      BOW00160
C-----CALLED BY SUBPROGRAM PANLSM                                      BOW00170
C                                                                      BOW00180
      REAL CM(136)                                                     BOW00190
      DO 100 I=1,136                                                   BOW00200
  100 CM(I)=0.                                                         BOW00210
C                                                                      BOW00220
C                                                                      BOW00230
      XM=XMO*TT                                                        BOW00240
      C1=XM*A*B                                                        BOW00250
      C2=C1*B                                                          BOW00260
      C3=C1*A                                                          BOW00270
      C4=C3*A                                                          BOW00280
      C5=C2*B                                                          BOW00290
C                                                                      BOW00300
      B10=13.*C1/105.                                                  BOW00310
      B11=11.*C2/630.                                                  BOW00320
      B12=B10/2.                                                       BOW00330
      B13=B11/2.                                                       BOW00340
      B14=3.*C1/70.                                                    BOW00350
      B15=13.*C2/1260.                                                 BOW00360
      B16=B14/2.                                                       BOW00370
      B17=B15/2.                                                       BOW00380
      B18=11.*C3/630.                                                  BOW00390
      B19=9.*C1/210.                                                   BOW00400
      B20=13.*C3/1260.                                                 BOW00410
      B21=B18/2.                                                       BOW00420
      B22=B20/2.                                                       BOW00430
      B23=C4/315.                                                      BOW00440
      B24=C4/420.                                                      BOW00450
      B25=B23/2.                                                       BOW00460
      B26=B24/2.                                                       BOW00470
      B27=C5/315.                                                      BOW00480
      B28=B27/2.                                                       BOW00490
      B29=C5/420.                                                      BOW00500
      B30=B29/2.                                                       BOW00510
C                                                                      BOW00520
      CM(1)=B10                                                        BOW00530
      CM(4)=B11                                                        BOW00540
      CM(5)=B12                                                        BOW00550
      CM(8)=B13                                                        BOW00560
      CM(9)=B14                                                        BOW00570
      CM(12)=-B15                                                      BOW00580
      CM(13)=B16                                                       BOW00590
```

```
      CM(16)=-B17                                                       BOWD0600
      CM(17)=B10                                                        BOWD0610
      CM(18)=B18                                                        BOWD0620
      CM(18)=B19                                                        BOWD0630
      CM(22)=-B20                                                       BOWD0640
      CM(25)=B12                                                        BOWD0650
      CM(26)=B21                                                        BOWD0660
      CM(29)=B16                                                        BOWD0670
      CM(30)=-B22                                                       BOWD0680
      CM(32)=B23                                                        BOWD0690
      CM(35)=B20                                                        BOWD0700
      CM(36)=-B24                                                       BOWD0710
      CM(39)=B21                                                        BOWD0720
      CM(40)=B25                                                        BOWD0730
      CM(43)=B22                                                        BOWD0740
      CM(44)=-B26                                                       BOWD0750
      CM(46)=B27                                                        BOWD0760
      CM(47)=B13                                                        BOWD0770
      CM(50)=B28                                                        BOWD0780
      CM(51)=B15                                                        BOWD0790
      CM(54)=-B29                                                       BOWD0800
      CM(55)=B17                                                        BOWD0810
      CM(58)=-B30                                                       BOWD0820
      CM(59)=B18                                                        BOWD0830
      CM(62)=B11                                                        BOWD0840
      CM(63)=B16                                                        BOWD0850
      CM(66)=-B17                                                       BOWD0860
      CM(67)=B14                                                        BOWD0870
      CM(70)=-B15                                                       BOWD0880
      CM(71)=B18                                                        BOWD0890
      CM(72)=-B18                                                       BOWD0900
      CM(75)=B16                                                        BOWD0910
      CM(76)=B22                                                        BOWD0920
      CM(79)=B12                                                        BOWD0930
      CM(80)=-B21                                                       BOWD0940
      CM(82)=B23                                                        BOWD0950
      CM(85)=-B22                                                       BOWD0960
      CM(86)=-B26                                                       BOWD0970
      CM(89)=-B21                                                       BOWD0980
      CM(90)=B25                                                        BOWD0990
      CM(92)=B27                                                        BOWD1000
      CM(93)=B17                                                        BOWD1010
      CM(96)=-B30                                                       BOWD1020
      CM(97)=B15                                                        BOWD1030
      CM(100)=-B29                                                      BOWD1040
      CM(101)=B18                                                       BOWD1050
      CM(104)=-B11                                                      BOWD1060
      CM(105)=B12                                                       BOWD1070
      CM(108)=-B13                                                      BOWD1080
      CM(109)=B10                                                       BOWD1090
      CM(110)=B18                                                       BOWD1100
      CM(113)=B14                                                       BOWD1110
      CM(114)=-B20                                                      BOWD1120
      CM(116)=B23                                                       BOWD1130
      CM(119)=B20                                                       BOWD1140
      CM(120)=-B24                                                      BOWD1150
      CM(122)=B27                                                       BOWD1160
      CM(123)=-B13                                                      BOWD1170
      CM(126)=B28                                                       BOWD1180
      CM(127)=B10                                                       BOWD1190
      CM(130)=-B11                                                      BOWD1200
      CM(131)=B10                                                       BOWD1210
      CM(132)=-B18                                                      BOWD1220
      CM(134)=B23                                                       BOWD1230
      CM(136)=B27                                                       BOWD1240
C                                                                       BOWD1250
      RETURN                                                            BOWD1260
      END                                                               BOWD1270
```

```
*DECK TSET                                                              TSE00020
      SUBROUTINE TSET(PV)                                               TSE00030
C                                                                       TSE00040
C-----SUBPROGRAM TO ASSEMBLE PERMUTATION VECTOR FOR FORMATION OF ELEMENTTSE00050
C     STIFFNESS AND MASS MATRICES FOR THE COMBINATION ELEMENT COMPOSED  TSE00060
C     OF THE BOGNER AND 8-O-H RECTANGLES                                TSE00070
C                                                                       TSE00080
      INTEGER PV(32)                                                    TSE00090
C                                                                       TSE00100
      PV(1)=3                                                           TSE00110
      PV(2)=4                                                           TSE00120
      PV(3)=5                                                           TSE00130
      PV(4)=8                                                           TSE00140
      PV(5)=11                                                          TSE00150
      PV(6)=12                                                          TSE00160
      PV(7)=13                                                          TSE00170
      PV(8)=16                                                          TSE00180
      PV(9)=19                                                          TSE00190
      PV(10)=20                                                         TSE00200
      PV(11)=21                                                         TSE00210
      PV(12)=24                                                         TSE00220
      PV(13)=27                                                         TSE00230
      PV(14)=28                                                         TSE00240
      PV(15)=29                                                         TSE00250
      PV(16)=32                                                         TSE00260
      PV(17)=25                                                         TSE00270
      PV(18)=26                                                         TSE00280
      PV(19)=30                                                         TSE00290
      PV(20)=31                                                         TSE00300
      PV(21)=17                                                         TSE00310
      PV(22)=18                                                         TSE00320
      PV(23)=22                                                         TSE00330
      PV(24)=23                                                         TSE00340
      PV(25)=1                                                          TSE00350
      PV(26)=2                                                          TSE00360
      PV(27)=6                                                          TSE00370
      PV(28)=7                                                          TSE00380
      PV(29)=9                                                          TSE00390
      PV(30)=10                                                         TSE00400
      PV(31)=14                                                         TSE00410
      PV(32)=15                                                         TSE00420
C                                                                       TSE00430
      RETURN                                                            TSE00440
      END                                                               TSE00450
```

```
*DECK BOWSTR                                                            BOW00010
      SUBROUTINE BOWSTR(EP,TP,PRP,XA,YB,XS,YS,D,SX,SY,SXY)              BOW00020
C                                                                       BOW00030
C-----SUBPROGRAM TO COMPUTE STRESSES SX, SY, SXY AT LOCATION (XS,YS)    BOW00040
C     FOR THE REFINED PLANE STRESS ELEMENT OF DIMENSIONS XA BY YB.      BOW00050
C     "D" IS THE VECTOR OF NODAL DISPLACEMENTS AND EP, TP, PRP ARE      BOW00060
C     THE ELEMENT ELASTIC MODULUS, THICKNESS, AND POISSON'S RATIO.      BOW00070
C                                                                       BOW00080
      REAL D(16)                                                        BOW00090
      I1=13                                                             BOW00100
      I2=14                                                             BOW00110
      I3=15                                                             BOW00120
      I4=16                                                             BOW00130
      J1=9                                                              BOW00140
      J2=10                                                             BOW00150
      J3=11                                                             BOW00160
      J4=12                                                             BOW00170
      K1=1                                                              BOW00180
      K2=2                                                              BOW00190
      K3=3                                                              BOW00200
      K4=4                                                              BOW00210
      L1=5                                                              BOW00220
      L2=6                                                              BOW00230
      L3=7                                                              BOW00240
      L4=8                                                              BOW00250
C                                                                       BOW00260
      E1=(EP*TP)/(1.-PRP*PRP)                                           BOW00270
      E2=(1.-PRP)/2.                                                    BOW00280
      E3=E1/TP                                                          BOW00290
      E4=E2/2.                                                          BOW00300
      YB3=(YS/YB)**3                                                    BOW00310
      YB2=(YS/YB)**2                                                    BOW00320
      T1=(2.*YB3-3.*YB2)/XA                                             BOW00330
      T2=(YB3-YB2)*YB/XA                                                BOW00340
      T3=(2.*YB3-3.*YB2+1.)/XA                                          BOW00350
      T4=(YB3-2.*YB2+YS/YB)*YB/XA                                       BOW00360
C                                                                       BOW00370
      STAX=T1*(D(I1)-D(J1)) + T3*(D(L1)-D(K1))                          BOW00380
     #     +T2*(D(I4)-D(J4)) + T4*(D(K4)-D(L4))                         BOW00390
      XA3=(XS/XA)**3                                                    BOW00400
      XA2=(XS/XA)**2                                                    BOW00410
      T1=(2.*XA3-3.*XA2+1.)/YB                                          BOW00420
      T2=(2.*XA3-3.*XA2)/YB                                             BOW00430
      T3=(XA3-2.*XA2+XS/XA)*XA/YB                                       BOW00440
      T4=(XA3-XA2)*XA/YB                                                BOW00450
C                                                                       BOW00460
      STAY=T1*(D(I2)-D(K2)) + T2*(D(L2)-D(J2))                          BOW00470
     #     +T3*(D(I3)-D(K3)) + T4*(D(J3)-D(L3))                         BOW00480
      SXI=E3*(STAX+PRP*STAY)                                            BOW00490
      SYI=E3*(STAY+PRP*STAX)                                            BOW00500
      T1=(1.-XS/XA)                                                     BOW00510
      T2=(1.-YS/YB)                                                     BOW00520
      T3=6.*(YB2-YS/YB)                                                 BOW00530
      T4=3.*YB2-2.*YS/YB                                                BOW00540
      T5=3.*YB2-4.*YS/YB+1.                                             BOW00550
      T6=6.*(XA2-XS/XA)                                                 BOW00560
      T7=3.*XA2-4.*XS/XA+1.                                             BOW00570
      T8=3.*XA2-2.*XS/XA                                                BOW00580
      SXYI=-T1*T3*D(I1)/YB - T1*T4*D(I4) - XS*T3*D(J1)/(XA*YB)          BOW00590
     #     -XS*T4*D(J4)/XA + T1*T3*D(K1)/YB - T1*T5*D(K4)               BOW00600
```

```
     #     +XS*T3*D(L1)/(XA*YB) - XS*T5*D(L4)/XA + YS*T6*D(I2)/(XA*YB)   BOW00600
     #     +YS*T7*D(I3)/YB - YS*T6*D(J2)/(XA*YB) + YS*T8*D(J3)/YB       BOW00610
     #     +T2*T6*D(K2)/XA + T2*T7*D(K3) - T2*T6*D(L2)/XA + T2*T8*D(L3) BOW00620
C                                                                       BOW00630
      SX=SX1                                                            BOW00640
      SY=SYI                                                            BOW00650
      SXY=SXYI*E3*E4                                                    BOW00660
C                                                                       BOW00670
      RETURN                                                            BOW00680
      END                                                               BOW00690
```

```
*DECK BFSSTR                                                            BFS00000
      SUBROUTINE BFSSTR(E,T,PR,A,B,X,Y,DN,MX,MY,MXY)                    BFS00010
C                                                                       BFS00020
C     THIS SUBPROGRAM COMPUTES THE STRESS RESULTANTS OF THE ELEMENT IE  BFS00030
C AT ANY POINT (X,Y) WITH RESPECT TO THE ELEMENT COORDINATES.           BFS00040
C     (BOGNER-FOX-SCHMIT 16 DOF PLATE BENDING ELEMENT)                  BFS00050
C                                                                       BFS00060
      REAL MX,MY,MXY,GMA(16),DN(1)                                      BFS00070
C GENERAL CUBIC BEAM FUNCTIONS AND THIER DERIVATIVES                    BFS00080
      F10(Z,C)=1.0-3.0*(Z/C)**2+2.0*(Z/C)**3                            BFS00090
      F11(Z,C)=-6.0*Z/C**2+6.0*Z**2/C**3                                BFS00100
      F12(Z,C)=-6.0/C**2+12.0*Z/C**3                                    BFS00110
      F20(Z,C)=3.0*(Z/C)**2-2.0*(Z/C)**3                                BFS00120
      F21(Z,C)=6.0*Z/C**2-6.0*Z**2/C**3                                 BFS00130
      F22(Z,C)=6.0/C**2-12.0*Z/C**3                                     BFS00140
      G10(Z,C)=Z-2.0*Z**2/C+Z**3/C**2                                   BFS00150
      G11(Z,C)=1.0-4.0*Z/C+3.0*(Z/C)**2                                 BFS00160
      G12(Z,C)=-4.0/C+6.0*Z/C**2                                        BFS00170
      G20(Z,C)=-Z**2/C+Z**3/C**2                                        BFS00180
      G21(Z,C)=-2.0*Z/C+3.0*(Z/C)**2                                    BFS00190
      G22(Z,C)=-2.0/C+6.0*Z/C**2                                        BFS00200
C                                                                       BFS00210
C                                                                       BFS00220
C COMPUTE THE GENERALIZED STRAINS                                       BFS00230
C (MXX)                                                                 BFS00240
      GMA(1)=F12(X,A)*F10(Y,B)                                          BFS00250
      GMA(2)=F12(X,A)*G10(Y,B)                                          BFS00260
      GMA(3)=-G12(X,A)*F10(Y,B)                                         BFS00270
      GMA(4)=-G12(X,A)*G10(Y,B)                                         BFS00280
      GMA(5)=F22(X,A)*F10(Y,B)                                          BFS00290
      GMA(6)=F22(X,A)*G10(Y,B)                                          BFS00300
      GMA(7)=-G22(X,A)*F10(Y,B)                                         BFS00310
      GMA(8)=-G22(X,A)*G10(Y,B)                                         BFS00320
      GMA(9)=F22(X,A)*F20(Y,B)                                          BFS00330
      GMA(10)=F22(X,A)*G20(Y,B)                                         BFS00340
      GMA(11)=-G22(X,A)*F20(Y,B)                                        BFS00350
      GMA(12)=-G22(X,A)*G20(Y,B)                                        BFS00360
      GMA(13)=F12(X,A)*F20(Y,B)                                         BFS00370
      GMA(14)=F12(X,A)*G20(Y,B)                                         BFS00380
      GMA(15)=-G12(X,A)*F20(Y,B)                                        BFS00390
      GMA(16)=-G12(X,A)*G20(Y,B)                                        BFS00400
      SUM=0.0                                                           BFS00410
      DO 100 I=1,16                                                     BFS00420
100   SUM=SUM+GMA(I)*DN(I)                                              BFS00430
      MXX=SUM                                                           BFS00440
C                                                                       BFS00450
C (MYY)                                                                 BFS00460
      GMA(1)=F10(X,A)*F12(Y,B)                                          BFS00470
      GMA(2)=F10(X,A)*G12(Y,B)                                          BFS00480
      GMA(3)=-G10(X,A)*F12(Y,B)                                         BFS00490
      GMA(4)=-G10(X,A)*G12(Y,B)                                         BFS00500
      GMA(5)=F20(X,A)*F12(Y,B)                                          BFS00510
      GMA(6)=F20(X,A)*G12(Y,B)                                          BFS00520
      GMA(7)=-G20(X,A)*F12(Y,B)                                         BFS00530
      GMA(8)=-G20(X,A)*G12(Y,B)                                         BFS00540
      GMA(9)=F20(X,A)*F22(Y,B)                                          BFS00550
      GMA(10)=F20(X,A)*G22(Y,B)                                         BFS00560
      GMA(11)=-G20(X,A)*F22(Y,B)                                        BFS00570
      GMA(12)=-G20(X,A)*G22(Y,B)                                        BFS00580
      GMA(13)=F10(X,A)*F22(Y,B)                                         BFS00590
```

```
      GMA(14)=F10(X,A)*G22(Y,B)                                         BFS00600
      GMA(15)=-G10(X,A)*F22(Y,B)                                        BFS00610
      GMA(16)=-G10(X,A)*G22(Y,B)                                        BFS00620
      SUM=0.                                                            BFS00630
      DO 200 I=1,16                                                     BFS00640
  200 SUM=SUM+GMA(I)*DN(I)                                              BFS00650
      MYY=SUM                                                           BFS00660
C                                                                       BFS00670
C (MXY)                                                                 BFS00680
      GMA(1)=F11(X,A)*F11(Y,B)                                          BFS00690
      GMA(2)=F11(X,A)*G11(Y,B)                                          BFS00700
      GMA(3)=-G11(X,A)*F11(Y,B)                                         BFS00710
      GMA(4)=-G11(X,A)*G11(Y,B)                                         BFS00720
      GMA(5)=F21(X,A)*F11(Y,B)                                          BFS00730
      GMA(6)=F21(X,A)*G11(Y,B)                                          BFS00740
      GMA(7)=-G21(X,A)*F11(Y,B)                                         BFS00750
      GMA(8)=-G21(X,A)*G11(Y,B)                                         BFS00760
      GMA(9)=F21(X,A)*F21(Y,B)                                          BFS00770
      GMA(10)=F21(X,A)*G21(Y,B)                                         BFS00780
      GMA(11)=-G21(X,A)*F21(Y,B)                                        BFS00790
      GMA(12)=-G21(X,A)*G21(Y,B)                                        BFS00800
      GMA(13)=F11(X,A)*F21(Y,B)                                         BFS00810
      GMA(14)=F11(X,A)*G21(Y,B)                                         BFS00820
      GMA(15)=-G11(X,A)*F21(Y,B)                                        BFS00830
      GMA(16)=-G11(X,A)*G21(Y,B)                                        BFS00840
      SUM=0.0                                                           BFS00850
      DO 300 I=1,16                                                     BFS00860
  300 SUM=SUM+GMA(I)*DN(I)                                              BFS00870
      MXY=SUM                                                           BFS00880
C                                                                       BFS00890
C COMPUTE THE GENERALIZED STRESSES                                      BFS00900
      D=E*T**3/(12.0*(1.0-PR*PR))                                       BFS00910
      MX=D*(MXX + PR*MYY)                                               BFS00920
      MY=D*(MYY + PR*MXX)                                               BFS00930
      MXY=D*(1.0 - PR)*MXY                                              BFS00940
      RETURN                                                            BFS00950
      END                                                               BFS00960
```

```
*DECK DYNAMIC                                                           DYNC0000
      SUBROUTINE DYNAMIC                                                DYNC0010
C                                                                       DYNC0020
C-----SUBPROGRAM TO COMPUTE FREQUENCIES, MODE SHAPES, AND DYNAMIC       DYNC0030
C     RESPONSE OF FRAME-PANEL STRUCTURES.  DISPLACEMENT RESPONSE TO     DYNC0040
C     SPECIFIED X, Y, Z DIRECTION PIECEWISE-LINEAR FORCING FUNCTIONS    DYNC0050
C     (APPLIED FORCES (IAF=1), GROUND ACCELERATION (IGA=1), OR          DYNC0060
C     INDEPENDENT SUPPORT MOTION (ISD=1)) IS COMPUTED, PRINTED (IF      DYNC0070
C     IDTH=1) AND PRINTER PLOTTED (IF NNPLOT>0).  SUPPORT REACTIONS AND DYNC0080
C     PANEL STRESSES ARE DETERMINED AT SPECIFIED TIMES OF INTEREST      DYNC0090
C     THROUGH BACKSUBSTITUTION.                                         DYNC0100
C                                                                       DYNC0110
      REAL NI,LF,MFF,MFR,LFXP,LFYP,LFZP,LFXPA,LFYPA,LFZPA               DYNC0120
      INTEGER PPV,FPV,PLIST                                             DYNC0130
C                                                                       DYNC0140
      COMMON                                                            DYNC0150
     2/C0NFJ/LFXP(32),LFYP(32),LFZP(32),LFXPA(32),LFYPA(32),LFZPA(32),  DYNC0160
     #       IFM(16),JJ(16),ITP(16)                                     DYNC0170
     3/C0NPFO/PPV(200),FPV(96),NFL(200),NRL(200),JFL(96)                DYNC0180
     4/C0STIF/XNI( 40, 40),S( 40, 40),MFF( 40, 40),TT(300),GAX(382),    DYNC0190
     #       GAY(300),GAZ(300),DX(300),DY(300),DZ(300),XDP(300),        DYNC0200
     #       VDP(300),LF(700),SFR( 40, 56),XP(100,198),MFR(120, 56),    DYNC0210
     #       SMM( 45, 45),SMR( 45, 56),SRR( 56, 56)                     DYNC0220
     5/C0TSTOR/XN1(80,80),FREQ(1000,3),PSQ(4060),XL0D(4060)             DYNC0230
     6/C0MISC/FX(46),FY(46),FZ(46),TX(46),TY(46),TZ(46),                DYNC0240
     #       BX(46),BY(46),BZ(46),BAX(46),BAY(46),BAZ(46),              DYNC0250
     #       AX(46),AY(46),AZ(46),G(32),NI(32),PD(32),TLF(103,3),       DYNC0260
     #       TPP(13),V1P(40),X1P(46)                                    DYNC0270
     7/C0DATA/EP,TP,PRP,DENSP,EF,GF,TF,DENSF,NS,SN,MCODE,ISM,           DYNC0280
     #       NRPN,NFT,NPT,NMT,NRT,NF,NP,NM,NR,NPN,NPE,NPD,NPDOF,       DYNC0290
     #       NFJ,NFM,NJ6,NFNSPR,NPNSPR,ISDA,NPR,NFR,NRFJ,              DYNC0300
     #       NFRT,IREAC,ISTRES,ISTAT,IL,IKKK,TIME                       DYNC0310
     8/C0DYND/PLIST(300),IND,INV,IAF,IGA,ISD,NDLC,LN,NPTS,NMODES,       DYNC0320
     #       IDMAX,IDTH,ND,D1,D2,FX0,FY0,FZ0,AX0,AY0,AZ0,SX,SY,SZ,      DYNC0330
     #       SXA,SYA,SZA,NTX,NTY,NTZ                                    DYNC0340
C                                                                       DYNC0350
C-----DETERMINE FREQUENCIES AND MODE SHAPES                             DYNC0360
C                                                                       DYNC0370
      CALL EIGENV                                                       DYNC0380
C                                                                       DYNC0390
C-----COMPUTE AND PRINT/PLOT DISPLACEMENT RESPONSE FOR STRUCTURE DOF'S  DYNC0400
C     FOR "NDLC" LOADINGS                                               DYNC0410
C                                                                       DYNC0420
      LN=0                                                              DYNC0430
   10 LN=LN+1                                                           DYNC0440
C                                                                       DYNC0450
C---1. INPUT DATA FOR DYNAMIC ANALYSIS (IF NDLC > 0)                    DYNC0460
C                                                                       DYNC0470
      CALL DYDATA                                                       DYNC0480
      IF(NDLC.EQ.0)RETURN                                               DYNC0490
C                                                                       DYNC0500
C---2. COMPUTE DYNAMIC RESPONSE                                         DYNC0510
C                                                                       DYNC0520
      CALL RESPON                                                       DYNC0530
C                                                                       DYNC0540
C---3. BACKSUBSTITUTE TO OBTAIN PANEL AND FRAME DISPLACEMENTS AT ALL    DYNC0550
C      NODES; SUPPORT REACTIONS; AND PANEL STRESSES AND STRESS RESULT-  DYNC0560
C      ANTS (AT SPECIFIED TIMES OF INTEREST ONLY)                       DYNC0570
C                                                                       DYNC0580
      READ(5,*) NSATI,IREAC,ISTRES                                      DYNC0590
```

```
      IL=0                                                              DYNC0600
      IF(NSATI.EQ.0)GO TO 11                                            DYNC0610
      PRINT 13                                                          DYNC0620
   13 FORMAT("1DYNAMIC RESPONSE - PANEL STRESSES AND SUPPORT",          DYNC0630
     #  " REACTIONS",/,1X,55("-"))                                      DYNC0640
      IF(NSATI.EQ.-1)GO TO 12                                           DYNC0650
      READ(5,*) (PLIST(I),I=1,NSATI)                                    DYNC0660
      GO TO 14                                                          DYNC0670
   12 NSATI=NPTS                                                        DYNC0680
      DO 15 I=1,NPTS                                                    DYNC0690
   15 PLIST(I)=I                                                        DYNC0700
   14 DO 16 I=1,NSATI                                                   DYNC0710
      IL=IL+1                                                           DYNC0720
      ISTAT=PLIST(I)                                                    DYNC0730
      TIME=TT(ISTAT)                                                    DYNC0740
      PRINT 17,TIME                                                     DYNC0750
   17 FORMAT(//,10X,50("*"),/,10X,"*",48(" "),"*",/,10X,"*",14(" "),    DYNC0760
     #  "TIME =",1PE14.5,14(" "),"*",/,10X,"*",48(" "),"*",/,10X,       DYNC0770
     #  50("*"),/)                                                      DYNC0780
      CALL STATIC                                                       DYNC0790
   16 CONTINUE                                                          DYNC0800
C                                                                       DYNC0810
   11 IF(LN.LT.NDLC)GO TO 10                                            DYNC0820
C                                                                       DYNC0830
      RETURN                                                            DYNC0840
      END                                                               DYNC0850
```

```
*DECK DYDATA                                                            DYDC0000
      SUBROUTINE DYDATA                                                 DYDC0010
C                                                                       DYDC0020
C-----SUBPROGRAM TO READ IN AND PROCESS DATA FOR DYNAMIC ANALYSIS       DYDC0030
C                                                                       DYDC0040
      REAL NI,LF,MFF,MFR,LFXP,LFYP,LFZP,LFXPA,LFYPA,LFZPA               DYDC0050
      INTEGER PLIST,FPV,FPV                                             DYDC0060
C                                                                       DYDC0070
      COMMON                                                            DYDC0080
     2/CBNFJ/LFXP(32),LFYP(32),LFZP(32),LFXPA(32),LFYPA(32),LFZPA(32),  DYDC0090
     #        IFM(16),JJ(16),ITP(16)                                   DYDC0100
     3/CBNPFD/FPV(200),FPV(96),NFL(200),NRL(200),JRL(96)                DYDC0110
     4/CBSTIF/XN( 40, 40),SI( 40, 40),MFF( 40, 40),TT(300),GAX(300),    DYDC0120
     #        GAY(300),GAZ(300),DX(300),DY(300),DZ(300),XDP(300),       DYDC0130
     #        WDP(300),LF(700),SFR( 40, 56),XP(100,198),MFR(120, 56),   DYDC0140
     #        SMM( 45, 45),SMR( 45, 56),SRR( 56, 56)                    DYDC0150
     5/CBTSTOR/XN1(80,80),FREQ(1000,3),PSQ(4060),XLBDA(4060)            DYDC0160
     6/CBMISC/FX(46),FY(46),FZ(46),TX(46),TY(46),TZ(46),                DYDC0170
     #        BX(46),BY(46),BZ(46),BAX(46),BAY(46),BAZ(46),             DYDC0180
     #        AX(46),AY(46),AZ(46),G(32),NI(32),PD(32),TLF(103,3),      DYDC0190
     #        TPP(13),V1P(40),X1P(40)                                   DYDC0200
     7/CBDATA/EP,TP,PRP,DENSP,EF,GF,TF,DENSF,NS,SN,MCODE,ISM,           DYDC0210
     #        NRPN,NFT,NPT,NMT,NRT,NF,NP,NM,NR,NPN,NPE,NPD,NPDOF,       DYDC0220
     #        NFJ,NFM,NJ6,NFNSPR,NPNSPR,ISDA,NPR,NFR,NRFJ,              DYDC0230
     #        NFRT,IREAC,ISTRES,ISTAT,IL,IKKK,TIME                      DYDC0240
     8/CBDYND/PLIST(300),IND,INV,IAF,IGA,ISD,NDLC,LN,NPTS,NMODES,       DYDC0250
     #        IDMAX,IDTH,ND,D1,D2,FX0,FY0,FZ0,AX0,AY0,AZC,SX,SY,SZ,     DYDC0260
     #        SKA,SYA,SZA,NTX,NTY,NTZ                                   DYDC0270
C                                                                       DYDC0280
C-----PRINT LOADING NUMBER                                              DYDC0290
C                                                                       DYDC0300
      IF(LN.GT.1)GO TO 2001                                             DYDC0310
      READ(5,*) NDLC                                                    DYDC0320
      IF(NDLC.EQ.0) RETURN                                              DYDC0330
      IKKK=0                                                            DYDC0340
      WRITE(11) ((XN1(I,J),J=1,NFT),I=1,NFT)                            DYDC0350
 2001 PRINT 200,LN,NDLC                                                 DYDC0360
  200 FORMAT("1",15X," LOADING CONDITION NUMBER",I3," OF",I3,/,15X,     DYDC0370
     # "  ---------------------------------")                           DYDC0380
C                                                                       DYDC0390
C-----INPUT CONTROL PARAMETERS                                          DYDC0400
C                                                                       DYDC0410
      READ(5,*) IND,INV,IGA,IAF,ISD                                     DYDC0420
      READ(5,*) NMODES,NNPLOT,NJPLOT,IDTH,IDMAX                         DYDC0430
      PRINT 201,IND,INV,IGA,IAF,ISD                                     DYDC0440
  201 FORMAT(" IND INV IGA IAF ISD",/,I3,4I4)                           DYDC0450
      PRINT 202,NMODES,NNPLOT,NJPLOT,IDTH,IDMAX                         DYDC0460
  202 FORMAT(" NMODES NNPLOT NJPLOT  IDTH IDMAX",/,I5,3I7,2I5)          DYDC0470
C                                                                       DYDC0480
      ND=NPD+NJ6                                                        DYDC0490
      DO 2022 I=1,ND                                                    DYDC0500
 2022 PLIST(I)=0                                                        DYDC0510
      IF(NNPLOT.EQ.0)GO TO 2030                                         DYDC0520
      PRINT 2023                                                        DYDC0530
 2023 FORMAT("0PLOT LIST FOR NODE DISPLACEMENT RESPONSE",/," NODE ",    DYDC0540
     # "  01  02  03  04  05  06  07  08")                               DYDC0550
      DO 2024 I=1,NNPLOT                                                DYDC0560
      READ(5,*) N,(ITP(K),K=1,8)                                        DYDC0570
      IL=8*N                                                            DYDC0580
      I1=IL-7                                                           DYDC0590
```

```
      I2=0                                                              DYD00630
      DO 2025 K=I1,IL                                                   DYD00640
      I2=I2+1                                                           DYD00650
 2025 PLIST(K)=ITP(I2)                                                  DYD00660
 2024 PRINT 2026,N,(PLIST(K),K=I1,IL)                                   DYD00670
 2026 FORMAT(I4,1X,8I4)                                                 DYD00680
 2030 IF(NJPLOT.EQ.L)GO TO 2021                                         DYD00690
      PRINT 2028,(I,I=1,6)                                              DYD00700
 2028 FORMAT("0PLOT LIST FOR JOINT DISPLACEMENT RESPONSE",/,            DYD00710
     #  " JOINT",6(" D",I1))                                           DYD00720
      DO 2032 I=1,NJPLOT                                                DYD00730
      READ(5,*) N,(ITP(K),K=1,6)                                        DYD00740
      IL=6*N+NPU                                                        DYD00750
      I1=IL-5                                                           DYD00760
      I2=0                                                              DYD00770
      DO 2029 K=I1,IL                                                   DYD00780
      I2=I2+1                                                           DYD00790
 2029 PLIST(K)=ITP(I2)                                                  DYD00800
 2032 PRINT 2031,N,(PLIST(K),K=I1,IL)                                   DYD00810
 2031 FORMAT(I5,1X,6I4)                                                 DYD00820
C                                                                       DYD00830
C-----MODAL DAMPING DATA ( G(I)=DAMPING FRACTION IN MODE I)             DYD00840
C                                                                       DYD00850
 2021 READ(5,*) (G(I),I=1,NMODES)                                       DYD00860
      PRINT 2409                                                        DYD00870
 2409 FORMAT(*0MODAL DAMPING RATIOS AND DAMPED FREQUENCIES(RAD/SEC)*)   DYD00880
      PRINT 2429                                                        DYD00890
 2429 FORMAT(* MODE  RATIO  DAMPED FREQUENCY(RAD/SEC)*)                 DYD00900
 2419 FORMAT(I4,F8.3,4X,1PE13.5)                                        DYD00910
      DO 203 I=1,NMODES                                                 DYD00920
      P=SQRT(PSQ(I))                                                    DYD00930
      NI(I)=G(I)*P                                                      DYD00940
      PD(I)=P*SQRT(1.-G(I)*G(I))                                        DYD00950
  203 PRINT 2419,I,G(I),PD(I)                                           DYD00960
C                                                                       DYD00970
C-----READ IN INITIAL CONDITIONS OF DISPLACEMENT (XOP) (IF INO=1) AND   DYD00980
C     VELOCITY (VOP) (IF INV=1) AND TRANSFORM TO NORMAL COORDINATES     DYD00990
C     (USE X1P(), V1P(), TPP() AND ITP() AS TEMPORARY STORAGE)          DYD01000
C                                                                       DYD01010
      DO 204 I=1,NPD                                                    DYD01020
  204 V0P(I)=X0P(I)=0.                                                  DYD01030
C-----PRINT DOF TABLE                                                   DYD01040
      PRINT 171                                                         DYD01050
  171 FORMAT(*0DOF TABLE*,/,* DOF   NODE   DISPL. TYPE*)                DYD01060
      DO 170 I=1,NPN                                                    DYD01070
      IL=8*I                                                            DYD01080
      I1=IL-7                                                           DYD01090
      I2=0                                                              DYD01100
      DO 173 K=I1,IL                                                    DYD01110
      I2=I2+1                                                           DYD01120
      IF(PPV(K).GT.NFT)GO TO 173                                        DYD01130
      PRINT 174,PPV(K),I,I2                                             DYD01140
  173 CONTINUE                                                          DYD01150
  174 FORMAT(I4,I5.7X,"D",I1)                                           DYD01160
  170 CONTINUE                                                          DYD01170
      IF(LN.EQ.1)GO TO 1701                                             DYD01180
      IF((IND+INV).EQ.0)GO TO 1701                                      DYD01190
      IF(IKKK.EQ.0)BACKSPACE 11                                         DYD01200
      READ(11) ((XN1(I,J),J=1,NFT),I=1,NFT)                             DYD01210
      IKKK=0                                                            DYD01220
 1701 IF(IND.NE.1)GO TO 205                                             DYD01230
      PRINT 206,(I,I=1,8)                                               DYD01240
  206 FORMAT("0INITIAL DISPLACEMENTS",/," NODE",9X,8("D",I1,11X))       DYD01250
      READ(5,*) NNIND                                                   DYD01260
      DO 2061 I=1,NNIND                                                 DYD01270
      READ(5,*) N,(TPP(K),K=1,8)                                        DYD01280
      IL=8*N                                                            DYD01290
      I1=IL-7                                                           DYD01300
      I2=0                                                              DYD01310
      DO 2060 K=I1,IL                                                   DYD01320
      I2=I2+1                                                           DYD01330
 2060 X0P(PPV(K))=TPP(I2)                                               DYD01340
 2061 PRINT 207,N,(X0P(PPV(K)),K=I1,IL)                                 DYD01350
  207 FORMAT(I4,1X,1P8E13.5)                                            DYD01360
      DO 208 K=1,NMODES                                                 DYD01370
      X1P(K)=0.                                                         DYD01380
      DO 208 I=1,NFT                                                    DYD01390
  208 X1P(K)=X1P(K)+XN1(K,I)*X0P(I)                                     DYD01400
      DO 209 K=1,NMODES                                                 DYD01410
  209 X0P(K)=X1P(K)                                                     DYD01420
  205 IF(INV.NE.1)GO TO 210                                             DYD01430
      PRINT 211,(I,I=1,8)                                               DYD01440
  211 FORMAT("0INITIAL VELOCITIES",/," NODE",9X,8("V",I1,11X))          DYD01450
      READ(5,*) NNINV                                                   DYD01460
      DO 2111 I=1,NNINV                                                 DYD01470
      READ(5,*) N,(TPP(K),K=1,8)                                        DYD01480
      IL=8*N                                                            DYD01490
      I1=IL-7                                                           DYD01500
      I2=0                                                              DYD01510
      DO 2110 K=I1,IL                                                   DYD01520
      I2=I2+1                                                           DYD01530
 2110 V0P(PPV(K))=TPP(I2)                                               DYD01540
 2111 PRINT 207,N,(V0P(PPV(K)),K=I1,IL)                                 DYD01550
      DO 212 K=1,NMODES                                                 DYD01560
      V1P(K)=0.                                                         DYD01570
      DO 212 I=1,NFT                                                    DYD01580
  212 V1P(K)=V1P(K)+XN1(K,I)*V0P(I)                                     DYD01590
      DO 213 K=1,NMODES                                                 DYD01600
  213 V0P(K)=V1P(K)                                                     DYD01610
  210 CONTINUE                                                          DYD01620
C                                                                       DYD01630
C-----CONSTRUCT VECTORS OF LOAD FACTORS IN PRINCIPAL COORDINATES        DYD01640
C     (LFXP, LFYP, LFZP) FOR THREE LOADING CASES                        DYD01650
C                                                                       DYD01660
      DO 215 K=1,NMODES                                                 DYD01670
  215 LFXP(K)=LFYP(K)=LFZP(K)=0.                                        DYD01680
      DO 216 I=1,NO                                                     DYD01690
  216 LF(I)=0.                                                          DYD01700
      IF(IGA.EQ.1)GO TO 217                                             DYD01710
      IF(ISO.EQ.1)GO TO 218                                             DYD01720
      IF(IAF.NE.1)GO TO 237                                             DYD01730
C                                                                       DYD01740
C-----APPLIED FORCING FUNCTION CASE (PROPORTIONAL LOADING ASSUMED)  IAF=DYD01750
C                                                                   1   DYD01760
C                                                                       DYD01770
      READ(5,*) NNLF                                                    DYD01780
      PRINT 219,(I,I=1,8)                                               DYD01790
  219 FORMAT("0LOAD FACTORS AT NODES; APPLIED FORCING FUNCTION CAS:",/,  DYD01800
     #  " NODE",8("     LF",I1))                                       DYD01810
      DO 220 I=1,NNLF                                                   DYD01820
```

```
      READ(5,*) N,(TPP(K),K=1,6)
      IL=6*N
      I1=IL-7
      I2=0
      DO 221 K=I1,IL
      I2=I2+1
  221 LF(PPV(K))=TPP(I2)
  220 PRINT 222,N,(LF(PPV(K)),K=I1,IL)
  222 FORMAT(I4,1X,6F9.3)
C
      DO 223 J=1,NMODES
      LFXP(J)=LFYP(J)=LFZP(J)=0.
      DO 223 K=1,NPN
      K1=6*K-7
      K2=K1+1
      K3=K1+2
      IF(NFL(K1).EQ.0)GO TO 225
      J1=PPV(K1)
      LFXP(J)=LFXP(J)+XN(J1,J)*LF(J1)
  225 IF(NFL(K2).EQ.0)GO TO 226
      J2=PPV(K2)
      LFYP(J)=LFYP(J)+XN(J2,J)*LF(J2)
  226 IF(NFL(K3).EQ.0)GO TO 223
      J3=PPV(K3)
      LFZP(J)=LFZP(J)+XN(J3,J)*LF(J3)
  223 CONTINUE
      GO TO 237
C
C-----GROUND ACCELERATION CASE (GROUND ASSUMED TO BE RIGID): IGA=1
C
  217 CONTINUE
C
C---1. COMPUTE (-)R = (S**-1)*SFR AND STORE IN XN1
C
      IF(LN.EQ.1)GO TO 2271
      REWIND 33
      READ(33) ((S(I,J),J=1,NFT),I=1,NFT)
      READ(33) ((SFR(I,J),J=1,NRT),I=1,NFT)
      READ(33) ((MFF(I,J),J=1,NFT),I=1,NFT)
      READ(33) ((MFR(I,J),J=1,NRT),I=1,NFT)
 2271 CALL OCOMP(NFT,S,NF,NF),RETURNS(227)
      GO TO 230
  227 PRINT 228
  228 FORMAT(///,' DECOMPOSITION OF S FAILS IN DYDATA',///)
      RETURN
  230 DO 231 I=1,NRT
  231 CALL SOLVE(NFT,S,SFR,XN1,I,1,NRT,NF,NF,NF,NR,NP,NP)
C
C---2. COMPUTE (MFF*R+MFR) WHERE R=-XN1: STORE RESULT IN SFR
C
      DO 232 I=1,NFT
      DO 232 J=1,NRT
      SUM=0.
      DO 233 K=1,NFT
  233 SUM=SUM-MFF(I,K)*XN1(K,J)
  232 SFR(I,J)=SUM+MFR(I,J)
C
C---3. COMPUTE (-)XN* * (MFF*R + MFR): STORE RESULT IN XN1
C
      DO 234 I=1,NMODES
      DO 234 J=1,NRT
      XN1(I,J)=0.
      SUM=0.
      DO 235 K=1,NFT
  235 SUM=SUM-XN(K,I)*SFR(K,J)
  234 XN1(I,J)=SUM
C
C---4. COMPUTE LOAD FACTORS IN PRINCIPAL COORDINATES (LFXP, LFYP, LFZP)
C
      DO 239 J=1,NMODES
      LFXP(J)=LFYP(J)=LFZP(J)=0.
      IF(NPR.EQ.0)GO TO 240
      DO 236 KN=1,NPN
      K1=6*KN-7
      IF(NRL(K1).NE.1)GO TO 2371
      LFXP(J)=LFXP(J)+XN1(J,PPV(K1)-NPDOF)
 2371 IF(NRL(K1+1).NE.1)GO TO 238
      LFYP(J)=LFYP(J)+XN1(J,PPV(K1+1)-NPDOF)
  238 IF(NRL(K1+2).NE.1)GO TO 236
      LFZP(J)=LFZP(J)+XN1(J,PPV(K1+2)-NPDOF)
  236 CONTINUE
  240 IF(NFR.EQ.0)GO TO 239
      DO 241 KJ=1,NFJ
      K1=6*KJ-5
      IF(JRL(K1).NE.1)GO TO 242
      LFXP(J)=LFXP(J)+XN1(J,FPV(K1)-NMT)
  242 IF(JRL(K1+1).NE.1)GO TO 243
      LFYP(J)=LFYP(J)+XN1(J,FPV(K1+1)-NMT)
  243 IF(JRL(K1+2).NE.1)GO TO 241
      LFZP(J)=LFZP(J)+XN1(J,FPV(K1+2)-NMT)
  241 CONTINUE
  239 CONTINUE
      GO TO 237
C
C-----INDEPENDENT SUPPORT MOTION CASE: ISD =1
C     (NOTE: ONLY TRANSLATIONAL SUPPORT MOTION INPUT IS ALLOWED IN
C      THE X, Y, AND Z DIRECTIONS)
C
  218 CONTINUE
C
C---1. READ IN FACTORS FOR SUPPORT MOTIONS AT RESTRAINED PANEL AND
C      FRAME NODES AND CONSTRUCT THE DISPL. TRANSFORMATION MATRIX TLF(,)
C      (WHERE OR() = TLF(,)*DG() )
C
      IF(LN.EQ.1)GO TO 2273
      REWIND 33
      READ(33) ((S(I,J),J=1,NFT),I=1,NFT)
      READ(33) ((SFR(I,J),J=1,NRT),I=1,NFT)
      READ(33) ((MFF(I,J),J=1,NFT),I=1,NFT)
      READ(33) ((MFR(I,J),J=1,NRT),I=1,NFT)
 2273 DO 250 I=1,NRT
      DO 250 J=1,3
  250 TLF(I,J)=0.
      IF(NPR.EQ.0)GO TO 260
      PRINT 2501,(I,I=1,8)
 2501 FORMAT("0LOAD FACTORS AT PANEL NODES AND FRAME JOINTS:",
     # " INDEPENDENT SUPPORT MOTION CASE",/," NODE",8(6X,"LF",I1))
      DO 251 J=1,NPPN
      READ(5,*) K,(TPP(L),L=1,8)
      K1=8*K-7
```

```
      IF(NRL(K1).EQ.1)TLF(PPV(K1)-NPOOF,1)=TPP(1)                       DYD03000
      IF(NRL(K1+1).EQ.1)TLF(PPV(K1+1)-NPOOF,2)=TPP(2)                   DYD03010
      IF(NRL(K1+2).EQ.1)TLF(PPV(K1+2)-NPOOF,3)=TPP(3)                   DYD03020
  251 PRINT 2502,K,(TPP(L),L=1,6)                                       DYD03030
 2502 FORMAT(I4,1X,6F9.3)                                               DYD03040
  260 IF(NFR.EQ.0)GO TO 270                                             DYD03050
      PRINT 2503,(I,I=1,6)                                              DYD03060
 2503 FORMAT("0JOINT",6(6X,"LF",I1))                                    DYD03070
      DO 261 J=1,NRFJ                                                   DYD03080
      READ(5,*) K,(TPP(L),L=1,6)                                        DYD03090
      K1=6*K-5                                                          DYD03100
      IF(JRL(K1).EQ.1)TLF(FPV(K1)-NMT,1)=TPP(1)                         DYD03110
      IF(JRL(K1+1).EQ.1)TLF(FPV(K1+1)-NMT,2)=TPP(2)                     DYD03120
      IF(JRL(K1+2).EQ.1)TLF(FPV(K1+2)-NMT,3)=TPP(3)                     DYD03130
  261 PRINT 2504,K,(TPP(L),L=1,6)                                       DYD03140
 2504 FORMAT(I5,1X,6F9.3)                                               DYD03150
C                                                                       DYD03160
C---2. COMPUTE (-XN' * SFR) AND STORE IN XN1                            DYD03170
C                                                                       DYD03180
  270 CONTINUE                                                          DYD03190
      DO 271 I=1,NNODES                                                 DYD03200
      DO 271 J=1,NRT                                                    DYD03210
      XN1(I,J)=0.                                                       DYD03220
      SUM=0.                                                            DYD03230
      DO 272 K=1,NFT                                                    DYD03240
  272 SUM=SUM-XN(K,I)*SFR(K,J)                                          DYD03250
  271 XN1(I,J)=SUM                                                      DYD03260
C                                                                       DYD03270
C---3. COMPUTE LFXP, LFYP, LF2P (FOR SUPPORT DISPLACEMENT CASE)         DYD03280
C                                                                       DYD03290
      DO 273 I=1,NNODES                                                 DYD03300
      LFXP(I)=LFYP(I)=LFZP(I)=0.                                        DYD03310
      SUM1=SUM2=SUM3=0.                                                 DYD03320
      DO 274 J=1,NRT                                                    DYD03330
      SUM1=SUM1+XN1(I,J)*TLF(J,1)                                       DYD03340
      SUM2=SUM2+XN1(I,J)*TLF(J,2)                                       DYD03350
  274 SUM3=SUM3+XN1(I,J)*TLF(J,3)                                       DYD03360
      LFXP(I)=SUM1                                                      DYD03370
      LFYP(I)=SUM2                                                      DYD03380
  273 LFZP(I)=SUM3                                                      DYD03390
C                                                                       DYD03400
C---4. COMPUTE (-XN' * MFR) AND STORE IN XN1                            DYD03410
C                                                                       DYD03420
      DO 275 I=1,NNODES                                                 DYD03430
      DO 275 J=1,NRT                                                    DYD03440
      XN1(I,J)=0.                                                       DYD03450
      SUM=0.                                                            DYD03460
      DO 276 K=1,NFT                                                    DYD03470
  276 SUM=SUM-XN(K,I)*MFR(K,J)                                          DYD03480
  275 XN1(I,J)=SUM                                                      DYD03490
C                                                                       DYD03500
C---5. COMPUTE LFXPA, LFYPA, LFZPA (FOR SUPPORT DISPLACEMENT CASE)      DYD03510
C                                                                       DYD03520
      DO 277 I=1,NNODES                                                 DYD03530
      LFXPA(I)=LFYPA(I)=LFZPA(I)=0.                                     DYD03540
      SUM1=SUM2=SUM3=0.                                                 DYD03550
      DO 278 J=1,NPT                                                    DYD03560
      SUM1=SUM1+XN1(I,J)*TLF(J,1)                                       DYD03570
      SUM2=SUM2+XN1(I,J)*TLF(J,2)                                       DYD03580
  278 SUM3=SUM3+XN1(I,J)*TLF(J,3)                                       DYD03590
      LFXPA(I)=SUM1                                                     DYD03600
      LFYPA(I)=SUM2                                                     DYD03610
  277 LFZPA(I)=SUM3                                                     DYD03620
C                                                                       DYD03630
C-----READ IN FORCING FUNCTION ORDINATES (FX,FY,FZ) AND CORRESPONDING   DYD03640
C     POINTS OF SLOPE CHANGE (TX,TY,TZ) (I.E., NTX POINTS IN FX,TX;     DYD03650
C     NTY PTS. IN FY,TY; AND NTZ PTS. IN FZ,TZ); ALSO, READ IN D1 =     DYD03660
C     TIME INTERVAL AT WHICH RESPONSE IS TO BE COMPUTED.                DYD03670
C     NOTE: READ IN SUPPORT ACCEL.-TIME FUNCTIONS ALSO IF ISD=1         DYD03680
C                                                                       DYD03690
  237 PRINT 330                                                         DYD03700
  330 FORMAT("0FORCING FUNCTION ORDINATES AND TIMES OF OCCURRENCE",/,   DYD03710
     # " ----------------------------------------")                    DYD03720
      READ(5,*) NTX,NTY,NTZ,D1                                          DYD03730
      PRINT 229,NTX,NTY,NTZ,D1                                          DYD03740
  229 FORMAT(" NTX =",I3,"  NTY =",I3,"  NTZ =",I3,6X,"RESPONSE TIME",  DYD03750
     # " INTERVAL (D1) =",1PE13.5,/)                                    DYD03760
      IF(ISD.NE.1)PRINT 331                                             DYD03770
      IF(ISD.EQ.1)PRINT 3310                                            DYD03780
  331 FORMAT("      FX",11X,"TX",11X,"FY",11X,"TY",11X,"FZ",11X,"TZ")   DYD03790
 3310 FORMAT(6X,"FX",11X,"TX",11X,"FY",11X,"TY",11X,"FZ",11X,"TZ",      DYD03800
     # 11X,"AX",11X,"AY",11X,"AZ")                                      DYD03810
      NTM=MAX0(NTX,NTY,NTZ)                                             DYD03820
      DO 244 I=1,NTM                                                    DYD03830
      AX(I)=AY(I)=AZ(I)=0.                                              DYD03840
  244 FX(I)=TX(I)=FY(I)=TY(I)=FZ(I)=TZ(I)=BX(I)=BY(I)=BZ(I)=0.          DYD03850
      READ(5,*) (FX(I),I=1,NTX)                                         DYD03860
      IF(ISD.EQ.1)READ(5,*) (AX(I),I=1,NTX)                             DYD03870
      READ(5,*) (TX(I),I=1,NTX)                                         DYD03880
      READ(5,*) (FY(I),I=1,NTY)                                         DYD03890
      IF(ISD.EQ.1)READ(5,*) (AY(I),I=1,NTY)                             DYD03900
      READ(5,*) (TY(I),I=1,NTY)                                         DYD03910
      READ(5,*) (FZ(I),I=1,NTZ)                                         DYD03920
      IF(ISD.EQ.1)READ(5,*) (AZ(I),I=1,NTZ)                             DYD03930
      READ(5,*) (TZ(I),I=1,NTZ)                                         DYD03940
      DO 332 I=1,NTM                                                    DYD03950
      IF(ISD.EQ.1)PRINT 333,FX(I),TX(I),FY(I),TY(I),FZ(I),TZ(I),        DYD03960
     # AX(I),AY(I),AZ(I)                                                DYD03970
      IF(ISD.NE.1)PRINT 333,FX(I),TX(I),FY(I),TY(I),FZ(I),TZ(I)         DYD03980
  332 CONTINUE                                                          DYD03990
  333 FORMAT(1P9E13.5)                                                  DYD04000
C                                                                       DYD04010
C-----CALCULATE SLOPES OF PIECEWISE-LINEAR FORCING FUNCTIONS            DYD04020
C                                                                       DYD04030
      J1=NTX-1                                                          DYD04040
      J2=NTY-1                                                          DYD04050
      J3=NTZ-1                                                          DYD04060
      DO 334 J=1,J1                                                     DYD04070
      DELT=TX(J+1)-TX(J)                                                DYD04080
      IF(ISD.EQ.1)BAX(J)=(AX(J+1)-AX(J))/DELT                           DYD04090
  334 BX(J)=(FX(J+1)-FX(J))/DELT                                        DYD04100
      DO 335 J=1,J2                                                     DYD04110
      DELT=TY(J+1)-TY(J)                                                DYD04120
      IF(ISD.EQ.1)BAY(J)=(AY(J+1)-AY(J))/DELT                           DYD04130
  335 BY(J)=(FY(J+1)-FY(J))/DELT                                        DYD04140
      DO 336 J=1,J3                                                     DYD04150
      DELT=TZ(J+1)-TZ(J)                                                DYD04160
      IF(ISD.EQ.1)BAZ(J)=(AZ(J+1)-AZ(J))/DELT                           DYD04170
  336 BZ(J)=(FZ(J+1)-FZ(J))/DELT                                        DYD04180
C                                                                       DYD04190
```

```
      RETURN                                                            0YD04230
      END                                                               0Y004210
```

```
*DECK RESPON                                                                RESL0030
      SUBROUTINE RESPON                                                     RESL0040
C                                                                           RESL0050
C-----SUBPROGRAM TO COMPUTE/PRINT/PLOT DISPLACEMENT RESPONSE                RESS0060
C                                                                           RESL0070
      REAL NI,LF,MFF,MFP,LFXP,LFYP,LFZP,LFXPA,LFYPA,LFZPA                   RESS0080
      INTEGER PLIST,PPV,FPV,RTCOL,DOF(100,3)                                RESC0090
C                                                                           RESL0100
      COMMON                                                                RESS0110
     2/CBNFJ/LFXP(32),LFYP(32),LFZP(32),LFXPA(32),LFYPA(32),LFZPA(32),      RESS0120
     #        IFM(16),JJ(16),ITP(16)                                       RESS0130
     3/CBNPFO/PPV(200),FPV(96),NFL(200),NRL(200),JRL(96)                    RESC0140
     4/CBSTIF/XN( 40, 40),S( 40, 40),MFF( 40, 40),TT(300),GAX(300),         RESS0150
     #        GAY(300),GAZ(300),DX(300),DY(300),DZ(300),XOP(300),           RESS0160
     #        VOP(300),LF(700),SFR( 40, 56),XP(100,198),MFR(120, 56),       RESS0170
     #        SMM( 45, 45),SMR( 45, 56),SRR( 56, 56)                       RESL0180
     5/CBTSTOR/XN1(80,80),FREQ(1000,3),PSQ(4060),XL8DA(4060)                RESS0190
     6/CBMISC/FX(46),FY(46),FZ(46),TX(46),TY(46),TZ(46),                    RESS0200
     #        BX(46),BY(46),BZ(46),BAX(46),BAY(46),BAZ(46),                 RESS0210
     #        AX(46),AY(46),AZ(46),G(32),NI(32),PD(32),TLF(103,3),          RESS0220
     #        IPP(13),V1P(40),X1P(40)                                       RESC0230
     7/CBDATA/EP,TP,PRP,DENSP,EF,GF,TF,DENSF,NS,SN,MCODE,ISM,               RESS0240
     #        NRPN,NFT,NPT,NMT,NRT,NF,NP,NM,NR,NPN,NPE,NPD,NPDOF,           RESS0250
     #        NFJ,NFM,NJ6,NFNSPR,NPNSPR,ISDA,NPR,NFR,NRFJ,                  RESS0260
     #        NFRT,IREAC,ISTRES,ISTAT,IL,IKKK,TIME                          RESS0270
     8/CBDYNO/PLIST(300),IND,INV,IAF,IGA,ISD,NDLC,LN,NPTS,NMODES,           RESS0280
     #        IDMAX,IDTH,ND,D1,D2,FX0,FY0,FZ0,AX0,AY0,AZ0,SX,SY,SZ,         RESS0290
     #        SXA,SYA,SZA,NTX,NTY,NTZ                                       RESS0300
      EQUIVALENCE (DOF(1,1),FX(1))                                          RESS0310
C                                                                           RESS0320
C-----INITIALIZE FORCING FUNCTIONS                                          RESC0330
      FX0=FX(1)                                                             RESS0340
      FY0=FY(1)                                                             RESS0350
      FZ0=FZ(1)                                                             RESS0360
      AX0=AY0=AZ0=AX1=AY1=AZ1=0.                                            RESS0370
      IF(ISD.NE.1)GO TO 701                                                 RESS0380
      AX0=AX(1)                                                             RESS0390
      AY0=AY(1)                                                             RESS0400
      AZ0=AZ(1)                                                             RESC0410
C-----INITIALIZE TX1, TY1, TZ1 = TOTAL TIME TO NEXT DATA PT. IN FX,FY,FZ    RESS0420
  701 TX1=TX(2)                                                             RESS0430
      TY1=TY(2)                                                             RESS0440
      TZ1=TZ(2)                                                             RESS0450
C-----T1=TIME TO NEXT CORRELATION PT.; T2=TOTAL TIME AT WHICH CURRENT       RESC0460
C       RESPONSE IS BEING COMPUTED (SUCCESSIVE VALUES OF T2 ARE STORED IN   RESS0470
C                                                                 TT( ).    RESS0480
      T1=T2=0.                                                              RESC0490
      KX=KY=KZ=1                                                            RESS0500
C-----INITIALIZE SLOPES OF FUNCTIONS FX, FY, FZ                             RESL0510
      SX=BX(1)                                                              RESS0520
      SY=BY(1)                                                              RESC0530
      SZ=BZ(1)                                                              RESS0540
      SXA=SYA=SZA=0.                                                        RESL0550
      IF(ISD.NE.1)GO TO 702                                                 RESS0560
      SXA=BAX(1)                                                            RESL0570
      SYA=BAY(1)                                                            RESS0580
      SZA=BAZ(1)                                                            RESS0590
  702 I=0                                                                   RESC0600
C-----I=NO. OF PTS. AT WHICH RESPONSE IS COMPUTED (=1,...,NPTS)             RESS0610
  300 I=I+1                                                                 RESS0620
```

```
      NPTS=I-1                                                          RESC0600
      IF((TX1.LE.TY1).AND.(TX1.LE.TZ1)) GO TO 100                       RESC0610
      IF((TY1.LE.TX1).AND.(TY1.LE.TZ1)) GO TO 101                       RESC0620
      TEMP=TZ1                                                          RESC0630
      T1=TZ1-T2                                                         RESC0640
      SX=BX(KX)                                                         RESC0650
      SY=BY(KY)                                                         RESC0660
      SZ=BZ(KZ)                                                         RESC0670
      IF(ISD.NE.1)GO TO 703                                             RESC0680
      SXA=BAX(KX)                                                       RESC0690
      SYA=BAY(KY)                                                       RESC0700
      SZA=BAZ(KZ)                                                       RESC0710
  703 KZ=KZ+1                                                           RESC0720
C-----NTZ=NO. OF DATA PTS. IN FZ(T)                                     RESC0730
      IF(KZ.GT.NTZ) GO TO 400                                           RESC0740
      FX1=FX0+SX*T1                                                     RESC0750
      FY1=FY0+SY*T1                                                     RESC0760
      FZ1=FZ(KZ)                                                        RESC0770
      IF(ISD.NE.1)GO TO 704                                             RESC0780
      AX1=AX0+SXA*T1                                                    RESC0790
      AY1=AY0+SYA*T1                                                    RESC0800
      AZ1=AZ0+SZA*T1                                                    RESC0810
  704 IF(KZ.EQ.NTZ) GO TO 102                                           RESC0820
      TZ1=TZ(KZ+1)                                                      RESC0830
      GO TO 102                                                         RESC0840
  101 TEMP=TY1                                                          RESC0850
      T1=TY1-T2                                                         RESC0860
      SX=BX(KX)                                                         RESC0870
      SY=BY(KY)                                                         RESC0880
      SZ=BZ(KZ)                                                         RESC0890
      IF(ISD.NE.1)GO TO 705                                             RESC0900
      SXA=BAX(KX)                                                       RESC0910
      SYA=BAY(KY)                                                       RESC0920
      SZA=BAZ(KZ)                                                       RESC0930
  705 KY=KY+1                                                           RESC0940
C-----NTY=NO. OF DATA PTS. IN FY(T)                                     RESC0950
      IF(KY.GT.NTY) GO TO 400                                           RESC0960
      FX1=FX0+SX*T1                                                     RESC0970
      FZ1=FZ0+SZ*T1                                                     RESC0980
      FY1=FY(KY)                                                        RESC0990
      IF(ISD.NE.1)GO TO 706                                             RESC1000
      AX1=AX0+SXA*T1                                                    RESC1010
      AY1=AY0+SYA*T1                                                    RESC1020
      AZ1=AZ0+SZA*T1                                                    RESC1030
  706 IF(KY.EQ.NTY) GO TO 102                                           RESC1040
      TY1=TY(KY+1)                                                      RESC1050
      GO TO 102                                                         RESC1060
  100 TEMP=TX1                                                          RESC1070
      T1=TX1-T2                                                         RESC1080
      SX=BX(KX)                                                         RESC1090
      SY=BY(KY)                                                         RESC1100
      SZ=BZ(KZ)                                                         RESC1110
      IF(ISD.NE.1)GO TO 707                                             RESC1120
      SXA=BAX(KX)                                                       RESC1130
      SYA=BAY(KY)                                                       RESC1140
      SZA=BAZ(KZ)                                                       RESC1150
  707 KX=KX+1                                                           RESC1160
C-----NTX=NO. OF DATA PTS. IN FX(T)                                     RESC1170
      IF(KX.GT.NTX) GO TO 400                                           RESC1180
      FY1=FY0+SY*T1                                                     RESC1190
      FZ1=FZ0+SZ*T1                                                     RESC1200
      FX1=FX(KX)                                                        RESC1210
      IF(ISD.NE.1)GO TO 708                                             RESC1220
      AX1=AX0+SXA*T1                                                    RESC1230
      AY1=AY0+SYA*T1                                                    RESC1240
      AZ1=AZ0+SZA*T1                                                    RESC1250
  708 IF(KX.EQ.NTX) GO TO 102                                           RESC1260
      TX1=TX(KX+1)                                                      RESC1270
C-----N1=NO. OF PULSES OF FULL WIDTH D1 BETWEEN CURRENT CORRELATION PTS. RESC1280
  102 N1=INT(T1/D1)                                                     RESC1290
      IF(N1.EQ.0) GO TO 120                                             RESC1300
      I=I-1                                                             RESC1310
C-----COMPUTE RESPONSE AT EACH OF N1 PTS. (PULSE WIDTH = D2) BETWEEN    RESC1320
C       CURRENT CORRELATION PTS.                                        RESC1330
C       IC = INITIAL CONDITION CODE: IF IC=1, COMPUTE I.C. AT NEXT      RESC1340
C       CORRELATION TIME.                                               RESC1350
      DO 200 J=1,N1                                                     RESC1360
      IF(J.EQ.N1) IC=1                                                  RESC1370
      I=I+1                                                             RESC1380
      D2=J*D1                                                           RESC1390
      T2=T2+D1                                                          RESC1400
C-----WHEN EXCITATION=GROUND ACCELERATIONS (IGA=1), SAVE THE X, Y, AND  RESC1410
C     Z RIGID BODY GROUND ACCELERATIONS IN GAX, GAY, GAZ (1.....NPTS)   RESC1420
C     FOR LATER USE IN SUPPORT REACTION CALCULATIONS (SEE "STATIC")     RESC1430
C     OR, WHEN ISD=1, USE DX,DY,DZ TO HOLD THE SUPPORT MOTION           RESC1440
C     AND GAX, GAY, AND GAZ TO HOLD THE SUPPORT ACCELERATION            RESC1450
C     TIME FUNCTIONS AT THE RESPONSE CALCULATION TIMES.                 RESC1460
C                                                                       RESC1470
      IF(IGA.NE.1)GO TO 1030                                            RESC1480
      GAX(I)=FX0+SX*D2                                                  RESC1490
      GAY(I)=FY0+SY*D2                                                  RESC1500
      GAZ(I)=FZ0+SZ*D2                                                  RESC1510
      GO TO 103                                                         RESC1520
 1030 IF(ISD.NE.1)GO TO 103                                             RESC1530
      DX(I)=FX0+SX*D2                                                   RESC1540
      DY(I)=FY0+SY*D2                                                   RESC1550
      DZ(I)=FZ0+SZ*D2                                                   RESC1560
      GAX(I)=AX0+SXA*D2                                                 RESC1570
      GAY(I)=AY0+SYA*D2                                                 RESC1580
      GAZ(I)=AZ0+SZA*D2                                                 RESC1590
  103 CONTINUE                                                          RESC1600
      TT(I)=T2                                                          RESC1610
      CALL RCALC(I,IC)                                                  RESC1620
  200 CONTINUE                                                          RESC1630
      IF((TEMP-T2).LT.0.001) GO TO 130                                  RESC1640
      I=I+1                                                             RESC1650
C-----FINALLY, COMPUTE RESPONSE AT NEXT CORRELATION TIME                RESC1660
  120 T2=TEMP                                                           RESC1670
      D2=T1                                                             RESC1680
      IC=1                                                              RESC1690
      TT(I)=T2                                                          RESC1700
      CALL RCALC(I,IC)                                                  RESC1710
  130 T2=TEMP                                                           RESC1720
      IG=0                                                              RESC1730
      FX0=FX1                                                           RESC1740
      FY0=FY1                                                           RESC1750
      FZ0=FZ1                                                           RESC1760
      IF(IGA.NE.1)GO TO 1310                                            RESC1770
      GAX(I)=FX1                                                        RESC1780
      GAY(I)=FY1                                                        RESC1790
```

```
      GAZ(I)=FZ1                                                        RES01800
      GO TO 131                                                         RES01810
 1310 IF(ISD.NE.1)GO TO 131                                             RES01820
      OX(I)=FX1                                                         RES01830
      OY(I)=FY1                                                         RES01840
      OZ(I)=FZ1                                                         RES01850
      GAX(I)=AX1                                                        RES01860
      GAY(I)=AY1                                                        RES01870
      GAZ(I)=AZ1                                                        RES01880
  131 CONTINUE                                                          RES01890
      DO 132 K=1,NMODES                                                 RES01900
      XOP(K)=X1P(K)                                                     RES01910
  132 VOP(K)=V1P(K)                                                     RES01920
      GO TO 300                                                         RES01930
C                                                                       RES01940
C---TRANSFORM THE NORMAL MODE RESPONSE TO PHYSICAL COORDINATES (X=XN*XP)RES01950
C     USING THE RESPONSE IN MODES 1 TO "NMODES."                        RES01960
C                                                                       RES01970
  400 CONTINUE                                                          RES01980
      DO 142 J=1,NPTS                                                   RES01990
      DO 141 L=1,NFT                                                    RES02000
      X1P(L)=0.                                                         RES02010
      DO 141 K=1,NMODES                                                 RES02020
  141 X1P(L)=X1P(L)+XN(L,K)*XP(K,J)                                     RES02030
      DO 140 LL=1,NFT                                                   RES02040
  140 XP(LL,J)=X1P(LL)                                                  RES02050
  142 CONTINUE                                                          RES02060
      LL1=NFT+1                                                         RES02070
      NFRT=NFT+NRT                                                      RES02080
      DO 1411 J=LL1,NFRT                                                RES02090
      DO 1411 I=1,NPTS                                                  RES02100
 1411 XP(J,I)=0.                                                        RES02110
C                                                                       RES02120
      IF(ISD.NE.1)GO TO 1427                                            RES02130
      IF(NPR.EQ.0)GO TO 1421                                            RES02140
      DO 1422 J=1,NPN                                                   RES02150
      K1=6*J-7                                                          RES02160
      K2=K1+1                                                           RES02170
      K3=K1+2                                                           RES02180
      IF(NRL(K1).EQ.0)GO TO 1423                                        RES02190
      DO 1424 I=1,NPTS                                                  RES02200
 1424 XP(PPV(K1)-NPT,I)=TLF(PPV(K1)-NPDOF,1)*OX(I)                      RES02210
 1423 IF(NRL(K2).EQ.0)GO TO 1425                                        RES02220
      DO 1426 I=1,NPTS                                                  RES02230
 1426 XP(PPV(K2)-NPT,I)=TLF(PPV(K2)-NPDOF,2)*OY(I)                      RES02240
 1425 IF(NRL(K3).EQ.0)GO TO 1422                                        RES02250
      DO 1420 I=1,NPTS                                                  RES02260
 1420 XP(PPV(K3)-NPT,I)=TLF(PPV(K3)-NPDOF,3)*OZ(I)                      RES02270
 1422 CONTINUE                                                          RES02280
 1421 IF(NFR.EQ.0)GO TO 1427                                            RES02290
      DO 1430 J=1,NFJ                                                   RES02300
      J1=6*J-5                                                          RES02310
      J2=J1+1                                                           RES02320
      J3=J1+2                                                           RES02330
      IF(JRL(J1).EQ.0)GO TO 1431                                        RES02340
      JX=FPV(J1)-NMT+NFT                                                RES02350
      JX1=JX-NFT                                                        RES02360
      DO 1432 I=1,NPTS                                                  RES02370
 1432 XP(JX,I)=TLF(JX1,1)*OX(I)                                         RES02380
 1431 IF(JRL(J2).EQ.0)GO TO 1433                                        RES02390
      JY=FPV(J2)-NMT+NFT                                                RES02400
      JY1=JY-NFT                                                        RES02410
      DO 1434 I=1,NPTS                                                  RES02420
 1434 XP(JY,I)=TLF(JY1,2)*OY(I)                                         RES02430
 1433 IF(JRL(J3).EQ.0)GO TO 1430                                        RES02440
      JZ=FPV(J3)-NMT+NFT                                                RES02450
      JZ1=JZ-NFT                                                        RES02460
      DO 1435 I=1,NPTS                                                  RES02470
 1435 XP(JZ,I)=TLF(JZ1,3)*OZ(I)                                         RES02480
 1430 CONTINUE                                                          RES02490
C                                                                       RES02500
C-----PRINT DISPLACEMENT-TIME HISTORY (IF IOTH=1)                       RES02510
C                                                                       RES02520
 1427 IF(IOTH.NE.1) GO TO 500                                           RES02530
      PRINT 150                                                         RES02540
  150 FORMAT("0DISPLACEMENT-TIME HISTORY FOR DEGREES OF FREEDOM",/,     RES02550
     $" ----------------------------------------------")               RES02560
C                                                                       RES02570
C-----FIRST, PRINT THE DEGREE-OF-FREEDOM TABLE                          RES02580
C                                                                       RES02590
      PRINT 171                                                         RES02600
  171 FORMAT("  DOF   NODE  DISPL. TYPE")                               RES02610
      DO 172 I=1,NPN                                                    RES02620
      IL=8*I                                                            RES02630
      I1=IL-7                                                           RES02640
      I2=0                                                              RES02650
      DO 173 K=I1,IL                                                    RES02660
      I2=I2+1                                                           RES02670
      IF(PPV(K).GT.NFT)GO TO 1731                                       RES02680
      DOF(PPV(K),1)=PPV(K)                                              RES02690
      DOF(PPV(K),2)=I                                                   RES02700
      DOF(PPV(K),3)=I2                                                  RES02710
      GO TO 173                                                         RES02720
 1731 IF(ISD.NE.1)GO TO 173                                             RES02730
      IF(NRL(K).NE.1)GO TO 173                                          RES02740
      DOF(PPV(K)-NPT,1)=PPV(K)-NPT                                      RES02750
      DOF(PPV(K)-NPT,2)=I                                               RES02760
      DOF(PPV(K)-NPT,3)=I2                                              RES02770
  173 CONTINUE                                                          RES02780
  172 CONTINUE                                                          RES02790
      ISUM=NFT                                                          RES02800
      IF(ISO.NE.1)GO TO 1740                                            RES02810
      ISUM=NFT+NPR                                                      RES02820
      DO 1732 I=1,NFJ                                                   RES02830
      J1=6*I-5                                                          RES02840
      J6=J1+5                                                           RES02850
      I2=0                                                              RES02860
      DO 1733 J=J1,J6                                                   RES02870
      I2=I2+1                                                           RES02880
      IF(JRL(J).NE.1)GO TO 1733                                         RES02890
      DOF(FPV(J)-NMT+NFT,1)=FPV(J)-NMT+NFT                              RES02900
      DOF(FPV(J)-NMT+NFT,2)=I                                           RES02910
      DOF(FPV(J)-NMT+NFT,3)=I2                                          RES02920
 1733 CONTINUE                                                          RES02930
 1732 CONTINUE                                                          RES02940
 1740 CONTINUE                                                          RES02950
      DO 1741 I=1,ISUM                                                  RES02960
 1741 PRINT 174,(DOF(I,J),J=1,3)                                        RES02970
  174 FORMAT(I4,I5,7X,"0",I1)                                           RES02980
      IF(ISD.NE.1)GO TO 1742                                            RES02990
```

```
      PRINT 1711                                                        RESU3000
 1711 FORMAT("0 DOF JOINT DISPL. TYPE")                                 RESU3010
      ISUM=ISUM+1                                                       RESU3020
      DO 1743 I=ISUM,NFRT                                               RESU3030
 1743 PRINT 174,(DOF(I,J),J=1,3)                                        RESU3040
      ISUM=NFRT                                                         RESU3050
 1742 CONTINUE                                                          RESU3060
C-----NOW, PRINT THE DISPLACEMENT-TIME HISTORY                          RESU3070
  151 FORMAT(* *,I4,2X,1P9E13.5)                                        RESU3080
      NPAGES=(NPTS-1)/9+1                                               RESU3090
      DO 153 I=1,NPAGES                                                 RESU3100
      LTCOL=9*(I-1)+1                                                   RESU3110
      RTCOL=9*I                                                         RESU3120
      IF(RTCOL.GT.NPTS)RTCOL=NPTS                                       RESU3130
      PRINT 154,(TT(K),K=LTCOL,RTCOL)                                   RESU3140
  154 FORMAT(*0TIMES*,1P9E13.5)                                         RESU3150
      PRINT 1541                                                        RESU3160
 1541 FORMAT(" -------")                                                RESU3170
      PRINT 155                                                         RESU3180
  155 FORMAT(*   DOF   DISPLACEMENT RESPONSE*)                         RESU3190
      DO 156 J=1,ISUM                                                   RESU3200
  156 PRINT 151,J,(XP(J,K),K=LTCOL,RTCOL)                               RESU3210
  153 CONTINUE                                                          RESU3220
C                                                                       RESU3230
C-----DETERMINE AND PRINT MAXIMUM DISPLACEMENT RESPONSE AND TIMES OF    RESU3240
C     OCCURRENCE                                                        RESU3250
C                                                                       RESU3260
  500 IF(IOMAX.NE.1)GO TO 600                                           RESU3270
      PRINT 160                                                         RESU3280
  160 FORMAT(*0MAXIMUM DISPLACEMENT RESPONSE*,/,* *,29(*-*),            RESU3290
     # /,* DOF  NODE  DISPL. TYPE     TIME      DISPLACEMENT*)         RESU3300
  161 FORMAT(I3,I6,8X,"0",I1,4X,1P2E13.5)                               RESU3310
      DO 162 I=1,ISUM                                                   RESU3320
      XM=XP(I,1)                                                        RESU3330
      TM=TT(1)                                                          RESU3340
      DO 163 J=2,NPTS                                                   RESU3350
      IF(ABS(XP(I,J)).LE.ABS(XM))GO TO 163                              RESU3360
      XM=XP(I,J)                                                        RESU3370
      TM=TT(J)                                                          RESU3380
  163 CONTINUE                                                          RESU3390
  162 PRINT 161,(DOF(I,J),J=1,3),TM,XM                                  RESU3400
C                                                                       RESU3410
C-----PLOT DISPLACEMENT-TIME HISTORIES FOR DOF'S SPECIFIED IN PLIST():  RESU3420
C     0=DO NOT PLOT, 1=DO PLOT                                          RESU3430
C                                                                       RESU3440
  600 CONTINUE                                                          RESU3450
      DO 601 IP=1,ND                                                    RESU3460
      IF(PLIST(IP).EQ.0)GO TO 601                                       RESU3470
      IF(IP.LE.NPD)GO TO 603                                            RESU3480
      IPF=IP-NPD                                                        RESU3490
      IF(JRL(IPF).NE.1)GO TO 601                                        RESU3500
      JT=(IPF-1)/6+1                                                    RESU3510
      TYP=5HJOINT                                                       RESU3520
      IOIR=IPF-(6*JT-6)                                                 RESU3530
      IROW=FPV(IPF)-NMT+NFT                                             RESU3540
      GO TO 606                                                         RESU3550
  603 JT=(IP-1)/8+1                                                     RESU3560
      IOIR=IP-(8*JT-8)                                                  RESU3570
      TYP=5H NODE                                                       RESU3580
      IROW=PPV(IP)                                                      RESU3590
      IF(NRL(IP).EQ.1)IROW=IROW-NPT                                     RESU3600
  606 PRINT 602,TYP,JT,IOIR                                             RESU3610
  602 FORMAT("1DISPLACEMENT-TIME HISTORY ", A5,I3," -  D",I1,           RESU3620
     # " DIRECTION", /,51("-"),/)                                       RESU3630
      CALL GRAPH(IROW,NPTS)                                             RESU3640
  601 CONTINUE                                                          RESU3650
      PRINT 6011                                                        RESU3660
 6011 FORMAT("1")                                                       RESU3670
      RETURN                                                            RESU3680
      END                                                               RESU3690
```

```
*DECK RCALC                                                          RCAL0000
      SUBROUTINE RCALC(I,IC)                                         RCAL0010
C                                                                    RCAL0020
C-----SUBPROGRAM FOR RESPONSE CALCULATIONS                           RCAL0030
C                                                                    RCAL0040
      REAL NI,LF,MFF,MFR,LFXP,LFYP,LFZP,LFXPA,LFYPA,LFZPA            RCAL0050
      INTEGER PPV,FPV,PLIST                                          RCAL0060
C                                                                    RCAL0070
      COMMON                                                         RCAL0080
     2/CBNFJ/LFXP(32),LFYP(32),LFZP(321,LFXPA(32),LFYPA(32),LFZPA(32),RCAL0090
     #        IFM(16),JJ(16),ITP(16)                                 RCAL0100
     3/CBNPFO/PPV(200),FPV(96),NFL(200),NRL(200),JRL(96)            RCAL0110
     4/CBSTIF/XN( 40, 40),S( 40, 40),MFF( 40, 40),TT(300),GAX(300), RCAL0120
     #        GAY(300),GAZ(300),OX(300),OY(300),OZ(300),XOP(300),    RCAL0130
     #        VOP(300),LF(700),SFR( 40, 56),XP(100,198),MFR(12), 56), RCAL0140
     #        SMM( 45, 45),SMR( 45, 56),SRR( 56, 56)                 RCAL0150
     5/CBISTOR/XN1(80,80),FREQ(1000,3),PSQ(4060),XLBDA(4060)        RCAL0160
     6/CBMISC/FX(46),FY(46),FZ(46),TX(46),TY(46),TZ(46),            RCAL0170
     #        BX(46),BY(46),BZ(46),BAX(46),BAY(46),BAZ(46),         RCAL0180
     #        AX(46),AY(46),AZ(46),G(32),NI(32),PO(32),TLF(103,3),  RCAL0190
     #        TPP(13),V1P(40),X1P(40)                                RCAL0200
     7/CBDATA/EP,TP,PRP,DENSP,EF,GF,TF,DENSF,NS,SN,MCODE,ISM,       RCAL0210
     #        NRPN,NFT,NPT,NMT,NRT,NF,NP,NM,NR,NPN,NPE,NPD,NPDOF,   RCAL0220
     #        NFJ,NFM,NJ6,NFNSPR,NPNSPR,ISOA,NPR,NFR,NRFJ,          RCAL0230
     #        NFRT,IREAG,ISTRES,ISTAT,IL,IKKK,TIME                   RCAL0240
     8/CBDYND/PLIST(300),IND,INV,IAF,IGA,ISO,NOLC,LN,NPTS,NMODES,   RCAL0250
     #        IOMAX,IOTM,NO,O1,O2,FXO,FYO,FZO,AXO,AYO,AZO,SX,SY,SZ,  RCAL0260
     #        SXA,SYA,SZA,NTX,NTY,NTZ                                RCAL0270
C                                                                    RCAL0280
      DO 100 K=1,NMODES                                              RCAL0290
      C1=COS(PO(K)*O2)                                               RCAL0300
      S1=SIN(PO(K)*O2)                                               RCAL0310
      E1=EXP(-NI(K)*O2)                                              RCAL0320
      E2=2*NI(K)/PSQ(K)                                              RCAL0330
      E3=(PO(K)*PO(K)-NI(K)*NI(K))/(PSQ(K)*PO(K))                    RCAL0340
      E4=(VOP(K)+NI(K)*XOP(K))/PO(K)                                 RCAL0350
C---DISPLACEMENT CALCULATIONS (EQU, 4.158A, P.358, "VIBR. PROBS. ENGRG."RCAL0360
C                                                                    RCAL0370
C     ON1 = FIRST LINE OF EQU. 4.158A                                RCAL0380
      ON1=E1*(XOP(K)*C1+E4*S1)                                       RCAL0390
      E5=(1.-E1*(C1+((NI(K)*S1)/PO(K))))/PSQ(K)                      RCAL0400
C-----ONX, ONY, ONZ = 2ND LINE, EQU. 4.158A, FOR X, Y, Z DIRECTIONS  RCAL0410
      IF(ISO.NE.1)GO TO 201                                          RCAL0420
      ONX=(LFXP(K)*FXO+LFXPA(K)*AXO)*E5                              RCAL0430
      ONY=(LFYP(K)*FYO+LFYPA(K)*AYO)*E5                              RCAL0440
      ONZ=(LFZP(K)*FZO+LFZPA(K)*AZO)*E5                              RCAL0450
      GO TO 202                                                      RCAL0460
  201 ONX=LFXP(K)*FXO*E5                                             RCAL0470
      ONY=LFYP(K)*FYO*E5                                             RCAL0480
      ONZ=LFZP(K)*FZO*E5                                             RCAL0490
C-----NOW ADD THE THIRD LINE OF EQU. 4.158A                          RCAL0500
  202 E6=(O2-E2+E1*(E2*C1-E3*S1))/PSQ(K)                             RCAL0510
      IF(ISO.NE.1)GO TO 203                                          RCAL0520
      ONX=ONX+(LFXP(K)*SX+LFXPA(K)*SXA)*E6                           RCAL0530
      ONY=ONY+(LFYP(K)*SY+LFYPA(K)*SYA)*E6                           RCAL0540
      ONZ=ONZ+(LFZP(K)*SZ+LFZPA(K)*SZA)*E6                           RCAL0550
      GO TO 204                                                      RCAL0560
  203 ONX=ONX+LFXP(K)*SX*E6                                          RCAL0570
      ONY=ONY+LFYP(K)*SY*E6                                          RCAL0580
      ONZ=ONZ+LFZP(K)*SZ*E6                                          RCAL0590

C-----COMPUTE XP(K,I) = NORMAL MODE RESPONSE FOR KTH MODE AT TIME NO. I RCAL0600
  204 XP(K,I)=ON1+ONX+ONY+ONZ                                        RCAL0610
C                                                                    RCAL0620
C-----DO NOT COMPUTE INITIAL VELOCITIES OR REINITIALIZE X1P() AND V1P() RCAL0630
C     UNLESS THE NEXT CORRELATION TIME HAS BEEN REACHED.             RCAL0640
      IF(IC.NE.1) GO TO 100                                          RCAL0650
C                                                                    RCAL0660
C---VELOCITY CALCULATIONS (EQU. 4.158B, P.358, "VIBR. PROBS. ENGRG.") RCAL0670
C     FIRST TWO LINES OF EQU. 4.158B                                 RCAL0680
      VN1=E1*(-XOP(K)*S1+E4*C1-(NI(K)/PO(K))*(XOP(K)*C1+E4*S1))      RCAL0690
C-----THIRD LINE OF EQU. 4.158B                                      RCAL0700
      F2=(E1*(1.+(NI(K)*NI(K))/(PO(K)*PO(K)))*S1)/PSQ(K)             RCAL0710
      IF(ISO.NE.1)GO TO 205                                          RCAL0720
      VNX=(LFXP(K)*FXO+LFXPA(K)*AXO)*F2                              RCAL0730
      VNY=(LFYP(K)*FYO+LFYPA(K)*AYO)*F2                              RCAL0740
      VNZ=(LFZP(K)*FZO+LFZPA(K)*AZO)*F2                              RCAL0750
      GO TO 206                                                      RCAL0760
  205 VNX=LFXP(K)*FXO*F2                                             RCAL0770
      VNY=LFYP(K)*FYO*F2                                             RCAL0780
      VNZ=LFZP(K)*FZO*F2                                             RCAL0790
C-----NOW, ADD THE FOURTH LINE OF EQU. 4.158B                        RCAL0800
  206 F3=E5/PO(K)                                                    RCAL0810
      IF(ISO.NE.1)GO TO 207                                          RCAL0820
      VNX=VNX+(LFXP(K)*SX+LFXPA(K)*SXA)*F3                           RCAL0830
      VNY=VNY+(LFYP(K)*SY+LFYPA(K)*SYA)*F3                           RCAL0840
      VNZ=VNZ+(LFZP(K)*SZ+LFZPA(K)*SZA)*F3                           RCAL0850
      GO TO 208                                                      RCAL0860
  207 VNX=VNX+LFXP(K)*SX*F3                                          RCAL0870
      VNY=VNY+LFYP(K)*SY*F3                                          RCAL0880
      VNZ=VNZ+LFZP(K)*SZ*F3                                          RCAL0890
C                                                                    RCAL0900
  208 V1P(K)=PO(K)*(VN1+VNX+VNY+VNZ)                                 RCAL0910
      X1P(K)=XP(K,I)                                                 RCAL0920
C                                                                    RCAL0930
  100 CONTINUE                                                       RCAL0940
C                                                                    RCAL0950
      RETURN                                                         RCAL0960
      END                                                            RCAL0970
```

```
*DECK GRAPH                                                          GRA00000
      SUBROUTINE GRAPH(M,N)                                          GRA00010
C                                                                    GRA00020
C-----SUBPROGRAM FOR PRINTER PLOT OF THE MTH ROW OF ARRAY DATA       GRA00030
C     WHICH CONTAINS N POINTS.                                       GRA00040
      COMMON                                                         GRA00050
     4/COSTIF/XN( 40, 40),S( 40, 40),MFF( 40, 40),TT(300),GAX(300),  GRA00060
     #        GAY(300),GAZ(300),OX(300),OY(300),OZ(300),XOP(300),    GRA00070
     #        YOP(300),LF(700),SFR( 40, 56),DATA(100,198),MFR(120, 56), GRA00080
     #        SMN( 45, 45),SMR( 45, 56),SRR( 56, 56)                 GRA00090
      REAL LINE(102)                                                 GRA00100
      DATA  DOT,EX,BLANK/1H.,1H*,1H /                                GRA00110
C      FORMATS                                                       GRA00120
 2000 FORMAT(1H ,///)                                                GRA00130
 2010 FORMAT("      TIME",8X,"DISPL.",2X,1PE13.5,38X,I1,37X,E13.5)  GRA00140
 2020 FORMAT(1H ,27X,102A1)                                          GRA00150
 2030 FORMAT(1H ,1P2E13.5,1X,102A1)                                  GRA00160
C                                                                    GRA00170
      WRITE(6,2000)                                                  GRA00180
C     BLANK ALL POINTS                                               GRA00190
      DO 50 I=1,102                                                  GRA00200
   50 LINE(I)=BLANK                                                  GRA00210
C     MAXIMUM VALUE OF DATA                                          GRA00220
      DMAX=0.0                                                       GRA00230
      DO 100 I=1,N                                                   GRA00240
      TEST=ABS(DATA(M,I))                                            GRA00250
      IF(TEST.GT.DMAX)DMAX=TEST                                      GRA00260
  100 CONTINUE                                                       GRA00270
C SCALE FACTORS                                                      GRA00280
      SCALE=DMAX                                                     GRA00290
      IZERO=0                                                        GRA00300
      SCLMIN=-DMAX                                                   GRA00310
      WRITE(6,2010) SCLMIN,IZERO,SCALE                               GRA00320
C PLACE DOT AT -SCALE, 0, +SCALE                                     GRA00330
      LINE(2)=DOT                                                    GRA00340
      LINE(52)=DOT                                                   GRA00350
      LINE(102)=DOT                                                  GRA00360
      WRITE(6,2020)(LINE(I),I=2,102)                                 GRA00370
C      DOT,PRINT, AND BLANK ENTIRE LINE                              GRA00380
      DO 200 I=2,102                                                 GRA00390
  200 LINE(I)=DOT                                                    GRA00400
      WRITE(6,2020)(LINE(I),I=2,102)                                 GRA00410
      DO 300 J=2,102                                                 GRA00420
  300 LINE(J)=BLANK                                                  GRA00430
C      PLOT DATA POINTS                                              GRA00440
      DO 400 I=1,N                                                   GRA00450
      LINE(2)=DOT                                                    GRA00460
      LINE(52)=DOT                                                   GRA00470
      LINE(102)=DOT                                                  GRA00480
      IF(SCALE.EQ.0.0) GO TO 350                                     GRA00490
      Y=DATA(M,I)*50./SCALE                                          GRA00500
      GO TO 360                                                      GRA00510
  350 Y=0.                                                           GRA00520
  360 CONTINUE                                                       GRA00530
      IY=Y                                                           GRA00540
      IPLOT=IY+52                                                    GRA00550
      LINE(IPLOT)=EX                                                 GRA00560
      WRITE(6,2030) TT(I),DATA(M,I),(LINE(J),J=2,102)                GRA00570
      LINE(IPLOT)=BLANK                                              GRA00580
  400 CONTINUE                                                       GRA00590
C      DOT, PRINT LINE                                               GRA00600
      DO 500 I=2,102                                                 GRA00610
  500 LINE(I)=DOT                                                    GRA00620
      WRITE(6,2020)(LINE(I),I=2,102)                                 GRA00630
      RETURN                                                         GRA00640
      END                                                            GRA00650
```